International Conference of Natural Products and Traditional Medicine (ICNPTM 2011)

December 8-10, 2011 Xi'an, China

Sponsors:

Northwest University
Xi'an National Bio-Pharmaceutical Incubator
eBioCenter Corporation

Scientific Research Publishing, USA
2012

ISBN: 978-1-61896-030-6

Printed copies of this publication are available by sending email to
service@scirp.org

Produced by Scientific Research Publishing

For information on producing a conference proceedings and receiving an estimate, contact
service@scirp.org
http://www.scirp.org

Conference Committee

Scientific Advisory Committee:

Prof. Michel Baltas, Universite Paul Sabatier, France

Prof. Maurizio Massi, University of Camerino, Italy

Prof. Sauro Vittori, University of Camerino, Italy

Prof. Prakash Nagarkatti, University of South Carolina School of Medicine, USA

Prof. Mitzi Nagarkatti, University of South Carolina Cancer Center, USA

Prof. Wenyun Gao, College of Life Science, Northwest University, China

Prof. Jin-Ming Gao, College of Science, Northwest A & F University, China

Prof. Minggao Zhao, Fourth Military Medical University, China

Prof. Hirohi Ashihara, Ochanomizu University, Japan

Prof. Thomas L. Casavant, University of Iowa, USA

Prof. Kenta Nakai, The University of Tokyo, Japan

Prof. Ji Chen, University of Houston, USA

Prof. Klaus Helmut Obermayer, University of Berlin, Germany

Prof. Joe Wiart, Orange Labs, USA

Prof. Kwoh Chee Keong, Nanyang Technological University, Singapore

Dr. Christiane Andre-Barres, Universite Paul-Sabatier, France

Dr. Yansheng Zhang, National Research Council Canada/Plant Biotechnology Institute, Canada

Preface

Natural Products and Traditional Medicine is one of the most important fields of organic chemistry and is the basis of many exciting new developments in production of drugs, vitamins, agrochemicals, etc. ICNPTM 2011 is international in scope and invites and encourages the submission of scientific abstracts and proposals for sessions from corporate scientists, academic researchers, educators and healthcare providers worldwide. The conference showed original traditional medicine research through keynote and plenary presentations, oral and poster presentations, and Parallel Sessions. The theme for the conference is “Natural Products and Human Health”.

The topics of interest include, but are not limited to those listed in the following:

- Natural Products Isolation and Structure Elucidation
- Methodology and Synthesis of Natural and Unnatural Products
- Biosynthesis of Natural Products
- Natural Products and Drug Discovery
- Catalysis and Synthetic Methodology
- Bioorganic and Medicinal Chemistry
- Pharmacology and Toxicology of Natural Products
- Natural Products and Chemical Communication
- Quality Control Methodology and Medicinal Analysis
- Marine Natural Products
- Chemical Biology
- Natural Products and Pharmaceutical Engineering
- Natural Products and Food
- Natural Products and Pesticides
- Quality, Safety and Efficacy of Natural Products
- Natural Products for Health and Beauty

Contents

Study on the Design and Synthesis of Lipid-Soluble Dihydromyricetin

Minhui CAO[1,2], Dejiang NI[3]
[1]*College of Science, Huazhong Agricultural University, Wuhan, China*
[2]*College of Horticulture and Forestry Sciences, Huazhong Agricultural University, Wuhan, China*
[3]*Colleges of Horticulture and Forestry Sciences, Huazhong Agricultural University / Key Laboratory of Horticultural Plant Biology, Ministry of Education, Wuhan, China*
Email: cmhxsz@mail.hzau.edu.cn, nidj@mail.hzau.edu.cn

Abstract: Dihydromyricetin is the main nature antioxidant, but its poor lipid-soluble property has restricted its application in oil food industry. In this paper, we have designed a new synthetic method of lipid-soluble dihydromyricetin which was prepared by chemical modification.

Keywords: Dihydromyricetin; lipid-soluble; antioxidation

1 Introduction

Ampelopsis grossedentata is a wild, flavonoid-rich plant found in South China. Its leaves can be used as food and medicinal materials. Dihydromyricetin (DMY, Fig.1), a 2, 3-dihydroflavonol compound, is extracted from A. grossedentata. It has been shown to be effective in inhibiting hypertension, relieving cough, protecting the liver, and decreasing blood sugar. In addition, DMY has antioxidant, antiviral, antibacterial and antitumor properties [1-4].

Recently their antioxidation has been shown to be as effective as tert-butyl hydroquinone (TBHQ) and superior to citric acid monohydrate, ascorbic acid [5].The molecular structure of DMY indicate that its hydrophilicity is well and lipophilicity is not well because of its multiple phenolic-hydroxyl groups [6]; therefore its application in lipid industry is impractical. Investigations have shown that antioxidation property of the compounds with multiple phenolic-hydroxyl groups depends on higher activity of phenolic-hydroxyl group. So the activity phenolic-hydroxyl groups should be remained. For this reason, we have made a study of three step of synthetic method which is a new chemical modification method. Firstly phenolic-hydroxyl groups of DMY were protected by esterification reaction. So we will obtain the first intermediate (ADMY）. Secondly ADMY was hydrocarbylated by lauryl alcohol to improve lipophilicity of ADMY. We can obtain the second intermediate (BDMY). Lastly BDMY was hydrolyzed to revive the phenolic-hydroxyl groups of DMY. Then the object product was lipid-soluble DMY (LDMY). The target compounds were synthesized in three steps as outlined in Scheme1. LDMY should hold both antioxidation property and lipophilicity to play the role of antioxidation in lipid system effective.

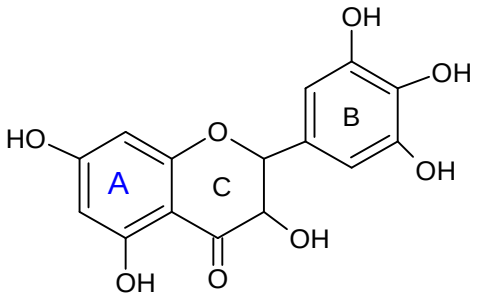

Figure 1. The molecular structure of DMY

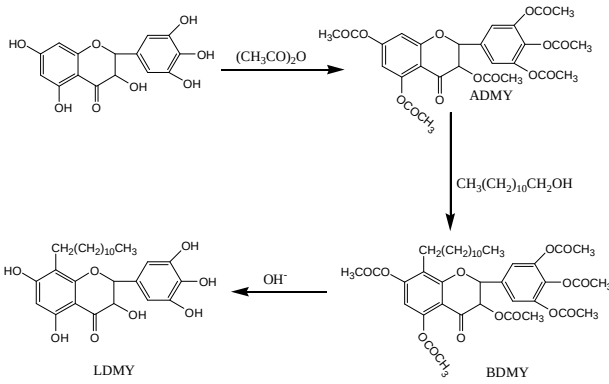

Scheme 1. Synthetic route for target compounds

2 Experimental

2.1 Apparatus

Infrared Spectroscopy (60SXB, America); Electro thermal constant-temperature dry box (SKFG-01, China); Electronic analytical balance (AW220, Japan); Electric-heated thermostatic water bath (HH-6, China); Vacuum pump of circulation water (SHZ-D(III), China).

2.2 Reagent

DMY (>95%) was prepared by our tea lab [7]. All other

978-1-61896-030-6

reagents were analytical reagent grade.

2.3 Experimental Method

2.3.1 Preparation of ADMY

Some DMY was stirred in 50ml of dry ethyl acetate at room temperature under a dry nitrogen atmosphere until all the DMY was dissolved in ethyl acetate. Some acetic anhydride was added drop from an additional funnel with constant stirring to the reaction mixture. The reaction mixture was then slowly heated to certain temperature and allowed to proceed with continuous stirring for certain time at certain temperature. The reaction mixture was washed with sodium bicarbonate solution in an extraction funne1. So process was repeated several times to remove the acetic acid and the unreacted DMY. Then extracted product was washed with distilled water 2～3 times to remove remainder impurities. ADMY was concentrated and dried in a vacuum desiccator.

2.3.2 Preparation of BDMY

Some ADMY was stirred in 50ml of dry acetone at room temperature under the dry nitrogen atmosphere until all the ADMY was dissolved in acetone. Some lauryl alcohol and catalyst was added drop from an additional funnel with constant stirring to the reaction mixture. The reaction mixture was then slowly heated to certain temperature and allowed to proceed with continuous stirring for certain time at certain temperature. The reaction mixture was washed with hot distilled water in an extraction funne1 in order to get rid of catalytic agent. Then it extracted by ether and concentrated to remove acetic ether. To increase the purity of BDMY, treatment of recrystallization in ethanol and dryness was performed.

2.3.3 Preparation of LDMY

Some BDMY was stirred in 10ml of NaOH methanol solution at certain temperature under a dry nitrogen atmosphere. The reaction mixture was washed with hydrochloric acid of which pH value was three in an extraction funnel in order to remove NaOH methanol solution. Then it was extracted by ether and concentrates to remove ether.

2.3.4 Determination of the Optimum Condition of Synthesis of Three Steps

Through single factor experiment the investigation analyzed the influence of factors such as pH, temperature, time and catalyst. In this paper, the optimal reaction conditions were determined.

3 Results and Discussions

3.1 Synthetic Principle

The first step was protection of phonetic-hydroxyl groups. There are six phenolic-hydroxyl groups that can react with acid anhydride or acylchloride in the molecular of DMY through theoretic analysis. In this experiment, we chose acetic anhydride to protect phenolic-hydroxyl groups, because acetic anhydride which is easy to hydrolyze is perfection protective group .The second reaction was hydrocarbylation. The 6 and 8 of A-ring of DMY which have a high nucleophilic activity are easy to react with electron-deficient reagents, such as alcohol, chloride. According to this principle lauryl alcohol was used to the benzene ring by Friedel alkylation, so long-chain aliphatic hydrocarbons can increase their lipid-soluble. Hydrolysis was the third step to remove the protective group. Under alkaline conditions acetate hydrolysis is general reaction.

3.2 Determination of Optimum Reaction

3.2.1 Synthesis Conditions of ADMY

The main purpose of this step was to protect phenolic hydroxyl by esterification reaction. However the phenolic hydroxyl under strong heat was prone to redox reactions. Therefore, to ensure the phenolic hydroxyl effectively transform into ester group, the conditions of the reaction temperature should be as low as possible and shorten the reaction time. Whether the infrared spectra of reaction products have telescopic vibratory absorption peak for–OH (3300～3400cm^{-1}) or not, that was a judgment of determination the optimum reaction.

3.2.1.1 Selection of Catalyst

We selected phosphoric acid, pyridine and potassium carbonate as a catalyst in experiments. The experimental results were as follows.

Table 1. Effect of catalyst type on the reaction

catalyst	phosphoric acid	pyridine	potassium carbonate
IR absorption peak for –OH	+	-	-

Note: + indicates the infrared spectra of reaction products at the 3300～3400cm^{-1} has the characteristic absorption peak of hydroxyl groups; - indicates that the infrared spectra of reaction products at the 3300～3400cm^{-1} free of the characteristic absorption peak of hydroxyl. The following Table 2, Table 3, Table 4, the + and - has the same meaning.

The results suggested that when phosphoric acid as a catalyst, the reaction was non-response. When pyridine and potassium carbonate as catalyst, the reaction was occured, but pyridine itself was odor and the reaction speed was very slow, so potassium carbonate was best catalyst for this reaction.

3.2.1.2 Effect of Acetic Anhydride Dosage

The amount of acetic anhydride directly affected the degree of esterification. Ensuring sufficient phenolic hydroxyl acylating with acetic anhydride, the amount of acetic anhydride should be as little as possible.

The following table showed the amount of acetic anhydride not less than 4 times the molar of DMY, the phenolic hydroxyl can be converted into esters. Therefore, we selected the amount of acetic anhydride (molar) 4 times to the amount for the DMY.

Table 2. Effect of acetic anhydride dosage

the molar ratio of DMY and acetic anhydride	1	2	3	4	5	6
IR absorption peak for –OH	+	+	+	-	-	-

3.2.1.3 Effect of Different Temperature and Different Time

We chose for the reaction temperature (30 ℃, 40 ℃, 50 ℃) and reaction time (2h, 4h, 6h) as a single factor experiment factors. The results showed that the response selection 4h and 40℃ was more appropriate.

Table 3. Effect of different temperature

Reaction temperature(℃)	30	40	50
IR absorption peak for –OH	+	-	-

Table 4. Effect of different time

Reaction time (h)	2	4	6
IR absorption peak for –OH	+	-	-

3.2.2 Alkylation

By Friedel-Crafst alkylation, long chain saturated hydrocarbon introduction into ADMY molecules can increase its lipid-soluble. There were two connected peaks in 2850cm^{-1} and 2920cm^{-1} for BDMY which was a telescopic vibratory absorption peak for C-H bond in fatty chain and indicates lauryl alcohol has been synthesized into DMY molecule while there was no such a peak for DMY. The characteristic absorption peak of IR and quality of the obtained product of unit mass ADMY was an indicator to determine whether the reaction was completed or not.

3.2.2.1 Effect of Catalyst Dosage

The catalyst such as $AlC1_3$、BF_3、$FeC1_3$、$ZnC1_2$ is commonly used in Friedel-Crafts alkylation reaction. As $AlC1_3$ is used in alcohol alkylation, hydrocarbon isomerization does not occur, $AlC1_3$ is a good catalyst. When the amount of lauryl alcohol was 2nADMY, reaction temperature was 70℃, in nitrogen atmosphere, the amount of catalyst were ADMY (quality) of 4%, 6%, 10%, 12%, 14%(w/w), the results in the following table indicated that the amount of catalyst directly affect reaction rate, the greater the amount of catalyst, the reaction time was shorter. When the amount in the range of 10% ~ 14% (w/w), the effect on the reaction is no longer obvious, the percent of 10% was best ration.

Table 5. Effect of catalyst dosage

catalyst dosage(w/w)	4%	6%	10%	12%	14%
IR absorption peak	+	+	+	+	+
quality of BDMY (g)	1.24	1.32	1.41	1.44	1.45

Note: + indicates the infrared spectra of reaction products at the 2850cm^{-1} and 2920cm^{-1}has the characteristic absorption peak; - indicates that the infrared spectra of reaction products at the 2850cm^{-1} and 2920cm^{-1} free of the characteristic absorption peak. The following Table 6, Table 7, Table 8, the + and - has the same meaning.

3.2.2.2 Effect of Lauryl Alcohol Dosage

When the amount of catalyst was 10% of ADMY quality, reaction temperature was 70℃, reaction time was 6h, in nitrogen atmosphere the results were showing in the following table.

Table 6. Effect of lauryl alcohol dosage

lauryl alcohol dosage (n_{ADMY})	1	1.2	1.4	1.6	1.8
IR absorption peak	+	+	+	+	+
quality of BDMY (g)	1.08	1.35	1.38	1.36	1.41

The results showed that when the amount of lauryl alcohol was 1.4 times molar of ADMY, there was no obvious effect on the reaction. So the best amount of lauryl alcohol was 1.4 times molar of ADMY.

3.2.2.3 Effect of Different Temperature

Temperature was a major factor of the alkyl isomerization. Isomerization was easy to occur under high-temperature. In order to avoid or reduce isomerization, it should try to reduce the temperature of alkylation. When the amount of catalyst was 10% of ADMY, the amount of lauryl alcohol was 1.4 times molar of ADMY, in nitrogen atmosphere, the effect of temperature on the reaction as follows. When the reaction temperature was higher than that of 50℃, the reaction can be carried out smoothly. Although increasing the reaction temperature can shorten the reaction time, but result in hydrocarbon isomerization. Significant increase of BDMY in quality, the reason is result of the isomerization reaction. At 50℃, although the reaction time was longer, but the reaction conditions were mild. Thus the temperature of 50℃ was more appropriate.

Table 7. Effect of different temperature

Reaction temperature（℃）	40	50	60	70	80
Reaction time(h)	12	8	6	4	2
IR absorption peak	-	+	+	+	+
quality of BDMY(g)	0	1.29	1.34	1.45	1.68

3.2.3 Hydrolysis

Many acetate hydrolysis methods were existence, but the hydrolysis reaction rate was fast in sodium hydroxide methanol solution, reaction conditions were mild. Whether the infrared spectra of reaction products have

978-1-61896-030-6 © 2012 SciRes.

telescopic vibratory absorption peak for ester (1710～1780cm^{-1}) or not, that was a judgment of determination the optimum reaction.

3.2.3.1 Effect of pH on the Reaction

To ensure hydrolysis of BDMY effectively it should try to reduce the pH value of solution, because of instability of the phenolic hydroxyl group.

Table 8. Effect of pH on the reaction

pH value	7.5	8	8.5
IR of ester	+	-	-

The results were as follows. When pH value was greater than 7.5, BDMY were able to fully hydrolyze. Therefore, we choose pH = 8 as better condition.

3.2.3.2 Effect of Different Temperature

To ensure hydrolysis of BDMY effectively, the reaction temperature should be as low as possible, because of instability of the phenolic hydroxyl group. The following table showed when the reaction temperature was not lower than 30℃; reaction time not less than 8h, BDMY was able to fully hydrolyze. Thus, 30 ℃ was more appropriate reaction temperature.

Table 9. Effect of different temperature on the reaction

Reaction temperature（℃）	20	30	40	50
Reaction time(h)	12	8	6	4
IR of ester	+	-	-	-

4 Conclusion

Three-step synthesis method is effective and new method to synthesize lipid-soluble DMY. The optimum reaction conditions of acylation are as follows: potassium carbonate as catalyst, DMY and acetic anhydride molar ratio of 1:4, the reaction temperature is 40 ℃, reaction time is 4h; The optimum reaction conditions of alkylation are as follows: the amount of catalyst is 10%(w/w), reaction temperature is 50℃, reaction time is 6h, the amount of lauryl alcohol (amount of substance) is 1.4 times ADMY; the optimum reaction conditions of hydrolysis are as follows: pH=8, the reaction temperature is 30℃.

Acknowledgement

The authors are grateful for financial support by the major special projects of technology of the Ministry of Agriculture (06208202B) and “the Fundamental Research Funds for the Central Universities” (2011JC002).

References

[1] Zhang Yousheng, Ning Zhengxian,Yang Weiling, Ampelopsis Grossedentat, Guangzhou: Guangdong science and Technology Press,pp220-246,2003.
[2] Weng Xinchu, Ren Guopu, Selection nature antioxidant, Journal of the Chinese Cereals and Oils Association, Vol4(13), pp46-48, 1998.
[3] Lin Shuying, Zhang Yousheng,Ye Hongqing, Study on antioxidation of dihydromyricetin in lard system. Food Science and Technology, Vol(4), pp7l-73,2003.
[4] Paola Montoro , Alessandra Braca, Cosimo Pizza, Nunziatin, De Tommasi, Structure–antioxidant activity relationships of flavonoids isolated from different plant species, Food-Chemistry, Vol92 (2005), pp349-355.
[5] Seung Mi Yoo , Sung yong Mun, Jin-Hyun Kim, Recovery and pre-purification of (+)-dihydromyricetin from Hovenia dulcis, Process,Biochemistry,Vol41(2006), pp567-570.
[6] Xianyong Yu, Ronghua Liu, Fengxian Yang, Danhong Ji, Xiao fang Li, Study on the interaction between dihydromyricetin and bovine serum albumin by spectroscopic techniques, Journal of Molecular Structure, Vol985 (2011), pp 407-412.
[7] Cao Minhui, Xie Yiping Chen Yuqiong, Ni Dejiang. Study of new Methods for Green Extraction and Purification of Dihydromyricetin from Ampelopsis.Food science and technology. Vol 6(2011), pp128-130.

Study on the Extraction Technology of Chlorgenic Acid in Huaiqing Chrysanthemum

Juan MIAO[1], Nannan WEI[1], Jingjing LI[1], Dexue FU[2]
[1]*Department of Physics and Chemistry Henan Polytechnic University, Jiaozuo, China*
[2]*Huaiyao Research Center Jiaozuo University, Jiaozuo, China*
Email: miaojuan@hpu.edu.cn

Abstract: The effects of the solvent concentration, the extracting time, and the liquid/solid ration were investigated to study the optimum technological conditions of the chlorogenic acid from Huaiqing chrysanthemum with the ethanol solution by the orthogonal experiment method in this paper. The optimum technological conditions were as follows. The ethanol volume fraction ¢ is 55%; the extracting time is 1 hour; the liquid/solid ratio is 20. The extraction process of the chlorogenic acid was also identified as a Quasi-first order reaction by researching the reaction kinetics, whose apparent rate constant k is 0.03935.

Keywords: Huaiqing chrysanthemum; chlorogenic acid; extraction; orthogonal experiment; reaction kinetics

1 Introduction

Huaiqing chrysanthemum is Jiaozuo specialty as one of Four Huaiqing Chinese Medicines (Yam, Chrysanthemum, Rehmannia, Achyranthes). It is a kind of high nutritional vegetable which used as both food and medicine in China. It has functions for dispelling wind and clearing heat, also benefit for liver and eyes[1]. Chlorogenic acid is one of the important active ingredients in the chrysanthemum.

Chlorogenic acid is a kind of synthetic phenylpropanoid substances in the process of aerobic respiration within plants[2], it has multiple effects such as free radicals, anti-bacterial anti-inflammatory, antiviral, hypoglycemic, lipid-lowering, liver gallbladder and so on. Chlorogenic acid has been found to have anti-cancer, anti-HIV effect, it can be used for design and development of anti-cancer, anti-AIDS drugs[3]. At the same time, chlorogenic acid and other polyphenols known as the "seventh class of nutrients," is widely used in health-care industry, with detoxification, beauty emollients, anti-aging characteristics of the digestive system, blood system and the reproductive system diseases have a significant effect. Extraction of chlorogenic acid has been reported rarely[4-6]. In this paper, the solvent heat extraction method was be used to extract the chlorogenic acid in the Huaiqing chrysanthemum. And then, the orthogonal experimental was done to make sure the optimum process conditions.

2 Materials and Methods

2.1 Materials, Instruments and Reagents

Huaiqing chrysanthemum was purchased from Jiaozuo. UV spectrophotometer (UV1900, Purkinje General Instrument Co., Ltd Beijing), circulating water pump (SHB-Ⅲ, Chang sheng Experiment Instrument Co., Ltd., Zheng zhou), precision pH meter (PHS-3CT, Grand & P Instrument Co., Ltd. Shanghai), constant temperature heating magnetic stirrer (CL-Z, Chang sheng Experiment Instrument Co., Ltd., Zheng zhou). Chlorogenic acid comparison products were purchased from the Chinese Identification of Pharmaceutical and Biological Products, production batch number 110753-200413; anhydrous ethanol, ethanol (¢ = 95%) for the AR; deionized water from the Experimental Center of Chemistry, Henan Polytechnic University, made.

2.2 Methods

The chlorogenic acid was extracted by hot extraction methods from the Huaiqing chrysanthemum which was crushed. The optimum extraction conditions were determined with the designed orthogonal experiments on the basis of single factor experiment. Under the optimum conditions, the dynamics of the chlorogenic acid extraction process was also studied by the linear fitting method.

2.3 Optimal Wavelength and Standard Curve

2.3.1 The Choice of the Maximum Absorption Wavelength

Chlorogenic acid reference substance was diluted by 95% ethanol. The absorption spectra of reference solution and extraction solution were scanned with UV spectrophotometer, which wavelength range from 200nm to 400nm. The results were shown in Fig1. The absorption spectra of reference solution and extraction solution have the same maximum absorption peak at 329nm, which is consistent with the literature[7]. So the wavelength of detection light was determined as 329 nm in our next experiments.

978-1-61896-030-6

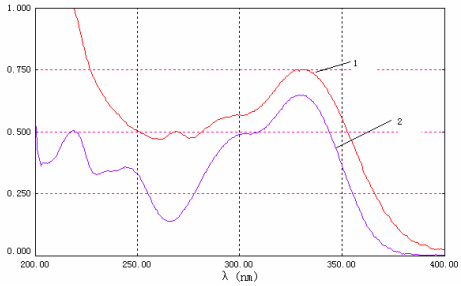

Figure 1. UV spectra of reference solution and extraction solution

1-Extraction solution; 2-Reference solution

2.3.2 Building Standard Curve

Firstly, the stock solution of the chlorogenic acid was obtained. 5.0 mg chlorogenic acid standard substance was weighed accurately in 100 mL of volumetric flask, dissolved and made up to the mark with ethanol solution of 95%. Secondly, a sequence of standard solutions with different concentration was obtained by diluting the stock solution with 95% ethanol. Thirdly, the absorbance of each standard solution was determined by the UV spectrophotometry at 329nm, and the reference solution was the 95% ethanol. And then, the standard curve was drawn in Fig2, ordinate representing absorbance (Y) and abscissa representing standard solution concentration (C), respectively. The regression equation concluded from the standard curve can be shown as Y = 0.06045 ×C-0.01149, where the linear range is 0 ~ 30μg/mL, and the correlation coefficient (R) is 0.9998. According to this regression equation, the mass of chlorogenic acid (m) can be calculated as the following formula (1).

$$m(g) = [(Y + 0.01149) \cdot 10^{-6} \cdot n \cdot V] / 0.06045 \quad (1)$$

$$\alpha = m / M \cdot 100\% \quad (2)$$

Equation (2) is the yield of chlorogenic acid; n is a multiple of dilution; V is the volume of solvent (mL); M is quality of the crude drugs.

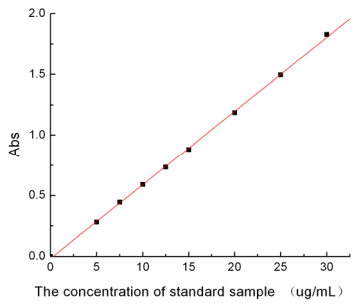

Figure 2. The standard curve of chlorogenic acid

2.4 Solvents to Choose

Chlorogenic acid molecule contains hydroxyl and pyrocatechol hydroxyl, so chlorogenic acid is soluble in water and organic solvents such as methanol, ethanol and acetone. However, the acetone has very low boiling point and the methanol is toxic. In this paper water and ethanol were used as the extraction solvents of chlorogenic acid and investigated their different effect on the yield of chlorogenic acid.

The UV absorption spectra of chlorogenic acid with different solvents were given in Fig 3. The spectrum of the extraction solvents with water is wide and has not obvious absorption peak at 329nm. But the absorption peak of the spectrum of the extraction solvents with ethanol is more obvious. This result shows that the ethanol should be suited to be the extraction solvent of chlorogenic acid from the Huaiqing chrysanthemum.

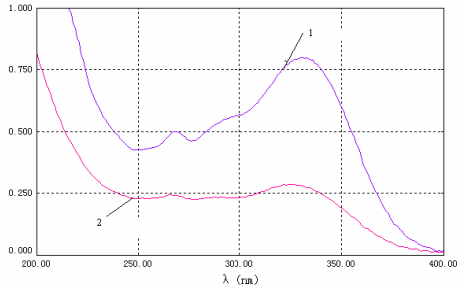

Figure 3. The comparison of the UV absorption spectra between water and ethanol solution

1-Extraction solution with ethanol; 2- Extraction solution with water

3. Results and Discussion

3.1 Orthogonal Experiments

According to the single factor experiment results, under the condition of pH6 and temperature for 80^0C, the orthogonal experiments were designed to determine the optimization technique conditions. As is shown in table1 that the extracting time (A), the solvent volume fraction (B) and the liquid/solid ratio (C) were treated as the orthogonal experimental investigation factor and taken three levels and chosen the orthogonal table L^9 (3^4).

Each experiment was repeated twice in orthogonal table in order to reduce experimental error[8]. The orthogonal experiment results were shown in table2.

The range analysis results show that the order of factors which affect the yield of chlorogenic acid is the solvent volume fraction, the liquid/solid ratio and the extracting time. According to the highest yield of chlorogenic acid, the optimum extraction technology is A1B1C3. That is to say, it is that the extracting time is 1 hour, and the ethanol volume fraction ¢ is 55% and the liquid/solid ratio is 20. The yield of chlorogenic acid is 5.5028% by calculation in this condition.

3.2 The Reaction Dynamics Research

Spiro M[9] et al. found the dynamic model that is

widely used in extraction of plant components in 1981. They have studied the extraction process of the Theaflavins and the thearubigins from black tea and the extraction of the caffeine from the coffee beans. Furthermore they established the dynamic equation of the solute diffusion, that is $\ln[C\infty/(C\infty-C)]=kt$, where C is the solute concentration of the solution at t moment, and C∞ is the balance concentration, and k is the apparent rate constant.

The extraction experiment was done in order to investigate the reaction dynamics under the optimum conditions. The UV absorbance of the chlorogenic acid would be measured every 20min until the UV absorbance almost unchanged. To that moment, the acquired concentration was the balance concentration C∞. The values of the $\ln[C\infty/(C\infty-C)]$ were gotten by contrasting the standard curve. And then, the relationship between these values and the time t was investigated by Origin7.5 and shown in the Fig4.

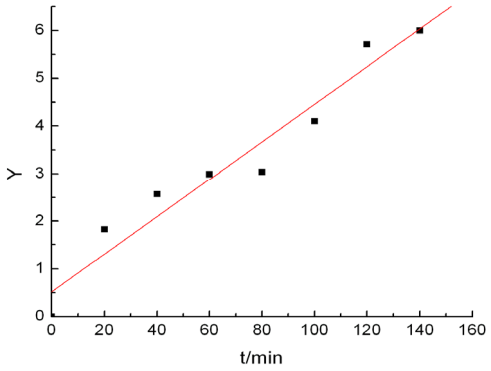

Figure 4. The relations between $\ln[C\infty/(C\infty-C)]$ (y axis) and time t (x axis) correlation coefficient R=0.97219

The linear fitting result shows that the $\ln[C\infty/(C\infty-C)]$ and the time t is a good linear relation whose curve equation is Y =0.52306 + 0.03935×X, the correlation coefficient R = 0.97219. This result demonstrates that the solute diffusion of the extraction process of the chlorogenic acid from the Huaiqing chrysanthemum is in accordance with the Spiro M equation. So the extraction process of the chlorogenic acid could be identified as the pseudo-first-order reaction whose apparent rate constant k is 0.03935.

Table 1. Factors and levels in orthogonal experiments

levels	The extracting time /min (A)	The solvent volume fraction /ø (B)	The liquid/solid ratio(C)
1	60	55	15
2	90	70	25
3	120	95	20

Table 2. Results of orthogonal experiments

Test number	A	B	C	Yield(%)	
				Y1	*Y2*
1	1	1	1	4.8252	4.8294
2	1	2	2	5.4627	5.4632
3	1	3	3	4.8196	4.792
4	2	1	2	5.2441	5.2326
5	2	2	3	5.2953	5.2953
6	2	3	1	3.7663	3.7663
7	3	3	3	5.2338	5.243
8	3	1	1	5.3500	5.3156
9	3	2	2	4.4629	4.4515
K1	30.192	30.797	27.853		
K2	28.6	30.431	30.317		
K3	30.057	27.621	30.679		
R	1.592	3.176	2.826		

4 Conclusion

The optimum technological conditions were determined by the orthogonal experiments with three revels and 4 factors. Under the condition of pH6 and temperature for 800C, the extract conditions were that the ethanol volume fraction ¢ is 55%, and the extracting time t is 1 hour, and the liquid/solid ratio is 20, The yield of the chlorogenic acid was 5.5028% under these conditions. And then, the reaction kinetics of the chlorogenic acid extraction process was identified preliminarily as the pseudo-first-order reaction kinetics process whose apparent rate constant k is 0.03935. This method can be used as a reliable and easy method for the extraction of chlorogenic acid from Huaiqing chrysanthemum.

Acknowledgement

Zhang Lei and Yang Lin in Henan polytechnic university provide the selfless help in this paper.

References

[1] Song Fu-hai,Guo Yong-sheng The quality, high yeild and pollution-free cultivation techniques of Huaiqing chrysanthemum [J].Agro-environment & development, 2005,22 (4),P23-24(Ch).

[2] Du Yan-bing, Qiu Ai-yong. Bioactivity, resources, extraction and purification of chlorogenic acid[J]. Modernfood science & technology, 2006,22(2),P250-252(Ch).

[3] Chen Shao-hua, Wang Ya-qin, Luo Li-xin.Advances in research on chlorogenic acid[J]. Food science and techology, 2008,33 (2),P195-198(Ch).

[4] Ling Guan-ting. Polyphenols are called as “Seventh Nutrients”[J]. China food additives, 2000,(1),P28-37(Ch).

978-1-61896-030-6

[5] Wei Qin, Ma Xi-han, Jing Qian-ping. Study on technique of extraction and isolation of chlorogenic acid from leaves of eucommia ulmoides[J]. Chemistry & iudustry of forest products, 2001,21(4), P27-32(Ch).
[6] Liu Zong-lin, Hui Jiu-zhen,Peng Yi-jiao. Extraction of functional components in the leaves of eucommia[J]. Food science, 2003,24 (8),P 62-63(Ch).
[7] Lu Jin-qing, Jiang Sheng-jun Lu hua. Determination of chlorogenic acid in dendranthema morifolium witj HPLC[J]. Lishizhen medicine and materia medica research, 2006,17 (4),P 549-551(Ch).
[8] Zheng Shao-hua, Jiang Feng-hua. Design of experiments and data processing[M]. Beijing: China building materials industry Press, 2004,64.
[9] Feng Nian-ping, Yu Wei-zhu. Chinese medicine principle and application of extraction and separation technology[M]. Beijing: Chinese medical science and technology Press, 2005,15-29.

Crystal Structure and Antimicrobial Activity of Bis(1-benzyl-2-phenyl-1H-benzimidazole) Copper(II) Dichloride Complex

Yufen LIU[1], Haitao XIA[1], Defu RONG[2]
[1]*School of Chemical Engineering, Huaihai Institute of Technology, Lianyungang, Jiangsu, China*
[2]*Beilun Entry-Exit Inspection and Quarantine Bureau of China, Ningbo, Zhejiang, China*
Email: liu222005@hhit.edu.cn

Abstract: One new copper(II) complex with 1-benzyl-2-phenyl-1H-benzimidazole [$Cu(C_{20}H_{16}N_2)_2Cl_2$] were synthesized, and characterized by elemental analysis and IR spectra. The structures were established by single crystal X-ray diffraction. The copper(II) ion is four-coordinated and exhibites parallelogram coordination geometry. The molecules of the complex are linked through hydrogen bonding and π…π bonding to form three-dimensional network. After studying the antimicrobial activity of copper(II) complex, we can find that the copper(II) complex was active against *Escherichia coli*, *Staphylococcus aureus* and *Bacillus subtilis*.

Keywords: Benzimidazole derivative; Cu(II) complex; crystal structure; antimicrobial activity

1 Introduction

Copper is a physiologically important metal [1,2], playing an important role in growth, scavenging harmful free radicals, and preventing oxidative damage to cells, protein synthesis, and the activity of metal enzymes [3], capable of participating in a variety of redox cycling reactions [4]. The benzimidazole derivant have the a wide range of biological activity involving the anticancer, antibacterial, anti-inflammation, therapy of hypoglycemia and physiological disorder and so on [5], the studies in the pharmaceutical chemistry have allimportant significance. The research indicated that many transition metal complexes with the benzimidazole exist in all kind of important biomolecules have become good model for many metalloenzymes and metal protein active spot [3]. By virtue of their variable oxidation states, flexible coordinate geometry, and rich photophysical and electrochemical properties, many transition metal complexes have been covalently linked to biomolecules for various purposes [6]. In this study, we report the crystal structures and antimicrobial activity of the new complex [$Cu(C_{20}H_{16}N_2)_2Cl_2$].

2 Experimental

2.1 Preparation of the Complex

To a solution of ligand (10mmol) in methanol (30ml) was added to $CuC1_2 \cdot 2H_2O$ (5mmol) in water (10ml). The mixture was stirred at 55-60℃ for 2h. The solvent was cooled to room temperature, a mass of green precipitation was collected by filtration, then washed with water and methanol successively, finally dried to afford green powder in 76.8% yield, recrystallization of the complex from ethanol at room temperature gave crystal suitable for X-ray single crystal diffraction analysis. m.p. 274-276℃. IR(KBr，ν/cm^{-1}): 3040, 1608, 1449, 1410, 1353, 1299, 1170, 1074, 1027, 978, 927, 824, 732, 690; Anal. calcd for $C_{40}H_{32}Cl_2CuN_4$ (%): C68.32, H4.59, N 7.97; found (%): C68.24, H4.53, N8.12.

Scientific Foundation of Huaihai Institute of Technology (Z2009022)

2.2 Physical Measurements

Element analyses were measured by Perkin-Elmer 2400c Element analyzer. Infrared spectra were recorded on a Nicolet 5DX FT-IR spectrophotometer in the range 4000 to 400 cm^{-1}.

2.3 X-Ray Crystal Structure Determination

A single-crystal of the complex suitable for X-ray crystallographic analysis was mounted in sealed glass capillaries. Diffraction data were collected with a Bruker SMART 1000 CCD diffractometer by the use of graphite monochromated Mo-Ka radiation (λ = 0.71073 Å) at 298(2) K. The crystal structure was solved by direct methods and all non-hydrogen atoms were located with successive difference Fourier syntheses. The structure was refined by full-matrix least-squares on F^2 with anisotropic thermal parameters for all non-hydrogen atoms. Hydrogen atoms were added according to theoretical models. All calculations were performed using the programs contained in the SHELXL package [7, 8]. A summary of crystallographic data and refinement parameters for the Cu(II) complex are given in table 1.

2.4 Antimicrobial Activity Determination

The test of antimicrobial activity adopts a method by

978-1-61896-030-6

agar diffusion using DMF as the solvent. Culture medium of antibiotic medium are consist of the Beef extract, albumens and agars. The culture medium, experiment wear and filter paper of 5 mm diameter were sterilized for 30 min at 120˚C, the culture medium was transferred to glass plates and cooled to about 37˚C. After *Escherichia coli* (*E.coli*), *Staphylococcus aureus* (*S.aureus*) and *Bacillus subtilis* (*B.subtilis*) were inoculated to the solid culture medium surface, the filter paper with 20μL samples were placed on the surface. They were allowed to incubate at 37˚C for 24 h. The inhibition zone around the disc was calculated as zone diameter in millimeters.

3 Results and Discussion

3.1 Crystal Structure of Complex

The molecular structure of Cu(II) complex is shown in Figure 1. The selected bond distances, bond angles and hydrogen bonds are summarized in Table 2. Bei *et al* [15] have reported the crystal structure of ligand, but they have no any explanation for intermolecular forces. There are hydrogen bonds and π…π bonds in the structure of the ligand and Cu(II) complex. The central Cu(II) ion is four-coordinated with two N atoms from two ligands and two chloridion. The two N atoms and two chloridion coordinated to Cu(II) ion define a parallelogram, the Cu(II) ion occupies center of parallelogram and is strictly coplane with the two N atoms and two chlorine atoms. The Cu–Cl bond distance is 2.2741(11)Å, Cu–N bond distance are 1.967(3)Å. The dihedral angles between benzimidazole plane and phenyl plane, benzyl plane are 35.02(10) º and 79.57(5) º for ligand, whereas corresponding to 44.13(15)º and 87.96(9)º for Cu(II) complex. This change is because of the N atom coordinated to Cu(II) ion, and there are C(7B)-H(7B)…Cl(1) and C(7C)-H(7C)…Cl(1A) hydrogen bonds in molecules. In addition, π…π stacking interactions exist between phenyl plane of adjacent molecules for ligand and Cu(II) complex, The center-to-center distance and vertical distance of adjacent phenyl plane are 4.879(2) Å and 3.366 Å for ligand, 4.309(3) Å and 3.321 Å for Cu(II) complex, respectively. The molecules of the ligand and Cu(II) complex are linked through hydrogen bonding and π…π bonding to form three-dimensional network.

Table 1. Crystal data and structure refinement for ligand and complex

compound	ligand	complex
Formula	$C_{20}H_{16}N_2$	$C_{40}H_{32}N_4CuCl_2$
Formula weight	284.35	703.14
Temperature (K)	298(2)	298(2)
Wavelength (Å)	0.71073	0.71073
Crystal system	Monoclinic	Monoclinic
Space group	$P2_1/c$	$P2_1/c$
Unit cells and dimensions (Å, ˚)		
a	6.0045(13)	10.5976(16)
b	16.924(2)	16.719(2)
c	15.181(2)	10.0340(10)
α	90	90
β	91.467(2)	113.398(2)
γ	90	90
Volume (Å^3), Z	1542.2(4), 4	1631.7(4), 2
D_{Calcd} (mg/m^{-3})	1.225	1.431
F(000)	600	726
Crystal size (mm^3)	0.40×0.23×0.21	0.18×0.11×0.05
θ Range for data collection (˚)	1.80-25.01	2.09-25.01
Reflections collected	7679 [R(int)=0.0553]	8217 [R(int)=0.1060]
Refinement method	Full-matrix least-squares on F^2	Full-matrix least-squares on F^2
Data/restraints/parameters	2709/0/199	2875/0/214
Goodness-of-fit on F^2	1.005	1.010
Final R indices [$I>2\sigma(I)$]	R_1=0.0452, wR_2=0.1206	R_1=0.0531, wR_2=0.1153
Largest difference peak and hole (eÅ^{-3})	0.140 and -0.162	0.605 and -0.612

Table 2. Selected bond lengths (A˚), hydrogen bond lengths (A˚) and bond angles (°) for ligand and complex

Cu(1)–N(1)^i	1.967 (3)
Cu(1)–N(1)	1.967 (3)
Cu(1)–Cl(1)^i	2.2741 (11)
Cu(1)–Cl(1)	2.2741 (11)
N(1)^i–Cu(1)–N(1)	180.00 (18)
N(1)^{ii}–Cu(1)–Cl(1)^i	90.24 (9)
N(1)–Cu(1)–Cl(1)^i	89.76 (9)
N(1)^i–Cu(1)–Cl(1)	89.76 (9)
N(1) –Cu(1)–Cl(1)	90.24 (9)
Cl(1)^i–Cu(1)–Cl(1)	180.0

	D–H…A	D–H	H…A	D…A	∠D–H…	A
ligand	C(8)–(8B)…N(2)^{ii}	0.97	2.55	3.515(3)	176	
complex	C(7)–H(7)…Cl(1)^{iii}	0.93	2.93	3.852(4)	171	

Symmetry codes: (i) −x+1, −y+1, −z+1; (ii) x−1, y, z; (iii) x, $-y+1\frac{1}{2}$, $z-\frac{1}{2}$

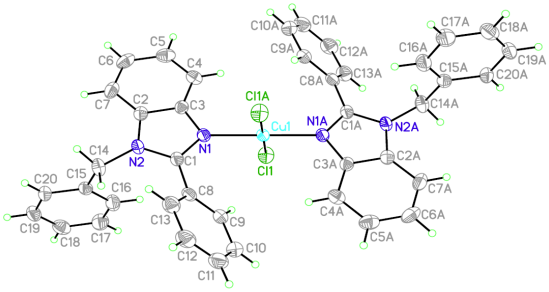

Figure 1. Molecular crystal structure of the Cu(II complex [symmetry code: A (1-x, 1-y, 1-z)])

3.2 Antimicrobial Activity

The test results of the ligand and the complex against *B. subtilis*, *E. coli* and *S. aureu* are presented in Table 3. It is evident that antibacterial activity of the Cu(II) complex and ligand increased with the increasing the concentration. The ligand showed higher activity against *B. subtilis*, *E. coli* and *S. aureu* as compared to the complex. Complexation could enhance the lipophilic character of the central metal atom, which subsequently favours its permeation through the lipid layers of cellular membrane, inhibit the growth of bacteria.

Table 3. The antibacterial activity of the complex and ligand

	Diameter of inhibition zone (mm)					
	complex			ligand		
	0.3mg/mL	1mg/mL	2mg/mL	0.3mg/mL	1mg/mL	2mg/mL
E.coli	9.6	11.2	15.1	8.8	19.1	23.0
S.aureu	7.1	12.3	16.6	9.6	17.0	21.2
B.sutilis	8.8	10.5	13.2	9.1	13.1	14.9

4 Conclusion

We synthesized a new copper complex $[Cu(C_{20}H_{16}N_2)_2Cl_2]$ and its structure was established by single crystal X-ray diffraction. The antimicrobial properties of the complex in DMF has been investigated. The complex sample showed good antimicrobial activity against *E. coli*, *S. aureu* and *B. subtilis*. But the ligand showed higher activity against *B. subtilis*, *E. coli* and *S. aureu* as compared to the complex.

References

[1] G. Crisponi, V.M. Nurchi, D. Fanni, C. Gerosa, S. Nemolato and G. Faa, "Copper-related diseases: From chemistry to molecular pathology", *Coordination Chemistry Reviews*, Vol. 254, No. 7-8, 2010, pp. 876-889.

[2] J. A. Drewry and P. T. Gunning, "Recent advances in biosensory and medicinal therapeutic applications of zinc(II) and copper(II) coordination complexes", *Coordination Chemistry Reviews*, Vol. 255, No. 3-4, 2011, pp. 459-472.

[3] Jian-Quan Lu, Fen Jin, Ting-Quan Sun and Xing-Wang Zhou, "Multi-spectroscopic study on interaction of bovine serum albumin with lomefloxacin–copper(II) complex", *International Journal of Biological Macromolecules*, Vol. 40, No. 4, 2007, pp. 299-304.

[4] H.Y. Shrivastava, M. Kanthimathi and B.U. Nair, "Copper(II) complex of a tridentate ligand: an artificial metalloprotease for bovine serum albumin", *Biochimica et Biophysica Acta*, Vol. 1573, No. 2, 2002, pp. 149-155.

[5] Zheng-Zhou MAO, Zhao-Yang Wang, Xiao-Na Hou, Xiu-Mei Song, and Yu-Fen Luo, "Research Progress in the Synthesis of Benzimidazoles", *J. Organ. Chem (Chinese)*, Vol. 28, No. 3, 2008, pp. 542-547.

[6] Jun Wang, Yun-Feng Wang, Jian Gao, Ping Hu, Hong-Yu Guan, Li-Qun Zhang, Rui Xu, Xia Chen and Xiang-Dong Zhang, "Investigation on damage of BSA molecules under irradiation of low frequency ultrasound in the presence of FeIII-tartrate complexes", *Ultrasonics Sonochemistry*, Vol. 16, No. 1, 2009, pp. 41-49.

[7] Sheldrick, G.M. SHELXL-97, Programof X-Ray Crystal Structure Solution; University of Göttingen: Göttingen, Germany, 1997.

[8] Sheldrick, G.M. SHELXL-97, Program for X-Ray Crystal Strucuture Refinement; University of Göttingen: Göttingen, Germany, 1997.

[9] Feng-Li Bei, Hai-Qun Chen, Xu-Jie Yang, Lu-De Lu and Xin Wang, "Synthesis, Crystal Structure and Quantum Chemical Calculation of Benzimidazole Derivatives", *J. Organ. Chem. (Chinese)*, vol. 24, 2004, pp. 300-305.

978-1-61896-030-6 © 2012 SciRes.

Ultrasound-Microwave Assisted Extraction of Ricinus Communis Allergen from Castor Bean Meal

Ailin ZHANG[1,2], Yufeng HU[1], Changlu WANG[1], Lijin ZHANG[2], Zhijiang ZHOU[3]
[1]*Tianjin Engineering Center of Food process, Tianjin, China*
[2]*Department of Food Science, Tianjin Agricultural University, Tianjin, China*
[3]*School of Chemical Engineering and Technology, Tianjin University, Tianjin, China*
Email: zhang_taohui2000@yahoo.com.cn

Abstract: The influence of ultrasound-microwave during extraction of Ricinus communis (L) allergen from castor bean meal (CBM) was investigated. The method was successfully applied for the ultrasound-microwave assisted extraction (UME) of allergen from CBM. The corresponding extraction parameters including the extraction temperature, ultrasonic-microwave power and extraction time were investigated. CBM was crushed, sifted, ground and suspended for 4 h in 25% ethanol water (1:4) at room temperature followed by ultrasound-microwave. The yield, polysaccharose and protein contents were determined after each processing step. The purity of extracted allergen was tested through HPLC and the Sephadex G-100 and Tricine-SDS-PAGE detection with unique electrophoresis strip documented that allergen was purifed. The paper describes the conditions of the temperature, time, and microwave-power for the method reliability with UME and suitability for the effective extraction of allergen from CBM.

Keywords: Ricinus communis L; allergen; ultrasound-microwave assisted extraction; castor bean meal

1 Introduction

Recent studies described the use of high-intensity ultrasound-microwave to extract a number of polysaccharides from a variety of sources, It was suggested significant reductions in time and solvent requirements leading to cost savings and increased production rates [1]. Ricinus communis with its derivatives has scores of industrial uses, while the pomace is used only as a fertilizer and this usage has some hazard because of the potent allergens it contains. The major byproduct of castor bean oil extraction can the main protein source for swine diets globally if we adopted of reasonable processing. Castor bean meal (CBM) contains not only rich Various nutrients protein that posses 33%-35% protein content, mineral elements, amino acids, protein, etc, but also the serveral harmful components, such as ricinines, allergens, ricin and hemagglutinins which cannot be directly used for feed protein. The toxicity of ricin is destroyed when its water solution is heated to boiling or even to the coagulation temperature of the protein. But the principal castor bean allergen retains immunt-precipitating and allergenic properties after heating at 100℃. Allergen belongs to the group of immunoglobulin G(IgE)-mediated urine protein. It is characterized by a higher frequency of severe reaction than foundin other plantallergies. Fatal plant-induced anaphylaxis affecting children as well as adults is often induced by exposure to castor oil plant [1-5]. Due to its prevalence and the potential severity of allergic reactions identification and molecular characterization of plant allergens is an essential step towards improving diagnosis and therapy. Today, there are many extraction methods used for this aim. Although the repeating solvent extraction method is the most widely used extraction method [5], it proves to be laborious, time-consuming and solvent-consuming. Nowadays, the ultrasound-microwave assisted extraction has been successively developed as the alternative extraction methods for this conventional extraction. Although this extraction method greatly lessen the extraction time and experimental operation, they do not meet the demand of green chemistry for the consumption of volatile or harmful solvents. This paper describes the conditions of temperature, time, microwave power for allergen, the use of ultrasound to improve the efficiency of the extraction process could lead to cost and time savings. The goal of this study was therefore to evaluate whether the use of high intensity ultrasound during the extraction may benefit allergen production In the present study, the ethanol-based UME was used for the extraction of allergen from CBM considering the alcohol of target compounds. Therefore, some chemical qualitative and quantitative analysis of allergen are necessary for the evaluation of this extraction method. Up to today, HPLC [2, 16, 17], polyacrylamide gel electrophoresis [18] and DSC melting point determination apparatus assay methods [19] have been used for this. On the basis of this, an efficient extraction method of allergen from CBM was established.

Identify applicable sponsor: Tianjin Municipal Rural Affair Committee of the People's Republic of China (0502170)

2 Experiment

2.1 Reagents and Materials

The resgents were Purchased from the National Institute for the Control of Pharmaceutical and Biological Products (shanghai, China), allergen was dissolved in ethanol and stored at -20 ℃. Bovine Serum Albumin (BSA) was obtained from Shanghai Chengjie Chemical Co., Ltd. (Shanghai, China). Other reagents were at least of analytical grade and purchased from Tianjin Chemical Factory (Tianjin, China). Reverse osmosis Milli-Q water (Millipore, USA) was used throughout the whole experiment.

The CBM was purchased from Tianjin Nankai university HaiTai castor production base (Tianjin, China).

2.2 Apparatus

HPLC used a Waters Millennium^{32} system including a Waters 996 photodiode array detection (DAD) system, a Waters 600 Multisolvent Delivery System, a Waters 600 System controller, a Waters 600 pump and a Millennium^{32} workstation (Waters, Milford, USA). The UME was carried out on an variable microwave power extraction bath of thermal energy converter,type of CW2000, shanghai xintuo Microwave sample-dispelling technology Co., Ltd., (Shanghai, China).

2.3 Ethanol-Based UME

The dried CBM (100.0 g) was ground and sieved into 40 sizes. 10.0 g sample powder was accurately weighed and suspended in 50 mL aqueous distilled water solution1:5solid-to-solvent ratio, w/v) at room temperature for 4 h, stirred for 4 hours After conversion, the sample was executed UME ,the temperature was controlled by the constant-temperature water. The ethanol concentration, extraction temperature, ultrasonicmicro-wave power and extraction time were optimized. Using bovine serum albumin as a standardsamples were scanned at least three times, and the average allergen values were reported (Fig1). After each extraction, the extract was filtrated through a 0.45 μm filter for the subsequent HPLC analysis Samples were scanned at least three times, and the average values were reported.

2.4 Traditional Extraction Method

To illustrate the feasibility and necessity of ethanol-based UME of allergen from CBM, it was firstly dissolved with ethanol-water solution which concen-tration was about 25 weight percent but separated out with ethanol-water solution which concentration was about 75 weight percent conditions. Furthermore, added to sugar of lead reagent ,the traditional extraction method was chosen as the control extraction method for the ethanol-based, that was, an aliquot (10.0 g) of sample was accurately weighed and extracted by boiling process with abundant ethanol repeatedly for 4 times. After four times extraction, the extracts were combined and concentrated into 20 mL. All final extracts were filtrated through a 0.45 μm filter for the subsequent HPLC analysis.

2.5 Chromatographic Conditions

The chromatographic column was KromasilC-18 column (150mm×4.6mm ID, 5μm) The eluent was a mixture of methylalcohol and deionized(25:75, v/v), the flow rate was 1.0 mL/min , the injection volume was 20 μL and the column effluent was monitored at the wavelength of 268 nm. All chromatographic measure-ments were operated at room temperature. Mean separation was achieved using orthogonal polynominal contrast.

2.6 Statistical Analysis

To determine possible correlations between the different extraction steps and treatments, results were subjected to statistical analyses using SAS, version 8 (SAS Institute Inc., Cary, NC).

3 Results and Discussion

3.1 Effect of Extraction time on the Extraction Efficiency

To some degree, the extraction time is in direct proportion to the extraction efficiency. Fig. 2 (a) illustrated that the extraction efficiency increased with the increase of the extraction time up to 200s. When the extraction time was longer than 200s, the extraction efficiency decreased. The decrease of extraction efficiency derives from the thermal disintegration of allergen caused by the excessive extraction time. As can be seen, 200s was enough for the extraction procedure.

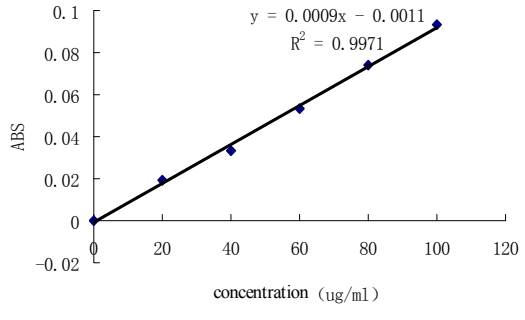

Figure 1. Standard curve of bovine serum albumin solution

978-1-61896-030-6 © 2012 SciRes.

3.2 Effect of Extraction Temperature on the Extraction Efficiency

Theoretically, the extraction temperature can increase the extraction rate, the extractionefficiency and the degradation of unstable compounds. Fig.2 (b) clarified this kind of opposite effects of extraction temperature on the extraction efficiency. The initial increase of extraction temperature had a positive effect on the extraction efficiency while extraction temperature higher than 75 ºC had a negative effect on the extraction efficiency, which was due to the thermal degeneration of allergen. So 75ºC was the maximum allowable extraction temperature in the present experiment.

3.3 Effect of Microwave Power on the Extraction Efficiency

The whole process of ultrasonic was opened. Microwave power is related to the dispersion of solvent into the solid sample. The second phase extraction time in 300s, the extraction and separation are the highest, for the contents of allergen 0.0889 mg/mL Fig. 2 (c) illustrated the effect of microwave power on the extraction efficiency. The initial increase of microwave power led to a small increase of extraction efficiency while an obvious decrease of the extraction efficiency was observed at microwave power higher than 400W. Generally, acoustic cavitation produced by the power is believed to bring the degradation of dissolved organic compounds in aqueous media [21]. Consequently, the increase in microwave power could accelerate the isomerization of Polysaccharide, unsaturated half of lactose residual base, as well as the thermal disintegration of allergen. Thus, the microwave power of 400 W was suitable for the extraction.

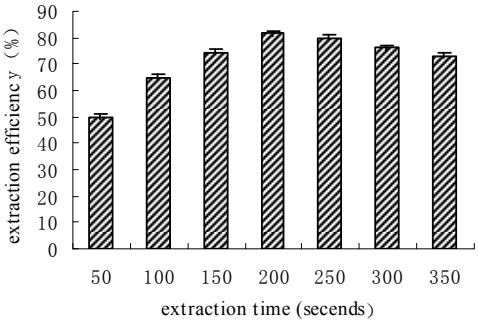

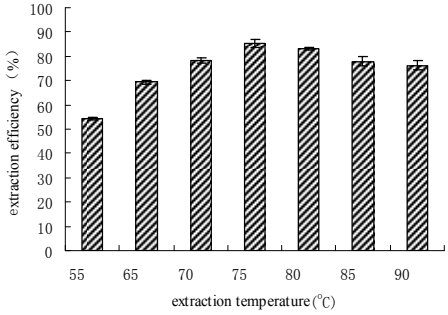

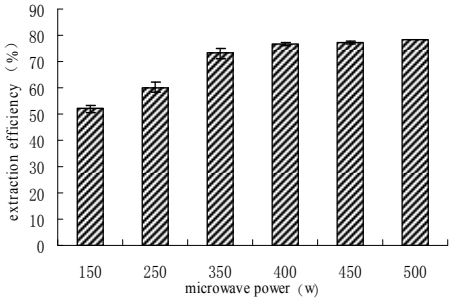

Figure 2. Effect of the different factors below on the extraction efficiency

The extraction efficiency is expressed as the observed value of allergen and the maximum amount in each curve was considered to be 100%). (a) extraction time. (b)extraction temperature ; (c) microwave power.

3.4 Comparison of the Proposed Extraction with the Traditional Method

The ethanol-based UME efficiency of allergen from CBM was compared with that of the REE. Under the same optimized UME conditions, the proposed ethanol-based UME produced higher efficiency than that of REE extraction (18.01% enhanced).

3.5 Method Validation

Based on the optimization of ethanol-based UME, the linearity, reproducibility and limit of detection of the proposed extraction were evaluated by the spiking experiments. The results showed that linear range of allergen was 0-120 ug/mL, the correlation coefficient of the linear equation was 0.9971. The further experiments revealed that the recovery ranged from 94.8% to 98.4% and the relative standard deviation (RSD) was lower than 1.28%. These results demonstrated the reliability of the extraction method. The Sephadex G-100 had done on with purification for the allergen. The Tricine-SDS-PAGE detection with unique electrophoresis strip documented that allergen was pured. Application Coomassie brilliant blue test and the alclan blue test staining the is appraisal double analyzed, and it is glycoproteins and the position was approximately equal to 19600 Dr.

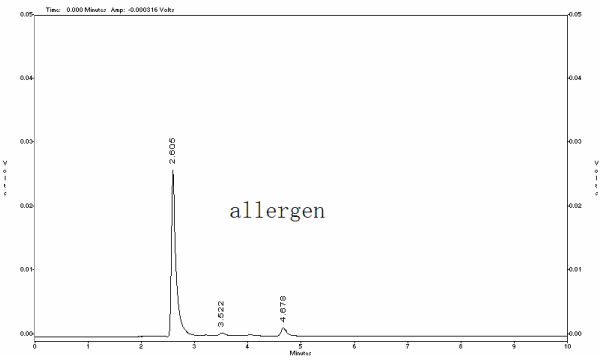

Figure 3. Chromatogram of allergen extracted from CBM

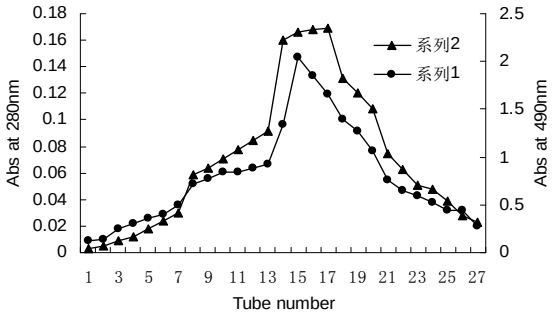

Figure 4. Elution of proteins precipitated on Sephadex G-100

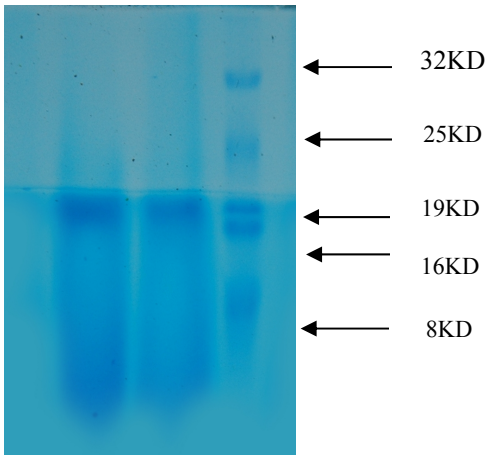

(a) alclan blue test staining

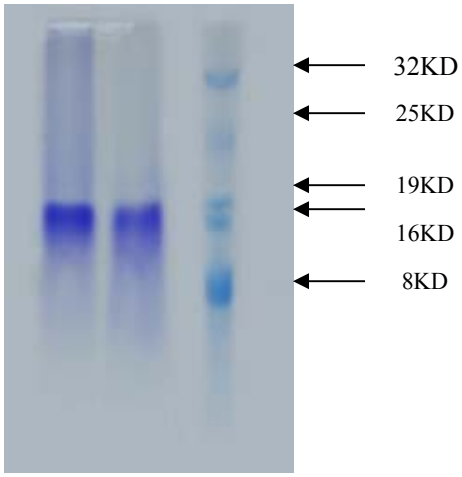

(b) Coomassie brilliant blue test staining

Figure 5. Tricine-SDS-PAGE electrophesis graph of allergen detection with unique electrophoresis strip documented that allergen

4 Conclusion

In the present study, the ethanaol-based UME parameters including the extraction temperature, microwave power and extraction time were studied to establish a simple and convenient extraction method. Based on the optimization of extraction parameters, the ethanol-based UME offered higher extraction efficiency and shorter extraction time than the traditional REE. Moreover, the validation of analysis method and the spiking experiments revealed that the proposed extraction is suitable for the effective extraction of allergen from CBM. By means of HLPC detection, allergen was purified. The Sephadex G-100 had done on with purification for the allergen. The Tricine-SDS-PAGE detection with unique electrophoresis strip documented that allergen was pured. Application Coomassie brilliant blue test and the alclan blue test staining the is appraisal double analyzed, and it is glycoproteins and the position was approximately equal to 19600 Dr.

Acknowledgement

We are grateful for the research support provided by Tianjin Municipal Rural Affair Committee of the People's Republic of China (0502170) and the Lab Science & Technology Program of Tianjin University of Science and Technology.

References

[1] China Pharmacopoeia Committee, Pharmacopoeia of the People's Republic of China, First Division, 2005 ed., China Chemical Industry Press, Beijing, 2005, pp. 152-153.

[2] Zhang, B., Yang, R.Y., Liu, C.Z., Sep. Purif.Technol.2008, 62, 480-483.
[3] G Ram Reddy, M R Reddy. Nutrient digesTableility and rumen meTableolism in buffaloes Fed castor-bean-meal in the concentrate feeds [J].Indian J Sci，1986，56 (5):567-572.
[4] Pablo F Polit，Valdcmiro C，Sgarbicri. Some physicalchemical and Nutritional properties of castor bean (Ricinus Communis) protein [J].J Agric Food Chem，1976, 24:795-798.
[5] Waller GR, Yang KS, Gholson RK. The pyridine nucleotide cycle and its role in the biosynthesis of ricinine by Ricinus communis L [J].J Biol Chem, 1966，241 (19):4411-4418.
[6] Jon D. Crystallization for ricin a chain obtained from a cloned gene expressed in Escherichia coli [J]. Biology Chemistry, 1987, 262: 19-20.
[7] Ambekar V R, and Dole K K. Detoxication of castor cake [J].Indian J. Dairy Sic, 1957, 10:107-122.
[8] Mottola A C, Hendrickson A P, O'Connell D E，et al. Pilot plant deactivation of castor meal bean—Lime process [J]. J Agric Food Chem., 1968, 16 (5): 725-729.
[9] G. Fuller, H G.Walker, A C Mottola. Potential for detoxified castor meal [J].Journal of the American Oil chemists Society, 1971, 48:616-618.
[10] Lehrer.S.B., Tayler.J., Salvaggio.J.E.. Castor bean allergens: evidence for distince head-liable and Stable entities [J]. Immunochemistry, 1981, 95: 4929.
[11] Luis E. Rodriguez-Saona.Use of Fourier Transform Near-Infrared Reflectance Spectroscopy for Rapid Quantification of Castor Bean in a Selection of Flour-Based Products [J]. J. Agric. Food Chem. 2000, 48: 5169-5177.
[12] Zhang B, Yang RY, Liu CZ (2008) Sep. Purif. Technol. 62: 480-483.
[13] Xiang ZN, Ning ZX (2008) Food Sci. Technol. 41:1189-1203.
[14] Zhang B, Yang RY, Zhao Y, Liu CZ (2008) J. Chromatogr. B 867:253-258.
[15] Wang ZL, Wang JH, Sun YS, Li SB, Wang HZ (2008) Sep. Purif. Technol. 63:721-724.
[16] Hu FL, Deng CH, Liu Y, Zhang XM (2009) Talanta 77: 1299-1303.
[17] Li ZB, Huang DN, Tang ZX, Deng CH, Zhang XM (2010) Talanta 82: 1181-1185.
[18] Lu ZY, Sun QX, Li HJ, *et al*. Molecular identification and marker-assisted selection of Pm21 gene conferring resistance to powdery mildew in wheat [J]. Yi Chuan Xue Bao, 1999, 26(6): 673-682.

Application Research on Extraction of Matrine from Radix Sophorae Tonkinensis by Microwave-Assisted and Ultrasonic Methods

Yan ZHANG[1], Shujie XIONG[2], Jie LIU[2], Yahong WANG[1], Yang ZHANG[1]
[1]*School of Chemical and Pharmaceutical Engineering, Jinlin Institute of Chemical Technology, Jilin, China*
[2]*The General Hospital of Jilin Chemical Industrial Group, Jilin, China*
Email: zyzxorange@126.com

Abstract: In this article, microwave-assisted and ultrasonic wave-assisted extraction of matrine from Radix Sophorae Tonkinensis were described, several experimental factors, including time, temperature, ratio of liquid to solid, microwave power, and ultrasonic frequency were optimized with orthogonal experiments. The optimal microwave-assisted extraction conditions were extraction time 20min, temperature 75℃, ratio of liquid to solid 40:1, microwave power 500W, and the ultrasonic method were time 120min, ethanol concentration 80%, ratio of liquid to solid 30:1, ultrasonic frequency 76kHz. The extraction was performed under the optimum conditions respectively, compared with ultrasonic method, the extraction rate by microwave-assisted method was much higher.

Keywords: Microwave-assisted extraction; ultrasonic wave-assisted extraction; matrine; Radix Sophorae Tonkinensis

1 Introduction

Radix Sophorae Tonkinensis is the root of Sophora Tonkinensis Gapnep, which is widely cultivated and used as traditional chinese medicine for the treatment of laryngopharyngitis. It has been demonstrated to be heat-clearing, detoxicating, and detumescent effects [1].Alkaloids, including matrine, oxymatrine, oxymatrine, and N-methylcytisine are the main effective components [2]. Matrine is the prominent compound, has been reported to have various bioactivities, such as the fuction of diuresis, anti-tumor, anti-inflammation, anti-hyper sensitivity, immunoregulation and antibacterial effect, etc[3].

Soxhelt extraction and reflux extraction, commonly considered as the traditional extraction techniques, were widely used for the extraction of bioactive components in medicinal plants. The two methods are often effective, but are labor intensive, time-consuming and large amounts of solvent and sample are required. Some novel extraction techniques have been developed over the past few years.

Microwave-assisted and ultrasonic wave-assisted extraction are effective methods for the rapid extraction of analytes from different matrices, and have been widely recognized as simple, time-saving, energy-saving, environment-friendly and versatile methods for the extraction of natural products. In this article, for the purpose of finding an effective and practical way to extract matrine from Radix Sophorae Tonkinensis, microwave-assisted and ultrasonic wave-assisted extraction method were described, and their extraction rates were also compared.

2 Instrument and Reagents

Multifunctional Grinder (RT-08, Rong Tsong Precision Technology Co., Ltd, Taichung City Taiwan, China), Normal Pressure Microwave Synthesis/ Extraction Reactor(MAS-1, Sineo Microwave Chemistry Technology Co., Ltd, Shanghai, China), Ultraviolet Visible Spectrophotometer(752N, Shanghai Precision & Scientific Instrument Co., Ltd, Shanghai, China), Rotary Evaporator(RE-52A, Ya Rong Biochemistry Instrument Co., Ltd, Shanghai, China), Thin Layer Chromatography Plate(GF-254, Qingdao Marine Chemical Plant, Qingdao, China),Radix Sophorae Tonkinensis samples, were purchased from Jiangcheng drugstores(Jilin, China). Matrine standard was obtained from National Institute for the Control of Pharmaceutical and Biological Products (Beijing, China). All other reagents were of analytical reagent grade.

3 Procedure

1000 g of Radix Sophorae Tonkinensis sample was grinded, and passed through 60 mesh sieve, then reserved after drying.

3.1 Microwave-Assisted Extraction

A total of 2 g of the sample was exactly weighed and placed into the conical flask, then proper amount of 80% of ethanol was added with certain ratio of liquid to solid.

978-1-61896-030-6

After soaking for 24 hours, the power, time and temperature of microwave were set to extract matrine from Radix Sophorae Tonkinensis, after extraction, filtered and introduced the filtrate to conical flaskes which were labeled previously.

Ultrasonic Wave-Assisted Extraction. A total of 2 g of the sample was exactly weighed and placed into the flask, then different concentration and volume of ethanol was added with certain ratio of liquid to solid. After soaking for 24 hours, the frequency and time of ultrasonic instrument were previously set, matrine of Radix Sophorae Tonkinensis was extracted on that condition, after extraction, filtered and introduced the filtrate to conical flaskes which were labeled in advance.

3.2 Determination of Matrine

The content of matrine was determined by TLC-UV method using matrine standard as reference substance at a wavelength of 412 nm. A total of 10 mg of matrine standard was exactly weighed and placed into a 5 mL volumetric flask, and diluted to 2.0 mg/mL with ethanol, then 2, 4, 8, 12, 16, 24 and 32 μL of standard solution were precisely absorbed on the TLC plate separately, chloroform- methanol-ammonia (5:0.6:0.2) were laid in 10℃,the subnatant as developing agent, with bismuth potassium iodide as chromogenic reagent. The wanted points were gathered, and put into the 1 cm×10 cm column, using 10 mL Ethanol-ammonia (50:1) solvent as eluent.The eluent was collected, removed the solvent, and extractly added 6.0 mL bromthymol blue buffer (2×10-4 mol·mL-1, pH 7.6), 6.0 mL chloroform to extract matrine. The absorbance of sample was tested at a wavelength of 412 nm, standard curve was plotted using the content of reference substance as abscissa and the corresponding absorbency as vertical coordinate, y=197.96x+0.0603, R=0.9999.

3.3 Process of Sample Liquid

The filtrate obtained from microwave-assisted and ultrasonic wave-assisted extraction was collected, removed the solvent, dissolved in anhydrous alcohol, filtered and discarded the residue. The absorbance of filtrate was measured by the method of TLC-UV, and the total content of matrine was calculated. The extraction rate of matrine from Radix Sophorae Tonkinensis = the total content of matrine from filtrate (g) / the amount of sample power (g) × 100 %.

4 Results and Discussion

4.1 Experiments of Microwave-Assisted Extraction Design of Orthogonal Test

According to the results of single factor test, four factors, microwave power, temperature, time and ratio of liquid to solid, were selected to design orthogonal experiment table. The results were shown in Tab. 1.

The Optimized Process of Microwave-Assisted Extraction. According to Tab. 1., the optimized process was $A_1B_3C_2D_2$ (B> C> A> D), that was, microwave power (500w), temperature (75℃), time (20 min), ratio of liquid to solid (40:1).

4.2 Confirmation Experiments

The three confirmation experiments were parallelly carried out according to orthogonal test, the results were shown in Tab. 2.

4.3 Experiments of Ultrasonic Wave-Assisted Extraction Design of Orthogonal Test

According to the results of single factor test, four factors, ultrasonic frequency, concentration of ethanol solution, time and ratio of liquid to solid, were selected to design orthogonal experiment table. The results were shown in Tab. 3.

The Optimized Process of Ultrasonic Wave-Assisted Extraction.According to Tab.3, the optimized process was $A_2B_3C_3D_3$ (A > C > B > D), that was, ratio of liquid to solid (30:1), concentration of ethanol solution (80 %), ultrasonic frequency (76 kHz), time (120 min).

4.4 Confirmation Experiments

The three confirmation experiments were parallelly carried out according to orthogonal test, the results were shown in Tab. 4.

Table 1. The orthogonal test results of microwave-assisted extraction

NO.	A Microwave Power /w	B Temperature /℃	C Time /min	D Ratio of Liquid to Solid /(V/W)	Absorbance	Extraction rate /%
1	500	45	15	30:1	0.289	0.578
2	600	60	20	30:1	0.350	0.732
3	700	75	25	30:1	0.428	0.929
4	600	75	15	40:1	0.279	0.829
5	700	45	20	40:1	0.264	0.772

Continued

NO.	A Microwave Power /w	B Temperature /℃	C Time /min	D Ratio of Liquid to Solid /(V/W)	Absorbance	Extraction rate /%
6	500	60	25	40:1	0.232	0.655
7	700	60	15	50:1	0.169	0.549
8	500	75	20	50:1	0.277	1.095
9	600	45	25	50:1	0.155	0.478
K1j	2.323	1.828	1.955	2.238		
K2j	2.039	1.931	2.598	2.251		
K3j	2.250	2.852	2.058	2.122		
k1j	0.774	0.609	0.652	0.746		
k2j	0.680	0.644	0.866	0.750		
k3j	0.750	0.951	0.686	0.707		
R	0.095	0.341	0.214	0.043		
Optimal Level	A1	B3	C2	D2		

Table 2. The results of experiments of microwave-assisted extraction

NO.	Absorbance	Extraction rate %
1	0.253	0.973
2	0.249	0.953
3	0.251	0.963

The average Extraction rate was 0.963%, RSD = 1.01%.

Table 3. The orthogonal test results of ultrasonic wave-assisted extraction

NO.	A Ratio of Liquid to Solid /(V/W)	B Concentration of Ethanol Solution /%	C Ultrasonic Frequency / kHz	D Time /min	Absorbance	Extraction rate /%
1	20:1	40	26	60	0.390	0.301
2	20:1	60	47	90	0.421	0.346
3	20:1	80	76	120	0.459	0.402
4	30:1	40	47	120	0.470	0.419
5	30:1	60	76	60	0.481	0.435
6	30:1	80	26	90	0.472	0.421
7	40:1	40	76	90	0.441	0.375
8	40:1	60	26	120	0.416	0.339
9	40:1	80	47	60	0.453	0.393
K1	1.049	1.095	1.061	1.129		
K2	1.275	1.120	1.158	1.142		
K3	1.107	1.216	1.212	1.160		
R	0.226	0.121	0.151	0.031		
k1	0.350	0.365	0.354	0.376		
k2	0.425	0.373	0.386	0.381		
k3	0.369	0.405	0.404	0.387		
R′	0.075	0.040	0.050	0.010		

Table 4. The results of confirmation experiments of ultrasonic wave-assisted

NO.	Absorbance	Extraction rate /%
1	0.376	0.699
2	0.301	0.657
3	0.448	0.711

The average Extraction rate was 0.689%, RSD = 2.75%.

5 Conclusion

The order of impact factors of microwave-assisted extraction as below: B> C> A> D, that was, microwave power (500w), temperature (75℃), time (20 min), ratio of liquid to solid (40:1). The order of impact factors of

978-1-61896-030-6 © 2012 SciRes.

ultrasonic wave-assisted extraction as below: A > C > B > D, that was, ratio of liquid to solid (30:1), concentration of ethanol solution (80 %), ultrasonic frequency (76 kHz), time (120 min).Compared with ultrasonic wave-assisted extraction, microwave-assisted extraction was improved with less time (20 min) and higher extraction rate (0.963%) on the extraction of matrine from Radix Sophorae Tonkinensis. In all, microwave-assisted extraction was a better method on the extraction of matrine from Radix Sophorae Tonkinensis, in contrast to ultrasonic wave-assisted extraction, one sixth of time was needed, and the extraction rate was hither 39.8%.

References

[1] Jia-Ping Lai, Xi-Wen He and Yue Jiang. "Preparative separation and determination of matrine from the Chinese medicinal plant Sophora flavescens Ait by molecularly imprinted solid-phase extraction", Anal Bioanal Chem, Vol. 375, No. 5, 2003, pp. 264-269.

[2] Liang Yan-ming, Yang Xiao-xiao and Guo Wei. "Comparative Study on Extraction of M artine from Radix Sophore Tonkinesis by Different Method", Technology & Development of Chemical Industry, Vol. 37, No. 4, 2008, pp. 17-19.

[3] Xiong Xiao-chun, A N Chun-mei. "An overview in the anti-tumor research on Matrine", China Medical Herald, Vol. 6, No. 37, 2009, pp. 10-12.

[4] Zou Gui-xin, You Xiang-min. "Determination of Matrine of Angelica Sinensis Particles by Thin Layer Chromatography-Spectrophotometry Method", Lishizhen Medicine and Materia Medica Research, Vol. 12, No.3, 2001, pp. 212.

Analysis of Different Harvest Period in Supercritical Fluid Extraction Obtained from *Bupleurum chinense* by GC-MS Spectrometry

Xue LEI, Qishuai WANG, Yun YANG, Xiaokun LI

College of Pharmacy, Henan University of Traditional Chinese Medicine, Zhengzhou, China, 450008

Email: leixue15003880050@163.com

Abstract: This paper studies chemical compositions and the dynamic change law of *Bupleurum chinense*. The extracts were extracted by supercritical fluid extraction (SFE). The composition of chemical constituents was determined by chromatography-mass spectrometry (GC-MS). There were 36 constituents accounting for 74.32%-90.45% of total extracts separated and identified. The relative content of the fatty acids which extracted by SFE-CO_2 was 45.10%-80.95%, the aldehydes was 1.61%-5.65%, the ketones was 0.65%-1.28%, and the esters was 4.80%-8.12%.

Keywords: Supercritical fluid extraction; chemical constituents; GC-MS

1 Introduction

Bupleurum chinense DC., a kind of perennial herb, belonging to umbelliferae plants[1] is mainly produced in Liaoning, Hebei, Shanxi, Henan, Shanxi and Gansu provinces[2]. Because of the different growth environment, growth and harvest period, and process method, the chemical composition have differences in different production area and growth cycle. It is shown that Saikosaponin, volatile oil, and the ethanol soluble extraction in *Bupleurum chinense* have obvious differences with different harvest period[3]. It means harvest time has some effect on the quality of *Bupleurum chinense* to some extent.

Some research have shown that supercritical fluid extraction can increase the convulsion threshold of rat cerebral cortex by electrical stimulation and have obvious antagonism effects on the max electric shock and convulsion model [4], so that it have anti-epilepsy and anti convulsion effect. At present, as author know there is no relative report for the dynamic change law of supercritical fluid extraction obtained from *Bupleurum chinense*. To make better use of *Bupleurum chinense* resources and to further perfect its quality evaluation system, this experiment choose *Bupleurum chinense* artificial cultivated at Songxian as research subject, using SFE and GC-MS method to extract the chemical composition and analysis the extracts separately. Further discussion on the influences of the growth cycle on chemical composition of *Bupleurum chinense* will provide references for the normalized cultivation and industrialization development of *Bupleurum chinense*.

2 Meterials and Methods

2.1 Plant Materials and Reagents

Bupleurum chinense was cultivated before tomb-sweeping day of 2008, and collected from May to December of 2009(Table 1) at Songxian, in Henan. The plant was authenticated by Prof**.** CM Dong (College of pharmacy, Henan University of Traditional Chinese Medicine) as *Bupleurum chinense* DC.. Remove the stem, leaves and sediments, *Bupleurum chinense* were dried for 24 hours at 40 ℃, and then were preserved in closed and low temperature. Samples are grinded to pass through 10-mesh sieve before measured for reserve.

Table 1. Collecting periods and sample number

Sample No.	Growth pattern	Collecting periods
C1	cultivated products	May 29,2009
C2	cultivated products	June 30,2009
C3	cultivated products	July 28,2009
C4	cultivated products	August 28,2009
C5	cultivated products	September 28,2009
C6	cultivated products	October 29,2009
C7	cultivated products	November 30,2009
C8	cultivated products	December 28,2008

2.2 Apparatus

Chemical composition analysis was performed on a spectrometry Thermo Trace DSQⅡ GC-MS analyzer (American Thermal Power Corporation); chromatography library are NIST98 and Wiley138; the type of SFE apparatus is HA221-50-06 (Nantong, Jiangsu).

2.3 Preparation of the SFE Extracts

After 160 g of *Bupleurum chinense* powder were weighted into 1 L capacity SFE extraction kettle and extracted by SFE, we got SFE extracts. The extraction

978-1-61896-030-6

condition were as followed: the temperature of the extraction kettle, separation kettle Ⅰand Ⅱ was 55 ℃, 65 ℃, 40 ℃, the pressure of them was 25 MPa, 12 MPa respectively, and all SFE studies took 120 min.

2.4 GC-MS Analysis

2.4.1 Preparation of the Test Liquid

Proper SFE extracts were got, dissolved in n-hexane, and were filtered through a 0.45 μm membrane, thus test liquid were remained.

2.4.2 GC-MS Analysis Condition

The GC-MS analysis was performed using a Thermo Trace DSQⅡ MS coupled to a Trace GC fitted with a DB-5MS (30 m ×0.25 mm×0.25 μm) column (Agilent, USA), injection(1 μL) was performed with a split ratio of 50:1(280 ℃), and the oven temperature was programmed at 100 ℃ for 1 min, ramped at 20 ℃·min^{-1} to 250 ℃ and maintained at this temperature for 20 min. the carrier gas was helium with a constant flow rate of 1 mL·min^{-1}. The transmission line temperature was set at 250 ℃. MS were obtained range of 33～450 amu for qualitative analysis, using EI ion source with an ionization energy of 70 eV and temperature at 250 ℃, the detection voltage was set at 1.3 KV. All the relative content was calculated by normalization method.

2.4.3 Sample Determination

Inject the sample with different collection periods of 1.0 μL and follow the GC-MS analysis condition above.

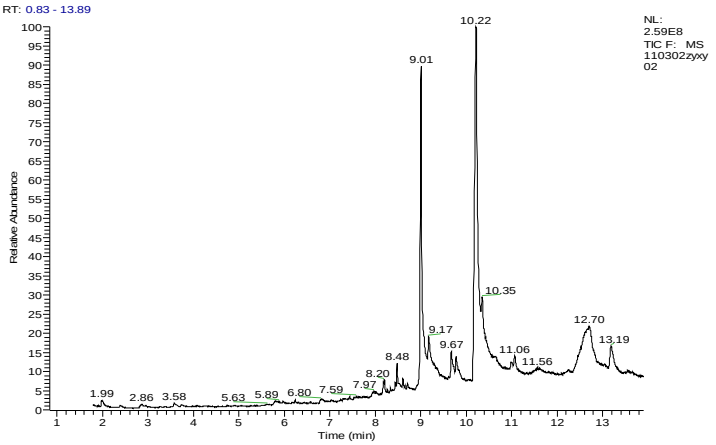

Figure 1. The GC-MS total ion chromatograms of *Bupleurum chinense* extracts by SFE

(collected by May 29, 2009)

Table 2. The main chemical compounds and relative content of SFE extraction products from *Bupleurum chinense* with different harvest period

Retention Time (min)	Name	Relative content of the main components (%)							
		C1	C2	C3	C4	C5	C6	C7	C8
1.99	Hexanal	0.67	0.37	0.41	0.41	0.56	0.28	0.33	0.22
2.39	Heptaldehyde	0.31	0.25	0.21	0.20	0.19	0. 19	0. 19	0. 13
2.86	Caproic acid	0.44	0.74	1.05	0.87	0.77	0.62	0. 82	0. 28
3.37	2-Octene aldehyde	0.17	0.22	0.14	0.13	0.15	0.13	0.14	0. 11
3.58	4-Nonyl aldehyde	0.45	0.22	0.38	0.31	0.41	0.27	0. 31	0. 20
3.74	2-Ethyl hexanoate	0.26	0.29	0.16	0.11	0.15	0.12	0.11	0.00
4.08	2-Nonyl aldehyde	0.18	0.26	0.19	0.15	0.15	0.14	0.14	0.12
4.91	Tridecane	0.22	0.11	0.19	0.17	0.18	0.16	0.16	0. 18
5.06	2,4-Twelve diene aldehyde	0.15	0.47	0.13	0.12	0.12	0.12	0.13	0.11
5.80	5-Ethyl-2-Thiophene acid	0.48	0.20	0.42	0.35	0.39	0.16	0.17	0.29
5.97	Caryophyllene	0.25	0.13	0.26	0.19	0.19	0.16	0.25	0.15

Continued

Retention Time(min)	Name	Relative content of the main component(%)							
		C1	C2	C3	C4	C5	C6	C7	C8
6.06	1a,2,3,5,6,7,7a,7b-Octahydro-1,17,7a-Tetramethyl-1 H-Cyclopropane (a)-naphthalene	0.14	0.18	0.20	0.12	0.11	0.22	0.17	0.16
6.18	1,2-Dihydro-2,2,4-trimethyl quinoline	0.18	0.24	0.17	0.18	0.16	0.16	0.17	0.21
6.24	Pentadecane	0.26	0.23	0.28	0.26	0.29	0.26	0.34	0.32
6.58	P-(1,2,2-Trimethyl cyclopentane-based)-toluene	0.18	0.23	0.32	0.25	0.34	0.25	0.28	0.26
6.8	1-(4-Isopropoxy-3-methoxy)-acetone	0.49	0.46	0.40	0.46	0.57	0.31	0.45	0.25
7.44	Hepatadecanoic	0.29	0.72	0.27	0.63	0.25	0.61	0.19	0.28
7.62	Octadecene aldehyde	0.26	0.40	0.25	0.62	0.22	0.87	0.18	0.14
7.93	Fourth carbonate	0.57	1.19	0.47	0.42	1.08	0.37	0.44	1.34
8.20	3,7,11,15-Tetramethyl-2-sixteen en-1-alcohol	0.91	0.62	0.53	0.51	0.58	0.55	0.47	0.45
8.27	6,10,14-Trimethyl-2-fifth ketone	0.19	0.25	0.20	0.24	0.17	0.25	0.17	0.19
8.48	Isobutyl phthalate	1.67	2.45	1.96	2.40	1.82	1.70	2.01	1.86
8.61	2-Seventeen ketone	0.60	0.32	0.22	0.28	0.36	0.29	0.24	0.21
8.71	Sixteen methyl carbonate	0.45	0.34	0.24	0.29	0.31	0.26	0.30	0.33
9.01	Sixteen carbonic acid	15.08	27.20	24.69	26.78	25.91	25.91	26.09	26.06
9.07	Sixteen ethyl carbonate	0.12	0.48	0.30	0.20	0.39	0.18	0.18	0.13
9.17	9,17-Eighteen carbon diene aldehyde	1.74	0.31	0.37	0.31	0.50	0.11	0.11	0. 11
9.67	Nineteenth carbon diene aldehyde	1.90	0.72	0.39	0.48	0.57	0.56	0.43	0.58
9.78	Octadecenoic acid methyl ester dienes	1.76	1.04	0.74	0.76	0.64	0.80	1.17	0.94
10.22	Linoleic acid	27.11	39.58	41.50	40.32	44.98	45.85	46.35	50.12
10.35	Eighth carbonate	1.16	2.94	2.77	2.99	3.04	2.40	2.57	2.86
10.99	Linoleic acid isopropyl	0.57	0.67	0.73	0.75	0.75	0. 83	0.94	0.67
11.06	Carbonic acid monoglyceride sixteen	1.04	0.59	0.67	0.53	0.45	0.54	0.60	0.29
12.67	Stigmasterol	11.34	0.23	0.11	0.16	0.12	0.11	0.23	0. 11
13.19	Glyceryllinoleate	2.51	1.68	1.86	0.95	1.07	1. 19	1.33	0. 58
The proportion of the identified components of the total		74.32	86.65	83.42	84.18	88.21	87.13	88.38	90.45

3 Results and Discussion

1. Analyzing the test liquid by GC-MS, we got the result of the total ion chromatogram (with samples on May as an example in Figure 1). After scanning through GC-MS Data System (NIST98 and Wiley138), we can retrieval and access to the relevant information to determine the compounds and calculate its relative content in the total extracts. The results showed in table 2.

2. Through the analyze of Fig.1 that: 59 constituents were separated and 36 with high proportion relative content were identified by GC-MS, which account for 74.32% to 90.45% of the total extracts.

3. According to retention time, we can see the time before 1.81 min is solvent peak thus we choose 1.99 as the starting time.

4. By analysing Table 2, we can see that: The relative content of the fatty acids which extracted by SFE-CO_2 was 45.10%-80.95%, the aldehydes was 1.61%-5.65%, the ketones was 0.65%-1.28%, and the esters was 4.80%-8.12%. Fatty acid (mainly composed of sixteen carbonated acid and linoleic) is the main compounds, the relative content increased monthly, the tiptop is on December(linoleic acid account for 50.12%), and highest relative content of sixteen carbonated acid accout for 27.20% is on July. Some studies shown that α-linoleic acid and linoleic acid at the ratio of 1 to 4 mixed can effectively anticonvulsive [5]. The research shown that the fatty acid in SFE extracts of *Bupleurum chinense* may have some anticonvulsant effect. The compounds of aldehydes, ketones and esters in extract is decreasing, and the highest proportion of the three compounds

978-1-61896-030-6 © 2012 SciRes.

occurs on May. All these analysis proved that the chemical composition changed constantly. The cultivate and process method can affect the quality of *Bupleurum* to a large extent.

4 Conclusions

36 compounds of *Bupleurum chinenese* SFE extracts which had highly relative content were Separated and identified. The main compounds are fatty acids, among which sixteen carbonated acid and linoleic have highest relative proportions. The relative content of aldehydes, ketones and esters in *Bupleurum chinenese* has obvious differences with harvest period. This analysis provides a scientific basis for the cultivation and harvest of *Bupleurum chinenese* to some extent.

References

[1] Chinese Pharmacopoeia Commission, Pharmacopoeia of People's Repubic of China(Vol.1), Chemical Industry Press, Beijing, 2005:198.

[2] Wang QS, Li XK, Yang Y, Xiao GS, Feng WS, "Study on dynamic accumulation of index components from *Bulplerum Chinese* in various collecting periods," J. journal of Chinese medicinal meterials, Vol 33, No. 8, pp 1204-1206, 2010.

[3] Huang QH, Liao WP, Ge FH, "The anticonvulsant effect of saikosaponin by SFE-CO_2 extract," J. journal of Chinese medicinal materials, Vol 25, No. 8, pp 576-577, 2002.

[4] Liu Y, Wu HQ, Ge FH, "Chemical constituents Analysis on anticonvulsive of three extracts from radix Bupleuri," J. journal of Chinese medicinal materials, Vol 25, No. 9, pp 635-636, 2002.

[5] Sh. Yehude, R. Carasso, D. Mostofsky. "Essential fatty acid preparation (SR-3) raises the seizure threshold in rats ," J..European Journal of Pharmacology, Vol 254 pp: 193-198, 1994.

Secondary Metabolites of *Fusarium solani*, an Endophytic Fungus in *Ficus carica* L.

Hongchi ZHANG[1], Rui LIU[1], Feng ZHOU[1], Kenming YU[1], Runmei WANG[1], Yangmin MA[2]
[1]*College of Agronomy and Life Science, Shanxi Datong University, Datong Shanxi, China.*
[2]*College of Chemistry and Chemical Engineering, Shaanxi university of Science & technology, Xi'an, Shaanxi, China.*
Email: zhanghclw@163.com

Abstract: Within our screening program for antimicrobial fungal secondary metabolites, eleven compounds were isolated from an endophytic fungus *Fusarium solani* of *Ficus carica*. Their structures were elucidated on the basis of spectroscopic analysis with the reported data in the literature. Among them, compound 5, 8 and 11 were isolated from endophytic fungi for the first time.

Keywords: Endophytic fungi; *Ficus carica* L.; *Fusarium solani*; secondary metabolites

1 Introduction

Endophytic fungi that inhabit normal tissues of the host plants without causing apparent pathogenic symptoms have been proven to be a rich source of new biologically active natural products because as a group they inhabit a relatively untapped ecological environment, and their secondary metabolism is activated by their metabolic interactions with their hosts [1,2]. Natural products from endophytic fungi have been observed to inhibit or kill a wide variety of harmful microorganisms including, but not limited to, phytopathogens, as well as bacteria, fungi, viruses, and protozoans that affect humans and animals [3].

In the course of our search for biologically active metabolites from endophytic fungi of Chinese medicinal plants, a subculture of an isolate of *Fusarium solani*, obtained from roots of *Ficus carica* L., was cultivated on potato dextrose agar (PDA). An EtOAc extract of the culture showed significant antimicrobial activity. This prompted us to carry out secondary metabolites studies on this fungus, which resulted in the isolation of eleven compounds. Herein we describe the isolation and structural elucidation of its secondary metabolites.

2 Experimental Section

2.1 General Experimental Procedures

The ^{1}H and ^{13}C NMR spectra were recorded on Bruker ADVANCE 400 MHz spectrometer, with TMS as an internal standard. Melting points were obtained on a Fisher-Johns apparatus and are uncorrected. EI-MS were recorded on a JEOL SX102A mass spectrometer. Column chromatography was performed with silica gel (200-300 mesh, Qingdao Marine Chemical Inc. Qingdao, China) and Sephadex LH-20 (Amersham Biosciences Inc. Shanghai, China). Analytical TLC was carried out with glass precoated silica gel GF_{254} plates and spots were detected under UV light and colored by spraying with 7 % H_2SO_4 in 95 % ethanol followed by heating. All the reagents used were AR grade.

2.2 Fungal Material and Identification

The fungal strain FR20 was isolated from the roots of *Ficus carica* L., collected in the Qinling Mountains, Shaanxi Province, China, on September 10, 2009. By classical microscopic analysis, the fungus was identified as a member of the genus *Fusarium*. It was further identified as *Fusarium solani* according to a molecular biological protocol by DNA amplification and sequencing of the ITS region. The fungal strain has been preserved at the Shaanxi university of Science & technology, Shaanxi Province, China.

2.3 Fermention, Extraction and Isolation

Starter cultures were maintained on PDA medium at 28 °C for 7 days. Plugs of agar supporting mycelial growth were cut and transferred aseptically to 1000 mL Erlenmeyer flasks containing 400 mL of liquid Czapek medium at 28 °C on a rotary shaker for 15 days. The fungal culture (60 L) was filtered through cheesecloth. The filtrate was concentrated to 3.5 L below 60 °C and then extracted five times with ethyl acetate (4.5 L). The dried mycelium (55 °C, 95 g) was extracted three times with methanol (4 L). All extracts were concentrated at reduced pressure to afford 17.2 g of a dark brown crude extract.

The crude extract was subjected to silica gel column chromatography eluting successively with ethyl acetate/methanol gradient (1:0, 50:1, 20:1, 10:1, 5:1, 2:1, 1:1, 0:1) and yielded eight fractions (A-H). Fraction A was separated by column chromatography on silica gel with a gradient of ethyl acetate in petroleum ether to give five subfractions (A1-5). Fraction A1 was separated by silica gel column chromatography with elution with petroleum

978-1-61896-030-6

ether/ethyl acetate (2:1) to give pure compound 1 and compound 2. Fraction A3 was separated by silica gel column chromatography with elution with petroleum ether/ethyl acetate (1:2) to give pure compound 3, together with crude compound 4 and compound 5. The crude compound 4 was then recrystallized from petroleum ether/ethyl acetate to give the pure compound 4. Similarly compound 5 was obtained from the crude compound 5 subjected to repeated chromatographic purifications using petroleum ether/ethyl acetate. Fraction B was subjected to repeated chromatographic purifications using ethyl acetate-methanol and Sephadex LH-20 with ethyl acetate-methanol, then compound 6, compound 7 and compound 8 were obtained. Similarly compound 9, compound 10 and compound 11 were obtained from fraction C after subjected to repeated chromatographic purifications using ethyl acetate-methanol and Sephadex LH-20 with ethyl acetate-methanol (1:1).

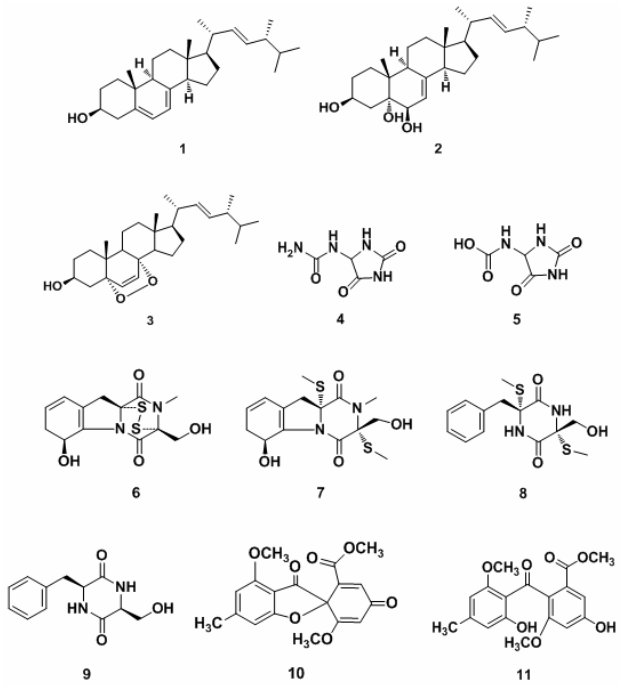

Figure 1. Compounds isolated from *Fusarium solani* of *Ficus carica* L.

The compounds were subjected to characterization using nuclear magnetic resonance spectroscopy (^{1}H-& ^{13}C-NMR) (Bruker). The secondary metabolites were identified as ergosterol (1) [4], cerevisterol (2) [5], ergosterol peroxide (3) [6,7], allantoin (4) [8], (2,5-dioxo-4-imidazolidinyl)-carbamic acid (5) [9], gliotoxin (6) [10], bis-N-norgliovietin (7) [11,12], bis(methylthio)gliotoxin (8) [12,13], cyclo- (Phe-Ser) (9) [14], trypacidin (10) [15] and monomethylsulochrin (11) [16] (Figure 1), by comparison of their spectral data with the reported data in the literature.

Ergosterol (1): $C_{28}H_{46}O$, Colorless needle, mp 155-157 ^{o}C, El-MS m/z 398 $[M]^+$. ^{1}H-NMR (400 MHz, $CDCl_3$): δ : 3.66 (1H, m, 3-H), 5.59 (1H, dd, *J*=8 and 4 Hz, 6-H), 5.41 (1H, dd, *J*=4Hz, 2 Hz, 7-H), 0.65 (3H, s, 18-H), 0.94 (3H, s, 19-H), 1.05 (3H, d, *J*=4 Hz, 21-H), 5.18 (1H, dd, *J*=16 and 8 Hz, 22-H), 5.22 (1H, dd, *J*=16 and 8 Hz 23-H), 0.85 (3H, d, *J*=8 Hz, 26-H), 0.83 (3H, d, *J*=8 Hz, 27-H), 0.93 (3H, d, *J*=8 Hz, 28-H). ^{13}C-NMR (100 MHz, $CDCl_3$): δ: 38.4(1-C), 32.0(2-C), 70.5(3-C), 40.8 (4-C), 139.8 (5-C), 119.6 (6-C), 116.3 (7-C), 141.4 (8-C), 46.2 (9-C), 37.0 (10-C), 21.1 (11-C), 39.1 (12-C), 42.8 (13-C), 54.6 (14-C), 23.0 (15-C), 28.3 (16-C), 55.7 (17-C), 12.1 (18-C), 17.6 (19-C), 40.5 (20-C), 21.1 (21-C), 132.0 (22-C), 135.6 (23-C), 42.8 (24-C), 33.1 (25-C), 19.7 (26-C), 20.0 (27-C), 16.3 (28-C).

Cerevisterol (2): $C_{28}H_{46}O_3$, Colorless needle, mp 240-242℃, El-MS m/z 430 $[M]^+$. ^{1}H-NMR (400 MHz, $CDCl_3$): δ: 4.08 (1H, m, 3-H), 3.62 (1H, d, *J*=4.8 Hz, 6-H), 5.35 (1H, m, 7-H), 0.60 (3H, s, 18-H), 1.09 (3H, s, 19-H), 1.03 (3H, d, *J*=6.5 Hz, 21-H), 5.17 (1H, dd, *J*=15.0Hz, 8.0 Hz, 22-H), 5.23 (1H, dd, *J*=15.0hz, 7.5 Hz, 23-H), 0.84 (3H, d, *J*=7.0 Hz, 26-H), 0.82 (3H, d, *J*=7.0 Hz, 27-H), 0.91 (3H, d, *J*=7.0 Hz, 28-H). ^{13}C-NMR (100 MHz, $CDCl_3$): δ: 32.8 (1-C), 30.6 (2-C), 67.5 (3-C), 39.7 (4-C), 78.1 (5-C), 76.4 (6-C), 115.1 (7-C), 143.9 (8-C), 43.7 (9-C), 37.4 (10-C), 22.3 (11-C), 39.6 (12-C), 43.9 (13-C), 55.2 (14-C), 23.2 (15-C), 28.8 (16-C), 56.3 (17-C), 12.5 (18-C), 18.4 (19-C), 40.8 (20-C), 19.8 (21-C), 132.3 (22-C), 135.9 (23-C), 43.2 (24-C), 33.4 (25-C), 20.1 (26-C), 21.3 (27-C), 17.8 (28-C).

Ergosterol peroxide (3): $C_{28}H_{44}O_3$, Colorless needle, mp 175-177 ^{o}C, EI-MS m/z: 428$[M]^+$. ^{1}H NMR (400 MHz, $CDCl_3$): δ: 4.06-3.93 (1H, m, H-3), 6.28 (1H, d, *J*=8.5 Hz, H-6), 6.53 (1H, d, *J*=8.5 Hz, H-7), 0.90 (3H, s, H-18), 0.92 (3H, d, *J* = 6.8 Hz, H-19), 1.02 (3H, d, *J* = 6.6 Hz, H-21), 5.15 (1H, dd, *J* = 15.2, 7.4 Hz, H-22), 5.24 (1H, dd, *J*=15.2, 7.4 Hz, H-23), 0.83 (3H, s, H-26), 0.82 (3H, s, H-27), 0.84 (3H, s, H-28). ^{13}C NMR (100 MHz, $CDCl_3$): δ: 34.65 (C-1), 30.08 (C-2), 66.45 (C-3), 36.88 (C-4), 82.16 (C-5), 135.40 (C-6), 130.73 (C-7), 79.42 (C-8), 51.02 (C-9), 36.93 (C-10), 20.61 (C-11), 39.76 (C-12), 44.54 (C-13), 51.65 (C-14), 23.38 (C-15), 28.66 (C-16), 56.14 (C-17), 12.86 (C-18), 18.17 (C-19), 39.30 (C-20), 20.87 (C-21), 135.19 (C-22), 132.27 (C-23), 42.75 (C-24), 33.04 (C-25), 19.95 (C-26), 19.64 (C-27), 17.55 (C-28).

Allantoin (4): $C_4H_6N_4O_3$**,** white powder, mp 230-232 ^{o}C. ^{1}H NMR (400 MHz, DMSO-d_6): δ: 8.07 (1H, s, 1-NH), 10.55 (1H, s, 3-NH), 6.89 (1H, d, *J* = 8.2 Hz, 4-NH), 5.80 (2H, s, 6-NH_2), 5.25 (1H, d, *J* = 8.2 Hz, H-4). ^{13}C NMR (100 MHz, DMSO-d_6): δ: 157.21 (C-2), 62.86 (C-4), 174.06 (C-5), 157.80 (C-6).

(2,5-dioxo-4-imidazolidinyl)-carbamic acid (5): $C_4H_5N_3O_4$, white powder, mp 243-245 ^{o}C. ^{1}H NMR (400

MHz, DMSO-d_6): δ: 8.06 (1H, s, H-1), 5.78 (1H, s, H-3), 5.25 (1H, d, J = 8.0 Hz, H-4), 6.88 (1H, d, J = 8.0 Hz, H-6), 10.54 (1H, s, 7-OH). ^{13}C NMR (100 MHz, DMSO-d_6): δ: 156.72 (C-2), 62.44 (C-4), 157.22 (C-5), 173.52 (C-7).

Gliotoxin (6): $C_{13}H_{14}N_2O_4S_2$, white needle. ^{1}H NMR (400 MHz, $CDCl_3$): δ: 4.43 (1H, dd, J=12.8, 5.4 Hz, H-3a), 4.25 (1H, dd, J=12.7, 9.5 Hz, H-3a), 4.82 (2H, s, H-5a, H-6), 5.78 (1H, d, J=9.3 Hz, H-7), 5.97-5.92 (1H, m, H-8), 6.00 (1H, s, H-9), 3.74 (1H, d, J=18.0 Hz, H-10), 2.96 (1H, d, J=18.0 Hz, H-10), 3.21 (s, 3H, 2-CH_3). ^{13}C NMR (100 MHz, CDCl3): δ: 166.03 (C-1), 77.17 (C-3), 60.59 (C-3a), 165.26 (C-4), 69.79 (C-5a), 73.13 (C-6), 129.92 (C-7), 123.35 (C-8), 120.23 (C-9), 130.72 (C-9a), 36.57 (C-10), 75.59 (C-10a), 27.50 (2-CH_3).

Bis-N-norgliovietin (7): $C_{14}H_{18}N_2O_3S_2$, white needle. ^{1}H NMR (400 MHz, DMSO-d_6): δ: 8.99 (1H, s, H-2), 8.46 (1H, s, H-5), 3.52 (1H, d, J=13.6 Hz, H-7), 3.00 (1H, d, J=13.6 Hz, H-7), 7.03-742 (5H, m), 2.29 (3H, s, H-14), 2.11 (3H, s, H-15), 3.39 (2H, s, H-16), 4.82 (1H, s, 16-OH). ^{13}C NMR (100 MHz, DMSO-d_6): δ: 165.89 (C-1), 66.27 (C-3), 165.67 (C-4), 66.07 (C-6), 43.66 (C-7),135.61 (C-8), 130.89 (C-9,13), 128.28 (C-10,12), 127.10 (C-11), 13.94 (C-14), 13.09 (C-15), 65.26 (C-16).

Bis (methylthio) gliotoxin (8): $C_{15}H_{20}N_2O_4S_2$, white needle. ^{1}H NMR (400 MHz, $CDCl_3$): δ: 4.31 (1H, d, J=11.5 Hz, H-3a), 3.90 (1H, d, J=11.5 Hz, H-3a), 4.62 (1H, d, J=13.3 Hz, H-5a), 4.90 (1H, d, J=13.2 Hz, H-6), 5.76 (d, J=9.7 Hz, 1H, H-7), 5.93-5.87 (m, 1H, H-8), 5.94-5.98 (1H, m, H-9), 2.94 (1H, d, J=16.4 Hz, H-10), 3.04 (1H, d, J=16.1 Hz, H-10), 3.12 (3H, s, 2-NCH_3), 2.20 (3H, s, 3-SCH_3), 2.46 (3H, s, 10-SCH_3). ^{13}C NMR (100 MHz, $CDCl_3$): δ: 164.44 (C-1), 71.71 (C-3), 64.21 (C-3a), 167.14 (C-4), 67.64 (C-5a), 74.24(C-6), 130.38 (C-7), 122.95 (C-8), 120.39 (C-9), 131.34 (C-9a), 38.58 (C-10), 69.14 (C-10a), 32.20 (2-NCH_3), 14.82 (3-SCH_3), 17.88 (10-SCH_3).

Cyclo (Phe-Ser) (9): $C_{14}H_{14}N_2O_3$, white powder, mp 246-248℃. ^{1}H NMR (400 MHz, DMSO-d_6): δ: 7.94 (1H, s, 1-NH), 4.05 (1H, t, J=6.3 Hz, H-3), 8.05 (1H, s, 4-NH), 3.68-3.61 (1H, m, H-6), 3.26-3.33 (1H, m, H-7), 2.87 -2.78 (1H, m, H-7), 3.10 (1H, dd, J=13.5, 6.1 Hz, H-8), 2.98 (1H, dd, J=13.5, 4.9 Hz, H-8), 7.19-7.15 (2H, m, H-2′ and H-6′), 7.28 (d, J=7.5 Hz, 2H, H-3′ and H-5′), 7.23 (dd, J=6.1, 3.8 Hz, 1H, H-4′), 4.90 (t, J=5.7 Hz, 1H, 7-OH). ^{13}C NMR (100 MHz, DMSO-d_6): δ: 166.99 (C-2), 55.95 (C-3), 166.20 (C-5), 57.61 (C-6), 40.36 (C-7), 63.60 (C-8), 137.11 (C-1′), 130.44 (C-2′ and C-6′), 128.59 (C-3′ and C-5′), 126.98 (C-4′).

Trypacidin (10): $C_{18}H_{16}O_7$, white powder. ^{1}H NMR (400 MHz, $CDCl_3$): δ: 6.46 (1H, s, H-5), 2.64 (3H, s, H-6a), 5.81 (1H, s, H-7), 7.20 (1H, d, J=2.2 Hz, H-2'), 6.60 (1H, d, J=2.2 Hz, H-4'), 3.91 (3H, s, 4-OCH_3), 3.69 (6H, s, 6'-OCH_3 and 5'-OCH_3). ^{13}C NMR (100 MHz, $CDCl_3$): δ: 83.96 (C-2), 190.44 (C-3), 107.95 (C-3a), 158.31 (C-4), 105.50 (C-5), 152.45 (C-6), 23.32 (C-6a), 105.77 (C-7), 173.85 (C-7a), 138.52 (C-1'), 137.34 (C-2'), 185.00 (C-3'), 103.20 (C-4'), 168.83 (C-5'), 163.11 (C-6'), 56.29 (4-OCH_3), 52.87 (6'-OCH_3), 56.87 (5'-OCH_3).

Monomethylsulochrin (11): $C_{18}H_{18}O_7$, white powder. ^{1}H NMR (400 MHz, $CDCl_3$): δ: 6.62 (1H, d, J=2.2 Hz, H-4), 7.04 (1H, d, J=2.2 Hz, H-6), 3.71 (6H, s, 7-O**C**H_3 and H-8), 6.48 (1H, s, H-3'), 6.08 (1H, s, H-5'), 2.31 (3H, s, H-7'), 3.39 (3H, s, H-9'), 13.01 (1H, s, 2'-OH). ^{13}C NMR (100 MHz, $CDCl_3$): δ: 128.35 (C-1), 127.94 (C-2), 156.27 (C-3), 102.92 (C-4), 157.02 (C-5), 107.98 (C-6), 166.24 (C-7), 56.19 (C-8), 111.00 (C-1'), 164.28 (C-2'), 110.37 (C-3'), 148.18 (C-4'), 103.23 (C-5'), 160.94 (C-6'), 22.54(C-7'), 199.76 (C-8'), 55.69 (C-9'), 52.31 (7-O**C**H_3).

3 Conclusion

The ethyl acetate extract was subjected to chromatography on silica gel eluting successively with different mobile phases which resulted in the isolation and characterization of eleven compounds.

The secondary metabolites were identified as ergosterol (1), cerevisterol (2), ergosterol peroxide (3), allantoin (4), (2,5-dioxo-4-imidazolidinyl)-carbamic acid (5), gliotoxin (6), bis-N-norgliovietin (7), bis(methylthio) gliotoxin (8), cyclo-(Phe-Ser) (9), trypacidin (10) and monomethylsulochrin (11).

Among them, compound 5, 8 and 11 were isolated from endophytic fungi for the first time.

The present study of screening secondary metabolites revealed that *Fusarium solani*, an endophytic fungi from *Ficus carica* L. is the sources for the production of bioactive metabolites. These secondary metabolites can be further exploited for the biotechnological applications in medicine and agriculture.

References

[1] O. Petrini, "In Endophytic Fungi in Grasses and Woody Plants: Systematics, Ecology and EVolution;" Redlin, S. C., Carris, L. M., Eds.; APS Press: Saint Paul, MN, 1996, pp. 87-93.

[2] B. Schulz, C. Boyle, S. Draeger, A.K. Rommert, K. Krohn, "Endophytic fungi: a source of novel biologically active secondary metabolites," *Mycological Research*, Vol. 106, No. 9, 2002, pp. 996-1004.

[3] G. Strobel, B. Daisy, U. Castillo, J. Harper, "Natural Products from Endophytic Microorganisms," *Journal Natural Products*, Vol. 67, No. 2, 2004, pp. 257-268.

[4] F. De Simone, F. Senatore, D. Sica and F. Zollo, "Sterols from some basidiomycetes," *Phytochemistry*, Vol. 18, No. 9, 1979, pp. 1572-1573.

[5] S. Gupta, C. Montllor, Y.S. Hwang, "Isolation of Novel Beauvericin Analogues from the Fungus Beauveria bassiana," *Journal Natural Products*, Vol. 58, No. 5, 1995, pp. 733-738.

[6] L. A. A. Gunatilaka, Y. Gopichand, F. J. Schmitz, C. Djerassi, "Minor and trace sterols in marine invertebrates. 26. Isolation and structure elucidation of nine new 5α,8α-epidioxy sterols

978-1-61896-030-6 © 2012 SciRes.

from four marine organisms," *Journal of Organic Chemistry*, Vol. 46, No. 2, 1981, pp. 3860-3866.

[7] Y. Takaishi, M. Uda, T. Ohashi, K. Nakano, K. Murakami, T. Tomimatsu, "Glycoside of ergosterol derivatives from Hericum erinacens," *Phytochemitry*, Vol. 30, No. 12, 1991, pp. 4117-4120.

[8] F. Yin, L. Hu, R. Pan, "Novel Dammarane-Type Glycosides from Gynostemma pentaphyllum," *Chemical Pharmaceutical Bull*, Vol. 52, No. 12, 2004, pp. 1440-1444.

[9] X.Z. Hui, Y.J. Shan, L.R. mian, L. yang, Z.J. Guo, Z.Q. Tai and Y.S. Song, "A new narutal product from Cistanche deserticola Y.C. Ma.," *Journal Chinese Pharmaceutical Sciences*, Vol. 8, No. 2, 1999, pp. 61-63.

[10] M. Kaouadji, "Gliotoxin: uncommon ^{1}H couplings and revised ^{1}H- AND ^{13}C-NMR assignments," *Journal Natural Products*, Vol. 53, No. 3, 1990, pp. 717-719.

[11] G.W. Kirby, G.V. Rao and D.J. Robins, "New co-metabolites of gliotoxin in Gliocladium virens," *Journal of Chemical Society, Perkin Transactions 1*, No. 2, 1988, pp. 301-304.

[12] Okamoto M, Yoshida K, Uchida I, Nishikawa M, Kohsaka M, Aoki H, "Studies of platelet activating factor (PAF) antagonists from microbial products. I. Bisdethiobis(methylthio)gliotoxin and its derivatives," *Chemical Pharmaceutical Bull*, Vol. 34, No. 7, 1986, pp. 340-344.

[13] G.W. Kirby, D.J. Robins, M.A. Sefton and R.R. Talekar, "Biosynthesis of bisdethiobis(methylthio)gliotoxin, a new metabolite of Gliocladium deliquescens," *Journal of Chemical Society, Perkin Transactions 1*, 1980, pp. 119-121.

[14] G.W. Kirby, G.L.Patrick, "Cyclo-(L-Phenylalanyl-L-seryl) as an intermediate in the biosynthesis of gliotoxin," *Journal of Chemical Society, Perkin Transactions 1*, No. 11, 1978, pp. 1336-1338.

[15] W.B. Turner, "The Production of Trypacidin and Monomethylsulochrin by Aspergillus fumigatus," *Journal of Chemical Society, Perkin Transactions 1*, No. 9, 1965, pp. 6658-6659.

[16] J.Y. Liu, Y.C. Song, Z. Zhang, L. Wang, Z.J. Guo, W.X. Zou and R.X. Tan, "Aspergillus fumigatus CY018, an endophytic fungus in Cynodon dactylon as a versatile producer of new and bioactive metabolites," *Journal of Biotechnology*, Vol. 114, No. 3, 2004, pp. 189-193.

Chemical Constituents from the Leaves and Stems of *Periploca sepium* Bunge

Rui LIU[1], Hongchi ZHANG[1], Feng ZHOU[1], Kenming YU[1], Runmei WANG[1], Yangmin MA[2]
[1]*College of Agronomy and Life Science, Shanxi Datong University, Datong Shanxi, China*
[2]*College of Chemistry and Chemical Engineering, Shaanxi university of Science & technology, Xi'an, Shaanxi, China*
Email: zhanghclw@163.com

Abstract: As part of our ongoing studies on chemistry of Chinese traditional medicines, the constituents of *Periploca sepium* Bunge was investigated. Five triterpenes (1-5) and six flavones (6-11), were isolated from the leaves and stems of *P. sepium*, collected in the Qinling Mountains. Their structures were determined mainly by spectroscopic and chemical analyses. Among them, compound 1, 2, 4, 5, 7 and 10 were isolated from *P. Sepium* for the first time.

Keywords: Chemical constituents; *Periploca sepium* Bunge; triterpenes; flavones

1 Introduction

Periploca sepium Bunge, a woody vine belonging to the family Asclepiadaceae, is a native species and widespread on the Loess Plateau of China which is a drought-prone region with infrequent precipitation and high levels of soil erosion [1]. As a dominant shrub, *P. sepium* plays an important role in plant community structure and succession in the Loess hilly regions where the ecosystems are largely barren [2]. In addition, the root barks of *P. sepium* had been used for the treatment of rheumatoid arthritis as a traditional Chinese medicine. Pharmacological studies on this plant had demonstrated its anti-inflammatory and immunosuppressive effects [3].

As part of our ongoing studies on chemistry of Chinese traditional medicines, we investigated the chemical constituents of the leaves and stems of *P. Sepium* collected from the Qinling Mountains, Shaanxi Province. This paper describes the isolation and structure elucidation of five triterpenes and six flavones from the ethanolic extract of the plant.

2 Experimental Section

2.1 General Experimental Procedures

The ^{1}H and ^{13}C NMR spectra were recorded on Bruker ADVANCE 400 MHz spectrometer, with TMS as an internal standard. Melting points were obtained on a Fisher-Johns apparatus and are uncorrected. IR spectra were recorded with a JASCO FT/IR-5300 spectrometer. EI-MS were recorded on a JEOL SX102A mass spectrometer. Column chromatography was performed with silica gel (200-300 mesh, Qingdao Marine Chemical Inc. Qingdao, China) and Sephadex LH-20 (Amersham Biosciences Inc. Shanghai, China). Analytical TLC was carried out with glass precoated silica gel GF_{254} plates and spots were detected under UV light and colored by spraying with 7 % H_2SO_4 in 95 % ethanol followed by heating.

2.2 Plant Material

The leaves and stems of *Periploca sepium* Bunge was collected from the Qinling Mountains, Shaanxi Province, China, in September 2009. The voucher specimens were deposited in the College of Forestry, Northwest A & F University, Yangling, Shaanxi Province, China.

2.3 Extraction and Isolation

The air-dried leaves and stems of *P. sepium* (1.5 kg) were powdered and extracted with 95 % ethanol at room temperature. The ethanol extract was evaporated in vacuum at 60 ^{o}C to give residue. The residue was suspended in water and successively treated with petroleum ether, ethyl acetate and *n*-butanol to afford the petroleum ether extract (8 g), the ethyl acetate extract (51 g) and the *n*-butanol extract (19 g). The ethyl acetate extract was subjected to silica gel column chromatography eluting successively with ethyl acetate/methanol (1:0, 50:1, 20:1, 10:1, 5:1, 2:1, 1: 1, 0:1) and yielded eight fractions (A-H). Fraction A was rechromatographed on silica gel column, eluted with ethyl acetate in petroleum ether to compound 1 (131 mg), compound 2 (77 mg) and compound 3 (68 mg). Fraction B was separated by column chromatography on silica gel with a gradient of ethyl acetate in petroleum ether to give four subfractions (B1- 4). Fraction B1 was separated by silica gel column chromatography with elution with ethyl acetate/methanol (15:1) to give pure compound 4 (95 mg) and compound 5 (78 mg). Fraction D was repeatedly subjected to silica gel column chromatography with a gradient of ethyl acetate in petroleum ether and Sephadex LH-20 with ethyl acetate–methanol (1:1) to yield compound 6 (167 mg). The *n*-butanol extract was subjected to silica gel column

978-1-61896-030-6

chromatography eluting successively with chloroform /methanol gradient (1:0, 20:1, 10:1, 5:1, 2:1, 1: 1, 0:1) and yielded seven fractions (A-G). Fraction B was separated by column chromatography on silica gel with a gradient of methanol in chloroform to give five subfractions (B1-5). Fraction B2 was separated by silica gel column chromatography eluting with chloroform /methanol (10:1) to give pure compound 7 (125 mg) and compound 8 (292 mg). Fraction C was separated by column chromatography on silica gel with a gradient of methanol in chloroform to give five subfractions (C1-5). Fraction C2 was rechromatographed on silica gel column eluted with chloroform /methanol (10:1) to give pure compound 9 (95 mg), compound 10 (190 mg), compound 11 (135 mg).

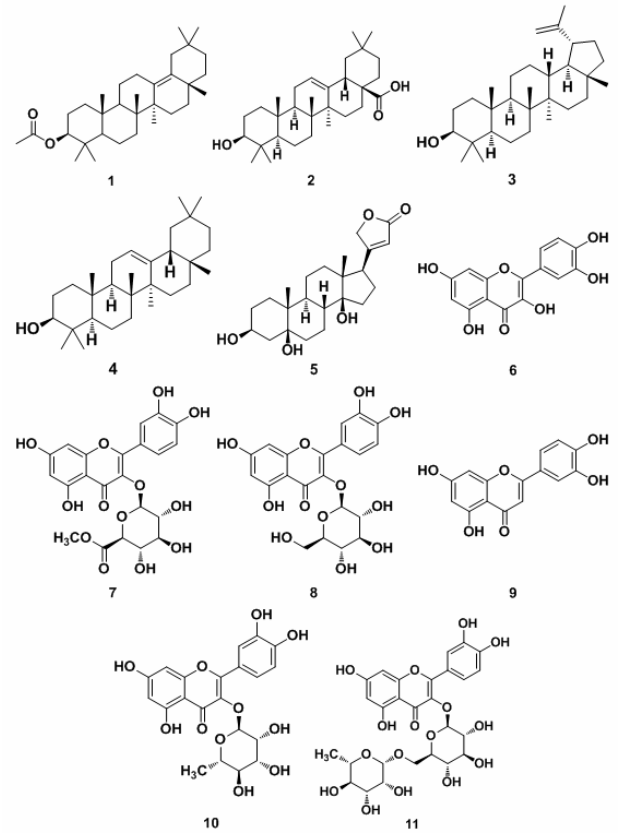

Figure 1. Compounds isolated from *P. sepium*

The structures of these compounds were elucidated by a combination of spectral analysis ^{1}H-NMR, ^{13}C-NMR, EI-MS and their physicochemical properties, and were identified as β-amyrin acetate (1) [4], oleanolic acid (2) [5], lupeol (3) [4,6], β-amyrin (4) [5], periplogenin (5) [7], quercetin (6) [8], quercetin-3-O-β-D-glucuronopyranoside methyl ester (7) [9], isoquercitrin (8) [10,11], luteolin (9) [12], quercetin-3-O-rhamnoside (10) [13], rutin (11) [14] (Figure 1), by comparison of their spectral data with the reported data in the literature.

β-Amyrin Acetate (1): $C_{32}H_{52}O_2$, mp 234-235 ^{o}C; colorless crystals; EI-MS m/z 468 $[M]^+$; ^{1}H NMR (400 MHz, $CDCl_3$) : δ: 5.17 (1H, t, *J*=3.6Hz, H-12), 4.49 (1H, m, H-3), 2.05 (3H, s, H-32), 1.12 (3H, s), 0.97 (3H, s), 0.92 (3H, s), 0.87 (6H, s), 0.81 (3H, s), 0.78 (6H, s); ^{13}C NMR (100 MHz, $CDCl_3$) : δ: 38.2 (C-1), 23.7 (C-2), 80.9 (C-3), 37.7 (C-4), 55.2 (C-5), 18.2 (C-6), 32.6 (C-7), 39.8 (C-8), 47.5 (C-9), 36.8 (C-10), 23.5 (C-11), 121.6 (C-12), 145.2 (C-13), 41.7 (C-14), 28.4 (C-15), 26.1 (C-16), 32.5 (C-17), 47.2 (C-18), 46.8 (C-19), 31.1 (C-20), 34.7 (C-21), 37.1 (C-22), 28.0 (C-23), 16.7 (C-24), 15.5 (C-25), 16.8 (C-26), 25.9 (C-27), 26.9 (C-28), 33.3 (C-29), 23.6 (C-30), 171.0 (C-31), 21.3 (C-32).

Oleanolic Acid (2): $C_{30}H_{48}O_3$, mp 302-304 ^{o}C; white powder; El-MS m/z: 456 $[M]^+$; IR(KBr)cm^{-1}: 3448 (-OH), 1693 (-C=O), 1403, 1 274, 1040; ^{1}H NMR (400 MHz, $CDCl_3$) : δ: 5.28 (1H, s, H-12), 3.26 (1H, m, H-3), 2.81 (1H, dd, *J*=10.0Hz, H-18), 0.74 (3H, s, H-26), 0.77 (3H, s, H-25), 0.90 (3H, s, H-24), 0.91 (3H, s, H-29), 0.92(3H, s, H-30), 0.98(3H, s, H-23), 1.13(3H, s, H-27); ^{13}C NMR (100 MHz, $CDCl_3$) : δ: 38.47 (C-1), 27.29 (C-2), 78.65 (C-3), 39.35 (C-4), 56.72 (C-5), 19.58 (C-6), 33.98 (C-7), 40.50 (C-8), 48.41 (C-9), 38.64 (C-10), 23.68 (C-11), 122.35 (C-12), 145.56 (C-13), 42.97 (C-14), 28.69 (C-15), 23.98 (C-16), 48.77 (C-17), 42.18 (C-18), 47.14 (C-19), 31.28 (C-20), 34.22 (C-21), 33.66 (C-22), 28.90 (C-23), 16.25 (C-24), 15.71 (C-25), 17.38 (C-26), 26.33 (C-27), 180.61 (C-28), 33.49 (C-29), 23.61 (C-30).

Lupeol (3): $C_{30}H_{50}O$, mp 210-212 ^{o}C; colorless needles; El-MS m/z: 426 $[M]^+$; ^{1}H NMR (400 MHz, $CDCl_3$) : δ: 4.62, 4.49 (each1H, d, *J*=1.8 Hz, H-29), 3.12 (1H, dd, *J*=11.2, 4.8 Hz, H-3), 1.68 (3H, s, H-30), 1.27 (1H, d, *J*=6.4 Hz, H-9), 1.03 (3H, s, Me-26), 0.97 (3H, s, Me-23), 0.89 (3H, s, Me-27), 0.81 (3H, s, Me-25), 0.92 (3H, s, Me-28), 0.74 (3H, s, Me-24); ^{13}C NMR (100 MHz, $CDCl_3$) : δ: 38.68 (C-1), 27.37 (C-2), 78.93 (C-3), 38.84 (C-4), 55.28 (C-5), 18.30 (C-6), 34.26 (C-7), 40.81 (C-8), 50.49 (C-9), 37.15 (C-10), 20.93 (C-11), 25.16 (C-12), 38.05 (C-13), 42.80 (C-14), 27.44 (C-15), 35.57 (C-16), 42.92 (C-17), 48.25 (C-18), 47.90 (C-19), 150.91 (C-20), 29.84 (C-21), 39.99 (C-22), 27.91 (C-23), 15.30 (C-24), 16.11 (C-25), 15.94 (C-26), 14.53 (C-27), 17.92 (C-28), 109.31 (C-29), 19.34 (C-30).

β-Amyrin (4): $C_{30}H_{50}O$, colorless crystals; mp 196-197 ^{o}C; EI-MS m/z 426 $[M]^+$; ^{1}H NMR (400 MHz, $CDCl_3$) : δ: 5.10 (1H, t, *J*=6.9Hz, H-12), 3.18 (1H, m, H-3), 1.12 (3H, s), 0.98 (3H, s), 0.96 (3H, s), 0.92 (3H, s), 0.87 (3H, s), 0.85 (3H, s), 0.81 (3H, s), 0.79 (3H, s); ^{13}C NMR (100 MHz, $CDCl_3$) : δ: 38.3 (C-1), 27.1 (C-2), 79.1 (C-3), 38.7 (C-4), 55.4 (C-5), 18.4 (C-6), 32.6 (C-7), 39.6 (C-8), 47.8 (C-9), 36.7 (C-10), 23.4 (C-11), 121.8 (C-12), 145.3 (C-13), 41.6 (C-14), 28.2 (C-15), 26.1 (C-16), 32.7 (C-17), 47.3 (C-18), 46.8 (C-19), 31.3 (C-20), 34.9 (C-21), 37.2 (C-22), 28.2 (C-23), 15.7 (C-24), 15.5

(C-25), 16.9 (C-26), 26.1 (C-27), 27.1 (C-28), 33.3 (C-29), 23.7 (C-30).

Periplogenin (5): $C_{23}H_{34}O_5$, colorless needles; mp 135-137 °C; EI-MS m/z 390$[M]^+$; ^{1}H NMR (400 MHz, $CDCl_3$) : δ: 5.89 (1H, s, H-22), 4.99 (1H, dd, *J*=18.0, 1.6, H-21), 4.82 (1H, dd, *J*=18.0, 1.6, H-21), 4.19 (1H, brs, H-3), 2.79 (1H, dd, *J*=9.2, 5.6, H-17), 0.95 (3H, s, H-19), 0.88 (3H, s, H-18); ^{13}C NMR (100 MHz, $CDCl_3$) : δ: 24.83 (C-1), 27.81 (C-2), 67.94 (C-3), 36.79 (C-4), 74.77 (C-5), 35.08 (C-8), 23.70 (C-7), 40.64 (C-8), 38.95 (C-9), 40.66 (C-10), 21.50 (C-11), 39.96 (C-12), 49.54 (C-13), 85.36 (C-14), 32.91 (C-15), 26.82 (C-16), 50.66 (C-17), 15.76 (C-18), 16.75 (C-19), 174.96 (C-20), 73.62 (C-21), 117.58 (C-22), 174.86 (C-23).

Quercetin (6): $C_{15}H_{10}O_7$, mp 312-314 °C; yellow powder; ^{1}H NMR (400 MHz, DMSO-d_6) : δ: 6.19 (1H, d, *J*=1.8Hz, 6-H), 6.41 (1H, d, *J*=1.8Hz, 8-H), 6.88 (1H, d, *J*=8.4Hz, 5′-H), 7.54 (1H, dd, *J*=2.0, 8.4Hz, 6′-H), 7.68 (1H, d, *J*=2.0Hz, 2′-H), 9.34 (1H, s, 3′-OH), 9.40 (1H, s, 4′-OH), 9.62 (1H, s, 3-OH), 10.80 (1H, s, 7-OH), 12.51 (1H, s, 5-OH). ^{13}C NMR (100 MHz, DMSO-d_6): δ: 147.24 (C-2), 136.19 (C-3), 176.29 (C-4), 161.17 (C-5), 98.63 (C-6), 164.34 (C-7), 93.79 (C-8), 156.58 (C-9), 103.46 (C-10), 22.40 (C-1'), 115.51 (C-2'), 145.51 (C-3'), 148.15 (C-4'), 116.05 (C-5'), 120.42 (C-6').

Quercetin-3-O-β-D-glucuronopyranoside methyl ester (7): $C_{22}H_{20}O_{13}$, mp 181-183 °C, yellow powder, IR (KBr) cm^{-1} : 3402 (OH), l73l (C=O), 1 647 C=O). ^{1}H NMR (400 MHz, DMSO-d_6) : δ: 6.21(1H, d, *J*=1.1Hz, H-6), 6.41(1H, d, *J*=1.1Hz, H-8), 7.51(1H, d, *J*=2.5Hz, H-2'), 6.83(1H, d, *J*=8.4Hz, H-5'), 7.56(1H, dd, *J*=2.5, 8.4Hz, H-6'), 5.46(1H, d, *J*=6.9Hz, H-1"), 3.71(3H, s, 6"-OCH_3). ^{13}C NMR (100 MHz, DMSO-d_6): δ: 156.77 (C-2), 133.62 (C-3), 177.59 (C-4), 161.67 (C-5), 99.27 (C-6), 164.79 (C-7), 94.07 (C-8), 156.91 (C-9), 104.36 (C-10), 121.36 (C-1'), 115.63 (C-2'), 145.37 (C-3'), 149.10 (C-4'), 116.57 (C-5'), 122.14 (C-6'), 101.88 (C-1"), 74.2 (C-2")3, 76.15 (C-3"), 71.85 (C-4"), 76.15 (C-5"), 169.35 (C-6"), 52.29 (6"-OCH_3).

Isoquercitrin (8): $C_{21}H_{20}O_{12}$, mp 225-227 °C, yellow needles, ^{1}H NMR (400 MHz, DMSO-d_6) : δ: 6.41 (1H, d, *J*=1.7Hz, 8-H), 6.20 (1H, d, *J*=1.7Hz,6-H), 7.57 (1H, d, *J*=1.9Hz, 2′-H), 7.58 (1H, dd, *J*=1.9, 8.9 Hz, 6′-H), 6.83 (1H, d, *J*=8.9Hz, 5′-H), 5.46 (1H, d, *J*=7.1Hz, H-1"). ^{13}C NMR (100 MHz, DMSO-d_6): δ: 156.68 (C-2), 133.86 (C-3), 177.93 (C-4), 161.73 (C-5), 99.15 (C -6), 164.62 (C -7), 93.98 (C-8), 156.81 (C-9), 104.46 (C -10), 121.68 (C-1'), 115.69 (C-2'), 145.28 (C-3'), 148.93 (C-4'), 116.72 (C -5'), 122.07 (C-6'), 101.45 (C -1"), 74.59 (C -2"), 77.02 (C-3"),. 70.46 (C-4"), 78.00 (C-5"), 61.49 (C-6").

Luteolin (9): $C_{15}H_{10}O_6$, mp 328-330 °C, yellow powder, ^{1}H NMR (400 MHz, DMSO-d_6) : δ: 7.42(1H, d, *J*=2.2, H-2′), 7.40 (1H, dd, *J*=2.2, 8.2, H-6′), 6.92 (1H, d, *J*=8.2, H-5′), 6.88 (1H, s, H-3), 6.49 (1H, *J*=2.1, H-8), 6.23 (1H, d, *J*=2.1, H-6). ^{1}H NMR (400 MHz, DMSO-d_6) : δ: 182.0 (C-4), 164.4 (C-7), 161.6 (C-5), 157.8 (C-9), 149.9 (C-4′), 146.0 (C-3′), 122.4 (C-1′), 119.5 (C-6′), 116.5 (C-5′), 113.7 (C-2′), 104.2 (C-10), 103.4 (C-3), 99.2 (C-6), 94.4 (C-8) [5].

Quercetin-3-O-rhamnoside (10): $C_{21}H_{20}O_{11}$, mp 185-187 °C, yellow needles, ^{1}H NMR (400 MHz, DMSO-d_6) : δ: 6.21 (1H, d, *J*=1.8 Hz, H-6), 6.39 (1H, d, *J*=1.8 Hz, H-8), 7.31 (1H, d, *J*= 2.1Hz, H-2'), 6.86(1H, d, *J*= 8.7Hz, H-5'), 7.26(1H, dd, *J*=2.1, 8.7 Hz, H-6'), 5.26 (1H, d, *J*=1.3 Hz, H-1"), 12.7 (1H, s, 5-OH), 10.8 (1H, s, 7-OH), 9.44 (1H, s, 4'-OH), 0.82(3H, d, *J*=6Hz, 6"-CH_3). ^{13}C NMR (100 MHz, DMSO-d_6): δ: 156.9 (C-2), 134.7 (C-3),178.2 (C-4), 161.8 (C-5), 99.2 (C-6), 164.7 (C-7), 94.1 (C-8), 157.8 (C-9), 104.5 (C-10), 121.6 (C-1'), 115.9 (C-2'), 145.7 (C-3'), 148.9 (C-4'), 116.1 (C-5'), 121.2 (C-6'), 102.3 (C-1"), 70.8 (C-2"), 71.0 (C-3"), 71.6 (C-4"), 70.5 (C-5"), 18.0 (C-6").

Rutin (11): $C_{27}H_{30}O_{16}$, mp 188-190 °C, yellow powder, ^{1}H NMR (400 MHz, DMSO-d_6) : δ: 6.19 (1H, d, *J*=2 Hz, H-6), 6.38 (1H, d, *J*=2 Hz, H-8), 7.53 (1H, d, *J*= 2.1Hz, H-2'), 6.84(1H, d, *J*= 8.0Hz, H-5'), 7.55(1H, dd, *J*=2.1, 8.0 Hz, H-6'), 5.35 (1H, d, *J*=7.3 Hz, H-1"), 4.39 (1H, s, H-11'"), 2.6 (1H, s, 5-OH), 10.7 (1H, s, 7-OH), 9.34 (1H, s, 4'-OH), 1.00(3H, d, J=6.2Hz, 6'"-CH_3). ^{13}C NMR (100 MHz, DMSO-d_6): δ: 157.0 (C-2), 133.8 (C-3),177.8 (C-4), 161.7 (C-5), 99.2 (C-6), 164.6 (C-7), 94.0 (C-8), 156.9 (C-9), 104.4 (C-10), 122.0 (C-1'), 115.7 (C-2'), 145.2 (C-3'), 148.9 (C-4'), 116.7 (C-5'), 121.6 (C-6'), 101.7 (C-1"), 74.5 (C-2"), 76.9 (C-3"), 71.0 (C-4"), 76.4 (C-5"), 67.4 (C-6"), 101.2 (C-1'"), 70.8 (C-2'"), 70.5 (C-3'"), 72.3 (C-4'"), 68.7 (C-5'"), 18.2 (C-6'").

3 Conclusion

The ethanolic extract of *P. sepium* was subjected to chromatography on silica gel eluting successively with different mobile phases which resulted in the isolation of eleven compounds, five triterpenes (1-5) and six flavones (6-11).

The structures of these compounds were elucidated by a combination of spectral analysis ^{1}H-NMR, ^{13}C-NMR, EI-MS and their physicochemical properties, and were identified as β-amyrin acetate (1), oleanolic acid (2), lupeol (3), β-amyrin (4), periplogenin (5), quercetin (6), quercetin-3-O-β-D-glucuronopyranoside methyl ester (7), isoquercitrin (8), luteolin (9), quercetin-3-O-rhamnoside (10), rutin (11).

Among them, compound 1, 2, 4, 5, 7 and 10 were isolated from *P. Sepium* for the first time.

References

[1] W. Li, Q.J. Wang, S.P. Wei, M.A. Shao, L. Yi, "Soil desiccation

978-1-61896-030-6 © 2012 SciRes.

for Loess soils on natural and regrown areas," *Forest Ecology and Management*, Vol. 255, No. 7, 2008, pp. 2467-2477.

[2] Z.D. Xue, Q.K. Zhu, Z.S. Liang, Y.X. Kang, L. Chang, "Dynamic changes of plant community on rehabilitated land in early succession stage in yan'an area," *Journal of Northwest Forestry University*, Vol. 22, No. 3, 2007, pp. 16-20.

[3] "State Administration of Traditional Chinese Medicine of the People's Republic of China," Shanghai: Shanghai Sci & Tech Press, 1998, pp. 1520-1522.

[4] D. Yang, N. Huu Tung, K. Sung In, K. Ha Won and K. Young Ho, "The regulation of inflammatory cytokine secretion in macrophage cell line by the chemical constituents of Rhus sylvestris," *Bioorganic & Medicinal Chemistry Letters*, Vol. 19, No. 13, 2009, pp. 3607-3610.

[5] L.N. Li, R. Tan, W.M. Chen, "Salvitmolic acid A, a new depside from roots of Salvia miltiorrhiza," *Planta Med*, Vol. 50, No. 3, 1984, 227.

[6] A. K. Ganguly, T. R. Govindachari, P. A. Mohamed, A. D. Rahimtulla and N. Viswanathan, "Chemical constituents of glochidion hohenackeri," *Tetrahedron*, Vol. 22, No. 4, 1966, pp. 1513-1519.

[7] T. Nakamura, Y. Goda, S. Sakai, K. Kondo, H. Akiyama and M. Toyoda, "Cardenolide glycosides from seeds of Corchorus olitorius," *Phytochemistry*, Vol. 49, No. 7, 1998, pp. 2097-2101.

[8] Z. Chen, Y.M. Liu, S. Yang, B.A. Song, G.F. Xu, P.S. Bhadury, L.H. Jin, D.Y. Hu, F. Liu, W. Xue and X. Zhou, "Studies on the chemical constituents and anticancer activity of Saxifraga stolonifera (L) Meeb," *Bioorganic & Medicinal Chemistry*, Vol. 16, No. 3, 2008, pp. 1337-1344.

[9] R.L. Zhang, X.C. Sun, W.X. Li, L.J. Wu, J. Huang and B.H. Sun, "Isolation and identification of chemical constituents of Polygonum perfoliatum L.," *Journal of Shenyang Pharmacesutical University*, Vol. 25, No. 2, 2008, pp. 105-107.

[10] C.Y. Wang, A. M. Pamukcu and G. T. Bryan, "Isolation of fumaric acid, succinic acid, astragalin isoquercitrin and tiliroside from Pteridium aquilinum," *Phytochemistry*, Vol. 12, No. 9, 1973, pp. 2298-2299.

[11] S. Tira, "Isoquercitrin from Orchis sambucina," *Phytochemistry*, Vol. 10, No. 8, 1971, pp. 1975-1976.

[12] C.F.F. Grael, S. Albuquerque and J.L.C. Lopes, "Chemical constituents of Lychnophora pohlii and trypanocidal activity of crude plant extracts and of isolated compounds," *Fitoterapia*, Vol. 76, No. 1, 2005, pp. 73-82.

[13] X.F. Ma, W.X. Tian, L.H. Wu, L.H. Wu and Y. Ito. "Isolation of quercetin-3-O-L-rhamnoside from Acer truncatum Bunge by high-speed counter-current chromatography," *Journal of Chromatography A*, Vol. 1070, No. 1-2, 2005, pp. 5211-5214.

[14] K. Kazuma, N. Naba, M. Suzuki, "Malonylated flavonol glycosides from the petals of Clitoria ternatea," *Phytochemistry*, Vol. 62, No. 2, 2003, pp. 229-237.

Isolation of Biosurfactant Producing Bacterium and Analysis of the Metabolite

Hongdan ZHANG[1], Jing WANG[1], Jinling WANG[1], Hanping DONG[2], Li YU[2]
[1]*Faculty of Chemical Engineering, China University of Petroleum, Beijing, China*
[2]*Fluid Flows in Porous Institute, Langfang Branch Institute, CNPC Beijing, China*
Email: wangjing36@hotmail.com

Abstract: An effective biosurfactant producing bacteria CK5-1 was isolated from Xinjiang crude oil and identified to be *Bacillus licheniformis* strain by biochemical tests together with 16S rDNA sequence analysis. Thin layer chromatography (TLC) and Fourier transformed infrared (FT-IR) worked together to reveal that CK5-1 produced lipopeptid biosurfactant. Under optimum condition, CK5-1 was able to reduce the surface tension of media from 72.4 mN/m to 28.726 mN/m after 72 h cultivation. Emulsification experiment indicated that CK5-1 had the ability to emulsify crude oil effectively, forming oil in water emulsion. CK5-1 could produce biosurfactant from 30℃ to 50℃. Under optimum temperature 30℃, the production of lipopeptid biosurfactant reached to its maximum 2 g/L. CK5-1 and its metabolite had a potential application in microbial enhanced oil recovery (MEOR).

Keywords: *Bacillus licheniformis*; lipopeptid; biosurfactant; metabolite

1 Introduction

Biosurfactants are surface-active compounds produced by wide range of microorganisms under specific condition [1, 2]. Biosurfactants are categorized by their chemical composition and microbial origin, including glycolipids, lipopeptides, polysaccharide–protein complexes, protein-like substances, lipopolysaccharides, phospholipids, fatty acids and neutral lipids [3].

In recent years, biosurfactant, identified as high biodegradability, low toxicity, low irritancy and various possible structures relative to chemical surfactants[4]have been widely employed in petroleum industries such as decomposition of spilled oils[5], cleaning of oil reservoirs[6], enhanced oil recovery [7,8]and reducing oil viscosity.

For microbial enhanced oil recovery (MEOR), biosurfactant is one of the most important metabolites. In the specific environment at reservoir, the most common biosurfactant-producers are *Bacillus* strains and *Pseudomonas* strains. And the isolated biosurfactants are usually glycolipids and lipopeptides [9].

The aims of this work were to isolate and characterize promising biosurfactant-producing microorganisms from Xinjiang oil field and to analyze the properties of the strain, purify and verify the biosurfactant and to evaluate the potentiality of the stain in MEOR.

2. Materials and Methods

2.1 Culture Media

In the present study, four culture media were used, and the compositions of these culture media were given in Table 1.

Table 1. Composition of the culture media used in the present study

Culture media	Component	Concentration (g/L)
Enrichment media	Crude oil *	5
	Glucose	2
	Yeast extract	0.1
	NH_4NO_3	0.5
	KH_2PO_4	1
	Na_2HPO_4	1
	$MgSO_4·7H_2O$	0.02
	Trace element solution	0.5 mL
Seed culture media	Peptone	10
	NaCl	5
	Glucose	10
	Beef extract	5
	Yeast powder	0.5
Fermentation media	NaCl	18
	$(NH_4)_2SO_4$	1
	NaH_2PO_4	3
	$K_2HPO_4·3H_2O$	6
	$MnSO_4$	0.01
	$MgSO_4$	0.05
	$FeSO_4·7H_2O$	0.01
	Crude oil	20

*crude oil was collected from Xinjiang oil field.

Initial pH of the seed culture media was adjusted to 7.0. In fermentation media, crude oil was used as the sole carbon and energy source to produce biosurfactant. Enrichment media and seed media were sterilized in autoclave at 110℃ for 30 min and fermentation media was sterilized at 121℃ for 15 min.

2.2 Microorganism Isolation

978-1-61896-030-6

5 mL crude oil was diluted with 95 mL sterile purified water, incubated at 30℃ in shaker for 2 h, after settlement, supernatant was inoculated into 90 mL enrichment culture and incubated at 30℃, 160 rpm for 3 d. Then 5 mL of the broth was transferred into fresh enrichment culture for totally 5 times. To isolate bacterial strains, samples (0.2 mL) of the nutrient solution were spread onto agar plates. Several colonies appeared and pure culture of each morphologically distinct colony was obtained by repetitive streaking onto agar plates. To obtain biosurfactant-producing microorganism, the above distinct colonies were transferred into 50 mL seed culture media and incubated at 30℃, 160 rpm for 24 h to obtain cells at logarithmic phase. Then 5% aliquot inoculum was transferred to 150 mL fresh fermentation media using crude oil as sole carbon, cultured at 30℃, 160 rpm for 2 d. After that, the surface tensions of culture samples were measured. The strain which could reduce the surface tension of broth to the lowest value was selected as the highest biosurfactant-producing strain and named CK5-1.

2.3 Identification of Strain CK5-1

The strain CK5-1 was identified biochemical according to <Bergey's Manual of systematic Bacteriology> [10]. For 16S rDNA sequencing, DNA was extracted using TIANGEN kit (China). Extracted DNA was amplified by PCR using universal set of primers 960f (5'-AAC GCG AAG AAC CTT AC-3') and 1392r (5'-ACG GGC GGT GTG TAC A-3'), A 40-bp GC clamp (5'-CGC CCG GGG CGC GCC CCG GGC GGG GCG GGG GCA CGG GGGG-3') was attached to the 5' end of the 960f. PCR amplification was performed in a total volume of 50 μL containing 2 μL template DNA, 5 μL 10× PCR buffer, 5 μL MgCl2(25 mM), 1 μL dNTP mixture(10 mM), 1 μL Taq DNA Polymerase(2.5 U/μL) and 1 μL of each primer(10 μM). The amplification fragments were V_6-V_8 regions of 16S rDNA [11]. PCR product (about 400 bp) was sent to Shanghai Sangon Biological Engineering Technology & Services Co, Ltd. (Shanghai, China) for sequencing. The resulting sequence was submitted to NCBI using BLAST service to determine its approximate phylogenetic affiliations.

2.4 Extraction of Biosurfactant

At the end of the incubation, pH of fermentation broth was adjusted to 8.0 using 2 M NaOH. After that the broth was centrifuged (8,000 rpm, 15 min) to remove cells and residual crude oil. Then pH of supernatant was adjusted to 2.0 by 1 M HCl and kept the supernatant at 4℃ over night to allow the precipitation of biosurfactant [12]. The precipitates were collected by centrifugation and extracted with an equal volume of chloroform/methanol (2:1, v/v) for 3 times. The solvent was concentrated in a rotary evaporator to obtain the crude biosurfactant. For further purification, n-hexane was added to the crude biosurfactant to scour off fatty acid, then the mixture was centrifuged to collect biosurfactant, dried and weighed the biosurfactant.

2.5 Biomass

Cell growth was monitored by measuring the optical density at 600 nm (OD_{600}). Cells were collected by centrifugation (8000 rpm, 15 min), and re-suspended in sterilized water to the original volume.

2.6 TLC Analysis

Preliminary characterization of the biosurfactant was done by thin layer chromatography (TLC). A portion of the extracted biosurfactant was firstly dissolved in chloroform and spotted on silica gel plates using the solvent system chloroform/methanol/double distilled water (65:25:4, V/V/V)[13]. The components on the TLC plate were visualized by hydrolizating at 110℃ for 1.5 h after spraying with 50% sulfuric acid. Ninhydrin reagent (0.5 g ninhydrin in 100 mL anhydrous acetone) was used to detect lipopeptide biosurfactant as red spots, and Phenol-sulfuric acid reagent(3 g phenol in 5 mL sulfuric acid mixed with 95 mL ethanol) to detect glycolipid biosurfactant as brown spots.

2.7 FT-IR Analysis

FT-IR spectra of the dried biosurfactant were recorded on a Bruker 113 VFT-IR spectrometer in wave number range of 4000–400 cm^{-1}. FT-IR analysis was performed with MAGNA-IR 560 E.S.P and carried out by the Center of Analytical Services of State Key Laboratory of Heavy Oil Processing, China University of Petroleum (Beijing).

3 Results and Discussion

3.1 Isolation and Identification of Biosurfactant-Producing Strain CK5-1

After a multi-step enrichment program, eight morphologically distinct microbial colonies had been selected as positive strains. Ultimately one of the isolates CK5-1, which can reduce the surface tension of the fermentation broth from 72.4 mN/m to below 30 mN/m was selected for the further studies. The 16S rDNA sequence analysis revealed that CK5-1 had 99 % homology with *Bacillus licheniformis*. Together with biochemical characteristics (Table2), CK5-1 was identified as *Bacillus licheniformis* strain.

Table 2. Biochemica characteristics of strain CK5-1

Experiments	Strain CK 5-1
Gram staining	+
Catalase	-
Oxidase	+
Urea enzyme	+
Methyl-red	-
Starch hydrolysis	+

The experiment is marked by plus sign "+" when the change in growth was observed; and marked by minus sign "–" when no change in growth was observed.

3.2 Preliminary Characterization of Biosurfactant

After adjusting pH of the fermentation broth to 2.0 and keeping the broth at 4℃, precipitate was observed, indicating the presence of lipopeptid.

TLC analysis showed that there was no brown spot on silica gel plates when using Phenol-sulfuric acid reagent as color developing reagent, suggesting that no glycolipids was found in this biosurfactant. Mean while, comparing the two results between hydrolization and nonhydrolization, the red spot which appeared only on the plate after hydrolization was recognized to contain amino acid from hydrolysis of lipopeptid.

FT-IR analysis (Figure 1) was utilized to confirm the biosurfactant following TLC detection. IR spectroscopy revealed that biosurfactant produced by CK5-1 showed strong absorption bands. The two absorption bands at 3302 cm^{-1} and 3067 cm^{-1}were result from the NH stretching, indicate the presence of peptide component. At 1650 cm^{-1}, the stretching mode of a C=O bond was observed and at 1539 cm^{-1} the deformation mode of the NH bond combined with C–N stretching mode occurred. The presence of an aliphatic chain was indicated by the C–H stretching modes at 2854–2960 cm^{-1} and 1464–1377 cm^{-1}. At 2925 cm^{-1} and 2854 cm^{-1} the stretching vibration of CH_2 occurred. The bonds at 1715 $cm^{-1}$and 1215 cm^{-1} were due to lactone carbonyl absorption. These results indicated that the biosurfactant contain aliphatic and carbonyl moieties.

According to all the above results biosurfactant produced by CK5-1 was identified as lipopeptid.

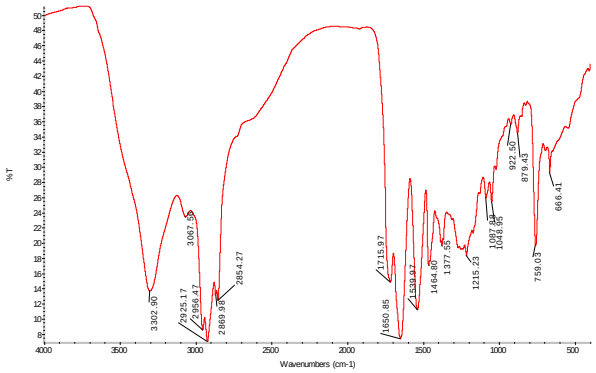

Figure 1. FT-IR spectrum of dried biosurfactant produced by CK5-1

3.3 Characteration of CK5-1

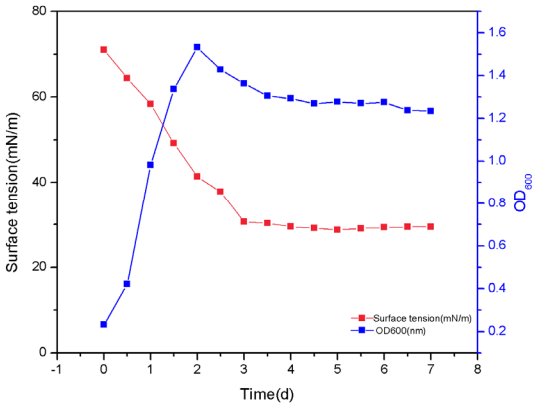

Figure 2. Growth and surface tension of strain CK5-1 under optimum condition

Previous studies (data not shown) had determined the optimum growing conditions of CK5-1 were temperature 30℃, pH =7.5, salinity 15-18.26 g/L. Under this optimum condition, the surface tension of the fermentation broth decreased from 72.4 mN/m to 28.726 mN/m (Figure 2). The lowest surface tension occurred when cell growth entered into stationary phase after 3 d of cultivation. The reduction of the surface tension of media was the result of biosurfactant production and accumulation along with cell growth during logarithm phase and stationary phases. It can be concluded that the biosurfactant produced by CK5-1 was a primary metabolite.

Good emulsification property is very important for biosurfactant to be promising in different applications [14]. The ability of CK5-1 to emulsify crude oil was investigated. Under optimum condition, CK5-1(5%) was inoculated into the fermentation media and incubated in a shaker at 160 rpm for 7 d.

978-1-61896-030-6 © 2012 SciRes.

Figure 3. Comparison macroscopic appearances of fermentation broth: left is without CK5-1 right is with CK5-1

Figure 4. Micro-emulsification of fermentation broth without CK5-1

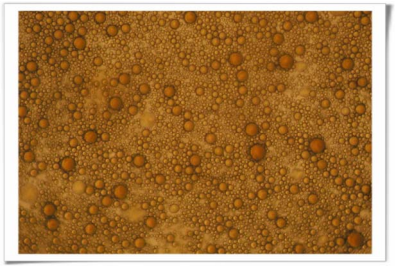

Figure 5. Micro-emulsification of fermentation after inoculated CK5-1 for 5 days

Figure.3 showed the emulsification of fermentation broth after inoculating CK5-1 for 2 d. Crude oil evenly dispersed in the broth, forming a homogeneous emulsion. Micro-emulsifying properties of the broth were also studied. After incubation, 100 μL broth was added onto the slide and observed with a microscope in 200× magnification, as figure.5 showed. For the blank controller (figure.4), most of the broth was aqueous. The five big oil drops were the result of mechanical shaking. After the action of CK5-1, the broth were full of small oil droplets, indicating that CK5-1 can act on the oil-water interface and make oil disperse in aqueous phase. The biosurfactant produced by CK5-1 promoted emulsification. Oil phase and water phase were well mixed forming oil in water emulsion.

3.4 Biosurfactant Production

In oil reservoirs, temperature is the most important factor that effect microbial growth and metabolism. The profiles of biomass concentration, biosurfactant production at different temperature were shown in figure.6-9. The production of biosurfactant was accumulated as the cell growth. Maximum biosurfactant production reached to about 2 g/L at optimum 30℃.

Although 30℃ is its optimal temperature, CK5-1 still had capacity to produce biosurfactant at 40℃ and 50℃, of which the concentration were 1.83 g/L and 1.54 g/L respectively, indicating that CK5-1 had a temperature resistance. The concentration of biosurfcatant reached to its maximum at about 4–5 days of fermentation, when the cell growth entered the decline phase.

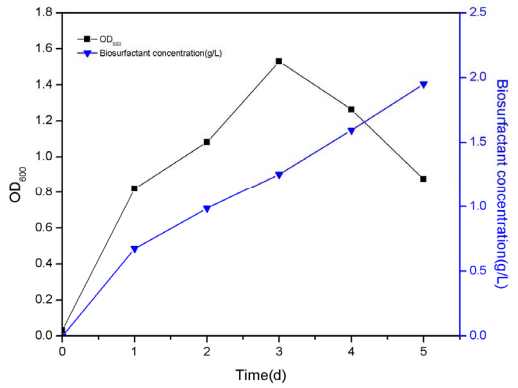

Figure 6. Time courses of biosurfactant production and biomass at 30℃

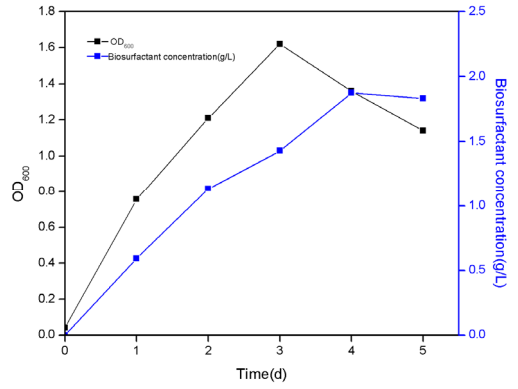

Figure 7. Time courses of biosurfactant production and biomass at 40℃

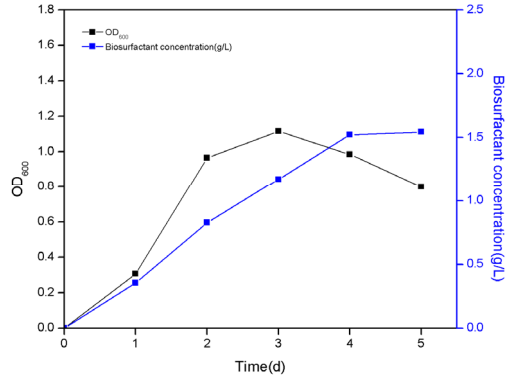

Figure 8. Time courses of biosurfactant production and biomass at 50℃

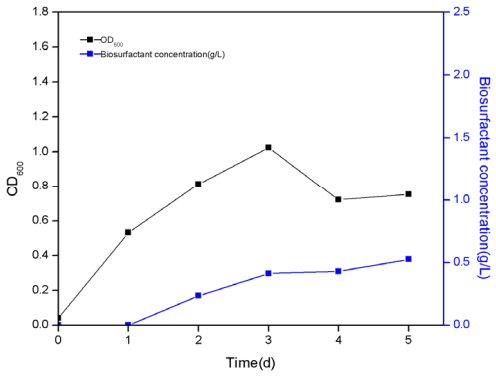

Figure 9. Time courses of biosurfactant production and biomass at 60℃

4 Conclusion

In the present study, we have successfully isolated the indigenous strain CK5-1. Results showed CK5-1 had the capacity to reduce the surface tension of the media to 28.726 mN/m by producing lipopeptid biosurfactant. The result is superior to those already published reports by other authors [15, 16]. It also showed a relative high emulsification capacity to emulsify crude oil and form water in oil emulsion. The advantage of this bacterium was the ability of biosurfactant production at wide range of temperature (20℃–50℃). In conclusion, the isolated strain CK5-1 had a potential application in petroleum and environmental application such as enhanced oil recovery and decomposition of spilled oils. What is more, the microbial products biosurfactant could be favorable for reservoirs with growth limiting conditions.

Acknowledgement

The supports of the China National 863 Hi-Tech R&D Plan (Grant No. 2009AA063504), China National Petroleum Corporation Science & Technology Management Program (2008A-1403) are gratefully acknowledged.

References

[1] B. Thanomsub, W. Pumeechockchai and A. limtrakul, "Chemical structures and biological activities of rhamnolipids produced by *Pseudomonas aeruginosa* B189 isolated from milk factory waste," *Bioresource Technology*, vol. 97, No. 5, 2006, pp. 1149-1153.

[2] N. Christofi and I. B. Ivshina, "Microbial surfactants and their use in field studies of soil remediation," *Journal of Applied Microbiology*, vol. 6, No. 6, 2002, pp. 915-929.

[3] O. Pornsunthorntawee, S. Maksung and O. Huayyai, "Biosurfactant production by *Pseudomonas aeruginosa* SP4 using sequencing batch reactors: effects of oil loading rate and cycle time," *Bioresource Technology*, vol. 100, No. 2, 2009, pp. 812-818.

[4] J. D. Van Hamme, A. Singh and O. P. Ward, "Physiological aspects. Part 1. In a series of papers devoted to surfactants in microbiology and biotechnology," *Biotechnology Advances*, vol. 24, No. 6, 2006, pp. 604-620.

[5] P. Bharali, S. Das and B. K. Konwar, "Crude biosurfactant from thermophilic Alcaligenes faecalis: Feasibility in petro-spill bioremediation," *International Biodeterioration & Biodegradation*, vol. 69, No.5, 2011, pp. 682-690.

[6] N. L. Olivera, M. L. Nievas and M. Lozada, "Isolation and characterization of biosurfactant-producing *Alcanivorax* strains: hydrocarbon accession strategies and alkanehydroxylase gene analysis," *Research in Microbiology*, vol. 160, No.1, 2009, pp. 19-26.

[7] G. Seghal Kiran, T. Anto Thomas, and Joseph Selvin, "Optimization and characterization of a new lipopeptide biosurfactant produced by marine *Brevibacterium* aureum MSA13 in solid state culture," *Bioresource Technology*, vol. 101, No. 7, 2010, pp.2389-2396.

[8] H. Amani, M. H. Sarrafzadeh and M. Haghighi, "Comparative study of biosurfactant producing bacteria in MEOR applications," *Journal of Petroleum Science and Engineering*, vol. 75, No.1-2, 2010, pp. 209-214.

[9] A. R. Najafi, M. R. Rahimpour and A. H. Jahanmiri, "Enhancing biosurfactant production from an indigenous strain of *Bacillus mycoides* by optimizing the growth conditions using a response surface methodology," *Chemical Engineering Journal*, vol. 163, No.3, 2010, pp. 188-194.

[10] J.G. Holt, N, R. Krieg and P. H. A. Sneath. "Bergey's Manual of Determinative Bacteriology," Shandong: Shandong University Press: Translated by Liu F.J, Shandong, 1988, pp. 78-83.

[11] W. T. Liu and K. Ritalahti, "Denaturing gradient gel electrophoresis (DGGE) protocol," M. ROME Lab DGGE Workshop, vol. 3, 1996, pp. 5-6.

[12] H. Yin, J. Qiang and Y. Jia, "Characteristics of biosurfactant produced by *Pseudomonas aeruginosa* S6 isolated from oil-containing wastewater,'' *Process Biochemistry*, Vol. 44, No. 3, 2009, pp. 302-308.

[13] N. I. A. Haddad, J. Wang, and B. Z. Mu "Isolation and characterization of a biosurfactant producing strain, *Brevibacilis brevis* HOB1," *Journal of Industrial Microbiology & Biotechnology*, vol. 35, No.12, 2008, pp. 1597-1604.

[14] M. Banat, R. S. Makkar and S. S. Cameotra, "Potential commercial applications of microbial surfactants," *Applied Microbiology and Biotechnology*, vol. 53, No.5, 2000, pp. 495-508.

[15] S. B. Batista, A. H. Mounteer and F. R. Amorim, "Isolation and characterization of biosurfactant/bioemulsifier-producing bacteria from petroleum contaminated sites," *Bioresource Technology*, vol. 97, No. 6, 2006, pp. 868-875.

[16] M. Shavandi, G. Mohebali, and A. Haddadi, "Emulsification potential of a newly isolated biosurfactant-producing bacterium, *Rhodococcus* sp. strain TA6," *Colloids and Surfaces B: Biointerfaces,* vol.82, No.2, 2011, pp. 477-482.

978-1-61896-030-6 © 2012 SciRes.

Protective Effect of N-Butanol Extraction from *Bupleurum chinense* DC. on CCl_4-Induced Injury in Mice and Study on the Features of Chemical Compositions

Bing WEI, Yun YANG, Qishuai WANG, Chengming DONG
Department of Pharmacy, Henan University of TCM, Zhengzhou, China
Email: Yyun@china.com.cn

Abstract: The effects of n-butanol extraction from *Bupleurum chinense* DC. on carbon tetrachloride(CCl_4) –induced liver injury were studied in mice and the features of chemical compositions in n-butanol fraction were studied at the same time. The drug group that pretreatment with saikosaponins could significantly decreased serum ALT and AST activities(P<0.05), at the same time, it could obviously enhance the activity of SOD and reduce the contents of MDA in liver tissue(P<0.05). The following study on the features of chemical compositions indicated that SSa and SSd were the two compositions of saikosaponins with the relatively high contents in the n-butanol fraction. The contents of total saikosaponins in the n-butanol fraction were 11.20 $mg \cdot mL^{-1}$.

Keywords: N-butanol extraction; *Bupleurum chinense* DC.; chemical compositions; saikosaponins

1 Introduction

The dried roots of *Bupleurum chinense* DC. from the umbelliferae were often used to treat Shao Yang diseases as traditional chinense medicine with the features of evacuation of antipyretic, relieving the depressed liver and lifting Yang Qi [1]. Modern studies [2-6] testified that water extraction and alcohol extraction from *Bupleurum chinense* DC. had effects of anti-liver fibrosis, protecting liver cells and inhibiting human liver cancer cells, in which many chemical compositions existed, such as flavonoids, carbohydrate, volatile oil and so on. As a result what kind of chemical compositions had the effects were not clear so far. Based on this, this experiment had a purification process of alcohol extraction and took the n-butanol fraction as the research object. Previous study on the n-butanol fraction was limited to one side of the pharmacological action or the features of chemical compositions, our present study was designed to evaluate the effects of n-butanol fraction on acute liver injury in mice induced by CCl_4 and study the features of chemical compositions in n-butanol fraction by using chromatographic analysis at the same time. The correlation between the chemical compositions and liver protection was preliminary studied.

2 Materials and Methods

2.1 Reagents and Instruments

Kits of ALT, AST, SOD and MDA (provided by Nanjing Jiancheng biological research institute of China with the batch number of 20100529), brifendate pills (provided by Zhejiang Wanbang pharmaceutical CO., LTD. of China with the batch number of 090906), Saikosaponin -a, -d, (SSa, SSd) were prepared by our laboratory [7], sample of *Bupleurum chinense* DC. was obtained from Dalian (Liaoning China), the sample was identified by botanists Prof. Cheng–ming Dong from Henan University of TCM.

SUMMIT HPLC instrument with "CHROMELE –ONTM" wokstation (DIONEX company USA) and ELSD (ALLTECH company USA), "Chromafinger" solution software (Version 1.5 Keman Medicine Research company Zhuhai China), Hydro-RP80A column (Guangzhou phnomenex company China), METLER AE240 analytical balance (Mettler-Toledo instruments company Switzerland), BS210S electronic balance (Sartorius automatic company Beijing China), SZ-93 double pure water distiller rotary evaporator (Yarong biochemistry instrument factory Shanghai China), PT2100 inscribed homogenizer (Polytron company USA), 3-18K high-speed freezing centrifuge (Sigma Germany), LDZ5-2 low-speed centrifuge (Jingli company Beijing China), UV-2000 uv-vis spectrophotometer (Unico company Shanghai China).

2.2 Animal Experiment

2.2.1 Animals

60 SPF kunming mice weighing 19-23 g were purchased from local breeders and were randomLy divided into 6 groups: blank group, model group, positive medicine group, three treatment groups (high, middle, low dose of saikosaponins extraction) with half male and half female in each group. The animals were housed in metal cages in animal experimental center of

Henan University Of TCM that was air-conditioned by means of a system designed to maintain the room temperature at an average of 24 ℃ and a relative humidity of about 30%-50%. Tap water and diet were available and libitum.

2.2.2 Preparation of Saikosaponins

201.0 g of *Bupleurum chinense* DC. meal was reflux extracted for two times with 8-fold volume of 95% alcohol for the first time and 6-fold volume of 95% alcohol for the second time, each time for 1h,vacuum filter and combine the filtrate, vacuum concentration to condensed paste which was dissolved by 1000 mL of n-butanol-saturated water (external therapeutic ultrasound (ETUC) for 20 min) and then water-saturated n-butanol extraction (equivalent) for three times,combine extraction liquid and vacuum concentration to condensed paste. Add 201 mL normal saline to dissolve the paste (ETUC for 5 min), centrifuge for 3min (3000 $r \cdot min^{-1}$) and the same to the precipitate, combine the supernatant and vacuum concentration to 201 mL to get the final extraction, the concentration was 1.0 $g \cdot mL^{-1}$ (1.0 mL solution contained 1.0 g crude drug). By diluting to get other dosage.

2.2.3 Dosage and Model Planning

The mice in the positive medicine group were pretreated with 7.5 $mg \cdot mL^{-1}$ DDB (compounding of 0.5 % (w/v) CMC-Na). The mice in the three treatment groups were respectively pretreated with 1.0 $g \cdot mL^{-1}$, 0.5 $g \cdot mL^{-1}$ and 0.2 $g \cdot mL^{-1}$ extraction of saikosaponins. The mice in the blank group and the model group were given equal volume of normal saline. Dosage of administration was 20 $mL \cdot kg^{-1}$ by continuous *ig* injection for 7 d. All mice were deprived of food after the final injection on the 7th day. 2 h after the final injection, the blank group was given vegetable oil by *ip* injection (10 $mL \cdot kg^{-1}$), the rest groups [8-9] were given 0.2% CCl_4 (CCl_4/vegetable oil (v/v)) by *ip* injection (10 $mL \cdot kg^{-1}$). The eyeballs were extracted and blood was drawn after 10 h, centrifuge for 4 min(2000 $r \cdot min^{-1}$) to get serum. The liver (0.5 g) perfused with ice-cold saline was homogenized with inscribed homogenizer in 4.5 mL saline, this homogenate was further centrifuged for 10 min (3000 $r \cdot min^{-1}$), 2 mL of supernatant was taken to reserve.

2.2.4 Serum and Liver Tissue Assay

ALT, AST activities in serum and SOD activity, MDA contents in liver tissue were assayed by using commercial kits.

2.3 Fingerprint of the Chemical Compositions

2.3.1 Preparation of Reference Solutions

Dissolve 3.00 mg of SSa and SSd in 5 mL of methanol respectively.

2.3.2 Preparation of Sample Solutions

1.0 g of the finely powdered root (sieve with 20mesh) was added to 40 mL methanol. The mixture was extracted by ultrasonic for 1 hour, filtered afterwards, and the leftover dissolved in 5 mL and filtered. The two filtrates were combined, evaporated to dryness in a fume cupboard and dissolved in 10 mL of water. The solution was extracted for three times with n-butanol which had been saturated by water, each volume was 10 mL, and three extractions were combined and evaporated to dryness. The residue was dissolved in 5 mL of methanol. The solution was filtered through a 0.45 μm membrane filter before use.

2.3.3 HPLC Conditions

HPLC conditions were shown as follows. The flow rate was 1.0 $mL \cdot min^{-1}$, The injection volume was 10 μL and the column temperature was maintained at 30℃. The mobile phase was consisted of water (A) and acetonitrile (B), which were applied in the following gradient elution: from 85A/15B to 70A/30B in 15min, in 10 min to 65A/35B, in 15min to 55A/45B, then in 20 min to 50A/50B, each run was following by a 10 min washing procedure. ELSD conditions: drifttube temperature, 110℃; carrier gas, compressed air; carrier gas flow, 3.0 $L \cdot min^{-1}$; splitter, off [10].

2.4 Total Saikosaponins Assay

2.4.1 Preparation of Sample Solution

0.2 g of *Bupleurum chinense* DC. meal was reflux extraction for two times with 10 mL of 95% alcohol for the first time and 8 mL of 95% alcohol for the second time, each time for 1h. Add 2 mL of alcohol to wash the leavings after natural filter and combine the filtrate. Drying the filtrate in a fume cupboard after measuring its volume. Add equal volume of n-butanol-saturated water to dissolve the paste and then water-saturated n-butanol extraction (equivalent) for three times, combine extraction liquid and evaporate to dryness. Constant volume was 25 mL with methanol.

2.4.2 Staining Method

0.8 mL aspiration of sample solution was evaporate to dryness. Add 0.10 mL of 1% paradimethylami -nobenzaldehyde solution in alcohol solution and evaporate to dryness. Then add 4.0 mL of phosphoric acid and heat in water bath (70 ℃) for 30 min. Cooled to room temperature.

2.4.3 Assay Method

Determine absorbability of sample solution and then use the formula curve as follows to calculate the contents

of total saikosaponins.

$$Y=3.1086X+0.0682(r=0.0996)$$

Where Y and X are absorbance and concentration of samples; RSD of precision test, stability test, replicate test and recovery test were all not more than 3.29%.

3 Results and Analysis

3.1 Statistical Analysis

The software package SPSS 13.0 was applied for one-way analysis of variance. Data of each group was expressed as mean±standard deviation ($\overline{X} \pm s$). The results were in table 1 and table 2.

As was shown in table 1, ALT and AST activities in serum were significantly higher in model group (P<0.05) than in blank group showed that the model building was successful. Compared with the control group, the serum ALT and AST activities in positive medicine group and high dose group were all significantly decreased (P<0.05). The middle and low dose group did not have these effects

Table 1. Effects of different dosage pretreatment on activities of serum ALT and AST in mice

Groups	Dosage/ g·kg^{-1}	ALT / U·L^{-1}	AST / U·L^{-1}
Blank group	saline	25.40±4.58*	30.30±5.76*
Model group	saline	47.80±4.29$^{\triangle}$	89.90±6.21$^{\triangle}$
Positive medicine group	0.15	30.10±4.07*$^{\triangle}$	47.70±8.25*$^{\triangle}$
High dose group	20	31.60±3.03*$^{\triangle}$	51.60±8.34*$^{\triangle}$
Middle dose group	10	45.50±4.35$^{\triangle}$	84.90±8.71$^{\triangle}$
Low dose group	4	47.70±5.19$^{\triangle}$	89.30±7.69$^{\triangle}$

*P<0.05, significant difference *vs* model group.
$^{\triangle}$ P<0.05, significant difference *vs* blank group

Table 2. Effects of different dosage on SOD activity and MDA contents of liver tissue in mice

Groups	Dosage /g·kg^{-1}	SOD/ $U{\cdot}mgprot^{-1}$	MDA /$nmol{\cdot}mgprot^{-1}$
Blank group	saline	285.89±25.10*	4.08±1.57*
Model group	saline	102.82±17.83$^{\triangle}$	7.37±1.19$^{\triangle}$
Positive medicine group	0.15	256.39±22.76*$^{\triangle}$	4.50±0.72*
High dose group	20	221.98±22.91*$^{\triangle}$	5.51±1.13*$^{\triangle}$
Middle dose group	10	197.48±18.37*$^{\triangle}$	7.81±1.32$^{\triangle}$
Low dose group	4	95.34±22.86$^{\triangle}$	7.71±1.23$^{\triangle}$

*P<0.05, significant difference *vs* model group.
$^{\triangle}$ P<0.05, significant difference *vs* blank group

As was shown in table 2, compared with blank group, the liver tissue SOD activity was significantly lower while the MDA contents were significantly higer(P<0.05) in model group showed liver tissue lipid peroxidation in mice appeared and the model building was successful. The decrease of liver tissue SOD activity and elevation of liver tissue MDA contents were significantly inhibited (P<0.05) in positive medicine group and high dose group by comparing with the model group. So saikosaponins could enhance the abilities of antioxidation and scavenging oxygen free radicals in mice.

3.2 Fingerprints Analysis

Fingerprints of SSa, SSd and the sample were shown in the figures as follows.

By comparing the retention time with figure 1 and figure 2, it can be confirmed that peak 15 was SSa and peak 17 was SSd in figure 3.

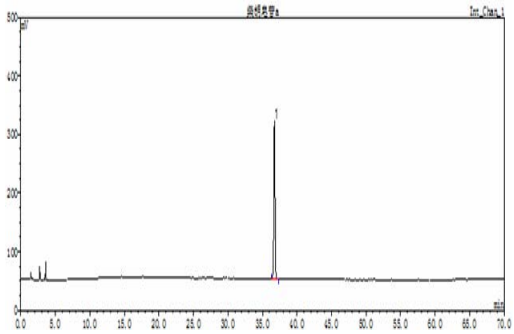

Figure 1. Characteristic spectrum of standard of SSa

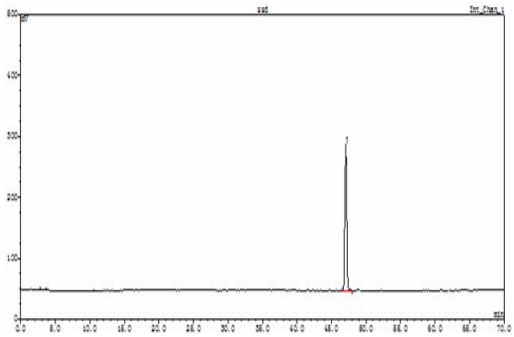

Figure 2. Characteristic spectrum of standard of SSd

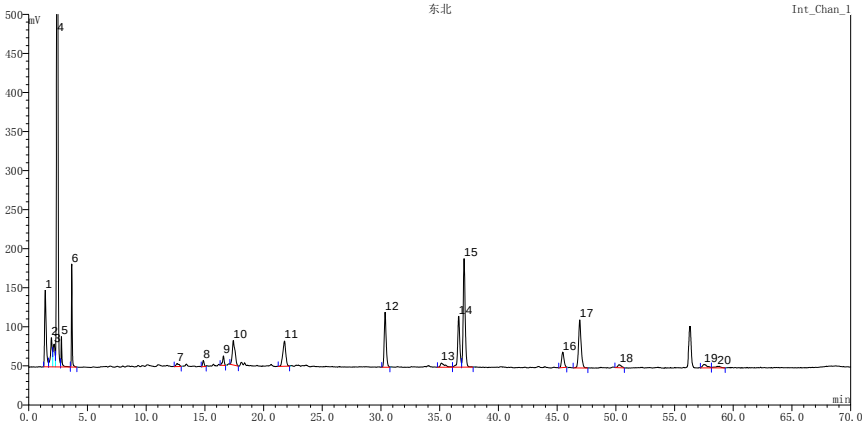

Figure 3. Characteristic spectrumof the n-butanol extraction from the sample

3.3 Contents of Total Saikosaponins

The contents of saikosaponins in high dose group (concentration was 1.0 g·mL^{-1}) was 11.20 mg·mL^{-1} using the formula curve to calculate.

4 Discussions

CCl_4 was one of the commonly used liver injury inducer. The method had the features of simple, remarkable effect and mature technology.

AST and ALT activities in liver tissue were 5000 times more than in blood, so massive transaminase entered into blood when the liver membrane permeability increased and as a result transaminase activities in blood were one of the sensitive indexes that reflected the degree of liver injury. As one of the main products of Lipid peroxides, MDA can not only reflect the degree of liver tissue lipid peroxidation, but also indirectly reflect the degree of free radicals attacking cells. SOD had the ability of scavenging $\bullet O_2$ in vivo, so it played an important role in the balance of oxidative and anti-oxidative in vivo. According to these, the activities of AST, ALT in serum and the liver tissue MDA contents, SOD activities were selected as the evaluation indexes.

Saikosaponins had an effective protective on actue liver injury when dosage was 20 g·kg^{-1}. The dosage was 15.5 times more than clinical dosage by calculating crude drug. It was equal to 224 mg·kg^{-1} of total saikosaponins and was equal to 1/21 of LD_{50} [11]. Analysis of liver protective mechanism was as follows：1. Inhibition of lipid peroxidation in vivo, its main process included the inhibition of $\bullet O_2$ generation, activation and enhancement of SOD activities. 2. Had protective effect on membrane so that free radicals can not damage the membrane.

The protective effect of the n-butanol fraction on acute liver injury in miceinduced by CCl4 was confirmed by the pharmacological experiment and the features of the n-butanol fraction were obtained by combiningwith the analysis of characteristic spectrum of the chemical compositions. It can be confirmed that SSa and SSd were the main compositions of total saikosaponins.Whether they were the main effective components with the effects of liver protective should be studied furtherly.

References

[1] Chinese Pharmacopoeia Commission, Pharmacopoeia of People's Republic of China [S].Vol.1.Chemical Industry Press, Beijing, 2005, P198.

[2] Shi Hui,Xie Donghao,Study on protective effect of acute liver injury in mice of water extraction from spring Chaihu and north Chaihu[J],Journal of Nanjing University of Traditional Chinense Medicine, 2009, 25(6), P461-462.

[3] Xie Donghao, Yuan Dongping, Cai Baochang. Comparative study on protective effect of dimethylnit -rosamine(DMN) –induced liver fibrosis in rats of north Chaihu and spring Chaihu[J],Chinense Journal of Hospital Pharmacy, 2008,28 (23) P2006-2009.

[4] Wang Zhanyi, Nan Jixing, Protective effects of Bupleurum Chinense Dc on tacrine induced fulminate hepatic failure[J], Journal of Binzhou Medical University, 2008, 31(2), P91-92.

[5] Li Yuanshi, Yan Guanghai,Li Gao, Analysis of constituents and its protective effects of ethanol extract of the Bupleurum Chinense DC for acute liver injury in mice[J],Journal of Medical Science Yanbian University, 2010, 33(2), P105-107.

[6] Song Jinggui,Xiao Zhengming,Li Shipeng,etc,Effects of the extraction from BCDC on human hepatoma SMMC-7721 cells and mice implanted S-180 tumor[J],Journal of Shan dong University of Traditional Chinese Medicine, 2001,25(4), P299-301.

[7] Yang Yun, Tian Runtao, Wang Zhongdong, etc, Study on the HPLC fingerprints of Bupleurum chinense from Henan[J], Chinese Journal of Modern Applied Pharmacy, 2007, 24(5), P380-383.

[8] Li Xia,Duan Lengxin,Wang Ya-nan,etc,Protective effects of velvet antler peptides on acute hepactic injury by carbon tetrachloride[J], Chinense Pharmaceutical Journal,2007,42 (24), P1864-1866.

[9] Xin nian, Xiong Jianxin, Han Shuying, etc, Protective effect of total flavonoids of buckwheat seed on acute hepatic injury by carbon tetrachloride[J],Acta Academiae Medicinae Militrais Tertiae, 2005, 27(14), P1456-1458.

[10] Wang Qishuai, Yang Yun, Xiao Gongsheng, etc, Fingerprint analysis of Bupleurum chinense by HPLC-ELSD and its chromate data[J],Chinense Traditional Patent Medicine, 2011, 33(3), P373-378.

[11] Jiangsu New Medical College, Dictionary of Chinese Medicine [M], People's publishing house of Shanghai,P1832- 1837.

978-1-61896-030-6 © 2012 SciRes.

Extraction of Essential Oil from Citrus Peel and Analysis of Its Components by GC-MS

Xu RU, Wenjie WU
College of Materials Science & Chemical Engineering, Tianjin University of Science & Technology, Tianjin, China
Email: xuru6666@163.com

Abstract: The essential oils were isolated by steam distillation method from the citrus peel and were identified by gas chromatography-mass spectrometry (GC-MS). More than thirty kinds of compounds were separated. Among their composition, the main components are limonene compounds, which account for 82.08% of essential oils extracted from citrus peel.

Keywords: Citrus peel; essential oil; extraction; gas chromatography-mass spectrometry

1 Introduction

Citrus, a member of the Rutaceac Citrus family, sexual-warm and humid climate, mainly in tropical and subtropical regions of geographical conditions are suitable for growth, includes many species, such as Orange, Pomelo and Sweet shaddock, and widely distributes in the region south of China. Citrus is one of the top producers in the world. Citrus peel, nearly accounting for 30% in total mass of citrus, is rich in essential oil [1].

Essential oil of citrus peel has sweet authentic aromas. The essential oil is mainly composed of tepenes, alcohol, aldehydes and esters. At present there are several methods to extract essential oil from citrus peel, such as distillation, Cold squeeze method, extraction, Supercritical fluid extraction and microwave-aid method [2]. In fact, supercritical carbon dioxide extraction method is higher essential oil quality and yield; however it is seldom used in industry because of its high cost and equipment demand. Distillation is widely used in industry not only easy operation and low cost but also high quality of essential oil. Essential oil of citrus peel can be used in food [3], medicine industry [4] and domestic chemical industry. Effective utilization of citrus castoffs, which are mostly citrus peel, will benefit the full use of the good citrus resources and improve its economic value.

In this research, essential oils of citrus peels were extracted by steam distillation and then analyzed and identified by gas chromatography-mass spectrometry. The research was expected to provide foundation for the extraction and application of essential oil from citrus peel.

2 Materials and Methods

2.1 Plant Material

Citrus purchased farm products market, Tianjin, China. Citrus peel ari-dried for about one week. All the chemicals used in this study were analytically pure.

2.2 Extraction of Essential Oil

About 200 g of Citrus peel was cut into about 1.0 cm lengths at 90 temperatures and then transferred immediately into a standard essential oil extractor to which 400 ml deionized water was added. The essential oil were obtained by steam-distillation. The oil samples from citrus peel were stored in air-tight containers after drying them over anhydrous sodium sulfate for GC-MS analysis.

2.3 GC-MS Analysis

The essential oil from Citrus peel by GC-MS electron impact ionization method on GC-MS Varian4000MS; fused silica capillary column (30 m x 0.25 mm; 0.25 mm film thickness), coated with VF-5; column temperature 60°C (2 min) to 250°C at the rate of 5°C/min; carrier gas, helium at constant pressure of 80 Kpa. Acquisition parameters full scan; scan range 50-500 amu.

2.4 Identification of the Compounds

Compound identification was done by comparing the NIST library data of the peaks. Percentage composition was computed from GC peak areas on VF-5 column.

3 Results and Discussion

According to the above experiment condition, the relative percentage content of various components of essential oils were calculated by gas chromatographic peak area normalization method and the chemical compositions were determined by gas chromatography/mass spectrometry technology. Chromatograms of the essential oils are shown in Figure 1.

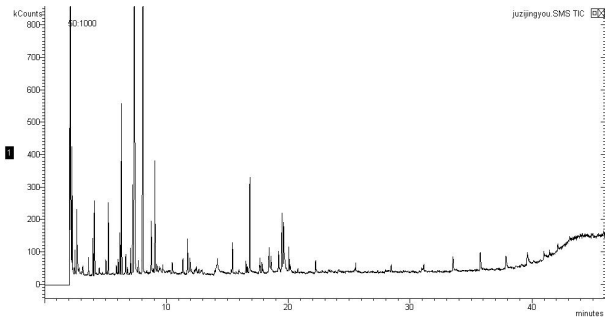

Figure 1. Total chromatograms of the essential oils of citrus peel

Through gas chromatography-mass spectrometry analysis, experiments show that the essential oil from citrus peel are presented with chemical constituents which are shown in table 1. Essential oil contains 38 constituents of which the major is limonene (82.08%). Other notable constituents are 1-methyl-4-(1-methylethyl)-1, 4-Cyclohexadiene (6.877%), β-pinene (1.259%), 3-methylcyclopentene (0.882%). The study reveals that the major constituent is limonene. Limonene is common in cosmetic products, used in food manufacturing and medicines [5, 6], for instance, Limonene has efficacy in preclinical models of breast cancer and may be an efficacious chemotherapeutic agent for human malignancies [7]. A broad overview of the anti-cancer activities only can be found in a review by Rabi and Bishayee [8]. Limonene has been shown to prevent or delay the growth of a number of cancer types including lymphomas [9], mammary [10], gastric, liver, lung, and prostate cancer [11]. Further more this study on essential oils of citrus peels provides scientific basis for further applications.

Table 1. Constituents of essential oils of citrus peel

SN L.o.	*Name of constituents in citrus peel*	*%*
1	3-methylcyclopentene	0.882
2	3-methyl-Hexane	0.816
3	Tetrahydro-2H-pyran-2-ol	0.005
4	Methylcyclohexane	0.149
5	Cycloheptatriene	0.051
6	4-Hydroxy-4-methyl-2-pentanone	0.120
7	2-methyl-5-(1-methylethyl) -bicyclo[3.1.0]hex-2-ene	0.091
8	(+)-α-Pinene	0.471
9	2-p-menthadiene	0.108
10	(1S,5S)-2(10)-Pinene	0.318
11	β-pinene	1.259
12	cis-5-Octen-1-ol	0.190
13	2-methyl-5-(1-methylethyl) -bicyclo[3.1.0]hex-2-ene	0.051
14	(+)-4-Carene	0.225
15	1-methyl-4-(1-methylethyl)- Benzene	0.690
16	limonene	82.08
17	3-Carene	0.119
18	1-methyl-4-(1-methylethyl) -1,4-Cyclohexadiene	6.877

Continued

SN L.o.	*Name of constituents in citrus peel*	*%*
19	1,3,4-trimethyl-3-Cyclohexene -1-carboxaldehyde	0.027
20	3,7,7-trimethyl-bicyclo [4.1.0]hept-2-ene	0.366
21	2-Isopropenyltoluene	0.038
22	3,7-Dimethyl-1,6-octadien-3-ol	0.965
23	3,7-Dimethyl-6-octenal	0.151
24	(+/-)-Terpinen-4-ol	0.159
25	α-Terpineol	0.365
26	4-ethenyl-4-methyl-1-propan-2-yl-3-prop-1-en-2-yl-cyclohexene	0.273
27	(-)-α-Cubebene	0.113
28	(-)-b-Elemene;	0.058
29	α-Bulnesene	0.948
30	(-)-trans-Caryophyllene	0.226
31	Elemene-gamma	0.055
32	Caryophyllene-alpha	0.123
33	(+)-valencene	0.185
34	Farnesene	0.538
35	1,3,6,10-Dodecatetraene,3,7,11 -trimethyl-, (3E,6E)-	0.574
36	1,6-dimethyl-4-propan-2-yl-2,3,4,4a,7 ,8-hexahydronaphthalene	0.235
37	Naphthalene	0.068
38	Cyclohexanemethanol	0.034

References

[1] YeXingQian. Citrus processing and comprehensive utilization of China light industry [M]. Press, 2005, 2-3.

[2] ChenChun jasmine, LaiXingHua, YuanYiHua extracted from orange peel. The technology essential oils [J]. Journal of foshan university, 1997, 15 (2): 68-72.

[3] T.-A. L. Do • J. Vieira • J. M. Hargreaves • B. Wolf • J. R. Mitchell .Impact of Limonene on the Physical Properties of Reduced Fat Chocolate. J Am Oil Chem Soc (2008) 85:911-920.

[4] David M. Vigushin á Grace K. Poon áAlan Boddy Jacqueline English á Gavin W. Halbert á Christos Pagonis á Michael Jarman á R. Charles Coombes Cancer Research Campaign Phase I/II Clinical Trials Committee.Phase I and pharmacokinetic study of D-limonene in patients with advanced cancer. Cancer Chemother Pharmacol (1998) 42:111-117.

[5] HIROTSUNE IGIMI, MD, TAKEHARU HISATSUGU, MD, MASAYA NISHIMURA, MD. The Use of d-Limonene Preparation as a Dissolving Agent of Gallstones. Digestive Diseases, Vol. 21, No.11 (November 1976), 926-939.

[6] MARK I.FRIEDMAN, PHD, GEORGE PRETI, PhD, RHONDA O. DEEMS, PhD, LAWRENCE S. FRIEDMAN, MD, SANTIAGO J. MUNOZ, MD, WILLIS C. MADDREY, MD .Limonene in Expired Lung Air of Patients with Liver Disease. Digestive Diseases and Sciences, Vol. 39, No. 8 (August 1994), 1672-1676.

[7] Pamela L. Crowell • Charles E. Elson • Howard H. Bailey • Abiodun Elegbede • Jill D.Haag • Michael N. Gould. Human metabollm of the experimental cancer therapeutic agent d-limonene. Cancer Chemother Pharmacol (1994) 35: 31-37.

[8] R abi T, Bishayee A (2009) Terpenoids and breast cancer chemoprevention.

[9] Del Toro-Arreola S, Flores-Torales E, Torres-Lozano C, Del Toro-Arreola A, Tostado-Pelayo K, Guadalupe Ramirez-Duenas M, Daneri-Navarro A (2005) Effect of D-limonene on immune response in BALB/c mice with lymphoma. Int Immunopharma-

978-1-61896-030-6 © 2012 SciRes.

col 5: 829-838.
[10] Maltzman TH, Hurt LM, Elson CE, Tanner MA, Gould MN (1989) The prevention of nitrosomethylurea-induced mammary tumors by D-limonene and orange oil. Carcinogenesis 10: 781-783.
[11] Jessica A. Miller • Patricia A. Thompson •Iman A. Hakim• H.-H. Sherry Chow •Cynthia A. Thomson. d-Limonene: a bio-active food component from citrus and evidence for a potential role in breast cancer prevention and treatment. Oncol Rev (2011) 5:31-42.

A New Insight into How Diethyl Maleate Affects the Conformation of BTB Domain of Keap1 via Direct Noncovalent Bonded Interaction

Shuchao CHEN[1], Xiuli LU[1,2], Yong ZHANG[1], Li ZHANG[1], Hongsheng LIU[1,2], Bing GAO[3]

[1]*The School of Life Science, Liaoning University, Shenyang, China*

[2]*Research Center for Computer Simulating and Information Processing of Bio-macromolecules of Liaoning, Shenyang, China, 110036*

[3]*The Institute of Basic Medical Sciences, Shenyang Medical College, Shenyang, China*

Email: gaobingdr@gmail.com

Abstract: Keap1 negatively regulates the function of Nrf2 that is a major activator of genes encoding phase 2 detoxifying enzymes via sequestering cytoplasmic Nrf2 and subsequent degradation through the proteasome system. Reactive cysteine residues of Keap1 could be modified by Michael reaction acceptor molecules. Previous studies have shown that adduction at Cys151 by diethyl maleate (DEM) can give rise to a significant conformational change in Keap1 that leads to the dissociation of Keap1 from CUL3, hence inhibits Nrf2 ubiquitylation. The BTB domain of Keap1 plays a crucial role in both forming self-dimerization and binding to CUL3. In order to better understanding the molecular mechanism how DEM interact with amino acid residues around Cys151, we performed two molecular dynamics (MD) simulations including Keap1-DEM complex and Keap1 alone (control group). Interestingly, we found that after a short period of lingering around Cys151, DEM ultimately stabilized in a gap between two specific helixes away from the cavity around Cys151 and induced a concomitant significant conformational change of BTB domain of Keap1. Similar phenomenon, however, was not observed in the control group. These results suggested that DEM could impair the normal function of Keap1 by inducing the conformational change of BTB domain via direct noncovalent bonded interaction. Our research provides a new insight into another way of interaction between Keap1 and DEM in spite of their known Michael addition reaction, by which novel phase2 enzyme inducer drugs with higher specificity could be discovered in the future.

Keywords: DEM; Keap1; BTB domain; molecular dynamics simulation; phase 2 enzymes

1 Introduction

Nrf2-dependent gene expression has been deemed to be involved in many major illnesses, such as cancer, inflammation, neurodegenerative diseases. Keap1 inhibits nuclear activation of antioxidant responsive elements by association with Nrf2 through binding to the N-terminal Neh2 domain, thereby down regulating the expression of phase 2 detoxifying and oxidative stress enzyme genes via a mechanism named Nrf2 nuclear shuttling [1]. Keap1 and Nrf2 form an important cellular sensor for oxidative stress. Upon exposure to electrophilic and oxidative stresses, the conformation of Keap1 can be altered, which undermines the inhibitive effect from Keap1, more Nrf2 can traverse from the cytoplasm to the nucleus and then activate the expression of phase 2 genes. Subsequent studies found that Keap1 functions as an adaptor for Cul3-based E3 ligase to engage in the process of proteasomal degradation of Nrf2 [2]. Moreover, the ability of Keap1 to assemble into a functional E3 ubiquitin ligase complex with Cul3 and Rbx1 also plays a critical role in controlling relative stable level of Nrf2 in cytoplasm [3]. It was reported that Keap1 negatively regulates Nrf2 function by targeting Nrf2 for ubiquitination through the CUL3-ROC1 ligase [4]. Further studies found that the actin cytoskeleton provides scaffolding that is indispensable for the anchoring of Keap1 to function appropriately [5]. In view of the attractive prospect of screening the lead drug candidates based on Keap1-Nrf2 regulatory pathway, two distinct cysteine motifs which could be modified to produce aberrant conformations by inducers have been identified by now, one is located at Cys151 in the BTB domain, the other is located in the intervening domain and centers around Cys 273 and 288 [6-7]. Some inducers disrupt Keap1-Nrf2 complex by modifying two (Cys273 and Cys288) through the formation of intermolecular disulfide bridges [8]. Many Michael reaction acceptor molecules like DEM can have addition reactions with sulfhydryl group of Cys151 of Keap1 [9]. Modification at Cys151 causes the dramatic conformational change of BTB domain that has a notable impact on the normal function of Keap1 such as self-dimerization, assembling into Nrf2-Keap1-Cul3 complex Self-dimerization of Keap1 via its BTB domain is required to sequester Nrf2 in cytoplasm [10]. It is clear that is very important to further explore the detailed mechanism of interaction between BTB domain of Keap1 and Michael reaction acceptor molecule.

978-1-61896-030-6

Molecular dynamics (MD) simulations have been broadly applied to the exploration of detailed molecular mechanism of how biomolecules interact with each other at the atomic level. Our previous preliminary research has shown that the cavity around Cys151 constitutes a special physical-chemical condition that has a crucial facilitation effect on final Michael addition reaction [11]. Docking results provide some simulative evidence for our original hypothesis, which assumes that noncovalent bonded interaction between protein and small molecule has a remarkable impact on bonded interaction. We performed two molecular dynamics (MD) simulations including the Keap1-DEM complex and Keap1 alone (control group) to further study the detailed molecular mechanism of the interaction between Keap1 and DEM. To our surprise, DEM did not stabilize in the cavity around Cys151, we have mentioned above. During most of the time of dynamics simulations (total time is 10 ns), it was found that DEM preferred to stay in a gap between two specific helixes away from the cavity around Cys151. Allowing for the limitations of MD in simulating bonded interaction, we could draw a preliminary conclusion that DEM may lead to the conformational change of Keap1 merely by direct noncovalent bonded interaction with the BTB domain (a.a. 61-179) of Keap1, where the Cys151 just right presents. In addition to the reported oxidative modification of DEM by Michael reaction at Cys151 of Keap1, DEM may induce the conformational change of Keap1 through two kinds of totally different mechanisms. In conclusion, our present simulation result provides a new insight into how DEM affect the conformation of BTB domain of Keap1 via direct noncovalent bonded interaction. This result leads us to speculate that this may provide a totally new perspective strategy to design drug molecules targeting to Keap1-Nrf2 pathway.

2 Experimental Section

In our previous study, we performed molecular docking between Keap1 and DEM by use of Autodock4.2 docking procedure [11]. The model of Keap1-DEM complex was chosen from a cluster of stable docking conformations. MGLTools-1.5.4 was employed as a software for visualization and saving complex [12]. Please note that the complex for dynamics simulation consists of DEM and BTB domain of keap1 rather its whole structure. The model was taken into the subsequent MD simulation for initial structure.

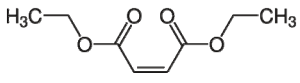

Figure 1. The molecular structure of DEM

All MD simulations were performed with the NAMD 2.6 [13] in a 15 nodes HPC cluster, and the AMBER all-atom force field was used. During the simulations, all bond lengths containing hydrogen atoms were constrained using the SHAKE algorithm, and the integration time step was set to 2 fs. First, the two systems (Keap1-DEM complex and control group) were respectively minimized by 20,000 steps with solutes constrained. The minimized systems then were slowly heated from 0 up to 310 K within 620ps leaving all C_α atoms and the Na^{2+} ions unconstrained. Finally, the non-constrained simulations were performed for 9.32 ns at a constant temperature of 310 K and a constant pressure of 1 atm through the Langevin piston method. Analyses of the simulation results were operated by VMD 1.9 [14].

3 Results and Discussion

Docking results suggest that DEM generates only a bunch of relative stable conformations (data not shown) according to the value of RMSD with relation to conformational change of small ligand (DEM), MD simulations were applied to systematically study the detailed molecular mechanism of the interaction between the cavity around Cys151 of Keap1 and DEM, nevertheless, this method has been mainly exploited in researching noncovalent bonded interaction among biomolecules. Our previous results suggested that such noncovalent bonded interaction between protein and small ligand plays a critical role in helping to form related bonded interaction [11]. The present study was aimed to further investigate whether such noncovalent bonded interaction between DEM and keap1 play some of important role in facilitating the induction of phase 2 enzyme through change of conformation of keap1 structure.

The root means square deviation (RMSD) for C_α atoms of Keap1 in these two groups (Keap1-DEM complex and Keap 1 alone) are shown in Figure 2 and Figure 3.

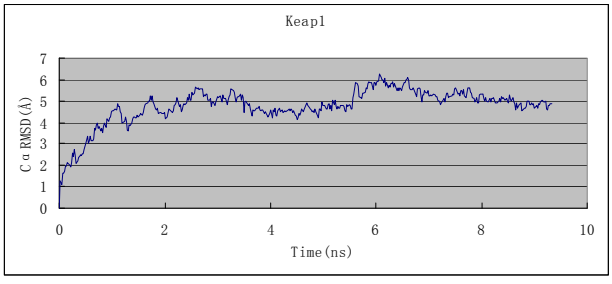

Figure 2. C_α RMSD of Keap1 from complex

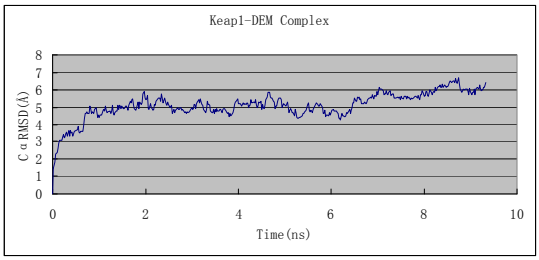

Figure 3. C_α RMSD of Keap1 from control group

As shown in Figure 2, the RMSD curve became relative flat after about 2 ns, indicating the conformations of the protein achieve equilibrium. When the simulative time is more than 7 ns, however, the curve revealed rising trend if compared to the equilibrium condition that lasted for 5 ns. From the Figure 3, it is apparent that the backbone of Keap1 arrives at equilibrium since 3 ns, and the curve goes up between 6ns and 7ns, and then became flat and stable. The relative values of RMSD of the BTB domains of keap1 were bigger which could be explained by that the 3-dimensional structure of Keap1 model we have built revealed dumbbell-like structure, which is more flexible than globular proteins. Considering the specific characteristic of Keap1, in a larger but confidential scale, we can conclude these two simulative systems have reached equilibrium in the end.

We have made animations that vividly display the change of the secondary structure of Keap1 during the whole simulation. We found that the secondary structure of BTB domain of Keap1 with DEM has been changed dramatically. It was found that DEM stayed in a gap between two specific helixes, which is away from the cavity around Cys151, while the BTB domain of Keap1 underwent significant change of the secondary structure. In contrast, the control group revealed relative stable consistency on the structures of keap1before and after simulation. We further examined the specific change of BTB domain through aligning one stable structure that is randomly sampled from stable period of RMSD of the backbone of Keap1 to the initial structure by use of Pymol [15]. We got two pictures respectively as displayed below in Figure 4 and Figure 5.

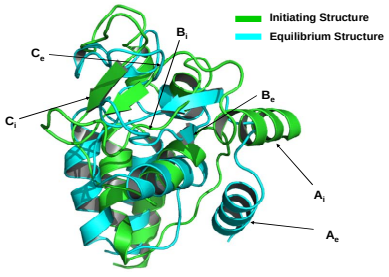

Figure 4. Superimposition of secondary structures of BTB domain of Keap1 from complex

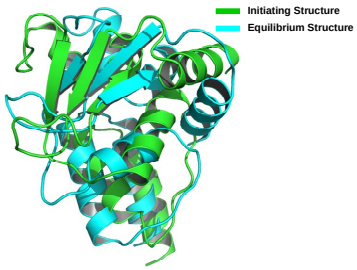

Figure 5. Superimposition of secondary structures of BTB domain of Keap1 from control group

As shown in Figure 4, the areas (including two pleated sheets and one helix) represented by A, B, C revealed these significant changes of secondary structures of Keap1 before and after simulation. The angle of Helix A and whole structure under the initiating and equilibrium condition was dramatically changed (from Ai to Ae). The short polypeptides Bi became a new sheet Be in the equilibrium condition. The sheet structure of Ci under the initiating condition disappeared under the equilibrium condition. Instead, the polypeptide of Ci sheet changed to random coils in the equilibrium structure. Based on these findings, we speculate that DEM can markedly affect the secondary structures of BTB domain of Keap1 which is crucial for both its formation of homodimerization and effectively binding to Cul3. This result suggested that DEM could disrupt the self-dimerization of Keap1 via direct noncovalent bonded interaction within BTB domain in spite of its inherent feature of addition to sulfhydryl group of Cys151 of Keap1. We also have examined the continuous changes of secondary structures of BTB of Keap1 during the whole simulation (shown in Figure 6 and Figure 7) to further attest our presumption.

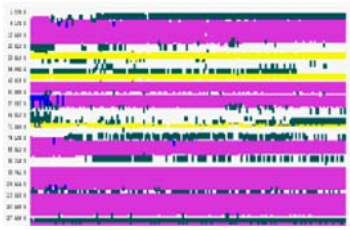

Figure 6. Continuous changes of secondary structures of BTB domain of Keap1 from complex

Different color in Figure 6 or Figure 7 represents different secondary structure type (green stands for Turn, yellow for Extended conformation, pink for Alpha helix, blue for 3-10 helix, white for Coil, brown for Isolated bridge and red for Pi-helix). The abscissa denotes amino acid residues, the ordinate denotes simulation time. These two Figures illustrate the continuous changes of secondary structures correspond to certain interval of amino acid residues of BTB. It is clear that the secondary structures of BTB of Keap1 from complex have under-

978-1-61896-030-6 © 2012 SciRes.

gone observable changes compared to the control group, among which the secondary structures correspond to the interval from Hip43 to Ser71 change most drastically.

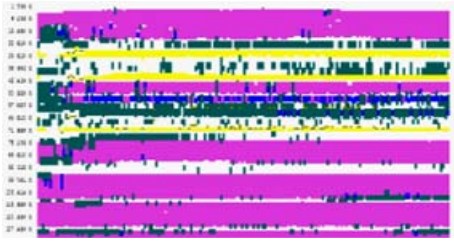

Figure 7. Continuous changes of secondary structures of BTB domain of Keap1 from control group

In addition to the analysis of changes of secondary structures of BTB of Keap1, we have also performed an analysis of interaction between BTB domain of Keap1 and DEM to explore which amino acid residues exactly facilitate the stabilization of DEM around BTB domain of Keap1. We analyzed the forming of hydrogen bond between DEM and residues of BTB domain. We randomly have chosen the model of Keap1-DEM complex from final simulation results, which are under the relative equilibrium station.

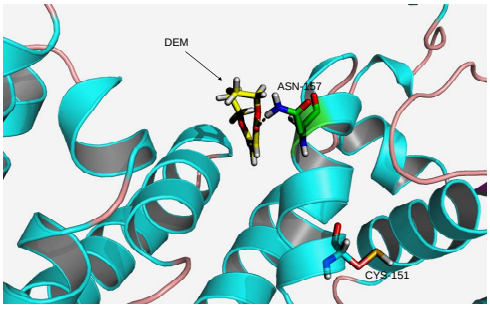

Figure 8. Analysis of hydrogen bonding between BTB domain of Keap1 and DEM

As shown in Figure 8, DEM ultimately stabilized in a gap between two specific helixes around BTB domain of Keap1, which is away from initial position (the cavity around Cys151). The hydrogen bond formed by the hydrogen of 4-amino group of Asn167 and the oxygen of carbonyl group of DEM is shown in Figure 8. This hydrogen bond seems to play an important role in facilitating DEM to interact with BTB domain of Keap1.

4 Conclusion

The Keap1-Nrf2 regulatory pathway plays a central role in the protection of cells against oxidative and xenobiotic damage. Multi-steps involved in assembling Keap1 into complex for the ubiquitination of Nrf2 all could be disrupted to allow more newly-synthesized Nrf2 to activate the expression of phase 2 genes. Researches in preceding years reveal that there are a large amount of Michael reaction acceptor molecules like DEM could have a similar addition reaction with sulfhydryl group of Cys151 of Keap1, thereby cause a significant conformational change of Keap1 which results in the disruption of assembling of Nef2-Keap1-Cul3 complex. This is anindispensable step for the ubiquitination of Nrf2.The significance of the position of Cys151 could be explained by its partial molar volume in determining the folding of 3-dimensional structure of Keap1 [16]. In this study, MD simulations were performed to systematically explore the detailed mechanism of interaction between DEM and BTB domain of Keap1. Simulation results suggested that DEM could disrupt the ubiquitination of Nrf2 by direct binding to BTB domain with non-covalent bonds that is a totally different mechanism, despite of the fact that DEM can have an addition reaction with Cys151 of Keap1. Our research provides a new insight into how DEM could affect the conformation of BTB domain of Keap1 through noncovalent bonded interaction.

References

[1] K. Itoh, N. Wakabayashi, et al. “Keap1 represses nuclear activation of antioxidant responsive elements by Nrf2 through binding to the amino-terminal Neh2 domain.” *Genes&Development*. vol. 13, 1999, pp. 76-86.

[2] Kobayashi, A., M. I. Kang, et al. “Oxidative Stress Sensor Keap1 Functions as an Adaptor for Cul3-Based E3 Ligase To Regulate Proteasomal Degradation of Nrf2.” *Molecular and Cellular Biology*. vol. 24, 2004, pp. 7130-7139.

[3] Zhang, D. D., S. C. Lo, et al. “Keap1 Is a Redox-Regulated Substrate Adaptor Protein for a Cul3-Dependent Ubiquitin Ligase Complex.” *Molecular and Cellular Biology*. vol. 24, 2004, pp. 10941-10953.

[4] Furukawa, M. and Y. Xiong. “BTB Protein Keap1 Targets Antioxidant Transcription Factor Nrf2 for Ubiquitination by the Cullin 3-Roc1 Ligase.” *Molecular and Cellular Biology*. vol. 25, 2004, pp. 162-171.

[5] Kang, M. I. “Scaffolding of Keap1 to the actin cytoskeleton controls the function of Nrf2 as key regulator of cytoprotective phase 2 genes.” *Proceedings of the National Academy of Sciences*. vol. 101, 2004, pp. 2046-2051.

[6] Sekhar, K. R., G. Rachakonda, et al. “Cysteine-based regulation of the CUL3 adaptor protein Keap1.” *Toxicol Appl Pharmacol*. vol. 244, 2010, pp. 21-26.

[7] Yamamoto, T., T. Suzuki, et al. “Physiological significance of reactive cysteine residues of Keap1 in determining Nrf2 activity.” *Mol Cell Biol*. vol. 28, 2008, pp. 2758-2770.

[8] Wakabayashi, N. “Protection against electrophile and oxidant stress by induction of the phase 2 response: Fate of cysteines of the Keap1 sensor modified by inducers.” *Proceedings of the National Academy of Sciences*. vol. 101, 2004, pp. 2040-2045.

[9] Kobayashi, M., L. Li, et al. “The Antioxidant Defense System Keap1-Nrf2 Comprises a Multiple Sensing Mechanism for Responding to a Wide Range of Chemical Compounds.” *Molecular and Cellular Biology*. vol. 29, 2008, pp. 493-502.

[10] Laurie M. Zipper and R. Timothy Mulcahy. “The Keap1 BTB/POZ dimerization function is required to sequester Nrf2 in cytoplasm.” *The Journal of Biological Chemistry*. vol. 277, 2002, pp. 36544-36552.

[11] Lu X., Chen S., Zhang Y., et al. “Study of expanded application of molecular docking on virtual screening”. *2011 international conference on remote sensing, environment and transportation*

engineering (RSETE 2011). Vol. 9, pp.7863-7866.

[12] Michel, F. S. P.. "Python: a programming language for software integration and development." *J Mol Graph Model*. vol. 17, 1999, pp. 57-61.

[13] James, C. P., Rosemary, B., et al. "Scalable molecular dynamics with NAMD." *Journal of Computational Chemistry*. vol. 26, 2005, pp. 1781-1802.

[14] W. Humphrey, A. Dalke, and K. Schulten. "VMD: visual molecular dynamics." *Journal of molecular graphics*. vol. 14, 1996, pp. 33-38.

[15] DeLano, W. L. The PyMOL Molecular Graphics System (2002) DeLano Scientific, San Carlos, CA, USA. http://www.pymol.org.

[16] Eggler, A. L., E. Small, et al. "Cul3-mediated Nrf2 ubiquitination and antioxidant response element (ARE) activation are dependent on the partial molar volume at position 151 of Keap1." *Biochem J*. vol. 422, 2009, pp. 171-180.

978-1-61896-030-6 © 2012 SciRes.

Studies on the Chemical Constituents from *Anemone rivularis* var. *flore-minore*

Yu DING[1,2], Haifeng TANG[1], Dan LIU[3], Guang CHENG[4], Xiaoyang WANG[1], Xiangrong TIAN[1], Minna YAO[1], Ning MA[1]

[1]*Department of Pharmacy, Xijing Hospital, Fourth Military Medical University, Xi'an, China*
[2]*Department of Pharmacy, Dalian Sanatorium of Shenyang Military Region, Dalian, China, 116013*
[3]*Department of Pharmacy, 210th Hospital of People's Liberation Army, Dalian, China, 116012*
[4]*Department of Neurosurgery, Xijing Hospital, Fourth Military Medical University, Xi'an, China*
Email: tanghaifeng71@163.com

Abstract: Fifteen compounds (**1**−**15**), including one labdane type diterpenoid glycoside (**13**), one tetrahydrofuran type lignan glycoside (**14**), one triterpene sapogenin (**15**) and twelve triterpenoid saponins (**1**−**12**) were obtained and elucidated from *Anemone rivularis* var. *flore-minore* for the first time, among which four were found in genus *Anemone* for the first time (**10**, **11**, **13** and **14**) and three are new compounds (**10**, **13** and **14**). Saponins **5** and **12** showed *in vitro* cytotoxicity against human BEL-7402 and HeLa tumor cells. Diterpenoid glycoside and lignan glycoside were found in genus *Anemone* for the first time. All these support that the title plant is a variation from *A*. *rivularis*. *A*. *rivularis* var. *flore-minore* was first proved to belong to genus *Anemone* from the chemical taxonomic point of view. Our studies established a homebase for further development of the title medicinal plant with abundant resources in China.

Keywords: *Anemone rivularis* var. *flore-minore*; triterpenoid saponin; diterpenoid glycoside; lignan glycoside; cytotoxicity

1 Introduction

Anemone rivularis var. *flore-minore* (Ranunculaceae), a perennial herbaceous plant, distributes mainly in the north and west of China, especially in the north and south slopes of Tsinling Mountains. The entire plants and rhizome were used as folk medicines. It has been reported to treat hepatitis, muscle and joint pain, stranguria, emission, edema, and so on [1].

The genus *Anemone* has been proved to be an especially valuable source of diverse saponin substances with potentially useful biological properties. However, no investigation has been reported on chemical constituents of this species of *Anemone*. As part of our ongoing investigation on new antitumor glycosides from natural source, the chemical studies on this plant led to the isolation of fifteen compounds from the *n*-BuOH extracts, including three new compounds (one gypsogenin saponin **10**, one diterpene glycoside **13** and one lignanoid glycoside **14**, see Fig. 1), one known triterpene sapogenin (**15**) and eleven known triterpenoid saponins (**1**−**9** and **11**, **12**, see Fig. 2). All these compounds were first isolated from the plant, and four of them (**10**, **11**, **13** and **14**) were found in genus *Anemone* for the first time. We described herein the isolation and structural elucidation of these compounds, as well as their cytotoxicity against human BEL-7402 and HeLa tumor cells.

2 Experimental

2.1 Materials and Instruments

The plant material was collected from the north of Tsinling Mountains in Shaanxi Province of China, in September 2009, and identified by Professor Ji-Tao Wang from Shaanxi University of Chinese Medicine. A voucher specimen was deposited in the Herbarium of Shaanxi University of Chinese Medicine. Instruments and reagents were omitted.

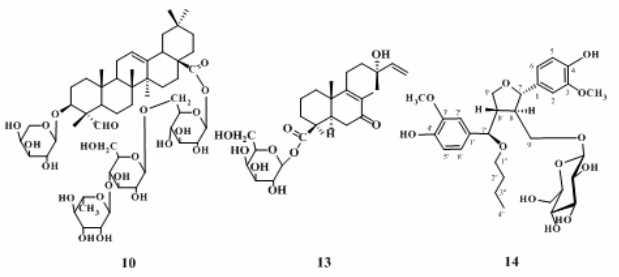

Figure 1. Structures of new compounds 10, 13 and 14 isolated from *Anemone rivularis* var. *flore-minore*

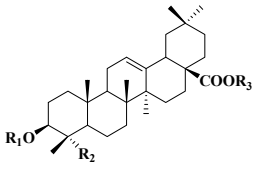

	R_1	R_2	R_3
1	Ara	CH_3	Rha-(1→4)-Glc-(1→6)-Glc
2	Ara	CH_2OH	Rha-(1→4)-Glc-(1→6)-Glc
3	Glc-(1→2)-Ara	CH_2OH	Rha-(1→4)-Glc-(1→6)-Glc
4	Rib-(1→3)-Rha-(1→2)-Ara	CH_2OH	Rha-(1→4)-Glc-(1→6)-Glc
5	Ara	CH_2OH	H
6	H	CH_2OH	Rha-(1→4)-Glc-(1→6)-Glc
7	Ara	CH_2OH	Glc
8	Glc-(1→2)-Ara	CH_3	Rha-(1→4)-Glc-(1→6)-Glc
9	Ara	CH_2OH	Glc-(1→6)-Glc
11	H	CH_2OH	Glc
12	Glc-(1→2)-Ara	CH_3	H
15	H	CH_2OH	H

Figure 2. Structures of known compounds 1−9, 11, 12 and 15 isolated from *Anemone rivularis* var. *flore-minore*

2.2 Extraction and Isolation

The air-dried whole plants of *A. rivularis* var. *flore-minore* (7.7 kg) were crushed and refluxed with 70% EtOH(3×6 L). The extracts were condensed in a rotary evaporator to obtain a syrupy residue (1.8 kg). The residue was suspended in H_2O and extracted successively with petroleum ether and *n*-BuOH. The *n*-BuOH extracts (150 g) was subjected to column chromatography (silica gel, ODS, Sephadex LH-20 and HPLC) to yield fifteen compounds **1**−**15**.

2.3 Structure Identification

Compound **14** was obtained as a yellow amorphous powder; $[\alpha]_D^{22}$-17.2 (*c* 0.12, MeOH). CD (*c* = 72 μmol/L, MeOH): +16.7 (206), +4.6 (237). ESI-MS (positive ion mode) *m/z*: 617 $[M+Na]^+$; ESI-MS (negative ion mode) *m/z*: 593 $[M-H]^-$; HR-ESI-MS (positive ion mode) *m/z*: 617.2570 $[M+Na]^+$ (calcd. for $C_{30}H_{42}NaO_{12}$: 617.2574). ^{1}H-NMR and ^{13}C-NMR data were shown in Table I.

Glycoside **14** (1 mg) was heated in 2 mol/L aq. CF_3COOH (1 mL) at 120 °C for 2 h. The mixture was evaporated to dryness, and the residue was partitioned between CH_2Cl_2 and H_2O. The aq. phase was concentrated to furnish a monosaccharide mixture. Pyridine (1 mL) and NH_2OH•HCl (2 mg) were added to the dried residue, and the mixture was heated at 90 °C for 1 h. The solution was concentrated, and the resulting aldononitrile peracetate was analyzed by GC-MS using authentic reference samples for identification. The derivative of D-glucose (Glc) was detected, with retention time (t_R) of 8.01 [2].

Spectral data and chemical reactions of other compounds were omitted.

Table 1. ^{1}H-(500 MHz) and ^{13}C-NMR (125 MHz) data of glycoside 14 in C_5D_5N (δ in ppm, *J* in Hz)

Position	δ_C mult.	δ_H
1	134.3 s	-
2	111.0 d	7.40 d (1.7)
3	148.7 s	-
4	147.6 s	-
5	116.3 d	7.22 m
6	119.8 d	7.30 dd (8.1, 1.7)
7	83.5 d	5.18 d (7.9)
8	51.7 d	2.34 m
9	68.8 t	3.36 dd (9.9, 4.9), 4.07 dd (9.7, 3.2)
1'	132.6 s	-
2'	111.2 d	7.24 m
3'	149.0 s	-
4'	147.9 s	-
5'	116.1 d	7.19 m
6'	121.3 d	7.02 dd (8.0, 1.7)
7'	84.6 d	4.41 d (8.9)
8'	48.7 d	3.21 m
9'	71.3 t	4.19 m, 4.56 dd (8.7, 4.8)
1"	68.2 t	3.26 m, 3.43 m
2"	32.3 t	1.50 m
3"	19.7 t	1.31 m
4"	14.0 q	0.79 t (7.4)
C-3-OMe	55.9 q	3.75 s
C-3'-OMe	55.9 q	3.83 s
Glc		
1	105.4 d	4.65 d (7.8)
2	75.3 d	4.03 m
3	78.6 d	4.17 m
4	71.5 d	4.22 m
5	78.4 d	3.81 m
6	62.6 t	4.33 dd (11.7, 4.9), 4.44 m

2.4 Antitumor Bioassay

The cytotoxicity of ten compounds which have relative more yields against human BEL-7402 and HeLa tumor cells was evaluated by MTT colorimetric assay described in previous papers, with doxorubicin (Sigma, ≥98%, USA) as positive controls. Dose response curves were plotted for the samples and the IC_{50} values were calculated as the concentrations of the test compounds resulting in 50% reduction of absorption compared to the control cells.

3 Results and Discussion

The structures of known compounds **1**−**9**, **11**, **12** and **15** were identified as 3-*O*-*α*-L-arabinopyranosyl-oleanolic acid-28-*O*-*α*-L-rhamnopyranosyl-(1→4)-*β*-D-glucopyranosyl-(1→6)-*β*-D-glucopyranosyl ester (**1**), 3-*O*-*α*-L-arabinopyranosyl-hederagenin-28-*O*-*α*-L-rhamnopyranosyl-(1→4)-*β*-D-glucopyranosyl-(1→6)-*β*-D-glucopyranosyl ester (**2**), 3-*O*-*β*-D-gluco-pyranosyl-(1→2)-*α*-L-arabinopyranosyl-hederagenin-28-*O*-*α*-L-rhamnopyranosyl-(1→4)-*β*-D-glucopyranosyl-(1→6)-*β*-D-glucopyranosyl ester (**3**), 3-*O*-*β*-D-ribopyranosyl-(1→3)-*α*-L-rhamnopyranosyl-(1→2)-*α*-L-arabinopyranosyl-hedera-

978-1-61896-030-6 © 2012 SciRes.

genin-28-*O*-*α*-L-rhamnopyranosyl-(1→4)-*β*-D-glucopyranosyl-(1→6)-*β*-D-glucopyranosyl ester (**4**), 3-*O*-*α*-L-arabinopyranosyl-hederagenin (**5**), hederagenin-28-*O*-*α*-L-rhamnopyranosyl-(1→4)-*β*-D-glucopyranosyl-(1→6)-*β*-D-glucopyranosyl ester (**6**), 3-*O*-*α*-L-arabinopyranosyl-hederagenin-28-*O*-*β*-D-glucopyranosyl ester (**7**), 3-*O*-*β*-D-glucopyranosyl-(1→2)-*α*-L-arabinopyranosyl-oleanolic acid-28-*O*-*α*-L-rhamnopyranosyl-(1→4)-*β*-D-glucopyranosyl-(1→6)-*β*-D-glucopyranosyl ester (**8**), 3-*O*-*α*-L-arabinopyranosyl-hederagenin-28-*O*-*β*-D-glucopyranosyl-(1→6)-*β*-D-glucopyranosyl ester (**9**), hederagenin-28-*O*-*β*-D-glucopyranosyl ester (**11**), 3-*O*-*β*-D-glucopyranosyl-(1→2)-*α*-L-arabinopyranosyl-oleanolic acid (**12**) and hederagenin (**15**), respectively, by comparison of their spectroscopic data and chemical evidences with published values.

Compound **14** was obtained as a yellow amorphous powder. The molecular formula of **14** ($C_{30}H_{42}O_{12}$) was deduced from HR-ESI-MS [*m/z* 617.2570 ([M+Na]$^+$)].

In the ^{1}H-NMR spectrum (500 MHz, C_5D_5N), one CH_3 proton signal at δ 0.79 (t, J =7.4 Hz, H-4''), two CH_2 proton signals at δ 1.50 (m, H-2'') and 1.31 (m, H-3''), three O-bearing CH_2 proton signals at δ 3.26 (1H, m, H-1'') and 3.43 (1H, m, H-1''), 3.36 (1H, dd, J =9.9, 4.9 Hz, H-9) and 4.07 (1H, dd, J=9.7, 3.2 Hz, H-9), 4.19 (1H, m, H-9') and 4.56 (1H, dd, J=8.7, 4.8 Hz, H-9'), two O-bearing CH proton signals at δ 5.18 (d, J=7.9 Hz, H-7) and 4.42 (m, H-7'), two MeO- proton signals at δ 3.75 and 3.83, two sets of 1,3,4-trisubstituted benzene ring signals at δ 7.40 (1H, d, J =1.7 Hz, H-2), 7.22 (1H, m, H-5), 7.30 (1H, dd, J=8.1, 1.7 Hz, H-6) and δ_H 7.22 (1H, m, H-2'), 7.19 (1H, m, H-5'), 7.02 (1H, dd, J=8.0, 1.8 Hz, H-6'), and an anomeric H-atom signal at δ 4.65 (d, J =7.8 Hz, Glc-H-1) were observed. In the ^{13}C-NMR spectrum (125 MHz, C_5D_5N), thirty carbon signals can be observed. Except six carbon signals belonging to a hexose, the other 24 carbons were ascribed to the aglycone part, which can be assigned as a CH_3 carbon at δ 14.0 (C-4''), two CH_2 carbon at δ 32.3 (C-2'') and 19.7 (C-3''), three O-bearing CH_2 carbon at δ 68.2 (C-1''), 68.8 (C-9) and 71.3 (C-9'), two O-bearing CH carbon at δ 83.5 (C-7) and 84.6 (C-7'), two MeO- carbon at δ 55.9 (2C, C-3-OMe and C-3'-OMe), two sets of 1,3,4-trisubstituted benzene ring carbons at δ 134.3 (C-1), 148.7 (C-3), 147.6 (C-4) and 132.6 (C-1'), 149.0 (C-3'), 147.9 (C-4'), and the other six carbons belonging to the two benzene rings at δ 111.0 (C-2), 116.3 (C-5), 119.8 (C-6), 111.2 (C-2'), 116.1 (C-5') and 121.3 (C-6').

The ^{1}H-^{1}H COSY experiment of **14** in combination with HMBC spectrum revealed the partial structures as shown by the bold lines in Fig. 3.

The sugar moiety of **14** was determined to be D-glucose by acidic hydrolysis with aqueous 2 mol/L trifluoroacetic acid and preparation of the corresponding aldononitrile peracetate which was analyzed by GC-MS. The *β*-configuration was suggested by the ^{13}C-NMR chemical shift of the anomeric carbon at δ 105.4 and the coupling constant of the anomeric proton at δ 4.65 (d, J = 7.8 Hz). The carbon and proton signals of the sugar were identified by analysis of the HSQC, TOCSY, ^{1}H-^{1}H COSY, NOESY and HMBC spectra of **14** (Table I). The linkage of the glucose unit was deduced from an HMBC experiment: a correlation peak was observed between H-1 (δ 4.65) of glucose and C-9 (δ 68.8) of the aglycone (Fig. 3).

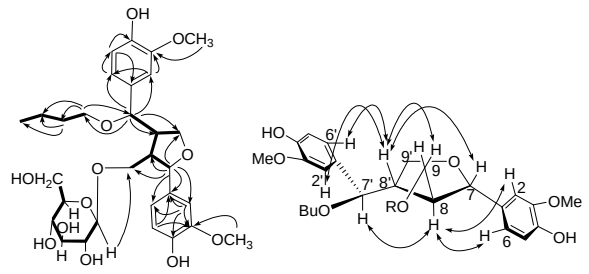

Figure 3. Key ^{1}H-^{1}H COSY, HMBC and NOESY correlations of glycoside 14

Except the 7′-butoxy group in **14** was replaced by a hydroxyl group, the above informations were similar to those of compound **14a** [**14a** = (7*S*,8*R*,7'*R*,8'*S*)-4,9,4'7'-tetrahydroxy--3,3'-dimethoxy-7,9'-epoxylignan 9-*O*-*β*-D-glucopyranoside] as reported in literature [3]. The linkage of the butoxy group to C-7′ was evident from the HMBC correlation from the H-1″ proton signal at δ 3.26 to the carbon signal at δ 84.6 (C-7′).

Hence, the planar structure of **14** was elucidated as 4,9,4'-trihydroxy-3,3'-dimethoxy-7'-butoxy-7,9'-epoxylignan 9-O-*β*-D-glucopyranoside.

There are four chiral carbon atoms (C-7, C-8, C-8′ and C-7′) in **14**. The anterior three carbon atoms were in the tetrahydrofuran ring, and their absolute configurations could be suggested by CD spectra data in comparison with those of **14a** with the similar structure. The CD spectrum of **14** showed two positive *Cotton* effects [$\Delta\varepsilon$ +16.7 (206 nm), +4.6 (237 nm)] similar to those of **14a** [$\Delta\varepsilon$ +15.2 (206 nm), +3.5 (235 nm)], indicating that the C-7, C-8, C-8' in **14** possess *S*, *R*, and *S* configurations, respectively. It has been reported that H_2-9' signal in the ^{1}H-NMR spectrum was upfield by the anisotropic effect between the aromatic group at C-7' and H_2-9' in **14a**. However, the H_2-9 and H-8 signals were upfield by the anisotropic effect between the aromatic group at C-7' and H_2-9 and H-8 in the 7'*S*-isomer of **14a** [3]. The ^{1}H-NMR chemical shifts of H-8, H_2-9 and H_2-9' in **14** were similar to those of **14a**, indicating that **14** has the same configu-

ration to **14a** (7'*R*). In addition, the coupling constant of H-7' (8.9 Hz) in **14** revealed an antiperiplanar orientation of H-7' and H-8'. In the NOESY spectrum (Fig. 3), H-8 showed NOE correlations with H-2, H-6 and H-7', whereas H-8' showed NOE correlations with H-7, H-9, H-2' and H-6'. However, no NOE correlations between H-8 and H-2', H-6' were observed. These evidences further verified the 7'*R* configuration of **14**.

Consequently, the structure of **14** was determined to be (7*S*,8*R*,7'*R*,8'*S*)-4,9,4'-trihydroxy-3,3'-dimethoxy-7'-butoxy-7, 9'-epoxylignan 9-*O*-*β*-D-glucopyranoside.

The structures of the new compounds **10** and **13** were identified, by extensive spectral analysis and chemical evidences according to a similar way, as 3-*O*-*α*-L-arabinopyranosyl-gypsogenin-28-*O*-*α*-L-rhamnopyranosyl-(1→4)-*β*-D-glucopyranosyl-(1→6)-*β*-D-glucopyranosyl ester and 13(*S*)-hydroxy-7-oxo-labda-8,14-diene-19-oic acid-*β*-D-galactosyl ester, respectively. Diterpene glycoside and lignanoid glycoside were obtained from genus *Anemone* for the first time. The aglycone of compound **10**, gypsogenin, was rare in nature, and was first found from genus *Anemone*, too.

The cytotoxicity of ten saponins which have relative more yields against human BEL-7402 and HeLa tumor cells was evaluated by MTT colorimetric assay and the results were shown in Table II. The data showed that saponins **5** and **12** exhibited cytotoxic activity against the two tumor cells *in vitro*. The preliminary structure-activity relationship was analyzed as followed: saponins **1**−**3** and **7**−**10** possessed sugar chains both at C-3 and C-28 of the oleanane skeletons, and saponin **6** possessed sugar chain at C-28. There are no free carboxylic group in all the eight saponins. However, saponins **5** and **12** possessed sugar chains at C-3 with free carboxyl groups at C-28. This suggested that those triterpenoid saponins with free carboxyl group at C-28 and sugar chain at C-3 exhibited significant cytotoxic activity against tumor cells *in vitro*.

Table 2. Cytotoxic activity of saponins 1−3, 5−10 and 12 against two cancer cell lines *in vitro* (IC_{50}, μg/mL)

Saponins	BEL-7402	HeLa
1	>50	>50
2	>50	>50
3	>50	>50
5	10.2 ± 0.5[a]	8.6 ± 0.8
6	>50	>50
7	>50	>50
8	>50	>50
9	>50	>50
10	>50	>50
12	9.1 ± 0.3	7.4 ± 1.2
Doxorubicin[b]	0.7 ± 0.1	0.9 ± 0.4

a. The data represent the mean plus SD of three independent experiments in which each compound concentration was tested in three replicate wells.
b. Doxorubicin as positive controls.

Many triterpenoid saponins, especially the oleanolic acid and hederagenin saponins have been isolated from genus *Anemone*. *A*. *rivularis* var. *flore-minore* was a variant of *A*. *rivularis*. Since this species was attributed to genus *Anemone* according to its morphological characteristics by the end of 19th century, no relevant report confirmed the conclusion from a point of chemical composition. Twelve of fifteen compounds identified in this study belonged to the above two types of saponins. Therefore, it was verified that the title species belonged to genus *Anemone* from the point of chemical composition for the first time. However, diterpene glycoside, lignan glycoside and saponin with gypsogenin as aglycone were found from genus *Anemone* for the first time. This suggested the particularity of *A*. *rivularis* var. *flore-minore* as a variety of *A*. *rivularis*.

This study filled in the blank of the chemical constituents of *A*. *rivularis* var. *flore-minore*, enriched the chemical constituents of genus *Anemone*, and provided the reference data for the research and development of the title medicinal plant with abundant resources in China.

Acknowledgement

This work was financially supported by the National Natural Science Foundation of China (No. 30873402).

References

[1] W. C. Wang, "Ranunculaceae," *In Flora Reipublicae Popularis Sinicae*, Beijing: Science Press, 1995, pp. 24-24.
[2] H. F. Tang, H. W. Lin and X. L. Chen, "Cytotoxic triterpenoid saponins from Ardisia pusilla," *Chinese Chem. Lett*., vol. 20, pp. 193-196, 2009.
[3] K. Machida, M. Yamauchi and E. Kurashina, "Four new lignan glycosides from *Osmanthus fragrans* Lour. var. *aurantiacus* Makino," *Helv. Chim. Acta*, vol. 93, pp. 2164-2175, 2010.

Study on the Spectrum-Effect Relationship of *Bupleurum chinense*

Yun YANG, Bing WEI, Qishuai WANG, Weisheng FENG
Department of Pharmacy, Henan University of TCM, Zhengzhou, China
Email: yyun@china.com.cn

Abstract: The study of spectrum-effect relationship was based on the method of using HPLC to build characteristic information of chemical compositions in the n-butanol fraction which was obtained from *Bupleurum chinense* and using the pharmacodynamics method to describe its liver protective efficiency in acute liver injury mice induced by CCl_4. Appropriate statistics methods and chemometrics analysis methods (cluster analysis and canonical correlation analysis) were used to analyze the data of spectrum-effect relationship. It was determined that SSa and SSd were the effective substance of *Bupleurum chinense* with the effect of liver-protective according to the analysis results.

Keywords: Spectrum-effect relationship; pharmacodynamics; cluster analysis; canonical correlation analysis

1 Introduction

Saikosaponins from *Bupleurum chinense* was proved to have protective effects on CCl_4-induced liver injury in mice. However, saikosaponins in different samples of *Bupleurum chinense* which were obtained from different origin and different harvest time had differences. It's unknown that the differences reflected through the saikosaponins would or not have effects on liver-protective. Whether existed the relevance between the liver-protective and the contents of saikosaponins. Were all the saikosaponins had the same effects in vivo. The spectrum-effect relationship study was going to do with these issues.

Spectrum-effect relationship based on the foundation of TCM fingerprint can obtain chemical information in maximum and can obtain the link between the pharmacodynamics results and the fingerprint which was used to mark the characteristic peak of chemical compositions. So it was used to research the determination of effective substance of TCM and make control standards reflected internal quality of products.

2 Materials and Methods

2.1 Regents and Materials

10 samples of *Bupleurum chinense* were shown in table 1.

2.2 Total Saikosaponins Assay

2.2.1 Preparation of Sample Solution

Meal of *Bupleurum chinense* was refluxed for two times with 10 times amount of alcohol for the first time and 8 times amount of alcohol for the second time, each time for 1h. Add proper alcohol to wash the leavings after natural filter and combine the filtrate. Drying the filtrate in a fume cupboard after measuring its volume. Add equal volume of n-butanol-saturated water to dissolve the paste (external therapeutic ultrasound (ETUC) for 20 min) and then water-saturated n-butanol extraction (equivalent) for three times, combine extraction liquid and evaporate to dryness. Constant volume was 25 mL with methanol.

2.2.2 Assay Method

Determine absorbability of sample solution after staining and then the following formula curve was used to calculate the contents of total saikosaponins.

$$Y=3.1086X+0.0682(r=0.0996) \quad (1)$$

Where Y and X are absorbance and concentration of samples. RSD of precision test, stability test, replicate test and recovery test were all not more than 3.29%.

Table 1. Sample information

Numbers	Growth pattern	Growth years/month	habitat
S1	cultivation	24	Dalian
S2	wild	perennial	Datong
S3	wild	perennial	Baoji
S4	wild	perennial	Xixia
S5	wild	perennial	Fengning
S6	wild	perennial	Chengde
S7	wild	perennial	Luanping
S8	wild	perennial	Luanchuan
S9	cultivation	20	Huixian
S10	cultivation	22	Songxian

2.3 Fingerprint of the Chemical Compositions

HPLC experiment [1] was performed on a Summit HPLC instrument form Dionex (USA), and equipped with a 2000ES ELSD detector from Allech (USA). A Hydro-RP80A C_{18} column (4.6 mm×250 mm, 5 μm) from phenomenex (USA) was used with a flow rate of 1.0 mL·min^{-1}. The injection volume was 10 μL and the column temperature was maintained at 30℃. The mobile phase was consisted of water (A) and acetonitrile (B), which were applied in the following gradient elution: from 85A/15B to 70A/30B in 15 min, in 10 min to 65A/35B, in 15 min to 55A/45B, then in 20 min to 50A/50B, each run was following by a 10 min washing procedure. ELSD conditions: drifttube temperature, 110 ℃; carrier gas, compressed air; carrier gas flow, 3.0 L/min.

2.4 Animal Experiment

2.4.1 Preparation of Saikosaponins

Referring to "2.1", the differences was that saline took the place of methanol when constant volume.

2.4.2 Animals

120 SPF kunming mice weighing 19-23 g were purchased from local breeders and were randomly divided into 12 groups: blank group, model group, twelve treatment groups with half male and half female in each group. The animals were housed in metal cages in animal experimental center of Henan University of TCM that was air-conditioned by means of a system designed to maintain the room temperature at an average of 24 ℃ and a relative humidity of about 30%-50%. Tap water and diet were available and libitum.

2.4.3 Dosage and Model Planning

The mice in the twelve treatment groups were pretreatment with 1.0 g·mL^{-1} extraction of saikosaponins. The mice in the blank group and the model group were given equal volume of normal saline. Dosage of administration was 20 mL·kg^{-1} by continuous *ig* injection for 7 d. All mice were deprived of food after the final injection on the 7th day. 2 h after the final injection, the blank group was given vegetable oil by *ip* injection (10 mL·kg^{-1}), the rest groups [2-3] were given 0.2% CCl_4 (CCl_4/vegetable oil (v/v)) by *ip* injection (10 mL·kg^{-1}). The eyeballs were extracted and blood was drawn after 10 h, centrifuge for 4min (2000 r·min^{-1}) to get serum. The liver (0.5 g) perfused with ice-cold saline was homogenized with inscribed homogenizer in 4.5 mL saline, this homogenate was centrituged for 10min (3000 r·min^{-1}), 2 mL of supernatant was taken to reserve.

2.4.4 Serum and Liver Tissue Assay

ALT, AST in serum and SOD, MDA in liver tissue were assayed using commercial kits (provided by Nanjing Jiancheng biological research institute of China with the batch number of 20100529).

3 Results and Analysis

3.1 Samples Assay

The contents of total saikosaponins of different samples were shown in table 2.

Table 2. Determination results of samples from different origin and harvest time

Groups	Sampling amount/g	Total saikosaponin	Relative content/%
S1	0.2038	2.679	1.31
S2	0.2016	3.153	1.56
S3	0.2022	3.302	1.63
S4	0.2029	3.925	1.93
S5	0.2009	2.381	1.19
S6	0.2034	2.325	1.14
S7	0.2042	2.377	1.16
S8	0.2034	4.163	2.05
S9	0.2009	2.494	1.24
S10	0.2007	3.298	1.64

3.2 Analysis of Fingerprint

3.2.1 Building of Common Pattern

Take the retention time of fingerprint of S5 as reference standards and take the fingerprint of SSd with steady larger peak area and better resolution as internal reference peak to match the fingerprints of ten samples. 12 peaks with 100% occurrence frequency were considered as common peaks and Gaussian curve was used to correct the baseline. The common pattern was shown in figure 1 and peak 7, peak 10 respectively represented SSa and SSd [1].

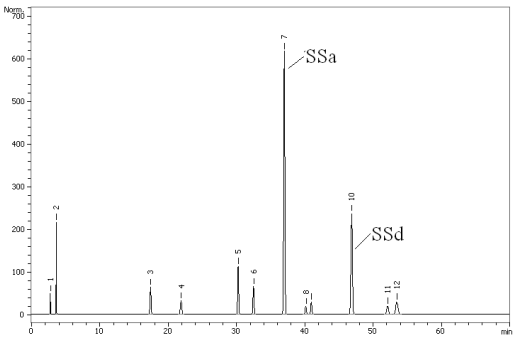

Figure 1. Fingerprint common pattern of 10 batches of samples

978-1-61896-030-6 © 2012 SciRes.

3.2.2 Similarity Analysis

"Chromafinger" solution software (Version 1.5) was used to calculate correlation coefficient of 10 samples based on the common pattern and evaluate the similarity of fingerprints of ten samples. The results were shown in table 3.

Table 3. Results of similarity analysis

Numbers	S1	S2	S3	S4	S5
Similarity	0.980	0.975	0.979	0.996	0.958
Numbers	S6	S7	S8	S9	S10
Similarity	0.949	0.952	0.998	0.988	0.981

As was drawn from the table 3, saikosaponins existed in the ten samples from different regions and harvest time were merely same (correlation coefficient was all more than 0.9) and the total non-common peak areas were less than 10% of total peak areas in the chromatogram. So the common peaks that we selected had representative and can be used to mark the features of saikosaponins from *Bupleurum chinense*.

3.2.3 Peak Areas of Common Pattern

Logarithm of peak areas in common pattern was resulted in table 4.

Table 4. Logarithm of peak areas in common pattern

TR/min	2.77	3.66	17.48	21.94	30.30	32.53	37.05	40.19	41.00	46.93	52.18	53.51
Nnumbers	peak1	peak2	peak3	peak4	peak5	peak6	peak7	peak8	peak9	peak10	peak11	peak12
S1	5.1022	7.4781	5.7856	6.1185	5.9465	5.9284	8.8833	5.1772	5.5931	7.8829	5.8121	6.0298
S2	5.8060	6.8825	7.6964	7.1881	7.4361	6.8375	9.1031	5.6705	6.1371	8.2469	6.2951	7.0814
S3	5.9632	6.9448	7.5618	6.9919	7.8120	7.3429	9.1653	5.8817	6.3251	8.4105	6.7998	7.3947
S4	4.5485	4.5272	5.6345	5.7330	7.3183	6.0575	9.4089	5.0295	5.5500	8.5266	5.0585	5.7887
S5	4.7847	6.5959	5.1774	5.3210	6.8232	6.4009	8.4118	5.8543	5.7193	8.2310	5.6933	6.2080
S6	4.6614	6.7086	5.1238	5.2075	6.3015	5.9852	8.3661	5.7440	5.8699	8.1931	5.4887	6.2755
S7	4.7304	6.8107	5.1118	5.2823	6.7843	6.0381	8.3766	5.7896	5.6845	8.0443	5.5390	6.1234
S8	5.6577	6.9686	5.9152	5.3337	7.6991	7.0910	9.5533	5.8494	6.6857	8.8213	5.7271	6.2310
S9	5.2580	5.7413	6.4093	6.3353	6.8228	6.5591	8.5112	5.5736	5.7817	7.6798	6.2601	6.7408
S10	5.8875	6.9448	7.5580	6.9919	7.8120	7.3429	9.1653	5.8817	6.5255	8.4288	6.4696	7.1859

3.2.4 Cluster Analysis

Take the common peaks of sample fingerprints as the variables to describe sample chemical features (data source was natural logarithm of common peak areas, deal the data with Z standardization, the same to the following).Software SPSS 13.0 for windows was applied to perform on cluster analysis of 10 batches of samples. A cluster of 10 samples was obtained (Figure 2).When the rescaled distance was 10, 10 samples would be divided into four clusters. Combine with the results of table 2, the classification was defined as follows: one cluster with S2,S3,S10 and the contents of total saikosaponins were in the range of 1.56%～1.64%; one cluster with S8 and the contents of total saikosaponins were 2.05%; one cluster with S1, S5, S6, S7, S9 and the contents of total saikosaponins were in the range of 1.14%～1.31%; one cluster with S4 and the contents of total saikosaponins were 1.93%. The results indicated that the common peaks which had been chosen could significantly characterize the chemical information of saikosaponins from samples.

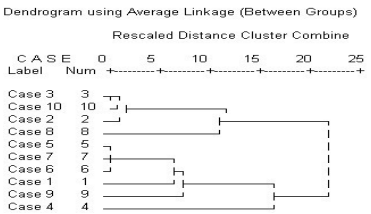

Figure 2. Dendrogram for samples

In order to explore the relationship of each peak in the common pattern, cluster analysis (Figure 3) of 12 common peaks was going on next (data source was natural logarithm of 12 common peak areas).

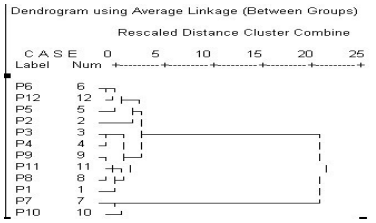

Figure 3. Dendrogram for variables

Our previous study indicated that SSa (p7) and SSd (p10) were the highest contents of saikosaponins in *Bupleurum chinense* [1], so we chose 5 as the rescaled distance and 12 common peaks were divided into 2 clusters with p7 and p10 in one cluster and other peaks in one cluster. The results showed that p7 and p10 had different change pattern compared with other peaks.

Above analysis showed that fingerprints of samples can not only reflect the common features of saikosaponins of *Bupleurum chinense*, but also can express the differences among the samples efficiently.

3.3 Results of Pharmacodynamics

3.3.1 Results of Liver Protective

Data of each group was expressed as mean ± standard deviation ($\bar{x}\pm s$) .The results were in table 5 and table 6.

As was shown in table 5, ALT and AST activities in serum were significantly higher in model group (P<0.05) than in blank group showed that the model building was successful. Compared with the control group, the serum ALT and AST activities in different treatment groups were all significantly decreased (P<0.05).

Table 5. Effects of the activities on serum ALT and AST among different samples ($\bar{X} \pm s$, n=10)

groups	ALT / U·L^{-1}	AST / U·L^{-1}
Blank group	19.30±3.40*	17.30±4.24*
Model group	41.20±2.82$^{\triangle}$	84.70±5.74$^{\triangle}$
S1	26.40±1.90*$^{\triangle}$	58.40±6.59*$^{\triangle}$
S2	25.70±2.71*$^{\triangle}$	64.20±6.13*$^{\triangle}$
S3	30.20±2.62*$^{\triangle}$	52.00±6.85*$^{\triangle}$
S4	25.60±1.90*$^{\triangle}$	58.00±5.62*$^{\triangle}$
S5	30.50±3.38*$^{\triangle}$	66.90±4.91*$^{\triangle}$
S6	34.40±2.63*$^{\triangle}$	64.10±4.86*$^{\triangle}$
S7	31.00±3.43*$^{\triangle}$	54.70±5.19*$^{\triangle}$
S8	28.90±2.56*$^{\triangle}$	56.10±5.67*$^{\triangle}$
S9	31.10±2.47*$^{\triangle}$	60.60±5.08*$^{\triangle}$
S10	28.30±2.41*$^{\triangle}$	58.40±5.78*$^{\triangle}$

*P<0.05, significant differences *vs* model group.

$^{\triangle}P$<0.05, significant differences *vs* blank group.

Table 6. Effects of SOD activity and MDA contents on liver tissue among different samples ($\bar{X} \pm s$, n=10)

Groups	SOD / *U·mgprot*$^{-1}$	MDA / *U·mgprot*$^{-1}$
Blank group	296.36±37.43*	3.04±0.60*
Model group	87.21±21.78$^{\triangle}$	7.57±1.15$^{\triangle}$
S1	236.53±45.26*$^{\triangle}$	4.91±1.11*$^{\triangle}$
S2	281.85±29.69*	5.81±0.94*$^{\triangle}$
S3	166.87±37.34*$^{\triangle}$	5.51±0.61*$^{\triangle}$
S4	276.80±26.24*	6.02±0.99*$^{\triangle}$
S5	157.21±23.41*$^{\triangle}$	5.01±0.66*$^{\triangle}$
S6	126.69±24.05*$^{\triangle}$	3.20±0.59*
S7	145.33±29.75*$^{\triangle}$	3.25±0.82*
S8	248.18±23.28*$^{\triangle}$	5.14±1.27*$^{\triangle}$
S9	157.80±29.57*$^{\triangle}$	3.91±0.99*$^{\triangle}$
S10	269.29±39.14*	4.77±1.10*$^{\triangle}$

*P<0.05, significant differences *vs* model group.

$^{\triangle}P$<0.05, significant differences *vs* blank group.

As was shown in table 6, compared with blank group, the liver tissue SOD activity was significantly lower while the MDA contents were significantly higher (P<0.05) in model group showed liver tissue lipid peroxidation in mice appeared and the model building was successful. The decrease of liver tissue SOD activity and elevation of liver tissue MDA contents were significantly inhibited (P<0.05) in different treatment groups by comparing with the model group.

3.3.2 Comparison between Groups and Cluster Analysis

Multivariate variables analysis on liver protective of different samples took the ALT, AST, SOD, MDA as parameters and the significant levels of four test were all zero, so they all had statistical significance (P<0.05). So it can be considered that ten samples had different effects of liver protective (Two samples had statistical significance at least).

Mean of four pharmacodynamics indexes were selected as variables to describe the differences of 10 samples by using cluster analysis. Four index variables were unified transformed for they expressing different implication. The higher of serum ALT, AST activities and liver tissue MDA contents, the better of these indexes while the opposite to the index of liver tissue SOD activity. The formula was as follows and the results were shown in table 7.

$$\bar{X}_{unified} = | \bar{X}_{sample} - \bar{X}_{model} | \qquad (2)$$

Where $\bar{X}_{unified}$, $\bar{X}_{sample}$ and $\bar{X}_{model}$ are mean of sample after unified transformed, mean of sample and mean of

978-1-61896-030-6 © 2012 SciRes.

model.

Table 7. Results of pharmacodynamics indexes after unified transformed

Numbers	Unified ALT/ $U{\cdot}L^{-1}$	Unified AST/ $U{\cdot}L^{-1}$	Unified SOD/ $U{\cdot}mgprot^{-1}$	Unified MDA/ $U{\cdot}mgprot^{-1}$
S1	14.80	26.30	149.32	2.66
S2	15.50	20.50	194.64	1.76
S3	11.00	32.70	79.66	2.06
S4	15.60	26.70	189.59	1.55
S5	10.70	17.80	70.00	2.56
S6	6.80	20.60	39.48	4.37
S7	10.20	30.00	58.12	4.32
S8	12.30	28.60	160.97	2.43
S9	10.10	24.10	70.59	3.66
S10	12.90	26.30	182.08	2.80

From the formula (2), we can see that the unified data will not have an effect on cluster analysis for the variables all subtracting the same constant at the same time, what is more the variables were all higher-better indexes after unified transformed and it was more beneficial to the requirement of data analysis, so we choose the unified data as the variables to perform on the cluster analysis of ten batches of samples. The results were shown in figure 4.

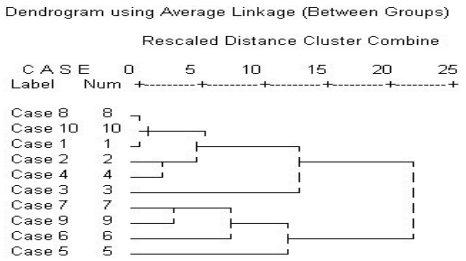

Figure 4. Dendrogram for unified data

When the rescaled distance was 15 in figure 5, 10 samples would be divided into two clusters. Combine with the results of table 2, the classification was defined as follows: one cluster with S1, S2, S3, S4, S8, S10 and the contents of total saikosaponins were in the range of 1.31%～2.05%; one cluster with S5, S6, S7, S9 and the contents of total saikosaponins were in the range of 1.14%～1.24%

3.3.3 Study of Spectrum-Effect Relationship

Above analysis showed that the fingerprints of saikosaponins from samples and the four pharmacodynamics indexes had the same identity when they were used as variables to describe the features of samples. So the following cluster analysis of samples took the common peaks of HPLC fingerprints and the four pharmacodynamics indexes as the common variables. The results were in figure 5.

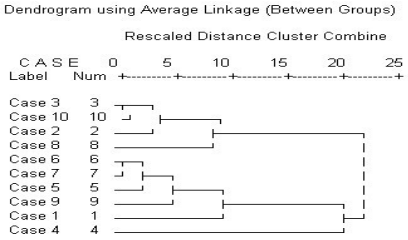

Figure 5. Dendrogram for samples

When the rescaled distance was 5 in figure 5, 10 batches of samples would be divided five clusters. The classification was defined as follows: one cluster with S2, S3, S10 and the contents of total saikosaponins were in the range of 1.56%～1.64%; one group with S8 and the contents of total saikosaponins were 2.05%; one cluster with S5, S6, S7, S9 and the contents of total saikosaponins were in the range of 1.14%～1.24%; one cluster with S1 and the contents of total saikosaponins were 1.31%; one cluster with S4 and the contents of total saikosaponins were 1.93%. As can be seen from the classification results no matter what type of index (fingerprint common pattern and efficacy mean) was chosen as the variables to describe the samples, the classification results had consistency, so some kind of relevance may existed among the variables. The following work was to perform on the cluster analysis of all the 16 variables. The results were in figure 6.

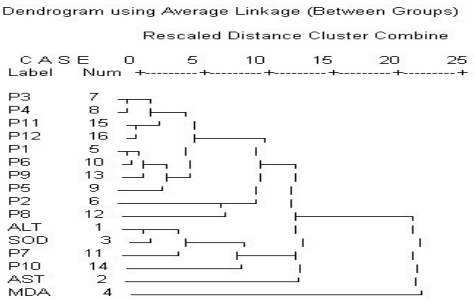

Figure 6. Dendrogram for variables

When the rescaled distance was 10, all variables were divided into four clusters. ALT, SOD of pharmacodynamics indexes and p7, p10 of common peaks were in one cluster indicated these two groups of variables had higher correlation.

Then SPSS 13.0 for windows was used to make correlation analysis of above two indexes with probable relevance. The canonical correlation analysis of these two

groups of variables extracted two pairs of canonical variables (U_1, V_1 and U_2, V_2).Correlation coefficient of the first pair of canonical variables (U_1, V_1) was 0.039 (P<0.05) and its correlation coefficient was 0.842, so it had linear positive correlation. Results of redundancy analysis indicated that U_1 of the first pair of canonical variable explained the information of original variables of spectrum peaks (p7, p10), and V_1 can also explained the information of efficacy variable group.

First pair of canonical variables (U_1, V_1) was retained based on the results of canonical correlation analysis and redundancy analysis and U_1, V_1 had already described all of the relevant information between efficacy variable group and spectrum peak variable. The formula was shown as follows.

$$U_1 = -1.257 InA_{SSa} + 0.398 InA_{SSd} \quad (3)$$

Where U_1, A_{SSa} and A_{SSd} are canonical variable of spectrum peak variable group; peak areas of SSa and peak areas of SSd

$$V_1 = -0.062\ \bar{X}_{\text{unified ALT}} - 0.943\ \bar{X}_{\text{unified SOD}} \quad (4)$$

Where V_1, $\bar{X}_{\text{unified ALT}}$ and $\bar{X}_{\text{unified SOD}}$ are canonical variable of efficacy variable group; mean of serum ALT in mice and mean of liver tissue MDA in mice.

From the formula we can see that U_1 which reflected the information of spectrum was determined by the interaction of SSa and SSd and V_1 which reflected the information of efficacy was determined by the interaction of $\bar{X}_{\text{unified ALT}}$ and $\bar{X}_{\text{unified SOD}}$. U_1 and V_1 can express the correlation of these two groups of variables. As the first pair of canonical variable had linear positive correlation (The correlation coefficient was 0.842.), we can consider that the variation of SSa and SSd reflected the change trend of $\bar{X}_{\text{unified ALT}}$ and $\bar{X}_{\text{unified SOD}}$. So we can have an overall grasp of $\bar{X}_{\text{unified ALT}}$ and $\bar{X}_{\text{unified SOD}}$ according to variation of SSa and SSd. The results indicated that SSa and SSd of *Bupleurum chinense* had an effect on the activities of ALT and AST in acute liver injury mice induced by CCl_4, the interaction of SSa and SSd can enhance the efficacy, they were the key chemical compositions of *Bupleurum chinense* with liver protective effect.

4 Discussion

SSa and SSd were the main saikosaponins of *Bupleurum chinense* that had liver protective effect according to the analysis of this paper. The content differences of SSa, SSd in different samples were the main factor that led to the different liver protective effect. T.Nishiura [4] reported that SSa and SSd can significantly suppress the increase in serum GOT (AST) and GPT (ALT) levels in comparison with the rats treated with phenobarbital, halothane and hypoxia, while SSc, SSb1, SSb2 had less effect. That was different saikosaponins had different liver protective effects. It matched the conclusion of this paper.

Clustering method was based on a specified standard (distance criterion as usual) to segment data to different clusters Different from the traditional classification, clustering method was, without any prior knowledge, based only on the similarity between data. As a result, data in the same group had higher similarity and data in different groups had higher differences at the same time [5]. So the clustering method had the features of similarity analysis, but its classification conditions were fuzzy [6] because of the gradual clustering. In this experiment, the contents of total saikosaponins were chosen as classification foundation and effectively made up for the disadvantages. From the results of clustering analysis, we can overall grasp the similarity and classification of different indexes, find correlation between variables, reject the variables with less similarity and provide thoughts and directions for deeply studying of data.

The combination of cluster analysis and canonical correlation analysis were firstly used in this in this experiment to analyze the spectrum-effect relationship data. Clustering analysis can effectively classify the multivariable and variables with higher correlation in the classification were the data for canonical correlation analysis. In this way the variables were screened and the variables with no correlation or less correlation would not be compulsory introduced into regression equation, at the same time it could also provide foundation for rejecting variables with collinearity.

References

[1] Wang Qishuai, Yang Yun, Xiao Gongsheng, etc, Fingerprint analysis of Bupleurum chinense by HPLC–ELSD and its chromate data[J], Chinense Traditional Patent Medicine, 2011, 33(3), P373-378.

[2] Li Xia, Duan Lengxin, Wang Ya-nan, etc, Protective effects of velvet antler peptides on acute hepactic injury by carbon tetrachloride [J], Chinense Pharmaceutical Journal, 2007, 42 (24), P1864-1866.

[3] Xin nian, Xiong Jianxin, Han Shuying,etc, Protective effect of total flavonoids of buckwheat seed on acute hepatic injury by carbon tetrachloride [J], Acta Academiae Medicinae Militrais Tertiae, 2005, 27(14), P1456-1458.

[4] Teruhiro Nishiura, Seishiro Marukawa, Hiroatsu Ishida, etc, Effects of saikosaponins onhepatic damage induced by halothane and hypoxia in phenobarbital-pretreated rats [J], Journal of Anesthesia, 1994, 8, P87-92.

[5] Yang Xiaobing, Research of key techniques in cluster analysis [D], Hangzhou, Zhejiang University, 2005.

[6] Hui Zhouli, The study and application of some issues for cluster analysis [D], Taiyuan, Zhongbei University, 2008.

978-1-61896-030-6 © 2012 SciRes.

Olfactory Responses of the Larvae(Hepialidae)—The Host of Cordyceps Sinensis (Berk.)Sacc. to Several Kinds of Foods

Mingchao LI[1], Meng YE[1], Zuji ZHOU[1], Yikai CHEN[1], Yong DAI[2]
[1]*College of Forestry Sichuan Agricultural University, Sichuan, China*
[2]*Chengdu Enwei Group Company, Sichuan, China*
Email: dzlimingchao@163.com

Abstract: Choose 12 kinds of foods to determine olfactory responses of the larvae to them, which showed that the order is *Gentiana macrophyllad*＞*Stachys seiboibi* Miq. ＞*Potentilla anserine* L.＞*Tibetia tongolensis* (Ulbr.)＞*Rheum palmatum L.*=*Solanum tuberosum*＞*Malus pumila*＞*Daucus carota* Linn. var. sativa Hoffm＞*Hordeum vulgare* Linn. var. nudum Hook.f.＞*Astragalus membranaceus* (Fisch.) Bunge.＞*Oxytropis densa Benth.*＞Anemone obtusiloba D.＞*Morina nepalensis* var.alba (Hand.-Mazz.) Y.C.Tang and summarized the allure of them.

Keywords: Y-type olfactory olfactometer; foodstuff; larvae

1 Introduction

Cordyceps is known as a rare traditional herb of China, it is a combo of Hepialidae larva and fungus, formed through parasitization of *Cordyceps sinensis* (Berk.)Sacc on the Hepialidae larva (Lepidoptera, Hepialidae)[1]. In recent years the researches on cordyceps have been widely done in many aspects, however, most are concentrated in its efficacy and property. There are little materials to sustain the industrialization of the production of cordyceps in the current circumstance of supply falls short of demand. Therefore the cultivation of the larvae (Hepialidae) is becoming important, the key of which is the feeding habits of the larvae.

When refers to the feeding habits of the larvae people always try to identify what they eat but not what they prefer. In cultivation the foods choice confused people for many years. The foods they chose such as *Polygonum viviparum* L., *Rheumpumilum Maxim*. and *Potentilla anserine* L. et al. mainly grew in where the larvae existed[2-9], which is the single principle people followed. Since the cultivation conditions and modes[10] have been put forward many firms began to take their action to the new field with the support from many graduate schools and universities. Now papers had given some information about the effect different feeds on weight of larvae[2], But before doing such works we should confirm the order of all foods larvae eat firstly under the man-made conditions that can be controlled easily.

Normally the methods to study the feeding habits are Olfactometer[11-13], Petri dish experiments[14-15] and EAG determination[16-18]. All can be used to the confirmation of the foods order relates to how the larvae like. EAG determination is useless in studying the larvae as the antennae of which are regressive. When carrying the Petri dish experiments it spends much time and the condition controlled hard. Among all olfactometers Y-type overmatch the two above in the studying. It can be used to distinguish the responses of two materials in short time and the results of which is clear at a glance.

In order to cognize the olfaction of larvae and provide scientific basis for culturing the larvae, the preference order of 12 materials(more information will be given in charge2) is shown in this paper with the utilization of Y-type olfactometer.

2 Materials and Methods

2.1 Materials

Most materials in the experiment are the underground part of the whole plant except *Malus pumila*, which fruit is selected. *Malus pumila*, *Solanum tuberosum*, and *Daucus carota* Linn. var. sativa Hoffm are normal and can be easily collected from market. Other materials are gathered from Xinduqiao Town (3600meters in elevation), Kangding County, Sichuan Province in Oct. 2009.

Table 1. Plants materials in the experiment

Sepcies	Family	Genus
Morina nepalensis var.alba (Hand.-Mazz.) Y.C.Tang	Dipsacaceae	Morina
Gentiana macrophylla	Gentianaceae	Gentiana
Hordeum vulgare Linn. var. nudum Hook.f.	Gramineae	Hordeum
Stachys seiboibi Miq.	Lamiaceae	Stachys
Oxytropis densa Benth.	Leguminosae	Oxytropis
Tibetia tongolensis (Ulbr.)	Leguminosae	Tibetia
Astragalus membranaceus (Fisch.) Bunge	Leguminosae	Astragalus
Rheum palmatum L.	Polygonaceae	Rheum
Anemone obtusiloba D.	Ranunculaceae	Anemone
Malus pumila	Rosaceae	Malus
Potentilla anserine L.	Rosaceae	Potentilla
Solanum tuberosum	Solanaceae	Solanum
Daucus carota Linn. var. sativa Hoffm	Umbelliferae	Daucus

The tested larvae are Hepialus xiaojinensis(Hepialidae, Hepialus), which are in 3 age phase[19], for the lengths of them are ranged from 2cm to 2.5cm, and most of which have just moulted. All are cultivated without foods for 7 days before the experiment.

2.2 Methods

Cut all plants materials into bits of 0.5cm × 0.5cm × 0.5cm size and deposit the bits in different cases with lids.

All subassemblies of Y-type olfactometer (Fig.1) are washed first with distilled water then with acetone for 2 times. At last put them into a oven heated to a temperature of 50℃ until they are dry. Then take them out and assembly the Y-type olfactometer as soon as they are cold.

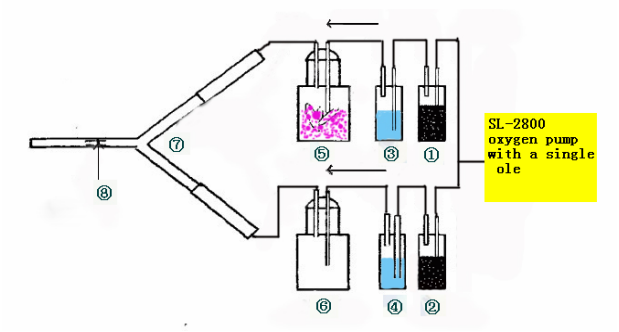

Figure 1. The sketch map of Y-type olfactometer

Note: ①、②conical flask with active carbon; ③、④conical flask with distilled water; ⑤conical flask with materials ⑥antitheses conical flask; ⑦Y-type glass pipe; ⑧location with larvae; the arrowheads show the direction of air current
The character of SL-2800 oxygen pump with a single hole
Rating voltage: 220V
Frequency: 50HZ
Air pressure: ≥0.012MPa
Exhaust volume: 2.5L/min
Weight: 0.26kg

Conical flask with *Solanum tuberosum* is contrast with the parallel conical flask with one of other 11 plants materials once in a test. There are 11 tests in the whole experiment.

The olfaction of larvae were tested in Y-tube of the 10cm×10cm×10cm size. The glass tubes were thoroughly washed and then heated to 200℃ after each experiment to make them free from any contamination or sample residue. The position of the Y- tube was continuously changed to compensate for the possible effects due to position, air or light. 10 larvae were observed for 5 times in each test. One larva was released at the common end of the tube and allowed to walk up and chose one of the arms, larvae which traveled 8 cm in the arm of Y-tube in 5 minute were considered to make a choice.

3 Results and Discussion

It's shown in Tab.2 that all foods had allure to the larvae, but there are differences, which shown a difference of individual and a difference of food.

A larva may choose both foods, only one of the two or neither of them. But as a whole there are no obvious differences when calculating the ten together to the two materials.

So it can calculate the total responses times the 10 larvae to one material and compare the various times to confirm the order of the 12 materials.

Table 2. Olfactory responses of each larva of 10 to 11 kinds of foods (amounts)

Foods	Amounts		
	Experiment	*Middle tube*	*Contrast*
Morina nepalensis var.alba(Hand.-Mazz.) Y.C.Tang	9	0	10
Gentiana macrophylla	9	0	8
Hordeum vulgare Linn. var. nudum Hook.f.	9	0	9
Stachys seiboibi Miq.	10	0	8
Oxytropis densa Benth.	8	0	9
Tibetia tongolensis (Ulbr.)	10	0	8
Astragalus membranaceus (Fisch.) Bunge	8	1	7
Rheum palmatum L.	9	0	9
Anemone obtusiloba D.	9	0	10
Malus pumila	9	0	10
Potentilla anserine L.	9	0	10
Daucus carota Linn. var. sativa Hoffm	9	0	8

As we can see from Tab3 that total 50 times were designed to observe the responses of the larvae toward the tested foods.

Among the foods the times larvae chose *Solanum tuberosum* are little than *Gentiana macrophylla* , *Stachys seiboibi* Miq., *Potentilla anserine* L. and *Tibetia tongolensis* (Ulbr.) in turn. By contrary which are more than *Malus pumila*, *Daucus carota* Linn. var. sativa Hoffm, *Hordeum vulgare* Linn. var. nudum Hook.f., *Oxytropis densa* Benth., *Anemone obtusiloba* D., *Morina nepalensis* var.alba (Hand.-Mazz.) Y.C.Tang in turn.

The extensive order of them can be confirmed that *Gentiana macrophylla*d ＞ *Stachys seiboibi* Miq. ＞ *Potentilla anserine* L.＞*Tibetia tongolensis* (Ulbr.) ＞ *Rheum palmatum* L.＞*Malus pumila*＞*Daucus carota* Linn. var. sativa Hoffm＞*Hordeum vulgare* Linn. var. nudum Hook.f. ＞*Oxytropis densa* Benth. ＞*Anemone obtusiloba* D. ＞ *Morina nepalensis* var.alba (Hand.-Mazz.) Y.C.Tang.

978-1-61896-030-6 © 2012 SciRes.

But there are 5 times the larvae didn't make a choice between the two materials(*Astragalus membranaceus* (Fisch.) Bunge and *Solanum tuberosum*.). just for which the order of them is *Hordeum vulgare* Linn. var. nudum Hook.f.＞*Astragalus membranaceus* (Fisch.) Bunge.

So the order is *Gentiana macrophylla*d＞*Stachys seiboibi* Miq.＞*Potentilla anserine* L.＞*Tibetia tongolensis* (Ulbr.)＞*Rheum palmatum* L.=*Solanum tuberosum*＞*Malus pumila*＞*Daucus carota* Linn. var. sativa Hoffm ＞ *Hordeum vulgare* Linn. var. nudum Hook.f. ＞ *Astragalus membranaceus* (Fisch.) Bunge.＞*Oxytropis densa* Benth.＞*Anemone obtusiloba* D.＞*Morina nepalensis* var.alba (Hand.-Mazz.) Y.C.Tang

The larvae lived a cave life under the soil, which is difficult to observe them in soil. The result is certainly suspected by many people. And the antennae of larvae are degenerate, which make the mechanism they response to the odor of foods is confusing. As a result, the terminate result should be discussed further when new method and new knowledge of the larvae are built.

Table 3. Olfactory responses of the larvae to 11 kinds of foods (times)

Foods	Times		
	Experiment	*Middle tube*	*Contrast*
Morina nepalensis var.alba (Hand.-Mazz.) Y.C.Tang	13	0	37
Gentiana macrophylla	30	0	20
Hordeum vulgare Linn. var. nudum Hook.f.	22	0	28
Stachys seiboibi Miq.	28	0	22
Oxytropis densa Benth.	21	0	29
Tibetia tongolensis (Ulbr.)	26	0	24
Astragalus membranaceus (Fisch.) Bunge	22	5	23
Rheum palmatum L.	25	0	25
Anemone obtusiloba D.	17	0	33
Malus pumila	24	0	26
Potentilla anserine L.	27	0	23
Daucus carota Linn. var. sativa Hoffm	23	0	27

Different larvae made different choice at the end of the mid-tube, which showed the otherness of the larvae's feeding habits

From the Tab.4 we can draw that different larvae respond variously to one food. Take the first group for example, there are 1,2,1,3,3,0 larvae reacting 0,1,2,3,4 times to *Solanum tuberosum*. The data about *Solanum tuberosum* of different test group illustrate the allure grade of different foods. Take the first and the second groups for example, when *Malus pumila* contrasting *Solanum tuberosum*, the larvae distributed mainly in 0-4 times to *Solanum tuberosum*, while *Morina nepalensis* var.alba (Hand.-Mazz.) Y.C.Tang contrasting *Solanum tuberosum*, the larvae distributed mainly in 2-5 times to *Solanum tuberosum*. The larvae tended to choose *Malus pumila* than *Morina nepalensis* var.alba (Hand.-Mazz.) Y.C.Tang. Similar results refer to the allure are *Malus pumila* ＞ *Anemone obtusiloba* D., *Malus pumila* ＞ *Hordeum vulgare* Linn. var. nudum Hook.f..

The whole order can't be made according the following data. Some unclear factors may influent the choice of larvae. In test some foods such as *Malus pumila*, *Daucus carota* Linn. var. sativa Hoffm and *Gentiana macrophylla* are with special odor to human, and they are more likely be chose by the larvae.

Table 4. Responses frequency of the tested larvae

		Times / Foods	0	1	2	3	4	5
Amounts	1	*Solanum tuberosum*	1	2	1	3	3	0
		Malus pumila	0	3	2	2	2	1
	2	*Solanum tuberosum*	0	0	2	1	5	2
		Morina nepalensis var.alba (Hand.-Mazz.) Y.C.Tang	2	5	1	2	0	0
	3	*Solanum tuberosum*	0	0	2	4	3	1
		Anemone obtusiloba D.	1	3	4	2	0	0
	4	*Solanum tuberosum*	1	1	1	4	2	1
		Hordeum vulgare Linn. var. nudum Hook.f.	1	2	4	1	1	1
	5	*Solanum tuberosum*	2	1	0	3	3	1
		Daucus carota Linn. var. sativa Hoffm	1	3	3	0	1	2
	6	*Solanum tuberosum*	2	1	2	3	1	1
		Astragalus membranaceus (Fisch.) Bunge	2	1	3	2	1	1
	7	*Solanum tuberosum*	0	4	1	4	0	1
		Potentilla anserine L.	1	0	4	1	4	0
	8	*Solanum tuberosum*	1	1	2	2	2	2
		Oxytropis densa Benth.	2	2	2	2	1	1
	9	*Solanum tuberosum*	2	3	1	2	1	1
		Gentiana macrophylla	1	2	1	1	3	2
	10	*Solanum tuberosum*	1	1	2	4	1	1
		Rheum palmatum L.	1	1	4	2	1	1
	11	*Solanum tuberosum*	2	1	1	3	3	0
		Tibetia tongolensis (Ulbr.)	0	3	3	1	1	2
	12	*Solanum tuberosum*	2	2	1	2	3	0
		Stachys seiboibi Miq.	0	3	2	1	2	2

4 Conclusion

The order reflects the choice larvae made when they are among the foods. According to the order, foodstuffs, accessible and inexpensive, such as *Solanum tuberosum* , *Daucus carota* Linn. var. sativa Hoffm, will easily be adopted when cultivating larva. But the one are preferred to eat don't mean the one is good to their growth. During their growth various nutrition are needed in different

phases. And one foodstuff is with different nutrition in different time of the year. In my opinion in the food range of the larvae all should be considered to take as fodder, mixed and offered in different times.

References

[1] Shuxiong Bai, Kanglai He, Zhenying Wang. A simple and convenient method for extracting plant volatiles—condensation by liquid nitrogen. Entomological Knowledge [J], 2003(4): 377-379.

[2] Hongshen Wang. The preliminary study on artificial rearing Hepialus spp.. Entomological Knowledge [J], 2002, 39(2): 144-146.

[3] Dinghua Yin, Xuemei Tang. Review on Study of Artificially Culturing Cordyceps. CHINA JOURNAL OF CHINESE MATERIA MEDICA [J] 1995, 20(12): 707-709.

[4] Lu Rao. Feeding host insects of Cordyceps sinensis. Gansu Science and Technology [J], 1994, 10(1): 36-36.

[5] Nanying Shen, Lu zeng, Xianchi Zhang. Study the Feeding Habit of the Hepialidae Larvae. Specialty scientific experiments [J], 1983(3): 19-20.

[6] Changxin Wang, Chunwei Yang. Cultivation Process of Cordyceps. Practical Pharmacy and Clinical Remedies [J], 2006, 9 (2): 111-112.

[7] Hongsheng Wang. The Preliminary Study of Artificial Feed of Fifth Instar Hepialidae larvae. Gansu Animal and Veterinary Sciences [J], 2001, 31(5): 15-16.

[8] Zhong Wang, Qilong Ma. Study on Bological Characteristics of H epialus minyuancus. Gansu Agricultural Science and Technology [J], 2001: 38-39.

[9] Zhong Wang, Qilong Ma. Gansu host insects of Cordyceps bat moth of artificial feeding techniques. Gansu Agricultural Science and Technology [J], 2001: 42-43.

[10] Zuxun Gao, Zhihong Zhao. Studies on artificial culture of Insect-herb—Research on the host swiftmoth (Hepialts oblifurcus Chu et Wang) of caterpillar fungus (Cordyceps sinensis (Berk.)Sacc.) in Kangding.. Journal of Zhejiang Agricultural University [J], 1991, 17(1): 1-5.

[11] Shuxiong Bai, Zhenying Wang, Kanglai He. Olfactory responses of Trichogramma ostriniae Pang et Chen to kairomones from eggs and different stages of female adults of Ostrinia furnacalis (Guenée). Acta Entomologica Sinica[J], 2004(1).

[12] Li Chen, Kewei Chen, Zaifu Xu. Olfactory Response of Telenomus remus Nixon to the Volatile Information Objects from Spodoptera exigua (Hübner). Journal of Changjiang Vegetables [J], 2010(18): 4-7.

[13] Siyue Ding, Qiuying Huang, Chaoliang Lei. Olfactory response of Culex pipiens pallens to four chemicals. Chinese Bulletin of Entomology [J], 2007(3): 389-392.

[14] Shufen Gong. Trichogramma parasitized host search and study of hormone regulation [D], Nanjing Agriculture University, 2004.

[15] Junhong Zhu, Fangping Zhang, Honggang Ren. Development and nutrition of Prodenia litura on four food plants. Entomological Knowledge [J], 2005, 42(6): 643-646.

[16] Youju Jin, Jiquan Li, Jianguang Li. Olfactory Response of Anoplophora glabripennis to Volatile Compounds from Ash-leaf Maple(Acer negundo) Under Drought Stress. Scientia Silvae Sinicae [J], 2004(1): 99-105.

[17] Sudhida GAUTAM. ctory responses of green lacewings, Chrysoperla sp. (carnea group) and Mallada desjardinsi on mealybug, Phenacoccus solenopsis (Homoptera: Pseudococcidae) fed on cotton. Acta Entomologica Sini [J], 2010(5): 497-507.

[18] Xiaosong Liang, Yong Liu, Shaohong Zhang. Olfactory Response and Electroantennal of Two Termites Species to Several Components. Journal of Nanjing Forestry University(Natural Sciences Edition)[J], 2007(2): 55-58.

[19] Quansen Li, Li Li. Biological properties of Cordyceps sinensis. Special Wild Economic Animal and Plant Research [J], 1991: 42-45.

978-1-61896-030-6 © 2012 SciRes.

Chemical Constituents and Their Bioactivity of *Anemone taipaiensis*

Xiaoyang WANG[1], Hui GAO[2], Haifeng TANG[1], Guang CHENG[3], Yi WANG[1], Liangjian HONG[1]
[1]*Department of Pharmacy, Xijing Hospital, Fourth Military Medical University, Xi'an, China, 710032*
[2]*Department of Stomatology, No.309 Hospital of Chinese PLA, Beijing, China, 100091*
[3]*Department of Neurosurgery, Xijing Hospital, Fourth Military Medical University, Xi'an, China, 710032*
Email: tanghaifeng71@163.com

Abstract: Ten new oleanane-type triterpenoid saponins **11**, **13**, **18**, **19**, **24** and **26**−**30**, a new natural product **8**, together with nineteen known compounds **1**−**7**, **9**, **10**, **12**, **14**−**17**, **20**−**23** and **25** were isolated from the rhizomes of *Anemone taipaiensis*. Their structures were elucidated by extensive spectroscopic analyses and chemical evidences. The six saponins **6**, **7**, **9**−**11** and **13**, possessed free carboxylic group at C-28, exhibited significant cytotoxicity against human leukemia HL-60 cells and human hepatocellular carcinoma Hep-G2 cells with IC_{50} values in the range of 1.31~10.12 μmol/L. Saponins **9**, **11** and **13** exhibited significant cytotoxicity against human glioma U-251MG cells. The most potent one was **9** with an IC_{50} value at 1.37 μmol/L in a 72 h test, which was almost as equivalent as the clinical commonly used anti-glioblastoma agent ACNU.

Keywords: *Anemone taipaiensis*; triterpenoid saponins; antitumor; bioactive constituent

1 Introduction

Anemone taipaiensis is only distributed in southwest part of Shaanxi Province [1]. The genus *Anemone* (Ranunculaceae) has been proved to be an especially valuable source of diverse saponin substances with potentially useful biological properties [2−5]. However, no investigation has been reported on chemical constituents of this species of *Anemone*. As part of our ongoing investigation on new antitumor glycosides from natural source [6−10], the chemical studies on this plant led to the isolation of ten new oleanane-type triterpenoid saponins **11**, **13**, **18**, **19**, **24** and **26**−**30**, a new natural product **8**, together with nineteen known compounds **1**−**7**, **9**, **10**, **12**, **14**−**17**, **20**−**23** and **25** (structures of saponins see Fig. 1 and Table 1). We described herein the isolation and structural elucidation of these compounds, as well as their potent cytotoxicity against human leukemia HL-60 cells, human hepatocellular carcinoma Hep-G2 cells and human glioma U251MG cells。

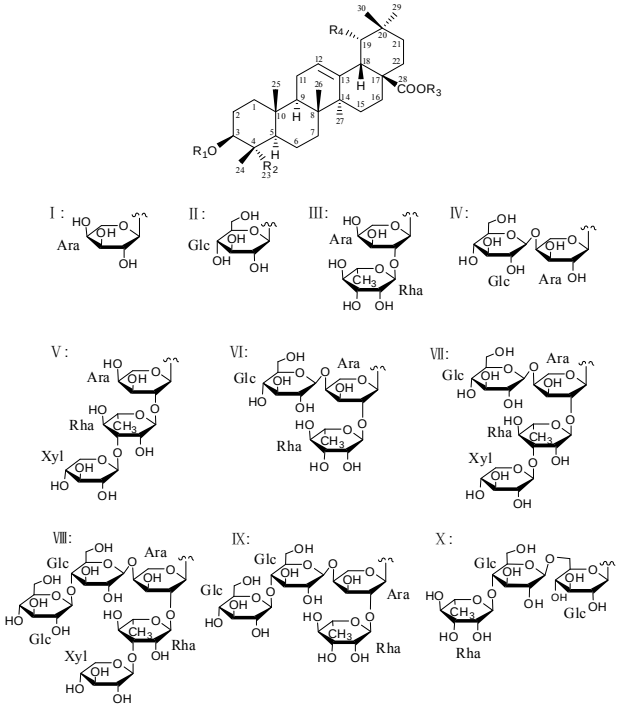

Figure 1. Structures of aglycones and sugar moieties of saponins 2 and 5−30 isolated from *Anemone taipaiensis*

2 Experimental

2.1 Materials and Instruments

The plant material was collected on Taibai Mountain, Shaanxi Province, China, in September 2009, and was identified by Prof. Ji-Tao Wang (Department of Pharmacog-nosy, School of Pharmacy, Shaanxi University of Chinese Medicine). A voucher specimen (NO.090918) was deposited in the Herbarium of Shaanxi University of Chinese Medicine. Instruments and reagents were omitted.

Table 1. Structures of saponins 2 and 5−30 isolated from *Anemone taipaiensis* (*represents new compound)

No.	R_1	R_2	R_3	R_4
2	I	CH_3	H	H
5	III	CH_2OH	H	H
6	V	CH_3	H	H
7	V	CH_2OH	H	H
8	V	CH_3	II	H
9	VI	CH_3	H	H
10	VI	CH_2OH	H	H
11*	VII	CH_2OH	H	H
12	VI	CH_2OH	II	H
13*	IX	CH_3	H	H
14	H	CH_3	X	H
15	VIII	CH_3	H	H
16	V	CH_3	X	H
17	I	CH_2OH	X	H
18*	IV	CH_3	X	OH
19*	V	CH_3	X	OH
20	VI	CH_2OH	X	H
21	IV	CH_2OH	X	H
22	V	CH_2OH	X	H
23	III	CH_2OH	X	H
24*	VIII	CH_3	X	H
25	VI	CH_3	X	H
26*	VIII	CH_3	X	OH
27*	VI	CH_3	X	OH
28*	IX	CH_2OH	X	H
29*	VII	CH_2OH	X	H
30*	VIII	CH_2OH	X	H

2.2 Extraction and Isolation

The air-dried rhizomes of *A. taipaiensis* (5 kg) were powdered and extracted with 70% EtOH (5 L × 3, 2 h/time) under reflux. The extract was concentrated under vacuum to give a residue (650 g) which was suspended in H_2O (8 L) and partitioned successively with petroleum ether (8 L × 2) and *n*-BuOH (8 L × 3). The *n*-BuOH extract (110 g) was subjected to column chromatography on silica gel (2200 g, 15 × 120 cm) and eluted with a $CHCl_3$-MeOH-H_2O gradient (10: 1: 0.05, 9: 1: 0.1, 8: 2: 0.2, 7: 3: 0.5, 6: 4: 0.8) to give 9 fractions (Fr.1−Fr.9). Compound **1** was crystaled from Fr.3 (18 g). Fr.4 (7.6 g) and Fr.5 (3.2 g) were chromatographed on silica gel (500 g, 5 × 100 cm; 280 g, 4 × 100 cm) with a $CHCl_3$-MeOH-H_2O gradient to yield sub-fractions from which compounds **2**−**4** and **5** were isolated. Fr.6 (4.5 g) and Fr.7 (3 g) were chromatographed on silica gel (400 g, 5 × 100 cm) with a $CHCl_3$-*n*-BuOH gradient to yield compound **6** and compound **7**, respectively. Fr.8 (15 g) was chromatographed on ODS C_{18} gel (300 g, 3 × 100 cm) with a MeOH-H_2O gradient to yield sub-fractions from which compounds **8**−**13** were isolated. Fr.9 (29.2g) was also chromatographed on ODS C_{18} gel (500 g, 3 × 100 cm) with a MeOH-H_2O gradient to yield four sub-fractions. Compounds **14**-**17**, **18**-**25**, **26**-**28** and **29**-**30** were isolated from Fr.9.1, Fr.9.2, Fr.9.3 and Fr.9.4, respectively. All sub-fractions were submitted to gel permeation chromatography on Sephadex LH-20 (900 g, 5 × 120 cm) in MeOH or $CHCl_3$-MeOH to remove the pigments and carbohydrates. Compounds **2** and **5**−**30** were isolated with repeating HPLC using mixtures of MeOH and H_2O: saponin **11** (30 mg, MeOH-H_2O, 86: 14, 8.0 mL/min, t_R 15.0 min from Fr.8.4); saponin **13** (70 mg, MeOH-H_2O, 86: 14, 8.5 mL/min, t_R 12.0 min from Fr.8.6); saponin **18** (12 mg, MeOH-H_2O, 56: 44, 6.5 mL/min, t_R 12.3 min from Fr.9.2.2); saponin **19** (12 mg, MeOH-H_2O, 56: 44, 6.5 mL/min, t_R 17.4 min from Fr.9.2.2); saponin **24** (45 mg, MeOH-H_2O, 65: 35, 7.0 mL/min, t_R 21.5 min from Fr.9.2.4); saponin **26** (23 mg, MeOH-H_2O, 54: 46, 6.0 mL/min, t_R 22.7 min from Fr.9.3.2); saponin **27** (28 mg, MeOH-H_2O, 54: 46, 6.0 mL/min, t_R 25.0 min from Fr.9.3.2); saponin **28** (55 mg, MeOH-H_2O, 55: 45, 6.0 mL/min, t_R 31.4 min from Fr.9.3.3); saponin **29** (44 mg, MeOH-H_2O, 55: 45, 6.0 mL/min, t_R 36.2 min from Fr.9.4.2); saponin **30** (250 mg, MeOH-H_2O, 55: 45, 6.0 mL/min, t_R 41.0 min from Fr.9.4.3).

2.3 Acid Hydrolysis and GC Analysis

Saponins **2** and **5**−**30** (each 3 mg) were heated with 1 mL 2 M/L CF_3COOH at 120 °C for 2 h, respectively. The reaction mixture was evaporated under vaccum and the residue was partitioned between CH_2Cl_2 and H_2O. The aqueous residue was evaporated under reduced preesure. Then 1 mL of pyridine and 2 mg of $NH_2OH{\cdot}HCl$ were added to the dry residue, and the mixtures were heated at 90 °C for 30 min. After the reaction mixtures were cooled, 0.5 mL of Ac_2O was added and the mixtures were heated at 90 °C for 1 h. The residue was partitioned between CH_2Cl_3 and H_2O. The organic layer was subjected to GC analysis. The sugar units were identified by comparing the retention times of the corresponding derivatives with those of the authentic samples prepared in the same manner.

2.4 Antitumor Bioassay

The cytotoxicity against human leukemia HL-60 cells, human hepatocellular carcinoma Hep-G2 cells and human glioblastoma U251MG cells was evaluated by MTT colorimetric assay described in previous papers [10,11], with doxorubicin (Sigma, ≥98%, USA) and nimustine hydrochloride (Sigma, ≥98%, USA) as positive controls. Dose response curves were plotted for the samples and the IC_{50} values were calculated as the concentrations of the test saponins resulting in 50% reduction of absorption compared to the control cells.

3 Results and Discussion

The nineteen known compounds were identified as *β*-sitosterol (**1**), 3*β*-O-(*α*-L-arabinopyranosyl} oleanolic acid (**2**), *β*-daucosterol (**3**), potengriffioside A (**4**), kalopanaxsaponin A (**5**), 3*β*-O-{*β*-D-xylopyranosyl-(1→3)-

978-1-61896-030-6 © 2012 SciRes.

α-L-rhamnopyranosyl-(1→2)-α-L-arabinopyranosyl} oleanolic acid (**6**), sapindoside B (**7**), 3β-O-{α-L- rhamnopyranosyl-(1→2)-[β-D-glucopyranosyl-(1→4)]-α-L-arabinopyranosyl} oleanolic acid (**9**), pulsatilla saponin D (**10**), cernusoide C (**12**), cussonside B (**14**), 3β-O-{β-D-xylopyranosyl-(1→3)-α-L-rhamnopyranosyl-(1→2)-[β-D-glucopyranos-yl-1→4)]-α-L-arabinopyranosyl} oleanolic acid (**15**), sieboldianoside B (**16**), cauloside D (**17**), hederacolchiside F (**20**), leontoside D (**21**), sieboldianoside A (**22**), kalopanaxsaponin B (**23**) and hederacolchiside E (**25**), respectively, by comparison of their spectroscopic analysis and chemical evidences with published values.

Table 2. ^{1}H- (500 MHz) and ^{13}C-NMR (125 MHz) chemical shifts of saponin 24 in pyridine-*d5*

C	δ_C	δ_H mult. (*J* in Hz)	C	δ_C	δ_H mult. (*J* in Hz)	C	δ_C	δ_H mult. (*J* in Hz)
1	38.9	1.44, 0.87 m	3-*O*-sugar			28-*O*-sugar		
2	26.7	2.02, 1.81 m	Ara			Glc II		
3	88.6	3.23 dd (4.0, 11.6)	1	105.2	4.71 d (7.0)	1	95.6	6.23 d (8.2)
4	39.5	–	2	75.5	4.51 m	2	73.8	4.11 m
5	56.0	0.75 d (11.5)	3	74.9	4.18 m	3	78.7	4.17 m
6	18.5	1.39, 1.23 m	4	80.2	4.20 m	4	70.8	4.29 m
7	33.0	1.37, 1.22 m	5	65.3	4.37,3.73 m	5	78.0	4.08 m
8	39.8	–	Rha I			6	69.1	4.63, 4.31 m
9	48.0	1.59 m	1	101.2	6.29 s	Glc III		
10	37.0	–	2	71.9	4.88 br s	1	104.8	4.97 d (7.8)
11	23.7	1.90, 1.85 m	3	82.8	4.74 d	2	75.3	3.92 m
12	122.8	5.38 br s	4	72.9	4.48 m	3	76.5	4.13 m
13	144.1	–	5	69.7	4.65 m	4	78.2	4.39 m
14	42.1	–	6	18.5	1.54 d (6.2)	5	77.1	3.64 dt
15	28.2	2.28, 1.13 m	Xyl			6	61.2	4.17, 4.06 m
16	23.3	2.03, 1.91 m	1	107.5	5.34 d (7.6)	Rha II		
17	47.0	–	2	75.6	4.05 m	1	102.7	5.84 s
18	41.6	3.16 dd (3.7, 13.4)	3	78.5	4.16 m	2	72.5	4.65 m
19	46.2	1.71, 1.20 m	4	71.1	4.17 m	3	72.7	4.52 m
20	30.7	–	5	67.4	4.33, 3.71 m	4	74.0	4.30 m
21	33.9	1.30, 1.08 m	Glc I			5	70.3	4.94 m
22	32.5	1.82, 1.74 m	1	106.7	5.10 d (7.9)	6	18.5	1.68 d (6.2)
23	28.1	1.29 s	2	75.4	4.03 m			
24	17.2	1.16 s	3	78.5	4.16 m			
25	15.6	0.85 s	4	71.2	4.22 m			
26	17.4	1.06 s	5	78.8	3.88 m			
27	26.0	1.23 s	6	62.5	4.47, 4.36 m			
28	176.5	–						
29	33.1	0.87 s						
30	23.6	0.87 s						

Compound **24** was positive to Liebermann-Burchard and Molish tests. The molecular formula was established as $C_{70}H_{114}O_{34}$ from the $[M+Na]^+$ ion at *m/z* = 1521.7081 (calcd. for $C_{70}H_{114}O_{34}Na^+$, 1521.7089) in the positive ion mode HR-ESI-MS. The analysis of the NMR data (Table 2) indicated that **24** was a saponin containing one triterpene aglycone and seven monosaccharides. The ^{1}H- and ^{13}C-NMR spectra showed seven tertiary methyl groups at δ_H = 0.85 (s, 1×CH_3), 0.87 (s, 2×CH_3), 1.06 (s, 1×CH_3), 1.16 (s, 1×CH_3), 1.23 (s, 1×CH_3), and 1.29 (s, 1×CH_3) and one trisubstituted olefinic proton at δ_H = 5.38 (br s) coupled with seven sp^3 carbons at δ_C = 15.6, 33.1, 23.6, 17.4, 17.2, 26.0 and 28.1 and two sp^2 olefinic carbons at δ_C = 122.8 and 144.1 (Table 2). The assignments of the NMR signals associated with the aglycone moiety were derived from ^{1}H-^{1}H COSY, TOCSY, HSQC, HMBC and NOESY experiments. The aglycone of **24** was identified as oleanolic acid [12]. The chemical shifts of C-3 (δ_C = 88.6) and C-28 (δ_C = 176.5) revealed that **24** was a bisdesmosidic glycoside. The correlations of H-3 with H_3-23 and H-5 observed in the NOESY spectrum indicated the β-configuration for the 3-*O*-sugar moiety (Fig. 2). The presence of L-arabinose (Ara), D-xylose (Xyl), L-rhamnose (Rha) and D-glucose (Glc) in a 1:1:1:2 ratio was established by acid hydrolysis followed by GC analysis of the corresponding derivatives. Meanwhile, the ^{1}H-NMR spectrum of saponin **24** exhibited seven anomeric protons at δ = 6.32 (s), 6.23 (d, *J* = 8.2 Hz), 5.84 (s), 5.34 (d, *J* = 7.6 Hz), 5.10 (d, *J* = 7.9 Hz), 4.97 (d, *J* = 7.8 Hz) and 4.71 (d, *J* = 7.0 Hz), and two methyl groups of 6-deoxy-hexopyranosyl moiety at δ 1.68 (d, *J* =6.2 Hz) and δ 1.54 (d, *J* =6.2 Hz). The β anomeric configurations for the xylose and glucose units were deduced from their $^3J_{H\text{-}1/H\text{-}2}$ coupling constants (7.6 and 7.8~8.2 Hz). The arabinose unit was determined to have an α anomeric configuration on the basis of the $^3J_{H\text{-}1/H\text{-}2}$ (7.0 Hz) value observed in the $^4C_1$ form. Although the anomeric proton of the rhamnose moiety was observed as a singlet in the ^{1}H-NMR spectrum, the ^{13}C-NMR shift of Rha C-5 at δ= 69.7 and 70.3 indicated the α anomeric configuration [13]. All proton signals due to sugars were identified by careful analysis of the ^{1}H-^{1}H COSY, TOCSY and NOESY spectra, and the carbon signals were assigned by HSQC and further confirmed by HMBC spectra (Table 2). Data from the above experiments indicated that the seven sugar residues are in their pyranose forms. In the HMBC spectrum of **24**, a cross peak between C-3 of the aglycone and H-1 of Ara indicated that Ara was connected to C-3 of the aglycone. The linkage of the terminal glucose at C-4 of Ara was indicated by the cross peak Glc I H-1/Ara C-4. Similarly the linkages of the terminal xylose at the C-3 of Rha I in turn linked to C-2 of Ara were indicated by cross peaks Xyl H-1/Rha I C-3 and Rha I H-1/Ara C-2; the linkages of terminal rhamnose at C-4 of Glc II in turn linked to C-6 of Glc III and in turn linked to C-28 of the aglycone were indicated by cross peaks Rha II H-1/Glc II C-4, Glc II H-1/Glc III C-6 and Glc III H-1/C-28. The conclusion was confirmed by the NOESY correlations as shown in Fig. 2. Accordingly, the structure of saponin **24** was elu-

cidated as 3β-O-{β-D-xylopyranosyl-(1→3)-α-L-rhamnopyranosyl-(1→2)-[β-D-glucopyranosyl-(1→4)]-α-L-arabinopyranosyl} oleanolic acid 28-O-{α-L-rhamnopyranosyl-(1→4)-β-D-glucopyranosyl-(1→6)-β-D-glucopyranoside}.

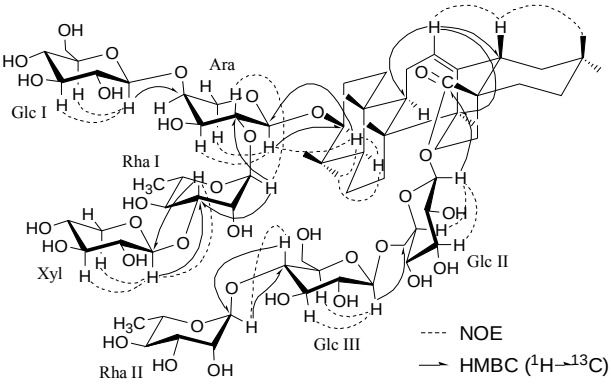

Figure 2. Key NOESY and HMBC correlations for saponin 24

The other nine new saponins **11**, **13**, **18**, **19** and **26**−**30**, and the new natural product **8** were identified, by extensive spectral analysis and chemical evidences, as 3β-O-{β-D-xylopyranosyl-(1→3)-α-L-rhamnopyranosyl-(1→2)-[β-D-glucopyranosyl-(1→4)]-α-L-arabinopyranosyl} hederagenin(**11**), 3β-O-{β-D-xylopyranosyl-(1→3)-α-L-rhamnopyranosyl-(1→2)-[β-D-glu-copyranosyl-(1→4)-β-D-glucopyranosyl-(1→4)]-α-L-arabinopyranosyl} oleanolic acid (**13**), 3β-O-{β-D-glucopyranosyl-(1→4)-α-L-arabinopyranosyl} siaresinolic acid 28-O-{α-L-rhamnopyranosyl-(1→4)-β-D-glucopyranosyl-(1→6)-β-D-glu-copyranoside} (**18**), 3β-O-{β-D-xylopyranosyl-(1→3)-α-L-rhamnopyranosyl-(1→2)-α-L-arabinopyranosyl} siaresinolic acid 28-O-{α-L-rhamnopyranosyl-(1→4)-β-D-glucopyranosyl-(1→6)-β-D-glucopyranoside} (**19**), 3β-O-{β-D-xylopyranosyl-(1→3)-α-L-rhamnopyranosyl-(1→2)-[β-D-glucopyranosyl-(1→4)]-α-L-arabinopyranosyl} siaresinolic acid 28-O-{α-L-rhamnopyranosyl-(1→4)-β-D-glucopyranosyl-(1→6)-β-D-glucopyranoside} (**26**), 3β-O-{α-L-rhamnopyranosyl-(1→2)-[β-D-glucopyranosyl-(1→4)]-α-L-arabinopyranosyl} siaresinolic acid 28-O-{α-L-rhamnopyranosyl-(1→4)-β-D-glucopyranosyl-(1→6)-β-D-glucopyranoside} (**27**), 3β-O-{β-D-xylopyranosyl-(1→3)-α-L-rhamnopyranosyl-(1→2)-[β-D-glucopyranosyl-(1→4)-β-D-glucopyranosyl-(1→4)]-α-L-arabinopyranosyl} hederagenin 28-O-{α-L-rhamnopyranosyl-(1→4)-β-D-glucopyra-nosyl-(1→6)-β-D-glucopyranoside} (**28**), 3β-O-{β-D-glucopy-ranosyl-(1→4)-β-D-glucopyranosyl-(1→4)-[α-L-rhamnopyranosyl-(1→2)]-α-L-arabinopyranosyl} hederagenin 28-O-{α-L-rhamnopyranosyl-(1→4)-β-D-glucopyranosyl-(1→6)-β-D-glu-copyranoside} (**29**), 3β-O-{β-D-xylopyranosyl-(1→3)-α-L-rhamnopyranosyl-(1→2)-[β-D-glucopyranosyl-(1→4)]-α-L-ar-abinopyranosyl} hederagenin 28-O-{α-L-rhamnopyranosyl-(1→4)-β-D-glucopyranosyl-(1→6)-β-D-glucopyranoside} (**30**) and 3β-O-{β-D-xylopyranosyl-(1→3)-α-L-rhamnopyranosyl-(1→2)-α-L-arabinopyranosyl} oleanolic acid 28-O-β-D-glucopyranoside (**8**), respectively.

The preliminary cytotoxic assay (Table 3) showed that saponins **6**, **7**, **9**-**11** and **13**, possessed free carboxylic group at C-28, displayed significant cytotoxicity against human leukemia HL-60 cells and human hepatocellular carcinoma Hep-G2 cells. Saponin **9** showed the most potent cytotoxicity with IC_{50} values of 1.31 and 2.81 μM/L. The preliminary structure-activity relationship was also elucidated. We postulated that the characteristic structural features of potent cytotoxic saponins were to have α-L-rhamnopyranosyl-(1→2)-α-L-arabinopyranosyl group at C-3 and a free carboxylic group at C-28 of the oleanane skeleton. Earlier studies on the cytotoxicity of similar compounds against other three human cancer cell lines have reached the same result [14].

Table 3. Cytotoxic activity of saponins 6−13 against three cancer cell lines *in vitro* (IC_{50}, μmol/L)

No.	HL-60	Hep-G2	U251MG		
	72 h	*72 h*	*24 h*	*48 h*	*72 h*
6	10.12 ± 0.54[a]	2.83 ± 0.21	14.82 ± 0.48	11.16 ± 0.56	9.50 ± 0.56
7	8.98 ± 0.48	5.62 ± 0.25	20.73 ± 0.78	23.54 ± 0.92	19.67 ± 0.45
8	24.77 ± 2.12	70.48 ± 5.74	>64	>64	>64
9	1.31 ± 0.12	2.81 ± 0.18	2.34 ± 0.34	1.47 ± 0.15	1.37 ± 0.22
10	9.39 ± 0.48	5.70 ± 0.32	7.64 ± 0.66	8.22 ± 0.68	15.35 ± 0.42
11	5.78 ± 0.28	3.41 ± 0.22	2.57 ± 0.18	1.72 ± 0.21	1.69 ± 0.32
12	>80	>80	>64	>64	>64
13	5.21 ± 0.32	3.82 ± 0.31	4.58 ± 0.63	2.63 ± 0.63	2.45 ± 0.42
D[b]	0.27 ± 0.02	0.46 ± 0.04	–	–	–
N[c]	–	–	1.32 ± 0.09	1.08 ± 0.05	0.95 ± 0.06

a. The data represent the mean plus SD of three independent experiments in which each compound concentration was tested in three replicate wells.
b. Doxorubicin (D) as positive controls.
c. Nimustine hydrochloride (N) as positive controls.

Saponins **9**, **11** and **13** exhibited significant cytotoxicity against human glioma U-251MG cells. The most potent one was **9** with an IC_{50} value of 1.37 μmol/L in a 72 h test, which was almost as equivalent as the clinical commonly used anti-glioblastoma agent ACNU (nimustine hydrochloride). Glioblastoma multiforme is the most common and lethal primary brain malignancy. Interstitial chemotherapy has been practiced for malignant brain tumors with administering chemotherapeutic compounds directly into the tumor which provide increased and prolonged drug concentration in the tumor, reduction of systemic toxicity and bypassing the blood-brain barrier. Meanwhile, interstitial chemotherapy can avoid the hemolysis effect of saponins. Therefore, saponins with anti-tumor activity could be developed as ideal chemotherapeutic agents. Clearly, the promising saponins **9, 11** and **13** merit further study as potential anti-glioblastoma agents. The mechanism of

978-1-61896-030-6 © 2012 SciRes.

these saponins to induce apoptosis of glioblastoma cells is now being investigated. Meanwhile, two relatively animal models for interstitial chemotherapy of glioblastoma have been established for the further studies on these saponins.

Acknowledgement

This work was financially supported by the National Natural Science Foundation of China (No. 30873402).

References

[1] Chinese Flora, vol. 28. Beijing: Science Press, 1980, pp. 53–54.
[2] M. K. Wang, F. E. Wu, and Y. Z. Chen, "Triterpenoid saponins from *Anemone hupehensis*," Phytochemistry, vol. 44, No. 2, 1997, pp. 333-335.
[3] W. C. Ye, Q. W. Zhang, G. S. Pan, S. X. Zhao, and C. T. Che, "Two unusual oleanane saponins from *Anemone anhuiensis*," Planta Med., vol. 67, No. 6, 2001, pp. 590-592.
[4] Y. Mimaki, K. Watanabe, Y. Matsuo, and H. Sakagami, "Triterpene glycosides from the tubers of *Anemone coronaria*," Chem. Pharm. Bull., vol. 57, No. 7, 2009, pp. 724-729.
[5] X. Chen, J. C. Lu, W. F. He, H. D. Chi, K. Yamashita, M. Manabe, and H. Kodama, "Antiperoxidation activity of triterpenoids from rhizome of *Anemone raddeana*," Fitoterapia, vol. 80, No. 2, 2009, pp. 105-111.
[6] H. F. Tang, Y. H. Yi, L. Li, P. Sun, S. Q. Zhang, Y. P. Zhao, "Three new asterosaponins from the starfish *Culcita novaeguineae* and their bioactivity," Planta Med., vol. 71, No. 5, 2005, pp. 458-463.
[7] H. Lin, X. Zhang, G. Cheng, H. F. Tang, W. Zhang, H. N. Zhen, et al, "Apoptosis induced by ardipusilloside III through BAD dephosphorylation and cleavage in human glioblastoma U251MG cells," Apoptosis, vol. 13, No. 2, 2008, pp. 247-257.
[8] Y. Tian, H. F. Tang, F. Qiu, X. J. Wang, X. L. Chen, and A. D. Wen, "Triterpenoid saponins from *Ardisia pusilla* and their cytotoxic activity," Planta Med., vol. 75, No. 1, 2009, pp. 70-75.
[9] H. F. Tang, J. Yun, H. W. Lin, X. L. Chen, X. J. Wang, and G. Cheng, "Two new triterpenoid saponins cytotoxic to human glioblastoma U251MG cells from *Ardisia pusilla*," Chem. Biodivers., vol. 6, No. 9, 2009, pp. 1443-1452.
[10] N. Ma, H. F. Tang, F. Qiu, H. W. Lin, X. R. Tian, and M. N. Yao, "Polyhydroxysteroidal Glycosides from the Starfish *Anthenea chinensis*," J. Nat. Prod., vol. 73, No. 4, 2010, pp. 590-597.
[11] B. S. Joshi, K. M. Moore, S. W. Pelletier, M. S. Puar, and B. N. Pramanik, "Saponins from *Collinsonia canadensis*," J. Nat. Prod., vol. 55, No. 10, 1992, pp. 1468-1476.
[12] T. H. Xu, Y. J. Xu, H. X. Li, D. Han, H. F. Zhao, S. X. Xie, et al, "Two new triterpenoid saponins from *Pulsatilla cernua* (Thunb.) Bercht. et Opiz.," J. Asian Nat. Prod. Res., vol. 9, No. 6-8, 2007, pp. 705-711.
[13] Q. Zheng, K. Koike, L. K. Han, H. Okuda, and T. Nikaido, "New biologically active triterpenoid saponins from *Scabiosa tschiliensis*," J. Nat. Prod., vol. 67, No. 4, 2004, 604-613.
[14] S. C. Bang, J. H. Lee, G. Y. Song, D. H. Kim, M. Y. Yoon, and B. Z. Ahn, "Antitumor activity of *Pulsatilla koreana* saponins and their structure-activity relationship," Chem. Pharm. Bull., vol. 53, No. 11, 2005, pp. 1451-1454.

The Research of Two Secondary Metabolites from the Plant Endophytic Fungus Pestalotiopsis Fici

Jing YU[1], Jing WANG[1], Chunming LIU[1], Zhiqiang LIU[2]
[1]*The Central Laboratory, Changchun Normal University, Changchun, China*
[2]*Laboratory of New Drug Research, Changchun Institute of Applied Chemistry, Chinese Academy of Sciences, Changchun, China*
Email: yujing5159@yahoo.com.cn

Abstract: Pestalofone E and Pestalofone F are new cyclohexanone derivatives from the plant endophytic fungus Pestalotiopsis fici. Pestalofone E and Pestalofone F, which isomeric compounds, have biological activities. It's important to develop a method of differentiating these. In this work, technology of mass spectrometry was established to analyze, distinguish them and evaluate its antioxidant activity.

Keywords: ESI-MS; Pestalofone E; Pestalofone F; antioxidant activity; secondary metabolites

1 Introduction

Plant endophytic fungi has attracted more attention due to producing a variety of bioactive secondary metabolites by culture technology in the past few decades, meanwhile, it will be become an important source for therapeutics. The fungal genus Pestalotiopsis is a common one in all of fungal types, which is widely distributed in various ecosystems. In recent years, new bioactive secondary metabolites with unique structural features were found in the fungal genus Pestalotiopsis [1-5]. The technology of mass spectrometry has been widely applied to many aspects [6-7]. Mass spectrometry applied to the study of antioxidant activity got a certain progress [8-10]. The research of mass spectrometry method in the analysis of these new metabolites is particularly important. Therefore, in this paper, two secondary metabolites from plant endophytic fungus Pestalotiopsis fici was preliminarily studied.

2 Experimental

2.1 Apparatus and Reagents

MS^n experiments were carried out on a Thermo Scientific LCQ Fleet mass spectrometer (Thermo Fnnigan, San Jose, CA, USA) equipped with an electrospray ionization (ESI) source. Methanol was of HPLC grade and purchased from Fisher Scientific Company chemical Ltd. (Pittsburg, PA, USA). Two secondary metabolites-Pestalofone E and Pestalofone F were provided by Institute of Microbiology, Chinese Academy of Sciences.

2.2 Experimental Procedure

100.0 μg two kinds of secondary metabolites were dissolved in 1 mL HPLC methanol. In this paper, two econdary metabolites were preliminarily studied by electrospray ionization mass spectrometry (ESI-MS). To get a better mass spectrum, at first, the experiment was carried out to optimize instrument parameters. Then, ESI-MS/MS of the two compounds and antioxidant research were analyzed. The operating parameters were as follows: The samples were introduced via a syringe pump at a flow rate of 3 μL/min. The capillary temperature was controlled at 275 ℃. Capillary Voltage was at -32 V, Tube lens was at -125 V, RT lens offset was at 1.5 V, lens 0 voltage was at 1.0 V, multipole 1 offset was at 9.0 V, multipole 0 offset was at 3.25 V, lens 1 voltage was at 8 V, gate lens voltage was at 40 V, front lens was at 48 V. The isolation width for ESI-MSn was 2.0 Da, and the collision energy (%) was 20-25%.

3 Results and Discussion

3.1 Optimization of ESI-MS Condition

Pestalofone E and Pestalofone F, which are isomeric compounds, are new cyclohexanone derivatives from the plant endophytic fungus Pestalotiopsis fici. Molecular formula and relative molecular mass are $C_{33}H_{36}O_{12}$ and 624, separately. The molecular structures of two compounds were illustrated in Figure 1. Its structure has been verified by ^1H, ^{13}C NMR and HMQC, as shown in Table 1[2]. In the negative and positive ion mode, the optimization of ESI-MS parameters were got using automatic adjustment. The sheath gas and auxiliary flow rates, the spray voltage and capillary temperature were obtained by manual adjustment. In the negative ion mode, the two compounds had an ideal mass spectrums, as shown in Figure 2.

978-1-61896-030-6

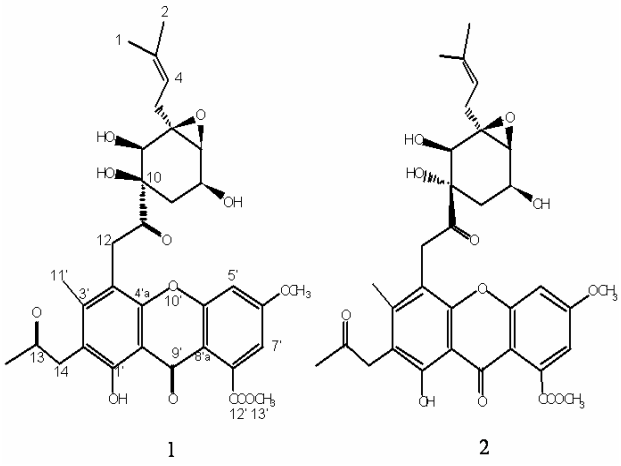

Figure 1. Structure of two secondary metabolites-Pestalofone E(1), Pestalofone F(2)

Table 1. NMR data of Pestalofone E and Pestalofone F (Acetone-d_6)

Position	Pestalofone E		Pestalofone F	
	$\delta_H{}^a$ (J in Hz)	$\delta_C{}^b$	$\delta_H{}^a$ (J in Hz)	$\delta_C{}^b$
1	1.66, s	18.1, CH_3	1.59, s	18.0, CH_3
2	1.72, s	25.9, CH_3	1.64, s	25.8, CH_3
3		135.4, qC		135.5, qC
4	5.22, t (6.5)	118.8, CH	5.18, t (6.5)	118.7, CH
5a	2.35, dd (15, 6.5)	34.5, CH_2	2.27, dd (15, 6.5)	32.6, CH_2
5b	2.69, dd (15, 6.5)		2.80, dd (15, 6.5)	
6		64.9, qC		65.9, qC
7	3.39, d (1.5)	63.9, CH	3.34, d (3.5)	62.3, CH
8	4.30, dddd (10, 5.5, 5.0, 1.5)	65.7, CH	4.25, ddd (6.0, 5.5, 3.5)	64.9, CH
9a	1.92, dd (16, 5.5)	30.4, CH_2	1.99, d (5.5)	30.3, CH_2
9b	2.04, dd (16, 10)			
10		80.8, qC		81.8, qC
11		208.4, qC		211.4, qC
12a	4.30, d (19)	35.9, CH_2	4.38, d (19)	36.3, CH_2
12b	4.58, d (19)		4.45, d (19)	
13		205.4, qC		205.6, qC
14	3.91, s	40.9, CH_2	3.92, s	40.9, CH_2
15	2.18, s	29.0, CH_3	2.19, s	29.2, CH_3
16	3.96, d (10)	72.5, CH	3.96, d (10)	70.5, CH
1'		158.4, qC		158.5, qC
2'		117.5, qC		117.4, qC
3'		148.9, qC		148.6, qC
4'		113.4, qC		113.4, qC
4'a		153.4, qC		153.2, qC
5'	7.17, d (2.0)	102.7, CH	7.27, d (2.0)	102.4, CH
6'		165.9, qC		166.1, qC
7'	6.96, d (2.0)	113.0, CH	6.96, d (2.0)	113.4, CH
8'		136.2, qC		136.1, qC
8'a		110.9, qC		111.3, qC
9'		181.0, qC		180.9, qC
9'a		106.7, qC		106.7, qC
10'a		159.0, qC		159.0, qC
11'	2.19, s	17.3, CH_3	2.19, s	17.2, CH_3
12'		169.1, qC		169.1, qC
13'	3.91, s	53.0, CH_3	3.91, s	53.0, CH_3
14'	4.00, s	56.9, CH_3	4.00, s	57.0, CH_3
OH-8	4.03, d (5.0)		4.32, d (6.0)	
OH-10	4.71, s		4.42, s	
OH-16	3.82, d (10)		4.05, d (10)	
OH-1'	12.81, s		12.82, s	

[a]Recorded at 400 MHz. [b]Recorded at 100 MHz.

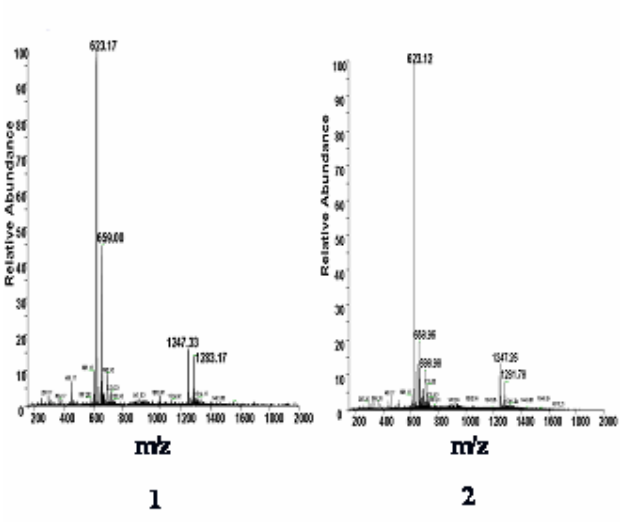

Figure 2. ESI-MS profiles of Pestalofone E(1), Pestalofone F(2) in the negative mode

3.2 ESI-MS/MS Study of Two Compounds

As shown in Figure 1, Pestalofone F and Pestalofone E have structural differences at C-10 position and they are epimer. The two compounds were analyzed by ESI-MS, the same molecular ion peak were found in negative ion mode. By means of ESI-MS^2, fragment ions were got, as shown in Figure 3. From the Figure 3, m/z 441 $[M-H]^-$) was a characteristic fragment ion and found in the Pestalofone F, meanwhile, the abudance of ion is 100%. This ion wasn't discovered in the Pestalofone E. Through the technology of mass spectrometry, the distinction of Pestalofone E and Pestalofone F is simple and fast.

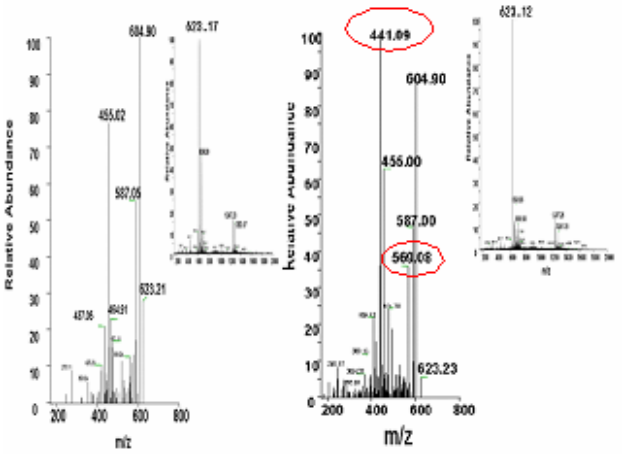

Figure 3. ESI-MS^2 profiles of Pestalofone E (left), Pestalofone F (right) in the negative mode

3.3 Antioxidant Activity of Two Compounds

The antioxidant activity of two secondary metabolites from the plant endophytic fungus Pestalotiopsis fici was studied by the technology of mass spectrometry. At first, ESI-MS was applied to the analysis of DPPH in methanol, as shown in Figure 4. Relative molecular mass of DPPH is 394, m/z 394 could be seen from the Figure 4, but, m/z 226 became the molecular ion peak. In the ESI-MS^2 experiment, m/z 394 ion yielded one main daughter ion at m/z 226. It can be seen m/z 226 would be fragment ion from m/z 394 ion. Later, excess DPPH methanol solution was mixed with two kinds of two compounds respectively at room temperature for 3 hours. Then, ESI-MS was applied to the analysis of two mixtures; two different mass spectrometry datas were got, as can be seen in Figure 5. From figure 5-1, the compound Pestalofone E at m/z 623 ion peak decreased significantly, the m/z 659 ion became the molecular ion peak. m/z 659 ion previously appeared in ESI-MS profile of Pestalofone E, The reason would be Pestalofone E combined with the methanol. From the Figure 5-2, the compound Pestalofone F at m/z 623 ion peak also decreased significantly, the m/z 227 ion became the molecular ion. The m/z 227, m/z 394, m/z 439 ions were present in ESI-MS profile of the single sample DPPH, which appeared in the negative ion mode. Possible reason was that Pestalofone F responsed fully with DPPH, excessive DPPH played a major role in negative mode.

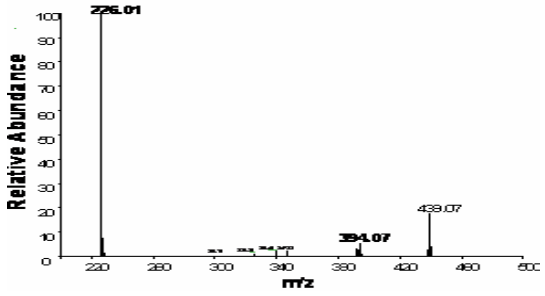

Figure 4. ESI-MS profile of DPPH in the negative mode

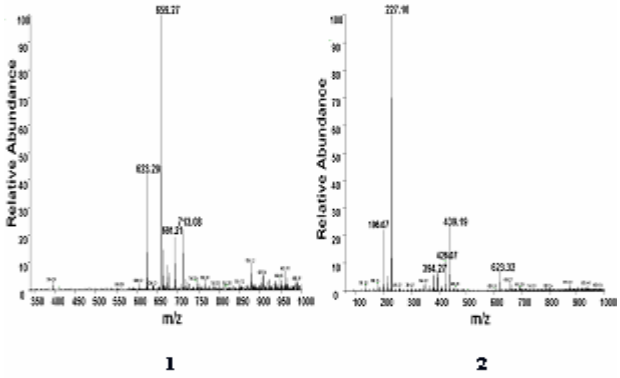

Figure 5. ESI-MS profiles of Pestalofone E+DPPH(1), Pestalofone F+DPPH(2) in the negative mode

4 Conclusion

This work studied two secondary metabolites from the plant endophytic fungus Pestalotiopsis fici using technology of mass spectrometry. Through the characteristic fragment ions of two secondary metabolites, it can quickly distinguish and analyze the secondary metabolites. Secondly, technology of mass spectrometry was applied into studying their antioxidant activities. The research showed that two compounds had some antioxidant activity; it will become the focus of follow-up work. This work has some value and practical significance.

Acknowledgement

Supported by the National Natural Science Foundation of China (No. 30970299), the Natural Science Foundation of Jilin Province of China (No. 20102203, 200905109, 20090936, 2009D206). Thanks for Liu Zhi-qiang teacher from Changchun Institute of Applied Chemistry, Chinese Academy of Sciences.

References

[1] L.Liu, S.C.Liu, X.L.Chen, etal. Pestalofones A–E, bioactive cyclohexanone derivatives from the plant endophytic fungus Pestalotiopsis fici [J]. Journal of Bioorganic&Medicinal Chemistry, 2009, 17:606-613.

[2] L.Liu. Chemical Investigation of the Plant Endophytic Fungus Pestalotiopsis fici[D]. Institute of Microbiology, Chinese Academy of Sciences, 2009, 5.

[3] S.C Liu, L. Liu. Isoprenylated chromones from the plant endophytic fungus Pestalotiopsis fici[J]. Journal of Mycosystema, 2010, 29(4):582-587.

[4] L.Liu, S.C.Liu, Shubin Niu, etal. Isoprenylated Chromone Derivatives from the Plant Endophytic Fungus Pestalotiopsis fici[J]. Journal of Natural Products, 2009, 72, 1482-1486.

[5] L.Liu, R.R.Tian, S.C.Liu, etal. Pestaloficiols A–E,bioactive cyclopropane derivatives from the plant endophytic fungus Pestalotiopsis fici[J]. Journal of Bioorganic&Medicinal Chemistry, 2008, 16, 6021-6026.

[6] J.Wang, H.LBai, C.M.Liu, etal. Isolation and Purification of Ginsenosides from Plant Extract of Panax quinque folium L. by High Performance Centrifugal Partition Chromatography Coupled with ELSD[J]. Chromato-graphia, 2010, 71 (3-4):267-271.

[7] J. Wang, C.M.Liu, L.Li,etal. Isolation of four high-purity dammarane saponins from extract of Panax notoginseng by centrifugal partition chromatography coupled with evaporative light scattering detection in one operation[J].Phytochemical Analysis, 2011.

[8] E.H.Liu, L.W.Qi, Y.B.Peng, etal. Rapid separation and identification of 54 major constituents in Buyang Huanwu decoction by ultra-fast HPLC system coupled with DAD-TOF/MS [J]. Journal of Biomedical Chromatography, 2009, 23, 828-842.

[9] D.Tang, H.J.Li, J.Chen, etal. Rapid and simple method for screening of natural antioxidants from Chinese herb Flos Lonicerae Japonicae by DPPH-HPLC-DAD-TOF/MS[J]. Journal of Separation Science, 2008, 31, 3519-3526.

[10] C.R.Sun, J.D.Fu, J.J.Chen, etal. On-line HPLC method for screening of antioxidants against superoxide anion radical from complex mixtures[J]. Journal of Separation Science, 2010, 33, 1018-1023.

978-1-61896-030-6 © 2012 SciRes.

Research on the Chromatographic Fingerprint of Herbal Preparations Fengliao Changweikang Oral Liquid

Xian YANG[1], Xue ZHANG[2], Xiaodong YU[1], Shuiping YANG[3]
[1]*College of Life Sciences, Chongqing Normal University, Chongqing, China*
[2]*Institute of Material Medical Planting, Chongqing Academy of Chinese Materia Medica, Chongqing, China*
[3]*College of Resources and Environment, Southwest University, Chongqing, China*
Email: yyxdsp@com

Abstract: A simple, reliable and repeatable method was based by high performance liquid chromatography-photodiode array detection (HPLC-DAD). The HPLC fingerprints of Fengliao Changweikang(FC)oral liquid and its ingredients were evaluated by the digital evaluation system of traditional Chinese medicines(TCMs). In addition, as the indicator components, contents of rutin, hyperin and isorhamnetinn were also determined. Chromatographic fingerprint, together with the contents of the markers were applied for quality control of FC oral liquid. FC oral liquid consists of two chinese herbs including: Niuerfeng, Laliao. In accordance with State Food and Drug Administration (SFDA) requirements, raw material medicine of FC oral liquid should be also established chromatographic fingerprint. Calculating similarity degree by the included-angle cosine method, and using correlation coefficient method to verify result.

Keywords: Fingerprinst; FC oral liquid; HPLC-DAD; TCMs

1 Introduction

Traditional Chinese medicines (TCMs), originated from nature, have been widely used in clinic practice [1]. However, in the development process of TCMs, their quality controls are always a bottleneck. The herbal medicines and their preparations for the establishment of the corresponding fingerprint are becoming an effective means to improve the inherent quality at this stage [2]. Since 2000, the SFDA required that all the injections made from herbal medicines or their raw materials should be standardized by chromatographic fingerprint [3]. Niuerfeng and Laliao are widely used as TCMs and are officially listed in the Chinese Pharmacopoeia (The Pharmacopoeia Commission of P. R. China, 2005). Niuerfeng, the branches and leaves of Daphniphyllum calycinum Benth., is mainly favonoid, such as rutin. Laliao, the whole grass of polygonum hydropiper Linn. is too mainly favonoids, such as rutin, hyperin and isorhamnetin[4,5]. Fengliao Changweikang (FC) oral liquid consists of two chinese herbs including: 2000g of Niuerfeng 1000g of Laliao. Preparation technological process are showed at SFDA, license number: Z20090296. The pharmacological screening and a wide range of clinical applications revealed that FC oral liquid carry many biological activities, such as strengthening stomach function, treating abdominal distension, abdominal pain, diarrhea and other symptoms of a definite therapeutic effect [6].

As a result of systemic investigations, high performance liquid chromatography-photodiode array detection (HPLC–DAD) application for fingerprint analysis of Niuerfeng, Laliao and FC oral liquid have not been reported in the literatures. So, the HPLC fingerprints of FC oral liquid and its ingredients were evaluated by the digital evaluation system of TCMs. In addition, as the indicator components, contents of rutin, hyperin and isorhamnetinn were also determined. Chromatographic fingerprint, together with the contents of the markers were applied for quality control of FC oral liquid.

2 The Model

2.1 Materials and Chemicals

Rutin, hyperin and isorhamnetin were all obtained from the National Institute for the Control of Pharmaceutical and Biological Products (Beijing, China).Niuerfeng and Laliao samples were collected from different regions in China. Their identities were confirmed in Chongqing Academy of Chinese Materia Medica, by Professor Shuiping Yang. 11 batches of FC oral liquid samples were obtained from different pharmaceutical factories in China.

Methanol and acetonitrile used for HPLC analysis were of chromatographic grade and purchased from Alltech Scientific (Beijing, China). Distilled water was purified with a Milli-Q Academic ultra-pure water system (Billerica, MA, USA) prior to the use as HPLC mobile phase. A.R. grade phosphoric acid, acetic acid and formic acid for analysis were purchased from the first chemical company of Nanjing (Jiangsu, China).

2.2 Apparatus and Conditions

An HP 1200 Agilent system equipped with a quaternary gradient pump, an autosampler and DAD photodiode array detector were used. The analytical column was a C18 of waters (250mm×4.6mm I.D., Waters, Milford,

MA, USA) protected with a 4.0mm×3.0mm I.D.guard column (Phenomenex, ANPEL scientific instrument Co.LTD, Shanghai, China). Detection wavelengths were acquired at: 359nm. Methanol constituted solvent A and formic acid-water (0.4: 99.6;v/v/v) constituted solvent B.The gradient elution program was applied as follows: 0-5min kept at 29%A, 5–35 min linear increased from 29% to 50%A, 35–45 min linear decreased from 50 to 40% A. 45–60 min linear decreased from 40 to 29% A. flow rate of 0.8 mL/min. The injection volume was 10μL.

2.3 Preparation of Standard Solutions

Accurately weighed solid portions of each standard were dissolved in methanol to prepare stock solutions: 0.856mg/mL for rutin, 1.061mg/mL for hyperin, 1.520 mg/mL for isorhamnetin. Then, each stock solution was diluted step by step with the combined solution.

2.4 Sample Preparation

2.4.1 Raw Material Medicine Sample Preparation

Samples of 1.0g of dried and powdered Niuerfeng or Laliao was refluxed in water bath with 50mL of 60% ethanol for 60min, respectively. Samples were cooled. 60% ethanol methanol was added to compensate the lost volume, samples were filtered by 0.45μm membrane filtration.

2.4.2 FC Oral Liquid Preparation

10mL of FC oral liquid were diluted with mobile phase to 50mL.ultrasound for 5 minutes, remove and put cold, mobile phase was added to compensate the lost volume. The solution was filtered through a 0.45 μm membrane.

3 Innovation, Technology Transfer, and Technology Intensity

3.1 Linearity, the Detection Limit (LOD) and Limit of Quantification (LOQ) Test

The linearity calibration curves were constructed by six concentration assays of each standard in triplicate. All measurements were done in duplicate. Table 1 showed the results of the standard calibration curves of integrated peak area (n=3) and linearity (r^2). Calibration curves were linear with correlation coefficients >0.999 for all analytes. LOD and LOQ were the concentrations of a compound at which its signal-to-noise ratios (S/N) were detected as 3:1 and 10:1, respectively. They were determined by serial dilution of sample solution using the described HPLC–DAD/MS conditions. The results are shown in Table 1.

Table 1. Linearity, LOD and LOQ for FC oral liquid using the optimized method

Standard	Linear range (μg/mL)	Slope(k)	Intercept(m)	Regressa r^2 (n=5)	LOD[b] (μg/mL)	LOQ[c] (μg/mL)
rutin	0.2372-18.976	356549	13246	r=0.9996	0.01581	0.05271
Hyperin	0.00535-2.140	3.14484×106	208.5	r=1.0000	0.0007197	0.002399
Isorhamnetin	0.04012-8.024	574379	34772	r=0.9996	0.002921	0.009738

a Regression coefficient. b Limit of detection (3 S/N). c Limit of quantitation (10 S/N).

3.2 Precision and Recovery Tests

The same sample solutions were successively injected into HPLC in 0, 2, 4, 8, 16, 24h .The day precision was studied. The RSD of contents of three components in 0.7-1.2%, that day precision was good (Table 2). At the same time, the same sample solutions were injected into HPLC six times for continuously six days to study the inter-day precision, the RSD of contents of three components in 1.1-2.6%, that inter-day precision was comparatively well (Table 2).

The recoveries were determined by the method of standard addition. Six portions of FC oral liquid were spiked with the standards of three components. Then the samples were pretreated as described in section “Sample preparation”, and the results were summarized in Table 2. All recoveries obtained were very well, suggesting that the good recovery of the method.

Table 2. Summary of intra-day, inter-day precision in FC oral liquid

Peak No.	Standard	Intra-day precisions (mg/g)		inter-day precisions(mg/g)		Recovery(%)	
		$\bar{x} \pm SD$	RSD（%）	$\bar{x} \pm SD$	RSD（%）	mean	RSD（%）
11	rutin	0.349±0.008	1.0	0.341±0.006	2.4	100.5	2.2
15	Hyperin	0.026±0.010	1.2	0.018±0.012	1.1	99.3	2.3
21	Isorhamnetin	0.032±0.006	0.7	0.038±0.007	2.6	98.4	1.5

978-1-61896-030-6 © 2012 SciRes.

3.3 Determination of Samples

According to section"Sample preparation". The 3 components from the 11 batches Niuerfeng, polygonum hydropiper Linn. And FC oral liquid were detected. The average contents of main components were showed in Table 3. According to herb-combined prescription of FC oral liquid 1mL of FC oral liquid was equivalent to the crude herb of 2g Niuerfeng and 1g polygonum hydropiper Linn. Through 11 batches raw material medicine, the contents of rutin was 0.224-0.352mg/g in Niuerfeng, 0.155-0.235mg/g in Laliao. The contents of hyperin and isorhamnetin were 0.0249-0.0542mg/g and 0.017-0.0359mg/g in Laliao, respectively. In addition, as the indicator components,contents of rutin, hyperin and isorhamnetinn were also determined in FC oral liquid, the yield of rutin was in the range of 76.0-81.4%. the yield of hyperin and isorhamnetin were 71.8-76.1% and 68.1-76.9%, respectively. The result showed that preparation of the extraction rate was good.

Table 3. The quantities of the 3 components from the 11 batches of raw material medicine and FC oral liquid (n = 3)

Sample No.	Content						
	Niuerfeng(mg/g)	Laliao (mg/g)			FC oral liquid(mg/mL)		
1	0.272±0.011	0.181±0.011	0.0343±0.008	0.0170±0.015	0.349±0.008	0.0261±0.010	0.0124±0.006
2	0.224±0.013	0.168±0.012	0.0517±0.004	0.0247±0.016	0.295±0.013	0.0393±0.011	0.0181±0.004
3	0.232±0.006	0.155±0.014	0.0632±0.006	0.0299 ±0.007	0.298±0.007	0.0480±0.013	0.0230±0.005
4	0.326±0.009	0.217±0.005	0.0249 0.009	0.0288 ±0.003	0.418±0.006	0.0189±0.013	0.0211±0.006
5	0.259±0.015	0.173±0.009	0.0338±0.003	0.0257 ±0.011	0.333±0.010	0.0257±0.012	0.0175±0.008
6	0.351±0.016	0.234±0.006	0.0468 0.011	0.0337 ±0.004	0.450±0.011	0.0336±0.003	0.0253±0.002
7	0.258±0.012	0.172±0.021	0.0542 0.013	0.0221 ±0.009	0.331±0.009	0.0412±0.012	0.0163±0.005
8	0.241±0.021	0.161±0.022	0.0541±0.016	0.0371 ±0.013	0.309±0.007	0.0411±0.012	0.0282±0.003
9	0.352±0.024	0.235±0.013	0.0311±0.021	0.0241 ±0.015	0.452±0.002	0.0236±0.017	0.0183±0.011
10	0.295±0.013	0.217±0.017	0.0353±0.018	0.0322 ±0.019	0.417±0.010	0.0268±0.011	0.0244±0.007
11	0.320±0.013	0.214±0.014	0.0428±0.013	0.0359 ±0.003	0.411±0.006	0.0325±0.006	0.0273±0.001

4 Conclusion

4.1 Fingerprint Analysis of Niuerfeng, Laliao and FC Oral Liquid

(1) Common peaks

By comparisive chromatograms, based on the determination of common peak, according to statistics of the samples in descending chromatogram of strong signal peaks, reference peak which retention time appeared the middle and existed in all chromatograms of 11 samples was randomly selected. Among these components, rutin indicated a high and stable content, therefore it was chosen as the reference substance.

10μL sample solution was injected into the HPLC system. By comparing the peak retention time, peaks existed in all chromatograms of 11 samples were assigned as "common peaks", indicating the integrity among various samples. From the 11 samples, the chromatograms of FC oral liquid consisted of 22 common peaks within 60min (As showed Fig.1.). Niuerfeng consisted of 15 common peaks (as showed Fig.2), and Laliao consisted of 14 common peaks within 60 min. (As showed Fig.3).

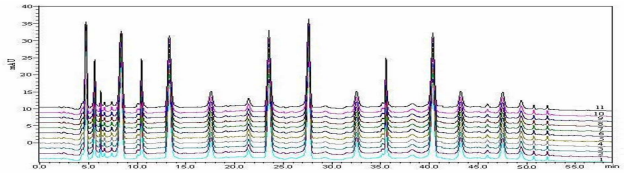

Figure 1. Chromatogram of FC oral liquid from different pharmaceutical factories

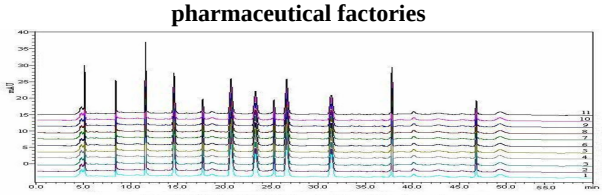

Figure 2. Chromatogram of Niuerfeng samples from different regions

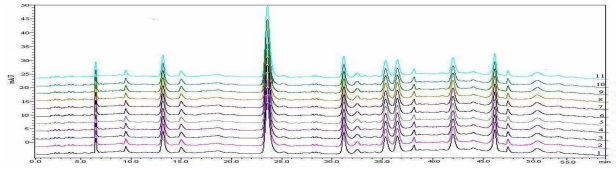

Figure 3. Chromatogram of Laliao samples from different regions

All common peaks' relative retention time and relative peak area were obtained with reference to rutin in FC oral liquid. R.S.D. values of the relative retention time of 22 common peaks in 11 batches samples were less than 1.0%, which means the common peaks were in good correspondence in all samples. Moreover, such low R.S.D. valves demonstrate that the fingerprint developed by HPLC had good stability and reproducibility. So, the peak profile of the 22 components made up the fingerprint of FC oral liquid. Likewise, values of the relative retention time of 15 common peaks in 11 batches samples were less than 1.0% in HPLC fingerprints of Niuerfeng from Table 9 to Table 10, R.S.D. values of the relative retention time of 15 common peaks in 11 batches samples were less than 1.0% in HPLC fingerprints of Laliao.

(2)Noncommon peaks

According to State Food and Drug Administration (SFDA) requirement, Besides the common peaks, there are about 5–16 noncommon peaks in each chromatogram, which represents the ambiguity,among the same kind of TCMs. Non-common peaks percentage of each batches Niuerfeng, Laliao and FC oral liquid preparations were calculated with the software of Excel 2003,respectively. According to above-mentioned methods to do strictly, The non-common peaks percentage of raw materials and FC oral liquid preparations in the respective total peak area were at 3.1 -6.5%, at 4.5 -7.1%, at 5.2 - 8.9% . less than the SFDA standard of 10%.

(3)The correlation between FC oral liquid preparations and their raw herbal medicines

SFDA suggested that all of herbal chromatograms should be evaluated by their similarities, which come from the calculation on the correlative coefficient and angle cosine value of original data [7]. With two different mathematic methods including correlation coefficient and the included angle cosine calculated with the software of Excel 2003, the data of fingerprints of 11 batches samples were processed to analyze similarity among these samples. According to the relative peak areas of 22 common peaks in the chromatograms of 11samples, the similarity analysis was conducted, and the results are showed that: two kinds of similarity calculations were more than 0.982. Which show that the technical specifications of the establishment of fingerprint was good stability and reproducibility.

Acknowledgement

This study was supported by the Fundamental Research Funds for the Central Universities, Project No.CDJXS11232241.

References

[1] Y.X. Liu, W.Wang, "Botanical drugs: Challenges and opportunities: Contribution to Linnaeus Memorial Symposium 2007,"*Life Sci*, Vol.82, No.9–10, 2008, pp.445-449.

[2] P.S. Xie, S.B. Chen, Y.Z. Liang, X.H. Wang, R.T. Tian, R. Upton, "Chromatographic fingerprint analysis-a rational approach for quality assessment of traditional Chinese herbal medicine," *J Chromatogr A* , Vol.1112, No.1–2, 2006, pp.171-180.

[3] Drug Administration Bureau of China,"Requirements for Studying Fingerprints of Traditional Chinese Medicine Injection," Drug Administration Bureau of China, Beijing, China. 2002.

[4] M.G. Derita, S.J. Gattuso, S.A. Zacchino, "Occurrence of polygodial in species of Polygonum genus belonging to Persicaria section," *Biochem Syst Ecol*, vol. 36, No.1, 2008, pp. 55-58.

[5] A. Hazarika, H.N. Sarma, "The estrogenic effects of Polygonum hydropiper root extract induce follicular recruitment and endometrial hyperplasia in female albino rats," *Contracept*, Vol.74, No.5, 2006, pp.426-434.

[6] M.G.Derita, M.L.Leivab, S.A. Zacchino,"Influence of plant part, season of collection and content of the main active constituent, on the antifungal properties of Polygonum acuminatum Kunth," *J Ethnopharmacol*, Vol.124, No.3, 2009, pp. 377-383.

[7] F,Gong, Y.Z. Liang, P.S. Xie, F.T. Chau, "Information theory applied to chromatographic fingerprint of herbal medicine for quality control," *J Chromatogr A*, Vol.1002, No.1–2, 2003, pp.25-40.

Effects of Brining, Drying and Roasting Conditions on Degradation of ATP and Its Related Compounds in Dried Duck Meat Slice

Gaojun SUN[1,2], Conggui CHEN[1], Bo YANG[1], Xiaoyan CHEN[1], Hongmei FANG[1], Wu WANG[1]
[1]*School of Biology and Food Engineering, Hefei University of Technology, Hefei, Anhui, China*
[2]*Anhui Tobacco Company, Hefei, Anhui, China*
Email: sun_gaojun@126.com, chen_conggui@hotmail.com, cplo@ntu.edu.tw

Abstract: The effects of brining, drying and roasting conditions on the degradation of adenosine triphosphate (ATP) in dried duck meat slice (DDMS) were studied. After brining for 2-3 h, adenosine monophosphate (AMP) degraded into inosine monophosphate (IMP) slowly, while easily into IMP when the brining time was 3-5 h, following sluggish transformation into inosine (I) which smoothly converted into hypoxanthine (HX). During the drying process, AMP converted into IMP with a low yield when drying time was 4-5 h, while IMP converted into I smoothly and I converted into HX tardily. Compared with the contents of the product roasted at 180°C for 2 min, IMP content was higher and I content was lower when roasted at 180°C for 6 min which were favorable to umami of the product. Generally, considering the effect of IMP and HX on the taste of DDMS, brining for 2 h with 1% NaCl, drying for 2 h at 65°C, and roasting for 6 h at 120°C favored the accumulation of IMP and low content of HX, which benefit for improving taste and declining off-taste. Those results indicated that above three treatments casted great impact on the degradation of ATP and the formation of its derivatives which were important to the flavor of DDMS.

Keywords: Brining; drying; roasting; ATP degradation; dried duck meat slice

1 Introduction

Flavor is one of the most important components of the eating quality of muscle foods [1-3]. The characteristic flavor substances of meat are formed during the cooking process in which the non-volatile flavor precursors transfer into flavor substances through a series of complex reactions [4-6]. Time, temperature and removal of water during the cooking process have influences on the development of the flavor compounds [7].

Flavor changes of meat are closely related with degradation of adenosine 5'-triphosphate disodium salt (ATP) and content of inosine 5'-monophosphate disodium salt (IMP). An important taste, "umami" (roughly translated as good taste or savory), is considered as a primary taste by Asian cultures even though Western science has somewhat accepted umami as the fifth basic taste sensation [8, 9]. IMP is a very important taste substance existed in meat tissues evoking an umami taste sensation [10] and the umami of several L-α-amino acids can be enhanced by adding IMP [11, 12]. Meat tissues in which the levels of IMP are very low have poor organoleptic acceptance.

The pathway of ATP catabolism in meat tissues has been demonstrated that ATP transferred in a sequence to adenosine 5'-diphosphate disodium salt (ADP), adenosine 5'-monophosphate (AMP), IMP, inosine (I) and hypoxanthine (HX) [13-15]. A few experimental results on thermal degradation of ATP in meat have been reported. Takashi, Maya, Hideyuki and Toshihiro studied the effect of retort conditions on ATP-related compounds in pouched fish muscle and found that IMP content was decreased by common retort process [16]. Kavitha and Modi investigated the effects of water activity and temperature on the degradation of IMP in chicken muscle [13]. Additionally, Kuda, Fujita, Goto and Yano examined the effect of freshness on ATP-related compounds in retorted fish [17]. Nguyen and Sporns reported the thermal degradation of ATP during canning of meat [18]. Macy, Naumann and Baily found that the concentration of AMP increased while that of IMP decreased during the heat treatment [19]. Chikuni found that IMP contents of pork decreased as a result of cooking treatment [20]. Tikk explored the degradation of IMP during the aging of pork and the potential relationship between IMP, HX, and sensory attributes of pork meat [14].

Dried meat slice is one of traditionally enjoyed meat products in China, which is produced by the procedures such as brining, drying and roasting. Cooked duck meat products have been widely popular among consumers in China and Southeast Asia because of its delicate flavor and texture [21, 22]. Dried duck meat slice (DDMS) is a new kind of dried meat slice.

Considering the importance of IMP to umami of meat, there is an urgent need to explore its formation and degradation under different meat processing conditions. Moreover, no study has been done to examine the effects

of binning, drying and roasting processes on the degradation of ATP in duck meat. The present work is an attempt to investigate the degradation of ATP during the binning, drying and roasting processes and provides basic theory for the flavor improvement of meat products.

2 Materials and Methods

2.1 Preparation of Initial Material

The proper amount of frozen duck legs, which were purchased from a local Hypermarket of the Carrefour Group, was thawed for 12 h at 2-4°C. Skin, bone, visible fat and connective tissue were removed from these legs, and then the legs were ground with a meat grinder (Shangyuan, SYP-MM12, Guangdong, China) fitted with a plate of 6 mm diameter holes. The ground meat was divided, packaged with a polyethylene bag (about 120 g/bag), sealed and finally stored in refrigerator (-20°C) for future use.

The proximate compositions of the ground meat were crude protein (19.54 ± 0.14)%, crude fat (6.73 ± 0.23)%, ash (0.94 ± 0.36)%, moisture (70.35 ± 0.19)% (all in triplicates). NaCl, white granulated sugar, five spice powder, soy protein isolate, monosodium glutamate and chill powder were purchased from a local Hypermarket of the Carrefour Group.

2.2 Brining of Duck Meat

The ground duck meats were thawed at 2-4°C for 24 h and mixed with NaCl (1-3%), white granulated sugar (3%), five spice powder (1%), soy protein isolate (2%), monosodium glutamate (0.1-0.5%) and chill powder (1-5%), then brined at 2-4°C for 0-5 h. The brined samples were dried at 65°C for 2 h and then roasted at 180°C for 4 min. The ATP-related compounds of the final products were determined by HPLC.

2.3 Drying of Duck Meat

The brined duck meats (2% NaCl, 4 h) were dried at 55-75°C for 1-5 h, and then roasted at 180°C for 4 min. The ATP-related compounds of the final products were determined by HPLC.

2.4 Roasting of Duck Meat

The brined duck meats (2% NaCl, 4 h) were dried at 65°C for 2 h, and then roasted at 120-240°C for 2-10 min. The ATP-related compounds of the final products were determined by HPLC.

2.5 Extraction of Nucleotides

The extraction of nucleotides was performed according to the method described by [23] with a slight modification. 5 gram of sample was minced and mixed with 30 mL 5% perchloric acid (PCA). The mixture was immediately homogenized (2×20 s at 10000 rpm) in the ice bath with a FS-2 blender (Jintan, China), centrifuged for 10 min at 10000 rpm and 4°C. The precipitate was extracted with 10 mL PCA and centrifuged again. The two supernatants were combined, and then adjusted to pH 6.5 by dropwise addition of 0.5 mol/L and 0.05 mol/L NaOH, respectively, subsequently diluted with ultrapure water to 100 mL. The resulted extract was filtered through 0.45 μm filter paper before HPLC analysis.

2.6 HPLC Analysis of Nucleotides

ATP, ADP, AMP and I were purchased from Amresco (Solon, United States). IMP and HX were purchased from Sigma (St. Louis, United States).

The determination of nucleotides (ATP, ADP, AMP, IMP, I, HX) in samples was completed at 254 nm using HPLC (Waters 2996, USA) with a Hypersil ODS-2 C18 column (25 cm × 4.6 mm ID and 5 μm particle size, China). The standards and above extracts were eluted using a mobile phase consisting of 0.72% triethylamine water solution (containing 0.35% phosphate buffer, pH 6.5)/methanol (96.5 : 3.5, v/v), the flow rate was 1.0 mL/min, the injection volume was 20 μL. Each nucleotide was identified using the retention time for its authentic compound and the concentrations were calculated using the area for each peak. Typical HPLC chromatograms of mixed standards and real samples were showed in Fig. 1A and 1B.

Ultrapure water was obtained with MilliQ-System (Millipore Corporation, USA). Methanol was HPLC grade and other reagents were AR grade. All solvents were filtered through membrane 0.45 μm and degassed using a KS-1500 ultrasonic instrument (Ningbo Kesheng, China) for 30 min before use.

2.7 Statistical Analysis

The Data were expressed as mean ± standard deviation (SD) and then analyzed by Excel 2003 (Microsoft official Excel 2003 for Windows). Analysis of variance (ANOVA) was introduced to determine the significance of samples at $P<0.05$ level.

978-1-61896-030-6 © 2012 SciRes.

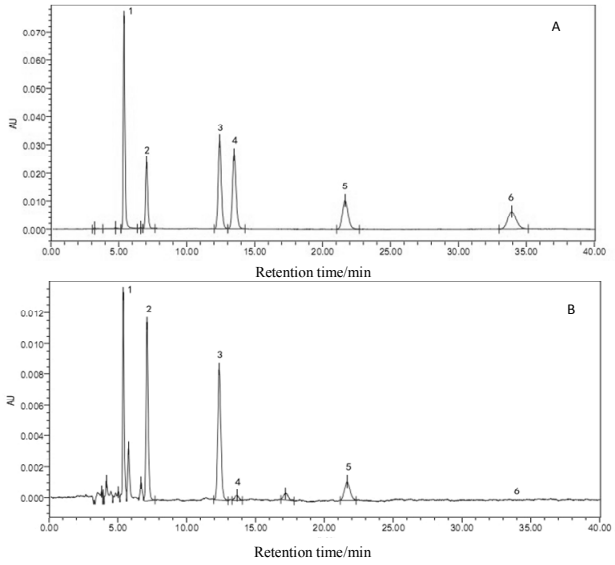

Figure 1. Typical HPLC chromatograms of (A) mixed standards and (B) real samples containing 1-HX, 2-IMP, 3-I, 4-AMP, 5-ADP, 6-ATP

3 Results and Discussion

3.1 Effect of Brining Conditions on Degradation of ATP

The degradation of ATP in DDMS influenced by brining time and NaCl level was showed in Fig. 2. From Figure 2a-2e, it seemed that the effecting trends of NaCl levels (1-3%) on ADP, AMP, IMP and I except HX were similar. Generally, higher the NaCl level, lower the contents of nucleotides except HX. High NaCl level could increase the osmotic pressure which might improve the dissolution of nucleotides resulting in the part loss of nucleotides [24]. When NaCl contents were 1% and 2%, ADP contents increased after 5-hour brining while the final ADP content level was similar to initial level (0 h) at 3%. From Fig. 2a, it could be concluded that high NaCl level did not favor the formation of ADP which might be relate to the low activity of ATP enzyme resulted from the high concentration of NaCl [25]. The contents of AMP decreased first, then increased, finally decreased despite different NaCl levels. IMP content decreased with the increase of NaCl level while first decreased and then increased in the duration of brining. The low content of IMP was attributed to the formation of I which could degrade to yield HX, this result was similar to the studies of Kuda [17] and Tikk [14]. In addition, NaCl did not significantly affect the IMP contents ($P > 0.05$) compared with NaCl-free sample, which is similar with the result of [24]. The change trend of I content was reverse to that of IMP, which might be due to the effect of endogenous enzyme [23]. Mateo, Domínguez, Aguirrezábal and Zumalacárregui found that the contents of nucleotides in sausages would decrease to undetectable levels in the long curing process [26], and Kohata, Numata, Kawaguchi, Nakamura and Arakawa also reported similar results in Parma Hams [27]. In present, the duration time of brining treatment was less than 1/4 day and the contents of IMP were about 15-60 ppm. Brining with 3% NaCl, HX content increased when the brining time ≤ 1 h, then decreased, finally increased to a little higher content level compared with the initial level (0 h). In addition, it could be speculated that the total nucleotides contents including ADP, AMP, IMP, I and HX nearly were not changed after 5-hour brining treatment, this result was inconsistent with the report of Liu [23].

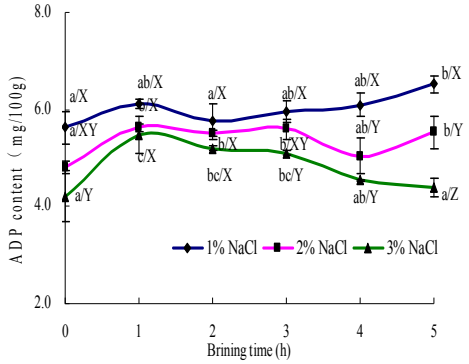

(a) ADP content at different brining time and NaCl content

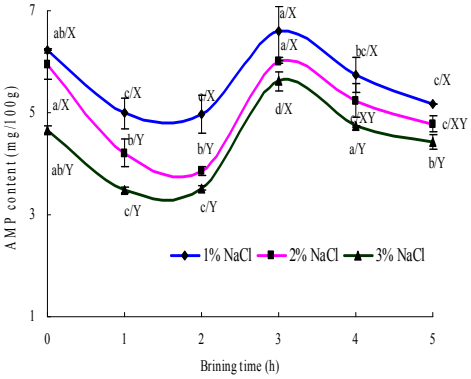

(b) AMP content at different brining time and NaCl content

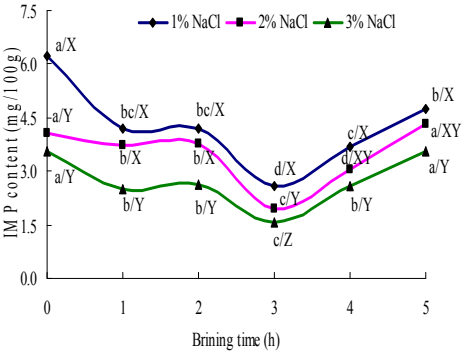

(C) IMP content at different brining time and NaCl content

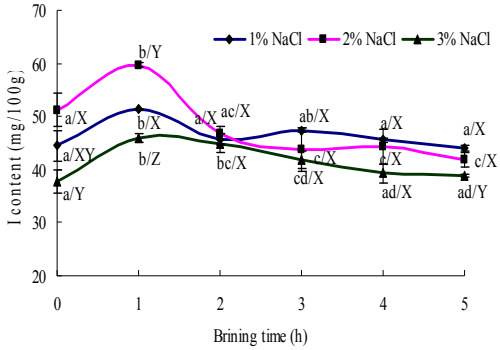

(d) I content at different brining time and NaCl content

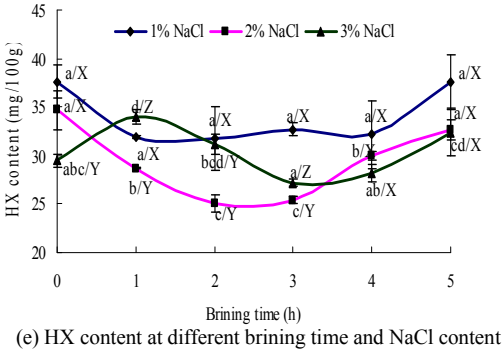

(e) HX content at different brining time and NaCl content

Figure 2. Degradation products of ATP

(a) ADP, (b) AMP, (c) IMP, (d) I, (e) HX in dried duck meat slice influenced by brining time and NaCl content, contents of ATP and degradation products on the basis of ground duck meat were expressed as means ± standard error (n = 3), values with different letters a-d among brining time (at same NaCl content) and X-Z among NaCl content (within the brining time) differ significantly (P<0.05).

For IMP contributes to umami taste and high content of HX is related with the bitterness, brining for 2 h with 1% NaCl favored the accumulation of IMP and low content of HX, which benefit for improving taste and declining off-taste of DDMS.

3.2 Effect of Drying Conditions on Degradation of ATP

The degradation of ATP in DDMS affected by drying temperature and time was presented in Fig. 3. ATP was not detected indicating that ATP in samples completely degraded. The content of ADP first increased and then decreased when the samples were treated at a temperature range from 55°C to 75°C. The content of ADP at 55°C was evidently higher than 65°C and 75°C when treated for more than 3 h. ADP was one of the degradation products of ATP and ATP was not detected in above samples, it could be concluded that ATP had various catabolites. The content of AMP increased during the treatment which was similar to the result reported by Macy [19], and its content at 55°C was markedly higher than 65°C and 75°C after 4 h. The taste profile contributed by AMP was dependent on the concentration in the samples. At a high concentration, AMP contributes to the umami taste, while at a low concentration; it contributes to the sweetness [28]. The content of IMP decreased after 5 h treatment, the result agreed with [19], and the content of IMP at 55°C was remarkably higher than 75°C when treatment time was more than 4 h. In similar studies carried out by Nguyen and Sporns [18]; Shaoul and Sporns [29], it was reported that the thermal degradation of IMP was temperature dependent. During cooking, the changes in the nucleotides are caused by a loss of cooking juice and thermal degradation of the nucleotides [30, 31]. So it was reasonable to speculate that the change of IMP in meat was mainly caused by loss of water and thermal treatment. IMP was one of intensive flavor enhancers to the umami taste, much stronger than monosodium glutamate (MSG). The synergistic effect of IMP with MSG-like components (Glu and Asp) greatly increases the umami taste [17, 32]. The content of I increased during the whole treatment. The content of I at 75°C was significantly higher than 65°C when treatment time was more than 3 h. I produced a bitter taste [26]. As a result, lower drying temperature was applicable to reduce the bitter level of sample resulted from I. The content of HX first increased and then decreased. HX also contributed to a bitter taste, which has a negative influence on the taste of aquatic product [33]. Hsiu, Ming, Deng and Lieh reported that IMP level increased in meat samples stored at –2°C whereas concentration of HX and I increased in samples stored at 20 °C [34]. It could be concluded that I and HX were also temperature dependent.

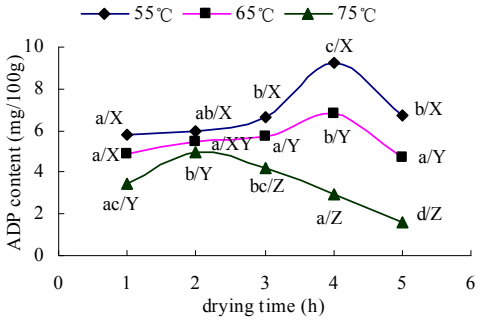

(a) ADP content at different drying temperature and time

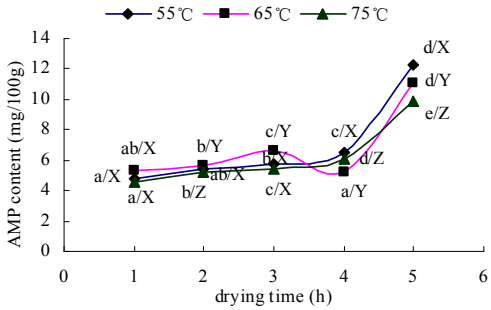

(b) AMP content at different drying temperature and time

978-1-61896-030-6 © 2012 SciRes.

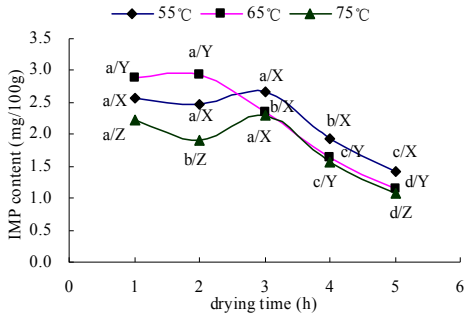

(C) IMP content at different drying temperature and time

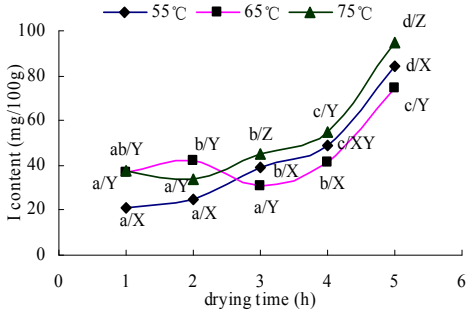

(d) I content at different drying temperature and time

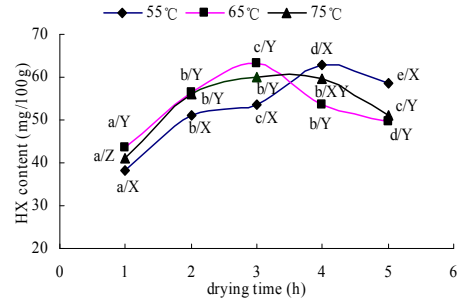

(e) HX content at different drying temperature and time

Figure 3. Degradation products of ATP

(a) ADP, (b) AMP, (c) IMP, (d) I, (e) HX in dried duck meat slice influenced by drying temperature and time, contents of ATP and degradation products on the basis of ground duck meat were expressed as means ± standard error (n = 3), values with different letters a-e among drying time (at the same drying temperature) and X-Z among drying temperature (within the same drying time) differ significantly (P<0.05).

From Fig. 3, it can be found that AMP converted into IMP with a low yield when drying time was 4 to 5 h and drying temperatures were 55°C to 75°C, while IMP converted into I smoothly and I converted into HX tardily.

So, drying for 2 h at 65°C favored the transformation of AMP to IMP and low content of HX, which would provide high content of IMP.

3.3 Effect of Roasting Conditions on Degradation of ATP

The degradation of ATP in DDMS influenced by roasting temperature and time was showed in Fig. 4. The content of ADP decreased under roasting conditions. The content of ADP at 240°C was significantly higher than 180°C when roasting time was more than 4 min. The content of AMP increased, the content of AMP at 240°C was observably higher than 120°C when roasting time was 2 min to 6 min, while differed insignificantly more than 6 min. Compared to drying treatment, the content of AMP was lower, it could be concluded that the change of AMP was also temperature dependent. The content of IMP first increased and then decreased. The content of IMP at 120°C, 180°C and 240°C differed insignificantly from 2 min to 4 min, while differed significantly after 4 min. During drying, the changes of IMP was caused by a loss of cooking juice and thermal degradation of the nucleotides [30, 31], roasting caused further loss of cooking juice, so it was reasonable to speculate that the change of IMP in meat was also mainly resulted from the loss of water and thermal treatment during roasting. IMP was the major nucleotide in muscle and its degradation resulted in formation of ribose in meat, which took part in the Maillard reaction [35]. Whitfield showed that temperatures above 110°C promote Maillard reactions in meat. So it was suggested that the difference between the change of IMP under drying and roasting conditions might originated from Maillard reactions under roasting condition [36]. The content of I at 240°C was markedly higher than the content of I at 120°C and 180°C when treatment time was more than 6 min. The content of I increased after 6 min. The content of HX first decreased and then increased when roasting treatment time was less than 8 min, while decreased after 8 min. This could be understood that HX might have been further broken into smaller units at higher temperature [18].

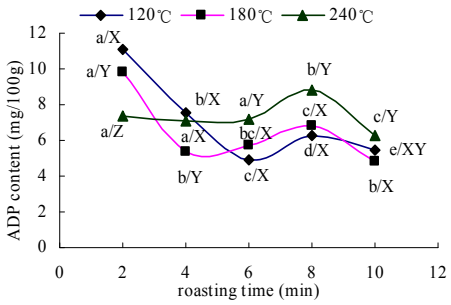

(a) ADP content at different roasting temperature and time

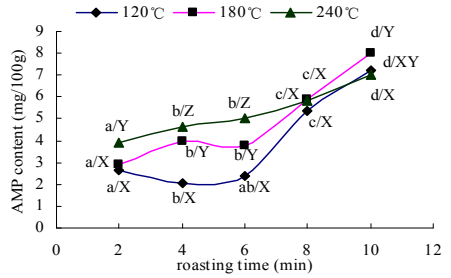

(b) AMP content at different roasting temperature and time

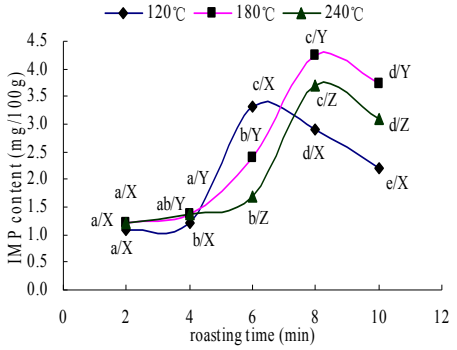

(C) IMP content at different roasting temperature and time

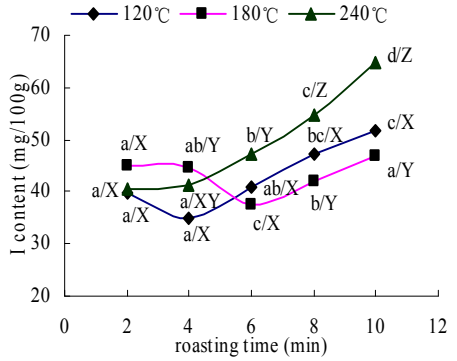

(d) I content at different roasting temperature and time

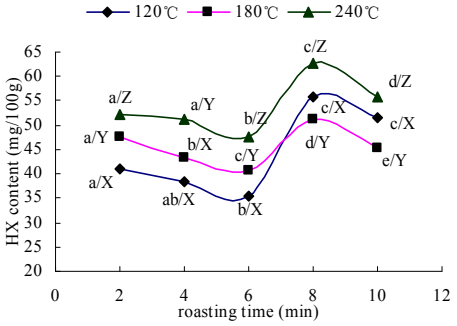

(e) HX content at different roasting temperature and time

Figure 4. Degradation products of ATP

(a) ADP, (b) AMP, (c) IMP, (d) I, (e) HX in dried duck meat slice influenced by roasting temperature and time, contents of ATP and degradation products on the basis of ground duck meat were expressed as means ± standard error (n = 3), values with different letters a-e among roasting time (at the same roasting temperature) and X-Z among roasting temperature (within the same roasting time) differ significantly ($P<0.05$).

From Fig. 4, it could be found that IMP content was higher and I content was lower when roasting temperature was 180°C and roasting time was 6 min compared to the contents of the product roasted at 180°C for 2 min, those roasting conditions were favorable to umami of the product. AMP converted into IMP tardily when roasting temperatures were 120°C, 180°C, 240°C and roasting time was 8-10 min, while IMP converted into I smoothly and I converted into HX tardily, those transformations led to decreased content of IMP and increased content of I.

Generally, considering the effects of contents of IMP and HX on the taste, toasting for 6 h at 120°C was good for the taste of DDMS.

4 Conclusion

Considering the effect of IMP and HX on the taste of DDMS, brining for 2 h with 1% NaCl, drying for 2 h at 65°C, and roasting for 6 h at 120°C favored the accumulation of IMP and low content of HX, which benefit for improving taste and declining off-taste.

Experimental results indicated that three treatments (brining, drying and roasting) casted great impact on the degradation of ATP and the formation of its derivatives which were important to the flavor of DDMS, and provided an insight into the degradation of ATP under brining, drying and roasting conditions which will be valuable for the processing of duck products.

Acknowledgement

This research work was financed by Project No.08010301080 of the Science and Technology Support in Eleventh Five Plan of Anhui Province in China and Creative Foundation for Young Teachers in Hefei University of Technology (No. 2011HGQC1020). We thank Dr Jing-Ke Liu, from food science and technology college of Huazhong agricultural university, for his help.

References

[1] J.-K. Liu, S.-M. Zhao, S.-B. Xiong and S.-H. Zhang, Influence of recooking on volatile and non-volatile compounds found in silver carp Hypophthalmichthys molitrix. Food Science and Technology, 75 (4), 2009, pp. 1067-1075.

[2] E. A. Bryhni, D. V. Byrne, M. Rødbotten, C. Claudi-Magnussen, H. Agerhem and M. Johansson, Consumer perceptions of pork in Denmark, Norway and Sweden. Food Quality and Preference, 2002, 13 (6), pp. 257-266.

[3] D. S. Mottram, Flavour formation in meat and meat products: A review. Food Chemistry, 1998, 62 (4), 415-424.

[4] I. Hornstein and P. F. Crowe, Flavor studies on beef and pork. Journal of Agricultural and Food Chemistry, 1960, 8 (6), pp. 494-498.

[5] G. MacLeod and J. M. Ames, The effect of heat on beef aroma: comparisons of chemical composition and sensory properties. Flavour and Fragrance Journal, 1986, 1 (3), pp. 91-104.

[6] D. S. Mottram, Meat. In H. Maarse (Ed.), Volatile compounds in foods and beverages, 1991, pp. 107–177. New York: Marcel Dekker, Inc.

[7] D. S. Mottram, The effect of cooking conditions on the formation of volatile heterocyclic compounds in pork. Journal of the Science of Food and Agriculture, 1985, 36 (5), pp. 377–382.

[8] H. Conn, "Umami" the fifth basic taste. Nutrition and Food Science, 92 (2), 1992, pp. 21-23.

[9] T. C. Wifall, T. M. Faes, C. C. Taylor-Burds, J. D. Mitzelfelt and E. R. Delay, An Analysis of 5'-Inosine and 5'-Guanosine Monophosphate Taste in Rats. Chemical Senses, 2007, 32 (2), pp. 161-172.

[10] P. Howgate, Kinetics of degradation of adenosine triphosphate in chill-stored rainbow trout (Oncorhynchus mykiss). International Journal of Food Science and Technology, 2005, 40 (6), pp. 579-588.

978-1-61896-030-6 © 2012 SciRes.

[11] M. Kawai, A. Okiyama and Y. Ueda, Taste enhancements between various amino acids and IMP. Chemical Senses, 2002, 27 (8), pp. 739-745.
[12] K. M. Manabe, T. Matoba and K. Hasegawa, Sensory changes in umami taste of inosine-5-monophosphate solution after heating. Journal of Food Science, 1991, 56 (5), pp. 1429-1432.
[13] S. Kavitha and V. K. Modi, Effect of water activity and temperature on degradation of 5-inosine-monophosphate in a meat model system. LWT-Food Science and Technology, 2007, 40 (7), pp. 1280-1286.
[14] M. Tikk, K. Tikk, M. A. Tørngren, L. Meinert, M. D. Aaslyng, A. H. Karlsson, et al. Development of inosine monophosphate and its degradation products during aging of pork of different qualities in relation to basic taste and retronasal flavour perception of the meat. Journal of Agricultural and Food Chemistry, 2006, 54 (20), 7769-7777.
[15] S., Fuke and S. Konosu, Taste-active components in some foods: A review of Japanese research. Physiology and Behavior, 1991, 49 (5), pp. 863-868.
[16] K. Takashi, F. Maya, G. Hideyuki and Y. Toshihiro, Effects of retort conditions on ATP-related compounds in pouched fish muscle. LWT-Food Science and Technology. 2008, 41 (3), pp. 469-473.
[17] T. Kuda, M. Fujita, H. Goto and T. Yano, Effects of freshness on ATP-related compounds in retorted chub mackerel Scomber japonicus. LWT-Food Science and Technology, 2007, 40 (7), 1186–1190.
[18] T. T. Nguyen and P. Sporns, Composition of flavour enhancers, monosodium glutamate, inosine-5-monophosphate and guanosine-5-monophosphate during canning. Journal of Food Science, 1985, 50 (3), pp. 812-814.
[19] R. L. Macy, H. D. Naumann and M. I. Baily,. Water soluble flavour and odour precursors of meat. Journal of Food Science, 1964, 29 (2), 142-148.
[20] K. Chikuni, K. Sasaki, T. Emori, F. Iwaki, F. Tani, I. Nakajima, et al. Effect of cooking on the taste and flavor related compounds in pork (in Japanese). Japanese Journal of Swine Science, 2002, 39 (3), pp. 191-199.
[21] W. M. Xu, X. L. Xu, G. H. Zhou, D. Y. Wang and C. B. Li, Changes of intramuscular phospholipids and free fatty acids during the processing of Nanjing dry-cured duck. Food Chemistry, 2008, 110 (2), pp. 279-284.
[22] C. G. Chen, R. Wang, G. J. Sun, H. M. Fang, D. R. Ma and S. L. Yi, Effect of high pressure level and holding time on properties of duck muscle gels containing 1% curdlan. Innovative Food Science and Emerging Technologies, 2010, 11 (4), pp. 538-542.
[23] Y. Liu, X. L. Xu and G. H. Zhou, Changes in taste compounds of duck during processing. Food Chemistry, 2007, 102 (1), pp. 22-26.
[24] K. Sasaki, M. Motoyama and M. Mitsumoto, Changes in the amounts of water-soluble umami-related substances in porcine longissimus and biceps femoris muscles during moist heat cooking. Meat Science, 2007, 77 (2), pp. 167-172.
[25] B. Holliman, N. Olden-Stahl and P. R. Pratap, ATP-dependence of Na+/K+-ATPase activity isolated from duck supraorbital salt glands measured with a fluorescence coupled-enzyme assay. Biophysical Journal, 2004, 86 (1), pp. 244A-244A.
[26] J. Mateo, M. C. Domínguez, M. M. Aguirrezábal and J. M. Zumalacárregui, Taste compounds in chorizo and their changes during ripening. Meat Science, 1996, 44 (4), pp. 245-254.
[27] H. Kohata, M. Numata, M. Kawaguchi, T. Nakamura and N. Arakawa, The effect of salt composition on taste development in prosciutto. In Proceedings of the 38th international congress of meat science and technology, 1992, pp. 1271-1274 France: Clermont-Ferrand.
[28] D. W. Chenand M. Zhang, Non-volatile taste active compounds in the meat of Chinese mitten crab (Eriocher sinensis). Food Chemistry, 2007, 104 (3), pp. 1200-1205.
[29] O. Shaoul and P. Sporns, Hydrolytic stability at intermediate pH of the common purine nucleotides in food, inosine-5-monophosphate, guanosine-5-mono- phosphate and adenosine-5-mono phosphate. Journal of Food Science, 1987, 52 (3), pp. 810-812.

Simultaneous Determination of Aconitine Compounds in the Plant Medicine by High Performance Capillary Electrophoresis

Suya GAO[1,2], Li WANG[1], Lining YANG[1], Hua LI[2]
[1]*Department of Pharmacy, Xi'an Medical University, Xi'an, China*
[2]*Institute of Analytical Science, Northwest University, Xi'an, China*
Email: gaosuya1972@163.com

Abstract: A simple and inexpensive high performance capillary electrophoresis (HPCE) was applied to separate three alkaloids in Radix Aconiti Praeparata simultaneously. The investigation was carried out by capillary zone electrophoresis (CZE). The best conditions for separation were obtained using 20 mM borax and 2 mM β-CD buffer (pH 8.9) containing 20% methanol (v/v). Online UV detection was performed at 235 nm. A voltage of 16 kV was applied and the temperature was controlled at 25℃. Injection was performed at 0.5psi for 10 s. The separation and determination were satisfactory and quick.

Keywords: High performance capillary electrophoresis (HPCE); aconitine; hypaconitine; mesaconitine; Radix Aconiti Praeparata

1 Introduction

Over the last two decades, high performance capillary electrophoresis (HPCE) has been proved to be a powerful efficient technique in the field of separation. Compared to other analytical techniques like HPLC, HPCE offers several advantages for separation analysis including implicity, short analytical times, high efficiencies, different separation mechanisms, small volumes and low running costs, and a tremendous flexibility for separations because of a wide variety of available additives. The most frequently used additives in HPCE are surfactants and selectors such as cyclodextrins (CDs). The mechanism of discrimination using CDs is the inclusion of the analytes into the cavity of the selector. Additionally, the secondary bonds between the rim of the CDs and the analyte stabilize the complex. Separation is achieved if the binding constants of both compounds for the CDs are different and/or if the mobilities of both compound-CDs complexes differ.

Aconitine, hypaconitine and mesaconitine are important alkaloids in Radix Aconiti Praeparata, a traditional Chinese medicine. It has the function of clearing rheumatism and removing the pain in menstruation. So it is used to cure rheumatism, joint pain and heart disease. Moreover, aconites are also a kind of high poisonous alkaloids. In recent years it has been studied by more and more researchers [1-5]. In addition, aconites alkaloids are complicated in structure and weak in stability. There is a great difference in the content and in the toxic about the effective components in the different condition such as the origin place, collected season, processing method, and etc. The cases are usually occurred in taking or mistaking an overdose of aconites alkaloids. Therefore, it is very important to determine three poisonous aconites alkali for controlling the qualification and ensuring the safety of the medicine. In this paper a new method was established to separate and determine three alkaloids simultineously in Radix Aconiti Praeparata by HPCE. During method development, no detailed investigation of the compounds by HPCE has so far been reported. In this investigation the several parameters that influence the separation were investigated including pH, concentration of buffer, applied voltage and so on. Moreover, the results of separation and determination were satisfactory.

2 Experimental

2.1 Instrumentation

A Beckman MDQ capillary electrophoresis system equipped with diode-array detector (DAD) (Beckman Instruments Inc., USA). All separations were performed in an uncoated fused-silica capillary (Hebei Yongnian Optical Fiber Factory, China) with a total length of 60 cm (50 cm to the detector) × 75 μm internal diameter. Instrument control and data acquisition were performed by the chromatography software 32Karat. Other apparatus also were used for analysis such as pH meter (Orion Research Incorporated, USA), ultrasonic cleaning instrument (Kun-shan Ultrasound Equipment Company, China) and UV-2450 ultraviolet-visible spectrophotometer equipped with UV-probe software (Shimadzu, Japan).

978-1-61896-030-6

2.2 Reagents and Solutions

Aconitine, hypaconitine and mesaconitine were bought from the National Institute for the Control of Pharmaceutical and Biological Products. Alcohol, Ethanol, methanol, acetomitrile, acetone and other reagents were of analytical grade. The stock solution of aconitine compounds were prepared with acetomitrile up to 25 mL in the ultrasonic generator for 30 min, respectively. These were stored at 4℃ in the refrigerator. Before injection, these stock solutions were diluted and mixed to the desired concentration with the separation buffer. If appropriate, organic modifier was added. The buffer and the solution were filtered through a 0.45 μm microporous membrane, respectively. The doubly distilled water used for preparing solution was obtained from a quartz sub-boiling high-water distiller.

2.3 Procedure for CE Analysis

Before the experiment everyday, the capillary was sequentially rinsed with 0.1M NaOH, water and 0.1M HCl, each for 10 min. Between runs, the capillary was rinsed for 5 min with water and for 3 min with the background electrolyte (BGE) solution. Online UV detection was performed at 235 nm. Unless stated otherwise, a voltage of 16 kV was applied and the capillary was temperature controlled at 25℃ by liquid cooling. Sample solutions were injected pressure (0.5 psi) for 10 s. When the components were separated baselinely, the spectral peaks were qualitatived according to peak height and migration time to respond to increasing the concentration of single-component respectively. The signal was displayed and integrated for a 0.1 s interval.

2.4 Procedure for Pharmaceutical Formulations

Firstly, Radix Aconiti Praeparata purchased from the local market was finely powdered (through 60 mesh), weighed 4.000g accurately and transferred into a 100 mL volumetric flask, and then diluted to volume with 80 mL alcohol concentration of 85%. Then it was placed in a water-bathing generator to be heated for 1.75 h. Secondly, The resulting mixture was centrifuged for 15 min at 3000 rpm, filtered. Lastly, the upper clear liquid was concentrated by water-bathing heater and was further diluted with acetonitrile so that the final concentration was within the working range. Before injection the formulations were filtered through a 0.45 μm microporous membrane, and then analyzed according to the procedure described above.

3. Results and Discussion

3.1 Choice of Detection Wavelength

The three aconitine compounds have a larger absorption at 235 nm by UV scanning (shown in Fig.1). Thus 235 nm was selected as detection wavelength and baselines instability could be avoided at shorter wavelength.

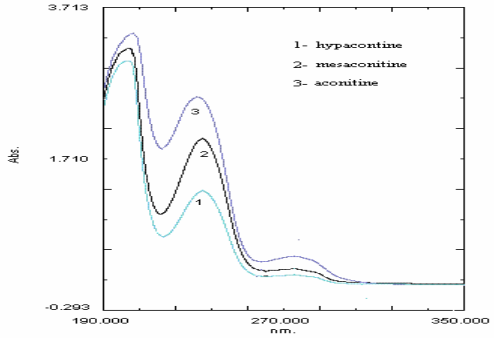

Figure 1. Spectral photograms of aconitine, hypacontine and mesaconitine

3.2 Optimized Procedure of HPCE Conditions

3.2.1 Concentration of the Buffer

Three kinds buffer system such as borax, phosphate and Tris-HCl buffer were investigated, respectively. When borax butter was chose, the migration time was short and the baseline was smooth. In addition, peak triangulation due to electrokinetic dispersion is a peak deformation mechanism that occurs when the sample solution has a higher conductivity than the BGE and during separations where the migration velocity of the sample and buffer ions of the same charge is different. Increasing the ionic strength of the BGE can reduce electromigration dispersion. Fig.2 illustrates the separation of the compounds by varying the concentration of the borax butter. Using an over 50 mM sodium tetraborate buffer, clearly peak dispersion occurred. More efficient peaks were observed with below 30 mM buffer. The best results were obtained from using 20 mM.

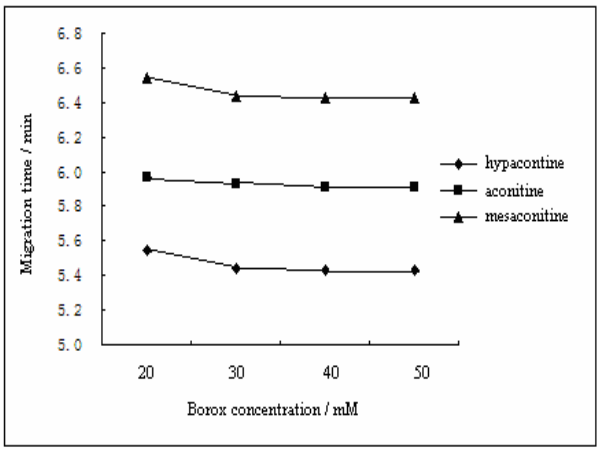

Figure 2. Effect of borax concentration on migration time

3.2.2 Effect of pH of Butter on Separation

The apparent charge of analytes is usually changed by pH of buffer. Thus the migration behavior was also seriously influenced by the pH of the buffer. The separation was investigated corresponding to the pH of the buffer from 7.3 to 9.5 containing 20 mM borax. Increasing the pH value of the buffer resulted in a decrease in migration time (shown in Fig.3). When pH value was set at 9.0, the separation and migration time were all good.

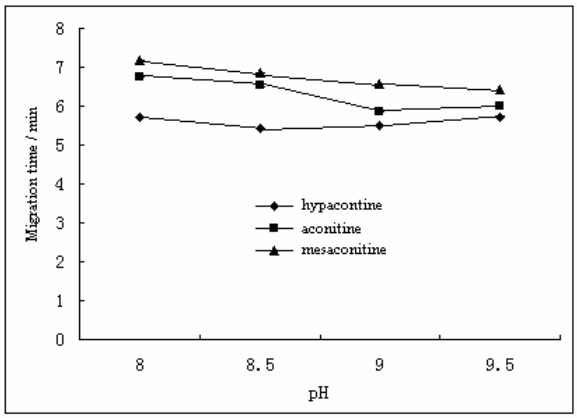

Figure 3. Effect of pH on migration time

3.2.3 Effect of β-CD and Organic Additives

The addition of β-CDs, surfactants and organic additives in buffer usually can improve separation including Rs and the shape of peaks. In this experiment we investigated surfactants SDS, β-CD and organic agents, respectively. Furthermore, the different concentration of β-CD from 1mM to 10mM also was investigated. Finally, 2mM β-CD and 20% methanol were selected to add into the buffer for separation.

3.2.4 Effect of Applied Voltage and Injection Time

In this experiment the voltage was varied from 10 kV to 24 kV. The migration time of the compounds decreased with increasing voltage. In addition, the intensity of the peaks was also increased. But higher voltages than 16 kV could not be used because of the generation of higher currents and noise. Therefore 16 kV was selected for further investigation. Moreover, the injection time was investigated from 4s to 15s. When the injection time was set at 10s, the peaks were good and their areas were suitable for quantification.

3.3 System Suitability Test

During method development it was observed that the *Rs* between the compounds decreased upon using the same β-CD stock solution for several days. For quantitative analysis of CE the *Rs* should exceed 2.0. If the *Rs* was lower than 2.0, a new stock solution of β-CD was prepared. It was found that the stock solution could be used for maximal ten consecutive days.

3.4 Standard Curve and Precision

Under the selected conditions described above, the calibration area of spectrum (y) versus personal concentration (x) was linear in the range of 21.6 ~ 128.0 μg/mL with a detection limit (3σ) of 0.8μg/mL. The linear regression equations of aconitine, hypacontine and mesaconitine were y = 108837 x – 1635.2, y = 170962 x – 2749.6, y = 90570 x – 313.36 with a correlation coefficient of 0.9997, 0.9998 and 0.9995 (n=6), respectively. Intraday precision was determined by comparing the relative corrected peak areas for six repeated injections of three concentrations. The mixed standard solution containing three compounds was repeated injection 6 times in the selected experimental conditions. And the interday one was determined on six different days. The relative standard deviation (RSD) values obtained for intra-and interday precision of three compounds were lower than 3.8%, respectively.

3.5 Reproducibility and Recovery Experiments

In order to assess the possible analytical application of the proposed method, the processed samples solution was repeated injection 6 times in the selected experimental conditions. Six replicate assays on 1 day were performed to assess repeatability of the method. Then interday method precision was assessed by injecting newly prepared samples on six different days in a period of 1 month. The RSDs of the migration time and the peak area of three compounds were all lower than 0.33% and 4.6%, respectively. Therefore, the reproducibility was good. Average recovery of aconitine, hypacontine and mesaconitine were 98.2%, 99.6% and 100.2%, respectively. The RSD values obtained for average recovery test were all lower than 1.8%. These results showed that the developed method was accurate for application.

3.6 Analysis of Real Sample

Following the procedure in the item "*Procedure for Pharmaceutical Formulations*" described previously, the proposed HPCE method was applied to the determination of aconitine, hypaconitine and mesaconitine in Radix Aconiti Praeparata (shown in Fig. 4). Three batches of Radix Aconiti Praeparata samples commercially available were determined. The average results of determination were 127.3 μg/g for aconitine, 275.7μg/g for hypaconitine and 230.7μg/g for mesaconitine, respectively.

978-1-61896-030-6 © 2012 SciRes.

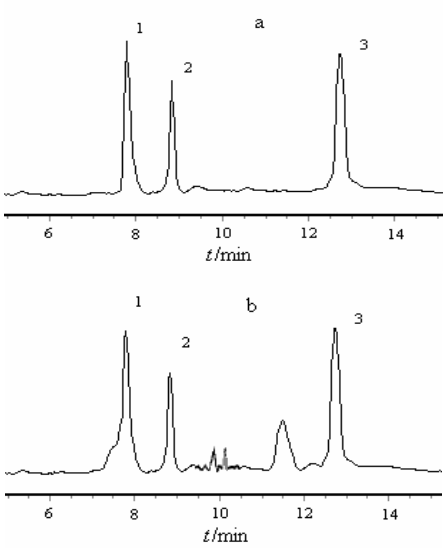

Figure 4. Electropherotograms of standards (a) and Radix Aconiti Praeparata sample (b)

(1-hypaconitine 2-aconitine 3-mesaconitine)

4 Conclusion

A simple HPCE method was developed for the separation of three effective compounds in Radix Aconiti Praeparata. Several experimental parameters that influence separation were investigated including pH of the buffer, β-CD and the concentration of borax, etc. The best conditions were 20 mM borax and 2 mM β-CD (pH9.0) containing 20% methanol (v/v). Online UV detection was performed at 235 nm. A voltage of 16 kV was applied and the capillary temperature was controlled at 25℃. The simultineous separation of three compounds was obtained in less than 15 min with Rs more than 2.0. The separation and determination were satisfactory, quick and reliable. The proposed method shows a larger potential application for simultineous separations and for quantification of compounds with similar structure by HPCE in pharmaceutical analysis.

Acknowledgement

This work was supported by the Scientific Research Program Funded by Shaanxi Provincial Education Department (Program No. 11JK0656).

References

[1] Mojun LI, Ye JIANG, Ting SUN. Determination of aconitine in Wenweishu particles by HPCE. Chinese Traditional and Herbal drugs, 2009, 40(10): 1577-1579.

[2] HOU Da-bin; ZHAO Xiang-sheng. Effects of Different Preparation Technologies on the Content Determination of Alkaloids in Aconitum carmichaeli by RP-HPLC. China Pharmacy, 2010, 21(19): 1763-1765.

[3] NIE Li-xing; ZHANG Yu-mei; LU Jing, et al. Study on Quality Standard of Fuzi and Fupian. Chinese Pharmaceutical Journal, 2009, 44(12): 946-950.

[4] SHU Xiao-yan; HOU Da-bin; LI Feng. Study on the Content of Alkaloids and Polysaccharide in Different Varieties of Aconitum carmichaeli. China Pharmacy, 2010, 21(31): 2765-2768.

[5] LIU Lan, FAN Zhi-chao, ZHANG Zhi-qi. HPLC Simultaneous Determination of Four Aconitine Alkaloids in Patent Medicine. 2010, 30(2): 236-239.

In Vitro Modulation of Melanization in Melanoma Cells by Isoliquiritigenin

Xiaoyu CHEN[1], Caixia WANG[2], Qiusheng ZHENG[1,2]

[1]*Key Laboratory of Xinjiang Endemic Phytomedicine Resources, Ministry of Education, School of Pharmacy, Shihezi University, Shihezi, China, 832002*

[2]*Ocean School of Yantai University, Yantai, Chian, 264005*

Email: zqsyt@sohu.com

Abstract: B16F0 murine melanoma cells were grown for 24 or 48 h in Dulbecco's modified Eagle medium in presence of 5-20μg/ml isoliquiritigenin. The intracellular melanin concentration and the melanin secreted in the extracellular medium were estimated by spectrophotometry. The results showed that 10 μg/ml isoliquiritigenin treatment (48 h) stimulates the increase of extracellular secretion and intracellular content of melanin in B16F0 melanoma cells, as well as stimulates the increase of the tyrosinase specific activity. The increased melanin synthesis may be due to the elevator of cellular tyrosinase activity induced by isoliquiritigenin. After 24 or 48 h isoliquiritigenin treatment, the cells exhibited a dose-depengent increase in inhibition and had a special morphological change. Isoliquiritigenin, a natural compound, is a unique molecule which may be involved in the regulation of melanin biosynthetic pathway; it enhances melanogenesis by increasing the activity of tyrosinase, a regulatory enzyme, in the pathway.

Keywords: Tyrosinase; melanogenesis; B16 melanoma; isoliquiritigenin; melanin synthesis

1 Introduction

The most important characteristic of differentiation in melanocytic cells is the presence of melanin pigment. Melanin synthesis is enzymatically regulated by the rate limiting enzyme, tyrosinase. Tyrosinase is a bifunctional, copper-containing enzyme which controls the modulation of melanin production [1–3]. Firstly, by catalyzing the hydroxylation of L-tyrosine to 3,4 dihydroxyphenyl-alanine(dopa) and in a second enzymatic step, by catalyzing the oxidation of dopa to dopaquinone (dopa oxidase activity).The hydroxylation reaction, also known as the cresolase activity of tyrosinase, is the rate regulatory step in the biosynthesis of melanin [1–3]. Melanin pigment is a heterogenous biopolymer formed from various intermediate products derived from dopaquinone.

To date, a large number of melanogenesis regulatory factors have been reported. Among these, phorbol-esters such as 12-0-tetradecanoyl phorbol 13-acetate (TPA) and phorbol dibutyrate were shown to have an inhibitory effect on melanin synthesis, while intracellular cyclic adenosine monophosphate inducers, such as melanocyte stimulating hormone and dibutyryl cyclic AMP (db cAMP) were shown to increase melanogenesis in murine melanoma cells [4–12].

However, natural compounds as activators of melanization in melanoma cells were reported less till recently [13]. Licorice (Glycyrrhiza uralensis) has been used for more than 4 millennia as a flavoring agent in foods, beverages, and tobacco, and been used to treat individuals with gastric or duodenal ulcers [14], sore throats, coughs, bronchitis, arthritis [15], adrenal insufficiency, and allergies[16]. Isoliquiritigenin (ISL), a simple chalcone-type flavonoid, has been evaluated in terms of its antioxidative effects [17], antiplatelet aggregation effects [18], and estrogenic properties [19].

B16F0 murine melanoma cells have been widely used to elucidate the regulatory mechanisms of melanogenesis. We hereby report the effects of ISL on melanogenesis of B16F0 murine melanoma cell line. These observations add new information to our knowledge of how melanogenesis is regulated and add further support to the ISL role of how to contribute in regulating melanin synthesis.

2 Materials and Methods

2.1 Materials

Isoliquiritigenin (ISL) was purchased from Jiangxi Herb Tiangong Technology Co., Ltd. (Jiangxi, China). Culture medium (DMEM) was purchased from Gibco. Fetal bovine serum (FBS) was purchased from Tianjin Hao Yang Biological Manufacture CO_2 Ltd (Tianjin, China); 3,4-Dihydroxyphenylalanine (L-dopa) and phenyl methyl sulfonyl fluoride (PMSF) were purchased from Sigma. Bradford kit was purchased from sangong (Shanghai, China). All other chemicals were of analytical grade and commercially available.

2.2 Cell Line

978-1-61896-030-6

B16F0 murine melanoma cell line was purchased from China Center for Type Culture Collection (Wuhan).

2.3 Cell Culture

The cells were cultured in Dulbecco's modified Eagle's medium (DMEM) medium supplemented with 10% fetal calf serum, 100 U/ml penicillin and 100 μg/ml streptomycin in 5% CO_2 and humidified in a 37°C incubator.

3 Experimental Procedures

3.1 Cell Viability Assay

The cell viability was assessed by using the MTT assay, which was based on the reduction of the dye MTT to formazan crystals, an insoluble intracellular blue product, by cellular dehydrogenases (Denizot and Lang, 1986). Cells were seeded on 96-wells plates with 4×10^3 cells in 200 μl medium per well and cultured 24 h and 48 h for stabilization. At the end of the exposure, 20 μl MTT was added to each well at a final concentration of 2 mg/ml, and then, the cells were cultured for 4 h at 37°C. The medium was then removed carefully and 150 μl DMSO was added and mixed with the cells thoroughly until formazan crystals were dissolved completely. This mixture was measured in a microplate reader（Thermo）with a wave length of 570 nm. Experiment was divided into control group and experimental group. The cell viability was expressed as a percentage of the viability of the control culture.

3.2 Analysis of Morphological Changes

After 48 h incubation with different concentrations of ISL, the cells were observed in inverted differ the microscope equipped with a camera.

3.3 Melanin Synthesis Level Assay in B16 Cells

B16F0 cells were taken suction of the supernatant and washed twice, in order to measure extracellular and intracellular melanin according to the method of Hill et al [20]. After 48 h incubation at 37°C in 5% CO_2, the culture medium was removed, centrifuged (700 x g, 10 min) and the supernatant was collected for extracellular melanin quantification; 1 ml of 0.4 M HEPES buffer (pH 6.8) and EtOH (9:1, v/v) was added to 1 ml of the medium and the OD at 405 nm was measured to quantify extracellular melanin by using a calibration curve obtained with synthetic melanin solutions. Cells were collected by trypsinization, pelleted, washed twice with PBS and digested in 1 ml 1 N NaOH for 16 h at room temperature; intracellular melanin was measured as described above.

3.4 Activity of B16 Melanocyte Tyrosinase Assay

Tyrosinase activity was assayed as DOPA oxidase activity using the method described previously [21]. The cells were washed twice with ice-cold phosphate-buffered saline (PBS) and lysed with 1% Triton X-100 (pH 7.5). Tyrosinase activity was then analysed by spectrophotometry. The concentration of dopachrome in the reaction mixture was measured at 475 nm. The reaction mixture, containing 220 ml of freshly prepared substrate solution 20 μl [1% L-DOPA in 0.1 M sodium phosphate (pH 6.0)] and 200 μl of enzyme solution, was incubated at 37°C. The change in absorbance was measured for the first 2 h of the reaction (i.e. while the increase in absorbance was linear). Corrections were made for the auto-oxidation of L-DOPA in the controls. Enzymatic activity was expressed as the percentage of that in the control cells. The values were normalised against the protein content of the samples. The protein concentration was determined by the Bradford method using a commercial kit (sangong).

4 Results

4.1 ISL Decreased B16 Cell Viability

The viability of the treated B16F0 cells was analyzed using the MTT assay. It was found that with the addition of ISL to the culture medium for 24 h or 48 h, the viability of the B16F0 cells was significantly reduced in a concentration-dependent manner compared with the control cells (Fig. 1).

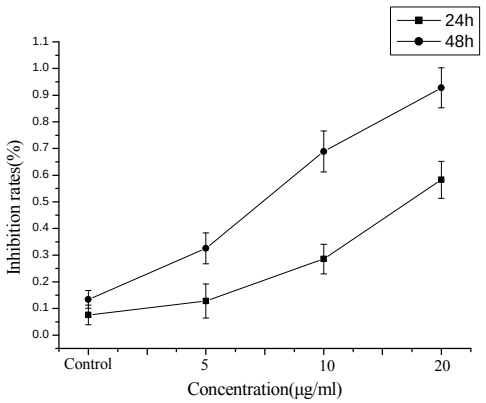

Figure 1. The effect of ISL on B16F0 cells viability

Cells were planted on the cell culture plates at the density of 4×10^4 cells/ml, and then treated with ISL at different concentrations (5, 10 and 20 μg/ml) for 24 h and 48 h. The results were presented as a percentage of control group viability. Data were expressed as mean ± SEM of five determinations.

4.2 Effects of ISL on Morphological Changes in Melanoma B16 Cells

A morphologic change accompanied by extended dendrites was induced in melanoma cells after treatment with different concentration of ISL.

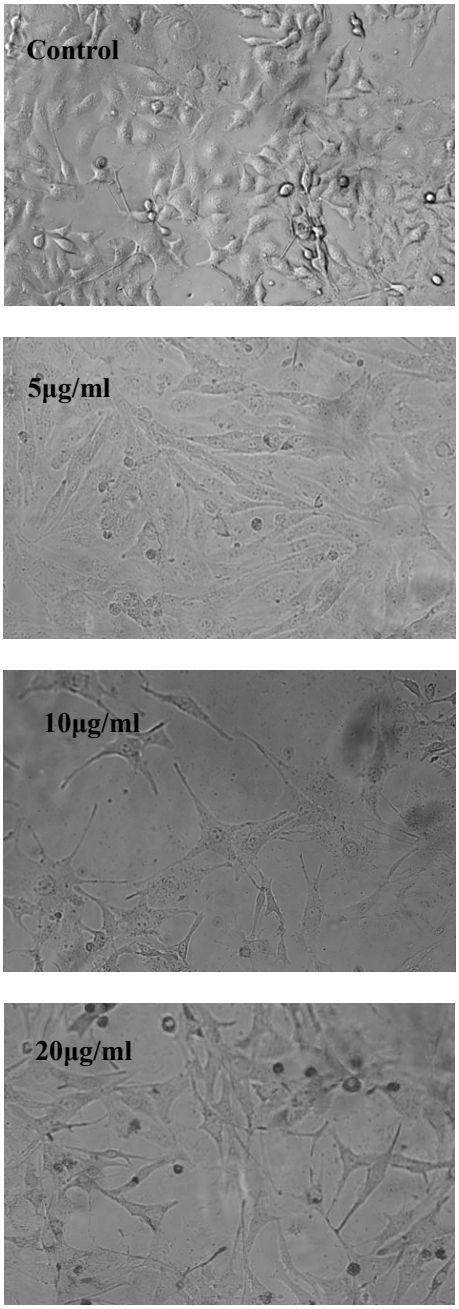

Figure 2. Effect of 5, 10, 20 μg/ml ISL with respect to control on B16F0 cell proliferation and morphology changes after 48 h incubation

Cells were seeded and treated as described in the materials and methods; then digital images were obtained by observation with an inverted microscope at x10.

4.3 ISL Induces Melanogenesis in Melanoma B16 Cells

The extracellular melanin secretion and the intracellular melanin synthesis in presence or absence of graded concentration of ISL were estimated. Data were expressed as the change of the melanin content level, 10μg/ml ISL could increase melanin content remarkably compared with control. The results are presented in Figs 3 and 4.

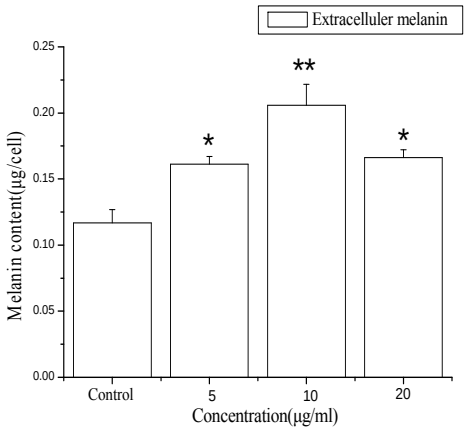

Figure 3. Effect of varying concentration of ISL on extracellular melanin levels in B16F0 cells

* P＜0.05 vs.control, ** P＜0.01 vs.control. Each experiment was done three times.

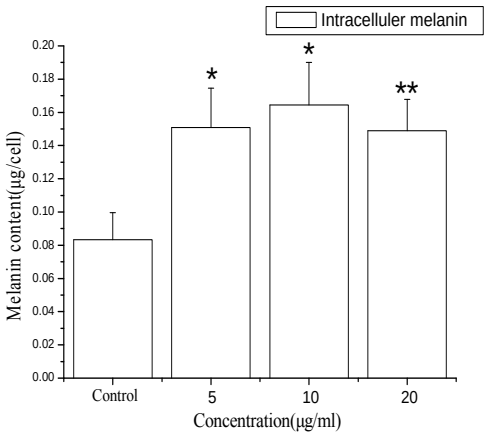

Figure 4. Effects of ISL on intracellular melanin level in B16F0 cells

* P＜0.05 vs.control, ** P＜0.01 vs.control. Each experiment was done three times.

4.4 Effects of ISL on Tyrosinase Activity in B16F0 Melanoma Cells

The effect of ISL on tyrosinase activity was examined because of the key role of this enzyme in melanogenesis.

978-1-61896-030-6 © 2012 SciRes.

The enzyme activity in the crude extracts of the treated cells was measured using L-dopa as an enzyme substrate. The results are shown in Fig. 5. The cellular tyrosinase activity in the crude extract was considerably increased after stimulation by 10 μg/ml ISL.

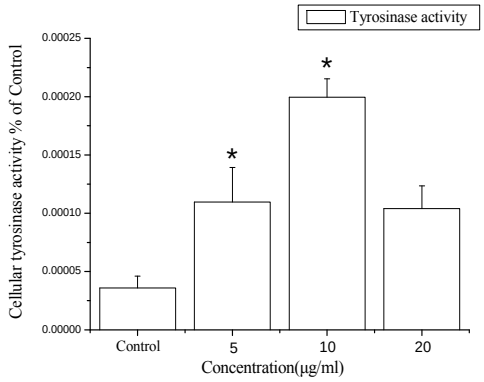

Figure 5. Effect of varying concentration of ISL on tyrosinase activity in B16F0 melanocyte cells

* P＜0.05 vs.control.

5 Discussion

The activity of tyrosinase is the rate regulatory step in melanin biosynthesis. Some agonists of tyrosinase activity are known, but ISL, a natural compound, has not been observed to activate tyrosinase activity under in vitro conditions.

Using a moderately melanotic B16F0 melanoma cell line, we studied the effects of ISL on cellular proliferation and melanogenesis. Following 24 or 48 h treatment with ISL, the cells exhibited a concentration-dependent increase in cellular inhibition. The growth inhibitory effect of ISL was due to retardation of proliferation. As shown in Fig. 1, the cells were determined by MTT assay.

The present results show unequivocally that ISL stimulates melanin biosynthesis by stimulating the tyrosinase activity in B16F0 murine melanoma cells in culture (Fig. 3 and Fig. 4). Because tyrosinase plays an essential role in the process of melanogenesis.

A morphologic change accompanied by extended dendrites was induced in melanoma cells after treatment with ISL. The altered morphology was similar to that of neural cells. Many of dendrites of neighboring cells and had synapse-like knobs on their dendrites.

In summary, the results presented here have demonstrated some evidence to suggest that ISL plays a positive regulatory role in melanogenesis through modulating the expression of tyrosinase.

Acknowledgement

This Study was supported by the National Natural Science Foundation of China (No. 30960451) and Major State Basic Research Development Program (2010CB535003). Funds of Xin Jiang Production and Construction Corps for Distinguished Young Scientists (No. 2011CD006).

References

[1] Hearing VJ, Ekel TM: Mammalian tyrosinase. A comparison of tyrosine hydroxylation and melanin formation. Biochem J 157: 549-557, 1976.
[2] Lerner AB, Fitzpatrick TB: Biochemistry of melanin formation. Physiol Rev 30: 91-126, 1950.
[3] Lerner AB, Fitzpatric TB, Calkins E, Summerson WH: Mammalian tyrosinase: Preparation and properties. J Biol Chem 178: 185-195,1949.
[4] Mufson RA, Fisher PB, Weinstein IB:Effect of phorbol ester tumor promoters on the expression of melanogenesis in B16 melanoma cells.Cancer Res 39: 3915-3919, 1979.
[5] Fuller BB, Viskochil DH: The role of RNA and protein synthesis in mediating the action of MSH on mouse melanoma cells. Life Sci 24:2405-2416, 1979.
[6] Ludwig KW, Niles RM: Suppression of cyclic AMP-dependent protein kinase activity in murine melanoma cells by 12-0-tetradecanoyl phorbol-13- acetate. Biochem Biophys Res Commun 95: 296-303, 1980.
[7] Laskin JD, Piccinini L, Engelhardt DL, Weinstein IB: Specific protein production during melanogenesis in B16/C3 melanoma cells. J Cell.Physiol 114: 68-72, 1983.
[8] Jimenez M, Kameyama K, Maloy WL, Tomita Y, Hearing VJ:Mammalian tyrosinase: Biosynthesis, processing and modulation by MSH. Proc Natl Acad Sci (USA) 85: 3830-3834, 1988.
[9] Niles RM, Lowey BP: Induction of protein kinase C in mouse melanoma cells by retinoic acid. Cancer Res 49: 4483-4487, 1989.
[10] Hoganson GE, Ledwitz-Rigby F, Davidson RL, Fuller BB: Regulation of tyrosinase mRNA levels in mouse melanoma cell clones by melanocyte-stimulating hormone and cyclic AMP. Somat Cell Mol Genet 15: 255-263, 1989.
[11] Fuller BB, Niekrasz I, Hoganson GE: Down regulation of tyrosinase mRNA levels by tumor promoters and by insulin. Mol Cell Endocrinol 72: 81-87, 1990.
[12] Park HY, Russakousky V,Gilchrest BA:Depletion of protein kinase C blocks alpha melanocyte-stimulating hormone- induced melanogenesis. J Invest Dermatol 98: 645, 1992.
[13] Devi CC, Tripathi RK, Ramaiah A: Citrate activates tyrosinase from B16 murine melanoma and human skin. Pigment Cell Res 2: 117-122, 1989.
[14] Fintelmann, V. Modern phytotherapy and its uses in gastrointestinal conditions.Planta Med. 57:S48-52; 1991.
[15] Kamei, J.; Saitoh, A.; Asano, T.; Nakamura, R.; Ichiki, H.; Iiduka, A.; Kubo, M.Pharmacokinetic and pharmacodynamic profiles of the antitussive principles of Glycyrrhizae radix (licorice), a main component of the Kampo preparation Bakumondo-to (Mai-men-dong-tang). Eur. J. Pharmacol. 507:163-168; 2005.
[16] Haggag, E. G.; Abou-Moustafa, M. A.; Boucher,W.; Theoharides, T. C. The effect of aherbal water-extract on histamine release from mast cells and on allergic asthma. J. Herb. Pharmacother. 3:41-54; 2003.
[17] Haraguchi, H.; Ishikawa, H.; Mizutani, K.; Tamura, Y.; Kinoshita, T. Antioxidative and superoxide scavenging activities of retrochalcones in Glycyrrhiza inflata.Bioorg. Med. Chem. 6:339-347; 1998.
[18] Tawata, M.; Aida, K.; Noguchi, T.; Ozaki, Y.; Kume, S.; Sasaki, H.; Chin, M.; Onaya, T.Anti-platelet action of isoliquiritigenin, an aldose reductase inhibitor in licorice.Eur.J. Pharmacol. 212:87-92; 1992.

[19] Tamir, S.; Eizenberg, M.; Somjen, D.; Izrael, S.; Vaya, J. Estrogen-like activity of glabrene and other constituents isolated fromlicorice root. J. Steroid. Biochem.Mol.Biol. 78:291-298; 2001.

[20] Hill SE, Buffey J, Thody AJ, Oliver I, Bleehen SS and Mac NS:Investigation of the regulation of pigmentation in alphamelanocyte-stimulating hormone responsive and unresponsive cultured B16 melanoma cells. Pigment Cell Res 2: 161-166,1989.

[21] Matsuda H, Nakamura S, Kubo M (1994) Studies of cuticle drugs from natural sources. II. Inhibitory effects of Prunus plants on melanin biosynthesis. Biol Pharm Bull 17: 1417-1420.

978-1-61896-030-6

UV-Induced Accumulation of Photoprotective Compounds in the Edible Terrestrial Cyanobacterium *Nostoc flagelliforme*

Shenghui PANG[1], Haifeng YU[1], Guodong SUN[2], Rong LIU[1]
[1]*Shandong Provincial Key Laboratory of Microbial Engineering, Shandong Institute of Light Industry, Jinan, China*
[2]*Heze Municipal Hospital, Heze, China*
Email: yhf0831@yahoo.com.cn

Abstract: Effects of UV-B and UV-C radiation on the accumulation of photoprotective compounds scytonemin and oligosaccharide-linked mycosporine-like amino acids (OS-MAAs) in *Nostoc flagelliforme* were studied. Results revealed that both UV-B and UV-C played a positive role in the production of scytonemin, though UV-C and high level (5W/m^2) of UV-B showed inhibition after exposure for 12h and 36h. Obviously different influences of UV-B and UV-C on OS-MAAs accumulation were observed. Results showed that the synthesis of OS-MAAs was affected by different UV-B levels but the UV-C maight play a negative role in its production. In this paper, we conclude that the optimal UV source and intensity is UV-B at 3 W/m^2 for stimulation of scytonemin and UV-B at 1 W/m^2 for OS-MAAs.

Keywords: Scytonemin; mycosporine-like amino acids; cyanobacteria; *Nostoc flagelliforme*; UV radiation

1 Introduction

With the substantial loss in the stratospheric ozone layer and consequent increase in solar ultraviolet radiation on the earth's surface, incidence of skin cancer and other photoaging complications is increasing [1]. Interest in searching for natural photoprotective compounds has been augmented in recent years [2]. Cyanobacteria are a group of Gram-negative, oxygen producing photosynthetic prokaryotes that have survived and flourished on the earth for more than two billion years with the creation of oxygenic environment [3]. During the long evolutionary process, cyanobacteria have possessed complete UV-protective mechanisms, one of which is the ability of secreting a series of photoprotective compounds [4].

The most two common photoprotective substances in cyanobacteria are scytonemin and mycosporine-like amino acids (MAAs). Scytonemin is an lipid-soluble dimeric pigment with a molecular weight of 544 Da and a structure based on indolic and phenolic subunits [5] (Fig.1a) and can be induced by high photon fluence rate in cyanobacteria. It absorbs significantly at 252, 278 and 300 nm, and remains chemically stable after it is synthesized. Due to the above unique properties scytonemin has been applied to develop a variety of daily sunscreens [2]. Furthermore, scytonemin is also an inhibitor of polo-like kinase 1 activity and of various other cell cycle-regulatory kinases that could be used to build up several novel classes of therapeutically valuable drugs [6].

Typically MAAs are intracellular, small (<400 Da), colorless and water-soluble compounds that consist of cyclohexenone or cyclohexenimine chromophores conjugated with the nitrogen substituent of amino acids or its imino alcoholb [7] (Fig.1b). In some cyanobacteria, extracellular oligosaccharide-linked MAAs (OS-MAAs) may also occur [8]. MAAs are favored as photoprotective compounds because they have maximum UV absorption between 310 and 362 nm, high molar extinction coefficients, the capability to dissipate absorbed radiation efficiently as heat without producing reactive oxygen species (ROS) [9]. Besides the production of sun care products, MAAs have been commercially explored in the manufacture of several non-biological materials such as photostabilizing additives in plastics, paints and varnishes [10].

Nostoc flagelliforme, a traditional edible cyanobacterium in China, is distributed in arid or semiarid areas with poor environments, especially accompanied by high intensity solar radiation [11]. L. Ferroni has reported the high levels of scytonemin and OS-MAAs contents in *N. flagelliforme* [12], which suggest that *N. flagelliforme* is a potential source for natural photoprotective compounds. However, studies on the accumulation of secondary metabolites under UV radiation in *N.flagelliforme* are still scarce. In this paper, different UV sources (UV-B and UV-C), different UV intensity and different radiation durations are employed to study the scytonemin and OS-MAAs accumulation in *N. flagelliforme*.

2 Materials and Methods

2.1 Organisms and Culture Conditions

The *N. flagelliforme* was collected from the eastern side of the HelanMountain in Yinchuan, Ningxia Hui Autonomous Region, China and was stored in dry conditions at room temperature for 36 months before being used in experiments. The dissociated cells were obtained according to the methods previously reported [13], and were cultured in 250mL $BG11_0$ axenic culture medium in 500-mL conical flask at 25°C under continuous illumination of 60 μ mol photon m^{-2} s^{-1} and were grown to its late growth phase as inoculums.

2.2 UV Lamps and UV Treatment

50mL homogenized suspension of *N. flagelliforme* cells from their exponential growth phase (5mg dry weight) was used and irradiated under UV-B and UV-C lamps (maximum output was at 313 and 254 nm, respectively, Nanjing Hua Qiang Electronic Co.,Ltd, China), using UV light meters to measure the UV irradiance. The culture suspension was placed in glass petri dishes of 90 mm diameter over a magnetic stirrer and irradiated for 3, 6, 12, 24, 36, 48 and 60h (triplicate for each treatment). Cultures maintained under continuous illumination of 60 μmol photon m^{-2} s^{-1} light intensity provided from fluorescent tubes were always treated as control. Deionized water was added to the petri dishes in order to avoid volume change due to evaporation.

2.3 Estimation of Scytonemin

Scytonemin was extracted with 100% acetone by grinding the cells in the solvent with a motor-driven tissue grinder. Extracts were clarified by centrifugation at 5000 rpm. The scytonemin content in supernatant was estimated at 384 nm in a UV-VIS spectrophotometer (Purkinje, TU-1810, China) using a extinction coefficient of 112.6 liters g^{-1} cm^{-1} [14].

2.4 Estimation of OS-MAAs

For extraction of OS-MAAs, 5 mL cell suspension was centrifuged at 5000 rpm for 10min and the pellet was extracted in 5 mL of methanol (30% vol/vol) for 30min at 50℃ water bath in darkness. The OS-MAAs concentration was calculated from recorded spectra of the methanol extracts by using a specific extinction coefficient of 17 liters $g^{-1}cm^{-1}$ at 312 nm [8].

2.5 Determination of Biomass

The cell dry weight (DW, $g.L^{-1}$) of N.flagelliforme was calculated through a method described by Yu [15].

2.6 Statistical Analysis

All the experiments were carried out in triplicates and results were presented as mean ± standard deviation (SD) from three different readings. The statistical analyses were carried out using SPSS 18.0 and Origin 8.0. Data obtained were analysed statistically to determine the degree of significance between treatments using two way analysis of variance (ANOVA).

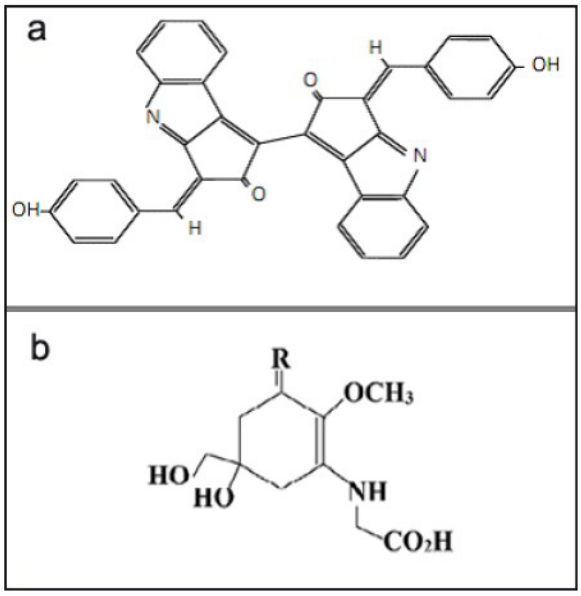

Figure 1.Structure of scytonemin (a) and basic structure of MAAs (b)

3 Results and Discussion

Cyanobacteria developed early during the Precambrian era (between 2.8 and 3.5×10^9 years), that was before the existence of the present ozone shield, it was presumed that these organisms faced high intense solar UV radiation (include UV-C) and this was the main reason for UV-C was used as a UV source in this experiment.

Fig.2 and Fig.3 showed the effects of UV-B and UV-C on the induction of scytonemin in *N.flagelliforme*. Results revealed that scytonemin content increased subsequently as the time of exposure increasing. Low levels (1 and 3 W/m^2) of UV-B continuously stimulated the synthesis of scytonemin, and the induction was 139.44% as compared to control after 60h of exposure to 3 W/m^2. However, high level (5 W/m^2) of UV-B had a adverse effect on the scytonemin production at the late stage of exposure time (from 36 h to 60 h). During the first 12h, significant inductive effects of UV-C on scytonemin synthesis were observed and 5 W/m^2 UV-C resulted in an increase of 67.61%.

978-1-61896-030-6 © 2012 SciRes.

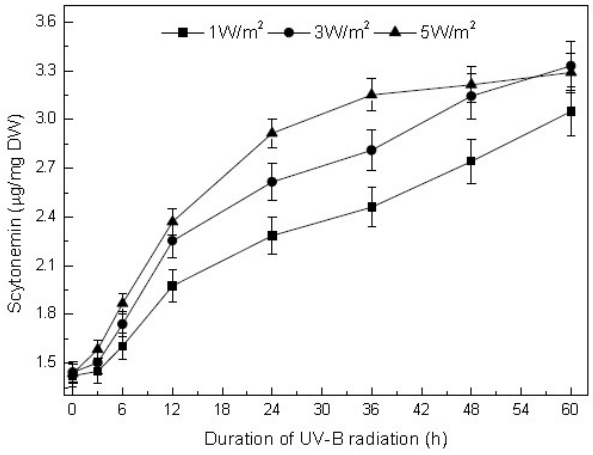

Figure 2. Scytonemin content changes in *N. flagelliforme* cells under different UV-B levels and different radiation durations

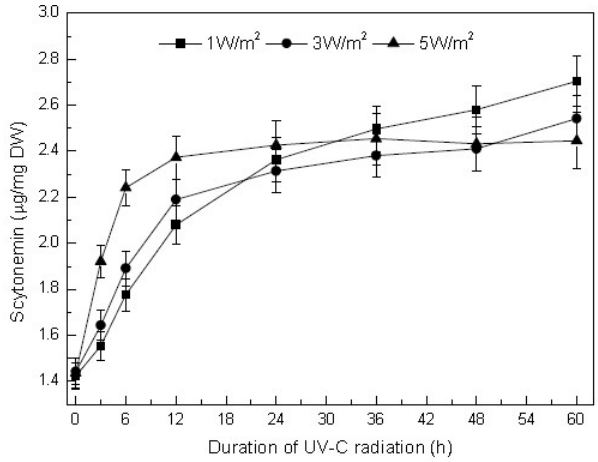

Figure 3. Scytoemin content changes in *N. flaglliforme* cells under different UV-C level and different radiation durations

Effects of UV-B and UV-C on the induction of OS-MAAs in *N.flagelliforme* were shown in Fig.4 and Fig.5. As shown in Fig.4, the effects of UV-B on OS-MAAs production were variable depending on the radiation intensity. 1 W/m^2 UV-B continuously induced the secretion of OS-MAAs, after 60 h continuous UV-B exposure, the content increased by 43.16%. However, decreases were observed at the end stage of exposure time both under the 3 and 5 W/m^2 UV-B levels. Effects of UV-C on the accumulation of OS-MAAs did not meet expectations (Fig.5). In addition to an slight enhancement in OS-MAAs content at the early exposure stage, UV-C caused rapid decrease of OS-MAAs as compared to control after 6 h of irradiation.

Scytonemin is thought to be synthesized from metabolites of aromatic amino acid biosynthesis and serves as the main photoprotective compound in cyanobacteria [5]. The reason for its accumulation may relate to the UV induced serious injury to cells. Through the analysis above, we supposed that the slow growth rate of scytonemin content under 5 W/m^2 UV-B and different levels UV-C during the later period was caused by the UV-induced metabolic inhibition. However, no decline in concentration finally indicated it possessed good photostability.

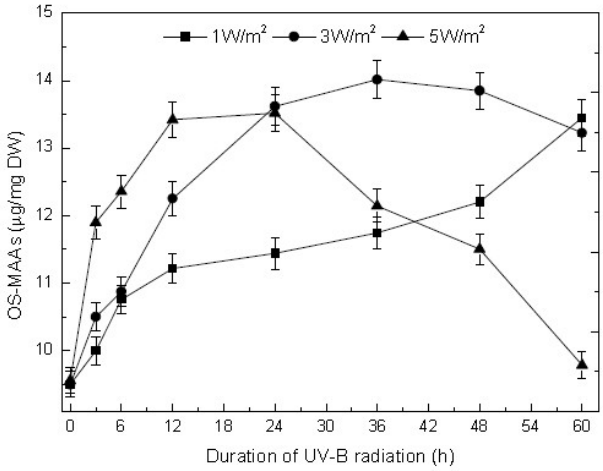

Figure 4. OS-MAAs content changes in *N. flagelliforme* cells under different UV-B levels and different radiation durations

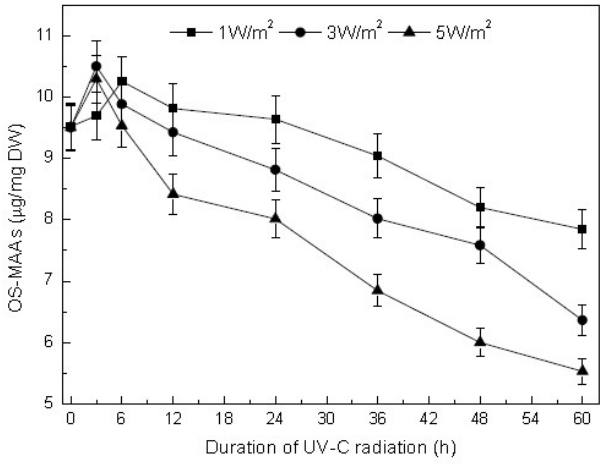

Figure 5. OS-MAAs content changes in *N. flagelliforme* cells under different UV-C levels and different radiation durations

The biosynthesis of MAAs is presumed to occur via the first part of shikimate pathway, MAAs are synthesized in bacteria, fungi, cyanobacteria, phytoplankton and macroalgae but not in animals, which lack the shikimate pathway[16]. Studies with cyanobacteria have shown that MAAs prevent 3 out of 10 photons from hitting cytoplasmic targets. Cells with high concentrations

of MAAs are approximately 25 % more resistant to ultraviolet radiation than those with no or low concentrations. UV-B induced overproduction of MAAs has been reported in many documents, however, the reasons for the decline in OS-MAAs content under high levels of UV-B needs further study.

4 Conclusion

In this experiment, both UV-B and UV-C can stimulate the synthesis of scytonemin in *N.flagelliforme* at the early stage of UV exposure and the effect of UV-C is more obvious. After an extended radiation time, the high-intensity (5 W/m^2) UV-B and three levels (1, 3 and 5W/m^2) of UV-C may inhibit the scytonemin production. With regard to OS-MAAs, it seems that the synthesis is influenced by the UV-B levels and the UV-C may play a negative role in its production. From the results described in this paper, we conclude that the optimal UV sources and intensities for stimulation of scytonemin and OS-MAAs are UV-B at 3 W/m^2 and UV-B at 1 W/m^2, respectively.

For thousands of years in China, *N. flagelliforme* is considered to be a functional food with high medicinal value. In recent years, the nutritional value, physiological and ecological characteristics, extracellular polysaccharide and training methods have been extensively studied in this organism. However, there is a lack of study on the secondary metabolism and related metabolites. We sincerely hope that our research can fill some gaps of knowledge in this field.

References

[1] R. Pallela, Y. Na-Young and S.-K. Kim, "Anti-photoaging and Photoprotective Compounds Derived from Marine Organisms," Mar. Drugs, vol. 8, 2010, pp. 1189-1202.

[2] R. P. Rastogi, Richa, R. P. Sinha, S. P. Singh and D. -P. Häder,"Photoprotective compounds from marine organisms," J Ind Microbiol Biotechnol, vol. 37, 2010, pp. 537-558.

[3] V. N. Sergeev, L. M. Gerasimenko, and G. A. Zavarzin, "The Proterozoic history and present state of cyanobacteria," Microbiology, vol. 71, 2002, pp. 725-740.

[4] J. Rozema, L. O. Björn, et al, "The role of UV-B radiation in aquatic and terrestrial ecosystems-an experimental and functional analysis of the evolution of UV-absorbing compounds," J Photochem Photobiol B Biol, vol. 66(1), 2002, pp. 2-12.

[5] S. P. Singh, S. Kumari, R. P. Rastogi, K.L. Singh, Richa and R. P. Sinha, "Photoprotective and biotechnological potentials of cyanobacterial sheath pigment, scytonemin," African Journal of Biotechnology, vol. 9, 2010, pp. 581-588.

[6] C. S. Stevenson, E. A. Capper, A. K. Roshak, et al, "Scytonemin-a marine natural product inhibitor of kinases key in hyperproliferative inflammatory diseases," Inflamm. Res, vol. 51, 2002, pp. 112-114.

[7] S. P. Singh, S. Kumari, R. P. Rastogi, K.L. Singh and R. P. Sinha, "Mycosporine-like amino acids (MAAs): chemical structure, biosynthesis and significance as UV-absorbing/screening compounds," Ind J Exp Biol. vol. 46, 2008, pp. 7-17.

[8] G. A. Böhm, W. Pfleiderer, P. Boger and S. Scherer, "Structure of a novel oligosaccharide-mycosporine-amino acid ultraviolet A/B sunscreen pigment from the terrestrial cyanobacterium Nostoc commune," J Biol Chem, vol. 270, 1995, pp. 8536-8539.

[9] F. R. Conde, M. S. Churio and C. M. Previtali, "The photoprotector mechanism of mycosporine-like amino acids. excited-state properties and photostability of porphyra-334 in aqueous solution," J Photochem Photobiol B Biol, vol. 56, 2000, pp.139-144.

[10] W. M. Bandaranayake, "Mycosporines: are they nature's sunscreens?," Nat Prod Rep, vol. 15, 1998, pp. 159-172.

[11] K.Gao, "Chinese studies on edible blue- green alga, Nostoc flagelliforme: a review," J Appl Phycol, vol. 10, 1998, pp. 37-49.

[12] L. Ferroni, M. Klisch, S. Pancaldi and D. P. Häder, "Complementary UV-Absorption of Mycosporine-like Amino Acids and Scytonemin is Responsible for the UV-Insensitivity of Photosynthesis in Nostoc flagelliforme," Marine Drugs, vol. 8, 2010, pp. 106-121.

[13] J. Su, S. Jia, X. Chen and H. Yu, "Morphology, cell growth, and polysaccharide production of Nostoc flagelliforme in liquid suspension culture at different agitation rates," Journal of Applied Phycology," vol. 20, 2008, pp. 213-217.

[14] F. Garcia-Pichel, N. D. Sherry and R. W. Castenholz, "Evidence for an ultraviolet sunscreen role of the extracellular pigment scytonemin in the terrestrial cyanobacterium Chlorogloeopsis sp.," Photochem Photobiol, vol. 56, 1992, pp. 17-23.

[15] H.Yu, S. Jia and Y. Dai, "Growth characteristics of the cyanobacterium Nostoc flagelliforme in photoautotrophic, mixotrophic and heterotrophic cultivation," Journal of Applied Phycology.vol. 21(1), 2009, pp. 127-133.

[16] A. I. Callone, M. Carignan, N. G. Montoya and J. I. Carreto, "Biotransformation of mycosporine like amino acids (MAAs) in the toxic dinoflagellate Alexandrium tamarense," J Photochem Photobiol B Biol, vol.84, 2006, pp.204-212.

978-1-61896-030-6 © 2012 SciRes.

Performance Evaluation of Beijing Water Resources System

Zhi LIU
Department of Basic Course, Shenyang University of Technology, Liaoyang, China
Email:liuzhi2099@163.com

Abstract: According to the variable weights combination prediction model are proposed based on traditional index smoothing prediction and grey system predinction, aiming at to minimize the error sum of squares. Beijing water resources system in 2009 is taken as an example to simulation. And using the same way forecast predicts 2010 Beijing water resources. A model based on the theory of fuzzy probability is used to calculate the risk degree in water. The sensitive factors of water shortage risk of Beijing in 2010 are identified by discrimination analysis.

Keywords: Index smoothing prediction; grey system; combination prediction; water shortage risk

1 Introduction

Combination prediction, proposed by Bates and Grange in 1969 [1], is a prediction method that is combining the useful information contained in all single prediction methods [2]. The objective of combination prediction is to improve the prediction accuracy as high as possible by using the information that is provided by various methods. Currently, the research of combination prediction method concentrates on the weights determination of each single prediction method, and the combination weights are normally divided into constant weights and time-varying weighs. Time-varying weighs is better than constant weights.

The shortage risk of water resources is to make regional water system of the probability of a water shortage happened and corresponding impact of water shortage due to water and water existing fuzzy and random character, in a specific environment conditions. Based on the theory of fuzzy probability，a model which can be used to comprehensively evaluate both the probability and the impact degree due to water shortage risk is developed. In the model a membership function is constructed to evaluate the fuzziness of water resources systems. On this basis, an evaluation model for water shortage risk based on fuzzy probability is obtained. The sensitive factors of water shortage risk are identified by discrimination analysis.

Beijing is a severe shortage of water resources in the world, its per capita water resources of less than 300 m3, for the national average per capita, 1/8 of the world, 1/30 of the severe water shortages of area. The shortage of water resources has influenced and restricted the capital social and economic development. So it is important to recognition the main factors on the shortage of water resources, take the corresponding effective measures to avoid risk or reduce the harm caused.

2 Model

2.1 Fixed Weights Combination Prediction Model Based on Grey-Index Smoothing

The weights are determined by optimal combination method, and the fixed weights combination prediction method is given based on minimum error sum of squares. Firstly, index smoothing prediction model and grey model GM(1,1) prediction[2] is used for single prediction to obtain the prediction errors, and then linear combination is carried out for single prediction values, and the minimum error sum of squares is taken as the object function to find the combination weights. Finally the optimal weights vector of every time is taken as occupied important degree of each single prediction model in combination prediction model to obtain the final fixed weights combination prediction model.

Assume that y_i is the actual observed value at time $i(i=1,2,\cdots,n)$; y_{ij} is the prediction value of the jth$(j=1,2,\cdots,m)$ prediction method at time i; w_j is the weights of the jth prediction; y_i is the prediction value at time i.

The normal combination prediction model is:

$$\begin{cases} \hat{y}_i = \sum_{j=1}^{m} w_j y_{ij}, \quad i=1,2,\cdots,n \\ \sum_{j=1}^{m} w_j = 1 \end{cases} \tag{1}$$

Assume that Y_{ij} is the ith$(i=1,2,\cdots,n)$ prediction value of the jth$(j=1,2,\cdots,m)$ prediction method; Y_i is the ith history data; $\varepsilon_{ji} = Y_{ji} - Y_i$ is the ith prediction deviation of the jth prediction method; w_j is the

combination weight coefficient of the jth prediction method.

The prediction deviation of combination model is:

$$\begin{aligned}\varepsilon_i &= \hat{Y}_i - Y_i \\ &= \sum_{j=1}^{m} w_j \hat{Y}_{ji} - Y_i \\ &= \sum_{j=1}^{m} w_j \hat{Y}_{ji} - Y_i \sum_{j=1}^{m} w_j \\ &= \sum_{j=1}^{m} w_j \varepsilon_{ji}\end{aligned} \tag{2}$$

Object function is the square sum of the difference between the prediction value of combination model and the prediction value of object variable, the optimal rule is established by minimizing the square sum of the difference, and the linear programming p_1 is obtained:

$$\begin{aligned}&\min Z = \sum_{i=1}^{n} [Y_i - Y_i]^2 \\ &\sum_{j=1}^{m} w_j = 1 \\ &w_j \geq 0,\ j = 1,2,\cdots,m\end{aligned} \tag{3}$$

Because of $z = \sum_{i=1}^{n} [Y_i - Y_i]^2 = \sum_{i=1}^{n} \left[\sum_{j=1}^{m} w_j \varepsilon_{ji} \right]^2$ The linear programming p_1 is transformed into the linear programming p_2:

$$\begin{aligned}&\min Z = \sum_{i=1}^{n} \left[\sum_{j=1}^{m} w_j \varepsilon_{ji} \right]^2 \\ &\sum_{j=1}^{m} w_j = 1 \\ &w_j \geq 0,\ j = 1,2,\cdots,m\end{aligned} \tag{4}$$

To solve the above linear programming problem, we can find the optimal combination prediction model based on grey-index smoothing is:

$$\hat{y}_i = w_1 y_{1i} + w_2 y_{2i} \tag{5}$$

Where y_{1i} is the prediction value of index smoothing prediction model at time i, and w_1 is its weight. y_{2i} is the prediction value of $GM(1,1)$ prediction model at time i, and w_2 is its weight. The analytic expression of weight is:

$$w_j = \frac{h_{jj}^{-1}}{h_{11}^{-1} + h_{22}^{-1}},\ j = 1,2 \tag{6}$$

Where $h_{jk} = h_{kj} = \sum_{i=1}^{n} \varepsilon_{ji} \varepsilon_{ki}$ is the covariance of deviation of two models.

2.2 Model for Evaluating Water Shortage Risk Based on Fuzzy Probability

Water resources system based on the fuzzy uncertainty [3], and constructs a suitable membership function to describe the water supply crash damage. Assume that $x = W_d - W_s$ is shortages of water, $\mu_w(x)$ is membership function of the shortages of water in the fuzzy sets:

$$W_e = \{x : 0 \leq \mu_w(x) \leq 1\} \tag{7}$$

$$\mu_w(x) = \begin{cases} 0, & 0 \leq x \leq W_a \\ \left(\dfrac{x - W_a}{W_m - W_a} \right)^p, & W_a < x < W_m \\ 1, & x \geq W_m \end{cases} \tag{8}$$

Where w_s is the supplying water; w_d the requirement of water; w_a is the minimum in the requirement of water; w_m is the maximum in the requirement of water; P is an integer which is greater than 1.

The shortage risk of water resources is defined as the probability of occurrence in A fuzzy events[4]-[6]:

$$P(A_f) = \int_{R^n} \mu_{A_f}(y) f(y)\, dy \tag{9}$$

Quick Clust process is used to intuitive that the shortage of water resources of the risk degree. Euclidean distance is the measure of interval for variable and Chsquaremeasure is the similarity between variables [7]-[8]:

$$EUCLD(x, y) = \sqrt{\sum_i (x_i - y_i)^2} \tag{10}$$

$$CHISQ(x, y) = \sqrt{\frac{\sum_i (x_i - E(x_i))^2}{E(x_i)} + \frac{\sum_i (y_i - E(y_i))^2}{E(y_i)}} \tag{11}$$

3 Example Analysis

Beijing water resources system is taken as an example to evaluate.The water resources data for 9 years is shown in table 1.

3.1 Fixed Weights Combination Prediction

Table 1. Water consumption and water resources in total from 2001 to 2009

2009	Real	Combination	Absolute error	Relative error
Water consumption	35.5	35.423	-0.077	-0.002
Water resources	21.8	21.939	0.139	0.006

978-1-61896-030-6 © 2012 SciRes.

Table 2. Index smoothing and GM (1,1) predictive value and error

Year	01	02	03	04	05	06	07	08	09
Water consumption（108 m3）	38.9	34.6	35.8	34.6	34.5	34.3	34.8	35.1	35.5
Water resources（108 m3）	19.2	16.1	18.4	21.4	23.2	24.5	23.8	34.2	21.8

(IS: Index smoothing)

Table 3. Combination predictive value and error

2009	Real	IS	Absolute error	Relative error	GM（1,1）	Absolute error	Relative error
Water consumption	35.5	35.612	0.112	0.003	35.034	-0.466	-0.013
Water resources	21.8	21.076	-0.724	-0.332	22.662	0.862	0.040

Water consumption and water resources in total in 2010. And the water consumption and water resources are 35.725 and 23.924. The water consumption and water resources from 2001 to 2010 are shown in figure 1.

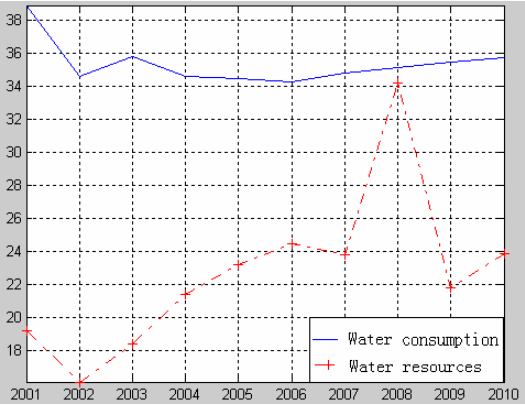

Figure 1. Water consumption and water resources from 2001 to 2010

3.2 Evaluate Water Shortage Risk

First, model (9) is used to calculate the lacks water risk degree in Beijing respectively from 2001 to 2010. The results are 1.00, 0.94, 0.88, 0.65, 0.55, 0.47, 0.54, 0, 0.68, 0.58.

Second, Quick Clust process is used to intuitive that the shortage of water resources of the risk degree. The final class centers and features of all kinds of risks such as shown in table 4.

Table 4. The final class centers and features

Category	Center	Characteristics
Min risk	0.03	Negligible
Lower risk	0.32	Acceptable
Med risk	0.54	Edge risk
More risk	0.73	More serious
Max risk	0.84	Cannot afforded

Final, according to the above evaluation model, the lacks water risk degree in Beijing in 2010 is 0.58 which is in the danger of edge.

4 Conclusions

In this paper, fixed weights combination prediction model based on grey-index smoothing is used to predicted the total water consumption and water resources of Beijing in 2010; and the fuzzy probability method is used to calculate the shortage risk of water resources in Beijing from 2001 to 2010, Quick Clust process is used to intuitive that the shortage of water resources of the risk degree. 2010 Beijing is modest level of water shortage So we must take the recycled water reuse and diversion measures to improve Beijing water shortages.

References

[1] J. M. Bates and C. W. Grang, Combination of forecasts, Operations Research Quarterly, vol.20, pp451-468, 1969.
[2] J. L. Deng The course of grey system theory, Wuhan: HUST Press, 1990.
[3] Hashimoto T, Stedinger J R, Loucks D P. Reliability, resiliency and vulnerability criteria for water resources system erformance evaluation[J]. Water Resour. Res. 1982, 18(1):14-20.
[4] Bagel MS, Das Gupta A, Nayak DK. A model for optimal allocation of water to competing demands[J]. Water Resources Management, 2005, 19(6):693-712.
[5] Bardossy A, Disse M. Fuzzy rule based models for infiltration[J].Water Resour.Res. 1993, 29(2), 373-382.
[6] Bogardi I, Bordossy A, Duckstein L. Regional management of an aqifer for mining under fuzzy environmental objectives [J].Water Resour. Res., 1983, 19(6): 1394-1402.
[7] Mujumdar P P, Sasikumar K. A fuzzy risk approach for seasonal water quality management of a river system[J].Water Resour. Res, 2002, 38(1): 1-9.
[8] Sasi Kumar K, Mujumdar P P. Application of fuzzy probability in water quality management of a river system[J].Int. J.Syst.Sci., 200030(5): 575-591.

Synthesis of Mandelic Acid and Analogues by Phase Transfer Catalysis under Microwave Irradiation

Qingfang CHENG[1], Qifa WANG[2], Guochuang ZHENG[1]
[1]*School of Chemical Engineering, Huaihai Institute of Technology, Lianyungang, Jiangsu, China*
[2]*Jiangsu Key Laboratory of Marine Biotechnology, Huaihai Institute of Technology, Lianyungang, Jiangsu, China*
Email: cheng_qingfang@yahoo.com.cn

Abstract: Mandelic acid and analogues were synthesized from benzaldehyde or substituted benzaldehydes with chloroform in the presence of 40% NaOH by the combination of catalytic amount of phase transfer catalysis cetyltrimethylammonium bromide (CTAB), and microwave irradiation. The catalyst CTAB possessed high catalytic activity for the reaction and mandelic acid and analogues were obtained with yields of 70.9%-93.6% within 12 to 27 minutes under microwave irradiation. Effects of different factors, such as catalyst concentration, reaction temperature, power of microwave, had been investigated to obtain the optimum condition.

Keywords: Mandelic acid; phase transfer catalyst; microwave irradiation; synthesis

1 Introduction

Mandelic acid (MA) is an important starting compounds for the resolution of (*R*)-mandelic acid and (*S*)-mandelic acid [1-4]. Mandelic acid derivatives have been widely employed for the manufacture of semisynthetic penicillins or cephalosporins, and for the synthesis of various other pharmaceuticals [5,6]. Many approaches for the synthesis of mandelic acid have been reported [7-9], and two pathways have risen into prominence. One is based on the hydrocyanation of benzaldehyde in the presence of chloroform, which gives rise to the corresponding cyanohydrin, followed by hydrolysis in the presence of strong acid such as concentrated acid (Scheme 1). This procedure involved poisonous raw materials, generated copious quantities of salt and is not compatible with sensitive functional groups. The other pathway is feasible by combining a chlorination of hypnone and a hydrolysis in alkaline water (Scheme 2), but it also involves many disadvantages, such as harsh condition, long reaction time and low yield.

Microwave-assisted reactions have received a great deal of attention since 1986 [10], because this technique is more convenient and easily controlled compared with traditional methods. A large number of organic reactions can be carried out in higher yields, shorter reaction time and milder conditions under microwave irradiation [11,12]. We have reported one-pot, three-component reaction of aromatic aldehydes, malononitrile and barbituric acid under microwave irradiation successfully [13].

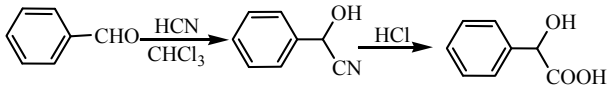

Scheme 1. Synthesis of mandelic acid via benzaldehyde and hydrocyanic acid

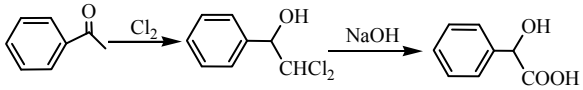

Scheme 2. Synthesis of mandelic acid via benzaldehyde and chlorine

In recent years, "green synthesis" is one of the most fascinating developments in organic synthesis. Wender defined the "ideal synthesis" as one in which the target molecule is prepared from readily available, inexpensive starting materials in one simple, safe, environmentally acceptable, and resource-effective operation that proceeds quickly and in quantitative yield [14]. To the best of our knowledge, the synthesis of mandelic acid and analogues from benzaldehyde or substituted benzaldehydes with chloroform by the combination of phase transfer catalysis and microwave irradiation has not yet been reported. In continuation of our research interest in the use of microwave irradiation and green synthesis [15], we report herein, the microwave-assisted synthesis of mandelic acid and analogues from benzaldehyde or substituted benzaldehydes with chloroform in the presence of 40% NaOH by the combination of a single phase transfer CTAB, and microwave irradiation.

2 Results and Discussion

To achieve suitable conditions for the synthesis of mandelic acid and analogues, various reaction conditions have been investigated in the model reaction of benzaldehyde

978-1-61896-030-6

with chloroform in the presence of 40% NaOH by the combination of phase transfer catalysis cetyltrimethyl-ammonium bromide (CTAB), and microwave irradiation to give mandelic acid (**2a**) (Scheme 3). Initially, we examined the effect of the catalyst cetyltrimethyl ammonium bromide (CTAB) on the model reaction of benzaldehyde with chloroform affording mandelic acid **2a** (Scheme 3). The results are presented in Table 1.

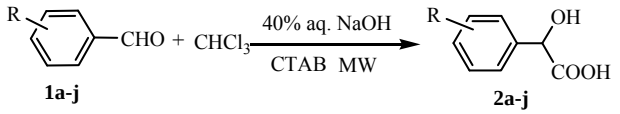

1a-j **2a-j**

Scheme 3. Synthesis of mandelic acid and analogues 2a-j

The phase transfer catalysis CTAB played a crucial role in the model microwave-assisted reaction. Without CTAB, the reaction time is long and the yield is only 20.6% (Table 1, Entry 1). The phase transfer catalysis CTAB is highly effective, the model reaction could be carried out with 1.0 mol% catalyst loading, affording 53.6% yield of mandelic acid **2a** after irradiated 15mins at 60 °C (Table 1, Entry 3). The increase of the amount of CTAB remarkably accelerated the reaction (Table 1, Entries 4-13). The model reaction in the presence of 5 mol% CTAB was found to be completed after 15 min. at 60 °C under microwave irradiation, giving mandelic acid **2a** in 89.5 % yield (Table 1, Entry 14). However, when the amount of CTAB exceeded 5 mol%, the yield decreased (Table 1, Entries 15-16).

Table 1. The effect of catalyst concentration on the model reaction[a]

Entry	Catalyst (mol%)	Irradiation time(min)	Yield[b] (%)
1	0.0	20	20.6
2	1.0	10	50.6
3	1.0	15	53.6
4	1.0	20	54.3
5	1.5	15	59.9
6	1.5	20	62.8
7	2.0	15	67.2
8	2.0	20	67.8
9	2.5	15	73.2
10	3.0	15	76.9
11	3.5	15	82.5
12	4.0	15	84.7
13	4.5	15	86.5
14	5.0	15	89.5
15	5.5	15	85.6
16	6.0	15	80.8

[a] Reaction conditions: benzaldehyde (20 mmol), chloroform (10 mL), 40% NaOH (15 mL), temperature 60 ^{0}C, microwave power 500W.
[b] Isolated yield.

The effect of reaction temperature on the model reaction was also examined. The model reaction at 30 °C for 10 min. gave only a 38.2% yield of desired mandelic acid **2a**; even when the reaction time was extended for 20 min. at 30 °C, the yield can only obtained 42.8% (Table 2, Entry 3). The increase of reaction temperature remarkably accelerated the reaction (Table 2, Entries 4-9). A high yield can be obtained within 15 min. when the model reaction was carried out at 60 °C (Table 2, Entry 8). However, for this reaction, a higher temperature was unfavorable (Table 2, Entries 10-11).

Table 2. The influence of temperature on the model reaction[a]

Entry	Temperature(°C)	Irradiation time (min.)	Yield[b] (%)
1	30	10	38.2
2	30	15	41.3
3	30	20	42.8
4	40	15	52.6
5	40	20	53.9
6	50	15	77.5
7	50	20	78.6
8	60	15	89.5
9	60	20	89.1
10	70	15	82.1

[a] Reaction conditions: benzaldehyde (20 mmol), chloroform (10 mL), 40% NaOH (15 mL), CTAB (1 mmol), microwave power 500W.
[b] Isolated yield.

The effect of microwave power on the model reaction was also examined. The microwave is another important factor for the reaction. In the absence of microwave, the reaction must be performed for 6 h to produce a low yield of 40.4% (Table 3, Entry 1). One can observe that microwave with different powers leads to various results (Table 3, Entries 2-13). The yield increased at first and then decreased with a variation of microwave power from 100 to 600 W. The addition of microwave can effectively enhance the yield up to 73.7% and reduce the reaction time to 10 min. (Table 3, Entry 9). The best yield (89.5%) was obtained with microwave power at 500 W (Table 3, Entry 11).

Table 3. The effect of microwave power on the model reaction[a]

Entry	Microwave power(W)	Reaction time(min)	Yield[b] (%)
1	0	3600	40.4
2	100	30	51.6
3	100	60	52.7
4	200	15	56.4
5	200	30	58.9
6	200	60	60.5
7	300	15	64.2
8	300	20	65.7
9	400	15	73.7
10	400	20	75.8
11	500	15	89.5
12	500	20	88.4
13	600	15	80.3

[a] Reaction conditions: benzaldehyde (20 mmol), chloroform (10 mL), 40% NaOH (15 mL), CTAB(1 mmol), temperature 60 ^{0}C.
[b] Isolated yield.

This method was further studied in several recations of substituted benzaldehydes **1b-j** with chloroform in the presence of 40% NaOH by the combination of phase transfer catalysis cetyltrimethylammonium bromide (CTAB), and microwave irradiation to give the respective mandelic acid analogues **2b-j**. The results are presented in Table 4.

Table 4. Synthesis of mandelic acid and analogues 2a-j catalyzed by CTAB under microwave irradiation[a]

Entry	Product	R	Irradiation time[b] (min.)	Yield[c] (%)
1	**2a**	H	15	89.5
2	**2b**	4-Me	12	93.6
3	**2c**	4-OMe	14	90.3
4	**2d**	4-OH	15	86.5
5	**2e**	3-OMe-4-OH	17	85.7
6	**2f**	4-F	20	79.6
7	**2g**	4-Cl	20	76.4
8	**2h**	4-Br	20	72.5
9	**2i**	3-Cl	25	65.8
10	**2j**	2-Cl	27	60.9

[a] Reaction conditions: substituted benzaldehyde (20 mmol), chloroform (10 mL), 40% NaOH (15 mL), CTAB (1 mmol), temperature, 60 ^{0}C, microwave power 500W. [b] Monitored by TLC.
[c] Isolated yield.

We found that the results were excellent in terms of yields using aromatic aldehydes carrying electron-donating substituents (Table 4, entries 2-5). Under the same conditions, however, the reactions with aromatic aldehydes carrying electron-withdrawing groups required a longer time and the yields of some products notably decreased (Table 4, entries 6-8). It was also found that the meta-and ortho-substituted aromatic aldehydes generally gave lower yields, probably due to the large steric effect (Table 4, entries 9-10). That is to say, steric factors played a key role in affecting the rates of reaction and the reactions required a longer time.

3 Experimental

Apparatus and Analysis

All reagents were purchased from commercial sources and used without further purification. The microwave irradiation reactions were carried out in a temperature-controlled single beam microwave oven for organic synthesis MARS5 (Microwave Apparatus CEM Corporation, Matthews, NC, USA). IR spectra were recorded on a Nicolet FT IR-500 spectrometer. ^{1}H NMR spectra were recorded on a Bruker DPX 300 MHz spectrometer, and shifts are given in ppm downfield from TMS as an internal standard, $CDCl_3$ as the solvent. Elemental analysis was performed on an Elementar Vario EL III analyzer. Melting points were determined on a XT-5A digital melting-points apparatus and are uncorrected.

General procedure for the synthesis of mandelic acid and analogues **2a-j** Preparation of mandelic acid (**2a**) is described as an example: Benzaldehyde (20 mmol), chloroform (10 mL) and phase transfer catalysis CTAB (1 mmol), were placed in a three-neck 100 mL flask and stirred in a microwave reaction vessel at 60 °C (the microwave power was set at 500 W). Then 15 mL 40% aq. sodium hydroxide was added dropwise under microwave irradiation. After addition, the reaction was continued to irradiated at 60 °C for some times until the benzaldehyde has completely reacted, as indicated by TLC. Then the reaction mixture was quenched in 30 mL water, the aqueous layer and organic layer were separated. The aqueous layer was acidified to a pH value of approximately one by using 50% aq. concentrated hydrochloric acid, and then extracted with ethyl acetate (2×20 mL). The combined extracts were distilled to remove ethyl acetate under reduced pressure. After recrystallization from toluene, pure mandelic acid **2a** was obtained by filtration.

Mandelic acid (2a) White solid, m.p. 188-189 $^\circ$C; IR (KBr) υ: 3412, 3215, 2918, 2849, 1726, 1503, 1452 cm^{-1}; ^{1}H NMR (300MHz, $CDCl_3$) δ: 9.06 (s, 1H, COO-H), 7.32-7.69 (m, 5H, ArH), 5.11 (s, 1H, O-H), 2.43 (s, 1H, C-H); MS-ESI (*m/z*): 152.9 (M+H).

4-Methyl mandelic acid (2b) White solid, m.p. 136-137 $^\circ$C; IR (KBr) υ: 3406, 3257, 2933, 2829, 1703, 1499, 1472 cm^{-1}; ^{1}H NMR (300MHz, $CDCl_3$) δ: 8.92 (s, 1H, COO-H), 8.17 (d, *J*=8.1 Hz , 2H, ArH), 7.32 (d, *J*=8.1 Hz, 2H, ArH), 5.36 (s, 1H, O-H), 2.45 (s, 1H, C-H), 2.37 (s, 3H, CH_3); MS-ESI (*m/z*): 167.1 (M+H).

4-Methoxyl mandelic acid (2c) White solid, m.p. 109-111°C; IR (KBr) υ: 3465, 3278, 2913, 2809, 1674, 1487, 1445 cm^{-1}; ^{1}H NMR (300MHz, $CDCl_3$) δ: 9.13 (s, 1H, COO-H), 8.29 (d, *J*=9.1 Hz , 2H, ArH), 7.11 (d, *J* =9.1 Hz, 2H, ArH), 5.67 (s, 1H, O-H), 3.91 (s, 3H, CH_3), 2.49 (s, 1H, C-H); MS-ESI (*m/z*): 181.3 (M-H).

4-Hydroxyl mandelic acid (2d) White solid, m.p. 83-85 $^\circ$C; IR (KBr) υ: 3465, 3278, 2913, 2809, 1674, 1487, 1445 cm^{-1}; ^{1}H NMR (300MHz, $CDCl_3$) δ: 10.9 (s, 1H, O-H), 9.22 (s, 1H, COO-H), 8.42 (d, *J*=8.1 Hz, 2H, ArH), 6.93 (d, *J*= 8.1 Hz, 2H, ArH), 5.61 (s, 1H, O-H), 2.46 (s, 1H, C-H); MS-ESI (*m/z*): 169.2 (M+H).

3-Methoxyl-4-hydroxyl mandelic acid (2e) White solid, m.p. 132-134 $^\circ$C; IR (KBr) υ: 3489, 3298, 2968, 2843, 1689, 1487, 1456 cm^{-1}; ^{1}H NMR (300MHz, DCl_3) δ: 10.82 (s, 1H, O-H), 9.31 (s, 1H, COO-H), 8.27 (s, 1H, ArH), 7.89(d, *J*=8.4 Hz, 1H, ArH), 6.95(d, *J*= 8.4 Hz, 1H, ArH), 5.67 (s, 1H, O-H), 3.86 (s, 3H, CH_3), 2.51 (s, 1H, C-H); MS-ESI (*m/z*): 199.1 (M+H).

4-Fluoro mandelic acid (2f) White solid, m.p. 134-136 $^\circ$C; IR (KBr) υ: 3408, 3226, 2926, 2839, 1713, 1499, 1436 cm^{-1}; ^{1}H NMR (300MHz, $CDCl_3$) δ: 9.26 (s, 1H, COO-H), 7.12-7.41 (m, 4H, ArH), 5.37 (s, 1H, O-H), 2.39 (s, 1H,

978-1-61896-030-6 © 2012 SciRes.

C-H); MS-ESI (*m/z*): 169.3 (M-H).

4-Chloro mandelic acid (2g) White solid, m.p. 117-119 °C; IR (KBr) *υ*: 3388, 3247, 2918, 2844, 1702, 1478, 1439 cm^{-1}; ^1H NMR (300MHz, $CDCl_3$) δ: 9.19 (s, 1H, COO-H), 7.39 (d, *J*=6.5 Hz, 2H, ArH), 7.27 (d, *J*= 6.5 Hz, 2H, ArH), 5.46 (s, 1H, O-H), 2.41 (s, 1H, C-H); MS-ESI (*m/z*): 187.4 (M+H).

4-Bromo mandelic acid (2h) White solid, m.p. 120-121 °C; IR (KBr) *υ*: 3399, 3256, 2903, 2852, 1713, 1489, 1452 cm^{-1}; ^1H NMR (300MHz, $CDCl_3$) δ: 9.25 (s, 1H, COO-H), 7.32 (d, *J*=7.2 Hz, 2H, ArH), 7.16 (d, *J*= 7.2 Hz, 2H, ArH), 5.41 (s, 1H, O-H), 2.42 (s, 1H, C-H); MS-ESI (*m/z*): 232.1 (M+H).

3-Chloro mandelic acid (2i) White solid, m.p. 112-113 °C; IR (KBr) *υ*: 3389, 3236, 2911, 2835, 1701, 1465, 1431 cm^{-1}; ^1H NMR (300MHz, $CDCl_3$) δ: 9.22 (s, 1H, COO-H), 7.29-7.41 (m, 4H, ArH); 5.58 (s, 1H, O-H), 2.48 (s, 1H, C-H); MS-ESI (*m/z*): 185.5 (M-H).

2-Chloro mandelic acid (2j) White solid, m.p. 117-119 °C; IR (KBr) *υ*: 3376, 3241, 2906, 2857, 1714, 1451, 1429 cm^{-1}; ^1H NMR (300MHz, $CDCl_3$) δ: 9.33 (s, 1H, COO-H), 7.21-7.34 (m, 4H, ArH); 5.52 (s, 1H, O-H), 2.42 (s, 1H, C-H); MS-ESI (*m/z*): 185.6 (M-H).

4 Conclusion

The reaction of benzaldehyde or substituted benzaldehydes with chloroform can be efficiently performed in the presence of 40% NaOH by the combination of catalytic amount of phase transfer catalysis CTAB, and microwave irradiation giving good to high yields of the respective mandelic acid or mandelic acid analogues **2a-j**. Phase transfer catalysis CTAB is promising for the development of green catalysts.

References

[1] K. David, N. Agnes, A Maria, F. Elemer, "Optical resolution of mandelic acid by cinchonine in different solvents," Tetrahedron: Asymmetry, Vol 5, 1994, pp.315-316.

[2] J. K. Whitesell, D. Reynolds, "Resolution of chiral alcohols with mandelic acid," J. Org. Chem., Vol 48, 1983, pp. 3548-3551.

[3] S. P. Zingg, E. M. Arnett, A.T. McPhail, A.A. Bothnerby, "Chiral discrimination in the structures and energetics of association of stereoisomeric salts of mandelic acid with alpha.-phenethylamine, ephedrine, and pseudoephedrine," J. Am. Chem. Soc., Vol 110, 1988, pp. 1565-1580.

[4] P. Saravanan, V. K. Singh, "An efficient synthesis of chiral nonracemic diamines: Application in asymmetric synthesis," Tetrahedron Lett., Vol 39, 1998, pp.167-170.

[5] Y. T. Yokohama, T. N. Saitama, S. Aoki, R. Nishizawa, "Process for preparing optically active amino acid or mandelic acid," US Patent: 4224239, 1980.

[6] J. Mill, K. K. Schmiegel, W. N. Shaw, "Phenethanolamines, compositions containing the same, and method for effecting weight control," US Patent: 4391826, 1983.

[7] M. A. K. Patterson, R. P. Szajewski, G. M. Whitesides, "Enzymic conversion of .alpha.-keto aldehydes to optically active .alpha.-hydroxy acids using glyoxalase I and II, " J. Org. Chem., Vol 46, 1981, pp. 4682-4685.

[8] T. Mori, M. Furui, K. Nakamichi, E. Takahashi,"Process for producing D-mandelic acid from benzoylformic acid," US Patent: 5441888, 1995.

[9] H. R. Huang, J. H. Xu, Y. Xu, J. Pan, X. Liu,"Preparation of (*S*)-mandelic acids by enantioselective degradation of racemates with a new isolate *Pseudomonas putida* ECU1009," Tetrahedron: Asymmetry, Vol 16, 2005, pp. 2113-2117.

[10] R. Gedye, F. Smith, K. Westaway, "The use of microwave ovens for rapid organic synthesis," Tetrahedron Lett., Vol 27, 1986, pp. 279-282.

[11] C. O. Kappe,"Controlled microwave heating in modern organic synthesis," Angew. Chem. Int. Ed. Engl., Vol 43, 2004, pp. 6250-6284.

[12] Loupy A, "Microwaves in organic synthesis," 2nd Eds. Wiley: New York, NY, 2006.

[13] Q. F. Cheng, X. Y. Xu, Q. F. Wang, J. L. Zhang, L. Zhang, X. J. Yang, "One-pot synthesis of pyrano [2,3-*d*] pyrimidine derivatives in aqueous media under microwave irradiation," Chin. J. Appl. Chem., Vol 27, 2010, pp. 673-676.

[14] P. A. Wender, "Introduction: Frontiers in organic synthesis," Chem. Rev., Vol 96, 1996, pp. 1-2.

[15] Q. F. Cheng, Q. F. Wang, X. Y. Xu, M. J. Ruan, H. L.Yao, X. J.Yang, "Solvent-free synthesis of monastrol derivatives catalyzed by NaHSO4," J. Heterocyclic Chem., Vol 47, 2010, pp. 624-628.

Synthesis of *N*-Maleoyl-Amino Acid-Curcumin under Ultrasonic Irradiation

Qingfang CHENG[1], Qifa WANG[2], Jianping TANG[1], Feng QIU[1]
[1]*School of Chemical Engineering, Huaihai Institute of Technology, Lianyungang, Jiangsu, China*
[2]*Jiangsu Key Laboratory of Marine Biotechnology, Huaihai Institute of Technology, Lianyungang, Jiangsu, China*
Email: cheng_qingfang@yahoo.com.cn

Abstract: *N*-maleoyl-amino acid-curcumins were synthesized from curcumin and *N*-maleoyl amino acids by using 1,3-dicyclo-hexylcarbodiimide (DCC) as a condensation agent at 30°C under ultrasonic irradiation. The condensation agent DCC possessed high activity for the reaction and *N*-maleoyl-amino acid-curcumins were obtained with yields of 71.2%-85.6% within 2.5 to 3.5 h under ultrasonic irradiation. Effects of different factors, such as concentration of condensation agent, reaction temperature, frequency of ultrasound, had been investigated to obtain the optimum conditions.

Keywords: DCC; *N*-maleoyl amino acid; ultrasonic irradiation; *N*-maleoyl-amino acid-curcumin; esterification

1 Introduction

Curcumin (diferuloylmethane, 1,7-bis(4-hydroxy-3-methoxyphenyl)-1,6-hepta-diene-3,5-dione), isolated as a yellow pigment from the root of Curcuma longa L., is a chemopreventive and chemotherapeutic natural product. Curcumin is commonly used as a food colourant, spice in India, better known as “Indian solid gold” due to its numerous therapeutic activities, its pharmacological safety and its colour [1]. This naturally occurring and synthetic compound has been reported to process anticarcinogenic [2], anti-inflammatory [3], antioxidative [4], anti-cancer [5] and anti-HIV [6] activities. Some studies on the cancer chemopreventive activities have been carried out with curcumin, which inhibits tumorigenesis during both the initiation and promotion stages in several animal models possibly through inhibition of cyclo-oxygenase and lipoxygenase [7] and blocking the formation of arachidonic acid metabolites. Other studies have also shown that curcumin inhibits COX-2 expression in human gastrointestinal epithelial cells [8].

Pharmacologically, curcumin is quite safe and doses as high as 8 g/day have been administered orally to humans with no side effects [9]. However, curcumin is unstable at a pH 7.4 and insolubility in water at acidic and neutral pH conditions. Another drawback is its very poor bioavailability [10]. Cellular uptake is slow and it gets metabolised fast once inside the cell, requiring repetitive oral doses in order to achieve significant concentration inside the cells for therapeutic activity. Moreover, the transportation across the cellular membrane of the infected cells is also changed, which necessitates the molecule to be transported to be well internalised with the changed environment of the cell.

It has also been reported that the activity of curcumin depends upon the presence of the phenolic groups and the α, β-unsaturated carbonyl moiety [11]. The α,β-unsaturated carbonyl moiety acts as a Michael reaction acceptor to covalently bind with sulfhydryl-rich proteins (Keap 1), signaling the up-regulation of phase 2 enzymes. On the other hand, other studies also concluded that the central methylene hydrogens of curcumin are important for antioxidant activity [12]. Recently, Litwinienko demonstrated that both the phenolic groups and the central methylene hydrogens may be involved in the mechanism of formation of the phenoxyl radical, depending on reaction conditions [13]. So, one of the accessible approaches was to make monooconjugates of curcumin by covalent attachment with some ligands, which internalise with cellular environment of infected cells. The amino acids, for example, glycine is essential components of bacterial cells. These components when linked covalently to curcumin molecule may act as carrier molecules as the cells recognise these molecules and thereby might increase the intracellular delivery of curcumin. The conjugates also are likely to be metabolised comparatively slowly.

Ultrasound has increas- ingly been used in organic synthesis in last three decades, this technique is more convenient and easily controlled compared with traditional methods. A large number of organic reactions can be carried out in higher yield, higher selectivity of reactions, shorter reaction time and milder conditions under ultrasonic irradiation. We have reported one-pot, three-component reaction under ultrasound irradiation [14]. To the best of our knowledge, the synthesis of curcumin monooconjugates with amino acids by the combination of DCC condensation agent and ultrasonic irradiation has not yet been reported. In continuation of our research interest in the use of ultrasonic irradiation and green

978-1-61896-030-6

synthesis, we report herein, the ultrasound-assisted synthesis of *N*-maleoyl-amino acid-curcumins from curcumin and *N*-maleoyl amino acids by using DCC as a condensation agent under ultrasonic irradiation.

2 Results and Discussion

During the synthesis, the amino function of amino acids was protected with maleic anhydride as *N*-maleoyl amino acids **2a-f**. These acylation reactions could be easy carried out in water with high yields without any catalyst. These obtained solid of *N*-maleoyl amino acids are relatively stable and could be easy saved. The *N*-maleoyl amino acids **2a-f** was subjected to esterification with curcumin to afford the corresponding *N*-maleoyl-amino acid-curcumins **4a-f** using DCC as a condensation agent under ultrasonic irradiation (Scheme 1).

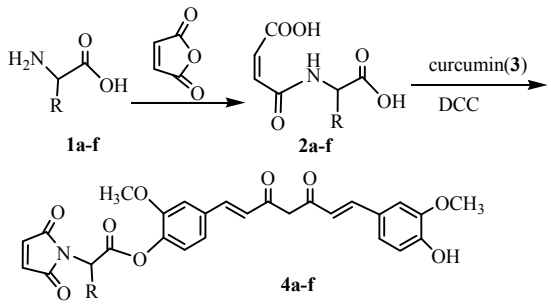

Scheme 1. Synthesis of *N*-maleoyl-amino acid-curcumins 4a-f

To achieve suitable conditions for the synthesis of *N*-maleoyl-amino acid-curcumins, various reaction conditions have been investigated in the model reaction of curcumin with *N*-maleoyl glycine **2a**. Initially, we examined the effect of the condensation agent DCC on the model esterification reaction of curcumin with *N*-maleoyl glycine **2a** affording *N*-maleoyl-glycine-curcumin **4a**. The results are presented in Table 1.

The condensation agent DCC is played a crucial role in the model reaction. Without the condensation agent DCC, the esterification reaction could not be carried out (Table 1, Entry 1). When DCC was added, the esterification reaction could be smoothly carried out. When the reactants were mixed in the molar ratio of curcumin to DCC 1:1, and exposed to ultrasonic irradiation at 30 °C for 2 h gave only a 54.4% yield of desired *N*-maleoyl-glycine- curcumin **4a** (Table 1, Entry 2); even when the reaction time was extended for 3 h at 30 °C, the yield can only obtained 61.4% (Table 1, Entry 4).

Table 1. The effect of DCC concentration on the model reaction[a]

Entry	*n*(DCC):*n* (**3**)	Irradiation time(h)	Yield[b] (%)
1	0	4.0	0
2	1.0	2.0	54.4
3	1.0	2.5	59.7
4	1.0	3.0	61.4
5	1.1	2.0	69.2
6	1.1	2.5	73.4
7	1.1	3.0	74.1
8	1.15	2.5	77.7
9	1.20	2.5	82.5
10	1.25	2.5	85.6
11	1.30	2.5	85.5
12	1.35	2.5	85.6

[a] Reaction conditions: curcumin (4 mmol), *N*-maleoyl glycine (4.4 mmol), *p*-toluenesulfonic acid (0.5 mmol), acetonitrile (15 mL), temperature 30 ^{0}C, ultrasound frequency 60 kHz;
[b] Isolated yield.

The increase of the amount of DCC remarkably accelerated the reaction. The model reaction in the molar ratio of curcumin to DCC 1:1.25 was found to be completed after 2.5 h under ultrasonic irradiation, giving *N*-maleoyl-glycine-curcumin **4a** in 85.6 % yield (Table 1, Entry 10). However, when the the molar ratio of curcumin to DCC exceeded 1:1.25, there is no apparent effect on the yield (Table 1, Entries 11-12).

Table 2. The influence of temperature on the model reaction[a]

Entry	Temperature(°C)	Irradiation time (h)	Yield[b] (%)
1	20	2.0	56.7
2	20	2.5	62.5
3	20	3.0	63.4
4	25	2.5	74.6
5	25	3.0	77.9
6	30	2.5	85.6
7	30	3.0	83.2
8	35	2.5	81.5
9	45	2.5	77.1
10	55	2.5	71.5

[a] Reaction conditions: curcumin (4 mmol), *N*-maleoyl glycine (4.4 mmol), DCC (5 mmol), *p*-toluenesulfonic acid (0.4 mmol), acetonitrile (15 mL), ultrasound frequency 60 kHz;
[b] Isolated yield.

Curcumin is heat-sensitive and susceptible to oxidation. So, the effect of temperature on the model esterification reaction was investigated as summarized in Table 2. Here it can be observed that there was much varied in the performance of the system, as the yield of *N*-maleoyl-glycine-curcumin 4a varied from 56.7% to 85.6%. Generally speaking, higher temperature accelerate the reaction rate and produces higher yields. But in this model esterification reaction, curcumin is heat-sensitive and gradually oxidation upon reaction with oxygen. Under a higher temperature, its oxidation speeds

up, which reduces the yield of product. Furthermore, *N*-maleoyl glycine **2a** is also easily oxidized at high temperature. Because of this, all the further experiments were carried out at 30 °C.

The effect of ultrasound frequency on the model reaction was also examined; the results are presented in Table 3. The pronounced effect of ultrasound can be easily demonstrated from the results shown by the entries 1-3 in Table 3. In the absence of ultrasound, the reaction must be performed for 5 h to produce a low yield of 40.1 %, even when the reaction time was extended for 8 h at 30 °C, the yield can only obtained 57.4% (Table 3, Entries 1-2). The addition of ultrasound can effectively enhance the yield up to 85.4% and reduce the reaction time to 3.0 h (Table 3, Entry 8). One can observe that ultrasound with different frequency leads to various results (Table 3, Entries 3-10). The yield increased at first and then decreased with a variation of ultrasound frequency from 25 to 100 kHz. The best yield (85.6%) was obtained with ultrasound frequency at 60 kHz (Table 3, Entry 7).

Table 3. The effect of the ultrasound frequency on the model reaction[a]

Entry	Frequency (kHz)	Reaction time(h)	Yield[b] (%)
1	None	5.0	40.1
2	None	8.0	57.4
3	25	2.5	68.5
4	25	3.0	72.6
5	40	2.5	74.1
6	40	3.0	77.8
7	60	2.5	85.6
8	60	3.0	85.4
9	80	2.5	77.5
10	100	2.5	70.8

[a] Reaction conditions: curcumin (4 mmol), *N*-maleoyl glycine (4.4 mmol), DCC (5 mmol), *p*-toluenesulfonic acid (0.4 mmol), acetonitrile (15 mL), temperature 30 ^{0}C; [b] Isolated yield.

Table 4. Synthesis of *N*-maleoyl-amino acid-curcumins 4a-f catalyzed by DCC under ultrasonic irradiation[a]

Entry	Compound	R	Timeb(h)	Yieldc(%)
1	4a	H	2.5	85.6
2	4b	CH(CH3)2	2.5	83.7
3	4c	CH2CH(CH3)2	3.0	78.8
4	4d	CH2CH2SCH3	3.0	80.4
5	4e	CH(CH3)CH2CH3	3.5	71.2
6	4f	CH2C6H5	3.5	72.9

[a] Reaction conditions: curcumin (4 mmol), *N*-maleoylamino acid (4.4 mmol), DCC (5 mmol), *p*-toluenesulfonic acid (0.4 mmol), acetonitrile (15 mL), temperature 30 ^{0}C, ultrasound frequency 60 kHz. [b] Monitored by TLC. [c] Isolated yield.

This method was further studied in several recations of *N*-maleoyl amino acids **2b-f** with curcumin under ultrasonic irradiation to give the respective *N*-maleoyl-amino acid-curcumins **4b-f**. The results are presented in Table 4. The result showed that all the yields achieved in the synthesis of *N*-maleoyl-amino acid-curcumins induced by DCC under ultrasonic irradiation were over 70% (Table 4) and all the reaction times were about 2.5-3.5 h, even for the *N*-maleoyl amino acids with long carbon chains or branched chains, such as in the case of **4e** and **4f** (Table 4, Entries 5-6), where the yields for synthesis of this two *N*-maleoyl-amino acid-curcumins respectively were 71.2%, 72.9% and the reaction time only 3.5 h. The yields of the *N*-maleoyl-amino acid-curcumins turned to be much lower as the atom numbers of the *N*-maleoyl amino acids became more or *N*-maleoyl amino acids with branched chain, such as in the case of **4e** (71.2%) and **4f** (72.9%) (Table 4, Entries 5-6). This may be due to steric hindrance in the *N*-maleoyl amino acids.

3 Experimental

Apparatus and Analysis

All reagents were purchased from commercial sources and used without further purification. Sonochemical reactions were carried out in a KQ-250E medical ultrasound cleaner and an output power of 250 W. IR spectra were recorded on a Nicolet FT IR-500 spectrometer. ^{1}H NMR spectra were recorded on a Bruker DPX 300 MHz spectrometer, and shifts are given in ppm downfield from TMS as an internal standard, $CDCl_3$ and DMSO-d_6 as the solvents. Elemental analysis was performed on an Elementar Vario EL III analyzer. Melting points were determined on a XT-5A digital melting-points apparatus and are uncorrected.

General procedure for the synthesis of *N*-maleoyl amino acids **2a-f** A 50 mL round-bottomed flask was charged with **2** (4.4 mmol), *p*-toluenesulfonic acid (0.4 mmol), DCC (4.4 mmol) and dry acetonitrile (15 mL), the reaction flask was located in the ultrasound cleaning bath, where the surface of reactants is slightly lower than the level of the water. The mixture was irradiated at 30 °C for 10 min, then, curcumin (4 mmol) was added. The mixture was continued to irradiate at 30 °C for the time period as indicated in Table 4. After the completion of the reaction (monitored by TLC), glacial acetic acid (5 mL) was added and the solution was stayed in a refrigerator overnight. The separated solid was filtered and the filtrate was concentrated under reduced pressure. The obtained crude products were washed with water. The collected precipitate was purified by recrystallization from 80% EtOH-H_2O, to afford the corresponding *N*-maleoyl-amino acid-curcumin **4a-f** .

***N*-Maleoyl-glycine-curcumin** (**4a**): m.p. 80-83 °C; IR (KBr) υ: 3417, 1739, 1635, 1607, 1463 cm^{-1}; ^{1}H NMR (300MHz, $CDCl_3$) δ: 3.13 (s, 2H, CH_2N), 3.79 (s, 2H, CH_2CO), 3.79 (s, 3H, CH_3), 3.92 (s, 3H, CH_3), 5.96 (s, 1H, OH), 6.52 (d, *J*=9.3 Hz, 2H, CH=); 6.88-7.49 (m, 8H,

978-1-61896-030-6 © 2012 SciRes.

ArH, CH=), 7.67 (d, *J*=9.3 Hz, 2H, CH=); Anal. Calcd for $C_{27}H_{23}NO_9$: C 64.15, H 4.59, N 2.77. Found: C 64.19, H 4.55, N 2.69.

***N*-Maleoyl-valine-curcumin(4b)**: m.p.105-108 °C; IR (KBr)*υ*: 3435, 1723, 1639, 1574, 1513, 1451 cm^{-1}; ^1H NMR (300MHz, DMSO-d_6) δ: 3.65 (s, 2H, CH_2CO), 3.74 (s, 3H, OCH_3), 3.83 (s, 3H, OCH_3), 5.36(s, 1H, OH), 6.79 (d, *J*=9.0 Hz, 2H, CH=); 6.78-7.61(m, 8H, ArH, CH=), 7.6 (d, *J*=9.0 Hz, 2H, CH=); Anal. Calcd for $C_{30}H_{29}NO_9$: C 65.80, H 5.34, N 2.56; Found:C 65.72, H 5.391, N 2.49.

***N*-Maleoyl-leucine-curcumin (4c)**: m.p. 108-111 °C, IR (KBr) *υ*: 3416, 1719, 16308 1574, 1527, 1446 cm^{-1}; ^1H NMR (300MHz, $CDCl_3$) δ: 1.03-1.21 (m, 6H, $2CH_3$), 2.03-2.17 (m, 2H, CH_2), 2.89-2.99 (m, 1H, CH), 3.48 (t, *J*=7.0 Hz, 1H, CHN), 3.76 (s, 2H, CH_2CO), 3.81 (s, 3H, OCH_3), 3.89 (s, 3H, OCH_3), 5.65 (s, 1H, OH), 6.41 (d, *J*=9.0 Hz, 2H, CH=); 6.53-7.46 (m, 8H, ArH, CH=), 7.78 (d, *J*=9.0 Hz, 2H, CH=); Anal. Calcd for $C_{31}H_{31}NO_9$: C 66.30, H 5.56, N 2.49; Found: C 66.24, H 5.49, N 2.41.

***N*-Maleoyl-methionine-curcumin (4d)**: m.p. 185-187 °C; IR (KBr) *υ*: 3431, 1639, 1621, 1573, 1526, 1450 cm^{-1}; ^1H NMR (300MHz, $CDCl_3$) δ: 1.89-1.99 (m, 2H, $C\underline{H}_2CH_2S$), 2.16 (s, 3H, SCH_3), 2.59 (dd, *J*=8.4, 5.8 Hz, 2H, CH_2S), 3.92 (s, 2H, CH_2CO), 3.79 (s, 3H, OCH_3), 3.92 (s, 3H, OCH_3), 4.38 (t, 1H, *J*=7.4 Hz, CHN), 5.75 (s, 1H, OH), 6.48 (d, *J*=9.3 Hz, 2H, CH=); 6.79-7.52 (m, 8H, ArH, CH=), 7.65 (d, *J*=9.1 Hz, 2H, CH=); Anal. Calcd for $C_{30}H_{29}NO_9S$: C 62.16, H 5.04, N 2.42; Found: C 62.03, H 4.96, N 2.51.

***N*-Maleoyl-isoleucine-curcumin (4e)**: m.p. 82-85 °C, IR (KBr) *υ*: 3421, 1726, 1639, 1593, 1527, 1462 cm^{-1}; ^1H NMR (300MHz, $CDCl_3$) δ: 0.95-1.07 (m, 6H, $2CH_3$), 1.26-1.33 (m, 2H, CH_2), 2.83-3.01 (m, 1H, CH), 3.78 (d, *J*=3.0 Hz, 1H, CHN), 3.85 (s, 2H, CH_2CO), 3.88 (s, 3H, OCH_3), 3.97 (s, 3H, OCH_3), 5.85 (s, 1H, OH), 6.54 (d, *J*=9.2 Hz, 2H, 2CH=); 6.82-7.68 (m, 8H, ArH, CH=), 7.69 (d, *J*=9.2 Hz, 2H, 2CH=); Anal. Calcd for $C_{31}H_{31}NO_9$: C 66.30, H 5.56, N 2.49; Found: C 66.22, H 5.51, N 2.42.

***N*-Maleoyl-phenylalanine-curcumin (4f)**: m.p. 110-113 °C; IR(KBr) *υ*: 3415, 1633, 1583, 1569, 1521, 1465 cm^{-1}; ^1H NMR (300MHz, $CDCl_3$) δ: 3.32(d, *J*=5.8 Hz, 2H, CH_2Ph), 3.72 (s, 3H, OCH_3), 3.83 (s, 2H, CH_2CO), 3.89 (s, 3H, OCH_3), 4.52 (t, *J*=7.2 Hz, 1H, CHN), 5.85 (s, 1H, OH), 6.58 (d, *J*=9.1 Hz, 2H, CH=); 6.92-7.63 (m, 13H, ArH, CH=), 7.71(d, *J*=9.1 Hz, 2H, 2CH=); Anal. Calcd for $C_{34}H_{29}NO_9$: C 68.56, H 4.91, N 2.35; Found: C 70.43, H 4.83, N 2.41.cm^{-1}; ^1H NMR (300MHz, $CDCl_3$) δ: 9.19 (s, 1H, COO-H), 7.39 (d, *J*=6.5 Hz, 2H, ArH), 7.27 (d, *J*= 6.5 Hz, 2H, ArH), 5.46 (s, 1H, O-H), 2.41 (s, 1H, C-H); MS-ESI (*m/z*): 187.4 (M+H).

4 Conclusion

The esterification of curcumin with *N*-maleoyl amino acids can be efficiently performed under ultrasonic irradiation in the presence of DCC condensation agent giving good yields of the respective *N*-maleoyl-amino acid-curcumins.

References

[1] Goel, A. B. Kunnumakkara, B. B. Aggarwal, "Curcumin as "curecumin": From kitchen to clinic," Biochem. Pharm., Vol 75, 2008, pp.787-809.

[2] J. K. Lin, S. Y. Lin-Shia, "Mechanisms of cancer chemoprevention by curcumin," Proc. Natl. Sci. Counc. Repub. China, Vol B 25, 2001, pp. 59-66.

[3] N. Chainani-Wu, "Safety and anti-inflammatory activity of curcumin: a component of turmeric (curcumin longa)," J. Altern. Complement. Med. Vol 9, 2003, pp.161-168.

[4] S. Daniel, J. L.Limson, A. Dairam, G. M. Watkins, S. Daya, "Through metal binding, curcumin protects against lead- and cadmium-induced lipid peroxidation in rat brain homogenates and against lead-induced tissue damage in rat brain," J. Inorg. Biochem., Vol 98, 2004, pp. 266-275.

[5] B. Aggarwal, A. Kumar, A. C. Bharti, "Anticancer potential of curcumin: Preclinical and clinical studies," Anticancer Research, Vol 23, 2003, pp.363-398.

[6] Mazumder, K. Raghavan, J. Weinstein, K. W. Kohn, Y. Pommier, "Inhibition of human immunodeficiency virus type-1 integrase by curcumin," Biochem. Pharmacol. Vol 49, 1995, pp. 1165-1170.

[7] M. T. Huang, W. Ma, Y. P. Lu, R. L. Chang, C. Fisher, P. S. Manchand, H. L. Newmark, A. H. Conney, "Effects of curcumin, demethoxycurcumin, bisdemethoxycurcumin and tetrahydrocur-cumin on 12-O-tetradecanoylphorbol-13-acetate-induced tumor promotion," Carcinogenesis, Vol 16, 1995, pp. 2493-2497.

[8] F. Zhang, N. K. Altorki, J. R. Mestre, K. Subbaramaiah, A. J. Dannenberg, "Curcumin inhibits cyclooxygenase-2 transcription in bile acid- and phorbol ester-treated human gastrointestinal epithelial cells," Carcinogenesis, Vol 20, 1999, pp. 445-451.

[9] S. K. Dubey, A. K. Sharma, U. Narain, K. Misra, U. Pati, "Design, synthesis and characterization of some bioactive conjugates of curcumin with glycine, glutamic acid, valine and demethylenated piperic acid and study of their antimicrobial and antiproliferative properties," Eur. J. Med. Chem., Vol 43, 2008, pp. 1837-1846.

[10] P. Anand, A. B. Kunnumakkara, R. B. Newman, B. B. Aggarwal, "Bioavailability of curcumin: Problems and promises," Molecular Pharm., Vol 4, 2007, pp. 807-818.

[11] T. Dinkova-Kostova, P. Talalay,"Direct and indirect antioxidant properties of inducers of cytoprotective proteins," Molecular Nutrition and Food Research, Vol 52, 2008, pp. S128-S138.

[12] S. V. Jovanovic, C. W. Boone, S. Steenken, M. Trinoga, R. B. Kaskey " How curcumin works preferentially with water soluble antioxidants," J. Am. Chem. Soc., Vol 123, 2001, pp. 3064-3068.

[13] G. Litwinienko, K. U. "Ingold Abnormal solvent effects on hydrogen atom abstraction. 2. Resolution of the curcumin antioxidant controversy. The role of sequential proton loss electron transfer," J. Org. Chem., Vol 69, 2004, pp. 5888-5896.

[14] Q. F. Cheng, X. Y. Xu, M. J. Ruan,Y. L. Wen, X. J. He, X. J. Yang, "One-pot three-component synthesis of pyrano [2,3-*d*]pyrimidine derivatives in aqueous media under ultrasonic irradiation," Chin. J. Org. Chem., Vol 29, 2009, pp. 1138-1141.

One-Pot Synthesis of Bis(indolyl)methanes Catalyzed by $FeCl_3 \cdot 6H_2O$

Qifa WANG[1], Qingfang CHENG[2], Yunpeng LIAO[2]
[1]*Jiangsu Key Laboratory of Marine Biotechnology, Huaihai Institute of Technology, Lianyungang, Jiangsu, China*
[2]*School of Chemical Engineering, Huaihai Institute of Technology, Lianyungang, Jiangsu, China*
Email: mifengw@yahoo.com.cn

Abstract: Bis(indolyl)methanes were synthesized by one-pot condensation reaction of aromatic aldehydes with indole using $FeCl_3 \cdot 6H_2O$ as green catalyst. The catalyst $FeCl_3 \cdot 6H_2O$ was found to be an effective catalyst for this one-pot condensation reaction and bis(indolyl)methanes were obtained with yields of 82.7%-93.5% within 1.5 to 3.5 h at 50 ^{0}C in benzene. Effects of different factors, such as class of solvent, catalyst concentration, reaction temperature, had been investigated to obtain the optimum condition.

Keywords: Bis(indolyl)methane; indole; $FeCl_3 \cdot 6H_2O$; aromatic aldehyde; synthesis

1 Introduction

Indoles and their derivatives have been shown to possess various pharmacological and biological properties, such as antibacterial, antioxidative, insecticidal, and cytotoxic activities [1,2]. Bis(indolyl)alkane, one of indole derivatives, constituted an important group of bioactive metabolites of terrestrial and marine origin [3-7]. During the past decade, a large number of natural products containing bis(indolyl) alkanes have been isolated from marine sources [8,9].

Consequently, the synthesis bis(indolyl)alkane derivatives have received an increasing attention, various methods for the preparation of bis(indolyl)alkane derivatives have been reported in the literaturare. In a general way, bis(indolyl)-alkane derivatives were synthesized by condensation reaction of indoles with various aldehydes and ketones catalyzed by various catalysts. Protic acid [10-11] and Lewis acid [12] are known to promote these reactions. However, these procedures suffered from some limitations when several substrates are sensitive to protic acids. Most recently, a great effort has been made to find mild and clean procedure in the synthesis of bis-indolylmethanes and some catalytic systems have been developed, such as metal salts $In(OTf)_3$ [13], $Dy(OTf)_3$ [14], $Ln(OTf)_3$ [15], $CeCl_3 \cdot 7H_2O$ [16], and molecular iodine [17], as well as solid acidic catalysts [18], such as clays and Zeolites, etc. However, some of these methods suffered from some drawbacks such as high reaction temperature, long reaction time, low yields, causing toxic wastes and expensive regents. Thus, there is still scope to develop simple and practical method for the synthesis of bis(indolyl)methanes.

The green chemistry advocated in the middle of 1990s suggests people to reduce or eliminate the utilization and producing of matters which are harmful to human health, social security and ecological environment, such as reactants, catalysts, solvents, products, by-products etc. One of the ultimate goals for organic reactions is to reduce the use of harmful catalyst. $FeCl_3 \cdot 6H_2O$ is a non-explosive, nontoxic, inexpensive, easy handling, and eco-friendly catalyst, so, in order to expand the application of bis(indolyl)alkane derivatives and in continuation of our research interest in green synthesis [19], we wish to report herein, a novel and efficient one-pot reaction of aromatic aldehydes with indole for the synthesis of some bis(indolyl)methanes using $FeCl_3 \cdot 6H_2O$ as green catalyst.

2 Results and Discussion

To achieve suitable conditions for the synthesis of bis(indolyl)methanes, various reaction conditions have been investigated in the model reaction of benzaldehyde with indole (Scheme 1).

To optimize the reaction conditions, initially, we studied the effect of different solvents on the reaction of benzaldehyde **1a** with indole **2** affording 3,3´-bis-indolyl phenylmethane **3a**. Deb has reported that the reactions of indoles with various aldehydes were carried out in a protic solvent to afford bis(indolyl)methanes in good yields [20], so, the solvents including THF, ethanol, acetone, acetonitrile, chloroform, dichloromethane and benzene were examined. The results were listed in Table 1.

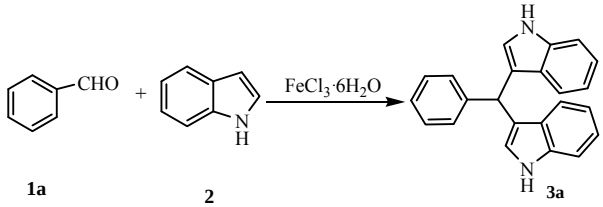

Scheme 1. Synthesis of 3,3´-bis-indolyl phenylmethane 3a

978-1-61896-030-6

Table 1. The influence of solvent on the model reaction[a]

Entry	Solvent	Time(h)	Yield[b] (%)
1	THF	3	85.6
2	Ethanol	3	81.8
3	Aacetone	3	80.3
4	Acetonitrile	3	88.4
5	Chloroform	3	84.7
6	Dichloromethane	3	87.2
7	Benzene	3	90.6
8	Benzene	2	90.4

[a] Reaction conditions: benzaldehyde (1 mmol), indole (2 mmol), solvent (4 mL), $FeCl_3 \cdot 6H_2O$ (0.05 mmol), temperature 50 ^{0}C. [b] Isolated yield.

All solvents examined afforded moderate yields of the desired products (Table 1). Nevertheless, the reaction using benzene as the solvent gave the best result (Table 1, entries 7-8). Thus, benzene was chosen as the solvent for all further reactions.

Next, we examined the effect of the catalyst $FeCl_3 \cdot 6H_2O$ on the model reaction of benzaldehyde with indole. The results are presented in Table 2.

Table 2. The effect of catalyst concentration on the model reaction[a]

Entry	Catalyst (mol%)	Time(h)	Yield[b] (%)
1	0.0	3.0	0
2	1.0	1.5	47.8
3	1.0	2.0	50.4
4	1.0	2.5	50.8
5	1.5	2.0	55.5
6	2.0	2.0	62.7
7	2.5	2.0	71.8
8	3.0	2.0	76.4
9	3.5	2.0	79.8
10	4.0	2.0	83.6
11	4.5	2.0	87.2
12	5.0	2.0	90.4
13	5.0	2.5	90.6
14	5.5	2.0	90.6
15	6.0	2.0	91.1

[a] Reaction conditions: benzaldehyde (1 mmol), indole (2 mmol), benzene (4 mL), temperature 50 ^{0}C. [b] Isolated yield.

The catalysis $FeCl_3 \cdot 6H_2O$ played a crucial role in the model reaction of benzaldehyde with indole. Without the catalyst $FeCl_3 \cdot 6H_2O$, the reaction cannot be carried out (Table 2, Entry 1). The yield of model reaction was significantly affected by the amount of catalyst $FeCl_3 \cdot 6H_2O$. The catalysis $FeCl_3 \cdot 6H_2O$ is highly effective, the reaction of benzaldehyde with indole could be carried out with 1.0 mol% catalyst loading, affording 50.4% yield of 3,3′-bis-indolyl phenyl-methane **3a** after 2 h (Table 2, Entry 3). The increase of the amount of catalyst $FeCl_3 \cdot 6H_2O$ remarkably accelerated the reaction (Table 2, Entries 5-11). The model reaction in the presence of 5 mol% $FeCl_3 \cdot 6H_2O$ was found to be completed at 50 ^{0}C after 2 h, giving 3,3′-bis-indolyl phenylmethane **3a** in 90.4 % yield (Table 2, Entry 12). However, when the amount of $FeCl_3 \cdot 6H_2O$ exceeded 5 mol%, the yield was not affected so much (Table 2, Entries 14-15).

We further examined the effect of reaction temperature on the model reaction of benzaldehyde with indole. The model reaction at 25 °C for 2 h gave only a 47.5% yield of desired 3,3′-bis-indolyl phenylmethane **3a** (Table 3, Entry 1); even when the reaction time was extended for 2.5 h at 25 °C, the yield can only obtained 50.3% (Table 3, Entry 2). The increase of reaction temperature remarkably accelerated the reaction (Table 3, Entries 3-8). A high yield can be obtained within 2 h when the model reaction was carried out at 50 °C (Table 3, Entry 9). However, for this reaction, a higher temperature was no advantage (Table 3, Entries 11-12).

Table 3. The influence of temperature on the model reaction[a]

Entry	Temperature(°C)	Time(h)	Yield[b] (%)
1	25	2.0	47.5
2	25	2.5	50.3
3	30	2.0	65.6
4	30	2.5	69.5
5	40	2.0	76.5
6	40	2.5	80.2
7	50	1.5	80.6
8	50	2.0	90.4
9	50	2.5	90.6
10	60	2.0	87.5
11	65	1.5	85.6
12	65	2.0	82.7

[a] Reaction conditions: benzaldehyde (1 mmol), indole (2 mmol), benzene (4 mL), $FeCl_3 \cdot 6H_2O$ (0.05 mmol). [b] Isolated yield.

To evaluate the effectiveness of the catalysis $FeCl_3 \cdot 6H_2O$ and explore the scope of this reaction, different substituted aromatic aldehydes (**1b-j**) were reacted with indole **2** under similar conditions furnishing the respective bis(indolyl)- methanes (**3b-j**) (Scheme 2). The results are summarized in Table 4.

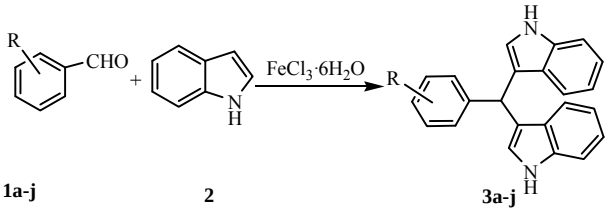

1a-j **2** **3a-j**

Scheme 2. Synthesis of bis(indolyl)methane 3a-j

The result showed that all the yields achieved in the synthesis of bis(indolyl)methanes induced by $FeCl_3 \cdot 6H_2O$ were over 80% and all the reaction times were about 1.5-3.5 h (Table 4). Aromatic aldehydes bearing either electron-withdrawing or electron-donating groups underwent the condensation reaction giving high yields of the corresponding bis(indolyl)methane derivatives.

Table 4. Synthesis of bis(indolyl)methanes 3a-j catalyzed by $FeCl_3·6H_2O$[a]

Entry	Product	R	Time[b](h)	Yield[c](%)
1	**3a**	H	2.0	90.4
2	**3b**	4-Me	2.5	86.7
3	**3c**	4-OMe	2.5	82.7
4	**3d**	4-OH	3.5	84.6
5	**3e**	3-OMe-4-OH	1.5	90.3
6	**3f**	3-Me	1.5	92.6
7	**3g**	3-OMe	1.5	93.5
8	**3h**	3-Cl	2.0	86.7
9	**3i**	3-NO_2	2.0	89.7
10	**3j**	2-Br	1.5	91.8

[a] Reaction conditions: aromatic aldehyde (1 mmol), indole (2 mmol), benzene (4 mL), $FeCl_3·6H_2O$ (0.05 mmol), temperature, 50 ^{0}C; [b] Monitored by TLC; [c] Isolated yield.

3 Experimental

Apparatus and Analysis

IR spectra were recorded on a Nicolet FT IR-500 spectrometer. ^{1}H NMR spectra were recorded on a Bruker DPX 300 MHz spectrometer, and shifts are given in ppm downfield from TMS as an internal standard, $CDCl_3$ as the solvent. Elemental analysis was performed on an Elementar Vario EL III analyzer. GC-MS were recorded using a Finnigan Trace 2000 GC/MS system. Melting points were determined on a XT-5A digital melting-points apparatus and are uncorrected.

General procedure for the synthesis of bis(indolyl)-methanes **3a-j** A 50 mL flask was charged with aromatic aldehyde(1 mmol), indole (2 mmol) and $FeCl_3·6H_2O$ (0.05 mmol) in benzene (4 mL). This mixture was stirred at 50 °C until aromatic aldehyde has completely reacted, as indicated by TLC. The reaction mixture was cooled and diluted with water. Then, the reaction mixture was extracted with ethyl acetate (20 mL) for twice. Organic phases were combined and dried over sodium sulphate and concentrated to dryness. Purification of the products was performed by a short column chromatography eluted with ethyl acetate/petroleum ether to give the desired products **3a-j** in high yields (Table 4).

3,3´-Bis-indolyl phenylmethane (3a) Pink solid, m.p. 126-127 °C; IR (KBr) *υ*: 3429, 3088, 1506, 1453 cm^{-1}; ^{1}H NMR (300 MHz, $CDCl_3$) δ: 7.76 (s, 2H, N-H), 7.40 (d, *J*=7.9 Hz, 2H, Ar–H), 7.39-7.33 (m, 3H, Ar-H), 7.31-7.26 (m, 3H, Ar-H), 7.28-7.24 (m, 1H, Ar-H), 7.22-7.18 (m, 2H, Ar-H), 7.09-7.01(m, 2H, Ar-H), 6.58 (s, 2H, Ar-H), 5.90 (s, 1H, C-H); MS (EI, 70 eV): *m/z* =323 $[M+H]^+$; Anal. Calcd for $C_{23}H_{18}N_2$: C, 85.68; H, 5.63; N, 8.69. Found: C, 85.69; H, 5.65; N, 8.73.

3,3´-Bis-indolyl-(4-methylphenyl)methane (3b) Pink solid, m.p. 93-95 °C; IR (KBr) *υ*: 3418, 3058, 1486, 1436 cm^{-1}; ^{1}H NMR (300 MHz, $CDCl_3$) δ: 7.93 (s, 2H, N-H), 7.36 (d, *J* =7.9 Hz, 2H, Ar-H), 7.33(d, *J*=8.2 Hz, 2H, Ar-H), 7.23(d, *J* =8.0 Hz, 2H, Ar-H), 7.25-7.16 (m, 2H, Ar-H), 7.13 (d, *J*=7.9 Hz, 2H, Ar-H), 7.05-6.99 (m, 2H, Ar-H), 6.66 (s, 2H, Ar-H), 5.85 (s, 1H, C-H), 2.38 (s, 3H, CH_3); MS (EI, 70 eV): *m/z* = 336 [M]; Anal. Calcd for $C_{24}H_{20}N_2$: C, 85.68; H, 5.99; N, 8.33. Found: C, 85.61; H, 5.90; N, 8.35.

3,3´-Bis-indolyl-(4-methoxyphenyl)methane (3c) Pink solid, m.p.185-186 °C; IR (KBr) *υ*: 3436, 3029, 1503, 1421 cm^{-1}; ^{1}H NMR (300 MHz, $CDCl_3$) δ: 8.97 (s, 2H, N-H), 7.29 (t, *J*=7.5 Hz, 4H, Ar-H), 7.19(d, *J*=7.1 Hz, 2H, Ar-H), 7.03 (t, *J* =7.4 Hz, 2H, Ar-H), 6.75 (t, *J* =7.5 Hz, 2H, Ar-H), 6.62 (s, 2H, Ar-H), 5.81 (s, 1H, C-H), 3.81 (s, 3H, CH_3); MS (EI, 70 eV): *m/z* = 352 [M]; Anal. Calcd for $C_{24}H_{20}N_2O$: C, 81.79; H, 5.72; N, 7.95. Found: C, 81.72; H, 5.65; N, 7.99.

3,3´-Bis-indolyl-(4-hydroxyphenyl)methane (3d) Pink solid, m.p. 210-212 ◦C; IR (KBr) *υ*: 3438, 3076, 1497, 1419 cm^{-1}; ^{1}H NMR (300 MHz, $CDCl_3$) δ: 9.69 (s, 2H, N-H), 8.61 (s, 1H, O-H), 7.26 (t, *J* =7.7 Hz, 4H, Ar-H), 7.16 (d, *J*=7.5 Hz, 2H, Ar-H), 7.06 (t, *J* =7.6 Hz, 2H, Ar-H), 6.89 (t, *J* =7.5 Hz, 2H, Ar-H), 6.69 (s, 2H, Ar-H), 5.75 (s, 1H, C-H); MS (EI, 70 eV): *m/z* = 339 $[M+H]^+$; Anal. Calcd for $C_{23}H_{18}N_2O$: C, 81.64; H, 5.36; N, 8.28. Found: C, 81.58; H, 5.42; N, 8.34.

3,3´-Bis-indolyl-(3-methoxy-4-hydroxyphenyl)-methane (3e) Pink solid, m.p. 99-101 °C ; IR (KBr) *υ*: 3506, 3055, 1632, 1392 cm^{-1}; ^{1}H NMR (300 MHz, $CDCl_3$) δ: 9.89 (s, 2H, N-H), 8.02 (s, 1H, O-H), 7.36-6.75 (m, 11H, Ar-H), 6.61 (s, 2H, Ar-H), 5.85 (s, 1H, C-H), 3.84 (s, 3H, CH_3); MS (EI, 70 eV): *m/z* = 369 $[M+H]^+$; Anal. Calcd for $C_{24}H_{20}N_2O_2$: C, 78.24; H, 5.44; N, 7.61. Found: C, 78.32; H, 5.39; N, 7.71.

3,3´-Bis-indolyl-(3-methylphenyl)methane (3f) Pink solid, m.p. 99-100 °C; IR (KBr) *υ*: 3408, 3052, 1602, 1461, 1422 cm^{-1}; ^{1}H NMR (300 MHz, $CDCl_3$) δ: 7.89 (s, 2H, N-H), 7.41 (d, *J*=7.9 Hz, 2H, Ar-H), 7.29(d, *J* =8.2 Hz, 2H, Ar-H), 7.21-7.15 (m, 5H, Ar-H), 7.09-6.93 (m, 3H, Ar-H), 6.59 (s, 2H, Ar-H), 5.82 (s, 1H, C-H), 2.33 (s, 3H, CH_3); MS (EI, 70 eV): *m/z* = 336; Anal. Calcd for $C_{24}H_{20}N_2$: C, 85.68; H, 5.99; N, 8.33. Found: C, 85.53; H, 5.91; N, 8.28.

3,3´-Bis-indolyl-(3-methoxyphenyl)methane (3g) Pink solid, m.p. 189-190 °C; IR (KBr) *υ*: 3429, 3075, 1458, 1269, 1163 cm^{-1}; ^{1}H NMR (300 MHz, $CDCl_3$) δ: 7.95 (s, 2H, N-H), 7.44 (d, *J*=7.8 Hz, 2H, Ar-H), 7.39 (d, *J* =8.2 Hz, 2H, Ar-H), 7.25 (d, *J*=7.8 Hz, 1H, Ar-H), 7.24-7.16 (m, 2H, Ar-H), 7.06-6.98 (m, 2H, Ar-H), 6.95 (d, *J*=7.7 Hz, 1H, Ar-H), 6.92 (d, *J*=2.2 Hz, 1H, Ar-H), 6.79-6.69 (m, 1H, Ar-H), 6.64 (s, 2H, Ar-H), 5.84 (s, 1H, C-H), 3.79 (s, 3H, CH_3); MS (EI, 70 eV): *m/z* =352 [M]; Anal. Calcd for $C_{24}H_{20}N_2O$: C, 81.79; H, 5.72; N, 7.95. Found: C, 81.76; H, 5.63; N, 7.91.

3,3´-Bis-indolyl-(3-chlorophenyl)methane (3h) Pink solid, m.p. 66-68 °C; IR (KBr) *υ*: 3408, 3033, 1459, 1099,

978-1-61896-030-6 © 2012 SciRes.

746 cm^{-1}; ^1H NMR (300 MHz, $CDCl_3$) δ: 7.85 (s, 2H, N-H), 7.44-7.35 (m, 5H, Ar-H), 7.28-7.15 (m, 5H, Ar-H), 7.06-6.99 (m, 2H, Ar-H), 6.61 (s, 2H, Ar-H), 5.88 (s, 1H, C-H); MS (EI, 70 eV): *m/z* =357 [M]; Anal. Calcd for $C_{23}H_{17}N_2Cl$: C, 77.42; H, 4.80; N, 7.85. Found: C, 77.51; H, 4.72; N, 7.76.

3,3´-Bis-indolyl-(3-nitrophenyl)methane (3i) Pink solid, m.p. 263-665 °C; IR (KBr) *υ*: 3412, 3063, 1526, 1349, 741 cm^{-1}; ^1H NMR (300 MHz, $CDCl_3$) δ: 8.26 (t, *J*=2.0 Hz, 1H, Ar-H), 8.13-8.08 (m, 1H, Ar-H), 8.05 (s, 2H, N-H), 7.75 (d, *J*=7.9 Hz, 1H, Ar-H), 7.48 (t, *J*=7.9 Hz, 1H, Ar-H), 7.35 (d, *J*=8.2 Hz, 2H, Ar-H), 7.26-7.19 (m, 2H, Ar-H), 7.06-7.01 (m, 2H, Ar-H), 6.69 (s, 2H, Ar-H), 5.98 (s, 1H, C-H); MS (EI, 70 eV): *m/z* = 368 $[M+H]^+$; Anal. Calcd for $C_{23}H_{17}N_3O_2$: C, 75.19; H, 4.66; N, 11.44. Found: C, 75.11; H, 4.58; N, 11.38.

3,3´-Bis-indolyl-(2-bromophenyl)methane (3j) Pink solid, m.p. 90-91°C; IR (KBr) *υ*: 3418, 3051, 1452, 1028, cm^{-1}; ^1H NMR (300 MHz, $CDCl_3$) δ: 7.93 (s, 2H, N-H), 7.62 (d, *J*=7.9 Hz, 1H, Ar-H), 7.46 (d, *J*=7.9 Hz, 2H, Ar-H), 7.34 (d, *J*=8.2 Hz, 2H, Ar-H), 7.24-7.15 (m, 4H, Ar-H), 7.14-7.09 (m, 1H, Ar-H), 7.05-6.98 (m, 2H, Ar-H), 6.63 (s, 2H, Ar-H), 6.16 (s, 1H, C-H); MS (EI, 70 eV): *m/z* =401 [M]; Anal. Calcd for $C_{23}H_{17}N_2Br$: C, 68.78; H, 4.21; N, 6.89. Found: C, 68.64; H, 4.05; N, 6.81.

4 Conclusion

The reaction of benzaldehyde or substituted benzaldehydes with indole can be efficiently performed in the presence of catalytic amount of $FeCl_3 \cdot 6H_2O$ giving good to high yields of the respective bis(indolyl)methane derivatives. The catalysis $FeCl_3 \cdot 6H_2O$ is promising for the development of green catalysts.

Acknowledgement

We acknowledgement the financial support from the Foundation of Jiangsu Key Laboratory of Marine Biotechnology (No. 2009HS04).

References

[1] M. Lounasmaa, A.Tolvanen, "Simple indole alkaloids and those with a nonrearranged monoterpenoid unit," Nat. Prod. Rep., Vol 17, 2000, pp.175-191.

[2] S. Hibino, T. Chozi, "Simple indole alkaloids and those with a nonrearranged monoterpenoid unit," Nat. Prod. Rep., Vol 18, 2001, pp. 66-87.

[3] E. Fahy, B. C. M. Potts, D. J. Faulkner, K. Smith, "6-Bromo tryptamine derivatives from the gulf of california tunicate didemnum candidum," J. Nat. Prod., Vol 54, 1991, pp. 564-569.

[4] T. Osawa; M. Namiki, "Structure elucidation of streptindole, a novel genotoxic metabolite isolated from intestinal bacteria," Tetrahedron Lett., Vol 24, 1983, pp. 4719-4722.

[5] R. Bell, S. Carmeli, N. Sar, A.Vibrindole, "A metabolite of the marine bacterium, vibrio parahaemolyticus, isolated from the toxic mucus of the boxfish ostracion cubicus," J. Nat. Prod., Vol 57, 1994, pp. 1587-1590.

[6] T. R. Garbe, M. Kobayashi, N. Shimizu, N. Takesue, M. Ozawa, H.Yukawa, "Indolyl carboxylic acids by condensation of indoles with α-keto acids," J. Nat. Prod., Vol 63, 2000, pp. 596-598.

[7] D. J. Faulkner, "Marine natural products," Nat. Prod. Rep., Vol 18, 2001, pp. 1-49.

[8] G. Bifulco, I. Bruno, R. Riccio, J. Lavayre, G. Bourdy, "Further brominated bis- and tris-indole alkaloids from the deep-water new caledonian marine sponge orina *sp*," J. Nat. Prod., Vol 58, 1995, pp.1254-1260.

[9] A. L. Smith, G. I. Stevenson, S. Lewis, S. Patel, J. L. Castro, "Solid-phase synthesis of 2,3-disubstituted indoles: discovery of a novel, high-affinity, selective h5-HT_{2A} antagonist," Bioorg. Med. Chem. Lett., Vol 10, 2000, pp. 2693-2696.

[10] A. Mahadevan, H. Sard, M.Gonzalez, J. C. McKew, "A general method for C3 reductive alkylation of indoles," Tetrahedron Lett., Vol 44, 2003, pp. 4589-459.

[11] A.V. Reddy, K. Ravinder, V. L. N. Reddy, T. V. Goud, V. Ravikanth, Y. Venkateswarlu, "Zeolite catalyzed synthesis of bis(indolyl) methanes," Synth. Commun., Vol 33, 2003, pp. 3687-3694.

[12] S. J. Ji, M. F. Zhou, D. J.Gu, Z. Q. Jiang, T. P. Loh, "Efficient Fe III-catalyzed synthesis of bis(indolyl)methanes in ionic liquids," Eur. J. Org. Chem., Vol 2004, 2004, pp. 1584-1587.

[13] R. Nagarajan, P.T. Perumal, "$InCl_3$ and $In(OTf)_3$ catalyzed reactions: Synthesis of 3-acetyl indoles, bis-indolylmethane and indolylquinoline derivatives,"Tetrahedron, Vol 58, 2002, pp. 1229-1232.

[14] G. Giannini, M. Marzi, G. P. Moretti, S. Penco, M. O. Tinti, S. Pesci, F. Lazzaro, F. D. Angelis, "Synthesis of cycloalkanoindoles by an unusual DAST-triggered rearrangement reaction," Eur. J. Org. Chem. Vol 2004, 2004, pp. 2411-2420.

[15] D. P. Chen, L. B. Yu, P. G. Wang, "Lewis acid-catalyzed reactions in protic media. Lanthanidecatalyzed reactions of indoles with aldehydes or ketones," Tetrahedron Lett., Vol 37, 1996, pp. 4467-4470.

[16] C. Silveira; S. R. Mendes, F. M. Líbero, E. J. Lenardão, G. Perin, "Glycerin and $CeCl_3 \cdot 7H_2O$: A new and efficient recyclable medium for the synthesis of bis(indolyl)-methanes," Tetrahedron Lett., Vol 50, 2009, pp. 6060-6063.

[17] B. P. Bandgar, K. A. Shaikh, "Molecular iodine-catalyzed efficient and highly rapid synthesis of bis(indolyl)methanes under mild conditions," Tetrahedron Lett., Vol 44, 2003, pp. 1959-1961.

[18] J. Li, M. Zhou, B. G. Li, G. L. Zhang, "Synthesis of triindolylmethanes catalyzed by zeolites," Synth. Commun., Vol 34, 2004, pp. 275-280.

[19] Q. F. Cheng, Q. F. Wang, X. Y. Xu, M. J. Ruan, H. L. Yao, X. J. Yang, "Solvent-free synthesis of monastrol derivatives catalyzed by NaHSO4," J. Heterocyclic Chem., Vol 47, 2010, pp. 624-628.

[20] M. L. Deb, P. J. Bhuyan, "An efficient and clean synthesis of bis(indolyl)methanes in a protic solvent at room temperature," Tetrahedron Lett., Vol 47, 2006, pp. 1441-1443.

.

A Convenient Synthesis of *N*-(l,2-dihydro-2-oxo-3*H*-indol-3-ylidene)-Amino Acid

Qifa WANG[1], Qingfang CHENG[2], Jianping TANG[2], Feng QIU[2]
[1]*Jiangsu Key Laboratory of Marine Biotechnology, Huaihai Institute of Technology, Lianyungang, Jiangsu, China*
[2]*School of Chemical Engineering, Huaihai Institute of Technology, Lianyungang, Jiangsu, China*
Email: mifengw@yahoo.com.cn

Abstract: A efficient protocol for the synthesis of Schiff bases of *N*-(l,2-dihydro-2-oxo-3*H*-indol-3-ylidene)-amino acids has been developed by the convenient condensation of isatin with amino acids. The catalyst *p*-toluenesulfonic acid (*p*-TSA) possessed high catalytic activity for the condensation reaction and *N*-(l,2-dihydro-2-oxo-3*H*-indol-3-ylidene)-amino acids were obtained with yields of 70.4%-85.5% within 3 to 4 h at 70 ^{0}C in methanol and dioxane (1:1). Effects of different factors, such as catalyst concentration, reaction temperature, class of solvent, had been investigated to obtain the optimum conditions.

Keywords: Isatin; amino acid; *p*-toluenesulfonic acid; Schiff base; synthesis

1 Introduction

Isatin, also named 1*H*-indol-2,3-dione, a nature oceanic antibiotics extracted from lobster [1], now has been confirmed existing in natural indigo [2], a traditional Chinese medicine and it is also an endogenous indole present in mammalian tissues and fluids [3]. Isatin is a privileged lead molecule for designing potential bioactive agents, and its derivatives have been shown to possess a broad spectrum of bioactivity, as many of which have been assessed as anti-HIV [4], antiviral [5], antitumor [6], antifungal [7] and anticancer [8] agents. These interesting properties have prompted many efforts toward the structure modification and biologieal activity optimization of isatin derivatives.

The Schiff base (or azomethine), named after Hugo Schiff, has a wide range of applications. For example, it can be used as a catalyst, nonlinear optical materials, electroluminescent materials and so on [9]. The synthesis of novel Schiff bases and the research of their physiological activities has become important due to their anticancer and antimicrobial activities [10,11]. As a part of drug development programs, numerous methods for the synthesis of various kinds of Schiff base have been reported [12-16].

The amino acids, for example, glycine is essential components of bacterial cells. These components when linked covalently to isatin molecule may act as carrier molecules as the cells recognise these molecules and thereby might increase the intracellular delivery of isatin. The conjugates also are likely to be metabolised comparatively slowly.

To the best of our knowledge, the synthesis of Schiff base of *N*-(l,2-dihydro-2-oxo-3*H*-indol-3-ylidene)-amino acids from isatin with amino acids in the presence of *p*-toluenesulfonic acid (*p*-TSA) has not yet been reperted. In order to expand the application of isatin derivatives, we wish to report a novel and efficient method for the synthesis of Schiff base of *N*-(1,2-dihydro-2-oxo-3*H*-indol-3-ylidene)-amino acids by the convenient condensation of isatin with amino acids.

2 Results and Discussion

To achieve suitable conditions for the synthesis of *N*-(l,2-dihydro-2-oxo-3*H*-indol-3-ylidene)-amino acids **3**, various reaction conditions have been investigated in the reaction of isatin **1** with glycine **2a** as a model reaction (Scheme 1).

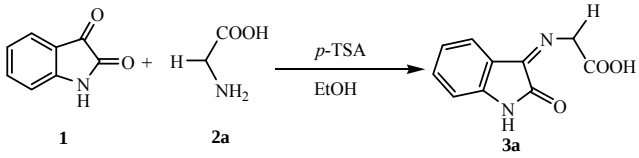

1 **2a** **3a**

Scheme 1. Synthesis of *N*-(1,2-dihydro-2-oxo-3*H*-indol-3-ylidene)-glycine 3a

Initially, we examined the effect of the catalyst *p*-toluenesulfonic acid (*p*-TSA) on the model reaction of isatin **1** with glycine **2a** affording *N*-(1,2-dihydro-2-oxo-3*H*-indol-3-ylidene)-glycine (**3a**) (Scheme 1). The results are presented in Table 1.

The *p*-TSA played a crucial role in the model reaction. Without *p*-TSA, the reaction time is long and the yield is only 46.2% (Table 1, Entry 1). The catalysis *p*-TSA is highly effective, the model reaction could be carried out with 1.0 mol% catalyst loading, affording 54.8% yield of *N*-(1,2-dihydro-2-oxo-3*H*-indol-3-ylidene)-glycine (**3a**) at 70 ^{0}C after 3 h (Table 1, Entry 3). The increase of the amount of *p*-TSA remarkably accelerated the reaction (Table 1, Entries 5-11). The model reaction in the presence of 5 mol% *p*-TSA was found to be completed at 70 ^{0}C after 3 h, giving *N*-(1,2-dihydro-2-oxo-3*H*-indol-3-

978-1-61896-030-6

ylidene)-glycine (**3a**) in 85.5% yield (Table 1, Entry 12). However, when the amount of *p*-TSA exceeded 5 mol%, the yield was not affected so much (Table 1, Entries 14-15).

Table 1. The effect of catalyst concentration on the model reaction[a]

Entry	Catalyst (mol%)	Time(h)	Yield[b] (%)
1	0.0	6	46.2
2	1.0	2	51.6
3	1.0	3	54.8
4	1.0	4	55.2
5	1.5	3	60.5
6	2.0	3	64.4
7	2.5	3	68.2
8	3.0	3	71.9
9	3.5	3	75.1
10	4.0	3	79.9
11	4.5	3	82.6
12	5.0	3	85.5
13	5.0	4	84.8
14	5.5	3	85.6
15	6.0	3	85.2

[a] Reaction conditions: isatin (10.5 mmol), glycine (10 mmol), dioxane (10 mL), methanol (10 mL), temperature 70 ^{0}C; [b] Isolated yield.

Next, we examined the effect of the solvent through some experiments. To search for the optimal solvent, the reaction of isatin with glycine was examined using methanol, ethanol, dioxane as solvent. The results were listed in Table 2.

Table 2. The influence of solvent on the model reaction[a]

Entry	Solvent	Time(h)	Yield[b] (%)
1	Methanol	3	66.2
2	Methanol	4	64.7
3	Ethanol	3	59.6
4	Ethanol	4	57.6
5	Dioxane	3	76.5
6	Dioxane	4	77.5
7	Dioxane:Methanol (1:1)	3	85.5
8	Dioxane:Methanol (1:1)	4	86.1
9	Dioxane:Methanol (1:2)	3	81.4
10	Dioxane:Methanol (2:1)	3	80.7

[a] Reaction conditions: isatin (10.5 mmol), glycine (10 mmol), solvent (20 mL), *p*-TSA(0.5 mmol), temperature 70 ^{0}C; [b] Isolated yield.

The results showed that when the reactions were alone carried out in methanol, ethanol, or dioxane, the reaction yields were lower (Table 2, entries 1-6). Combination of methanol and dioxane afforded good yields of the desired product (Table 2, entries 7-10). Nevertheless, the reaction using methanol and dioxane (1:1) as the solvent gave the best result (Table 2, entries 7-8). Thus, methanol and dioxane (1:1) was chosen as the solvent for all further reactions.

We attempted to further improve the yield by performed the model reaction in different temperature. The model reaction at 30 °C for 2 h gave only a 39.4% yield of desired *N*-(1,2-dihydro-2-oxo-3*H*-indol-3-ylidene)-glycine (**3a**) (Table 3, Entry 1); even when the reaction time was extended for 4h at 30 °C, the yield can only obtained 45.2% (Table 3, Entry 3). The increase of reaction temperature remarkably accelerated the reaction (Table 2, Entries 4-11). A high yield can be obtained within 3 h when the model reaction was carried out at 70 °C (Table 3, Entry11). However, for this reaction, a higher temperature was unfavorable (Table 3, Entries 12-13).

Table 3. The influence of temperature on the model reaction[a]

Entry	Temperature(°C)	Time(h)	Yield[b] (%)
1	30	2	39.4
2	30	3	44.7
3	30	4	45.2
4	40	2	48.6
5	40	3	54.7
6	50	2	64.5
7	50	3	68.8
8	60	2	73.4
9	60	3	77.7
10	70	2	82.1
11	70	3	85.5
12	80	2	80.6
13	80	3	75.7

[a] Reaction conditions: isatin (10.5 mmol), glycine (10 mmol), dioxane (10 mL), methanol (10 mL), *p*-TSA(0.5 mmol); [b] Isolated yield.

This method was further studied in several recations of isatin with amino acids (**1b-j**) under similar conditions furnishing the respective *N*-(1,2-dihydro-2-oxo-3*H*-indol-3-ylidene)-amino acids (**3b-j**) (Scheme 2). The optimized results are presented in Table 4.

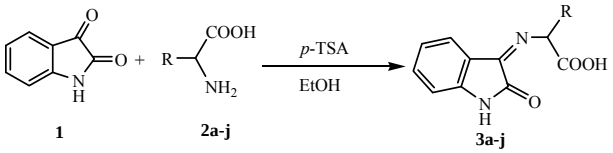

1 **2a-j** **3a-j**

Scheme 2. Synthesis of *N*-(1,2-dihydro-2-oxo-3*H*-indol-3-ylidene)-amino acids 3a-j

The result showed that under the same conditions, all the yields achieved in the synthesis of *N*-(1,2-dihydro-2-oxo-3*H*-indol-3-ylidene)-amino acids **3a-j** induced by *p*-TSA at 70 ^{0}C were about 70% (Table 4) and all the reaction times were about 3-4 h. It was also found that amino acids with long carbon chains (Table 4, entries 2-6) or with aromatic ring (Table 4, entries 7-10) generally gave lower yields, probably due to the large steric effect. That is to say, steric factors played a key role in affecting the rates of reaction and the reactions required a longer time.

Table 4. Synthesis of *N*-(1,2-dihydro-2-oxo-3*H*-indol-3-ylidene)-amino acids 3a-j catalyzed by *p*-TSA[a]

Entry	Product	2	Time[b](h)	Yield[c] (%)
1	**3a**	Gglycine (**2a**)	3.0	85.5
2	**3b**	L-Alanine (**2b**)	3.5	82.6
3	**3c**	L-Valine (**2c**)	3.5	80.7
4	**3d**	L-Methionine (**2d**)	3.5	78.2
5	**3e**	L-Aspartic acid (**2e**)	4.0	75.4
6	**3f**	L-Arginine (**2f**)	4.0	72.6
7	**3g**	L-Phenylalanine (**2g**)	4.0	70.5
8	**3h**	L-Histidine (**2h**)	4.0	72.8
9	**3i**	L-Tyrosine (**2i**)	4.0	73.7
10	**3j**	L-Tryptophane (**2j**)	4.0	67.4

[a] Reaction conditions: isatin (10.5 mmol), amino acid (10 mmol), dioxane (10 mL), methanol (10 mL), *p*-TSA(0.5 mmol), temperature, 70 ^{0}C; [b] Monitored by TLC; [c] Isolated yield.

3 Experimental

Apparatus and Analysis

IR spectra were recorded on a Nicolet FT IR-500 spectrometer. ^{1}H NMR spectra were recorded on a Bruker DPX 300 MHz spectrometer, and shifts are given in ppm downfield from TMS as an internal standard, DMSO-d_6 as the solvent. Elemental analysis was performed on an Elementar Vario EL III analyzer. Melting points were determined on a XT-5A digital melting-points apparatus and are uncorrected.

General procedure for the synthesis of *N*-(1,2-dihydro-2-oxo-3H-indol-3-ylidene)-amino acids **3a-j** A 100 mL flask was charged with isatin **1** (10.5 mmol), amino acids (10 mmol) and *p*-TSA (0.5 mmol) in methanol (10 mL) and dioxane (10 mL). This mixture was stirred at 70 °C until amino acid has completely reacted, as indicated by TLC. After the completion of the reaction, the reaction mixture was allowed to cool and a lot of precipitation was isolated by filtration, and then washed three times with cold methanol to afford the pure product as solid.

***N*-(1,2-dihydro-2-oxo-3*H*-indol-3-ylidene)-glycine (3a)** White solid, m.p. 287-288 °C; IR (KBr) *υ*: 3439, 3188, 1665, 1630, 1613, 1503, 1403, 1337, 1128 cm^{-1}; ^{1}H NMR (300 MHz, DMSO-d_6) δ: 10.15 (s, 1H, N-H), 9.76 (s, 1H, COO-H), 6.83-7.68 (m, 4H, ArH), 4.25 (s, 2H, CH_2); Anal. Calcd for $C_{10}H_8N_2O_3$: C 58.82, H 3.95, N 13.72; found C 58.76, H 3.89, N 13.76.

***N*-(1,2-dihydro-2-oxo-3*H*-indol-3-ylidene)-L-alanine (3b)** White solid, m.p. 267-268 °C; IR (KBr) *υ*: 3418, 3036, 2969, 1637, 1586, 1479, 1411, 1369, 1338, 1149 cm^{-1}; ^{1}H NMR (300 MHz, DMSO-d_6) δ: 10.51 (s, 1H, N-H), 9.98 (s, 1H, COO-H), 7.48-7.89 (m, 4H, ArH), 3.35 (q, *J*=3.9 Hz, 1H, CH), 1.19 (d, *J*=3.9 Hz, 3H, CH_3); Anal. Calcd for $C_{11}H_{10}N_2O_3$: C 60.54, H 4.62, N 12.84; found C 60.51, H 4.58, N 12.78.

***N*-(1,2-dihydro-2-oxo-3*H*-indol-3-ylidene)-L-valine (3c)** White solid, m.p. 295-296 °C; IR (KBr) *υ*: 3456, 3337, 1673, 1632, 1516, 1494, 1408, 1325, 1161 cm^{-1}; ^{1}H NMR (300 MHz, DMSO-d_6) δ: 10.45 (s, 1H, COO-H), 7.18-7.29 (m, 4H, ArH), 3.89 (d, *J*=6.1 Hz, 1H, CH), 3.51(s, 1H, N-H), 3.23-3.31 (m, 1H, CH), 1.22 (d, *J*=4.5 Hz, 6H, 2CH_3); Anal. Calcd for $C_{13}H_{14}N_2O_3$: C 63.40, H 5.73, N 11.38; found C 63.46, H 5.81, N 11.31.

***N*-(1,2-dihydro-2-oxo-3*H*-indol-3-ylidene)-L-methionine (3d)** White solid, m.p. >300 °C; IR (KBr) *υ*: 3289, 3198, 1703, 1622, 1487, 1456, 1359, 1123 cm^{-1}; ^{1}H NMR (300 MHz, DMSO-d_6) δ: 10.41(s, 1H, COO-H), 7.02-7.31 (m, 4H, ArH), 3.39 (t, *J*=5.6, 3.9 Hz, 1H, CH), 2.47-2.53 (m, 2H, CH_2), 2.47 (t, *J*=4.8, 3.9 Hz, 2H, CH_2), 2.45 (s, 1H, N-H), 1.75(s, 3H, CH_3); Anal. Calcd for $C_{13}H_{14}N_2O_3S$: C 56.11, H 5.07, N 10.07; found C 56.17, H 5.13, N 10.13.

***N*-(1,2-dihydro-2-oxo-3*H*-indol-3-ylidene)-L-aspartic acid (3e)** White solid, m.p. 290-292 °C; IR (KBr) *υ*: 3447, 3345, 1674, 1628, 1519, 1453, 1401, 1312, 1151 cm^{-1}; ^{1}H NMR (300 MHz, DMSO-d_6) δ: 10.49 (s, 1H, COO-H), 10.42 (s, 1H, COO-H), 6.83-7.61 (m, 4H, ArH), 3.96 (t, *J*=6.5, 4.6 Hz, 1H, CH), 3.25 (s, 1H, N-H), 3.29 (d, *J*=4.6 Hz, 2H, CH_2); Anal. Calcd for $C_{12}H_{10}N_2O_5$: C 54.92, H 3.84, N 10.69; found C 54.97, H 3.76, N 10.61.

***N*-(1,2-dihydro-2-oxo-3*H*-indol-3-ylidene)-L-arginine (3f)** White solid, m.p. >300 °C; IR (KBr) *υ*: 3336, 3256, 1706, 1684, 1626, 1478, 1429, 1345, 1107 cm^{-1}; ^{1}H NMR (300 MHz, DMSO-d_6) δ: 10.72 (s, 1H, COO-H), 10.21 (s, 1H, N-H), 9.74(s, 1H, N-H), 7.63 (s, 1H, N-H), 6.73-7.58 (m, 4H, ArH), 5.56 (s, 2H, NH_2), 3.46 (t, *J*=6.0, 4.2 Hz, 1H, CH), 3.11-3.23 (m, 2H, CH_2), 2.02-2.14 (m, 2H, CH_2), 1.39-1.56 (m, 2H, CH_2); Anal. Calcd for $C_{13}H_{17}N_5O_3$: C 53.59, H 5.88, N 24.05; found C 53.64, H 5.94, N 23.98.

***N*-(1,2-dihydro-2-oxo-3*H*-indol-3-ylidene)-L-phenyl alanine (3g)** White solid, m.p. 296-297 °C; IR (KBr) *υ*: 3417, 3262, 1708, 1623, 1521, 1479, 1325, 1189 cm^{-1}; ^{1}H NMR (300 MHz, DMSO-d_6) δ: 10.47 (s, 1H, N-H), 8.36 (s, 1H, COO-H), 6.83-7.42 (m, 9H, ArH), 3.59 (t, *J*=5.2, 3.6 Hz, 1H, CH), 3.39 (d, *J*=3.6 Hz, 2H, CH_2); Anal. Calcd for $C_{17}H_{14}N_2O_3$: C 69.37, H 4.80, N 9.52; found C 69.31, H 4.74, N 9.59.

***N*-(1,2-dihydro-2-oxo-3*H*-indol-3-ylidene)-L-histidine (3h)** White solid, m.p. >300 °C; IR (KBr) *υ*: 3334, 3254, 1730, 1689, 1621, 1475, 1403, 1342, 1109 cm^{-1}; ^{1}H NMR (300 MHz, DMSO-d_6) δ: 10.62 (s, 1H, COO-H), 10.26 (s, 1H, N-H), 8.96 (s, 1H, N-H), 8.09 (d, *J*=4.1 Hz, 1H, =CHN), 6.71-7.63 (m, 4H, ArH), 6.81 (d, *J*=3.6 Hz, 1H, =CHN), 3.87 (t, *J*=5.8, 4.1 Hz, 1H, CH), 3.15 (d, *J*=4.1 Hz, 2H, CH_2); Anal. Calcd for $C_{14}H_{12}N_4O_3$: C 59.15, H 4.26, N 19.17; found C 59.21, H 4.32, N 19.25.

***N*-(1,2-dihydro-2-oxo-3*H*-indol-3-ylidene)-L-tyrosine (3i)** White solid, m.p. >300 °C; IR (KBr) *υ*: 3211, 3026,

978-1-61896-030-6 © 2012 SciRes.

1612, 1593, 1558, 1516, 1458, 1417, 1363, 1154 cm^{-1}; ^1H NMR (300 MHz, DMSO-d_6) δ: 10.72 (s, 1H, COO-H), 10.22 (s, 1H, N-H), 6.75-7.66 (m, 4H, ArH), 7.09-7.18 (m, 2H, ArH), 6.48-6.57 (m, 2H, ArH), 5.78 (s, 1H, O-H), 3.21 (t, *J*=5.6, 3.9 Hz, 1H, CH), 3.13 (d, *J*=3.9 Hz, 2H, CH_2); Anal. Calcd for $C_{17}H_{14}N_2O_4$: C 65.80, H 4.55, N 9.03; found C 65.87, H 4.51, N 9.08.

***N*-(1,2-dihydro-2-oxo-3*H*-indol-3-ylidene)-L-tryptophan (3j)** Brown solid, m.p. 297 °C (Dec.); IR (KBr) *υ*: 3416, 3295, 3138, 1641, 1597, 1428, 1399, 1303, 1225, 1112 cm^{-1}; ^1H NMR (300 MHz, DMSO-d_6) δ: 10.62 (s, 1H, COO-H), 10.27 (s, 1H, N-H), 8.57 (s, 1H, N-H), 6.69-7.99 (m, 8H, ArH), 7.52 (d, *J*=15.8 Hz, 1H, CH=), 3.49 (t, *J*=5.2, 3.7 Hz, 1H, CH), 3.36 (d, *J*=3.7 Hz, 2H, CH_2); Anal. Calcd for $C_{19}H_{15}N_3O_3$: C 68.46, H 4.51, N 12.61; found C 68.51, H 4.57, N 12.69.

4 Conclusion

In conclusion, we have found an efficient and convenient procedure for the preparation of Schiff bases of *N*-(1,2-dihydro-2-oxo-3*H*-indol-3-ylidene)-amino acids from isatin and amino acids in the presence of *p*-TSA in combination of methanol and dioxane (1:1) at 70 °C. The reaction of isatin with amino acids can be efficiently performed giving good to high yields of the respective *N*-(1,2-dihydro-2-oxo-3*H*-indol-3-ylidene)-amino acids. This method is the most simple and convenient and would be applicable for the synthesis of different types of isatin Schiff base derivatives.

Acknowledgement

We acknowledgement the financial support from the Foundation of Jiangsu Key Laboratory of Marine Biotechnology (No. 2009HS04).

References

[1] N. I. Kalinovskaya, E. P. Ivanova, Y.V. Alexeevaetal, N. M. Gorshkova, T. A. Kuznetsova, "Low-molecular-weight, biologieally active compounds from marine pseudoalteromonas species," Curr. Mierobiol. Vol 48, 2004, pp. 441-446.

[2] E. Medvedev, V. Glover, "Tribulin and endogenous MAO-inhibitory regulation in vivo," NeuroToxicology, Vol 25, 2004, pp. 185-192.

[3] V. Glover, J. M. Halket, P. J. Watkins, A. Clow, B. L. Goodwin, M. Sandler, "Isatin: identity with the purified monoamine oxidase inhibitor tribulin, " J. Neurochem. Vol 51, 1988, pp. 656-659.

[4] T. R. Bal, B. Anand, P. Yogeeswari, D. Sriram, "Synthesis and evaluation of anti-HIV activity of isatin β-thiosemicarbazone derivatives," Bioorg. Med. Chem. Lett. Vol 15, 2005, pp. 4451-4455.

[5] T. Jiang, K. L. Kuhen, K. Wolff, H. Yin, K. Bieza, J. Caldwell, B. Bursulaya, T. Tuntland, K. Zhang, D. Karanewsky, Y. He, "Design, synthesis, and biological evaluations of novel oxindoles as HIV-1 non-nucleoside reverse transcriptase inhibitors. Part 2," Bioorg. Med. Chem. Lett. Vol 16, 2006, pp. 2109-2112.

[6] R. Tripathy, A. Reiboldt, P.A. Messina, M. Iqbal, J. Singh, E. R. Bacon, T. S. Angeles, S. X. Yang, M. S. Albom, C. Robinson, H. Chang, B.A. Ruggeri, J. P. Mallamo, "Structure-guided identification of novel VEGFR-2 kinase inhibitors via solution phase parallel synthesis," Bioorg. Med. Chem. Lett. Vol 16, 2006, pp. 2158-2162.

[7] A. Raj, R. Raghunathan, M. R. Sridevikumaria, N. Raman, "Synthesis, antimicrobial and antifungal activity of a new class of spiro pyrrolidines," Bioorg. Med. Chem. Vol 11, 2003, pp. 407-419.

[8] S. Holla, B. S. Rao, K. Shridhara, P. M. Akbaerali, "Studies on arylfuran derivatives: Part XI. Synthesis, characterisation and biological studies on some Mannich bases carrying 2,4-dichlorophenylfurfural moiety" Farmaco, Vol 55, 2000, pp. 338-344.

[9] R. Irie, K. Noda, Y. Ito, N. Matsumoto, T. Katsuki, "Catalytic asymmetric epoxidation of unfunctionalized olefins," Tetrahedron Lett. Vol 31, 1990, pp. 7345-7348.

[10] Heine, G. DeSantis, J. G. Luz, M. Michael, W. Chi-Huey, "Observation of covalent intermediates in an enzyme mechanism at atomic resolution," Science, Vol 294, 2001, pp. 369-374.

[11] Uchida, T. Ando, N. Fukami, K. Yoshida, M. Hashimoto, T. Tada, S. Koda, Y Morimoto, "The structure of vinigrol, a novel diterpenoid with antihypertensive and platelet aggregation-inhibitory activities," J. Org. Chem., Vol 52, 1987, pp. 5292-5293.

[12] Bolognese, M.V. Diurno, O. Mazzoni, F. Giordano, "On the azetidin-2-one ring formation. A ^1H NMR investigation," Tetrahedron, Vol 47, 1991, pp. 7417-7428.

[13] Capon, Z. P. Wu, "Comparison of the tautomerization and hydrolysis of some secondary and tertiary enamines," J. Org. Chem. Vol 55, 1990, pp. 2317-2324.

[14] M. Paventi, A. S. Hay, "Novel synthesis of *N,N*-diarylaryl -methanamines from N-(arylmethylene)arenamines and (aryl-methoxy)arenes," J. Org. Chem. Vol 56, pp. 5875-5882, 1991.

[15] Hunter, D. G. Neison, T. J. R. Weakley, "Rearrangement reactions of 1,3,6-triaryl-1,4-dihydro-*s*-tetrazines leading to 2,4-diarylquinazolines, 1-anilino-3,5-diaryl-1*H*-1,2,4-triazoles, 1, 3,5-triaryl-1*H*-1,2,4-triazoles, and 2,5-diaryl-1*H*-1,3,4-oxadiazoles. *X*-Ray structure determination of 6-isopropyl 2,4-diphenylquinazoline," J. Chem. Soc. Perkin Trans 1, 1985, pp. 2709-2712.

[16] T. B. Francoise, "A simple, convenient and mild synthesis of imines on alumina surface without solvent," Synthesis, Vol 6, 1985, pp. 679-680.

The Time and Concentration-Effect Relationships of Maxingshigan Decoction in Citric Acid-Guinea Pig Cough

Bo LIU[1], Qinghua LIU[2], Zuoyong LI[1], Peng XU[1], Liping HUANG[1], Guoliang XU[3], Wenting TONG[1], Riyue YU[1]

[1]*College of Pharmacy, Jiangxi University of Traditional Chinese Medicine, Nanchang, China, 330004*
[2]*College of Pharmacy, Fujiang University of Traditional Chinese Medicine, Fuzhou, China, 350108*
[3]*Key Laboratory of Modern Preparation of Ministry of Education, Jiangxi University of Traditional Chinese Medicine, Nanchang, China, 330004*
Email: yry59@126.com

Abstract: Citric acid inhalation causes cough in guinea pigs, which could be prevented and cured after administering Maxingshigan decoction for continuous several times. However, the time and concentration-effect relationships have not been fully clarified. In this paper, Maxingshigan decoction (nine doses and four time phases) was set for treating citric acid-guinea pig cough, which was detected by the System of Biomechanical parameter Collection, amicrophone and visual observation. The results showed citric acid-guinea pig cough number could also be decreased after administering Maxingshigan decoction only 1 time. And the best time for detecting cough number was 1 h after administering Maxingshigan decoction. The concentration-effect relationship of Maxingshigan decoction on cough likes wave, and the dose of Maxingshigan decoction (3.24g/kg) is the best for treating cough. The citric acid-guinea pig cough number was also decreased at 4 h after administering Maxingshigan decoction, but it is lower than that at 1 h. The time and concentration-effect relationships of Chinese Medicinal Herbs may be set as modern medicine.

Keywords: Time and concentration-effect relationships; cough; Maxingshigan decoction

1 Introduction

Inhalation of a citric acid aqueous solution is commonly used experimentally to evoke cough in guinea-pig and man. Acid-induced cough may be directly relevant to the chronic cough [1]. That pH value in airway is associated with inflammatory diseases, which contribute to cough [2]. Lots of Chinese Medicinal Herbs, considered anti-inflammatory and anti-bacterial, are known to prevention and treatment of cough [3]. In a long time, Chinese Medicinal Herbs may be administered long-term for treatment of disease. However, the time and concentration-effect relationships of cough change after administering Chinese Medicinal Herbs are not fully known.

Maxingshigan decoction is a formula of Traditional Chinese Medicine, which is a combination of plant species and minerals such as *Herba Ephedrae*, *Semen Armeniacae Amarum*, *Gypsum Fibrosum* and *Radix et Rhizoma Glycyrrhizae* [4]. On a basis of clinical experiences, the Maxingshigan decoction plays an important role in prevention and treatment of cough. Citric acid inhalation causes cough in guinea pigs, which could be prevented and cured by Maxingshigan decoction in our study. However, the time and concentration-effect relationships have not been fully clarified.

In this paper, Maxingshigan decoction was administered only 1 time or continuous several times for treatment of cough in guinea pigs. The cough number was detected at 1 h and 4 h by cough transfer-signal, voice and visual observation. The results showed Maxingshigan decoction (3.24g/kg) could decrease cough number after administering for 1 h. The concentration-effect relationship of Maxingshigan decoction on cough likes wave, and the dose of Maxingshigan decoction (3.24g/kg) is the best for treating cough.

2 Materials and Methods

2.1 Animals

Male guinea pigs (weighting 200～250 g, obtained from the Dongchang Center of Laboratory Animal, Changsha, China) were used in our study. All animals were kept in a temperature-controlled environment, with common laboratory food and water freely available.

2.2 Measurement of Cough

Unanesthetized male guinea pigs, which bound by respiratory-flow transducer, were placed in an individual transparent chamber and exposed to citric acid (0.4 M) generated with an ultrasonic nebulizer (Yuyue Medicine Technologies, China). The time of exposure to the citric acid was 4 min, followed by a further observation period of 6 min. Individual cough number was detected by the System of Biomechanical parameter Collection, amicrophone placed inside transparent chamber and individual visual observation. The animal exposed to citric acid for

978-1-61896-030-6

1 min and cough number was counted for 3 min before experiments. Only animals, which cough number was counted between 10 and 30 times, were chosen for further studying.

2.3 Experimental Design

To examine the effect of Maxingshigan decoction on citric acid-guinea pig cough. Guinea pigs were randomly divided into five groups such as control, codeine, high-dose Maxingshigan decoction (4.86g/kg, High-Ma), middle-dose Maxingshigan decoction (3.24g/kg, Middle-Ma) and low-dose Maxingshigan decoction (2.16g/kg, Low-Ma). Maxingshigan decoction had been continuously administered for 7 days before citric acid-induced guinea pig cough model having been founded. Numbers of cough were counted with the System of Biomechanical parameter Collection, amicrophone and visual observation, which are responsible for cough transfer-signal, voice recording and individual counting.

To investigate the time-effect relationships of citric acid causes cough in guinea pigs after administering Maxingshigan decoction. Guinea pigs were randomly divided into five groups such as control, 0.5h, 1h, 2h and 4h group. Four different administering time groups, but the concentration of Maxingshigan decoction was only 3.24 g/kg. The cough number was counted at 0.5 h, 1 h, 2 h and 4h, respectively.

To explore the concentration-effect relationships of citric acid causes cough in guinea pigs after administering different doses Maxingshigan decoction. Guinea pigs were randomly divided into 10 groups such as control, 0.96, 1.44, 2.16, 3.24, 4.86, 7.29, 10.94, 16.41 and 24.61 g/kg group. The cough number was counted at 1 h and 4h after administering Maxingshigan decoction, respectively.

2.4 Drugs

Citric acid was obtained from Sigma (USA.). Codeine was purchased from Qihai pharmacy Pharmacy Co., Ltd (Qihai, China). *Herb Ephedrae*, *Semen Armeniacae Amarum*, *Gypsum Fibrosum* and *Radix et Rhizoma Glycyrrhizae* obtained from professor Rao Y. (The National Pharmaceutical Engineering Center for Solid Preparation in Chinese Medicinal Herbal Medicine, Nanchang, China). All Herbs were checked on basis of medicine law. And Maxingshigan decoction was prepared by traditional method.

2.5 Statistical Analysis

Data were analysed with SigmaPlot (SPSS Inc., Chicago, IL, USA). All data were shown as mean ± SEM in this text and figures. Statistical significance between two groups was tested by Student's *t*-test. The *p* value less than 0.05 was considered significant.

3 Results

3.1 Maxingshigan Decoction Decrease Cough Number

Numbers of cough was measured by the combination of transfer-signal, voice and individual counting. The results showed citric acid could induce guinea pig cough (58.86 ± 11.73 times). Both Low-Ma and Middle-Ma decrease cough number (40.71±18.63 times, 35.1±3.85 times) after adiministering Maxingshigan decoction for continuous several times, but not High-Ma (49.33±12.58 times) (Figure1.). The results showed the dose (3.24g/kg) of Maxingshigan decoction is the best concentration for treatment of cough.

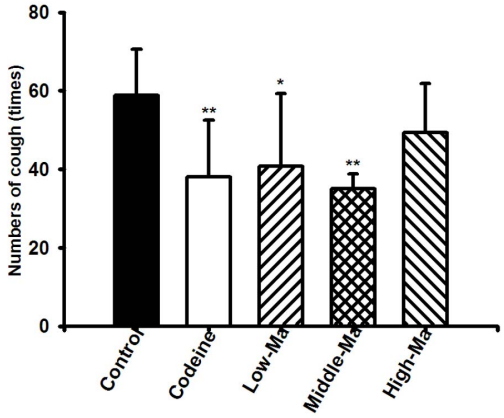

Figure 1. The effect of Maxingshigan decoction on cough

*, mean $p<0.05$, **,mean $p<0.01$,*VS* control, $n=8$.

3.2 Time-Effect Relationships of Maxingshigan Decodtion on Cough

The concentrations of Maxingshigan decoction (3.24g/kg) was set for treatment of cough in these experiments. Cough number was detected after administering various times up to 4 h (0.5 h, 1h, 2h, 4h) in citric acid-guinea pig cough. Figure2. showed that citric acid could induce guinea pig cough (53.63 ± 10.78 times). Cough number was decreased after administering Maxingshigan decoction for 1 h (34.83±9.15 times) and 4 h (42.83± 9.04 times), but not 0.5 h (48.83 ±10.23 times) and 2 h (52.17 ± 3.06 times). The 1 h after administering is the best phase for treatment of disease in Chinese Medicinal Herbs.

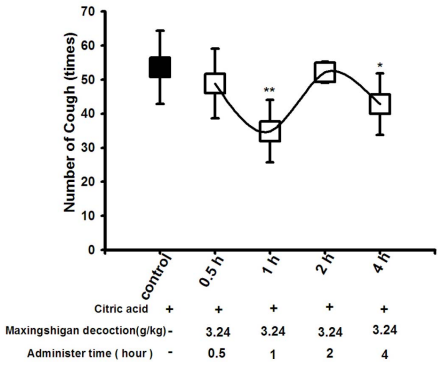

Figure 2. Time-effect relationships of Maxingshigan decodtion on cough

*, mean $p<0.05$, **,mean $p<0.01$,*VS* control, $n=6$.

3.3 Concentration-Effect Relationships of Maxingshigan Decoction on Cough

That effect of Maxingshigan decoction on citric acid-guinea pig cough was discovered. As nine doses were set for detecting the effect of Maxingshigan decoction on cough, the concentration-effect relationship was discovered. The results showed both 1 h and 4 h after administering, but the concentration-effect relationship of Maxingshigan decoction on cough likes wave. At 1 h after administering, the concentration of Maxingshigan decoction from 0.96g/kg to 3.24g/kg or from 10.94 g/kg to 24.61 g/kg, the concentration was increased and the cough number was decreased, but not the concentration of Maxingshigan decoction from 3.24g/kg to 7.29g/kg (Figure3.A). At 4 h after administering, the concentration of Maxingshigan decoction from 2.16g/kg to 4.86g/kg, the concentration was increased and the cough number was decreased, but not the concentration of Maxingshigan decoction from 4.86g/kg to 10.94g/kg (Figure3.B). The effect of Maxingshigan decoction on cough at 4 h after administering less than that 1 h after administering.

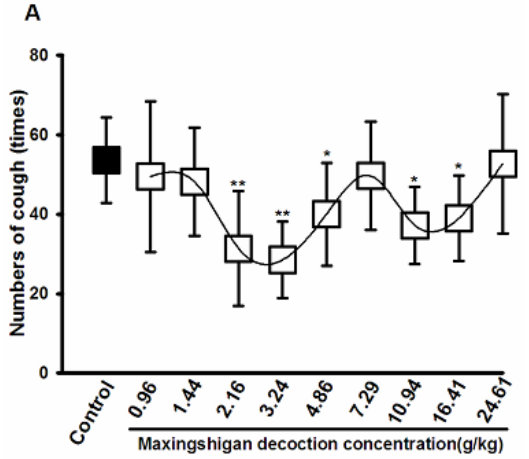

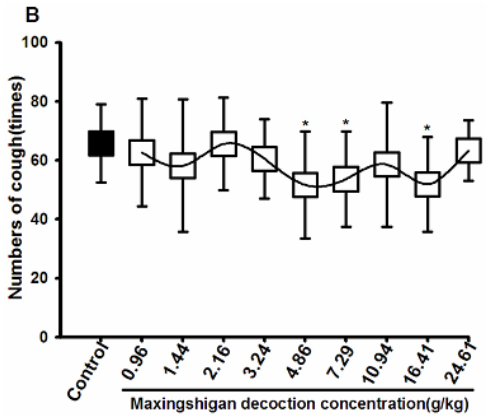

Figure 3. Concentration-effect relationships of Maxingshigan decodtion on cough

A, count number of cough after administering Maxingshigan decodtion for 1 h. B, count number of cough after administering Maxingshigan decodtion for 4 h. *, mean $p<0.05$, **,mean $p<0.01$,*VS* control, $n=8$.

4 Discussion

Cough is one of the most common symptoms of respiratory disease. Maxingshigan decoction, a traditional Chinese formula, has been considered to be a good classic prescription for treatment of cough. The time and concentration-effect relationships of Maxingshigan decoction on cough likes wave line was demonstrated in this paper. Maxingshigan decoction (3.24g/kg) could decrease cough number after administering for 1 h, and the dose of Maxingshigan decoction (3.24g/kg) is the best concentration for treating cough. In this paper, cough number was counted by the System of Biomechanical parameter Collection, amicrophone placed inside transparent chamber and individual visual observation. The results would be more accurate than that individual visual observation only.

In a long time, time and concentration-effect relationships are indistinguishable in Traditional Chinese Medicine. On a basis of clinic experiences, Chinese Medicinal Herbs may be administered long-term for treatment of disease [5]. And time and concentration-effect relationships of Chinese Medicinal Herbs are not same as modern medicine. In this paper, cough number was decreased after administering Maxingshigan decoction only 1 time. And found that the concentration-effect relationship of Maxingshigan decoction on cough was a wave line. It is not same as concentration-dependent manner in modern medicine. The complexes of compound may play an important role in these differences.

The 1 h after administering is the best phase for treatment of disease in Chinese Medicinal Herbs. Lots of pharmacokinetic are nonlinear in rats and humans with decreased total clearance at higher doses [6]. In this pa-

978-1-61896-030-6 © 2012 SciRes.

per, the change of symptom was used to detecting time and concentration-effect relationships. Results would be an example for blooding in serum-pharmacology methods [7].

In conclusion, the time and concentration-effect relationships of Chinese Medicinal Herbs may be set as modern medicine, but it would be more difficult than that in modern medicine.

Acknowledgement

This work was supported by The National Basic Research Program of China (2010CB530603).

References

[1] D. Jaspersen, "Extra-esophageal disorders in gastroesophageal reflux disease", *Dig Dis*, vol. 22, 2004, pp. 115-119.

[2] J.F. Hunt, K. Fang, R. Malik, et al. "Endogenous airway acidification: implications for asthma pathophysiology", *Am J Respir Crit Care Med*, vol. 161, 2000, pp. 694-699.

[3] X. Liu, Y. Han, K. Peng, et al. "Effect of traditional chinese medicinal herbs on *Candida* spp. from patients with HIV/AIDS", *Advances in Dental Research*, vol. 23, 2011, pp. 56-60.

[4] X.M. Zhang and J.B. Luo, "Effects of herba ephedrae, honey -fried herba ephedrae and maxingshigan decoction on autonomic activities of mice", *Zhong Yao Cai*, vol, 33, 2010, pp. 236-239.

[5] J. Lu, J.S. Wang and L.Y. Kong, "Anti-inflammatory effects of Huang-Lian-Jie-Du decoction, its two fractions and four typical compounds", *J Ethnopharmacol*, vol. 134, 2011, pp. 911-918.

[6] T. Kuwabara, Y. Kato, S. Kobayashi, et al. "Nonlinear pharmacokinetics of a recombinant human granulocyte colony-stimulating factor derivative (nartograstim): species differences among rats, monkeys and humans", *J Pharmacol Exp Ther*. Vol. 271, 1994, pp. 1535-1543.

[7] Y.H. Zhang, J.T. Liu, "Mechanisms of inhibiting proliferation of vascular smooth muscle cells by serum of rats treated with Dahuang Zhechong pill", *J Ethnopharmacol*. Vol, 124, 2009, pp. 125-129.

Attenuation of Sepia Ink Glycosaminoglycan towards Immune System Injury Induced by Cyclophosphamide

Yinyan HUANG[1], Guang WANG[2], Bin WU[2], Huazhong LIU[1]
[1]*Education Example Center, Guangdong Ocean University, Zhanjiang, China*
[2]*College of Food Science & Technology Guangdong Ocean University, Zhanjiang, China*
Email: 270101917@163.com

Abstract: In order to explore the attenuation of sepia ink glycosaminoglycan (SIGG) towards immune system injury, S.D. rats were employed to be administered with intraperitoneal cyclophosphamide (CP) and/or oral sepia ink glycosaminoglycan. The results showed that cyclophosphamide can induce the immune system injury by determination of number of leukocytes and lymphocytes in sera, and the antioxidant capacity in spleen. The SIGG at different doses all can inhibit the damage induced by cyclophospahmide to some extent.

Keywords: Sepia ink glycosaminoglycan; cyclophosphamide; immune system

1 Introduction

Cyclophosphamide (CP), a most commonly used anti-tumor drug which belongs to alkylating agent that mainly used in bone marrow transplantation, chronic and acute leukemias, multiple myeloma, lymphomas and rheumatic arthritis[1,2]. It is inactive until undergoing the activation in liver, and it can induce many side effects like hemorrhagic cystitis[3], decline of leukocytes[4] because of the toxic metabolin, which limit its application in practice.

Sepia is a kind of invertebrate Mollusca who can eject the dark ink to protect themselves. Recently, there is an increasing interest in functions of sepia ink and researches have showed that sepia ink possesses multiple biological functions like hemostasis[5], anti-tumor[6], anti-oxidation[7], anti-bacteria [8, 9] etc.. Actually, the history that sepia ink used as medicine in China can trace back to Ming Dynasty according to the Compendium of Materia Medica compiled by a famous doctor called Shi-Zhen Li. Previous researches demonstrated that the main compositions of fresh ink were melanin and peptidoglycan, and the peptidoglycan was the primary active ingredient. Researchers have done some work on separation and purification of sepia ink polysaccharides, they found that glycan chain was a new structural glycosaminoglycan consisting of glucuronic acid (GlcA), N-acetylgalactosamine (GalNAc) and Fucose (Fuc)[10, 11]. Sepia ink polysaccharide was a group of fucose-rich glycosaminoglycans (GAGs). They obtained three fucose-rich GAGs with biochemical technology and discovered that the three GAGs had the same repeating unit of trisaccharide structure { -3GlcA β 1-4(GalNAc α 1-3)Fuc α 1-)} n. Currently, rarely information about the activity of purified sepia ink glycosaminoglycan was unveiled. With all these consideration in mind, the objective of this work is to explore the amelioratory effect of sepia ink glycosaminoglycan on immune system injury induced by cyclophosphamide.

2 Materials and Methods

2.1 Drugs and Chemicals

Cyclophosphamide was procured from Pu-de Pharmacy Limited Co., Shanxi, China. DEAE-sepharose F.F., SephadexG-15 were bought from Amersham Pharmacia Biotech company. Fresh sepia ink was obtained from fishermen and rapidly brought to the laboratory and stored at -40℃ before use. All other chemicals and solvents used are of analytical grade.

2.2 Preparation of Sepia Ink Polysaccharide

Extraction of SIGG from sepia ink was done according to the method[12]: Fresh ink taken directly from ink sacs of sepia was acidified to pH 4–5 with 0.1 M HCl and the solution was allowed to stand for 24 h at 4°C to participate melanin. Melanin was removed after centrifugation at 5,000 g for 1 h. Melanin-free ink was then digested with 2 volumes of 1% (w/v) papain in Tris–HCl buffer (50 mM, pH 6.8; containing 5 mM Cys and 5 mM EDTA) at 60°C for 24 h. Digestion was repeated twice to ensure the cleavage of the protein/peptide moiety. Crude melanin-free SIGG was obtained after precipitation with 4 volumes of ethanol. Protein was removed by the method of savage (chloroform: n-Butanol= 4: 1) for several times. Crude SIGG was dehydrated in freeze drier and grinded sufficiently in mortar. At last, SIGG was purified by using the DEAE-sepharose F.F. and desalted by using Sephadex G-15. (Fig.1 showed the maximum adsorbtion peak of SIGG) The samples were freeze-dried at 50 C for 24 h.

2.3 Animals and Experimental Protocol

Healthy S.D. rats at 12 weeks of age were served as

978-1-61896-030-6

experimental animals for the study. All animals were acclimatized 7 days prior to the commencement of the treatment and allowed free access to food and water. Rats were randomly divided into 6 groups; each group has 10 animals, male and female share equal quantity in each group. Control animals (group A) were administered with normal saline throughout the experimental period (7 days) and intraperitoneal normal saline at the beginning of experiment, respectively. Model animals (group B) were fed saline and intraperitoneally injected CP dissolved in saline at a dose of 100 mg/kg body weight at the beginning of experiment. Animals in group C and D were administrated with SIGG at dose of 10, 20 mg/kg/d body weight respectively during the experimental period and intraperitoneally injected normal saline at the beginning of experiment. Co-treated animals (group E and F) were injected with CP (as in model group) and SIPS (as in group C, D respectively). At the end of experiment (the 7^{th} day), animals were sacrificed via cervical decapitation, spleen was excised and washed with ice-cold normal saline, take a portion of tissue and make a 10% homogenate in ice-cold physiological saline to determine the antioxidant ability. Sera were prepared for investigation of peripheral lymphocytes and leukocytes.

2.4 Organ Index of Spleen Determination

Organ index of spleen was calculated and expressed as the ratio of organ weight to body weight, gram per gram (g/g).

2.5 Peripheral Blood Profile Determination

Blood was collected and sera was separated by centrifugation at 3000×g for 10 minutes. The level of leukocytes, lymphocytes in sera was determined by automatic hematocyte counter (Micros60, HORIBA ABX, France).

2.6 Determination of Antioxidant Ability in Spleen

The level of SOD, CAT, T-AOC and MDA was assessed by kit procured from Jiancheng Bioengineering research institute (Nanjing, China).

2.7 Data Analysis

The results were given as mean ± standard deviation (S.D.). Differences between groups were assessed by one-way ANOVA using SAS software for windows. Post hoc testing was performed using the least significance difference test. P values less than 0.05 were considered to be statistically significant.

3 Results

3.1 Organ Index of Spleen

The changes of organ index of spleen as shown in Fig.2 that cyclophospahmide can obviosly decrease the index of spleen compared with control group ($P<0.05$). High dose SIGG can significantly inhibit the decrease of index of spleen($P<0.05$), while low dose SIGG had no obvious effect on it ($P>0.05$).

3.2 Changes of Leukocytes and Lymphocytes in Sera

Fig.3 and Fig.4 showed that cyclophosphamide markedly declined the number of leukocytes and lymphocytes ($P<0.01$), and the SIGG at different doses all can enhance the decline of leukocytes and lymphocytes induced by cyclophosphamide ($P<0.05$ or $P<0.01$).

3.3 Changes of Antioxidant Capacity in Spleen and Sera

Table 1 unveiled the changes of the antioxidant capacity in spleen. The data in the table demonstrated that spleen was attacked by the free radical severely. However, all SIGG groups cotreated with CP showed the attenuation effect of SIGG towards free radical in spleen compared with model group($P<0.05$ or $P<0.01$).

4 Discussions

Spleen is the largest immune organ in body, which contains lots of immune cells that can induce T lymphocytes and B lymphocytes and macrophage. What's more, spleen is not only the important position of humoral immunoresponse, but also the important place of cellullar immunologic response.

Determination of organ index of spleen and antioxidant capacity in spleen showed that spleen was attacked by free radical and damaged to some extent, which markedly affect the immunologic function of body. There is an effective antioxidation defense system including some antioxidase and nonenzymatic anti- oxidative substance in organism, which can clear up the excessive free radicals and protect the histocyte. So, the activity of SOD, CAT, T-AOC and the content of MDA in tissue can indirectly reflect the degree of injury of histocytes. Combining with the examination of peripheral blood leukocytes and lymphocytes, we can arrive at a conclusion that cyclophosphamide has resulted in immune system injury. On the other side, SIGG at different doses showed the inhibiting effect on the parameters metioned above, which demonstrated the attenuation effect towards immune system injury induced by cyclophospahmide. The mechanism would be that SIGG undergo activating immune cells and cleaning up the superabundant free radicals, thereby play an important part in immune system protection.

Acknowledgement

This work was supported by the project of Science & Technology Plan in Guangdong Province and granted from Natural Science Foundation of Guangdong Ocean University.

References

[1] M.A.Goldberg, J.H.Antin, E.C.Guinan, J.M. Rappeport, Cyclophosphamide cardiotoxicity: an analysis of dosing as a risk factor. Blood 1986, 68, pp.1114-1118.
[2] C.Dollery, Cyclophosphamide. In: Dollery C, editor. Therapeutic Drugs. Churchill Livingstone, Edinburg, 1999, pp. 349-353.
[3] L.A.Levine,J.P.Richie, Urological complications of cyclophosphamide. J. Urol. 1989. 141, pp. 1063-1069.
[4] J.P.Zhong, G.Wang, J.H.Shang, J.Q.Pan, K.Li, Y.Huang,et al. Protective effects of squid ink extract towards hemopoietic injuries induced by cyclophosphamine. Mar. Drugs 2009, 7, pp. 9-18.
[5] G.L Xie, C.L. Lv, M.B. Hong, Experimental study of the effective machenisms of sepia in promoting coagulation of blood. Journal of china medical university.1994; 23 (6) 530-531.
[6] Y. Takaya, H. Uchisawa, H.Matsue, B.Okuzaki, F. Narumi, J. Sasaki, et al. An investigation of the antitumor peptidoglycan fraction from squid ink. Biol. Pharm. Bull. 1994, 17, pp.846-849.
[7] M.Lei, J.F.Wang, L Pang, Y.M.Wang, S.G. Chen, C.H.Xue, Effects of sepia on the metabolization of blood lipid and antioxidant ability in hyperlipidemia rats. Chin. J. Mar. Drugs .2007, 3, pp.30-33.
[8] Y. Funatsu, K.Fukami, H.Kondo, S.Watabe, Improvement of "kurozukuri ika-shiokara" (fermented squid meat with ink) odor with Staphylococcus nepalensis isolated from the fish sauce mush of frigate mackerel Auxis rochei. Nip. Suis. G. 2005, 71, pp. 611-617.
[9] S.Sadok, A. Abdelmoulah, A.E.Abed, Combined effect of sepia soaking and temperature on the shelf life of peeled shrimp Penaeus kerathurus. Food Chem. 2004, 88, pp.115-122.
[10] Y.Takaya, H. Uchisawa, K.Hanamatsu, F.Narumi, B.Okuzaki, H. Matsue, Novel fucose-rich glycosaminoglycans from squid ink bearing repeating unit of trisaccharide structure (-6GalNAc alpha 1-3GlcA beta 1-3Fuc alpha 1-)n. Biochem. Biophys. Res. Commun. 1994, 198, pp.560-567.
[11] Y.Takaya, H.Uchisawa, F. Narumi, H.Matsue, Illexins A, B, and C from squid ink should have a branched structure. Biochem. Biophys. Res. Commun. 1996, 226, pp.335-338.
[12] S.G.Chen, J. Xu, C.H.Xue, P.Dong, W.J.Sheng, J.L.Yu, et al. Sequence determination of a non-sulfated glycosaminoglycan-like polysaccharide from melanin-free ink of the squid Ommastrephes bartrami by negative-on electrospray tandemmass spectrometry and NMR spectroscopy, Glycoconj. J. 2008, 25, pp.481-492.

Table 1. Antioxidant capacity in spleen

	SOD (U/mg prot)	*CAT (U/mg prot)*	*MDA (nmol/mgprot)*	*T-AOC (unit/milligram prot)*
A	17.2±1. 18	0.94±0. 14	0.53±0. 11	6.17±1.45
B	27.6±2. 54*	1.41±0.09**	0.67±0. 06*	10.11±1.54**
C	15.8±1. 98	0.87±0.15	0.52±0. 13	5.94±1.31
D	14.9±1. 29	0.91±0.11	0.49±0. 05	6.19±1.78
E	19.2±3. 07	1.1±0.43#	0.55±0. 09#	8.57±2.59#
F	20.6±2. 85#	0.99±3.99#	0.51±0. 08#	8.79±0.71#

Note: A: control group; B: model group; C: low dose SIGG; D: high dose SIGG; E:cotreated CP and low dose SIGG; F: cotreated CP and high dose SIGG. "*" or "**" means P<0.05 or P < 0.01 VS control group, "#" or "##" means P <0.05 or P<0.01VS model group.

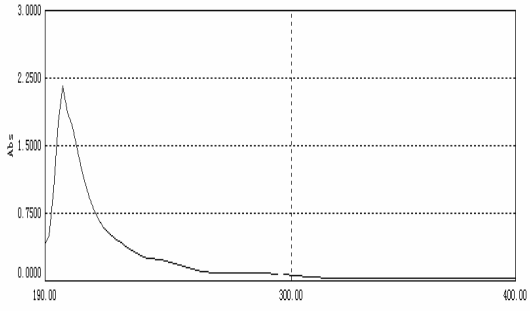

Figure 1. Maximum adsorbtion peak of SIGG

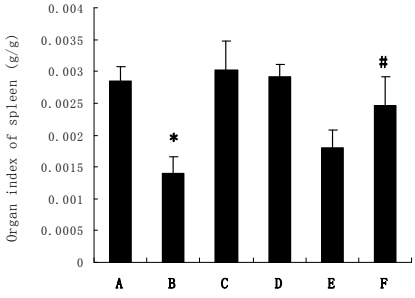

Figure 2. Changes of organ index of spleen

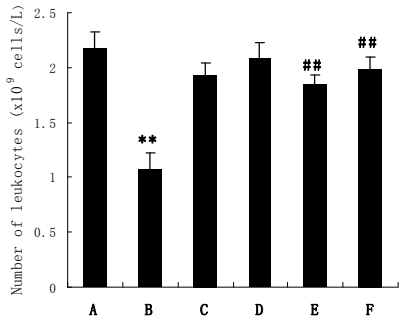

Figure 3. Changes in number of leukocytes in sera

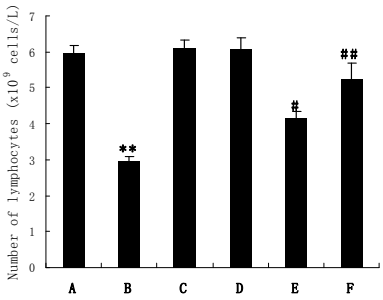

Figure 4. Changes in number of lymphocytes in sera

978-1-61896-030-6 © 2012 SciRes.

Optimization of Sulforaphane Extraction Protocol through Orthogonal Design

Zhansheng LI[1], Yumei LIU[1], Zhiyuan FANG[1], Limei YANG[1], Mu ZHUANG[1], Yangyong ZHANG[1], Peitian SUN[1], Wen ZHAO[2]

[1]*Chinese Academy of Agricultural Sciences, Chinese Institute of Vegetables and Flowers, Beijing, China*
[2]*Chinese Academy of Agricultural Sciences, Supervision and Testing Center for Vegetable Quality, Ministry of Agriculture, Beijing, China*
Email: liuym@mail.caas.net.cn, 2005lzsheng@163.com

Abstract: To optimize the extraction process of sulforaphane from vegetables and make sure the key factors to affect sulforaphane yield. orthogonal test L_9 (3^4) was designed to investigate the effect of pH value, the ratio of material to buffer (g/mL) (solid to buffer), zinc concentration ($Zncl_2$, mM/L) and reaction time (hour) on the amount of sulforaphane generated at room temperature. The results showed the ratio of material to buffer influencing on the formation of sulforaphane was significantly higher than factors of zinc concentration, pH value and reaction time ($P < 0.05$), and the final protocol was decided: material to buffer ratio 1:20 (g/mL), pH value 7.0, zinc ($Zncl_2$) concentration 8.0 mM/L and reaction time 2.0 h. The optimal extract process increased sulforaphane yield of 31.9% at maximum. The reasons why four factors affected the yield of sulforaphane was also discussed in detail through enzyme engineering and bioinformatics in the paper.

Keywords: Sulforaphane; orthogonal design; enzyme engineering; bioinformatics; high performance liquid chromatography (HPLC); glucosinolates; glucoraphanin

1 Introduction

The cruciferous vegetables are rich in glucosinolate, which are modified by amino acids, bearing an N-sulfate and an S-glucose moiety, but not all fruits and vegetables are equally effective. When cruciferous vegetables are crushed, bittern by insect or the human as well as in the harsh environment, gulcosinolate in special protein can be released and reacted with myrosinase, producing different second products in different pH condition, such as D-glucose, sulfate and intermediates. Then these intermediates change into bioactivities. Broccoli (*Brassica oleraceae* var. *italica*) typically has as its major aliphatic glucosinolate, methionine-derived glucoraphanin (4-methylsulphinylbutyl glucosinolate, RAA) [1]. Epidemiological studies suggest that sulforaphane is considered to be responsible for the major part of cancer prevention by up-regulating phase II detoxification enzymes that might clear chemical carcinogens and reactive oxygen species [2-4]. More and more papers are reporting sulforaphane can reduce the risk of most cancers of liver, lung, stomach, breast, colon, prostate and so on [5-9].

The first report about sulforaphane determination is Spencer and Daxenbichler (1980) [10] by gas chromatography-mass (GC/MS). Chiang (1988) [11] and Bertelli (1988) [12] also study the determination method of sulforaphane by GC/MS and high performance liquid chromatography (HPLC). But sulforaphane is unstable and depredated at high temperature. Most reported protocols are too complex or time-wasting. Liang (2006) [13] and Zhang (2007) [14] develop the extraction methods of sulforaphane, yet there are no detailed parameters about the pretreatment. Zhang (2009) [15] optimize hydrolysis conditions of sulforaphane by orthogonal design on solid to liquid, pH value and reaction time. Besides, sulforaphane yield is also affected by metal ions. Liang (2006) [16] studies effects of several metal ions on enzyme related with sulforaphane generation and reveals that zinc ion can significantly improve sulforaphane generation, while iron, calcium and other metal ions inhibit sulforaphane generation. But there is little research about the effect of pH, the ratio of solid to liquid, zinc ion concentration and reaction time on sulforaphane generation.

Sulforaphane is becoming a hot topic on studies ofclinical medical, food chemistry and nutrition. So the study focus on optimization process of extracting sulforahane from broccoli seed by orthogonal design, analyzing the reasons affecting the yield of sulforaphane and bioactivity of myrosinase according to enzyme engineering and bioinformatics. Finally optimization process might provide basis for cancer research, sulforaphane extraction, as well as nutrition.

2 The Materials and Methods

Broccoli (*Brassica oleraceae* var. *italica*) seed "zhongqing 2" was harvested in field in December 2008 at Institute of Vegetables and Flowers, Chinese Academy

of Agricultural Sciences (Beijing).

Sulforaphane standard was purchased form LKT Biochemical Company (USA), and the purity was above 99%. HPLC grade methanol, double-distilled water Milli-Q quality water system (Millipore, Bedford, USA) were obtained from Supervision and Testing Center for Vegetable Quality, Ministry of Agriculture (Beijing, China). Phosphates (K_2HPO_4 and KH_2PO_4), ethyl acetate of analysis reagent were purchased from Beijing chemical works (Beijing, China).

Firstly, broccoli seed was crushed into powder by grinder. Then 0.50 gram powder was exactly weighed and hydrolyzed with phosphate buffer, and then the mixture was extracted by ethyl acetate. Extraction and mixture was together centrifuged at 6000 rpm (×*g*) 10 minutes, repeating another two times based on the residuals. The collected three times supernatant were evaporated by rotator at 35 ℃, and the residuals were dissolved by 10 mL methanol, filtered through Agela (China) No. 0.22 μm (D 13 mm) nylon filter paper and stored at -20℃ for analysis.

Orthogonal design L_9 (3^4) was set for the study based on three levels and four factors. Four factors were individually pH value, solid to buffer (g/mL), zinc concentration ($mM \cdot L^{-1}$, $Zncl_2$) and reaction time (hour), following relatively three levels (Table 1).

Table 1. Factors and levels of orthogonal design

	Factors			
Levels	pH value /A	Solid to buffer （g/mL）/B	Zinc concentration （mM/L）/C	Reaction time （h）/D
1	5.0	1:05	1.0	1.0
2	6.0	1:10	8.0	2.0
3	7.0	1:20	20.0	3.0

A SHIMADZU LC-20A HPLC system equipped with a SPD-20 UV detector and a reverse-phase C_{18} column (250 × 4.6 mm, 5μm, SHISEIDO^{TM}) was used for sulforaphane analysis. A gradient mobile phase which consisted 5% tetrahydrofuran (Pump A) and 100% methanol (Pump B) was chosen, pump B solvent was 40% initially and then changed linearly to 60% in 10th min, and return to 100% after 10th min, equilibrating for 15 min at a flow rate of 0.80 mL/min. The absorbance was at 254 nm and the column oven temperature was set at 32 ℃. The HPLC chromatograms of sulforaphane from extracted samples and standard were shown in Figure 1, 2.

The standard of sulforaphane (1.0 mg/mL) was diluted into different concentrations: 5.0 μg/mL, 5.0 μg/mL, 50.0 μg/mL, 10.0 μg/mL, 200.0 μg/mL and 300.0 μg/mL. The linear equation based on the peak area responses (Y) and theoretical concentration (X). One standard solution and one sample were analyzed by recording peak areas, the precision of the HPLC system was calculated by the relative standard deviation (RSD). And recovery and stability related to extraction were examined by spiking known amounts of sulforaphane standard in extracted solution with six repeats every treatment.

Data was represented as average ± standard devation (Mean±SD) (n=3), and a *t-test* was performed for analyzing the data (a=0.05) by SAS Version 8.0 (Chinese Academy of Agricultural and Sciences).

3 The Results and Discussion

The linear equation based on peak area responses (Y) and theoretical concentration (X) was Y = 4623.7 + 516.2X, R^2 = 0.9998 at the range of 5.0 to 300.0 μg/mL standard samples. The RSD (%) for standard and extract samples were $2.5E^{-9}$ and 0.81 (RSD %) respectively (n=6). The average recovery of sulforaphane was 96.2 ± 1.3% (Mean ± RSD, n=6). In our study, we detected one same standard samples by keeping the record every two hours, the RSD of stability was 0.22% (n=5).

The chromatograms shown in figure 1 and 2 were standard and extract samples, both of them were with the same retention time based on the peak areas. The data suggested that different treatment had a different result (Table 2), and there were a significant difference among them (α=0.05). The ranges of sulforaphane detected in nine treatments of the orthogonal test were 5.319-7.015 g/kg DW. And the highest content 7.015 g/kg DW was 1.32 time than the lowest content 5.319 g/kg DW. The result revealed that optimal treatment No. 9 was better than the other treatments in the experiment.

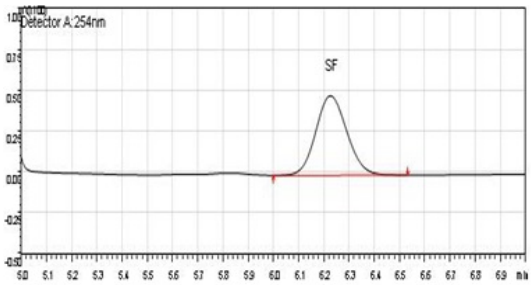

Figure 1. HPLC chromatograms of standard sulforaphane

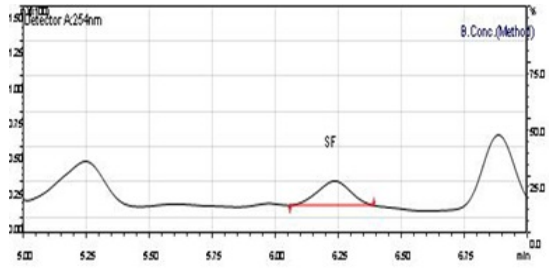

Figure 2. HPLC chromatograms of extract sulforaphane sample

978-1-61896-030-6 © 2012 SciRes.

Table 2. Data analysis of orthogonal design

NO	A	B	C	D	SF content（g/kg）
1	1（5）	1(1:05)	1(1)	1(1)	5.539 BC
2	5	2(1:10)	2(8)	2(2)	6.672 AB
3	5	3(1:20)	3(20)	3(3)	6.309 ABC
4	2（6）	1:05	8	2	5.319 C
5	6	1:10	20	1	6.913 AB
6	6	1:20	1	3	6.582 ABC
7	3（7）	1:05	20	3	6.088 ABC
8	7	1:10	1	1	6.242 ABC
9	7	1:20	8	2	7.015 A
T_{1j}	18.52	16.946	18.363	18.694	
T_{2j}	18.814	19.827	19.006	19.006	T= 56.679
T_{3j}	19.345	19.906	19.31	18.979	
R_j	0.825	3.446	0.947	0.312	

Note: Different capital letters show significant difference at *P*=0.01.

The highest content of sulforaphane all the treatments 7.015 g/kg DW was 1.46 time higher than Nathan (2001) report's data, which was more meaningful for industry production of sulforaphane.

Data analysis of variance showed the factor of solid to buffer was at significant level (α=0.05) (Table 3). The range data (Table 2) suggested four factors had different effects on sulforaphane content. The first was solid to buffer, the followings were separately zinc concentration, pH and reaction time. The treatment of No. 9 might be better protocol: solid to buffer (g/mL) 1:20, zinc concentration 8.0 mM/L, pH 7.0 and reaction time 2.0 hours.

Table 3. Data analysis of variance

Factor	Devsq	Df	F value	F critical value	significant level
pH	0.117	2	0.857	6.940	
Solid to buffer	1.896	2	13.890	6.940	*
Zinc concentration	0.156	2	1.143	6.940	
Reaction time	0.526	2	3.853	6.940	
Error	0.27	4			

The same broccoli seed was validated by the protocol of No. 9 treatment. Data were recorded dividedly with three repeats and final result were 6.985 g/kg DW, 7.002 g/kg DW and 7.051 g/kg DW. The result of validation suggested the protocol of No. 9 treatment was repeatable and stable, as well as consistent with No. 9 detection data. So No. 9 treatment was chosen as optimal protocol for hydrolysis of glucoraphanin into sulforaphane.

Solid to buffer: enzyme kinetics studies show that enzyme reactions not only depend on pH, temperature and activation agent, but also relevant substrate concentration. When substrate concentration is at low level, there is a positive correlation between reaction rate and substrate concentration, and the reaction is often shown as one order reaction. According to the performance level for mixed reaction as increase of the substrate concentration, there is no longer increase of reaction rate. When substrate concentration at a certain level, the reaction rate decreases gradually, and finally the reaction rate achieves maximum level (V_{max}) so that the reaction performance shows that zero level. In this study, solid to buffer (g/mL) 1:20 might increase the content of sulforaphane. We speculated that substrate concentration promoted the reaction achieve the maximum level (V_{max}).

Zinc concentration: myrosinase becomes the main factor influencing sulforaphane content when glucoraphanin is constant. The reaction of enzyme and substrate not only needs optimum temperature and pH, but also a right activator. Myrosinase belongs to the binding-protein family. Bioinformatics analysis reveals there are some ligand in the structure of myrosinase, such as fucose, glucose, xylose, BMA, liew, zinc ion and so on (Fig 4). The same ligand zinc ion may stable its structure, performancing as one activator (Figure 4). At the same time, when $ZnSO_4$ meets myrosinase, the yield of sulforaphane will decrease, which might caused by existing of $SO4^{2-}$ reversing the reaction.

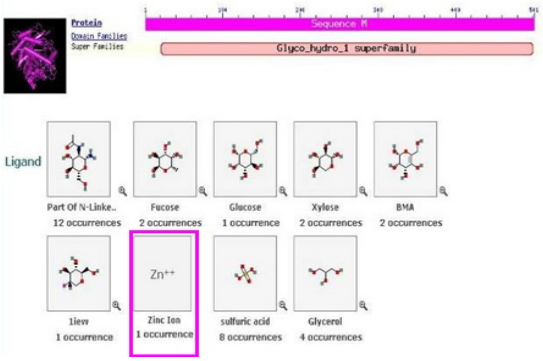

Figure 4. The ligands of myrosinase protein

(Zinc ligand showed in pink box)

pH: different enzymes require different pH condition, and most of them are changing from pH 5.0-8.0, animal pH value is pH 6.5-8.0, while plant and microbial pH 4.5-6.5. Higher or lower pH value may decrease bioactivities of relative enzymes by changing their structures. So glucoraphanin hydrolyzes into different products at different pH conditions, and sulforaphane is the major product in neutral condition [17], while nitrates in alkaline condition. In our study, the result was consistent with previous reports.

Reaction time: along with the reaction of enzyme continuing, the concentration of the substrate decreases, and the collision frequency of enzyme and substrate also decrease gradually so that the activity of enzyme begin to

decrease. At the same time, due to the instability of sulforaphane, it easily changes into its similar nitriles or other products, which also reduces the product of sulforaphane. In the study, there was a higher yield of sulforaphane in one to two hours. Liang (2004) report about the determination of vegetable seeds by HPLC and show that broccoli seed (Zhongqing 2) is with higher content of sulforaphane 4.618 mg/kg [17]. We had also tested the same style broccoli seed (Zhongqing 2) and got a higher content 7.015 mg/kg by optimized process, which was about 1.52 times higher than his reported result. Then we validated the optimal protocol and proved it to be with a stable and repeatable character. At the same time, we discovered ethyl acetate as solvent instead of methylene chloride and acetone also making the experiment stable, easy and lower toxicity. There were few impurity peaks based on extracting sulforaphane from broccoli seed. In a word, the optimal protocol and the higher sulforaphane content in broccoli seed might be useful and meaningful for medical, food chemistry research as well as nutrition.

4 Conclusion

The study provided one development method for extracting higher sulforaphane by orthogonal test L_9 (3^4). The optimization condition for sulforaphane hydrolysis was validated with a good yield comparing to the other treatments. So the study laid the foundation for sulforaphane extract and medical research.

References

[1] J. W. Fahey, Y. Zhang and P. Talalay, "Broccoli sprouts: an exceptionally rich source of inducers of enzymes that protect against chemical carcinogens." *Proceedings of the National Academy of Sciences*, Vol. 94, NO. 19, 1997, pp. 10367-10372.

[2] W. Xia, X. J. Zhao, K. Wu and L. H. Yuan, "Determination of sulforaphane in vegetables of north diet." *Chinese Journal of Disease Control & Prevention*, Vol. 9, NO. 3, 2005, pp. 209-211.

[3] P. Talalay and J. Fahey, "Phytochemicals from cruciferous plants protect against cancer by modulating carcinogen metabolism." *The Journal of Nutrition*, Vol. 131, NO. 11, 2001, pp. 3027S-3033S.

[4] E. H. Jeffery and A. S. Keck, "Translating knowledge generated by epidemiological and in vitro studies into dietary cancer prevention." *Molecular Nutrition & Food Research*, Vol. 52, 2008, pp. S7-S17.

[5] J. D. Brooks, V. G. Paton and G. Vidanes, "Potent induction of phase 2 enzymes in human prostate cells by sulforaphane." *Cancer Epidemiol Biomarkers Prevention*, Vol. 10, NO. 9, 2001, pp. 949-954.

[6] K. J. Hintze, K. A. Wald and H. Zeng, "Thioredoxin reductase in human hepatoma cells is transcriptionally regulated by sulforaphane and other electrophiles via an antioxidant response element." *The Journal of Nutrition*, Vol. 133, NO. 9, 2003, pp. 2721-2727.

[7] A. T. Dinkova-Kostova, W. D. Holtzclaw and R. N. Cole, "Direct evidence that sulfhydryl groups of Keap1 are the sensors regulating induction of phase 2 enzymes that protect against carcinogens and oxidants." *Proceedings of the National Academy of Sciences*, Vol. 99, NO. 18, 2002, pp. 11908-11913.

[8] N. Juge, R. Mithen and M. Traka, "Molecular basis for chemoprevention by sulforaphane: a comprehensive review." *Cellular and Molecular Life Sciences*, Vol. 64, NO. 9, 2007, pp. 1105-1127.

[9] J. W. Fahey, X. Haristoy and P. M. Dohn, "Sulforaphane inhibits extracellular. intraceHular, and antibiotic-resistane strains of helicobacter pylori and prevents benin (a) pyrene-induced stomach tumor." *Proceedings of the National Academy of Sciences*, 2002, pp. 7610-7615.

[10] A. S. Keck, Q. Qiao and E. H. Jeffery, "Food matrix effects on bioactivity of broccoli-derived sulforaphane in liver and colon of F344 rats." *Journal of Agricultural and Food Chemistry* , Vol. 51, NO. 11, 2003, pp. 3320-3327.

[11] G. F. Spencer and E. Daxenbichler, "Gas chromato-graphy-masss spectrometry of nitriles, isothiocyanates and oxazolidinethiones derived from cruciferous glucosinolates." *Journal of the Science of Food and Agriculture*, Vol. 31, 1980, pp. 359-367.

[12] W. C. Chiang, D. J. Pusateri and R. E. Leitz, "Gas chromatography/mass spectrometry method for the determination of sulforaphane and sulforaphane nitrile in broccoli." *Journal of Agricultural and Food Chemistry* , Vol. 46, NO. 3, 1988, pp. 1018-1021.

[13] M. Bertelli, D. Braghiroli and A. Monzani, "Separation by solid phase extraction and quantification by reverse phase HPLC of sulforaphane in broccoli." *Food Chemistry*, Vol. 63, NO. 3, 1998, pp. 417-421.

[14] H. Liang, Q. P. Yuan, H. R. Dong and Y. M. Liu, "Determination of sulforaphane in cabbage and broccoli by high performance liquid chromatography." *Journal of food and composition analysis*, Vol. 19, NO. 5, 2006, pp. 473-476.

[15] C. J. Zhang, X. L. Guo, Y. Q. Meng and Y. F. Feng, "HPLCanalysis of sulforaphane in different kinds of broccoli seeds." *Journal of Guangdong College of Pharmacy*, Vol. 23, NO. 5, 2007, pp. 506-508. (Chinese).

[16] H. Liang, Q. P. Yuan and Q. Xiao, "Effects of metal ions on myrosinase activity and the formation of sulforaphane in broccoli seed." *Journal of Molecular Catalysis B: Enzymatic*, Vol. 43, NO. 4, 2006, pp. 19-22.

[17] H. Liang, Q. Q. Yuan, H. R. Dong, Z. M. Qian and Y. M. Liu, "Comparison of sulforaphane content in seeds of cruciferous plant." Chinese Pharmaceutical Journal, Vol. 39, NO. 12, 2004, pp. 898-899. (Chinese).

978-1-61896-030-6 © 2012 SciRes.

Correlation between Apoptosis and Protein p53 Induced by Cordyceps Militaris(Fr) Link Polycarbohydrate in Hepatocellular Carcinoma H22

Lixin GUO[1,2], Ruishu LIU[2], Min ZHAO[1]
[1]*Department of Microbiology, College of Life Science, Northeast Forestry University, Harbin, China*
[2]*Department of Biochemistry, Heilongjiang University of Chinese Medicine, Harbin, China*
Email: 82191513@163.com

Abstract: The aim of the study is to discuss the anti-tumor mechanism of CMPGF (Cordyceps militaris(Fr) Link polycarbohydrate GF), which can induce H22 cell (mice transplanted ascites hepatoma cell lines) apoptosis in vivo. We established H22 transplanted tumor model in mice and observed ultrastructural changes of H22 tumor tussues by electron microscope. Apoptosis changes and apoptotic cells were present in tumor tissue in the eary stage after H22 mice were treated with CMPGF. To study the promoting-apoptosis effect of CMPGF. Annexin Ⅴ FITC/PI double marking quantitative method was performed in the early stage of H22 cells. The apoptotic cell percentages of CMPGF low-dose group, medium-dose group and high-dose group were 5.08%, 9.77% and 5.17% respectively. Medium-dose group increased obviously. Because we were not sure whether the apoptosis was associated with the expression of p53, immunohistochemistry methods were used to detect p53 protein in tumor tissue treated with CMPGF. Immunohistochemistry analysis demonstrated the expression level of mutatant p53 decreased.

Keywords: Cordyceps militaris(Fr) Link polycarbohydrate; apopotosis; H22; p53

1 Introduction

The relationship of apoptosis and tumorigenesis is a hot research in recent years. The induced apoptosis can make cancer cells shrink or disappear, so it is an important and promising approach to try to induce tumor cells apoptosis to cure the tumors. Apoptosis has become a new outcome to assess the curative effect. Improving the ratio of tumor cell apoptosis and proliferation is a new requirement in clinical chemotherapy; apoptosis test is also a fast and effective screening method of anti-cancer drugs.

Cordyceps militaris(Fr) Link is one of medicinal caterpillar fungus. Its main medicinal ingredients include caterpillar fungus acid, caterpillar fungus element and caterpillar fungus polysaccharide. Cordyceps militaris （Fr） Link has some effect such as anti-fatigue; improve immunity and anti-cancer and so on [1].so it is a medicinal fungus of high medical and economic value. The effectiveness of its artificially propagated products more unveiled its broad developmenting prospect. It has become a serious problem to be solved to learn the role of specific active substances and their mechanisms. This study is designed to uncover the tumor cell apoptosis induced by CMPGF, cultured artificially Cordyceps militaris(Fr) Link extract in H22 mice. We hope further development and application experiment basis can be provided.

2 Materials and Method

2.1 Materials

Male Kunming mice used in present study, which body weight were 20 ± 2 gram were provided by the Experimental Animal Center of Heilongjiang University of Chinese Medicine, Production License: SCXK (Beijing No. 2007-0001) .Cordyceps militaris(Fr) Link were planted by the department of Microbiology of Northeast Forestry University. Cordyceps militaris(Fr) Link polysaccharide GF was extracted according to Sasak's method and identified by Molish's method.H22 tumor cell line was purchased from the Cancer Institute of Heilongjiang Province. Cyclophosphamide (sigma), Annexin Ⅴ (BD), PI (BD), buffer (BD). Flow cytometry FACScalibur (BD). Transmission electron microscopy T12 D 326(Philips).

2.2 Methods

2.2.1 Influence of CMPGF on the Ultrastructure of H22 Tumor Tissue Observed by Electron Microscope

Select 7-9d tumor strains growing well and take ascites sterilely. Dilute ascites with saline to 2×10^6 / ml, stain with 0.2% trypan blue and account the total number of viable cells which was more than 95%. 0.2ml ascites / each mouse was inoculated in the subcutaneous of the right forelimb axillary after disinfection. Then the inoculated mice were randomly divided into 5 groups: CMPGF low-dose group (25mg/kg), CMPGF medium-

dose group of (50mg/kg), CMPGF high-dose groups (100mg/kg), cyclophosphamide group and negative control group (equal volume saline), normal feeding. After 6h of inoculation, one times every day and continuous administration of 12d. observe the animal tumor growth until the tumors of negative control group up to over 1 g, after 24 h of the last administration, mice were sacrified by neck dislocation method and fixed in the supine position, disinfect the chest with 75% alcohol, dissect right axillary and get the tumors and wash them with cold saline, then blot with filter paper.

Take 3 copies of tumor tissues of each group, which were placed in petri dishes and put a small amount of fixative in dishes, cut the tissue size of $2mm^3$ and then the following procedure were performed: prefixed (3%glutaraldehyde) →washed (phosphorylation liquid) → postfixed (osmium tetroxide) → rinsed (distilled water) → acetone gradient dehydration (50%, 70%, 90%, 100%) → soaked (24 hours) → polymerization (24 hours) → embedded (embedding Agent 812 #) →semi-thin section → ultrathin sections →electron staining →observing ultrastructure of tumor cells by electron microscope half thin section-ultra-thin slices and electron microscope and dyeing ultrastructures of tumor cells.

2.2.2 Detecting of H22 Tumor Cell Apoptosis Effect in the Early Stage Induced by CMPGF by Annexin Ⅴ / PI Double Staining Quantificative Assay

Take each tumor tissue, prepare conventionally cell suspension liquid, wash 2 times with PBS and regulate cell concentration to 1 x 106 / ml, prepare three QC samples to set fluorescent compensation and cross-door range of flow cytometric analysis. No dyeing cells, and only use annexin V dyeing cells which were fluorescently labeled, with only the PI dyeing of cells. Following kit instructions, add FITC Annexin V and PI, analysize with computer. Each sample collected 10 000 cells.

2.2.3 The Influence of CMPGF on the Expression of p53

Take the tumor tissues of negative control group and CMPGF low, medium and high-dose group, by conventional fixed, paraffin-embedded sections of 5μm. routine dewaxing to water, immersed in 3% H2O2 and incubated for 10min at room temperature to eliminate endogenous peroxidase activity, washed with distilled water, PBS for 5 minutes, antigen Microwave repair ed with 0.lmol / L citrate buffer. Dropping closed normal goat serum at room temperature for 10-15 minutes, pour out, plus p53 antibody of 1:50 dilution and incubated overnight at 4 ℃, washed with PBS, 3 minutes × 3 times. Add biotin-labeled secondary antibody, incubated in 37 ℃ for 10-15 minutes. Washed with PBS again plus avidin labeled with horseradish enzyme, washed with PBS, dropping DAB staining, hematoxylin, conventional dehydration, mounted with neutral gum. And then use a series of conventional means testing.

The statistical treatment: Data use average said ±Standard deviation and compare between groups with t test mean.

3 Results

3.1 Influence of CMPGF on the Ultrastructure of H22 Tumor Tissue Observed by Electron Microscope

Electron microscopy showed the polygonal or diamond cells were present in negative control group. These cells have round nucleus, clear nucleolus, cytoplasm rich in organelles (Fig. 1A); most of the microvilli dropped out, necrotic cell debris can be seen and most of the nuclear heterochromatin marginate and aggregate in CMPGF low-dose group (Figure 1B); a large number of apoptotic cells or apoptotic disintegration of necrotic cells were fount in CMPGF medium-dose group showed (Fig. 1C); part of the nuclear fragmentation, cytoplasmic vacuoles of varying sizes and nuclear structure like apoptosis appeared in High-dose group(Fig. 1D); part of the collapsed and necrotic cells, the nuclear heterochromatin margination and blurred organelles were present in cyclophosphamide group.

3.2 Detecting of H22 Tumor Cell Apoptosis Effect in the Early Stage Induced by CMPGF by Annexin Ⅴ / PI Double Staining Quantificative Assay

Flow cytometry analysis showed that compared with negative control group, H22 tumor cell apoptosis was significantly increased in each CMPGF group. Apoptosis rate was 2.79% in negative control (Figure 2A), 5.08% in CMPGF low-dose group (Figure 2B), 9.77% in CMPGF medium-dose group (Figure 2C), 5.17% in high-dose group (Figure 2D), and2.74% in cyclophosphamide group (Figure 2E).

3.3 The Influence of CMPGF on the Expression of p53

It can be seen from Table 1 that the expression of mutant p53 protein was significantly down-regulated in H22 tumor tissues of CMPGF groups, compared with the negative control group ($P < 0.05$).

4 Discussion

Apoptosis is a cell autonomous process, genetically controlled and expressed as cell shrinking, nuclear

978-1-61896-030-6 © 2012 SciRes.

chromatin condensation, nuclear marginalization, membrane foaming, and formation of apoptotic bodies and so on. It is different from cell necrosis. Cell necrosis is non-autonomous process, loss of integrity of its membrane and chemical gradients, leakage of cytoplasm contents inducing the cell lysis and death [2] can be seen in cell necrosis. Qualitative detection of apoptosis depends on the morphological observation. in this study, electron microscopy analysis showed an initial presentation of apoptosis in CMPGF low-dose group, significant structural features of apoptosis in the medium and high-dose groups. All these indicated that CMPGF can induce apoptosis. Flow cytometry are required in the quantitative detection of apoptosis. In 1992, Fadok reported phospholipids phosphatidylserine (PS) in the inner membrane migrate to the outside of cells in the early stage of apoptosis [3]. In 1995, Vermes detected the apoptotic cells by phospholipids binding protein Annexin V, which have a high affinity for PS. Since PS also expose surface of necrotic cells to present the Annexin V-positive, PI (DNA dye) staining must be used at the same time to distinguish the necrotic cells. Annexin V/PI double-parameter method can distinguish apoptotic cells from normal cells and dead cells. It is the preferred method of quantitative apoptosis detection by flow cytometry at present [4-5]. Flow cytometry analysis showed that apoptosis rate was 2.79% in the negative control group, indicating that H22 tumor cells in mice have spontaneous apoptosis, apoptosis rate significantly increased in CMPGF low, medium and high-dose group, indicating that CMPGF can induce apoptosis and the medium-dose group was the best.

p53 gene is a apoptosis-related cancer suppressive gene, located in the nucleus, it is a phosphorus protein of molecular weight 53kD including 393 amino acids. p53 gene have two types, wild-type and mutant [6]. Wild-type p53 acts as "molecular policeman", monitoring the integrity of cell gene, it can prevent gene mutation cells which have a tendency to convert cancer cells by cell suicide through apoptosis induction. Wild-type p53 play a tumor suppressor role. When the p53 gene mutates, it lost the ability to monitor cell cycle and initiate apoptosis program, leaving the cell proliferation control, and is closely related to the development of many tumors [7-8]. Wild-type p53 protein expressed in normal cells has a very short half-life, its expression cannot usually be detected by immunohistochemistry; but the expression protein of mutant p53 gene, which is cancer-causing gene, has a longer half-life, so it can be detected by immunohistochemistry method [9]. In the present study, p53 protein in H22 tumor tissues were detected by immunohistochemistry, the results showed that mutant p53 protein expression of H22 tumor tissues were down-regulated in CMPGF low, medium and high-dose ($P < 0.05$).

All above showed that CMPGF can induce H22 tumor cells apoptosis, associated with down-regulate the expression of mutant p53. But further mechanisms need to be explored.

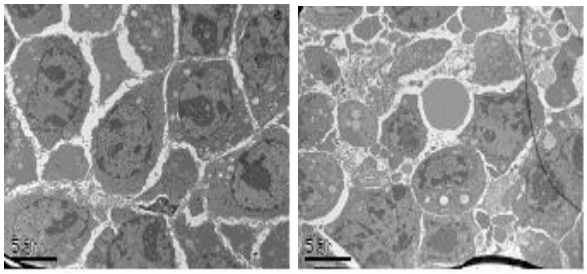

A. Negative control B. CMPGF low-dose group

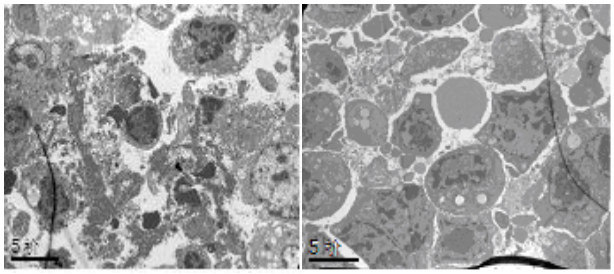

C. CMPGF medium-dose group D. CMPGF high-dose group

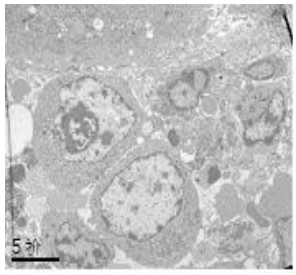

E. Cyclophosphamide group

Figure 1. Ultrastructure of tumor cells under different treated(×2550)

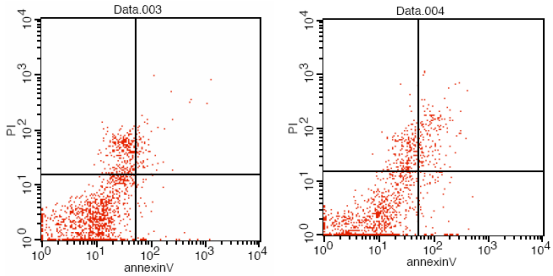

A. Negative control B. CMPGF low-dose group

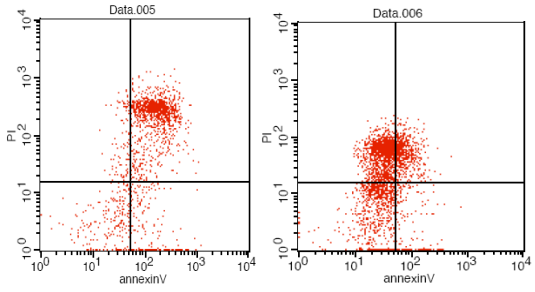

C. CMPGF medium-dose group D. CMPGF high-dose group

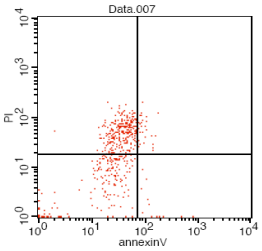

E. Cyclophosphamide group

Figure 2. H22 cell apoptosis induced by CMPGF detected by Annexin V /PI technique

Table 1. The influence of CMPGF on the expression of p53

Groups	mice numbers	p53 expression value	P value
Negative control	30	40.01±3.88	
Low-dose group	30	34.57±3.50	<0.05*
Medium-dose group	30	33.23±3.08	< 0.05*
High-dose group	30	33.90±3.46	< 0.05*

Note: * compared with negative control P<0.05.

References

[1] XL Jiang,BL Ge,XK Hu, "Cordyceps militaris. Drug-induced immune suppression of the antagonism,"*Journal of China Ocean University* , Vol. 32, No. 1, 2002, pp. 46-50.

[2] Y Hu, ZQ Liu, XY Shan, "Apoptosis Molecular Medicine," *Military Medical Sciences Press*, 2002, pp. 3-10.

[3] Fadok V A, Voelker D R, Campbell P A *et al* , " Exposure of phosphatidylserine on the surface of apoptotic lymphocytes triggers specific recognition and removal by macrophage," *J Immuol* , Vol. 148, No.7 , 1992 , pp. 2207-16.

[4] JN Zheng,SL Xie,JC Chen et al, "Comparison of 3 apoptosis methods by flow cytometry,"*Chinese Journal of Immunology*, Vol.15, No.10,1999, pp. 467-469.

[5] J Huang, YS Shen, HP Zhou, et al, " comparation of AnnexinV / PI,TdT and PI to detect cell apoptosis ," *Chinese Journal of Microbiology and Immunology*, Vol. 20, No. 4, 2000, pp. 387-388.

[6] S Li,JP SuMr.et al, "Tumor markers and p53 expression in cancer related research in progress," *Chinese General Practice*, Vol. 9, No. 11, 2006, pp.934-936.

[7] Chem P L, Chen Y, Brookstein R , et al, "Genetic mechanisms of tumor suppression by the human p53 gene," *Science*, Vol. 250, No. 4987, 1990, pp. 1576-1580.

[8] Baker SJ, Preisinger AC, "p53 gene mutations occur in combination with 17p allelic deletions as late events in colorectal tumorigenesis," *Cancer Res*, Vol. 50, No. 23, 1990, pp. 17-22.

[9] AM Ren, YY Hou, et al, "clinical and pathological features compared wild-type and mutant p53 in epithelial ovarian cancer," *Chinese Clinical Medicine*, Vol.16, No.2, 2009, pp.247-248.

978-1-61896-030-6 © 2012 SciRes.

Study on the Rivalry of Cordyceps Militaris Polycarbohydrate for the Micronucleus and Chromosome Aberration Induced by Cyclophosphamide

Lixin GUO[1,2], Shilong WANG[2], Yan QI[2], Min ZHAO[1]
[1]*Department of Microbiology, College of Life Science, Northeast Forestry University, Harbin, China*
[2]*Department of Biochemistry, Heilongjiang University of Chinese Medicine, Harbin, China*
Email: 82191513@163.com

Abstract: The study is to discuss the influence of *Cordyceps militaris (L.ex Fr) Link* polysaccharides GF(CMPGF) to the micronucleus formation rate of polychromatic erythrocyte (PCE) of bone marrow cells in mice and chromosome aberration rates induced by cyclophosphamide (CP), and to explore its anti-mutagenic effect. Micronucleus test and chromosome aberration test techniques were used in this study; we can get the results by microscopy and counting. The micronucleus inhibition rates were 29.75%, 36.20% and 44.48% respectively in MPGF low, medium and high-dose group. Inhibition rates were increased with the dose increasing. Compared with the cyclophosphamide group, each dose group were significantly different ($P < 0.05$); The aberration rates which were decreased with the dose increasing were 36.7 ± 5.46, 20.8 ± 3.52 and 18.1 ± 3.28 respectively in MPGF low, medium and high-dose group's CMPGF can reduce the micronucleus inhibition rates of PCE of bone marrow cells in mice and the aberration rates induced by CP, CMPGF have antimutagenic activity.

Keywords: Cordyceps militaris polycarbohydrate; micronucleus; chromosome aberration; cyclophosphamide

1 Introduction

Cordyceps militaris (L.ex Fr) Link and *cordyceps sinensis* belong to eumycota, Ascomycotina, pyrenomycetes, sphaeriales, claviticpitaceae and oedyceps[1]. It has some effect such as anti-fatigue; improve immunity and anti-cancer and so on [2]. Chinese medicine usually used to treat tuberculosis, the elderly chills, cough, weakness, anemia, maternal and elderly weakness, spontaneous sweating, waist and knee pain, weakness, coughing up blood, vomiting blood, etc. modern studies have shown that cordyceps has anti-tumor, anti-aging, and enhance Immunity and so on.

Mutation is the genetic variation of the genetic material of organisms (chromosome or gene). Modern research shows that many human healths-threaten diseases such as cancer, aging and certain degenerative diseases are associated with the occurrence of mutation effects. Reducing chromosome mutation rate of the body's normal cells and chromosomes by drugs with anti-mutant has far-reaching significance for the health of human life. This project examines the influence of CMPGF to micronucleus formation and chromosome aberration ratio of PCE in bone marrow cells of mice induced by cyclophosphamide to lay the foundation for further application.

2 Materials and Methods

2.1 Materials

Kunming mice used in present study, which body weight was 20 ± 2 gram and gender were half for males and half for females were provided by the Experimental Animal Center of Heilongjiang University of Chinese Medicine, Production License: SCXK (Beijing No. 2007-0001). Cordyceps militaris were planted by the department of Microbiology of Northeast Forestry University. CMPGF was extracted according to Sasak's method and identified by Molish's method. Cyclophosphamide (Batch number: K06R045) was produced by sigma. Biological microscopy (CHK-213) was produced by Olin Olympus Corporation of Japan.

2.2 Methods

2.2.1 Micronucleus Test of PCE

The mice were randomly divided into 5 groups: negative control group, CP group, CMPGF low-dose group, CMPGF medium-dose group and CMPGF high-dose group. The mice of negative control group and CP group received intramuscular injection with saline respectively on 1 ~ 10 days. The mice of CMPGF low, medium and high-dose groups were injected with CMPGF of 25 mg/kg, 50mg/kg and 100mg/kg respectively. The mice of CMPGF group and CP group received intraperitoneal injection of CP (CP 40mg/kg) on 9 and 10 days. The mice were killed by cervical dislocation 6h after injection on the 10th day. Get the double side of the femur, remove muscles with 75% ethanol soaked gauze, cut the femoral head, wash he bone

marrow cells with 3ml normal saline, centrifuged to 1000rpm/min for 5 minutes, discard the supernatant and make the slices regularly. Three slices were made in each mouse, then numbered, dried naturally, fixed with methanol, stain with 1:9 of Giemsa and observed by oil microscope. Count 1000 PCE of cell-integrity and distributed evenly, appropriately colored area in each slide by double-blind count. Record the micronucleus cells (MN) and calculate rate of micronuclei per thousand (MN ‰). Inhibition rate according to the following formula:

Inhibition rate (%) = [(the MN number of positive group-the MN number of experimental group)/the MN number of positive group] × 100%.

Data presented as mean ± standard deviation, mean comparison between groups using t test.

2.2.2 Chromosome Aberration Test of Mouse Bone Marrow Cells

Animal species, grouping, and pre-treatment were same with the micronucleus test, and finally, 2 h after the injection of CP, Colchicines (4ug/g) was injected intraperitoneally; the mice were killed by cervical dislocation 4h after the injection. Get the Bilateral of the femur, remove muscles with 75% ethanol soaked gauze, cut the femoral head, wash the bone marrow cells into centrifugal tubes with physiological saline sucked in syringe, wind and percuss with a straw evenly, centrifuge with 1000rpm/min for 8 minutes, discard the supernatant, add 9ml 0.075MKCL solution to the centrifuge tube, wind and percuss to cell suspension with a straw evenly, Treat it with hypotonic solution at 37℃for 30 minutes, fix, dry, stain with 1:9 of Giemsa for 8 minutes, observe by oil microscope. Count 100 metaphase cells of each animal which were well dispersed and colored clearly, record the number of chromosome structure abnormalities and abnormal cells. Each set of data as mean ± standard deviation, mean comparison between groups with t test.

3 Results

3.1 Influence of CMPGF to the PCE Micronucleus of Mice Bone Marrow Cells Induced by CP

3.1.1 The Cytological Features of PCE

Micronucleus were mostly single, round, smooth edges and tidy, caryochrome same as nuclear was blue-violet, the diameter was usually 1/20 ~ 1/5 under Oil immersion (Figure 1A). The micronucleated cells of PCE treated with CP, in one field of vision, cell micronucleus appear simultaneously in two Cells (Figure1B.1C).

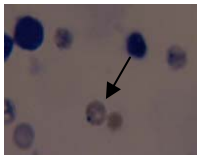

Figure 1A

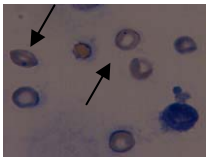

Figure 1B

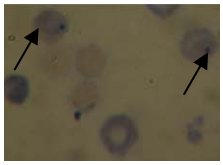

Figure 1C

Figure 1. Micronucleus map marrow

(Giemsa staining, ×100)

3.1.2 Influence of CMPGF to the Micronucleus Rate of PCE Induced by CP

The results of Table 1 showed that: CMPGF can reduce the bone marrow cell micronucleus rate induced by CP. Inhibition rates of micronuclei increased with the increasing doses in low, medium and high-dose groups, which were significantly different (P <0.05), compared with the CP group.

Table 1. Influence of CMPGF to the PCE micronucleus bone marrow cells induced by CP

Groups	PCE	micronucleus rate (‰)	Inhibition rate (%)
Negative control	1000	1.90±0.74	
CP group	1000	32.6±5.58	
Low-dose group	1000	22.9±3.93	29.75
Medium-dose group	1000	20.8±3.52	36.20
High-dose group	1000	18.1±3.28	44.48

3.2 Influence of CMPGF to the Chromosome Aberration of PCE Induced by CP

Chromosomal aberrations cytological features of bone marrow cells treated with CP were the fracture and partial deletion of chromosome.

The results of Table 2 showed that: CMPGF can reduce the rate of chromosomal aberrations induced by CP. The rate of chromosomal aberrations in CMPGF high-dose group was low. Compared with the CP group, CMPGF low, medium and high-dose groups were significantly different (P <0.05).

978-1-61896-030-6 © 2012 SciRes.

Table 2. Influence of CMPGF to the chromosome aberration of PCE induced by CP

Groups	Observed cell numbers	aberration rate (%)	P
Negative control	100	20.7 ±3.58	
CP group	100	43.5 ±6.17	
Low-dose group	100	36.7 ±5.46	<0.05
Medium-dose group	100	34.9 ±3.87	<0.05
High-dose group	100	28.5 ±4.53	<0.05

4 Discussion

Micronucleus formation is a genetic end point of cells by the genetic toxicology. Breaking of the chromosome and deferring to the late cell division or the destruction of chromosomes and spindle association of genetic damage can be detected by micronucleus test [3], the number of cells was observed by the number of micronuclei to determine the mitotic chromosome replication and whether these two processes is abnormal. Therefore, the micro-nuclear is often as an observation of whether there are indicators of mutagenicity induced by chemical substances. There has been a large number of applications in the genetic toxicity test of the foreign compounds (such as pharmaceuticals, food additives, pesticides, cosmetics, environmental pollution, etc.) and genetic damage detection of occupational exposure group and detection of Ecological Environment. Mammalian red blood cells in the ripening process can discharge the main nucleus and remain the micronuclei in the cell. Easy to identify, the results are stable and repeatable [3-4]. The study used the mouse bone marrow micronucleus test.

Analysis of bone marrow cell chromosome aberration test can observed chromosome aberration of intermitosis and prophase. It can reflect such as broken pieces cracks, circular chromosomes, polyploidy and other distortion results, and the results are reliable, able to reflect directly the level of incidence of bone marrow cell chromosome aberration and can judge whether the test substances have mutation effect [5].

Micronucleus test, chromosome aberration test are widely used in detection of chromosomal damage in the classic techniques, including the cellular level and chromosome level of detection range. Micronuclei and chromosomal aberrations exists a direct relationship, but not the same, Micronuclei can reflect the structure aberrations of part chromosome, this mainly refers to the instability of distortion; addition to fragments of chromosome aberrations in the micronucleus can be formed, the chromatic breaks, single or multiple Article lagging chromosomes can form micronuclei, and chromosome aberration test is more precise in form of chromosome damage observed in the genetic toxicology screening in the two detection methods are often used.

"Anti-mutant" and "mutation" are relative, according to the determination of relevant indicators of genetic toxicology; they can guide the anti-mutation screening material. Resistance mutation is to prevent gene mutations or chromosomal aberrations and other genetic material injury.

CP as a mutagen can induce the formation of micronuclei and chromosomal aberrations. In the use of mutagens, CMPGF were given to observe the anti-mutation effect at the same time. The micronucleus test in the present study showed that the micronucleus rate was 1.90 ‰ in negative control group, in a spontaneous mutation of the 1‰ ~ 3‰ range. three doses of CMPGF groups can significantly inhibit the micronucleus formation of PCE induced by CP and have significant differences compared with CP ($P<0.05$); chromo-some distortion analysis showed that three-dose CMPGF can reduce the chromosome aberration rates induced by CP and have significant differences compared with CP($P<0.05$). The results of the study suggest that CMPGF with anti-mutation effects can reduce the damage to the chromosomes, it can prevent genetic damage such as chromosomal aberrations have a very good effect, and there is a good prospect.

References

[1] Y Yu, JY An, JX Ma et al, "Cordyceps EPS extraction and purification,"Light Industry of Dalian Institute Jounal, Vol. 19, No. 4, 2000, pp. 268-270.

[2] XL Jiang, BL Ge, XK Hu, "Cordyceps militaris. Drug induced immune suppression of the antagonism," Journal of China Ocean University, Vol. 32, No. 1, 2002, pp.46-50.

[3] FT Tu,L Li, "Micronucleus formation mechanism," Modern Laboratory Medicine Jounal , Vol. 22 No. 4, 2007, pp. 19-22.

[4] Hosseinimehr SJ, Ahmadashrafi S, Naghshvar F, Ahmadi A, Ehasnalavi S, Tanha M, "Chemoprotective effects of Zataria multiflora against genotoxicity induced by cyclophosphamide in mice bone marrow cells," Integr Cancer Ther, Vol. 9, No. 2, 2010, pp. 219-223.

[5] SQ Liu,W Xiong,YM Du et al, "CMC bone marrow cell chromosome aberration tes," Toxicology Jounal, Vol. 22 , No. 1, 2008, pp. 70-71.

Review on Food Habits of Hepialidae Larvae

Mingchao LI[1], Meng YE[1], Zuji ZHOU[1], Yikai CHEN[1], Yong DAI[2]
[1]*College of Forestry, Sichuan Agricultural University, Sichuan, China*
[2]*Chengdu Enwei Group Company, Sichuan, China*
Email: dzlimingchao@163.com

Abstract: This review is focused on the research development in food habits of Hepialidae larvae, in which, the distribution of the Hepialidae insects, the common research methods on food habits of insects and the favourite plant species of Hepialidae larvae were discussed in detail.

Keywords: Hepialidae; larva; distribution; food habit

1 Introduction

Cordyceps sinensis, as one of the well-known medical herbs in China, is beneficial to lung and kidney. It is a combo of Hepialidae larvae and fungus, formed through parasitization of *Hirsutella sinensis* on the Hepialidae larva (Lepidoptera，Hepialidae) [1]. The parasite will soon be filled with all the mycelium and become stiff when the Hepialidae larvae have been infected, which lead to the death of the parasite at last. Spring to summer, the stroma of *Cordyceps sienesis* (Berkeley) Saccardo sprout from the head of the parasite in appropriate conditions, such as the temperature and humidity. In recent years, wild Cordyceps sinensis resources are decreasing while the demand for *Cordyceps sinensis* is increasing, which leads to the result that the yield of agrestal *Cordyceps sinensis* cannot meet the demand. Besides, plants which are enjoyed by the Hepialidae larvae have decreased sharply. Consequently, the conservation and artificial cultivation of *Cordyceps sinensis* become necessary choices. The cultivation of Hepialidae larvae is the base of the artificial cultivation of *Cordyceps sinensis*. Food habits research of Hepialidae Larvae has been researched for many years, and many results have been acheived.

2 The Distribution of the Hepialidae

The insects of Hepialidae belongs to Insecta, Lepidoptera, Hepialidae, which is mainly distributed in Sichuan, Yunnan, Gansu, Qinghai, Tibet and other provinces. Research has shown that 95% of the *Hepialidae* distribution areas are very narrow, and different species are usually distributed in different ranges, and sometimes there even are various species in different slopes and elevations in the same mountain [2].

The distribution center of the *Hepialidae* sp. is the area of latitude 27°~30°, longitude 95°~103°, which shows obviously zonal distribution, regional combination landscape and vertical distribution [3]. The Hepialidae is mainly distributed in the elevation of 3200~5100 m high plateau and high mountain gorge, and the most suitable elevation range for their growth is 3600~4800m[4]. The climate of these areas is the Tibetan Plateau climate, which character is low temperature, large temperature difference between day and night, no absolute frost-free period, long time frozen soil and sunny and strong ultraviolet light, modern glaciers in local area, various microclimates [5]. The soil most suitable for the growth of the Hepialidae is alpine meadow soil. Douxi Zhu [6] *et al.* discovered that fertile humus soil was suitable for the survival of the Hepialidae larva. And the soft black soil is formed by the dense rot roots with normal thickness of 20 cm ~ 30 cm. The distribution of plant communities in meadow significantly limits the distribution of the Hepialidae populations. Moreover, the plant seasonal aspect has a very close relationship with the populations and biomass of the Hepialidae [7].

The geographical distribution of the Hepialidae is controlled by integrated multiple ecological factors, such as food, vegetation, soil structure, temperature and humidity [4]. But the temperature, humidity, the content of soil salt and the soil pH are not major factors which influence the growth of the Hepialidae larvae, and biological factors (e.g. vegetation) may play a leading role [8].

Compared with the adult stage, the larval stage of the Hepialidae is very long, varying from 2 to 5 years [9]. Larvae live in the soil [9-10], they create tunnels about 20cm deep in the soil to the need of feeding and activity, and generally they live in (0)5~20(30) cm soil layer, but the active ones may concentrate in the scope of 10~15cm [5].

3 The Study Methods in Insects Food Habits

The option and utilization of food are necessary conditions to the growth of insect [11]. Insects play irreplaceable roles in nature and human life, they can meet the physical and spiritual needs of human. The exploitation of medicinal materials and feed, such as the Hepialidae and the *Tenebrio molitor*, the prevention of harmful in-

Fund project: The manuscript is subsidized by Chengdu Enwei Group Company.

978-1-61896-030-6

sects and the breeding of economic insects (e.g. silkworm), do need the study of insect food habit, which may contribute to the more efficient use of insects and bring greater social and economic benefits. Now the insects feeding habits are carefully researched in the food preference, the quantitative and qualitative analysis of food choice, food utilization, and so on [11]. Moreover, these elements are not isolated studied but studied together at one time to get the relationships between each other.

Direct observation and artificial breeding methods are often used in studying insects feeding habits [11-13]. Usually these two methods are combined closely in a research. Zhonggui Lin *et al*. [14] adopted both methods to study the feeding habit of Hylobitelus xiaoi Zhang and its hazard and prevention technology. They confirmed feeding site, type and style of Hylobitelus xiaoi Zhang, Yunbing Wang *et al*. [15] used these two methods to conclude that 58 insect species of the Scarabaeoidea were sorted to herbivorous, omnivorous and saprophagous insects. Qunfang Yang *et al.* [16] determined the food intake of grasshoppers using leaf area method and the proportion method, which can directly calculate the intake of certain insects except those living in the soil, feeding less, growing slowly, taking plants roots. However, Di Chen *et al*.[17] analyzed the stable carbon isotopic compositions of the Hepialidae larvae in Mountain Sejila on the Tibetan Plateau. And the local Hepialidae larvae were divided into plants roots feeding and humus substance feeding. The method can accurately track the diet composition of certain insects, which was suitable to study the feeding habit of insects, such as the Hepialidae larvae, but it cannot accurately figure out the ratio of every food composition in the total food intake. In order to get an appropriate proportion of food for the Hepialidae larvae, molecular identification of foregut contents, which can identify different kinds of food debris, has been applied in researches [10]. All methods above should be adopted at one time to analyze the natural food components of the Hepialidae larvae in quality and quantity.

Other researches come down to the effects that foods bring to the growth and propagation of insects. Junhong Zhu *et al.* [18] recorded and analyzed the growth cycle, pupae weight, livability of the Spodoptera litura feeding different foods, and identified the foods fitting the growth of Spodoptera litura. The flow of the research failed to get an appropriate food combination satisfying the basic growth of the Spodoptera litura Fab. and keeping them healthy and weight increase. Tapia D H[19] found the consanguineous relationship between food and the competitive exclusion of Myzus persicae. It can be concluded that individuals, populations, macro nutrition and micro chemical signals are the research direction for food utilization. Yikai Chen[20] detemined the nutritional components of the plants preferred by the Hepialidae larvae. It provided an idea that analysis system, such as the nutrition comparison of food-Hepialidae larvae-Cordyceps sinensis, can be established through similar methods, which may contribute to the industrial development and the generalize of artifical Cordyceps sinensis.

In summary, there are various research methods and burdensome complex content in studying insect feeding habits. When studying a certain insect feeding habits workable, effective methods should be chosen based on its characteristic and the research task.

4 The Plants that Hepialidae Larvae Feeding

Researches had been done on the feeding habits of Hepialidae larvae. From 1950 to 1961, Tailu Chen *et al*. firstly found the altitude distribution of *Cordyceps sinensis* and *Polygonum viviparom* were similar. In the following researches, they fed larvae the roots of *Polygonum viviparom* in room, and the larvae grew normally, which confirmed the opinion for the first time that Hepialidae larvae eat *Polygonum viviparom* [21]. In 1973, Tailu Chen [21] pointed out that the Hepialidae larva was a kind of phytophagous insect and could resist hunger for a long time while the imagos eat nothing.

Studies have shown that Hepialidae larvae eat many plants. Tab. 1 shows the plants known that preferred by the Hepialidae larvae [4, 6-7, 9].

Table 1. Plant list that Hepialidae larvae prefer to eat

Family	Genus	Species	Characters	Distribution
Polygonaceae	*Polygonum*	*Polygonum capitatum*	Rhizome hypertrophy	Jiangxi, Hunan, Hubei, Sichuan, Guizhou, Guangdong, Guangxi, Tibet. North India, Nepal, Sikkim, Bhutan, Myanmar and Vietnam
		Polygonum viviparum	Rhizome hypertrophy，rich in starch	Jilin, Inner Mongolia, Xinjiang, Shaanxi, Gansu, Qinghai, Sichuan, Tibet, Korea, Japan, Mongolia, India, Europe and North America, in alpine humid grassland
		Polygonum macrophyllum	Rhizome hypertrophy	Yunnan, Guizhou, Sichuan, Qinghai, Gansu, Shaanxi, Tibet; India. In alpine grasslands, altitudes 3000-5000m

Continued

Family	Genus	Species	Characters	Distribution
		Polygonum angusstifolium	Perennial herb	Distributed in eastern Siberia, Mongolia, China (Inner Mongolia).
		Polygonum glaciale	Small annual herb	Hebei, Shanxi, Gansu, Qinghai, Sichuan, Yunnan, Tibet.
		Polygonum orientale	Annual herb, 2-3 m	In whole China; Korea, Japan, the Philippines, India, Australia, Russia. in the village street and the waterfront edge of the wetland.
	Rheum	*Rheum pumilum*	Small perennial grass, 10-20 cm high	Distributed in Tibet and Qinghai.
	Oxyria	*Oxyria digyna*	Perennial herb, 15-30 cm high	Jilin, Shaanxi, Qinghai, Sichuan, Yunnan, Tibet; Korea, Japan, Mongolia, Europe and North America. in the valley slopes or mountain regions.
	Rumex	*Rumex acetosa*	Perennial herb, 30-80 cm high	Jilin, Liaoning, Hebei, Shaanxi, Xinjiang, Jiangsu, Zhejiang, Hubei, Sichuan and Yunnan; northern and eastern Asia, Europe and America, in the humidity fertile mountains.
		Rumex madaio	Perennial herb, about 1 m high. Root hypertrophy and large, yellow.	Sichuan, Guizhou, Jiangsu, Fujian, Hunan.
Rosaceae	*Potentilla*	*Potentilla anserina*	Roots fleshy, fusiform	Northeast, North, Northwest, Southwest; other parts of the world's temperate there. In the valley or wet meadow.
		Potentilla fruticosa	Deciduous shrub, 1.5m high	Liaoning, north, northwest, Sichuan, Yunnan; Japan, Mongolia, Russia, Siberia, Europe, North America, too. In High Peak thickets.
	Malus	*Malus pumila*	Arbor,15m high	Liaoning, Hebei, Shanxi, Shandong, Shaanxi, Gansu, Sichuan, Yunnan
Gentianaceae	*Gentiana*	*Gentiana macrophylla*	Perennial herb, 20-60 cm high, thick taproot, long and conical	Heilongjiang, Inner Mongolia, Hebei, Shanxi, Shaanxi, Ningxia, Gansu, Qinghai, Sichuan and northwest; Russia, Mongolia, in the mountains 2000-3000m altitude grassland or forest edge.
		Gentiana algida	Perennial herb, 15-25 cm high, fibrous roots	Jilin, Gansu, Xinjiang, Sichuan; Russia.
Umbelliferae	*Daucus*	*Daucus carota Linn. var. sativa Hoffm.*	Roots fleshy, long conical, fleshy, yellow or red	Usually planted everywhere.
	Ligusticum	*Ligusticum scapiforme*	Perennial herb, 5-25 cm high	Sichuan, Yunnan, near the hillside turf.
Gramineae	*Hordeum*	*Hordeum vulgare Linn. var. nudum Hook.f.*	Whisker roots	Tibet, Qinghai, Sichuan Yunnan, Gansu elevation 4200-4500 m.
		Hordeum vulgare	Annual grass, whisker roots	Yangtze River, Yellow River and Qinghai-Tibet Plateau.
	Festuca	*Festuca ovina*	No rhizome	Distributed in the temperate regions of Eurasia and North America, China's northwest and southwest
	Deyeuxia	*Deyeuxia arundinacea*	Perennial herb	Distributed in southwest, central, east, north, northeast, northwest in China.
	Poa	*Poa crymophila*	Perennial herbs, whisker roots, with a sand cover, with rhizomes, tillering ability	Mainly distributed in Qinghai, Gansu, Tibet, Sichuan, Xinjiang; India.
Solanaceae	*Solanum*	*Solanum tuberosum*	Herbal high 0.3-1m, massive rhizome, flat rounded spherical or moment	Widely planted in temperate regions around the world.
Liliaceae	*Polygonatum*	*Polygonatum sibiricum*	Perennial herbs. Roots will occur, mast fleshy, yellow-white, slightly flat, circle	Hebei, Inner Mongolia, Shaanxi, Guizhou, Hunan, Yunnan, Anhui, Zhejiang Guangxi.
Compositae	*Pyrethrum*	*Pyrethrum tatsienense*	Perennial herb, 7-25 cm high	Sichuan, Yunnan, in alpine meadow.
	Saussurea	*Saussurea pinnatidentata*	Perennial herb, 25-80cm high, fusiform root	Inner Mongolia, Gansu, Qinghai. In natural meadow, saline and farm, elevation 2200-3200m.
		Saussurea laniceps	Perennial herb, 15-30 cm high, thick rhizomes	Southwestern Sichuan, northwestern Yunnan and eastern Tibet.
	Artemisia	*Artemisia annua*	Perennial herb	All over in China.
Juncaginaceae	*Triglochin*	*Triglochin maritimum*	Perennial herb of wet	Distributed in northeast, north, northwest, southwest provinces in China; also widely distributed in the north temperate zone and the north frigid zone.

978-1-61896-030-6

Continued

Family	Genus	Species	Characters	Distribution
Ranunculaceae	*Caltha*	*Caltha scaposa*	Perennial herb, 10-15 cm high	Southern and eastern Tibet, northwest Yunnan, western Sichuan, southern Qinghai, southern Gansu; Nepal, India, in elevation 2800-4100m in the wet meadow or valley.
	Oxygraphis	*Oxygraphis glacialis*	Perennial grass, 2-9cm high. Rhizome roots short, , slender	Tibet, northern Yunnan, western Sichuan, southern Shaanxi, Gansu, Qinghai and Xinjiang; Central Asia, Russia, Siberia, Mongolia in 3000-4800m altitude alpine meadow.
	Ranunculus	*Ranunculus tanguticus*	Perennial herbs. Thin roots, the upper part slightly swollen.	Distributed in Shanxi, Shaanxi, Gansu, Qinghai, Sichuan, Yunnan, Tibet provinces; Nepal, India.
	Paeonia	*Paeonia lactiflora*	Perennial herb, 60-80 cm high	Gansu, Shaanxi, Shanxi, Hebei, Northeast Inner Mongolia and; Mongolia, Russia, Siberia.
	Thalictrum	*Thalictrum alpinum*	Perennial herb	Tibet and Xinjiang; in 2500-4750m altitude meadow or marsh grass slopes.
Caryophyllaceae	*Arenaria*	*Arenaria bryophylla*	Cushion-like perennial herb. Roots thick, lignified	In elevation of 4200-5400 meters alpine meadow and alpine rubble. Distributed in Tibet and Qinghai. Kashmir, Nepal, Sikkim.
		Arenaria lancangensis	Cushion-like perennial herb. Roots, 4-11 cm high	In northwestern Yunnan, western Sichuan, southeastern southeast Qinghai, southeast Tibet, in alpine meadow of elevation 3500-4800m.
Primulaceae	*Primula*	*Primula pinnatifida*	Perennial herb	Northwestern Sichuan, Yunnan, southeastern Tibet.
Cyperaceae	*Carex*	*Carex schneideri*	Perennial herb, rhizome clusters	Sichuan, Yunnan, Tibet.
		Carex atrofusca	Perennial herb, 15-30 cm high, sparse clusters, rhizome with short stolons.	Distributed in Gansu, Qinghai, Sichuan, Yunnan, Tibet.
	Kobresia	*Kobresia pygmaea*	Cushion-like herb	Distributed in Inner Mongolia, Hebei, Shanxi, Gansu, Qinghai alpine meadow and alpine shrub meadow, altitude 3200-5400m.
		Kobresia humilis	Short rhizome	Xinjiang, in sunny slopes of subalpine meadow at an elevation of 2500-3000m.
Campanulaceae	*Codonopsis*	*Codonopsis lanceolata*	Trailing perennial herb	Mainly in the Northeast of China.
Leguminosae	*Astragalus*	*Astragalus yunnanensis*	Perennial herbs, thick taproot.	Distributed in Sichuan and Yunnan. In slopes or grassland of elevation 3000-4300m
		Astragalus balfourianus	Perennial herb	Distributed in Sichuan, Yunnan, growing in altitude of 2,650-4,000m.
		Astragalus frigiolus	Perennial herb, 20-60cmhigh, erect stem.	In North America, Pakistan, Central Europe, Russia, India and Sichuan, Yunnan, Xinjiang in china, growing in altitude of 2,000m.
		Astragalus levitubus	Perennial herb	Western Sichuan and northwestern Yunnan. In elevation of 4,000m.
		Astragalus floridus	Perennial herb Roots stout, Straight.	Gansu, Qinghai, Sichuan and Tibet. In the elevation of 2600-4300m.
		Astragalus xiaojinensis	Perennial herb,40cm high	In northern Sichuan. In elevation of 3500m on the slopes.
		Astragalus tongolensis	Perennial herb Roots stout, Straight.	In Sichuan. In the hillside above 3000m altitude.
		Astragalus ernestii	Perennial herb Roots stout.	Western Sichuan, northwestern Yunnan and eastern Tibet. In 3900-4500m altitude.
Convolvulaceae	*Convolvulaceae*	*Ipomoea batatas*	Herbaceous perennial vine, white, red or yellow root.	Planted widely in China.
Salicaceae	*Salix*	*Salix lindleyana*	Cushion-like shrubs, prostrate trunk and rooting.	Tibet and northwestern Yunnan, in 4000m altitude
Ericaceae	*Rhododendron*	*Rhododendron amesiae*	Shrub, 2-4 m high	western Sichuan, altitude 2200-3000 m.
		Rhododendron capitatum	Evergreen shrub, about 1m high	Qinghai, Gansu, altitude 2500-3600m.
		Rhododendron przewalskii	Evergreen shrub, near 3m high	Qinghai, Gansu, Shaanxi, Sichuan, altitude 4000m.
		Rhododendron anthopogonoides	Evergreen shrub, 1-3m high	Gansu, Qinghai and Sichuan, altitude 2900-3700m.
		Rhododendron keysii	Evergreen shrub, about 4m high	Southern Tibet, Bhutan. Altitude 2800-4500m.
		Rhododendron microgynum	Shrub, 0.6-1.6 m high	Northwestern Yunnan and southeastern Tibet, altitude 3350-4250m.
		Rhododendron chamaethomsonii	Erect shurb,15-90cm high	Northwestern Yunnan and southeastern Tibet, altitude 4200-4500m.

Continued

Family	Genus	Species	Characters	Distribution
		Rhododendron pumilum	Small evergreen shrub, about 20 cm high.	Southwest Yunnan, southern Tibet, Sikkim, Myanmar, altitude 4000m around.

Explanation: Characteristics and distribution of plant in the table are neatened according to Flora of China and Atlas of higher plants in China.

Plants Hepialidae larvae prefer are distributed in 33 Genera of 18 Families, most of which are distributed in altiplano area, such as Sichuan, Yunnan, Qinghai and Tibet, which shows an identical distribution with the distribution of Hepialidae larvae. As we can see from the table, most plants are Perennial herb with fleshy roots or rhizome. Researches had shown that plants in Polygonaceae, Leguminosae, Cyperaceae, Gramineae, Ranunculaceae are Hepialidae larvae's favorite food[28], of which plants in *Polygonum* (*Polygonum viviparum*, *Polygonum macrophyllum*), *Rheum(Rheum pumilum)*, *Astragalus* are often firstly be chosen to feed the larvae. Other plants such as carrots, apples and potatoes are also the food Hepialidae larvae prefer to take. Food with *Rheum pumilum* showed an obvious increase in avoirdupois to the antitheses without *Rheum pumilum* [24]. Carrots can be used to be the food feeding the Hepialidae larvae, while potatoes are not appropriate as they rot and go moldy easily [25]. The Hepialidae larvae usually take the fresh and tender roots growing in current year [29]. Under artificial conditions, plants are easier to be chosen than in nature [30]. It had been reported that the Hepialidae larvae feed every few days [25], they had an ability of anti-hunger and took the soil humus in hunger [28].

Fei Liu *et al.* [31] detected the nutrition of different *Polygonum viviparum* from Sichuan and Chongqing and showed that the ash and total sugar contents of *Polygonum viviparum* in Chongqing were significantly higher than those in Sichuan, and the contents of K elements in Chongqing Polygonum roots were significantly higher than that in Sichuan Polygonum root, and Mg, Fe, and Mn elements were significantly lower than those in Sichuan Polygonum roots.

5 Discussion

Up to date, 63 kinds of Hepialidae have been found in China[8, 21, 32-47], and 10 of which have been researched on biological characteristics. The ten Hepialidae are *Hepialus armoricanus*[21], *H. menyuanicus*[28, 40], *H. yushuensis*[40], *H. gonggaensis* [48], *H. obliforcus*, *H. baimaensis*[39], *H. renzhiensis*, *H. deqinensis*, *H. altaicola* and *H. jianchuanensis*[51]. There are various biological characteristics in different Hepialidae, and deeper and wider researches are needed.

Hepialidae feed only at larval stage, and larvae make tunnel in the soil living in caves, which is not conducive for observational study[10]. Therefore, strict control of temperature and humidity are required when using soilless culture, and isolated breeding is also important as the larvae often attack each other when they encounter. Accordingly, one of the key factors to reveal the Hepialidae larvae feeding habits is the designing of research methods.

Although researches on the feeding habits of Hepialidae larvae have made great progress, the order of plants taken by Hepialidae larvae is not clear, and the feeding habits of larvae in different ages have not been identified respectively, and no results show the effect of different organs of plant material on the larvae. The Hepialidae larvae take many kinds of plants, most of which are wild plants with limited production, so that the development of artificial food is hot.

References

[1] Directed by National Pharmacopoeia Committee. the Chinese Pharmacopoeia (Part I) [M]. Beijing: Chemical Industry Press, 2005.

[2] Darong Yang, Chaoda Li, Chang Shu,et.al. STUDIES ON THE CHINESE SPECIES OF THE GENUS HEPIALIDAE AND THEIR GEOGRAPHICAL DISTRIBUTION[J]. ACTA ENTOMOLOGICA SINICA, 1996, 39(4): 413-422.

[3] Tianfu Huang, Shijiang Chen, Shanquan Fu, et.al. Studies on ecological types of the insects infected by Kangding Cordyceps sinensis fungus[J]. SHIZHEN JOURNAL OF TRADITIONAL CHINESE MEDICINE RESEARCH, 1996, 7(3): 178-179.

[4] Shijiang Chen, Shiyong Jin. Overview on host of domestic Cordyceps [J]. SHIZHEN JOURNAL OF TRADITIONAL CHINESE MEDICINE RESEARCH, 1992, 3(1): 37-39.

[5] Quansen Li, Zhengquan Cao. Elcoligical investigate in Cordyceps sinensis[J]. Journal of Chinese Medicinal Materials, 1990, 13(4): 3-7.

[6] Douxi Zhu, Ronghua He, Yang Wang, et.al. Study on ecological characteristic of Hepialidae in Tibet [J]. Edible Fungi of China, 2007, 26(2): 10-11.

[7] Darong Yang, Zhaoda Li, Chang Shu,et.al. RELATIONSHIP BETWEEN ALPINE MEADOW VEGETATION AND HEPIALIDAE MOTHS DISTRIBUTION [J]. Southwest China Journal of Agricultural Sciences, 1992, 5(2): 68-73.

[8] Xingcai Liang, Darong Yang, Farong Shen, et.al. FOUR NEW SPECIES OF THE GENUS HEPIAWS (GHOST MOTH) FROM YUNNAN, CHINA [J]. Zoological Research, 1988, 9(4): 419-425.

[9] Liping Liu, Qixin Long, Changqing Zhou. THE HOST INSECT OF THE CORDYCEPS SINENSIS FUNGUS-HEPIALIDS [J]. Natural Enemies of Insects, 1995, 17(4): 184-190.

[10] Hai Chen. Study on the Feeding Habits of Hepialidae pui [D]. Guang Zhou: Zhongshan university, 2009: 84.

[11] Lin Yan, Jinghua Lan. Feed Selection and Utilization of Grassland Caterpillar in the Field Cage Condition [J]. Acta Agrestia Sinica. 1995, 3(4): 257-268.

[12] Dejun Qin. HOST SPECIFICITY AND NUTRITION OF PHYTOPHAGOUS INSECTS [J]. Acta Entomologica Sinica. 1962, 11(2): 169-185.

[13] Xiulian Wan, Weiguo Zhang. Feeding Habit and Spatial Pattern of Gynaephora Alpherakii Larvae [J]. Acta Agrestia Sinica. 2006,

978-1-61896-030-6 © 2012 SciRes.

14(1): 84-88.
[14] Zhong Guilin, Yulan Lei, Zhenbao Peng, et al. Feeding habits,damage characters and control techniques of the larvae of Hylobitelus xiaoi [J]. FOREST PEST AND DISEASE. 2004, 23(1): 9-12.
[15] Yunbing Wang, Zhongyin Zhang, Xiaowa Xu, et al. Feeding Habits of Scarabaedidea [J]. Hubei Agricultural Sciences. 2007, 46(6): 928-930.
[16] Qunfang Yang, Zhichang Liao, Qing Li, et al. Feeding habits and economic threshold of Locusta migratoria tibetensis [J]. Acta Phytophylacica Sinica. 2008, 35(5): 399-403.
[17] Di, C., JianPing, Y., ShiPing, X.,et.al.Stable carbon isotope evidence for tracing the diet of the host Hepialidae larva of Cordyceps sinensis in the Tibetan Plateau[J]. Science in China Series D: Earth Sciences, 2009, 52(5): 655-659.
[18] Junhong Zhu, Fangping Zhang, Honggang Ren. Development and nutrition of Prodenia litura on four food plants [J]. Entomological Knowledge. 2005, 42(6): 643-646.
[19] Tapia D H, Troncoso A J, Vargas R R, et al. Experimental evidence for competitive exclusion of Myzus persicae nicotianae[J]. Eur. J. Entomol., 105: 643-648.
[20] Yikai Chen, Meng Ye, Mingchao Li, Li Xiang. Determination and Analysis of Nutritional Components in Rhizome (Tuber) of Three Host Plants of Hepialidae Larva. PROCEEDINGS OF 2010 INTERNATIONAL CONFERENCE OF NATURAL PRODUCT AND TRADITIONAL MEDICINE, Xi'an: Scientific and Technical Development Press, 2010:551-553.
[21] Tailu Chen, Jiajun Tang, Jinlong Mao. A PRELIMINARY STUDY ON THE BIOLOGY OF THE "INSECT HERB", HEPIALIDAE ARMORICANUS OBERTHUR [J]. Acta Entomologica Sinica, 1973, 16(2): 198.
[22] Zhong Wang, Qilong Ma, Zhengqiang Qiao, et.al. Artificial Feeding Techniques of the Host Hepialidae minyuancus of Cordyceps sinensis(Berkeley)Saccrdo in Gansu Province[J] . Gansu Agricultural Science and Technology, 2001, (7): 42-43.
[23] Hongsheng Wang. Preliminary Study on Artificial Feeding of the Host Hepialidae of Cordyceps in Fifth Instar Larvae [J]. Gansu Animal and Veterinary Sciences, 2001, 31(5): 15-16.
[24] Hongsheng Wang. The preliminary study on artificial rearing Hepialidae spp. [J]. Entomological Knowledge, 2002, 39(2): 144-146.
[25] Nanying Shen, Lu Zeng, Xianchi Zhang. Study on the Feeding Habit of the Hepialidae larva [J]. Special Wild Economic Animal and Plant Research, 1983, (3): 19-20.
[26] Qilong Ma, Zhong Wang, Fuquan Ma. Study on the Biological Characteristic of the Host Hepialidae of Cordyceps in Gansu [J]. GANSU AGRICULTURAL SCIENCE AND TESHNOLOGY, 1995, (12): 36-37.
[27] Tianfu Huang, Shanquan Fu, Qingming Luo. Experiments on Feeding Habit of Hepialidae armoricanus Larvae in Kangding [J]. Sichuan Journal of Zoology, 1989, 8(3): 8-10.
[28] Fei Liu, Deli Zhang, Wei Zeng, et.al. Studies on the Biological Characters of the First Breed of Hepialidae gonggaensis [J]. Lishizhen Medicine and Materia Medica Research, 2010, 21(11): 2978-2980.
[29] Farong Shen, Drong Yang, Yuexiong Yang, et.al. Observe on the Feeding Habit of H. baimaensis Liang Larvae [J]. Entomological Knowledge, 1990, 27(1): 36-37.
[30] Darong Yang, Yongcheng Long, Farong Shen, et.al. RESEARCH ON THE ECOLOGY OF YUNNAN HEPIALIDS —— Ⅰ.REGIONAL AND ECOGEOGRAPHICAL DISTRIB TION [J]. Zoological Research, 1987, 8(1): 1-11.
[31] Fei Liu, Xiaoli Wu, Min Qian, et.al. Analysis Comparative of Nutritional Components in Rhizoma of Polygonum viviparum L. Main Food of Insect of Cordyceps sinensis(Berk.)Sacc [J]. Special Wild Economic Animal and Plant Research, 2007, (4): 52-55.
[32] Hongfu Zhu, Linyao Wang, Hongxiang Han. Fauna Sinica (Insecta Lepidoptera thirty-eighth volume Lepidoptera Hepialidae Epiplemidae) [M]. Beijing: Science Press, 2004.
[33] Guren Zhang, Dexiang Gu, Xin Liu. A NEW SPECIES OF HEPIALIDAE (LEPIDOPTERA,HEPIALIDAE) FROM CHINA [J]. Acta Zootaxonomica Sinica, 2007, 32(2): 473-476.
[34] Darong Yang, Yuexiong Yang, Sanyuan Zhang. THREE NEW SPECIES OF THE GENUS HEPIALIDAE FROM QINGHAI AND GANSU, CHINA (LEPIDOPTERA: HEPIALIDAE) [J]. ACTA ENTOMOLOGICA SINICA, 1995, 38(3): 359-362.
[35] Darong Yang, Farong Shen, Yuexiong Yang, et.al. BIOLOGICAL STUDIES AND NOTES ON A NEW SPECIES OF THE GENUS HEPIALIDAE FROM YUNNAN, CHINA [J]. Acta Entomologica Sinica, 1991, 34(2): 218-224.
[36] Darong Yang, Zhaoda Li, Farong Shen. THREE NEW SPECIES OF THE GENUS HepidusFROM YUNNAN AND XIZANG, CHINA(LEPIDOPTERA. HEPIALIDAE) [J]. Zoological Research, 1992, 13(3): 245-250.
[37] Darong Yang, Changping Jiang. TWO NEW SPECIES OF THE GENUS HEPIALIDAE (LEPIDOPTERA: HEPIALIDAE) FROM NORTH XIZANG, CHINA [J]. ENTOMOTAXO-NOMIA, 1995, 17(3): 215-218.
[38] Darong Yang. FOUR NEW SPECIES OF THE GENUS Hepialidae FROM YUNNAN AND XIZANG, CHINA (Lepidoptera: Hepialidae) [J]. Zoological Research, 1994, 15(3): 5-11.
[39] Darong Yang. TWO NEW SPECIES OF THE GENUS HEPIALIDAE FROM YUNNAN, CHINA (LEPIDOPTERA: HEPIALIDAE) [J]. Acta Zootaxonomica Sinica, 1993, 18(2): 184-187.
[40] Zhong Wang, Qilong Ma, Fuquan Ma, et.al. Biological Property of Insect Host Hepialidae minyuancus of Cordyceps sinensis(Berkeley)Saccrdo [J]. Gansu Agricultural Science and Technology, 2001, (7): 38-39.
[41] Yongqin Tu, Kaisen Ma, Deli Zhang. A New Species of the Genus Hepialidae (Lepidoptera: Hepialidae) from China [J]. Entomotaxonomia, 2009, 31(2): 123-126.
[42] Farong Shen, Yousheng Zhou. TWO NEW SPECIES OF THE GENUS HEPIALIDAE FROM YUNNAN, CHINA (LEPI-DOPTERA: HEPIALIDAE) [J]. ACTA ENTOMOLOGICA SINICA, 1997, 40(2): 198-201.
[43] Fei Liu, Xiaoli Wu, Dinghua Yin, et.al. Overview on Species and Distribution of Host Insects of Cordyceps sinensis [J]. Chongqing Journal of Research on Chinese Drugs and Herbs, 2006, (1): 47-50.
[44] Xingcai Liang. FOUR NEW SPECIES OF THE GENUS Hepialidae (GHOST MOTH)FROM YUNNAN, SICHUAN OF CHINA(Lepidoptera: Hepialidae) [J]. Zoological Research, 1995, 16(3): 207-212.
[45] Zhaoda Li, Darong Yang, Farong Shen. A NEW SPECIES OF THE GENUS HEPIALIDAE FROM YUNNAN, CHINA (LEPIDOPTERA:HEPIALIDAE) [J]. Acta Entomologica Sinica, 1993, 36(4): 495-496.
[46] Shanquan Fu, Tianfu Huang, Qingming Luo. A NEW SPECIES OF HEPIALIDAE (LEPIDOPTERA: HEPIALIDAE) [J]. Acta Entomologica Sinica, 1991, 34(3): 362-363.
[47] Shanquan Fu, Tianfu Huang, Qingming Shijiang Chen, et.al. A new species of Hepialidae (Lepidoptera:Hepialidae) [J]. Acta Entomologica Sinica, 2002, 45: 56-57.
[48] Tianfu Huang, Shanquan Fu, Qingming Luo. BIONOMICS OF HEPIALIDAE GONGGAENSIS FROM KANDING [J]. Acta Entomologica Sinica, 1992, 35(2): 250-253.
[49] Darong Yang, Zhaoda Li, Farong Shen, et.al. STUDIY ON THE REPRODUCTIVE BEHAVIOR OF Hepialidae baimaensis LIANG [J]. Zoological Research, 1991, 12(4): 361-366.
[50] Heng Zhao, Xinlan Qu, Jihai Huang. Observe on reproductive law of Altai Hepialidae [J]. XINJIANG AGRICULTURAL SCIENCES, 1998, (4): 181-183.
[51] Fei Liu, Xiaoli Wu, Deli Zhang, et.al. Study on biological character of Hepialidae introduced from Yunnan province [J]. China Journal of Chinese Materia Medica, 2009, 34(4): 379-381.

Analysis of Global Genomic DNA Methylation Levels of Wheat-Rye Translocations Lines by HPLC

Shuangrong LI, Yong ZHANG, Kejun DENG, Meize DU, Yu LIU, Zhenglong REN
School of Life Sciences and Technology, University of Electronic Science and Technology of China, Chengdu, China, 610054
Email: zhangyong916@uestc.edu.cn

Abstract: Introduction of alien germplasm from different species into crop plants is commonly used in wide hybridization-based plant breeding programs. Alien introduction may cause the frequent observation of novel traits in hybridization-derived offspring. The origin of novel traits in the derived hybrid progenies may be explained, in part, by structural changes of chromosomes and perturbation of epigenetic state of the recipient genome (e.g., DNA methylation patterns). Therefore, it is necessary to analyze the levels and patterns of genomes DNA methylation when study the hybrid progenies. This paper presented a sensitive and reproducible method for determining global genomic DNA methylation (GDM) alterations using high-performance liquid chromatography (HPLC). All results of injection precision, stability, repeatability and recovery test indicate that this method was adequate, valid and applicable. Furthermore, thirteen wheat-rye translocation lines were analyzed to obtain their global genomic DNA methylation (GDM) changes using this method, respectively in shoot and root samples. The results showed that DNA methylation levels were diverse among these cultivars. Meanwhile, the GDM levels showed significantly differences between different tissues, shoots and roots, of same cultivar. These results demonstrated that this developed method was feasible for quality evaluation of global genomic DNA methylation (GDM) for wheat (*Triticum aestivum L*) and its derived hybrid progenies, even could be applied to its close relatives. It is meaningful for further studies of interspecific hybridization and crop breeding programs.

Keywords: Wheat-Rye translocations lines; HPLC; global genomic DNA methylation (GDM)

1 Introduction

Introduction of superior alien germplasm from different species to crop plants is an important and efficient way for the improvement of crop breeding because of the origin of many adaptive traits. Lots of studies have focused on genetic and epigenetic changes caused by hybridization to explore the underlying mechanism for the origin of novel traits in the derived hybrid progenies [1, 2].

DNA methylation, the addition of a methyl group to a cytosine base, is one of epigenetic modifications. It is evolutionarily ancient and plays essential roles in multiple cellular activities, including maintenance of genomic integrity, formation and perpetuation of heterochromatin, controlling of gene expression and genomic imprinting [3]. In plants, DNA methylation commonly occurs at cytosine bases within all sequence contexts: the symmetric CG and CHG contexts (where H=A, T, or C) and the asymmetric CHH context. DNA methylation in plants predominantly occurs on transposons and other repetitive DNA elements [4]. In plants, de novo methylation is catalyzed by DOMAINS REARRANGED METHYLTRANSFERASE 2 (DRM2) and maintained by three different pathways: CG methylation by DNA METHYLTRANSFERASE 1 (MET1), CHG methylation by CHROMOMETHYLASE (CMT3) and asymmetric CHH methylation through persistent de novo methylation by DRM2 [5].

Patterns of DNA methylation can be analyzed in total DNA, site-specific DNA sequences, or in sequences that undergo rapid changes in methylation status. The quantification of total DNA methylation is useful for determining global genomic changes that site-specific sequence techniques may not detect. While this approach does not differentiate between coding and non-coding sequences of DNA, nor detect subtle differences in the methylation status of individual genes, it is an appropriate technique for assessing the larger-scale epigenetic effects of hybridization, stress and acclimation responses in plants [6]. High-performance liquid chromatography (HPLC) is considered the most reliable and sensitive technique to determine total DNA methylation [7]. HPLC analysis can also resolve and detect modified bases other than 5-methylcytosine that may have biological significance. The procedure for HPLC analysis of DNA from plants was first reported by Wagner and Capesius [8]. Methods were also established for mammalian and microbial DNA by Kuo et al. and Gehrke et al. [9], which have since formed the basis of HPLC analysis of DNA for a wide range of tissues. Then, the procedures were reviewed and developed for plants tissues by Jason W. Johnston [6].

This paper optimized and presented a sensitive and re-

978-1-61896-030-6

producible method for determining 2`-deoxycytidine and 5-methyl-2`-deoxycytidine using HPLC system. Furthermore, thirteen wheat-rye translocation lines were analyzed to obtain their global genomic DNA methylation (GDM) changes using this method, respectively in shoot and root samples. The results showed that there were significant differences of GDM between these translocation lines and between the two parts in same line.

2 Material and Methods

2.1 Chemicals and Reagents

Standards of 2`-deoxycytidine and 5-methyl-2`-deoxycytidine with purity of 100% were supplied by Sigma-Aldrich. Nuclease (S1) and alkaline phosphatase (CIAP) were purchased from TaKaRa. HPLC grade acetonitrile and methanol (Tedia, USA) were used for the HPLC analysis. The potassium dihydrogen phosphate (KH2PO4) was of AR grade. The water used in all experiments had a resistivity of 18.2 MΩcm.

2.2 Instrumentation and Chromatographic Conditions

HPLC analysis was performed using a quaternary pump, a manual simple injector with a 20 μl loop and a photo diode-array detector set to 280 nm.

An gradient elution protocol was performed, consisted of 8 min with buffer A (10mM KH2PO4 adjusted to pH 3.7 with phosphoric acid, 0.22 μm filtered), followed by a linear gradient from 8 to 23 min to buffer B (25% v/v acetonitrile in 10 mM KH2PO4 adjusted to pH 3.7 with phosphoric acid, 0.22 μm filtered), followed by a linear gradient from 23–28 min to buffer A, followed by 28-38 min with buffer A, on a YMC-Pack ODS-A C18 column (150 × 4.6 mm I.D. S-5μm,12nm), with a flow rate of 1.0 ml/min. The effluent was monitored at a wave length of 280 nm. Injection volume was 10 μL and the analyses were carried out at temperature 25℃. Deoxycytidine methylation (%) was calculated as 5-methyl-2`-deoxycytidine concentration divided by the combined concentration of 2`-deoxycytidine and 5-methyl-2`-deoxycytidine, multiplied by 100.

2.3 Plant Material, DNA Extraction and DNA Digestions

Thirteen wheat-rye chromosome translocation lines "Chuan-nong" series were analyzed in the present study, including Chuan-nong10 (CN10), Chuan-nong11 (CN11), Chuan-nong12 (CN12), Chuan-nong17 (CN17), Chuan-nong18 (CN18), Chuan-nong19 (CN19), Chuan-nong21 (CN21), Chuan-nong22 (CN22), Chuan-nong23 (CN23), Chuan-nong24 (CN24), Chuan-nong25 (CN25), Chuan-nong62 (CN26) and Chuan-nong27 (CN27). Pedigree of these cultivars was according to REN Tian-heng [10].

Mature seeds were surface-sterilized with 75% ethanol and were placed in 15 cm Petri dishes on two layers of soaked filter paper. After germination, plant seedlings were grown in an incubator at (25±0.5) ℃ under 16 h of daylight and 8 h of darkness for 20 d. Then, the genomic DNA was isolated from shoots and roots respectively using cetyltrimethyl-ammonium bromide (CTAB) procedure according to Murray and Thompson [11]. The genomic DNA was checked for quality and quantity by agarose gel electrophoresis (0.8% agarose) and fluorimetry (BioSpec-mini, Shimadzu, Japan).

The method employed for DNA enzymatic hydrolysis was adapted from Johnston [6]. Nuclease S1 and alkaline phosphatase digestions were performed using 10μg of nucleic acid. Nucleic acids were denatured by heating to 95 °C for 8 min and held on ice quickly for 5 min. Digestion reactions were according to Johnston with some modifications. Samples were centrifuged at 10,000 × g for 5 min after digestion and the supernatant were then filtered (0.22 μm) prior to HPLC analysis.

3 Results and Discussion

Peaks were identified using standards. Chromatogram of standards was shown in Fig. 1.

3.1 Methodology Validation

3.1.1 Calibration, Linearity and Limit of Detection

Under the optimized experimental conditions, calibration curves of 2`-deoxycytidine showed good linearity in 2.5–315 ng, and 5-methyl-2`-deoxycytidine showed good linearity in 3.5–445 ng. Correlation coefficients (r) of these calibration curves were 1.0 (Fig. 2). The detection limits were all no less than 0.05ng/mL.

3.1.2 Injection Precision

The injection precision was determined by replicate injections of the same sample six times in one day. The relative standard deviations (RSD) of relative retention time (RRT) and relative peak area (RPA) for 2dC were lower than 0.61% and 0.13%, respectively. The RSDs of RRT and RPA for 5mdC were lower than 0.67% and 0.14%, respectively.

3.1.3 Sample Stability Test

The sample stability test was determined with one sample during four weeks. In this period, the solution was stored at temperature -20℃. The RSDs of RPA for 2dC and 5mdC were lower than 1.14% and 0.93%, respectively. The results indicated that the sample remained stable for four weeks.

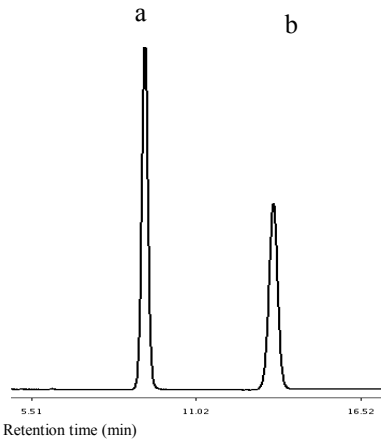

Figure 1. The chromatograms of standard compounds

a stand for 2`-deoxycytidine (2Dc) and b stand for 5-methyl-2`-deoxycytidine (5mdC).

3.1.4 Repeatability

The repeatability was assessed by analyzing six independently prepared samples of DNA. The RSDs of RPA for 2Dc and 5mdC were lower than 2.86% and 4.71%, respectively.

All results of injection precision, stability and repeatability test indicate that this method was adequate, valid and applicable.

3.2 Global Genomic DNA Methylation (GDM) Levels of Thirteen Wheat-Rye Translocation Lines

Samples of thirteen wheat-rye translocation cultivars in different tissues were investigated (Table 1). Their average relative standard deviations (R.S.D.) were all below 4.3%. As deduced from HPLC analyses, genomic DNA methylation levels were found to be diverse among these cultivars in both tissues. The rate varies from 11.22% (CN21) to 24.42% (CN25) in shoots and from 3.80% (CN24) to 7.51% (CN10) in roots. Meanwhile, the GDM levels showed significantly differences between different tissues, shoots and roots, of same cultivar (Figure 4). Chromatograms were shown in Fig. 3a and b.

3.3 Recovery Test

The wheat-rye translocation cultivar CN17 was used for recovery test. Sample with known content was accurately weighed and mixed with equal, 80% and 120% standard solutions, respectively. They were pretreated and analyzed using the method above. The average recoveries were found to be more than 93% and R.S.D. were all less than 6.9%.

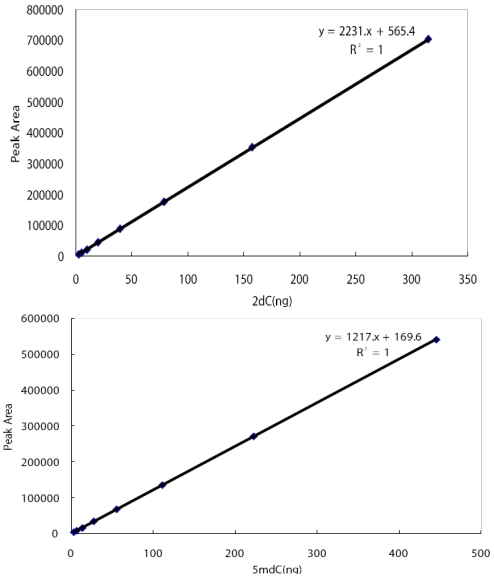

Figure 2. Calibration curves of 2`-deox ycytidine (2Dc) and 5-methyl-2`-deoxycytidine (5mdC)

Table 1. Global genomic DNA methylation (GDM) levels of thirteen wheat-rye translocation lines (n=5) [a]

	Shoot		Root	
	Mean (%)	R.S.D. (%)	Mean (%)	R.S.D. (%)
CN10	23.34	1.5	7.51	1.9
CN11	11.94	2.4	4.94	3.3
CN12	11.70	3.9	4.09	3.4
CN17	15.42	1.2	5.41	1.7
CN18	14.42	1.3	4.82	3.3
CN19	13.51	3.1	6.41	2.0
CN21	11.22	2.0	4.75	1.6
CN22	11.58	4.1	4.97	1.9
CN23	21.55	2.4	6.74	1.4
CN24	17.42	2.7	3.80	2.7
CN25	24.42	2.4	4.82	1.4
CN26	19.53	1.4	3.95	1.9
CN27	18.75	2.0	4.95	2.1

978-1-61896-030-6 © 2012 SciRes.

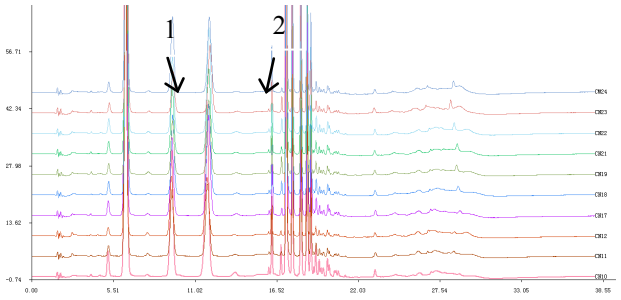

(a) Retention time (minute)

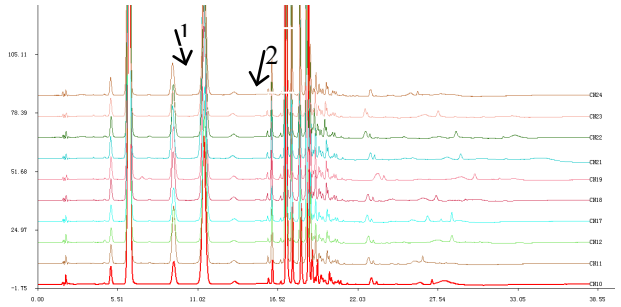

(b) Retention time (minute)

Figure 3. HPLC chromatograms for: (a) root samples; (b) shoot samples

1 stand for 2`-deoxycytidine (2Dc) and 2 stand for 5-methyl-2`-deoxycytidine (5mdC).

4 Conclusion

In summary, the whole method optimized and presented in this paper was stable, sensitive and eproduceble. The results demonstrated that this method was feasible for quality evaluation of global genomic DNA methylation (GDM) for wheat (*Triticum aestivum L*) and its relatives.

Acknowledgement

This work was supported by funding from the National Natural Science Foundation of China (Grant numbers 30730065, 30900779) and the Youth Science Foundation of University of Electronic Science and Technology of China.

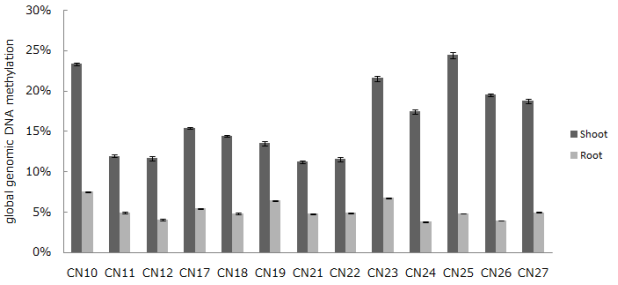

Figure 4. Global genomic DNA methylation (GDM) levels of thirteen wheat-rye translocation lines in shoots and roots, respectively

Data are mean (±) S.E of five replicates

References

[1] Shaked H, Kashkush K, Hakan Ozkan, Moshe Feldman and Avraham A. Levy, "Sequence Elimination and Cytosine Methylation Are Rapid and Reproducible Responses of the Genome to Wide Hybridization and Allopolyploidy in Wheat," The Plant Cell, Vol. 13, pp. 1749-1759, 2001.

[2] Moira Scascitelli, Marie Cognet and Keith L. Adams, "An Interspecific Plant Hybrid Shows Novel Changes in Parental Splice Forms of Genes for Splicing Factors," Genetics 184: 975-983, 2010.

[3] Bourchis D, Bestor TH, "Meiotic catastrophe and retrotransposon reactivation in male germ cells lacking Dnmt3L," Nature 431:96-99, 2004.

[4] Dario Cantu et al, "Research article Small RNAs, DNA methylation and transposable elements in wheat," BMC Genomics, 11:408, 2010.

[5] Julie A. Law and Steven E. Jacobsen, "Establishing, maintaining and modifying DNA methylation patterns in plants and animals," Nat Rev Genet, 11(3): 204-220.

[6] Jason W. Johnston, Erica E. Benson, et al, "HPLC analysis of plant DNA methylation: a study of critical methodological factors," Plant Physiology and Biochemistry 43: 844-853, 2005.

[7] M.F. Fraga, M. Esteller, "DNA methylation: a profile of methods and applications," BioTechniq. 33 632-649, 2002.

[8] I. Wagner and I. Capesius, "Determination of 5-methylcytosine from plant DNA by high-performance liquid chromatography," Biochim. Biophys. Acta 654 52-56, 1981.

[9] K.C. Kuo, R.A. McCune, C.W. Gehrke, R. Midgett and M. Ehrlich, "Quantitative reversed-phase high performance liquid chromatographic determination of major and modified deoxyr i-bonucleosides in DNA," Nucleic Acids Res. 8, 4763-4776, 1980.

[10] REN Tian-heng et al., "Application of 1RS.1BL Translocation in the Breeding of "Chuangnong" Series Wheat Cultivar," Journal of Triticeae Crops, 31(3):430-436, 2011.

[11] Murray M G, Thompson W F, "Rapid isolation of high molecular weight plant DNA," Nucleic Acids Res, 8(19): 4321-432.

Synthesis and Water Solubility of m-PEG Supported Oleanolic Acid

Xu ZHAO, Peng YU, Hua SUN
College of Biotechnology Tianjin University of Science and Technology, Tianjin, China
Email:sunhua@tust.edu.cn

Abstract: Oleanolic acid (OA), a triterpenoid found in many plant species, has attracted attention due to its important pharmacological properties. However the poor water solubility affects its bioavailability. A m-PEG supported OA with a succinate linker was synthesized. The product was characterized by ^{1}HNMR. The water solubility studies showed that the water solubility of m-PEG supported OA improved more than 500 times than OA.

Keywords: Oleaolnic acid; polyethylene glycol; m-PEG; synthesis

1 Introduction

Oleanolic acid (OA) (Fig.1) is a facile pentacyclic triterpenoid which is widely present in natural plants in the form of free acids or aglycones [1]. This triterpenoid compound has attracted considerable interest owing to its significant biological activities and promising clinical application as chemotherapeutic and chemopreventive agent (anti-tumor, anti-HIV and anti-inflammation, as well as many others [2]). OA has been marketed in China as an oral drug for liver disorder. OA is relatively non-toxic, and have been used in cosmetic and health product [3].

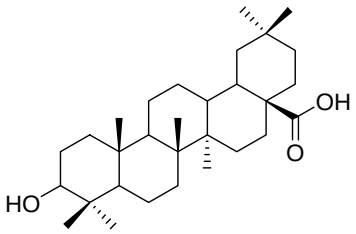

Figure 1. Structure of oleanolic acid

However the poor water solubility of OA and its derivatives affect their absorption in vivo. Derivatives obtained by chemical structural modifi cation to increase the water solubility were the important methods to increase the bioavailability and the clinical therapeutic effect. Poly (ethylene glycol) (PEG) is a water soluble amphiphilic polymer showing excellent biocompatibility is frequently used in biomedical applications [4]. Drugs modified with PEG carriers also benefit from lowered immunogenicity and better tumor uptake. In this study, m-PEG supported OA was prepared with a succinate linker.

2 Result and Discussion

The synthetic route of the m-PEG supported OA (4) is shown in Scheme 1. Commercially available m-PEG was successfully converted to m-PEG-DA 2 in high yield. Compound 3 can be obtained with oxalylchloride from 2. The compound 3 was reacted with OA to give m-PEG supported Oleanolic acid 4 successfully.

The water solubility of m-PEG supported OA 4 and OA was compared. The result showed that water solubility of m-PEG supported OA was improved more than 500 times from 4.4×10^{-3} mg/mL (OA) to 2.4 mg/mL (Table 1).

Table 1. Water solubility of m-PEG supported OA and OA

compound	Solubility in water (mg/mL)
OA	4.4×10^{-3}
4	2.4

3 Experiment

3.1 Procedure for the Preparation of m-PEG-1, 4-Succinic Acid Single Ester (2)

m-PEG-2000 (20 g, 10 mmol) was added to a mixture of 1,4-Succinic anhydride (2.5 g, 50 mmol) and pyridine (2 mL) in $CHCl_3$ (150 mL) at room temperature. The reaction mixture was heated to 80°C for 48 h and then cooled to room temperature. The mixture was filtered through a Celite pad, and the filtrate was subjected to evaporation under reduced pressure. The crude product was dissolved in a saturated solution of sodium bi-carbonate (150 mL), and extracted with ethyl acetate (10 mL ×3), then cooled to 0˚C - 5˚C. The pH was adjusted to 2-3 by progressively adding HCl solution (1 mol/L).

978-1-61896-030-6

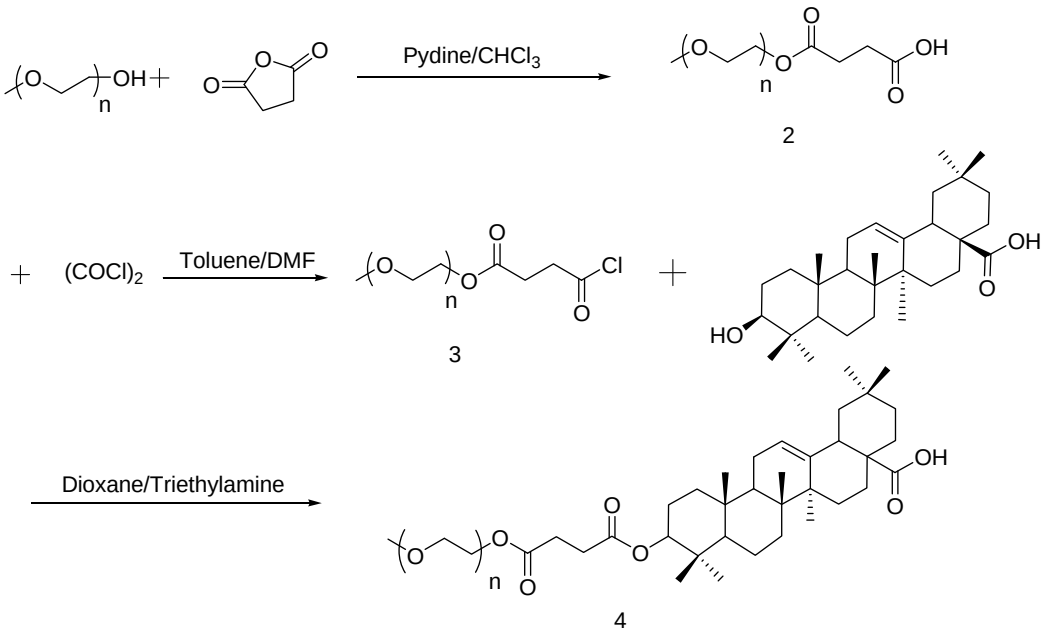

Scheme 1. The synthesis route of m-PEG-OCOCH$_2$CH$_2$CO-OA (4)

The aqueous layer was extracted with chloroform (100 mL×3). The organic layer was washed with water (20 mL×3) and the dried over anhydrous sodium sulfate. The solution was concentrated and the residue was purified by recrystallization in cold ethyl ether in yield 90 %. ^{1}HNMR(400 MHz, $CDCl_3$), δ_H 2.52 (t, 4H, CH_2CH_2), 3.3 (s, 3H, CH_3), 3.4~3.8 (br, PEG-CH_2CH_2O), 4.2 (t, 2H, CH_2).

3.2 Procedure for the Preparation of m-PEG-OCOCH$_2$CH$_2$COCl (3)

m-PEG-DA 2 (2.1 g, 1.0 mmol) was dissolved in dry toluene (25 mL). The reaction mixture was cooled to 0℃, followed by the addition of oxalyl chloride (0.3 g, 2 mmol) and one drop of dimethylformamide. This mixture was stirred for 3 h at 30-40℃under argon. The solvent was removed by distillation in vacuo. Compound 3 was used for next step without further purification.

3.3 Procedure for the Preparation of m-PEG-OCOCH$_2$CH$_2$CO-OA (4)

The compound 3 was dissolved in dry toluene (25 mL), and oleanolic acid (1.36 g, 3 mmol) and triethylamine (0.3 mL, 3 mmol) were added. The reaction mixture was refluxed for 16h, followed by removal of the solvent by distillation in vacuo and then cooled to room temperature. Water (30 mL) was added and extract with chloroform (10 mL×3)，the organic layer was washed with water (10 mL×3) and dried over anhydrous sodium sulfate. The solvent was removed in vacuo and the residue was crystallized with cold ethyl ether. The crude product was purified by column chromatography on silica gel eluted with (DCM/Petroleum Ether=1:10→1:5→1:3) to give the compound (1.3 g , 51%) as a pale yellow solid. ^{1}HNMR (400 MHz，$CDCl_3$), δ_H 0.83 (s, 3H, CH_3), 0.91 (s, 3H, CH_3), 0.91 (s, 3H, CH_3), 1.02 (s, 3H, CH_3), 1.03 (s, 3H, CH_3), 1.08 (s, 3H, CH_3), 1.14 (s, 3H, CH_3), 2.36 (m, 1H, H-2), 2.52（t, 4H, CH_2CH_2）, 2.54 (m, 1H, H-2), 2.68 (dd, 1 H, *J*=4.5 Hz, H-18), 3.3 (s, 3H, CH_3), 3.4~3.8 (br, PEG-CH_2CH_2O), 4.2 (t, 2H, CH_2), 5.30 (t , 1H , *J* = 3.3 Hz, H-12).

References

[1] K. H. Lee, Y. M. Lin, T. S. Wu, D. C. Zhang, T. Yamagishi, T. Hayashi, I. H. Hall, J. J. Chang, R. Y. Wu, and T. H. Yang, "The cytotoxic principles of Prunella vulgaris, Psychotria serpens, and Hyptis capitata: ursolic acid and related derivatives," *Plant. Med.* Vol. 54, 1988, pp. 308-311.

[2] H. Sun, W. S. Fang, W. Z. Wang, C. Hu,"Structure-activity relationships of oleanane- and ursane type triterpenoids." *Botan. Stud*. vol. 47, 2006, pp. 339-368.

[3] J. liu, "Pharmacology of oleanolic acid and ursolic acid," *J. Ethnopharmacol*, vol. 49, 1995, pp. 57-68.

[4] S. Zalipsky, "Chemistry of Polyethylene-Glycol Conjugates with Biologically-Active Molecules," *Adv. Drug Delivery Rev.* vol. 16, 1995, pp. 157-182.

Optimized Option System Based on Fuzzy Cluster Analysis for the Microbial Enhanced Oil Recovery

Yongjun ZHOU[1], Jing WANG[1], Jinling WANG[1], Hanping DONG[2], Li YU[2]
[1]*College of Chemical Engineering, China University of Petroleum (Beijing), Beijing, China*
[2]*Fluid Flows in Porous Institute, Langfang Branch Institute, CNPC, Beijing, China*
Email: wangjing36@hotmail.com

Abstract: In this paper we present a study of optimized option system of the microbial enhanced oil recovery (MEOR) via a fuzzy clustering technique. At First, in order to arrange a large number of strains information, strains database was established. Then based on the fuzzy clustering analysis method, similarity matrix about the concrete reservoir and strains data was established with the use of angle cosine and then Transitive closure method was applied to make clustering analysis. Finally the most suitable strain for specific reservoir was singled out; the whole process was systematized by VB.

Keywords: Microbial enhanced oil recovery; fuzzy cluster analysis; optimized option system; VB

1 Introduction

Two-thirds of the oil ever found is still in the ground even after primary and secondary production [1]. MEOR is a tertiary oil recovery process where microorganisms or their metabolites are used to retrieve unrecoverable oil from an oil reservoir. MEOR represents a truly eco-friendly petroleum recovery process employing biotechnological resources and techniques that can be used to replace and augment the traditional EOR processes and flooding chemicals [2, 3]. MEOR refers to petroleum recovery methods, which involve the use of a mixed microbial population and the metabolic products including biosurfactants, biopolymers, acids, solvents, gases and also enzymes to increase recovery of oil from depleted and marginal reservoirs, thereby extending the life of the oil wells [4]. In selective plugging approaches, microbial cell mass and/or biopolymers plug high-permeability zones and lead to a redirection of the water-flood [5]. Biosurfactants are produced in situ which leads to increased mobilization of residual oil and reduces interfacial tension between oil and water, oil and rock interfaces. Biopolymers are used to increase viscosity of water-flood. Acids, gases and solvents are used to increase the permeability through the porous network and to re-pressurize the oil reservoir [6].

Specific operations are divided into ground fermented and underground fermented. The cost of Underground fermentation is lower, and the process is simpler [7, 8]. But microorganisms must survive in the extreme environment of the oil reservoirs. MEOR, to be economically viable, demands the use of microbial strains, which best fit at such reservoir conditions as temperatures, pressure, pH and salinity. All in all, with the exhaustion of oil, MEOR must be one of the important methods.

Clustering analysis is a fundamental but important tool in statistical data analysis. In real life, due to the vagueness and uncertainty of information as well as the vagueness of human feeling and recognition, it is difficult to exactly evaluate and convey the feeling [9, 10]. Furthermore, a cluster method based on fuzzy equivalence relation is presented to tackle the cluster analysis under fuzzy environment.

Every year there are many micro-organisms are filtered out which might apply in MEOR, but in the specific field application, there are a lot of strains data and messy environment factors. How to filter out the most efficient strain which is adapted to specific mine scientifically and rapidly will be the contents of the study. In this paper, the fuzzy clustering analysis method is used in microbial enhanced oil recovery, and the entire process is systematic.

2 The Model

Fuzzy clustering analysis which is used in microbial enhanced oil recovery needs some improvement to change into cluster selection method. In order to make it more convenient to manage and apply strains. Create a strain database and a table, then input the information of strains data such as temperature, salinity, pH, and surface tension reduction value which are best adapted to the growth conditions. The strains data can be applied into MEOR.

2.1 Build an Application Interface

First, build an application interface by VB.

978-1-61896-030-6

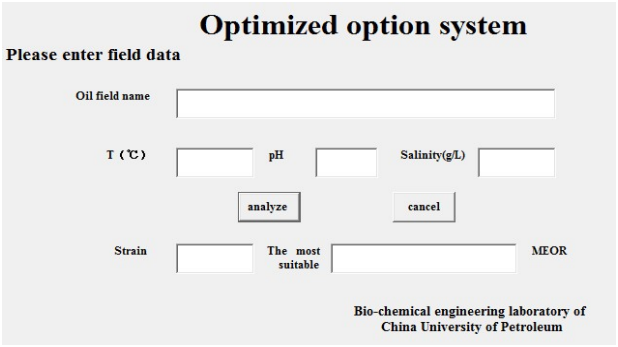

Program in analyze control by VB. Define the corresponding variables and a two-dimensional array a(i, j), then use adodc to build the links between database and VB. Finally read the strains information of the strain database in array a(i, j). Calculate the number of strains in the database and suppose the number is count.

2.2 Data Correction [11]

Strains data were transformed using Specific field data by formula, the optimal stain was clustered first which was the closest to field environment. In the meantime, biosurfactant was produced more than other strains.

The information of strains data, pH and salinity correction formula is:

X'=（k-|x-k|）/k

k is the data of field

the correction formula of surface tension is:

X'=M-x

where M equals one.

The corresponding code for Data correction process:

```
p = Text3.Text '   p represents   the input value of   pH in the field .
k = Text4.Text '   k represents   the input value of   salinity   in the field .
For i = 1 To count
        For j = 2 To 4
                If   j = 2 Then
                        a(i, j) = (p - Abs(p - a(i, j))) / p
                ElseIf j = 3 Then
                    a(i, j) = (k - Abs(k - a(i, j))) / k
                ElseIf j = 4 Then
            a(i, j) = 1 - a(i, j)
        End If
  Next j
Next i
```

2.3 Data Standardization [12]

In order to reduce the influence of different outline, standard deviation method was adopted to data standardization:

$$X'_{ik} = \frac{x_{ik} - x_k}{s_k} \qquad (1)$$

(i=1,2,3…,count; k=1,2,3,4)

where X_{ik} were the measured values, X_k the sample mean and S_k the sample standard deviation. Suppose the number of strain was i while the strain data indicator was k.

The corresponding code for Data standardization process:

```
M = 0
For i = 1 To count
   M=M + a(i, 1)
Next i
   M= M / count
F = 0
For i = 0 To count
      F = F + (a(i, 1) - M) ^ 2
Next i
F = Round(Sqr(F / count), 3)
For i = 1 To count
    a(i, 1) = Round((a(i, 1) - M) / F, 3)
Next i '     Standardization the first column data
M = 0
For i = 1 To count
      M = M+ a(i, 2)
Next i
M = M / count
F = 0
For i = 1 To count
  F = F + (a(i, 2) - M) ^ 2
Next i
F = Round(Sqr(F / count), 3)
For i = 1 To count
   a(i, 2) = Round((a(i, 2) - M) / F, 3)
Next i '   Standardization the second column data
M = 0
For i = 1 To count
   M = M + a(i, 3)
Next i
M = M / count
F = 0
For i = 1 To count
   F = F + (a(i, 3) - M) ^ 2
Next i
F = Round(Sqr(F / count), 3)
For i = 1 To count
   a(i, 3) = Round((a(i, 3) - M) / F, 3)
Next i '   Standardization the third column data
M = 0
For i = 1 To count
   M = M + a(i, 4)
Next i
M = M / count
```

```
F = 0
For i = 1 To count
  F = F + (a(i, 4) - M) ^ 2
Next i
F = Round(Sqr(F / count), 3)
For i = 1 To count
   a(i, 4) = Round((a(i, 4) - M) / F, 3)
Next i '   Standardization the fourth column data
```

2.4 The Establishment of Similarity Matrix [12, 13]

There are several methods for calculating the similarity matrix R, such as the maximum-minimum method, the similarity coefficient method and the angle cosine method. We used the angle cosine method which used the following formula:

$$r_{ij} = \frac{\left|\sum_{k=1}^{m} x_{ik} x_{jk}\right|}{\sqrt{\sum_{k=1}^{m} x_{ik}^2 \sum_{k=1}^{m} x_{jk}^2}} \qquad (2)$$

(i = 1, 2, ···, count; j = 1, 2, 3, 4).

where m was the count of each column, and i the order of data.

The corresponding code for similar matrices process :

```
For i = 1 To count
          For j = 1 To count
    t(i, j) = Round(Abs(a(i, 1) * a(j, 1) + a(i, 2) * a(j, 2) +
a(i, 3) * a(j, 3) + a(i, 4) * a(j, 4)) / Sqr((a(i, 1) ^ 2 + a(i, 2)
^ 2 + a(i, 3) ^ 2 + a(i, 4) ^ 2) * (a(j, 1) ^ 2 + a(j, 2) ^ 2 +
a(j, 3) ^ 2 + a(j, 4) ^ 2)), 3)
          Next j
Next i     'The establishment of similarity matrix by Cosine method
```

2.5 Matrix Transformation

Use the square method to obtain the equivalent matrix: $R \times R = R^2$, $R^2 \times R^2 = R^4$…Until $R^n = R^{2n}$ was obtained, the equivalent matrix was $R = R^n$ [14, 15].

According to calculation rules of fuzzy mathematics, A×B equals A and A plus B equals B, where the value of B is larger than A. The corresponding code for equivalent matrix process was as follows:

```
For i = 1 To count
                For j = 1 To count
                    For k = 1 To count
                        If t(i, k) <= t(k, j) Then
                            dmin(k) = t(i, k)
                        Else
                        dmin(k) = t(k, j)
                        End If
                    Next k
                dMax = dmin(1)
For k = 1 To count
                If dmin(k) >= dMax Then
                    dMax = dmin(k)
                        End If
                    Next k
                R(i, j) = dMax
            Next j
        Next i
  For i = 1 To count
            For j = 1 To count
                If t(i, j) <> R(i, j) Then
                    For i1 = 1 To count
                        For j1 = 1 To count
                            t(i1, j1) = R(i1, j1)
                        Next j1
                    Next i1
                GoTo 100
                End If
            Next j
Next i
```

2.6 Cluster Analysis [16]

After finding out the largest number in the equivalent matrix, two strains were obtained. Finally use the mine temperature to filter out the best strain. It was the MEOR strain which was most suitable in interface mine. The corresponding code for cluster analysis process was as follows:

```
  M = R(1, 1)
  For i = 1 To count
        For j = 1 To count
            If   i < j And R(i, j) > M Then
              M = R(i, j)
          End If
        Next j
    Next i
    For i = 1 To count
        For j = 1 To count
            If i < j And R(i, j) = M Then
          Text7.Text=i
          Text8.Text=j ' text7 and text8 are embedded
textboxes
        End If
      Next j
Next i
max1 = Val(Text7.Text)
max2 = Val(Text8.Text)
If a(max1, 1) < a(max2, 1) Then
      temp = max2
ElseIf a(max1, 1) = a(max2, 1) Then
      If a(max1, 4) < a(max2, 4) Then
```


978-1-61896-030-6 © 2012 SciRes.

```
            temp = max1
        Else
            temp = max2
        End If
Else
            temp = max1
End If
```

Text5.Text = jzName(temp) ' It manifested the name of optimal strain which was selected by the system
Text6.Text = Text1.Text ' It manifested the name of field which was adapted to the optimal strain.

2.7 System Integration

Program in cancel control: Unload Me.

Make this process exe file and complete the construction of MEOR optimization option system.

3 Conclusion

Based on fuzzy equivalence relation, this paper presented a cluster analysis method to solve MEOR problem. In this paper, fuzzy clustering analysis was applied in microbial enhanced oil recovery. Use database to manage the strain information, then make the process of fuzzy clustering programme. So that it can process the large amounts of data rapidly and play an important part in the field of microbial enhanced oil recovery. But in this paper, construction method of Optimal Microorganism community in microbial enhanced oil recovery was not involved. It wound be the direction and goal of future research.

Acknowledgement

The supports of the China National 863 Hi-Tech R&D Plan (Grant No. 2009AA063504), China National Petroleum Corporation Science&Technology Management Program (2008A-1403) are gratefully acknowledged.

References

[1] Lewis R Brown, “Microbial enhanced oil recovery (MEOR),” *Current Opinion in Microbiology*, 2010, 316-320.

[2] H. Volk, K. Liu, ” Oil Recovery: Experiences and Economics of Microbially Enhanced Oil Recovery (MEOR),” *Handbook of Hydrocarbon and Lipid Microbiology*.

[3] Banat. IM, “Biosurfactants production and possible uses in microbial enhanced oil recovery and oil pollution remediation,” *Bioresource Technol*, 51, 1995, 1-12.

[4] O. Pornsunthorntaweea, N. Arttaweeporna, S. Paisanjit, P. Somboonthanatea, M. Abeb, R. Rujiravanita, S. Chavadeja, “Isolation and comparison of biosurfactants produced by Bacillus subtilis PT2 and Pseudomonas aeruginosa SP4 for microbial surfactant-enhanced oil recovery,” *iochemical Engineering Journal*, vol. 42, 2008, 172-179.

[5] H. Suthar, K. Hingurao, A. Desai, A. Nerurkar, “Evaluation of bioemulsifier mediated Microbial Enhanced Oil Recovery using sand pack column,” *Journal of Microbiological Methods*, vol. 75, 2008, 1. 225-230.

[6] R. Sen, “Biotechnology in petroleum recovery: The microbial EOR,” *Progress in Energy and Combustion Science*, vol. 34, 2008, 714-724.

[7] I. Lazar, I. G. Petrisor, T. F.Yen, “Microbial enhanced oil recovery (MEOR),” *Petroleum Sci Technol*, vol. 25, 2007, 1353-1366.

[8] D. L. Zhou，D. Ma, W. L. Liang, “Microbial enhanced oil recovery technology,” *Inner Mongolia Petrochemical*, 2008.

[9] T. Wang, Y. P. Wang, J. T. Tang, “Fuzzy Mathematics and its Applications,” *Northeastern University Press*, 2005.

[10] D. R. Xiao, Z. J. Cao, K. Kang, “Analysis on the development of heavy using fuzzy clustering method,” *Microcomputer Information*, 2010.

[11] Y. H. Ng, “Compr ehensive Compar ison of Fuzzy Cluster Analysis Method on New Introduced Flue Cured Tobacco Var ieties,” *Inner Mongolia Agricultural Science And Technology*, vol. 5, 2007, 36-38.

[12] J. C. Wei, Z. J. Li, L. Q. Shi, Y. Z. Guan, H. Y. Yin, “Comprehensive evaluation of water-inrush risk from coal floors,” *Mining Science and Technology*, vol, 20, 2010, 2. 0121-0125.

[13] B. Y. Song, L. L. Cheng, X. B. Kong, L. B. Yang, L. Tian, Method of a fuzzy cluster analysis to apply the process of crude,” *Petrochemical Technology & Application*, 2008.

[14] Y. J. Wang, “A clustering system for data sequence partitioning,” *Expert Systems with Applications*, vol. 38, 2011, 659-666.

[15] Y. J. Wang, “A clustering method based on fuzzy equivalence relation for customer relationship management,” *Expert Systems with Applications*, vol. 37, 2010, 6421-6428.

[16] Z. H. Xu, J. Chen,J. J. Wu, “Clustering algoritHm for intuitionistic fuzzy sets,” *Information Sciences*, vol. 178, 2008, 12. 3775-3790.

Essential Oils Yield of Aqueous Extracts and Antioxidant Capacity of Rhizoma et Radix Notopterygii

Zhen WANG[1,2], Shilin CHEN[1], Linfang HUANG[1]

[1]*Institute of Medicinal Plant Development, Chinese Academy of Medical Sciences & Peking Union Medical College, Beijing, China, 100193*

[2]*School of Chinese Materia Medica, Beijing University of Chinese Medicine, Beijing, China, 100102*

Email: wangzhen392346@163.com

Abstract: This paper mainly described the yield of essential oils which were obtained by hydrodistillation and the antioxidant capacity of essential oil of Rhizoma et Radix Notopterygii. The yield of volatile oils ranged 0.5% from 4.6% (ml/100g). The antioxidant activities of essential oils of Rhizoma et Radix Notopterygii were investigated from two aspects: the capacity of removing superoxide anion radical ($O_2^{\bullet-}$) and the clearance of hydroxyl radical(· OH). The antioxidant and antiradcal scavenging properties of the selected oils were tested by 1,10-phenanthroline Spectrophotometry and the visible lightmediated pro-oxidant effects of Vitamin B2. All examined oils exhibited a free radical scavenging activities, ranging of 0.85 %- 7.08% of $O_2^{\bullet-}$ clearance and 2.73%-3.68% · OH inhibition.

Keywords: Rhizoma et Radix Notopterygii; essential oil; yield; antioxidant

1 Introduction

Qianghuo, *Notopterygium incisum* Ting ex H.T.Chang and *N. franchetii* H.de Boiss (Apiaceae)[1] is an perennial herb that has been widely used in traditional Chinese medicine as well as in some ethnics, such as Tibetan and Qiang minorities. The underground part of the herb has been traditionally used in the treatment of pain relieving, cold-expelling and dampness-dispersing. In previous research[2-3], the chemical composition of volatile oils from Radix et Rhizoma Notopterygii had been studied, however, there are few reports on the study of the antioxidant capacity of aqueous extracts by 1,10-phenanthroline Spectrophotometry and the visible light mediated pro-oxidant effects of Vitamin B_2.

The biological activity of Notopterygii, such as antimicrobial [4] and anti-inflammatory[5] have been investigated .To the best of our knowledge, there is no report on the antioxidant activity of the essential oils from Notopterygium. We emphasized on the antioxidant capacities of volatile oils by removing $O_2^{\bullet-}$ and · OH produced by radical systems. Surrounded by kinds of pollution that it increased the damage of free radicals: food, health products and medicines we took is an important way of reducing the risk of them in body[6]. With the emerge of · OH and $O_2^{\bullet-}$, they led to cell damage and degradation. Since ancient times, our ancestors used their wisdom and ShenNong who had tasted the herbs to test which were useful, toxic or dental, with the time passing by, more and more attentions having been paid to natural products (terrestrial plants, animal products, marine organisms and products of microorganisamal fermentation), since the tendency of modern society, people have put more effort on the their own health. In this article the author would mainly report the yield of essential oils from Notopterygium and their antioxidant capacity: the removing of superoxide anion and clearance of hydroxyl radicals.

2 Materials and Methods

2.1 Materials

Chemical reagents and apparatus : 1,10-phenanthroline monohydrate, $FeSO_4 \cdot 7H_2O$, H_2O_2(30%), KH_2PO_4, Nitro blue tetrozolium (NBT), NaOH(Sinopharm Chemical Reagent Co.,Ltd), Volatile oil, UV2550 spectrophotometer (Shimadzu), heated water bath (Beijing Jingkehuarui Co.,Ltd), vortex (Haimen Kylin-Bell apparatus Co.,Ltd), Biotek Synergy 2(Gene Company Limited). Others were high grade chemical reagents.

2.2 Plant Material

The samples were selected on the basis of different provinces and three counties were chosen in each province, plus three commercial use according to morphological differences (table1). The Rhizoma et Radix Notopterygium were collected from 12 cities of Sichuan, Gansu and Qinghai provinces in November, 2010. Specimen were taxonomically identified by professor Lin Yulin and vouchers were deposited at the Herarium of Institute of Medicinal Plant Development (IMPLAD). Samples were dried in the local place after harvesting.

2.3 Methods

2.3.1 Isolation of the Essential Oil

According to the reported literature[7] ,the essential oils were obtained by hydrodistillation. 90 g (through No.2 sieve) dried and ground powder of Rhizoma et Radix of Notopterygii together with 500 ml water were

978-1-61896-030-6

submitted to hydrodistillation to a 1 L round-bottomed flask, 4 glass beads, and soaked for an hour, heated gently till to boiling in a heating thermostat set, maintained about 6 hours. At the end of each distillation the oils were collected, dried over anhydrous Na_2SO_4 and after filtration, measured and kept at a temperature of 4°C for further analysis. The respective colors of volatile oils at first were transparent and turned to light green gradually. On the day of assay, the extracts were vortexed for ten seconds and cooled to room temperature.

2.3.2 Antioxidant Activity Riboflavine

Photosensitization

Use the buffer to prepare the radical system[8-9]: composition of $3.3*10^{-6}$mol/L vitamin C, 0.01mol/L Methionine, $4.6*10^{-5}$mol/L NBT (prepare when needed, protected from light). Mixed 3 ml of radical system and 0.1ml essential oil from different producing areas together, 4000lx light for 30 min at room temperature, with distillation water as reference solution, to detect the largest absorbance wavelength at 560nm, A; Water as the control group, A_0. To calculate the clearance of radical according to the formula:

$$O_2^{\bullet-} \text{ clearance} = \frac{A_0 - A}{A_0} \times 100$$

2.3.3 1,10-phenanthroline Spectrophotometry

The antioxidant activity was determined by 1,10-phenanthroline spectrophotometry assay, using hydroxyl radical ·OH, according to the procedure described by Wang Duoning [10] with some modification. The assay was performed by UV2550 and Biotek Synergy 2 simultaneously. Take 0.5ml of 1,10-Phenanthroline(5mmol/L) to 0.75mol/L phosphate (pH7.4) 2.4ml, mixed on the vortex, adding 7.5mmol/L Ferrous sulfate solution 0.5ml, votexed after each ones, then add 0.1ml essential oil to test tube, add 3% H_2O_2 0.5ml. Finally, keep the reaction solution in 310K incubation for half an hour, then measured at 510nm. The experiment was divided into three groups: A_0 (no essential oil and no H_2O_2), A_1(no essential oil but with H_2O_2),M(essential oil and H_2O_2). To calculate the clearance of ·OH, i.e., I%

$$I\% = [(M - A_1) / (A_0 - A_1)] \times 100$$

The antioxidant activity (· OH clearance) was performed on different instruments. The reaction solution was fulllength-scanned by UV2550 spectrophotometer system. The max absorbance wavelength was 510nm in this situation. While in Biotek Synergy 2, combined with the reported literature [11-12], two wave-length 510nm and 536nm was chosen to detect the absorbance of the antioxidant of the reaction solution. The analysis was carried out using a 96-well microplate, 100μl were added. All the essential oil samples were analyzed three times. All the data collected for each assay are the averages of triplicate experiments.

3 Results and Discussion

The yield of essential oils of the different origins of the Rhizoma et Radix Notopterygii were shown in Table 1. The mean oil yields of *Notopterygium. incisum* and *N. franchetii* were 0.5% ~4.6% and 1.1%~2.7%(ml/100g), respectively(Table 1). Samples from Qinghai provinces were all lower than the required criteria of the Chinese Pharmacopoeia (2010 edition), 1.4% (ml/100g), and so did the specimen from Lintao, Gansu province. Noteworthy, samples from Sichuan were all higher than 1.4% (ml/100g). Three commercial specifications were all fit the criteria of the Chinese Pharmacopoeia (2010 edition) ranging 2.7% from 3.4%, the striped and irregular-nodal Notopterygium had the similar content of essential oils. According to the table 1 and Fig.1, ABa has the highest yield among the 12 batches of the samples.

Table 1. The yield of essential oil in Notopterygium

origin	sciespe	essential oil % (ml/100g)	ondescripti	collection date
Banma, Qinghai	*N.incisum*	0.9	wild	Oct,2010
Gande, Qinghai	*N.incisum*	0.5	wild	Oct,2010
Dari, Qinghai	*N.incisum*	0.7	wild	Oct,2010
Aba, Sichuan	*N.incisum*	4.6	wild	Oct,2010
Rangtang, Sichuan	*N.incisum*	2.4	wild	Oct,2010
Dege, Sichuan	*N.incisum*	2.0	wild	Oct,2010
Kangding, Sichuan	*N.incisum*	3.4	wild	Oct,2010
Xining[1], Qinghai	*N.franchetii*	2.7	wild	Oct,2010
Xining[2], Qinghai	*N.franchetii*	2.7	wild	Oct,2010
Minxian, Gansu	*N.franchetii*	1.7	cultured	Oct,2010
Weiyuan, Gansu	*N.franchetii*	1.9	cultured	Oct,2010
Lintao, Gansu	*N.franchetii*	1.1	cultured	Oct,2010

The discrimination of morphological identification[13]:Kangding was silkworm Notopterygium,Xining1 was striped Notopterygium; Xining2 was irregular-nodal Notopterygium.

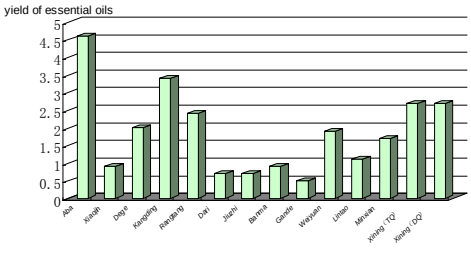

Figure 1. The yields of essential oils from different areas

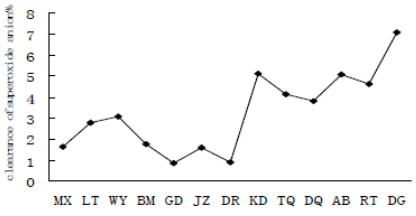

Figure 2. The clearance of superoxide anion

Fig.2. showed the X axis, the origins of samples, the Y axis described the removing capacity of superoxide anion produced by the visible light-mediated pro-oxidant effects of Vitamin B_2, Riboflavine. The 12 batches of antioxidant capacity range 0.85% from 7.08% per gram, respectively. GD showed the lowest superoxide anion clearance, DG explained the highest capacity among 12 batches, while KD, AB and RT had the similar antioxidant capacity, samples from Qinghai province described the lower superoxide anion removing capacity compared to other two provinces.

As shown in Fig.3 described the same specimen detected by two instrument, left column was UV2550 detection value ,and the right column was obtained by Biotek Synergy 2, the full length scan of 400nm-800nm by UV2550 showed that 510nm have the largest absorption, so both of them were compared the 510nm absorption values. The coefficient of variation between the triplet value of UV2550 was 1.09%- 35.64%, as a consequence of the low reproducible of the free hydroxyl radical clearance, and according to the reported literature[14] , then Biotek Synergy 2 was introduced to this experiment. Fig.3. showed that DQ has the most antioxidant capacity among the 12 batches by Synergy 2, and higher than UV2550 in the majority samples.

Fig.4. described the two absorbance wavelength by Biotek Synergy 2, it clearly showed that 1,10-phenanthroline spectrophotometry had more absorbance under 536 nm than 510 nm. Both of the two wavelengths showed the same tendency of the absorbance, but under 536nm detection had higher value than 510nm. It indicated that 536 nm was more suitable for the 510nm in this hydroxyl radical clearance experiment.

Compared Fig.3 with Fig.4, Synergy 2 was time-saving, convenient and with less amount of test samples, but the reuse of the 96 well-microplate would minimize the quantitative of samples, Biotek Synergy 2 could be simultaneously detected at dual wavelength. According to Fig.3 and Fig.4, 536nm have the more absorption in the 1,10-phenanthroline spectrophotometry.

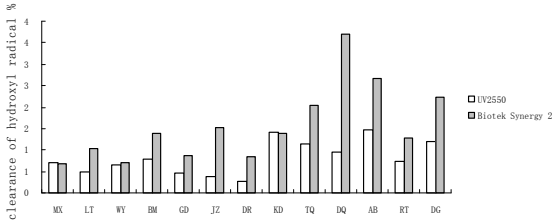

Figure 3. Different instrument under the 510nm absorption

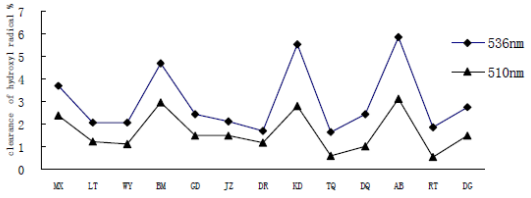

Figure 4. Comparison of two different wavelengths

From the Fig.2 and Fig.4, of the three commercial specification, KD was in accord with in the removing of superoxide anion and hydroxyl radicals. During the clearance of hydroxyl radicals, cultured *N. franchetii* were superior to wild *N. franchetii,* while in the removing of superoxide anions, cultured *N. franchetii* were inferior to wild *N. franchetii*. Among the three producing areas, Sichuan province has the most antioxidant activities. It was in accordance with traditional conception that Sichuan's Notopterygium is relatively good quality.

Acknowledgement

This research is financially supported by Beijing Tong Ren Tang Group Co., Ltd. (D08080203640901).

References

[1] Chinese Pharmacopoeia,Vol Ⅰ, Beijing: China Medical Science and Technology Press;2010,175.

[2] Qiu Y Q, Lu X, Pang T, Zhu S K, Kong H W, Xu G W. Study of traditional Chinese medicine volatile oils from different geographical origins by comprehensive twodimensional gas chromatography-time-of-flight mass spectrometry (GC × GC-TOFMS) in combination with multivariate analysis[J]. J Pharm Bio Anal, 2007, 43 (5):1721-1727.

[3] Yang X W, Zhang P, Tao H Y, Jiang S Y, Zhou Y. GC-MS analysis of essential oil constituents from Rhizome and Root of Notopterygium forbesii[J]. J Chin Pharm Sci, 2006, 15(4): 200-205.

[4] Noriko Sato. The active ingredients in inhibition of Staphylocollus aureus from Notopterygium[J]. Foreign Med Sci, 2002, 24 (4), 249.

[5] Zhang M F, Shen Y Q, Zhu Z P, Wang H W. The analgesic, anti-inflammatory and antithrombotic effect of Notopterygium [J]. Res tradit Chin Med, 1996, (06): 51-53.

[6] Kris-Etherton,P.M., Hecker, K.D., Bonanome,A.,et al. Bioactive compounds in foods:their role in the prevention of cardiovascular disease and cancer. Amer J med, 2002, 30, 71-88.

[7] Zhong G. Studies on optimum extraction technology for volatile oil in Notopterygium by orthogonal test[J]. Chin J Mod Drug , 2008, 2(11):26-27.
[8] Beauchamp C, Fridovich Irwin. Superoxide dismutase: Improved assays and an assay applicable to acrylamide gels[J]. Anal Biochem, 1971, 44: 276-287.
[9] Ilhami Gvlcin I. G Sat, S. Beydemir, M. Elmastsa, O.I. Kufrevioglu. Comparison of antioxidant activity of clove (Eugenia caryophylata Thunb) buds and lavender (Lavandula stoechas L.) Food Chem, 2004, 87:393-400.
[10] [10] Wang D N, Zhang X L, Yang Y, Reng L J, Mi M. Clearing hydroxy free base with Lily Polysaccharide[J]. J Shannxi Tradit Chin Med, 2006.29(4):53-55.
[11] Guo X F, Yue Y D, Meng Z F, et al. Detection of antioxidative capacity of bamboo leaf extract by scavenging hydroxyl free radical[J]. Spectroscopy Spectral Anal, 2010, 30 (2): 508-511.
[12] Zhong F, Wang X C, Lin Li. An experimental study on the effects of Pueraria on oxygen free radicals[J].J TCM Univ. Hunan.2004,24(2)17-18
[13] Liu X, Jiang S Y, Xu K J, et al. Quantitative analysis of chemical constituents in different commercial parts of Notopterygium incisum by HPLC-DAD-MS.[J] J Ethnopharma, 2009, 126(3): 474-479.
[14] Xu D, Zhou N L, Shen J. Hemocompatibility of carboxylic grapheme oxide[J].Chem J Chin Univ 2010,31(12):2354-2359.

Recent Progress in Dopamine D_3 Receptor (Partial) Agonists

Benhua ZHOU[1,2], Jin CAI[1], Chengliang FENG[1], Min JI[1]
[1]*School of Chemistry and Chemical Engineering, Southeast University, Nanjing, China, 211189*
[2]*School of Chemical and Biological Engineering, Yancheng Institute of Technology, Yancheng, China, 224051*
Email: jimin@seu.edu.cn

Abstract: Dopamine is a major neurotransmitter in the brain, and is implicated in the regulation of motion, cognition, drug addiction and so on through acting on dopamine receptors. The D_3 receptor is an important therapeutic target of central nervous system diseases, such as drug addiction, Parkinson's disease and schizophrenia. Dopamine D_3 receptor agonists and partial agonists are of extremely high value to research. Some representative D_3 receptor agonists and partial agonists reported in recent years were classified according to their structural characteristics in this article. At the same time their basic properties and applications were stated simply, the structure-activity relationships were summarized, and the outlook was raised in the end in order to provide a reference for the development of novel dopamine D_3 receptor agonists and partial agonists with high affinity and selectivity.

Keywords: Dopamine; D_3 receptor; agonist; partial agonist; structure-activity relationship

1 Introduction

Dopamine (DA) is one of the most important neurotrans-mittters in the central nervous system (CNS), and is implicated in the regulation of motion, cognition, emotion, drug addiction and so on by activation of dopamine receptor subtypes which are members of the G protein coupled receptor (GPCR) protein superfamily.

There are five functionally active dopamine receptor subtypes which have been classified into two major types of dopamine receptors, D_1-like and D_2-like dopamine receptors. The D_1-like receptor subtypes include the D_1 and the D_5 dopamine receptors, the D_2-like receptor subtypes include the D_2, D_3 and D_4 dopamine receptors according to the similarities in primary structure and pharmacologic properties[1]. The destruction of balance of dopamine neurotransmitter and dopamine D_3 receptor can cause diseases, such as Parkinson's disease (PD), schizophrenia, etc, so the dopamine D_3 receptor is a critical drug target for CNS disease.

2 Structure Classification

2.1 Type of Single Basic Core

Some representative compounds of this type are pramipexole, ropinirole, etc., and the common structural feature of these compounds is that each ligand contains only one core which has an aromatic ring or heterocycle generally. In addition, the hydrophilic amino nitrogen combines one or two n-propyls.

National Key Basic Research Program (973) (No. 2011CB933500) funding

7-OH-DPAT is a selective agonist. It possess a moderate binding affinity to the D_3 receptor with 1000 and 10000-fold selectivity over the D_2 and D_4 receptor respectively, and has no binding affinity to σ、5-HT1A and other receptors, representing for potent and high selective D_3 ligands at present[2].

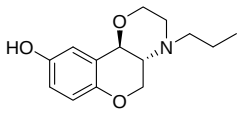

1 (PD-128907)

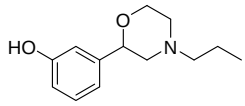

2

Compound **2** has a K_i value of 8nM for its binding affinity to the D_2 receptor and has >1250-fold selectivity over the D_2 receptor[3]. Since the structure of Compound **2** is novel and simple, dopamine D_3 receptor-selective ligands with better activity and selectivity would bring about if compound **2** is modified as a lead compound.

Compound **3** (pramipexole) which belongs to second-generation non-ergot alkaloids, is a drug for Parkinson's disease(PD), and it is a D_3 receptor agonist with a K_i value of 0.78nM for its binding affinity to the

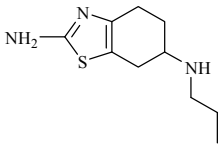

3 (Pramipexole)

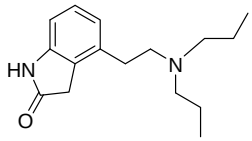

4 (Ropinirole)

D_3 receptor. In addition, compound **3** showed more than 80-fold selectivity for the D_3 receptor versus the D_2 receptor in cells expressing the mitogenic response of D_2

978-1-61896-030-6

and D_3 receptors [4]. Pramipexole is mainly a drug for PD, and is also effective for depression [5].

Compound **4** (ropinirole) which also belongs to second-generation non-ergot alkaloids, is another drug for Parkinson's disease(PD). ropinirole showed the characteristic of D_3 receptor agonists, and had a moderate binding affinity to the D_3 receptor with a 16-fold selectivity versus the D_2 receptor in the mitogenic function tests[4]. It is fit for Parkinson's disease and moderate to severe restless legs syndrome. Pramipexole and ropinirole are all available through a single therapy or in combination with levodopa to treat PD in various stages of treatment, especially patients with early PD[5,6]. Further more, D-264, pramipexole and ropinirole can increase synthesis and secretion of tyrosine hydroxylase positive neurons, brain-derived neurotrophic factor and glial cell line-derived neurotrophic factor, so they are suggested to have a neuroprotective function[7, 8].

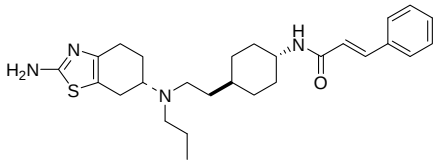

5 (CJ-51073)

Chen, *et al*. reported that structural modification of pramipexole resulted in a series of analogues which had higher binding affinity. Compound **5** is the best compound in these analogues, and displayed a K_i value of 0.41 nMfor its binding affinity to the D_3 receptor with 800-fold selectivity over the D_2 receptor. This compound was found to be a partial agonist at the D_3 receptor with no detectable binding activity at the D_2 receptor in vivo functional assays [9].

2.2 Type of Aryl Methanamide

After relevant literature was studied, it was found that most D_3 receptor (partial) agonists have the common structure characteristic, i.e. they contain a functional group of methanamide, in another words, they are characteristic of the structure model of "H-L-T". "H" stands for the part of basic core structure, "T" stands for the part of tail attached with "H" by a link which can be a alkylene or trans-olefinic bond carbon chain or trans-1,4-cyclohexyl, and all of them constitute the basic skeleton of this class of ligands.

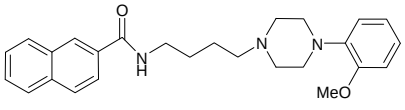

6 (BP897)

Naphthalene carboxamide derivative **6** (BP897) is a potent D_3 receptor partial agonist with better pharmaco-logical activity. It has a K_i value of 0.9nM for its binding affinity to the D_3 receptor with 70-fold selectivity versus the D_2 receptor, and has no binding affinity to D_1, D_4, α_1, α_2, 5-HT_{1A} and 5-HT_7 receptors[10].

In 2000, Foll and his collaborators reported that BP897 itself was not addictive, and did not affect cocaine self-administration behavior of its excitation, but it could cause mouse to reduce drug intake induced by cocaine-related suggestion in the secondary program, which showed that BP897 could reduce environmental relapse in the case of tiny dependence of itself [11]. However, later experiment displayed that BP897 could reduce cocaine craving behavior in mouse body mainly because of the function of its antagonizing of D_3 receptor, rather than as partial agonists[12]. In 2004, Hsu, *et al.* reported that BP897 was efficient to patients with Parkinson's movement disorders, but the effect was not significant as previously expected[13].

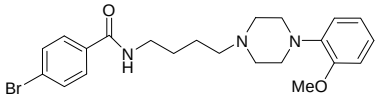

7

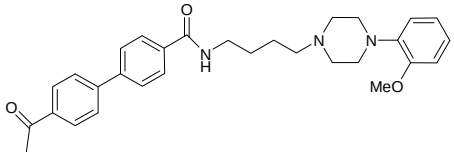

8

A new series of phenylpiperazine analogs has been developed by replacing the naphthamide in BP 897 with other aromatic groups, such as compound **7**($K_i(D_3)$= 0.5nM and compound **8**($K_i(D_3)$=0.3nM) which both attain subnanomolar level[14].

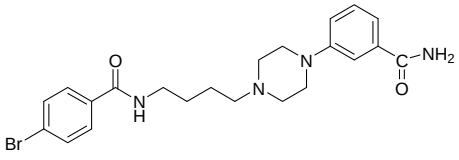

9 (RGH-237)

Compound **9** (RGH-237) is a dopamine D_3 receptor partial agonist, and its binding affinity to the D_3 receptor of human and mouse is $K_i(D_3)$=6.7nM and 1.6nM respectively with a good selectivity of more than several hundred folds over the D_2 receptor, and its intrinsic activity is about 50%. The results further demonstrated that the ligand compound is effective to treat cocaine abuse, and the results support the conclusion that

dopamine D_3 receptor partial agonist is effective to cope with cocaine abuse [15].

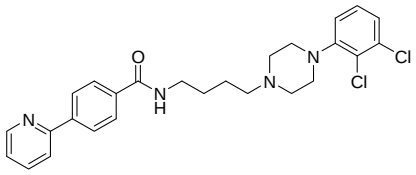

10 (CJB090)

Coumpound **10** was found to have a K_i value of 0.5±0.2nM to the D_3 with a D_3:D_2 selectivity ratio of 50[16]. In 2009, Achat-Mendes, et al. reported that animal tests did not confirm that CJB090 could dilute cocaine-enhanced or cocaine-induced effects, but a certain dose of CJB090 could dilute to identify the stimulus effects of cocaine by acting on the D_3 receptor with no harmful side effects [17].

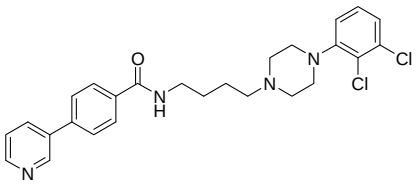

11 (PG01042)

Compound **11**(PG01042) has a high binding affinity (0.5±0.1nM) to the D_3 receptor with a 36-fold selectivity over the D_2 receptor [16]. In 2011, Riddle and his colleagues reported that PG01042 was a D_3 receptor-selective (partial) agonist, and had potential therapeutic effect to L-dopa induced dyskinesia with good prospect [18].

2.3 Type Derived by Combining Predominant Structures

Except for those types of structural patterns, another part of the D_3 receptor (partial) agonists have relatively novel structures, such as D-237, D-264, and so on. These ligand compounds are characterized of a certain length of alkylene connecting two different pharmacophores (predominant structure), and most ligands of this type contain phenylpiperazine fragment with good affinity and selectivity to the D_3 receptor and are suggested with promising application.

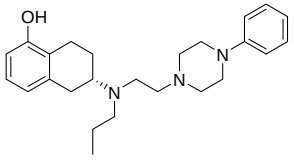

12 ((-)-D-237)

In 2008, Biswas, et al. reported that a novel hybrid approach combining 2-aminotetralin and arylpiperazine pharmacophoric moieties resulted in a series of ideal D_3 receptor ligands. For example, the representative compound **12**(the L-isomer) displayed a K_i value of 0.82±0.13nM to the D_3 receptor with a D_3:D_2 selectivity ratio of 31.5. The researchers also did an experiment on animals with compound **12** and found that it showed the characteristics of partial agonists [19].

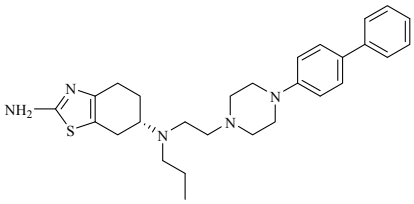

13 (D-264)

In 2008, Biswas, *et al.* also reported that a novel hybrid approach combining pramipexole and arylpiperazine pharmacophoric moieties resulted in a series of novel D_3 receptor ligands with high binding affinity for the D_3 receptor. For example, compound **13** (D-264) had a K_i value of 0.92±0.23nM to the D_3 with a D_3:D_2 selectivity ratio of 253[20]. In 2010, Li and his collaborators reported that D-264 was a D_3 receptor agonist with potential treatment and neuroprotective effect to Parkinson's disease patients according to experiments [21].

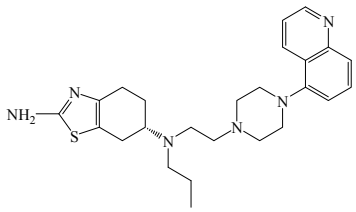

14

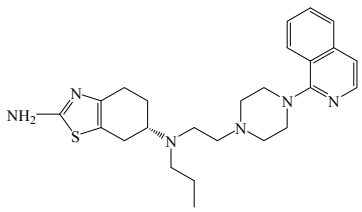

15

Ghosh, *et al.* also synthesized a novel hybrid series of D_3 receptor ligands with high affinity for D_3 receptors. Compound **14** possessed a K_i value of 1.21±0.16nM to the D_3 receptor with a D_3:D_2 selectivity ratio of 47.7 and compound **15** possessed a K_i value of 12.23±0.60nM to the D_3 receptor with a D_3:D_2 selectivity ratio of 121. In addition, whether they have neuroprotective effect to PD

978-1-61896-030-6 © 2012 SciRes.

patients will be studied in the future [22].

The hybrid ligands have novel structures with high affinity and selectivity to the D_3 receptor, and represent one of the development trends of D_3 receptor (partial) agonists with good prospect, so deserve further study.

3 The Structure-Activity Relationships of D_3 Receptor (Partial) Agonists

3.1 Type of Aryl Methanamide

This type of D_3 receptor (partial) agonists contain part I (basic core), part II (alkylene) which is generally a butylene, and part III (aromatic amide) (Figure1). Specifically, part I can be aminotetralin, tetrahydro isoquinoline, isoindole and 4-phenyl piperazine, etc., and generally contains polar groups or atoms with larger electronegativity which can produce binding affinity at key amino acid residues of the dopamine D_3 receptor so that the ligands show corresponding affinity and selectivity to the D_3 receptor. As far as ideal ligand activity is concerned, the most appropriate distance from aromatic ring center to the nitrogen atom is 4.8-5.5Å according to the structure analysis of some D_3 receptor ligands with good activity. In addition, if the ligand only has part I and part II, it has better activity provided that the nitrogen atom at part II combines one n-propyl.

Part II is alkylene, and generally butylene in the middle of ligand which adjusts the distance and geometrical conformation between part I and part III so that the ligand has appropriate afinity to the D_3 receptor. However, Flexible butyl chain may reduces the selectivity, so some researchers attempt to introduce rigid alkyl chains, such as (1,4-cyclohexane-yl) ethyl chain. By the way, the stereochemistry of the compounds impacts its performance and the trans-substituted compounds have higher selectivity to the D_3 receptors than the cis-substituted compounds.

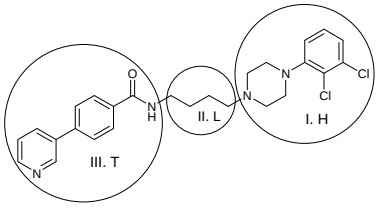

Figure 1. Structure of aryl methanamide type of D_3 receptor (partial) agonists

Part III affects affinity and other performance of ligands largely, and its structure can be reformed easely. It is very important to maintain co-planar structure of the aromatic ring or aromatic heterocycle, otherwise the binding affinity between the compound and the D_3 receptor will be reduced greatly.

There are many methods to raise affinity and selectivity between this type of ligands and the D_3 receptor, for example, make structural modification of part I or/and part II through bioisosterism and other medicinal chemistry methods, adjust the length of carbon chain connecting part I and part III, change the methylene carbon chain flexibility through introduction of double bond or cyclohexane and other means. But later literature reported that rigidification was a good strategy to improve selectivity, but it was shown detrimental for D_3 R affinity when applied to the linker. It is more desirable to incorporate the hydrogen bond acceptor and the aromatic moiety into a heterocycle. Moreover, rigidification can improve bioavailability and suppression of the hydrophile amide bond should be beneficial to brain permeation [23].

3.2 Type Derived by Combining Predominant Structures

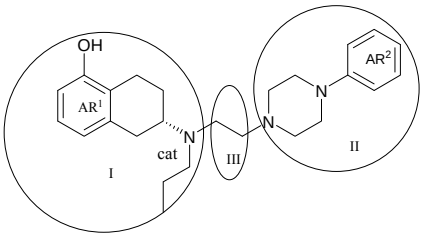

Figure 2. Structure of hybrid type of D_3 receptor agonists/partial agonists

Hybrid type D_3 receptor (partial) agonists generally consists of two different pharmacophores (predominant structure) and a alkylene connecting part I and part II(Figure 2). The docking of D_3 receptor agonists/partial agonists and the D_3 receptor with corresponding interfeature distances are depicted in Figure 3. Ar^1 denotes the aromatic ring of either aminotetralin or 2-aminothiazole moieties, Ar^2 is the phenyl ring attached to one of the piperazine nitrogens, and cat. denotes cationic. The distance between Ar^1 and Ar^2 is generally 11.4-12.5Å, the distance between Ar^1 and cat is 4.9-5.4 Å, and the distance between Ar^2 and cat is 7.6-8.3 Å[24].

Since this type of ligands has been gradually developed in recent years with a small number, so only the initial structure-activity relationships can be summed up: 1) Part I contains a tetrahydro benzene ring with no substituent. 2) The nitrogen atom at etrahydro benzene ring generally combines a alkylene, and the ligand has good activity and selectivity when the nitrogen atom combine a n-propyl. 3) In general, The benzene ring connected to the nitrogen atom of piperazine can only combine a phenyl in the opposite position. In addition, the ligand has high selectivity and activity when the

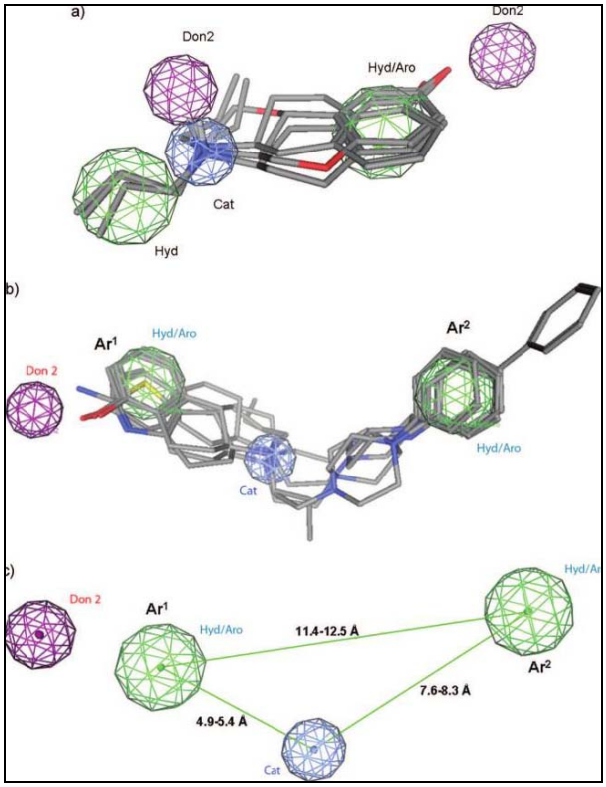

Figure 3. Schematic of docking of D_3 receptor agonists/partial agonists and D_3 receptor [24]

nitrogen atom connects a bulky aromatic heterocycle. 4) Part III is an alkylene which has great influence on affinity and selectivity of ligands, and is generally a ethylene.

As for the three-part structures, there is minor change in part III, and it is useful to the ligand selectivity to introduce phenyl piperazine structure (II). It is relatively easy to change or modify part I. Consequently, we should pay more attention to part I when design hybrid class of D_3 receptor (partial) agonists in the future.

4 Outlook

The dopamine D_3 receptor regulates dopamine synthesis, release and the function of dopaminergic neurons, is related to drug addiction and other CNS diseases, and it is a critical drug therapeutic target of CNS diseases. The (partial) agonists developed according to the dopamine D_3 receptor have broad and important applications in CNS field, and also have important reference values in in-depth studying of the detailed structure of dopamine receptors and the structural differences between receptor subtypes.

At present, the dopamine D_3 receptor (partial) agonists have made some applications in Parkinson's disease, and the research machine in drug addiction has also made some progress. I believe that more novel dopamine D_3 receptor (partial) agonists with high activity and selectivity to the D_3 receptor will be developed and so the researchers can further study the detailed structure and physiological functions of dopamine receptors and explore new applications of the D_3 receptor in the field of CNS diseases.

References

[1] E.Y.T. Chien, W. Liu, Q. Zhao, V. Katritch, G.W. Han, M.A. Hanson, L. Shi, A.H. Newmann, J.A. Javitch, V. Cherezov and R.C. Stevens, "Structure of the human dopamine D_3 receptor in complex with a D_2/D_3 selective antagonist", *Science,* Vol.330, No. 6007, 2010, pp. 1091-1095.

[2] van Vliet L A, Rodenhuis N, Wikström H, et al., "Thiazoloindans and thiazolobenzopyrans: a novel class of orally active central dopamine (partial) agonists", *Journal of Medicinal Chemistry,* Vol.43, No.19, 2000, pp. 3549-3557.

[3] Blagga J, Allerton M N, Batchelor V J, et al., "Design and synthesis of a functionally selective D_3 agonist and its in vivo delivery via the intranasal route", *Bioorganic & Medicinal Chemistry Letters*, Vol.17, No.24, 2007, pp. 6691-6696.

[4] S. Perachon, J.C. Schwartz and P. Sokoloff, "Functional potencies of new antiparkinsonian drugs at recombinant human dopamine D-1, D-2. and D-3 receptors", *European Journal of Pharmacology*, Vol.366, No.2-3, 1999, pp. 293-300.

[5] A. Antonini, P. Barone and R. Ceravolo, "Role of pramipexole in the management of Parkinson's disease", *CNS Drugs.,* Vol.24, No.10, 2010, pp. 829-841.

[6] D. Murdoch, S.M. Cheer and A.J. Wagstaff, "Management of Parkinson disease-defining the role of ropinirole", *Disease Management & Health Outcomes*, Vol.12, No.1, 2004, pp. 39-54.

[7] C. Li, S. Biswas and X. Li, "Novel D_3 dopamine receptor preferring agonist D-264: Evidence of neuroprotective propertyin Parkinson's disease animal models induced by 1-methyl-4-phenyl-1,2,3,6-tetrahy-dropyridine and lactacystin", *Journal of Neuroscience Research.,* Vol.88, No.11, 2010, pp. 2513-2523.

[8] J.N. Joyce, M.J. Millan, "Dopamine D_3 receptor agonists for protection and repair in Parkinson's disease", Current Opinion in Pharmacology, Vol.7, No.1, 2007, pp. 100-105.

[9] Chen J Y, Collins G T, Zhang J, et al., "Design, synthesis, and evaluation of potent and selective ligands for the dopamine 3 (D_3) receptor with a novel in vivo behavioral profile", *Journal of Medicinal Chemistry*, Vol.51, No.19, 2008, pp. 5905-5908.

[10] Preti, BP-897 (Bioprojet), *Current Opinion in Investigational Drugs*., Vol.15, No.2, 2000, pp. 110-115.

[11] B.L. Foll, J.C. Schwartz and P. Scokoloff, "Dopamine D-3 receptor agent as potential new medication for drug addiction", *European Psychiatry*, 2000, pp. 140-146.

[12] K. Wicke, J.G. Ladona, "The dopamine D_3 receptor partial agonist, BP 897, is an antagonist at human dopamine D_3 receptors and at rat somatodendritic dopamine D_3 receptors", *European Journal of Pharmacology*, Vol.424, No.2, 2001, pp. 85-90.

[13] Hsu A, Togasaki D M, Bezard E. et al. "Effect of the D_3 dopamine receptor partial agonist BP897[N-[4-(4-(2-me-hoxyphenyl) pipera zinyl)butyl]-2-naphthamide] on L-3,4 -dihydroxypheny lalanine- induced dyskinesias and parkinsonism in squirrel monkeys", *Journal of Pharmacology and Experimental Therapeutics,* Vol.311,No.2, 2004, pp. 770-777.

[14] Audinot V, Newman-Tancredi A, Gobert A, et al., "A comparative in vitro and in vivo pharmacological characterization of the novel dopamine D_3 receptor antagonists (+)-S 14297, nafadotride, GR 103,691 and U 99194", *Journal of Pharmacology and Experimental Therapeutics,* Vol.287, No.1, 1998, pp. 187-197.

978-1-61896-030-6 © 2012 SciRes.

[15] Gyertyan I, Kiss B, Gal K, et al., "Effects of RGH-237[N-{4-[4-(3-aminocarbonylphenyl)-piperazin-1-yl]-butyl}-4-bromo-benzamide], an orally active, selective dopamine D-3 receptor partial agonist in animal models of cocaine abuse", *Journal of Pharmacology and Experimental Therapeutics*, Vol.320, No.3, 2007, pp. 1268-1278.

[16] Grundt P, Carlson E E, Cao J J, et al., "Novel heterocyclic trans olefin analogues of N-{4-[4-(2,3-dichl-orophenyl)piperazin-1-yl] butyl} arylcarboxamides as selective probes with high affinity for the dopamine D_3 receptor", *Journal of Medicinal Chemistry*, Vol.48, No.3, 2005, pp. 839-848.

[17] Achat-Mendes C, Platt D M, Newman A H, et al., "The dopamine D_3 receptor partial agonist CJB 090 inhibits the discriminative stimulus but not the reinforcing or priming effects of cocaine in squirrel monkeys", *Psychopharmacology*, Vol.206, No.1, pp. 2009, 73-84.

[18] Riddle L R, Kumar R, Griffin S A, et al., "Evaluation of the D_3 dopamine receptor selective agonist/partial agonist PG01042 on L-dopa dependent animal involuntary movements in rats", *Neuropharmacology*, Vol.60 No.2-3, 2011, pp. 284-294.

[19] Biswas S, Zhang S H, Fernandez F, et al., "Further structure-activity relationships study of hybrid 7-{[2-(4-phenylpiperazin-1-yl) ethyl] propyla-mino}-5,6,7,8-tetrahydronaphtha-len-2-ol analogues: Identification of a high affinity D3-preferring agonist with potent in vivo activity with long duration of action", *Journal of Medicinal Chemistry*, Vol.51 No.1, 2008, pp. 101-117.

[20] Biswas S, Hazeldine S, Ghosh B, et al., "Bioisosteric heterocyclic versions of 7-{[2-(4-phenyl-piperazin-1-yl) ethyl]propylamino}-5, 6, 7, 8-tetrahydr onaphthal-en-2-ol: identification of highly potent and selective agonists for dopamine D_3 receptor with potent in vivo activity", *Journal of Medicinal Chemistry*, Vol.51, No.10, 2008, pp. 3005-3019.

[21] Li C, Biswas S, Li X G, et al., "Novel D_3 dopamine receptor-preferring agonist D-264: Evidence of neuroprotective property in parkinson's disease animal models induced by 1-methyl-4-phenyl-1,2,3,6-tetrahydro-pyridine and lactacystin", *Journal of Neuroscience Research*, Vol.88, No.11, 2010, pp. 2513-2523.

[22] B. Ghosh, T. Antonio, J. Zhen, P. Kharkar, M.E.A. Reith and A.K. Dutta, "Development of (S)-N-(2-(4-(isoquinolin-1-yl)piperazin-1-yl)ethyl)-N-propyl-4, 5,6, 7-tetrahydrobenzo[d]-thiazole-2, 6-dia-mine and its analogue as a D_3 receptor preferring agonist: Potent in vivo activity in parkinson's disease animal models", *Journal of Medicinal Chemistry*, Vol.53, No.3, 2010, pp. 1023-1037.

[23] M. Jean, J. Renault and N. Levoin, "Synthesis and evaluation of amides surrogates of dopamine D_3 receptor ligands", *Bioorganic & Medicinal Chemistry Letters*, Vol.20, No.18, 2010, pp. 5376-5379.

[24] D.A. Brown, P.S. Kharkar and I. Parrington, "Structurally constrained hybrid derivatives containing octahydrobenzo[*g* or *f*]quinoline moieties for dopamine D_2 and D_3 receptors: Binding characterization at D_2/ D_3 receptors and elucidation of a pharmacophore model", *Journal of Medicinal Chemistry*, Vol.51, No.24, 2008, pp. 7806-7819.

Tong Luo Jiu Nao Injection Induces Neuroprotection by Regulating Paracrine of Brain Microvascular Endothelial Cells

Weihong LI
School of Preclinical Medicine, Beijing University of Chinese Medicine, Beijing, China
Email: liweihong.403@163.com

Abstract: Historically, the study of CNS diseases has focused on intraneuronal mechanisms, but clinical trials that followed have not been successful. In recent years, this neuron-based autonomous model has perceptibly shifted to a more integrative paradigm that emphasizes interactions between different types of brain cells. In this study we investigated the effect of Tong Luo Jiu Nao injections (TLJN), a traditional Chinese medicine preparation, on signal transmission between brain microvascular endothelial cells (BMECs) and neurons. First, an in vitro model of cerebral ischemia in BMECs or neurons was established by oxygen-glucose-deprivation. Injured neurons were cultured in the conditioned media from normal and injured BMECs treated with TLJN, and the activity, lactate dehydrogenase (LDH) leakage, free Ca^{2+} concentration of neurons were determined. In addition, differential proteins in the conditioned media of BMECs were analyzed and identified by comparing proteomic technology. The results showed the activity of injured neurons was significantly increased when they were grown in conditioned media of normal or injured BMECs treated with TLJN, compared with that of normal or injured BMECs, The changes of LDH leakage, free Ca^{2+} concentration were consistent with the changes of neuronal activity. Proteomic analysis showed there were varied differential proteins in the conditioned media of BMECs, which meant that in the different conditions the MVEC could secrete different active substances that could influence survival of the injured neurons. The results suggested that regulating the paracrine of BMECs could be the important target of the drug action on injured-neurons, which may be a novel path for therapeutic intervention in ischemic injury.

Keywords: Brain microvascular endothelial cells; neuroprotection; Tong Luo Jiu Nao injection; calciumion; proteomics

1 Introduction

In recent 10 years chemical drug and biologic agent, aimed directly at the injured neurons, showed favorable result in preclinical study. However, it was very sorry that the result presented negative or neutral in crucial clinical trial. Besides ambiguous results, none could escape the termination of failure [1]. According to the viewpoint about the blood-brain barrier (BBB), medicine must be transmitted across the BBB to achieve blocking the damage of neurons or improving the function of neurons, but major solutes from circulatory system are prevented from entrying into brain by the BBB [2], only high-liposoluble and micromolecular (＜400-500Da) solutes can be transmitted across the BBB. Macromolecular drugs and biologic agent, such as monoclonal antibodies, recombination proteins, gene therapy, can not be diffused across the BBB [3]. Therefore, permeability of the BBB becomes bottleneck of developing of cerebropathy medicine. A new pathway of medicine action on the brain disease should be explored.

In the previous clinic work, we found that the traditional Chinese medicine had reliable curative effect on the stroke, could effectively reduce neurologic deficit and facilitate functional recovery after stroke. However, it is difficult for the chemical composition of Chinese medicine to transmit across the BBB. Accordingly, we consider there was another pathway to mediate medical effect on neurons in brain. Based on these considerations, we simulated pathology process of cerebral ischemia in vitro, and collected the conditioned media from various cultured brain microvascular endothelial cells (BMECs) groups. Then the conditioned media were added into the culture fluid of the neurons, and the viability, nomadic calcium ion concentration of neurons were determined. We found that the conditioned media of BMECs caused the change of above-mentioned items. We further analyzed differential proteins in conditioned media of various MVEC groups by proteomics techniques. Thus we gained the evidence of the BMECs mediating effect of medicine on the neurons, and proposed the hypothesis that the BMECs might be the important target of the drug action on injured-neurons in ischemic injury.

This work was supported by the Key Project of Chinese Ministry of Education (Grant No. 109023), by the National Program on Key Basic Research Project ("973" Program, Grant No. 2005CB523311).

978-1-61896-030-6

2 Materials and Methods

2.1 Materials

DMEM-H and horse serum were purchased from Gibco-BRL (Gaithersburg, MD). Endothelial cell growth supplement (ECGS), MTT and DMSO, Fluo-3/AM molecule probe were from Sigma (St. Louis, MO). A CytoTox assay kit was from Promega (Madison, WI).

Tong Luo Jiu Nao injections were provided by Kang Yuan Pharmaceutical Engineering Limited Company (Neimenggu, China), which were extracted from the Chinese herbs Panax notoginseng and Gardenia jasminoides. Its main component was determined as geniposide (4.95 mg/ml), ginsenoside (1.02 mg/ml) and geniposidic acid (1.73 mg/ml). The chemical structure of each component and the HPLC analysis spectrum had been described in a previous publication [4].

2.2 Culture and Identification of Rat Brain BMECs

Refering to protocol reported by Baiguera S, et al [5], ten male SD rats(3-4 weeks old) were anesthetized and decapitated, the cerebral hemispheres were quickly isolated. Then surface vessels were removed using a sterile swab applicator, the cerebral cortex were carefully dissected out and finely minced into small pieces. After homogenization the suspension was filtered in turn through the 200μm and 74μm nylon mesh. The microvessels were collected by washing the 74μm mesh, and then were digested with 0.2% coilagenase (in DMEM) at 37°C for 20 min. The microvessels were resuspended in MVEC growth medium and were plated in culture dishes precoated with 0.1% A-gelatin. After becoming a confluent monolayer, cells were passed by splitting with 0.05% Trypsin-EDTA. BMECs were used between passages 3 and 5 in this study. Identification of cells possessing Factor VIII-related antigen was performed by the immunoperoxidase method.

2.3 Primary Culture and Identification of Rat Cortical Neurons

The newborn (in 24 hours) rats were swabbed with 75% ethanol, then were decapitated. The cerebral cortexes were removed and minced into small pieces. The piece was dissociated by using 0.125% trypsin at 37°C for 20 min. The digestion was stopped by DMEM supplemented with 10% FBS, followed by pipetting and passage through a 74μm mesh. The cells were resuspended in complete culture medium (DMEM-H, 3.7 mg/ml NaHCO3, 4.766 mg/ml Hepes, 10% FBS, 10% horse serum, 2 mM L-glutamine, 100 U/ml penicillin and 100 μg/ml streptomycin, pH 7.2-7.4) at a concentration of 1.0×106/ml and seeded on poly-d-lysine-coated Petri dishes and cultured at 37 °C. At day 3, cytarabine was added to the medium to inhibit non-neuronal growth. The medium was changed at 48 hour intervals and the cells at day 12 were used for the experiments. The neurons were identified by immunofluorescence labeling with NSE antibody.

2.4 Collection of the Conditioned Media from BMECs

According to the method of Zhang Wandong, et al [6], the injured model of BMECs was prepared by Oxygen-Glucose Deprivation (OGD). The cells were exposed to sugar-free Krebs solution (NaCl 6.9 g, KCl 0.35 g, KH2PO4 0.16 g, NaHCO3 2.1g, CaCl2 0.28 g, MgCl2 0.2 g, dissolved into 1 L water, pH 7.3) in 93% N2 and 7% CO2 environment for 6 hours. The BMEC-culture medium was replaced with serum-free medium, and the supernatant fluids of cells were harvested as conditioned media after six hours. Four kinds of conditioned media from BMECs in various culture conditions were harvested: (1) conditioned medium from normal BMECs (N-CM), which were normally cultured without treatment; (2) conditioned medium from normal BMECs treated with TLJN (NT-CM) for 10 hours at a concentration of 2 μl/ml (which is the optimal concentration of TLJN determined in a previous study); (3) conditioned medium from OGD-injured BMECs (I-CM); (4) conditioned medium from OGD-injured BMECs treated with TLJN (IT-CM) at a concentration of 2 μl/ml for 10 hours.

2.5 Groups and Treatment of Neurons

A group of neurons were cultured in 100% neuron culture medium as normal control. The other neurons were injured by Oxygen-Glucose Deprivation according to the method of Tauskela et al [7]. and then divided into groups. Injured neurons were cultured respectively in 100% neuron culture medium as model control, in N-CM, in NT-CM, in I-CM, in IT-CM (the neuron culture medium to BMEC-conditioned medium ratio was 1:1). The neurons were cultured for 12 h for the following experiments.

2.6 MTT Assay

The neuronal mitochondrial activity was determined by MTT assay. About 5,000 normal or injured neurons/well were plated in a 96-well plate and incubated with a mixture of neuron culture media and various rBMEC-cultured media (at a 1:1 ratio). After a 12 hour culture, 10 μL of MTT wor 4 hours at 37 °C, 100μl DMSO was added to each well. The absorbance of each well was measured using a microculture plate reader with a test wavelength of 570 nm.

2.7 Lactate Dehydrogenase Assay

A CytoTox assay kit (Promega, Madison, WI) was used for enzymatic assessment of LDH release, following the manufacturer's instructions. The neurons were cultured for 12 hours as described above and medium was replaced with serum-free medium for further culturing for 24 hours. Fluorescence emission at 590 nm was measured with a Safire plate reader (Tecan, Switzerland). LDH leakage rate was expressed as the result of the following equation: LLR = (OD value of the supernatant of the medium/OD value of the supernatant of lysed cells) × 100%.

2.8 Measurement of Intracellular Calcium

Measurement of intracellular calcium in cultured neurons was performed as previously described [8]. Neurons were loaded with fluorescent dye fluo-3/AM (Molecular Probes, OR, USA) at a concentration of 10 μmol/L, supplemented with 0.0025% pluronic acid, and kept in the dark for 50 min. Then the cells were washed with D-Hanks' solution 2 times and kept in the dark for a further 20 min before fluorescence was measured. The cells were subjected to Ca^{2+} imaging with an Argus-20 fluorescent imaging processor (BMG Lab Technologies, Offenburg, German), with an excitation wavelength of 485 nm and an emission wavelength of 520 nm.

2.9 Compared Proteomic Analysis of Various BMECs Conditioned Media

To further explore the molecular basis of BMECs conditioned media exerting different effects, the differential proteins in two pair of the conditioned media, N-CM and I-CM, I-CM and IT-CM were analyzed and identified using unidimensional SDS-PAGE and the nano-liquid chromatography electrospray ionization tandem spectrometry (nanoLC-ESI-MS-MS) association technology.

At first the salts in the conditioned media were removed by dislysis, then the samples were condensed, and total quantities of protein were determined by Bradford. The samples were evaluated by means of SDS-PAGE and silver staining. If they are qualified, the proteins of samples were separated by SDS-PAGE and stained with Coomassie brilliant blue. Gray scale of the protein straps were quantitatively analyzed with scanning software ImageQuant (version 5.2, Amersham Bio-sciences). According to the result of image analysis, the difference straps were cut and treated with the process of reduction, alkylation, in-gel digestion and peptide extraction. Finally differential proteins were identified with nanoLC-ESI-MS-MS. Through the SWISS-PROT database retrieval, each protein's related information was searched for and then analyzed.

2.10 Statistical Methods

All measures were summarized as mean ± SD. The data were analyzed with the SPSS 10.0 statistical package. One-way analysis of variance (ANOVA) was used to determine statistically significant differences among the groups. A P-value of <0.05 was considered statistically significant.

3 Results

3.1 Change of Neuronal Mitochondrial Activity

The MTT assay was used to detect the mitochondrial activity of neurons. As shown in Table.1, the OD value in the model control was significantly decreased compared with the normal control, indicating that viability of the neurons was decreased by OGD. Compared with the model control, the OD values in N-CM and NT-CM groups were increased, which indicates that N-CM and NT-CM can improve the viability of the injured neurons, and the effect of NT-CM was more significant than that of N-CM (P<0.05). The OD value in the I-CM group was significantly decreased, which indicates that I-CM can further aggravate the damage of neurons. Compared with the I-CM group, the OD value in the IT-CM group was significantly increased (P<0.05).

Table 1. Changes of activity of neurons

groups	n	OD value
Normal control	6	0.295±0.047
Modle control	6	0.248±0.024*
N-CM	6	0.274±0.045
NT-CM	6	0.284±0.022#
I-CM	6	0.205±0.033#
IT-CM	6	0.254±0.024△

*P< 0.05 versus normal control group; # P< 0.01 versus model group; △P< 0.05 versus I-CM group.

3.2 Change of Neuronal LDH Leakage Rate

The degree of neuronal injury was determined by measuring the LDH leakage rate. As shown in Table. 2, the LDH release of the model control was significantly increased. N-CM as well as NT-CM, especially NT-CM, could reduce the leakage of LDH in injured neurons (P<0.05, P<0.01). The LDH leakage rate increased in the I-CM group (P<0.05), and that in the IT-CM group was significantly decreased compared with I-CM (P<0.05).

978-1-61896-030-6 © 2012 SciRes.

Table 2. Changes of leakage rate of LDH in neurons

groups	n	LDH leakage rate
Normal control	6	0.289±0.015
Modle control	6	0.335±0.024**
N-CM	7	0.311±0.016#
NT-CM	6	0.306±0.012##
I-CM	6	0.381±0.040#
IT-CM	6	0.315±0.016△

**P< 0.01 versus normal control group; # P< 0.05, # # P< 0.01 versus model group; △P< 0.05 versus I-CM group.

3.3 Change of Neuronal Ca^{2+} Concentration

Neuronal cytoplasmic Ca^{2+} was labelled by the fluorescent dye fluo-3/AM. As shown in Table. 3, the concentration of Ca^{2+} in the model control group was significantly increased compared with that of the normal control group, which suggests that OGD induced a calcium overload in neurons. N-CM and NT-CM reduced the concentration of Ca^{2+} in neurons, and the decrease induced by NT-CM was more significant than that induced by N-CM (P<0.05). Compared with the model control, the fluorescence value was increased in the I-CM group (P<0.05), suggesting that injured BMEC paracrine signals could further deteriorate the calcium overload in neurons. Compared with I-CM, the fluorescence value decreased in the IT-CM group (P<0.01), indicating that the calcium overload induced by injured BMEC paracrine signaling could be alleviated by the intervention of TLJN.

Table 3. Changes of [Ca2+]i in neurons

groups	n	fluorescence value
Normal control	10	31.23±5.61
Modle control	9	42.26±7.37***
N-CM	9	41.65±8.69
NT-CM	8	36.08±5.37#
I-CM	9	47.32±5.32
IT-CM	9	36.06±8.09#△△

***P< 0.01 versus normal control group; # P< 0.05 versus model group; △△P< 0.01 versus I-CM group.

3.4 Compared Proteomics Study on Various BMECs Conditioned Media

Glue image of silver staining showed that the protein of samples was successfully separated by SDS-PAGE. There were difference straps presented clearly among four samples. Then the samples were divided into two groups: group A including N-CM and I-CM, group B including I-CM and IT-CM. Paired samples were detected and analyzed. According to the result of image analysis, four significant different straps were cut, further identified with nanoLC-ESI-MS-MS.

There were altogether 103 differential proteins identified in group A of samples (N-CM and I-CM). Among them, 70 proteins only appeared in N-CM and 33 proteins in I-CM. There were altogether 64 differential proteins identified in group B of samples (I-CM and IT-CM). Among them, 35 proteins appeared in I-CM and 29 proteins in IT-CM. Subcellular localizations of these proteins were listed as follows: Secretion protein, cellular membrane, cytoplasma, cellular nucleus, cell organ, or unknown. The percentage of secretion protein in group A and B is 15.4%, 16.2% respectively. The functions of these differential proteins is involve in many aspects like energy metabolism, the protein synthesis and degradation, oxidative stress, the signal conduction, DNA transcription and repairing after damage as well as cell growth and proliferation, and so on. Fig. 1A shows functional classification of proteins identified in A group of samples (N-CM and I-CM). Fig. 1B shows functional classification of proteins identified in B group of samples (I-CM and IT-CM).

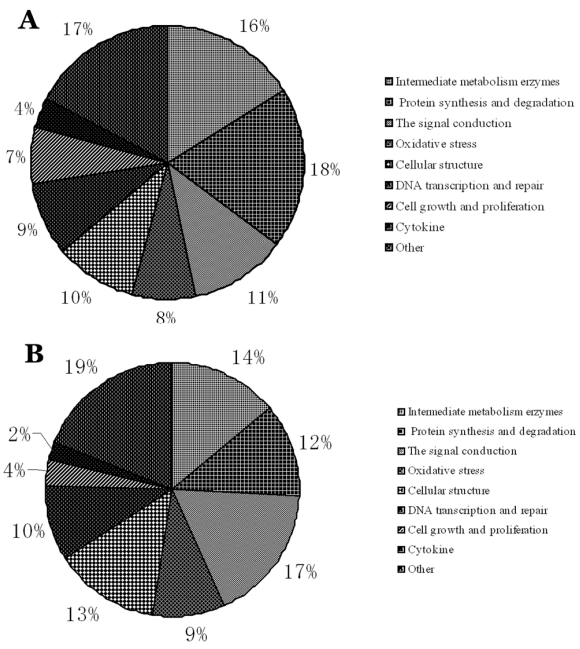

Figure 1. Functional classification of differential proteins in BMECs media

4 Discussion

Homeostasis of brain depends on cooperation of the central nervous system and the circulation of blood. However, traditionally nervous system and blood vessel system were often isolated to research. The blood-brain barrier (BBB) may be unique integrating site of both, and is principally researched as a mechanical isolation barrier

in drug transport system. Nowadays study of drug transport involves in carrier-mediated transmembrane transport (CMT) and receptor-mediated transmembrane transport (RMT). Relative carriers include organ anion-transporter, P-glucoprotein, multidrug resistance protein, nucleoside transporter and macromolecule amino acid transporter. Relative receptors include transferrin receptor, scavenger receptor et al [9]. Nevertheless ideal pathway of drug transmembrane transport is not obtained. The BBB is a dynamic door possessing powerful biological function, some of which may be undiscovered. Studying the BBB only from the angle of barrier function inhibited the research of drug effect on cerebropathy. Recently the conception of neurovascular unit (NVU), which is a functional unit formed by the tight contact of MVEC, astrocyte and neuron, was introduced in study of cerebropathy [10]. According to this theory, inter-cell tight contact and information transfer regulate homeostasis of internal environment in brain. Functional disorder of NVU could lead to occurrence of cerebral vascular diseases. Thus inter-cell information communication has been paid attention by more and more people.

Previous studies showed that the traditional Chinese medicine had reliable curative effect on the cerebropathy, but it is difficult for the chemical composition of Chinese medicine to transmit across the BBB. From this phenomenon we presume that the Chinese medicine could regulate the paracrine secretion of the brain BMECs, then through information transfer of active factors to achieve to resist damage of neurons. From the study we obtained the important conclusion that the MVEC could secrete some active substance that could influence survival of the neurons, internal mechanism involves in regulating calcium overload and mitochondrium function of neuron. Tong Luo Jiu Nao Injuction, through altering secretion function of BMECs, achieve to improve the damage of neunous. Main manifestation include: (1) N-CM displayed protective effect on the survival of injured neuron, especially NT-CM on injured neuron; (2) I-CM could further aggravate the damage of neurons. While IT-CM did not display this harmful effect; (3) Increased concentration of $[Ca^{2+}]i$ in model group suggested OGD led to calcium overload. N-CM and NT-CM reduced the concentration of $[Ca^{2+}]i$ in the neurons. IT-CM significantly reduced the concentration of $[Ca^{2+}]i$ in the neurons compared with I-CM, which suggested the effect of IT-CM is significant in the respect of reducing the concentration of $[Ca^{2+}]i$.

Analysis of compared proteomics showed protein composition of various conditional media presented significantly difference, which provided the information of function factor involved in various effects of the MVEC. According to the result of compared proteomics, we consider that the effect of the MVEC on the neuron is a multi-molecular event accompanying the changes of many proteins; some of them are possible key proteins during the pathophysiological change, while some other proteins may be accompanying changes of the key proteins. The BMECs brought about protective function on the injured neurons, meanwhile the function proteins expressed by BMECs happened to change, which suggested that the protective function of BMECs may be relative with the change of proteins. Now we initially have gained some significant information from the proteomic results. For instance, Urocortin-2, a cortical hormone, can enhance the tolerance of cells to sugar deficiency in the stress state, and relieve the inflammatory reaction. In this study Urocortin-2 was identified in IT-CM, but not in N-CM and I-CM, which suggests that Urocortin-2 is possibly one of the factors blocking the decrease of viability of neurons. Qur following works should be continued to verify the existence and function of these interested proteins, the result of study will be reported in time.

Therefore, in the process of pathological change the BMECs are not only passive target cells, but also effector organ possessing complicated function, and have important influence on circumambient nerve cells. On one hand, secretion of normal BMECs has a tendency to protect the injured neurons, Tong Luo Jiu Nao Injuction can enhance this action. On the other hand, once the BMECs are damaged, they could generate some active substance, which could directly poison neurons. This conclusion is similar to one of Betz Al [11]. Tong Luo Jiu Nao Injuction can significantly relieve this poisonous effect of the BMECs and indirectly protect the injured neurons. So we consider the MVEC may be the important target of the drugs, mediating drug effect on brain diseases. This conclusion may provide a new pathway for the study of drug effect on brain diseases.

Acknowledgement

This work was supported by the Key Project of Chinese Ministry of Education (Grant No. 109023), by the National Program on Key Basic Research Project ("973" Program, Grant No. 2005CB523311).

References

[1] L. A. Labiche, J. C. Grotta, "Clinical Trials For Cytoprotection In Stroke". *The American Society for Experimental NeuroTherapeutics*, Vol. 1, No. 1, 2004, pp. 46-70.

[2] M. A. Petty, E. H. Lo, "Junctional complexes of the blood-brain barrier: permeability changes in neuroinflammation". *Progress in Neurobiology*, Vol. 68, No. 5, 2002, pp. 311-323.

[3] W. M. Pardridge, "The Blood-Brain Barrier: Bottleneck in Brain Drug development". *The American Society for Experimental NeuroTherapeutics*, Vol. 1, No. 2, 2005, pp. 3-14.

[4] Q. Hua, X. Qing, P. Li, W. Li, J. Hou, J. Hu, Q. Hong, P. Sun, X. Zhu, "Brain microvascular endothelial cells mediate

neuroprotective effects on ischemia/reperfusion neurons". *Journal of Ethnopharmacology*, Vol. 129, No. 3, 2010, pp. 306-313.

[5] S. Baiguera, MT. Conconi, D. Guidolin, "Ghrelin inhibits in vitro angiogenic activity of rat brain microvascular endothelial cells". *International Journal of Molocular Medicine*, Vol. 14, No.5, 2004, pp. 849-854.

[6] W. Zhang, C. Smith, A. Shapiro, R. Monette, J. Hutchison, D. Stanimirovic, "Increased expression of bioactive chemokines in human cerebromicrovascular endothelial cells and astrocytes subjected to simulated ischemia in vitro". *Journal of Neuroimmunology*, Vol. 101, No.2, 1999, pp. 148-160.

[7] J. S. Tauskela, G. Mealing, T. Comas, E. Brunette, R. Monette, D. L. Small, P. Morley, "Protection of cortical neurons against oxygen-glucose deprivation and N-methyl-D-aspartate by DIDS and SITS". European Journal of Pharmacology, Vol. 464, No.1, 2003, pp. 17-25.

[8] W. Li, P. Li, Q. Hua, J. Hou, J. Wang, H. Du, H. Tang, Y. Xu, The impact of paracrine signaling in brain microvascular endothelial cells on the survival of neurons. Brain Research, Vol. 1287, No. 9, 2009, pp. 28-38.

[9] W. M. Pardridge, R. J. Boado, K. L Black, P. A. Cancilla, "Blood-Brain Barrier and New Approaches to Brain Drug Delivery". The Western Journal of Medicine, Vol. 156, No.3, 1992, pp. 281-286.

[10] J. H. McCarty, "Cell biology of the neurovascular unit: implications for drug delivery across the blood-brain barrier". ASSAY and Drug Development Technologies, Vol. 3, No. 1, 2005, pp. 89-95.

[11] A. l. Betz, "Alterations in cerebral endothelial cell function in ischemia", Advance in Neurology, Vol. 71, 1996, pp. 301-311.

A Study on the Germination Characteristics Differences of Ligusticum Seeds in Different Harvest Period

Jing TANG, Meng YE
College of Forest and Horticulture, Sichuan Agricultural University, Sichuan, China
Email: 1027905227@qq.com, yemeng5581@yahoo.com.cn

Abstract: The influence on germination characteristics of Ligusticum seed in four harvest time had been studied in this paper. The results showed that germination characteristics of Ligusticum seeds were significant differences in four harvest period. The seeds picked on October 15th had no germinating ability; the seeds picked on October 20th had germinating ability. To germinate the Ligusticum seeds in the dish of the four harvest periods, we discovered that seeds picked on October 25th was above 4 periods better on the germination rate, germination energy and germination index, germination rate was 36.67%, 15.34% higher than October 30th, 26.67% than October 20th; germination energy was 30%, 15% higher than October 30th, 12% than October 20th; germination Index was 11.98%, 4.59% higher than October 30th, 9.32% than October 20th. These results suggested that Ligusticum seeds germination rate would be increased in timely harvest period.

Keywords: Ligusticum; harvest period; germination characteristics

1 Introduction

Ligusticum(Ligusticum L, Umbelliferae), Liao Ligusticum(Ligusticum L, Umbelliferae)and Xinjiang Ligusticum(Conioselinum, Umbelliferae) are traditional Chinese herb whose rootstalk are used in oriental medicine for the treatmeat of cold, parietal headache, rheumatic limb bitong and alpine abdominal pain. Two Ligusticum, namely China and the Liao Ligusticum are collected in Chinese Pharmacopoeia of 2005 edition,which have the efficacy Of inhibition , bulk cold and pain dampness[1]. The study of Ligusticum mainly focused on the chemical composition and pharmacology, but the germination characteristics of Ligusticum rarely reported. Study confirmed that the main chemical components of Ligusticum as terpenes, phthalides, allyl benzene, coumarins, sesquiterpene Bisabolol ketones and other types of physiologically active substances[2-9]. As a broad-spectrum traditional Chinese medicine, because of the long-term excavation, Ligusticum which mainly based on wildlife rarelv cultivated is difficult to meet the market demand[10]. The germination of Ligusticum seeds research characteristics is particularly important, it can be improved to some extent, the number of Ligusticum seedlings, and tubers can be reduced as part of the use of Ligusticum that mainly by asexual reproduction. Therefore, this important development and use value, and concern has been extensively studied. This paper by studying three indicators of germination rate, germination energy, germination index and discount rate of dry in four harvest period(Which represents the amount of dry matter accumulation in different periods), then identify the characteristics of different harvest time difference between the germination by using significant analysis of the application.

2 Materials and Methods

2.1 Sampling Sites

It that locates in Yaan, Liangshan, Meishan and Leshan City at the junction of four and calls Yongsheng Township Jinkouhe District in Leshan City stands in southwest Sichuan, Emei Mountain, a small cold mountain hinterland, with elevation 1647m, (E103° 04.299 ", N29° 22.954"), the average annual temperature is 16.3℃, the average annual rainfall 946mm, a typical dry-hot valley climate.

2.2 Test Materials

Based on the Color of Ligusticum seed, traditional harvest period of it was in mid-October to early November. The experimental seeds picked in the traditional harvest period in four times, time interval was five days, seed respectively picked on October 15th (Denoted by Harvest period Ⅰ), October 20th (Denoted by Harvest periodⅡ), October 25th(Denoted by Harvest periodⅢ) and October 30th(Denoted by Harvest period Ⅳ). and then dried the seed in the shade with ventilation. Seeds of four different harvest periods stored in the refrigerator 5℃ after harvest with initially removing of impurities, were collecting from annual plants in Yongsheng Township Jinkouhe District.

The first phase of seeds (HarvestingⅠ): Green

978-1-61896-030-6

double-hanging fruit seeds, with many filaments, was still tightly together long picked on October 15th, 2010.

The second phase of seeds (Harvesting Ⅱ): The seeds of double-hanging fruit that few filaments attached to has basically been separate, seeds picked on October 20th, 2010 had turn yellow-green.

The third phase of seeds (Harvesting Ⅲ): Seeds is no longer present state of double-hanging fruit, but performances pale yellow and fruit of separation harvesting on October 25th, 2010.

The fourth phase of seeds (Harvesting Ⅳ): Picking on October 30th, 2010, Seeds has appeared on tan falling off naturally.

2.3 Test Methods

2.3.1 Seeds Treatments

Seeds with pellet full and the same size of Ⅰ, Ⅱ, Ⅲ, Ⅳ period 150 each grain (3 replicates, each repeated 50) is for germination test of 25℃ after 0.5% $KMnO_4$ disinfection 30min, distilled water rinsed in dishes of moist single filter paper. The total germination time needs 20days from December 9, 2010 to December 29. Adding distilled water every day for the seeds during the test, germinated grains daily statistics from the sixth day (White radicle reaching half length of seed is the standard of germination). Germination rate: It is the percentage that normal germination of seeds in the total number of tested seeds with the 20days.

Germination energy: It is the percentage that normal germination of seeds in the total number of tested seeds in 13days reaching the peak of seed gemination.

Germination index:

GI =Σ (Gt/Dt) (Gt is the number of germination in day t; Dt the number of days to germination). (1)

2.3.2 Measurement of Seeds in Physical Parameters

Determination of TKW (Thousand Kernel Weight):It is the average weight multiplied by 10 of the seeds that is dry in the shade of 100 in the eight times weighing in the One over ten thousand electronic balance by using one hundred weighing method[11].

Determination of discount rate of dry: Accumulation of nutrients in four harvest periods is measured by using Low temperature drying method [11].

Formula:

Water content=$(M_2-M_3)/(M_2-M_1)\times100\%$ (2)

M_1: the weight of sample box and lid (g)

M_2: the weight of sample box, lid and seeds before drying (g)

M_3: the weight of sample box, lid and seeds after drying (g)

The rate of dry matter accumulation=(1-Water content)×100% (3)

2.4 Data Handling

Use the Statistical software of SPSS 11.5, and then do significant analysis with Duncan.

3 Results and Analysis

3.1 TKW and Dry Matter Accumulation of Ligusticum Seeds in Four Harvest Periods

TKW and the rate of dry matter accumulation is different in four harvest periods through the figure 1 and figure 2. TKW of Ligusticum seeds is gradually rising trend With the extension of the harvest time, TKW in October 30th is the heaviest is 1.3350g, 0.3570g higher than that of October 25th, 0.7401g than October 20th and 1.0211g than October 15th.

It performances a gradually rising trend with the extension of the harvest time in aspects of dry matter accumulation. However, it is down in October 25th whose rate of dry matter accumulation is 73.2%, 1.7% higher than October 30th, 4.3% than October 20th and 4.6% than October 15th.It states that the rate of dry matter accumulation is the most in October 25th.

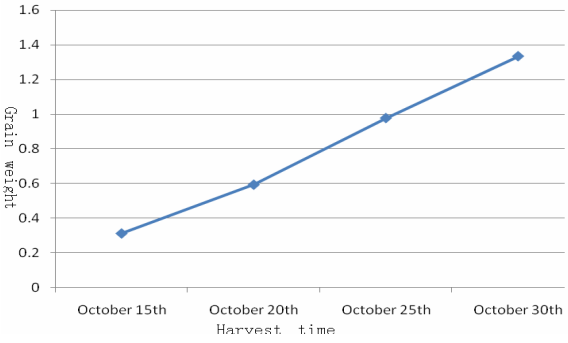

Figure 1. The change of TKW of Ligusticum seeds in different harvest periods

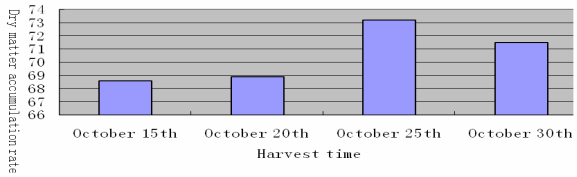

Figure 2. The change of the rate of dry matter accumulation of Ligusticum seeds in different harvest periods

3.2 The Influence of the Germination Process of Ligusticum Seeds in Different Harvest Periods

Harvest period plays a important part in the germination of Ligusticum seeds. Germination process appears clear differences in four harvest time, seeds on October 30th regardless of the length of time, will not germinate, which is possible due to the lack of nutrition matter accumulation that meets the need of germination. Seeds of the other 3 periods basically finish germination in 16 days. The peak of germination of October 25th is in 16d (18.3 grain), October 30th in 17d (10.7 grain),and October 20th in 15d (5 grain).The process of germination of seeds on October 25th that is the fast is present state of rising sharply from the outlook analysis of the four curves. Relatively, the curves of October 20th and October 30th are gentle, and the process of germination is relatively slow. Variance analysis showed that seeds of four periods all reached significant difference ($p<0.05$). These phenomena explains that the germination rate will rising in the appropriate period, however, it will slow down the germination rate in the harvest periods which is too late or early.

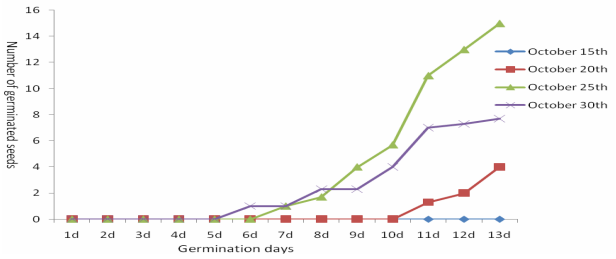

Figure 3. The germination process of Ligusticum seeds in different harvest periods

(for a total of 50 grain sprout)

3.3 The Influence of the Germination Condition of Ligusticum Seeds in Different Harvest Periods

3.3.1 The Influence of the Germination Rate Ligusticum Seeds in Different Harvest Periods

The germination of October 25th is 36.67% through Table 1.seeds of October 15th will not germinate, which is possible due to the lack of nutrition matter accumulation that meets the need of germination. Test results show that the average germination rate of October 25th is significantly higher than the rate of October 30th, October 20th and October 30th, October 30th significantly higher than the rate of October 20th and October 15th, October 20th and October 15th had reached a significant level. Pairwise comparison reached a significant level.

Table 1. Germination rate multiple comparison results

(the method of SSR)

Harvest period after flowering（d）	The average of germination rate（%）	Significant level of 5%	Significant level of 1%
October 25th	36.67	a	A
October 30th	21.33	b	B
October 20th	10.00	c	C
October 15th	0	d	D

Recording: Letters of different present significant, same is no significant (Lowercase letters $p < 0.05$, significant; Capital letters $p < 0.01$, extremely significant.)

3.3.2 The Influence of the Germination Energy Ligusticum Seeds in Different Harvest Periods

The germination energy of October 25th which is 15% higher than October 30th, 12% than October 20th is the highest in the four harvest periods. It expressed that germination uniformity of the seeds showed a high degree. The germination energy of October 15th is 0 because of no germination. Results show that the average germination energy of October 25th is significantly higher than the rate of October 30th and October 15th, higher than October 20th. October 30th is significantly higher than October 15th, but no significant difference with October 20th. The germination of October 20th and October 15th is not significant.

Table 2. Germination energy multiple comparison results

(the method of SSR)

Harvest period after flowering（d）	The average of germination energy（%）	Significant level of 5%	Significant level of 1%
October 25th	30.00	a	A
October 30th	15.00	b	B
October 20th	8.00	b	B
October 15th	0	c	C

Recording: Letters of different present significant, same is no significant(Lowercase letters $p < 0.05$, significant; Capital letters $p < 0.01$, extremely significant.)

3.3.3 The Influence of the Germination Index Ligusticum Seeds in Different Harvest Periods

the germination index of October 25th which is 4.59% higher than October 30th, 9.32% than October 20th is the highest in the four harvest periods. The average germination index of October 25th is significantly higher than that of October 30th, October 20th and October 15th. October 30th is significantly higher than October 20th and October 15th. The difference between October 20th and October 15th is in the significance level of 0.05.

978-1-61896-030-6 © 2012 SciRes.

Table 3. Germination index multiple comparison results
(the method of SSR)

Harvest period (d)	The average of germination index (%)	Significant level of 5%	Significant level of 1%
October 25th	11.98	a	A
October 30th	7.39	b	B
October 20th	2.66	c	C
October 15th	0	d	CD

Recording: Letters of different present significant, same is no significant(Lowercase letters $p < 0.05$, significant; Capital letters $p < 0.01$, extremely significant.)

4 Results and Discussion

4.1 TKW and the Rate of Dry Matter Accumulation

TKW is different in four harvest periods, TKW of Ligusticum seeds tends rising gradually. With the extension of the harvest time the seeds is in the completion of the accumulation of nutrients. The rate of dry matter accumulation of October 25th is preferable. Results directed that it is not good for germination because of the lack or loss of nutritional substances accumulation or loss in the harvest time which is too early or late.

4.2 The Influence of the Germination Process

Seeds of October 15th did not germinate in 20days, which is possible due to the lack of nutrition matter accumulation that meets the need of germination. The peak of germination of October 25th is in 16days (18.3 grain), October 30th in 17 days (10.7 grain),and October 20th in 15days (5 grain). The process of seeds germination of October 25th that is the fast is present state of rising sharply from the outlook analysis of the four curves. Relatively, the curves of October 20th and October 30th are gentle, and the process of germination is relatively slow.

4.3 The Difference of the Seeds in Germination rate, Germination Energy and Germination Index

The germination rate of Ligusticum seeds in four collection periods are extreme significant positive correlations ($p<0.01$). The seeds collected on October 25th get the highest position on germination rate, germination energy and germination index, is respectively 36.67%, 30%, 11.98%, the index of the three of October 15th that is the lowest is 0, October 30th which is in the second location is separately 21.33%, 15%, 7.39%, October 20th in the third location is separately 10%, 8%, 2.66%. The results of this study show that germination characteristics of Ligusticum seeds can be increased in the appropriate harvest period. The harvest period in this paper is October 25th when the germination rate, germination energy and germination index are preferable. It has some theoretical guidance in improving the number of Ligusticum plants when the definition of the harvest period. Simultaneously, it can save the resources of rootstalk of Ligusticum plants to be used as medicine.

References

[1] State Pharmacopeia Committee of China, The pharmacopoeia of PRC, Chemical Industry Press,Beijing. 2004: 263.
[2] Huang Yuanzheng,Fu Fading.Essential oil chemical composition analysis of the plants of Ligusticum L,Journal of Pharmacetical Analysis, 1989, 9(3):147-151.
[3] Xi Yugui,Sun Jieming ,Li Weiming. Studies on the Chemical Constituents of Ligusticum sinensis Olive, Chinese Herbal Medicine, 1987, 18(2): 6-7.
[4] Zhang Jinlan,Zhou Zhihua,Chen Ruoyun. Study on chemistry and pharmacology of genus Ligusticum, Chinese Pharmaceutical Journal, 2002, 37(9): 654-657.
[5] Zhang Jinlan,He Xiufeng, Zhou Zhihua. HPLC Determination of five constituents in plants of genus Ligusticum,Acta Pharmaceutica Sinica, 1996, 31(8): 622-625.
[6] YU DQ,Chen RY,Xie FZ. Structure Elucidation of Ligustilone from Ligusticum Sinensis Oliv, Chinese Chem Lett, 1995, 6(5): 391.
[7] Yu DQ, Xie FZ, Chen RY,et al.. Studies on the structure of ligustiphenol from Ligusticum sinense Oliv. Chin Chem Let t. 1996. 7: 721.
[8] Huang Yanhe, Yu Dequan. Studies on the Synthesis of dl-Ligustiphenol and its analogues, Acta Pharmaceutica Sinica, 1997, 32(9): 675-681.
[9] Dai Bing.Comparison of chemical constitvents of essential oil from four species of Ligusticum by GC-MS analysis, Acta Pharmaceutica Sinica, 1988, 23 (5): 361-369.
[10] Ding Liwei.The present situation of production and marketing hind city analysed of Ligusticum, Special Economic Animal and Plant, 2010, 12.
[11] Zheng Guanghua. Seed physiology studies, Science Publishing Company,Beijing, 2004, 4.

Flavonol Glycosides and Its Antioxidant Activity from the Flower of *Siraitia grosvenorii*

Yueyuan CHEN[1], Dianpeng LI[1], Fenglai LU[1], Tsuyoshi Ikeda[2], Toshihiro Nohara[2]
[1]*Guangxi key Laboratory of Functional Phytochemicals Research and Utilization, Guangxi Institute of Botany, Guangxi Zhuangzu Autonomous Region and Chinese Academy of Science, Guilin, China, 541006*
[2]*Faculty of Medical and Pharmaceutical Science, Kumamoto University, 5-1 Oe-honmachi, Kumamoto, Japan, 862-0973*
Email: phytoldp @ hotmail.com

Abstract: Ten flavones were isolated from the flower of *Siraitia grosvenori*. Their Structures were established by spectroscopic and chemical methods and by comparison with authentic samples. Their structures were identified as: 3-O-β-D-glucopyranosyl kaempferol 7-O-[β-D-glucopyranosyl-(1→2)-α-L-rhamnopyrano-side] (1), 7-O-α-L-rhamnopyranosyl kaempferol 3,4'-di-*O*-β-D-glucopyranoside (2), 3-*O*-α-L-rhamnopyranosyl kaempferol 7-*O*-[β-D-glucopyranosyl(1-2)-α-L-rhamnopyranoside](3), kaempferol 3,7-*O*-α-L-dirhamnopyranoside(4), kaempferol-7-*O*-α-L–rhamno-pyranoside(5), 7-methoxyl kaempferol 3-*O*-β-D-glucopyranoside (6), 7-methoxyl kaempferol 3-*O*-α-L-rhamnopyranoside (7), 3-*O*-β-D-glucopyranosyl kaempferol 7-*O*-α-L-rhamnopyranoside (8), kaempferol 3-*O*-α-L-rhamnopyranoside (9), kaempferol (10). This is the first time that these compounds are reported from the plant. All compounds were evaluated for antioxidant activity using FRAP and TEAC assays, where compound 2, 5, 10 proved to possess the most potent activity.

Keywords: *Siraitia grosvenori*; flavonol glycosides; antioxidant activity

1 Introduction

Siraitia grosvenorii SWINGLE (formerly Momordica grosvenori SWINGLE), a traditional Chinese fruit, belongs to Cucurbitaceae and has been used as a pulmonary demulcent and emollient for the treatment of dry cough, sore throat, dire thirst, and constipation in folk medicine [1]. The flower of S. grosvenori is usually used as a tea in China, being drinked with hot water or mixed with green tea. It can smooth dry throat and comfort intestine [2]. Previously we have obtained a number of cucurbitane triterpene saponins from the fruits [3-4]. In our serial studies on this plant, we present herein the isolation and characterization of the ten flavonols from the flower of S. grosvenori (Fig. 1). This is the first time that these compounds are reported from the plant. At the same time, biological evaluation for antioxidant activities of compounds **1—10** were carried out using the FRAP (Ferric reducing ability of plasma) and TEAC (Trolox equivalent antioxidant capacity) assays. Details of the isolation, structure elucidation, and antioxidant properties of these compounds are discussed in this paper.

2. Result and Discussion

2.1 Phytochemical Study

Fresh flower of S. grosvenori were extracted with methanol. A suspension of methanol-extract in water was subjected to a highly-porous polystynene gel, Diaion HP-20, which was successively eluted with H_2O and 30%, 80%, and 100% methanol. The 80% MeOH-eluted fraction was chromatographed on silica gel. The obtained fractions were further purified by Sephadex LH-20, normal and reverse-phase silica gel to afford ten flavonol glycosides (Fig.1).

Compound 1-10 are kaempferol glycosides. Comparing the H and C –NMR data (TABLE 1) with the literature values [5-14], they were determined as : 3-O-β-D-glucopyranosyl kaempferol 7-O-[β-D-glucopyranosyl-(1→2)-α-L-rhamnopyranoside] (**1**), 7-O-α-L-rhamnopyranosyl kaempferol 3,4'-di-*O*-β-D-glucopyranoside (**2**), 3-*O*-α-L-rhamnopyranosyl kaempferol 7-*O*-[β-D-gluco-pyranosyl-(1-2)-α-L-rhamnopyranoside] (**3**), kaempferol 3,7-*O*-α-L-dirhamnopyranoside (**4**), kaempferol-7-*O*-α-L-rhamnopyranoside (**5**), 7-methoxyl kaempferol 3-*O*-β-D-glucopyranoside (**6**), 7-methoxyl kaempferol 3-*O*-α-L-rhamnopyranoside (**7**), 3-*O*-β-D-glucopyranosyl kaempferol 7-*O*-α-L-rhamnopyranoside (**8**), Kaempferol 3-*O*-α-L-rhamnopyranoside (**9**), kaempferol (**10**).

978-1-61896-030-6

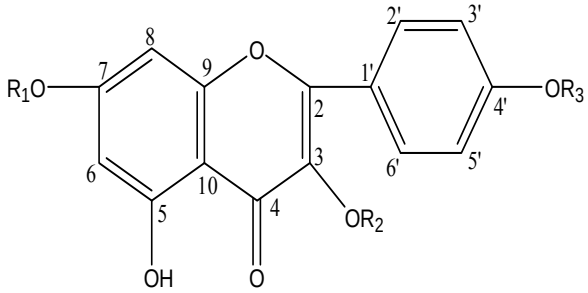

	R_1	R_2	R_3		R_1	R_2	R_3
1	-Rha(2←1)Glc	-Glc	-H	**6**	-CH3	-Glc	-H
2	-Rha	-Glc	-Glc	**7**	-CH3	-Rha	-H
3	-Rha(2←1)Glc	-Rha	-H	**8**	-Rha	-Glc	-H
4	-Rha	-Rha	-H	**9**	-H	-Rha	-H
5	-Rha	-H	-H	**10**	-H	-H	-H

Figure 1. The structures of 1-10

Table 1. ^{13}C-NMR data for compound 1-10 from the flower of *Siraitia grosvenori* (DMSO-d_6)

C NO.	1	2	3	4	5	6	7	8	9	10
2	158.6	156.1	156.1	156.0	156.1	156.2	156.4	155.9	156.1	146.8
3	134.6	134.1	134.6	134.5	134.5	133.2	134.4	133.5	134.5	135.6
4	177.9	177.7	177.9	177.9	177.9	177.4	177.9	177.4	177.9	175.9
5	160.9	160.9	160.9	160.9	160.9	161.2	160.9	160.8	160.9	160.7
6	99.6	99.4	99.5	99.4	98.7	98.6	97.9	99.3	98.7	98.2
7	162.4	161.7	161.4	161.7	164.1	165.0	165.2	161.6	164.1	163.9
8	94.6	94.6	94.6	64.5	93.6	93.6	94.4	94.4	93.6	93.4
9	157.0	156.2	157.7	157.7	156.7	156.8	157.5	156.7	156.7	156.2
10	106.4	105.8	105.8	105.7	105.8	103.8	105.1	105.6	105.8	103.0
1’	121.6	123.6	120.3	120.3	120.3	120.8	120.4	120.7	120.3	121.7
2’	131.3	130.7	130.6	130.6	130.6	130.8	130.6	130.9	130.6	129.5
3’	115.0	115.9	115.4	115.3	115.4	115.0	115.4	115.1	115.4	115.4
4’	160.4	159.4	160.1	160.1	160.1	159.9	160.1	160.0	160.1	159.2
5’	115.0	115.9	115.4	115.3	115.4	115.0	115.4	115.1	115.4	115.4
6’	131.3	130.7	130.6	130.6	130.6	130.8	130.6	130.9	130.6	129.5
R_1-Rha-1	97.8	98.5	97.2	98.5	101.8			98.4		
- 2	80.4	70.0	79.8	70.3	70.2			70.0		
- 3	70.6	69.8	70.6	70.6	70.6			70.2		
-4	72.9	71.6	72.1	71.1	71.6			71.6		
-5	70.4	69.7	70.2	69.7	70.0			69.8		
-6	16.9	16.8	17.7	17.8	17.4			17.8		
R_1-Glc-1	105.8		105.5							
2	74.4		73.9							
3	76.9		76.2							
4	70.8		69.8							
5	77.3		76.7							
6	61.6		61.0							
R_1-CH_3						48.5	48.3			
R_2-1	102.7	100.8	101.9	101.8		100.8	101.7	100.8	101.8	
-2	74.6	74.2	70.1	70.2		74.2	70.2	74.2	70.2	
-3	77.9	77.6	70.3	70.6		76.6	70.1	76.6	70.6	

Continued

C NO.	1	2	3	4	5	6	7	8	9	10
-4	71.0	70.3	71.1	71.5		69.9	71.6	69.9	71.6	
-5	76.9	77.6	70.0	70.0		77.4	70.1	77.5	70.0	
-6	61.5	60.9	17.4	17.4		60.8	17.4	60.8	17.4	
R_3-1		100.0								
-2		73.2								
-3		77.1								
-4		70.1								
-5		77.1								
-6		60.6								

2.2 Antioxidant Activity

Among the flavonoids, kaempferol(10), kaempferol 7-O-α-L-rhamnopyranoside(5), 7-O-α-L-rhamnopyranosyl kaempferal 3, 4'-di-O-β-D-glucopyranoside (2) have significant activity (TABLE 2). All of flavonoids aglycone is kaempferol. Based on the correlation between the structure and activity, we found that the 7, 3-hydroxyl groups at the aglycone are well related to the activity, if the 7-hydroxyl groups is methylated and 3- hydroxyl groups is glycoslated, the activity is decreased. Such as 7-methoxyl kaempferol 3-O-β-D-glucopyranoside(**6**), 7-methoxyl kaempferol 3-O-α-L-rhamnopyranoside (**7**), kaempferol 3,7-O-α-L-dirhamnopyranoside(**4**) and kaempferol 3-O-α-L-rhamnopyranoside(**9**) expressed no strong activity as that of kaempferol(**10**). If the 7-position of the aglycone connects to two sugar moieties, such as 3-O-α-L-rhamnopyranosyl kaempferol 7-O-[β-D-glucopyranoside-(1→2)- α-L-rhamnopyranoside](**3**) and 3-O-β-D-glucopyranosyl kaempferol 7-O-[β-D-glucopyranosyl-(1→2)-α-L-rhamnopyranoside] (**1**),they also showed no activity. In general, the hydroxyl group in the aglycone is contributed to the antioxidant activity. The occurrence of the hydroxyl group of kaempferol was considered to be crucial for the activity. This fact was coincident with the previously report [15].

3 Experimental

3.1 General

Optical rotations were measured with a P-1010 polarimeter (JASCO, Japan) at 25°C. TLC was performed on precoated silica gel 60 F254 plate (Merck), and detection was by spraying 10% aq. H_2SO_4. Column chromatographies were carried out on Kiesel gel (40-100 mesh and 230-400 mesh, Kanto Chem.), Diaion HP-20 (Mitsubishi Chemical Ind.). Sephadex LH-20 (25-100 mm, Pharmacia Fine Chemicals), Wakogel 50 C18 (36-212 mm, Wako Pure Chemical Industuies, Ltd.), Chromatorex ODS (30-50 μm, Fuji Silysia Chemical Ltd.). FAB-MS were measured by JEOL JMS-DX303HF spectrometer (Xe atom beam, accel. voltage 2-3 kV, matrix glycerol), 200-300 mA. NMR spectra were recorded at 500 MHz for ^1H and 125 MHz for ^{13}C by JNC-A500 NMR spectrometer and chemical shifts were given on a δ (ppm) scale with tetramethylsilane as internal standard.

Table 2. Total antioxidant capacity of compounds determined using the FRAP TEAC assay

Compounds(1mg/ml)	FRAP(umol trolox/g)	TEAC(umol trolox/g)
1	61.21±0.4	94.98±8.45
2	2854.69±33.54	2394.62±56.18
3	102.67±0.17	98.81±5.9
4	188.4±2.43	105.3±5.44
5	6425.71±25.44	6368.31±100.38
6	1430.62±0.58	1147.47±70.78
7	486.59±2.37	472.98±39.89
8	134.11±2.2	84.07±11.6
9	357.18±4.51	298.69±10.52
10	8712.9±79.79	7747.77±87.29

2, 4, 6-tripyridyl-s-triazine; 2-2'-Azinobis (3-ethylbenzoth-iazoline-6-sulfonic acid) diammonium salt (ABTS) and 6-hydroxy-2, 5, 7, 8-tetramethylchroman-2-carboxylic acid (Trolox) were obtained from Sigma chemical Co (St. Louis, MO). Manganese dioxide was obtained from Merck (no. 805958). Buffer salts and all other reagents were of analytical grade.

3.2 Plant Materials

Flower of S. grosvenori were collected from Lingui county, Guilin city of Guangxi province, China, in October 2005 and identified by Professor Wei Huanan. A voucher specimen (FSG0510) of the plant is deposited at the Herbarium of Guangxi Institute of Botany, China.

978-1-61896-030-6 © 2012 SciRes.

3.3 Extraction and Isolation

Fresh flower (3 kg) of Siraitia grosvenori was extracted with methanol (8L × 3) at room temperature for 10 days. The extract was evaporated under reduced pressure to afford methanol extract (36.7 g). The extract was chromotograped on Diaion HP-20, with successive elution with H_2O and 20%, 80%, and 100% methanol. The 80% methanol eluate (15.0 g) was submitted to silica gel column and eluted with $CHCl_3$-MeOH-H_2O (9:2:0.1; 7:3:0.5; 6:4:1, v/v), gradient, to afford ten fractions. Fr. 10 (600 mg) were repeatedly subjected to silica gel column chromatography with $CHCl_3$-MeOH-H_2O (8:2:0.2, v/v), followed by further purification with Wakogel C18 column chromatography (50-60% MeOH) afford **1** (16.2 mg) and **2** (25 mg). Fr. 9 (400 mg) followed by further purification with Chromatorex ODS (55-65% MeOH) to give **3** (56.0mg). Fr. 8 (400 mg) were repeatedly subjected to silica gel column chromatography with $CHCl_3$-MeOH-H_2O (8:2:0.2, 7:3:0.5, v/v) to afford **4** (91.6 mg) and **9** (6.9 mg). Fr. 7 (795 mg) were repeatedly subjected to silica gel column chromatography with $CHCl_3$-MeOH-H_2O (8:2:0.2, v/v), followed on crystallization to afford **8** (128 mg). Fr. 5 (210 mg) were repeatedly subjected to silica gel column chromatography with $CHCl_3$-MeOH-H_2O (9:2:0.1; 8:2:0.2, v/v), followed on crystallization to yield **6** (10.1mg). Fr. 3 (613 mg) were repeatedly subjected to silica gel column chromatography with $CHCl_3$-MeOH-H_2O (9:2:0.1, v/v), followed on crystallization to yield **5** (55.6 mg). Fr. 1 (970 mg) were subjected to Wakogel C18 column chromatography (50-60% MeOH), followed by further purification with Sephadex LH-20 (30-50% MeOH) and to afford **7** (32 mg) and **10** (23 mg).

3.4 Ferric Reducing Ability of Plasma (FRAP) Assay

FRAP assay was carried out by the method of Benzie and Strain (1996) [13] with a minor modification. FRAP assay measures the change in absorbance at 593 nm owing to the formation of a blue colored Fe (II)-2, 4, 6-tripyridyl-s-triazine compound from colorless oxidized Fe (III) form by the action of electron donating antioxidants. Standard curve was prepared using different concentrations (1-10 µmol /ml) of $FeSO_4 \times 7\ H_2O$. All solutions were used on the day of preparation. In the FRAP assay the antioxidant efficacity of the antioxidant under the test was calculated with reference to the reaction signal given by an Fe^{2+} solution of known concentration, this representing a one-electron exchange reaction. The results were corrected for dilution and expressed in µmol Fe (II)/ml. 10 mg of sample powder was dissolved in 10 ml of distilled water or 50% ethanol solution. The sample to be measured within 5 min., it be adequately diluted to fit within the linearity range. All determinations were performed in triplicate.

3.5 Trolox Equivalent Antioxidant Capacity (TEAC) Assay

The Trolox equivalent antioxidant capacity (TEAC) was evaluated applying the ABTS radical cation decolorization assay [16, 17]. This spectrophotometric technique measures the relative ability of antioxidants to scavenge a longlived specific radical cation chromophore in relation to that of Trolox (6-hydroxy-2, 5, 7, 8-tetramethyl-chroman-2-carboxlic acid), the water-soluble vitamin E analogue. Hence, the TEAC represents the concentration of Trolox with the same antioxidant activity as 1 mM solution for the examined samples. 1.25 mM Trolox was prepared in phosphate buffered saline (PBS) for use as a stock standard. Fresh working standards were prepared daily by diluting this stock solution with PBS. ABTS·+ radical cation was prepared by passing a solution of ABTS through manganese dioxide on a filter paper. Excess manganese dioxide was removed from the filtrate by passing it through a 0.2 µm syringe filter. This solution was diluted in 5 mM PBS pH 7.4 to an absorbance of 0.70 at 734 nm and pre-incubated at room temperature for 2 h prior to use. All samples were dissolved in 50% ethanol. Trolox or sample solutions (40µl) were added to 2.0 ml of diluted ABTS·+ solution (1.25 mM), The absorbance at 734 nm of the lower phase was taken in a Perkin Elmer (Lambda 25) spectrophotometer exactly 5 min after initiation of mixing. PBS blanks and 50% ethanol blanks were run in each assay. The scavenging activity is estimated within the range of the dose-response curve of Trolox and expressed as TEAC, which is defined as the concentration (mM) of Trolox having the antioxidant capacity equivalent to a 1.0mM or the tested sample solution. All determinations were performed in triplicate.

References

[1] "The Pharmacopoeia of the People's Republic of China," Part Ⅰ, The Pharmacopoeia Commission of PRC, Chemical Industry Publishing Press. Beijing, 2005, pp 147-148.

[2] Takasaki M, Konoshima T, Murata Y, Sugiura M, Nishino H, Tokuda H, Matsumoto K, Kasai R, Yamasaki K. "Anticarcinogenic activity of natural sweeteners, cucurbitane glycosides, from Momordica grosvenori." Cancer Lett, 2003, 198, pp. 37-42.

[3] Dianpeng Li, Tsuyoshi Ikeda, Toshihiro Nohara, Jinlei Liu, Yongxin Wen, Tatsunori Sakamoto and Gen-Ichiro Nonaka. "Cucurbitane Glycosides from Unripe Fruits of Siraitia grosvenori", Chem. Pharm. Bull. , 2007, 55, 7, pp. 1082-1086.

[4] Dianpeng Li, Tsuyoshi Ikeda, Nanae Matsuoka, Toshihiro Nohara, Hourui Zhang, Tatsunori Sakamoto and Gen-

Ichiro Nonaka. “Cucurbitane Glycosides from Unripe Fruits of Lo Han Kuo (Siraitia grosvenori)”, Chem. Pharm. Bull. , 2006, 54, 10, pp. 1425-1428.

[5] Hanan M. El-Youssef, Brian T. Murphy, Masouda E. Amer,Maged S. Abdel-Kader and David J. I. Kingston. “Phytochemical and biological study of the aerial parts of Lotus lalambensis growing in Saudi Arabia”, Saudi Pharmaceutical Journal, 2008, 16, 2, pp.122-134.

[6] Kroll,U; Reif,K; Lederer,I; Forster,G; Zapp,J; “Kaempferol-3,4'-di-O-beta-glucopyranoside-7-O-alpha-rhamnopyranoside as a new flavonoid from Iberis amara L.” Pharmazie Die, 2009, 64, 2, pp. 142-144.

[7] Iwona Wawer and Agnieszka Zielinska. “13C/MAS NMR studies of flavonoids.” Magn Reson Chem, 2001, 39, pp.374-380.

[8] Lawrence O. Arot Manguro, Ivar Ugi, Peter Lemmen, Rudolf Hermann. “Flavonol glycosides of Warburgia ugandensis leaves”, Phytochemistry, 64, 4, pp.891-896.

[9] Hatem Braham, Zine Mighri, Hichem Ben Jannet, Susan Matthew, and Pedro M. Abreu. “Antioxidant Phenolic Glycosides from Moricandia arvensis”, 2005, 68, pp. 517-522.

[10] V.Mohan Chari, Rence J. Grayer-Barkmeijer, Jeffrey B. Harborne, Bengt-Göran Österdahl. “An acylated allose-containing 8-hydroxyflavone glycoside from Veronica filiformis”, Phytochemistry, 1981,20, Issue 8, pp. 1977-1979.

[11] Antônio A.L. Mesquita, Dirceu De B. Corrêa, Adolfo P. De Pádua, Mário L.O. Guedes, Otto R. Gottlieb. “Flavonoids from four compositae species”, Phytochemistry, 1986, 25, 5, pp.1255-1256.

[12] Vicente Martínez, Oscar Barberá, J. Sánchez-Parareda, J. Alberto Marco. “Phenolic and acetylenic metabolites from Artemisia assoana”, Phytochemistry, 1987, 26, 9, pp. 2619-2624.

[13] Takeshi Kinoshita, Kurnia Firman. “Highly oxygenated flavonoids from Murraya paniculata”, Phytochemistry, 1996, 42, 4, pp. 1207-1210.

[14] Jia-Ming Sun, Jun-Shan Yang and Hui Zhang. “Two New Flavanone Glycosides of Jasminum lanceolarium and Their Anti-oxidant Activ ities”, Chem. Pharm. Bull., 2007, 55, pp.474-476.

[15] Re R, Pellegrini N, Proteggente A, Pannala A, Yang M, Rice-Evans C. “Antioxidant activity applying an improved ABTS radical cation decolorization assay”, Free Radical Biology & Medicine. 1999, 26, pp. 1231-1237.

[16] Benzie IFF, Strain JJ. “The ferric reducing ability of plasma (FRAP) as a measure of “antioxidant power”: the FRAP assay”, Anal. Biochem., 1996, 239, pp.70-76.

[17] Miller NJ, Sampson J, Candeias LP, Bramley PM, Rice-Evans CA. “Antioxidant activities of carotenes and xanthophylls”, FEBS lett., 1996, 384, pp.240-242.

978-1-61896-030-6 © 2012 SciRes.

Current Status of Galium aparine L. in Chemical Composition and Medical Research

Guoqing SHI[1,2], Wen'en ZHAO[1]

[1]*School of Chemical Engineering and Energy, Zhengzhou University, Zhengzhou, Henan, China*
[2]*School of Food and Bioengineering, Zhengzhou University of light industry, Zhengzhou, Henan, China*
Email: guoqings@163.com

Abstract: Current status of Galium aparine L. in chemical composition and medical research was reviewed in this paper. Pointing out that establishing screening model to confirm relationship between its various biological activities and chemical composition, developing clear component, clear efficacy Modern Chinese medicine, should take advantage of this plant resources in future using.

Keywords: Galium aparine L.; tumor; renal failure

Galium aparine L., a common weed in cornfield, is an herbaceous plant belonging to genus Galium of family Rubiaceae which is widely distributed over the wold. In the roadside, wilderness, ridges and meadows, it can be found, and it can harm the crops of winter wheat, winter rape and etc. At present, there are many research on Galium aparine L. most of them are on the control of Galium aparine with different herbicides in agricultural field, and the others are concentrate on the chemical composition and the application of traditional chinese medicine. In view of this, the current status of Galium aparine L. in chemical composition and medical research were summarized in this article, it was to use the Galium aparine L. effectively.

1 Chemical Composition Research

Chemical composition had been studied systematically on Galium aparine L. The results showed that the aerial parts of it are containing protopine[1], harmine, vasicinone 8-hydroxy-2,3-dehydrodeoxy-peganine and other alkaloids; monotropein, aucubin, asperu-loside[2] class of iridoid composition; rutin, quercetin galactlside and other flavonoids; chlorogenic acid, succinic acid, lactic acid and other organic acids; and coumarin, tannins, anthraquinones composition. The fruit of Galium aparine L. contains hordenine, jaligonic acid, luteolin, mannitol, inositol, ceryl alcohol, sitosterol and other ingredients.

Chemical composition research on Galium aparine L. in China concentrated in the last two years. Yang Juan and Cai Xiaomei, Guizhou Province and Chinese Academy of Sciences, who were obtain six phenolic and eight flavonoids isolated from Galium aparine L., respectively, they are 1-(4-hydroxyphenyl)-ethanone, vanillic acid, 3,4-dihydroxybenzoic acid, p-hydroxy-cinnamic acid, gallic acid, 4-hydroxytruxillic acid, chrysoeriol, apigenin, luteolin, quercetin, chrysoeriol-7-*O*-*β*-*D*-gluco side, apigenin-7-*O*-*β*-*D*-glucoside, luteo-lin-4′-*O*-*β*-*D*-glucoside and luteolin-7-*O*-*β*-*D*-glucoside [3,4]; Li Jian, Dong Junxing and others who from the Institute of Radiation Medicine, Military Medical Sciences, obtained eleven compounds from Galium aparine 60% alcohol extracts, they were 4-hydroxy-benzoic acid, vanillic acid, protocatechuic acid, cytosine, cytidine, uracil, uridine, adenosine, xanthopurpurin, 2-methyl-1,3,6-trihydroxy-9, 10-allthraquinone-3-O-α-rhamnosyl(1 → 2)-β-D-glucoside, 2-carbomethoxy-3-prenyl-1,4-naphthohydroquinone-di-*O*-*β*-*D*-glucoside[5], and that the compounds of methyl anthraquinone and naphthalene, there may be the basis of the active substance for treatment of cancer.

2 Medical Research

As traditional Chinese medicine, Galium aparine is first recorded in Materia Medica of South Yunnan which was written by Lan Mao (AD 1396~1476) in the Songming County of Yunnan Province, it has been collected by the "Chinese Pharmacopoeia of the People's Republic", a volum of 1977 edition, and it aslo included in the "great dictionary of chinese materia medica", "China Herbal". According to the Chinese medicine theory, Galium aparine L. is characteristic of eliminating wet heat, dissipating blood stasis, reducing swelling and detoxifying that could be used in the treatment of stranguria with turbid discharge, hematuria, traumatic injury, acute appendicitis, boils, otitis media and other diseases. The book of "Materia Medica of South Yunnan" has taken on the Experiment prescription of decoction and taken with liquor, using 15g Galium aparine, 10g talcum, 5g liquorice, 10g Veronica persica; "Hunan drugs" records that the use of 10g of Galium aparine decoction with water can treat the women's amenorrhea; "Chinese herbal medicine of Yunnan" aslo

have the experiment methods of using the Galium aparine and other Chinese medicine to cure the bruises, colds, swollen boil in early, acute appendicitis, breast cancer, gum bleeding and otitis. But the clinical research of modern chinese medicine mostly focuses on the anti-tumor, and the treatment of renal failure and so on.

2.1 Anti-Tumor

"The book of Universal medical health," it recorded the using of Galium aparine, Barbed skullcap herb, Caulis lonicerae, Hedyotis diffusa, Indian mock-strawberry herb with decoction to treat the cancer of anus; and the Galium aparine, Caulis lonicerae, Barbed skullcap herb, Black nightshade herb, Salvia miltiorrhiza, Cortex lycii radicis, Herba dichondrae, Solomonseal, with decoction to treatment completed of leukemia. "Chinese herbal medicine of anti-cancer" provides us a prescription of Nux vomica semen strychni 0.9g and Rheum officinale, Galium aparine, Barbed skullcap herb and etc 30g respectively, with decoction (1 dose everyday) to treat acute leukemia. Yang Yijian and Yang Yongxian reported that the case of illness to use Galium aparine and other herbs to cure the left buttock carbuncle[6]. He Zongjian and Zheng Xiuchun adopted Galium aparine to completed the treatment of acute leukemia by strengthening qi and nourishing yin, there are 3 cases with life cycle of more than 9 years[7]. The health-center in San Dian district Xin Zhou County of Hubei Province reported that the use of fresh Galium aparine juice 0.25kg and dried Galium aparine 50g with wash, cut up and boiled with water for 30-60 minutes, and added brown sugar properly in it, then take it after mixing with water to cure breast cancer, esophageal cancer, jaw cancer, cervical cancer, there are 9 cases have achieved a certain effect[8].

At present, the patent of Chinese medicinal formulae in China which containing herbal ingredients such as Galium aparine to treat cancer is nearly twenty, and there are eleven patents for the treatment of leukemia. In all of them, Chen Fengzhuan made the XUE AI SAN ZHENG JI who made by Galium aparine account for 20% to 30%, Fringed iris herb account for 8% ~ 10%, Suncured ginseng account for 8%~10%, Prismatomeris tetrandra (Roxb.)K.Schum account for 10% to 20%, 8% ~ 10% of the Isatis indigoti-ca fort, Tuber fleeceflower stem account for 4% to 5%, Fructus corni account for 8% to 13%, 8% to 10% of Lovage and animal bone proper for the treatment of blood cancer leukemia[9].Pan Wenguang execut the anti-leukemia tea with Chinese herbs such as Galium aparine and some active ingredients of anti-cancer drugs, microelement to treat leukemia, he thinks that these can replace chemotherapy and bone marrow transplantation, and the treatment effect is good. Zhou Guosheng invented a kind of Chinese medicine to cure leukemia, it included 10-20 copies of Galium aparine, Cortex lycii radicis, and Black nightshade herb, 6-10 copies of Barbed skullcap herb, Caulis lonicerae, 4-6 copies of dichondra repens forst and other supporting components, and it can used in the treatment of leukemia with various reasons by the conjunction of the main and auxiliary components of these, and it has good results. Wang Diliang invented the XUE KANG Pill of Chinese medicine, it was composed of Astragalus root, Red-rooted salvia, Root of rehmannia, Natural indigo, Cortex moutan, Root bark of the peony tree, Herba hedyotis diffusae, Kirilow groundsel herb, Barbed skullcap herb, and Galium aparine. It can healed leukocythemia availably. Zhao Shanzhi and Zhao Chuangong achieved a patent of prescription with 1-4 copies of Natural indigo, 1-2 copies of Madagascar periwinkle herb, 0.7-4 copies of Fructus camptothecae acuminatae, 0.5-10 copies of Galium aparine, 10-20 copies of the Bark of cephalotaxus hainanensis Li., 15-30 copies of Securinega suffruticosa rehd, and 2-4 copies of Ovate tylophora root and Rhizome. They claimed that it is effective against leukemia quickly, no negative effects, high cure rate, and no recurrence after healing[11]. Zhao Shanzhi also applied for the treatment of erythro leukemia, megakaryocytic leukemia, chronic myelogenous leukemia, lymphocytic leukemia and blood diseases with Chinese medicine composition. These patents all contain Galium aparine.

In addition to the leukemia, Galium aparine can also be used for treatment of other tumour. Chen Jianmin published a drug to treat lung cancer, he blend the Rumex madaio of 4-5.715g, Acvi of 3.2-3.43g, Celandine 10g, Wild buckwheat rhizome of 10g, Common sage herb of 9.71-10.4g, Galium aparine of 9.71-10.4g, Ginseng of 6.3-7.2g, Astragalus root of 10g, largehead atractylodesrhizome of 4-5.715g, Patrinia heterophylla of 10g, English walnut seed of 9.71-10.4g, subprostrate sophora of 9.71-10.40g proportionally, and infuse, decoct them into decotion or take internally after grinding them into capsule[12]. Chen Daming aslo invented a treatment of Chinese medicine for lung cancer; it was composed of Spreading hedyotis herb, barbed skullcap herb, mulberry leaves, Galium aparine, Pseudo-ginseng, astragalus root, Donkey-hide gelatin by a certain percentage of prescriptions for Cough, Bloody sputum, Pneumonia, especially lung cancer patients. Ling Zhixian made an invention about Chinese medicine to treat cancer blood of stool. The drugs were made from Common selfheal fruit-spike, Dindygulen peperomia herb, Galium aparine of 15-18g, and Camellias, Japanese thistle herb or root of 9-12g respectively, it has the characteristics of low cost, easy to prepare, small toxicity and adverse reaction, and Significant effect[13]. Men Lianshe published the Chinese herbal formula of cancer

978-1-61896-030-6 © 2012 SciRes.

using Galium aparine for different modified tumor and disease; it has significant effect on tumors and cancers. Dong Li aslo invented a traditional Chinese medicine preparation for cancer, she blend the active ingredient of Spreading hedyotis herb of 80g, Radix scutellariae of 40g, Honey-fried radix asteris of 30g, Buffalo horn cornu bubali of 40g's, Barbed skullcap herb of 50g, Galium aparine of 60g, Bezoar of 5g, English walnut seed of 80g, Pinellia tuber of 15g, Cattail pollen of 30g, Common bletilla tuber of 60g, Solomonseal of 30g, Unibract fritillary bulb of 40g, Lily of 50g, Licorice root of 15g evenly. It can cure lung cancer with effective treatment, no side effects, and easy to take. Li Chenglin get extract from Chinese herbal medicine such as Vietnamese sophora root, Spreading hedyotis herb, Common selfheal fruit-spike, Zedoary, Galium aparine, Black nightshade herb for anti-cancer and tumor with certain processing technology. Xu Zhongting blend the Rheum officinale, Croton seed, Scorpion, Realgar, Polyphylla, Araceae, centipedes, Galium aparine, Euphorbia, Strychnos, Angelica, Gelatin with fried pasting yellow rice to pill for cancer. Zhou Wei made a drug with toad, lizards, black nightshade, ginseng, white dragon and snake grass, barbata, Galium aparine, TCS and other drugs at a certain ratio. The drug's feature is short course, long-term increase in immune function, and the prevention and treatment of inhibition to kill cancer cells. The abroad aslo hold the relevant patents. The Russia Bojko Igor A published a patent for cancer with Galium aparine and other herbal medicine in 1995[14]. Kirillov N A, who use herbal medicine such as Galium aparine for the treatment and prevention of cancer[15]. The Bulgarian Girginov Girgin P aslo provided the patent for anticancer substances. All of these patents have Galium aparine.

2.2 Renal Failure

Dan Hua, Tian Yun, Hu Junhong and other people, who use drugs such as Galium aparine to cure 42 cases of Chronic renal failure early and mid renal failure with spleen and kidney blood detoxification method, and the curative effect is effective[16]. Xiang Shaowei and He Xiaoping and some others think that the Compound Immortality Capsules has the function of reduce serum transforming growth factor β1（TGF-β1）in patients with chronic glomerular disease. Xiang Shaowei, Xiang Chunlai and others made a clinical observation on the using of Nephritis Kang Tang to cure the 48 cases of chronic glomerulonephritis. The study found that the combination of Nephritis Kang Tang and Benazepril (ACEI) can improve clinical effect evidently, reduce urinary protein, ameliorate kidney function, and it also have the function of lower the patients' serum TGF-β1, make the patients' Serum laminin（LN）and Collagen Ⅳ (ColⅣ)better, and its index is more better than that in the western single-use medicine significantly. All of these were speculated that the Nephritis Kang Tang may have the function to against renal fibrosis[17]. He Xiaoping who comes from The Second Affiliated Hospital of Guangxi Medical College, use Grass jelly soup to cure 30 cases of chronic renal failure by Galium aparine melts into Shaoyin Channel to clear heat and dampness, stasis, swelling, detoxification, diuretic. She agrees that Galium aparine could delay Glomeruloscle-rosis and Interstitial fibrosis[18].

2.3 Other

Wen Haibin in the 10th of "Family Medicine" in 2001 described a clinical medicine prescription who contains the Galium aparine to treat breast hyperplasia. Feng Dekuan exploited the function of detoxification of Eight Immortals grass, and developed Ba Xian Fu Gan Tang as its main drug to cure 30 cases of Hepatic diabetes by himself, 10 patients were cured after 4 weeks of treatment. Wang Yanfan use Shuang Zhu Ba Xian Tang which composed of Lacoste grass and Eight Immortals grass as the main medicines for the treatment of 30 cases of acute and chronic epididymitis, it was caused by ineffective antibiotic and without suppuration. The results were satisfactory[19]. Xu Yongzheng and Lu Zhifang also published the findings of Smilax glabra and Galium aparine to becomes the the main medicines to treatment ulcerative colitis. Wang Yan, Cao Dong, who is made the Herbs of Eight Immortals grass to Suppository. It was provided with the effect of analgesic and antimicrobial. The Russia is also using it to Cook Tincture, to improve their own immunity [20].

3 Pharmacological Research

The related reports of pharmacological experiment mainly focused on the area of bring high blood pressure down, antibacterial and anticancer. The results showed that Galium aparine's extract can lower blood pressure but not heart rate, and it has an effect on dogs with intravenous dozes of 1-1.5g (crude drug), and no toxicity. The components of clover saponins car in Galium aparine can lower blood pressure. The results of antibacterial test with flat paper method showed that the Galium aparine decoction has inhibition on staphylococcus aureus, E. coli and Shigella dysenteriae. The animal tumor can be removed by Dawu cancer injection, which was composed of the contract of Galium aparine and other Chinese medicine. The alcohol extract of Galium aparine can inhibit the MLV L615 with the dose of 2.2g/kg take orally every day or abdomen injection for 6 days, the inhibition ratio is 28.5%. The Screening Test of methylene blue tube agglutination

technique demonstrated that the crude Galium aparine of 5g/ml reacted positively to immunophenotype in acute lymphoblastic leukemia and acute myeloblastic leukemia.

4 Conclusions and Prospects

In summary, the study on Galium aparine in abroad is mainly focused on chemical analyse, and there is aslo a few patents to use it for anticancer and improve immunity. But the chemical analyse in domestic is small, and the majority of them were utilized the function of Galium aparine's detoxification and activating blood circulation to dissipate blood stasis to anticancer, ARF and other disease, most of them are the patent of Chinese medicinal formula. The pharmacological test showed that the Galium aparine can lower blood pressure, anti-bacterial and anti-cancer, and no toxicity.

In addition to the Asperuloside have the function of lowering blood pressure of rabbits, Dong Junxing and some other people, who speculated that it contains compounds of anthraquinones and methyl naphthalene class, they thinks that these may be the active principles to cyberknife of Galium aparine, and the study on Galium aparine at home and abroad not to mention its chemical composition or the relationship between its active site and biological activity. But Galium aparine is monarch drug in the prescription of cancer and kidney disease, and it proved that the Galium aparine may contain the eliminating evil energy ingredients to kill cancer cells and the active ingredient to improve the oliguresis, azotemia and tubular necrosis, furtherly, it aslo have the potential to develop into modern medicine relatively. Our study found that the component of aether petrolei and n-butyl alcohol of Galium aparine alcohol extract has strong proliferative capacity of inhibit leukemia cells K562 in vitro, but the activity of crude extract is weak. The value of Chinese herbal medicine is not only new compounds which isolated from themselves, but more important is to find the relationship between the compounds and their biological activity, it can improve our lives better, and it aslo provide new sources and ideas for us. It would establish relevant screening models by oriented-bioactivity from the extraction and separation of Galium aparine with relevant functional components, and thus confirming its chemical composition or the relationship between its active site and various biological activities to study its mechanism, and then develop a modern medicine with clear composition and pesticide effect. It should be the future development direction to take advantage of these rich plant resources adequately.

References

[1] Sener B,Ergun F. "The first isolation of anisoq uinoline alkaloid from Galium aparine L," *Faculty Pharm Gazi University*, Vol. 8, No. 1, 1991, pp. 13-15.

[2] Deliorman D, et al. "Iridoids from Galium aparine,"*Pharmaceutical Biology*, Vol. 39, No. 3, 2001, pp. 234-235.

[3] YANG Juan, CAI Xiaomei, MU Shuzhen, YANG Xiaosheng. "Phenolic compounds from Galium aparine var. tenerum," *China Journal of Chinese Materia Medica*,2009,34(14):182-184. Vol. 34, No. 14, 2009, pp. 182-184.

[4] CAI Xiaomei, YANG Juan, RAO Qiongjuan. "Studies on Flavonoids from Galium aparine," *China Journal of Chinese Materia Medica*, , No. 19, 2009, pp. 1475-1477.

[5] Li Jian, LI Bing, CHEN Li, LIU Shi-jun, DONG Jun-xing. "Chemical constituents of Galium aparine," *Bulletin of the Academy of Military Medical Sciences*, 34(3):269-271. Vol. 34, No. 3 2010, pp. 269-271.

[6] YANG Yijie, YangYongxian. "upper body stone flat-abscess," *Acta Universitatis Medicinalis Anhui*, No. 5, 1975, pp. 823-839.

[7] He Zhongjian,Zheng Xiuchun. "Yiqiyangyin Therapy for three cases of survival for more than 9 years of reports of acute leukemia," *Shanghai Journal of Traditional Chinese Medicine*, No. 11, 1994, pp. 823-839.

[8] "Xinzhou County, Hubei Province, SanDian area hospitals, Galium aparine treatment of cancer a preliminary report of 15 cases," N*ew Medicine*, No. 9, 1972, pp. 26-27.

[9] Chen Fenzhuang. "A method of preparing Xue Ai San," China: 1339304A, 2002-03-13.

[10] Wang Diliang. "Leukemia treated with the Chinese medicine," China: 1695703A, 2005-11-16.

[11] Zhao Shanzhi,Zhao Changong. "A kind of leuke mia treated with the combination of chinese medicine," China: 1733008A, 2006-02-15.

[12] Li Suzhen, Chen Jianmin. "A lung cancer treatment for drug," China: 1530133A, 2004-09-22.

[13] Ling Zhixian. "One noticed the soup of the medicine to cure colorectal cancer drugs," China: 1733008A, 2009-04-22.

[14] Bojko, Igor A. "A method for treating tumor," Russ: 2028808, 1995-02-20.

[15] Kirillov N A, Mitrasov Yu N, Ionova E A, et al. "A medicated liquor containing medicinal comp osition for treating and preventing diseases," Russ: 2192877, 2002-11-20.

[16] Tan Hua, Tian Geng, Hu Junhong. "Strengthen ing Spleen and Kidney plus Activating Blood Circulation and Eliminating Toxin for Chronic Renal Failure," *Shanxi Journal of Tradtional Chinese Medicine*, Vol. 23, No. 4, 1977, pp. 292.

[17] Xiang Shaowei, Xiang Chunlai, Shi Hongbin, Tang Liping. "Shen Yan Kang treating chronic nephritis glomerulonephritis 48 cases observed," *Journal of New Chinese Medicine*, Vol. 40, No. 1, 2008, pp. 32-34.

[18] He Xiaoping, Xiang Shaowei, Meng Murong. "Immortality treating 30 cases of chronic renal failure," *Shanxi Journal of Traditional Chinese Mediticne*, Vol. 23, No. 4, 2002, pp. 293-294.

[19] Wang Yan-fan. "Lacoste Sin treating acute and chronic epididymitis 30 cases," *Zhejiang Journ al of Traditional Chinese Medicine*, Vol. 43, No. 7, 2008, pp. 407.

[20] Zakharov, Yu A. "Method for treating on colo gical diseases with a phytopreparation," Russ: 2161040, 2000-12-27.

978-1-61896-030-6 © 2012 SciRes.

Interaction of Isoliquiritigenin with Bovine Serum Albumin as Studied by a Fluorescence Quenching Method

Bo HAN[1,2,3], Wen CHEN[1], Akber Aisa Haji[2], Xinchun WANG[1], Le LI[1]
[1]*Key Laboratory of Xinjiang Phytomedicine Resources, Shihezi, China, 832002*
[2]*Xinjiang Technological Institute of Physics and Chemistry, Chinese Academy of Sciences, Urumqi, China, 830011*
[3]*Graduate School, Chinese Academy of Sciences, Beijing, China, 100049*
Email: chen-wen2000@126.com

Abstract: Isoliquiritigenin (ISL) is the main active component of a commonly used traditional Chinese medicine (TCM) *Glycyrrhiza uralensis*. In this study, ISL interactions. with bovine serum albumin (BSA) were investigated using fluorescence quenching. The number of binding sites (*n*) and apparent binding constant (*K*) were measured. Thermodynamic parameters (ΔH^0, ΔG^0, ΔS^0) were calculated at different temperatures. The distance (*r)* between the fluorescent donor (BSA) and fluorescent acceptor (ISL) were obtained using Förster's theory of non-radiative energy transfer. The results of synchronous fluorescence spectra and UV–Vis absorption spectra both showed that the conformation of BSA changed upon interaction with ISL.

Keywords: Isoliquiritigenin; bovine serum albumin; thermodynamic parameters; energy transfer

1 Introduction

Isoliquiritigenin (4,2',4'-trihydroxychalcone, ISL), which exists in licorice and in vegetables including shallots and bean sprouts[1], is a member of the flavonoids, has been shown to exhibit a variety of biological activities, such as antioxidant [2,3], anti-inflammatory [4], estrogenic [5], chemopreventive [6] and antitumor activities [7] attenuating brain injury in cerebral ischemia–reperfusion [8]. ISL has also been reported to inhibit cell proliferation and/or induce apoptosis in lung, gastric, breast, prostate, colon and melanoma cancer cells [9].Our findings show that ISL affects the proliferation and redifferentiation in HL-60 cells [10].

Serum albumins are the most abundant proteins in the circulatory system of a wide variety of organisms. Being the major macromolecule contributing to the osmotic blood pressure [11], they can play a dominant role in drug disposition and efficacy [12]. Many drugs and other bioactive small molecules bind reversibly to albumin and other serum components, which then function as carriers. Serum albumin often increases the apparent solubility of hydrophobic drugs in plasma and modulates their delivery to cells in vivo and in vitro. Consequently, it is important to study the interactions of drugs with this protein. The effectiveness of drugs depends on their binding ability.

Fluorescence and UV–vis absorption spectroscopies are powerful tools for the study of the reactivity of chemical and biological systems. The aim of this work was to determine the affinity of ISL to bovine serum albumin (BSA), and to investigate the thermodynamics of their interaction. We also tried to find the stoichiometry of the ISL–BSA complex. To resolve this problem, the UV and fluorescent properties of ISL as well as BSA were investigated.

2 Experimental

2.1 Materials

ISL (≥95%, Tian Ye Biotechnology Co., Ltd), Xian, China) and BSA (being electrophoresis-grade reagents, was obtained from Sigma) were used. The samples were dissolved in Tris–HCl buffer solution (0.05 mol L^{-1} Tris, 0.10 mol L^{-1} NaCl, pH = 7.4). All reagents were of analytical reagent grade and doubly distilled water was used throughout.

2.2 Apparatus

All fluorescent measurements were carried out on an F-2500 fluorescence spectrophotometer (Hitachi, Kyoto, Japan) equipped with a xenon lamp source and 1.0 cm cell. A UV-2401 recording spectrophotometer (Shimadzu, Kyoto, Japan) equipped with 1.0 cm quartz cells was used for the UV spectrum scanning. All pH measurements were made with a pHS-3 digital pH-meter (Shanghai Lei Ci Device Works, Shanghai, China) with a combined glass-calomel electrode. The mass of sample was accurately weighed with a microbalance (Sartorius).

2.3 Spectroscopic Measurements

The absorption spectra of BSA, ISL and their mixture

were performed at room temperature. The fluorescence measurements were performed at different temperatures (298, 310 and 315 K). Excitationwavelength was 286 nm. The excitation and emission slit widths were set at 10 nm and 700V PMT. Appropriate blanks corresponding to the buffer were subtracted to correct background fluorescence.

3 Results and Discussions

3.1 Fluorescence Characteristics of BSA

The concentrations of BSA were stabilized at10^{-5} mol L^{-1}, and the content of ISL varied from 0 to 2.205×10^{-6}mol/L at the step of 0.9600×10^{-6}mol/L. The effect of ISL on BSA fluorescence intensity is shown in Fig. 1. The intensity of fluorescence can be decreased by a wide variety of processes. Such decreases in intensity are called quenching. It is apparent from Fig. 2 that the fluorescence intensity of BSA decreased regularly with the increasing of ISL concentration. The fluorescence quenching data are usually analysed by the Stern–Volmer equation [13]:

$$F_0/F = 1 + K_q\tau_0[Q] = 1 + K_{sv}[Q] \qquad (1)$$

where K_q, K_{sv}, τ_0 and [Q] are the quenching rate constant of the biomolecule, the dynamic quenching constant, the average lifetime of the molecule without quencher and concentration of quencher, respectively. Because fluorescence lifetime of biopolymer is 10^{-8}s[14], quenching constant (Kq: L mol^{-1} s^{-1}) at pH 7.40 can be obtained by the slope: 298 K, Ksv = 1.307×10^5, r = 0.9892; 310 K, Ksv = 1.518×10^5, r = 0.9885 and 315K, Ksv = 1.745×10^5, r = 0.9864 Fig. 2 shows that curves have fine linear relationships, but changes of slopes with the increase of temperature. These results indicate that the probable quenching mechanism of fluorescence of BSA by ISL is a dynamic quenching procedure, because the K_{SV} increased with the rising temperature[13].

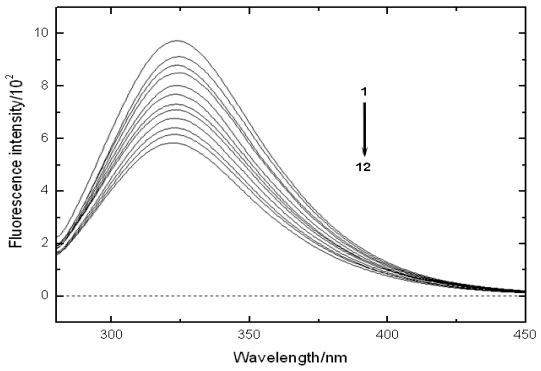

Figure 1. Emission spectra of BSA in the presence of various concentrations of ISL

c (BSA) = c_{BSA}=2.205×10^{-6}mol/L; *c* (ISL)/(10^{-6}mol/L), c_{ISL}(10^{-6}mol/L) : 1-12: 0，0.9600, 1.920，2.880，3.840，4.800，5.760，6.720，7.680，8.640，9.600，10.56 (T = 298 K)

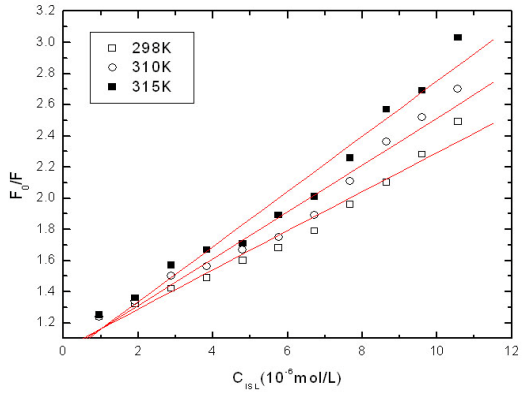

Figure 2. The Stern–Volmer curves for quenching of ISL to BSA

3.2 The Determination of the Force Acting between ISL and BSA

The interaction forces between a drug and biomolecule may include hydrophobic force, electrostatic interactions, van der Waals interactions, hydrogen bonds, etc. The slope of a plot of the bimolecular quenching constant versus 1/*T* (*T*, absolute temperature) allows one to calculate the energy change for the quenching process [14]. If the enthalpy change (ΔH^0) does not vary significantly over the temperature range studied, then its value and that of entropy change (ΔS^0) can be determined from the van't Hoff equation:

$$\ln K = -\frac{\Delta H^0}{RT} + \frac{\Delta S^0}{R} \qquad (2)$$

where *K* is the Stern–Volmer quenching constant at the corresponding temperature and *R* is the gas constant. The temperatures used were 298, 310 and 315 K. The enthalpy change (ΔH^0) is calculated from the slope of the van't Hoff relationship. The free energy change (ΔG^0) is estimated from the following relationship:

$$\Delta G^0 = \Delta H^0 - T\Delta S^0 \qquad (3)$$

Table 1 shows the values of ΔH^0 and $T\Delta S^0$ obtained for the binding site from the slopes and ordinates at the origin of the fitted lines.

Table 1. Stern–Volmer quenching constant K_{SV} and relative thermodynamic parameters of ISL–BSA at pH = 7.4

ΔH^0(kJ·mol^{-1})	ΔS^0(*J*·mol^{-1}·K^{-1})	*T*(K)	ΔG^0(kJ·mol^{-1})
		298	-29.18
12.5	139.8	310	-30.75
		315	-31.61

978-1-61896-030-6 © 2012 SciRes.

From Table 1, it can be seen that the negative sign for free energy (ΔG^0) means that the interaction process is spontaneous. The positive enthalpy (ΔH^0) and entropy (ΔS^0) values of the interaction of ISL and BSA indicate that the binding is mainly entropy-driven and the enthalpy is unfavorable for it, the hydrophobic forces playing a major role in the reaction [15].

3.3 Energy Transfer between ISL and BSA

The Förster theory of molecular resonance energy transfer[16] points out: in addition to radiation and reabsorption, a Fig. 3. Spectral overlap of ISL absorption with BSA fluorescence c (BSA) = c (ISL) = 2.205 ×10^{-6} mol/L. transfer of energy could also take place through direct electrodynamic interaction between the primarily excited molecule and its neighbors. According to this theory, the distance r of binding between ISL and BSA could be calculated by the equation (Eq. (4)) [17]:

$$E = R^6_0/(R^6_0 + r^6) \quad (4)$$

where E is the efficiency of transfer between the donor and the acceptor, R_0 is the critical distance when the efficiency of transfer is 50%.

$$R^6_0 = 8.8 \times 10^{-25} K^2 n^{-4} \Phi_D J \quad (5)$$

In Eq. (5), K^2 is the space factor of orientation; n the refracted index of medium; Φ the fluorescence quantum yield of the donor; J the effect of the spectral overlap between the emission spectrum of the donor and the absorption spectrum of the acceptor (Fig. 3), which could be calculated by the equation:

$$J = \frac{\int_0^\infty F(\lambda)\varepsilon(\lambda)\lambda^4 d\lambda}{\int_0^\infty F(\lambda) d\lambda} \quad (6)$$

where F (λ) is the corrected fluorescence intensity of the donor in the wavelength range λ–(λ+$\Delta\lambda$); $\varepsilon(\lambda)$ is the extinction coefficient of the acceptor at λ. The efficiency of transfer (E) could be obtained by the equation:

$$E=1-F/F_0 \quad (7)$$

In the present case, K^2 = 2/3, N = 1.336, and φ = 0.15 [18]. According to the Eqs. (4)–(7), we could calculate that J=4.87 ×10^{-15}cm^3 ·L·mol^{-1}; R_0 = 2.12 nm; E = 0.0693 and r =3.27nm. The average distance r < 8nm [19], and 0.5R_0 < r< 1.5R_0 [20] indicate that the energy transfer from BSA to ISL occurs with high probability.

c (BSA)= c (ISL) =2.205 ×10^{-6} mol/L.

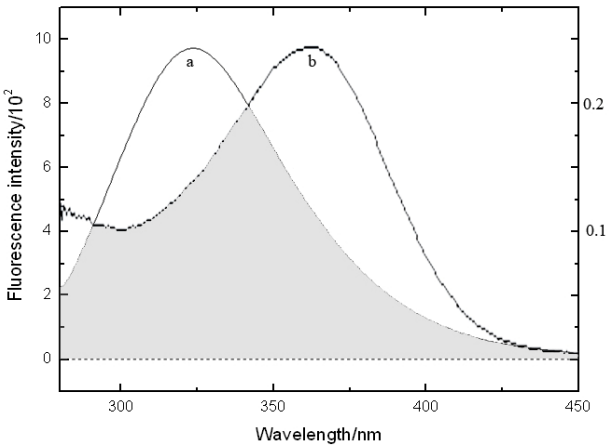

Figure 3. Spectral overlap of ISL absorption with BSA fluorescence

3.4 Conformation Investigation

The synchronous fluorescence spectra give information about the molecular environment in a vicinity of the chromosphere molecules. In the synchronous spectra, the sensitivity associated with fluorescence is maintained while offering several advantages: spectral simplification, spectral bandwidth reduction, and avoiding different perturbing effects. The authors[21] suggested a useful method to study the environment of amino acid residues by measuring the possible shift in wavelength emission maximum λ_{max}, the shift in position of emission maximum corresponding to the changes of the polarity around the chromophore molecule. When the D-value ($\Delta\lambda$) between excitation wavelength and emission wavelength were stabilized at 15 nm or 60 nm, the synchronous fluorescence gives the characteristic information of tyrosine residues or tryptophan residues[22]. The effect of ISLon BSA synchronous fluorescence spectroscopy is shown in Fig. 4. It is apparent from Fig. 4 that the maximum emission wavelength moderate shifts towards long wave when $\Delta\lambda$=60 nm. The shift effect expresses that the conformation of BSA was changed. It is also indicated that the polarity around the tryptophan residues was increased and the hydrophobicity was decreased [23].

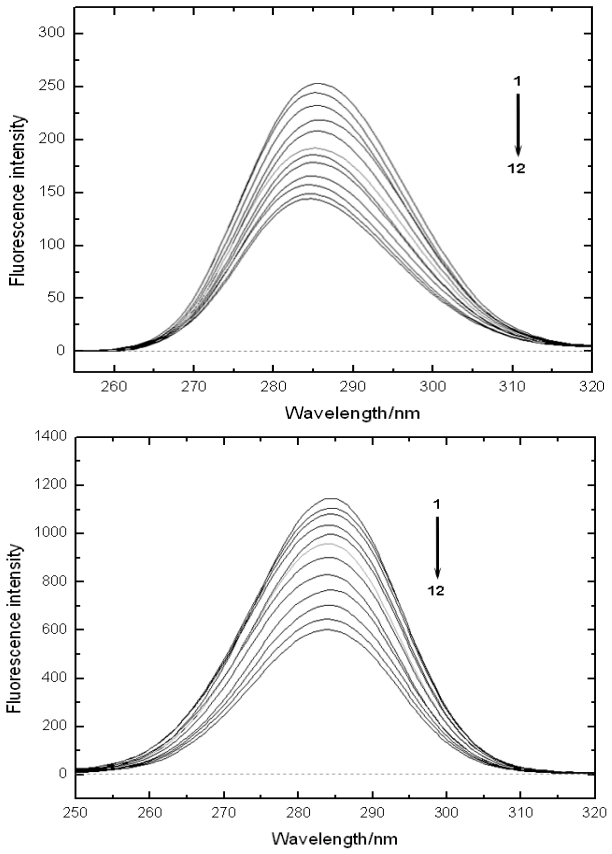

Figure 4. Synchronous fluorescence spectrum of BSA

(a) $\Delta\lambda$= 15 nm; (b) $\Delta\lambda$= 60 nm; c_{BSA} = 2.205 ×10^{-6} mol/L ; C_{ISL}/(10 - 5 molPL) : 1 ~ 12 :0, 0.13756, 0.17512, 1.11269, 1.15025, 1.18781, 2.12537, 2.16293, 3.10049, 3.13806, 3.17562, 4.11318. T = 298 K

4 Conclusions

In this paper, the interaction of ISL with BSA was studied by Spectroscopic methods including fluorescence spectroscopy and UV–vis absorption spectroscopy. The results of synchronous fluorescence spectroscopy and indicate that the secondary structure of BSA molecules is changed dramatically in the presence of ISL. The experimental results also indicate that the probable quenching mechanism of fluorescence of BSA by ISL is a dynamic quenching procedure, the binding reaction is mainly entropy driven, and hydrophobic interactions played a major role in the reaction.

Acknowledgement

This work was supported by a grant from the National Natural Science Foundation of China (Grant No. 30960515, 30760058). grant from University of Shihezi (No. ZRKXYB-13, RCZX200763 and ZRKX2008067).

References

[1] R. Kape, M. Parniske, S. Brandt, D. Werner, "Isoliquiritigenin a strongnod gene- and glyceollin resistance-inducing flavonoid fromsoybean root exudate," *Appl. Environ. Microb.*,Vol. 58, No. 5, 1992, pp. 1705-1710.

[2] H. Haraguchi, H. Ishikawa, K. Mizutani, Y. Tamura, T. Kinoshita, "Antioxidative and superoxide scavenging activities of retrochalcones in Glycyrrhiza inflate," *Bioorg. Med. Chem.*, Vol. 6, 1998, pp. 339-347.

[3] Y.W. Chin, H.A. Jung, Y. Liu, B.N. Su, J.A. Castoro, W.J. Keller, M.A. Pereira, A.D. Kinghorn, "Anti-oxidant constituents of the roots and stolons of licorice (Glycyrrhiza glabra)," *J. Agric. Food Chem.*, Vol.12, No. 55, 2007, pp. 4691-4697.

[4] J.Y. Kim, S.J. Park, K.J. Yun, Y.W. Cho, H.J. Park, K.T. Lee, "Isoliquiritigenin isolated from the roots of Glycyrrhiza uralensis inhibits LPS-induced iNOS and COX-2 expression via the attenuation of NF-kappaB in RAW 264.7 macrophages," *Eur. J. Pharmacol.*, Vol. 584, No. 1, 2008, pp. 175-184.

[5] S. Tamir, M. Eizenberg, D. Somjen, S. Izrael, J. Vaya, "Estrogen-like activity of glabrene and other constituents isolated from licorice root," *J. Steroid Biochem. Mol., Biol.* Vol. 78, No. 3, 2001, pp. 291-298.

[6] M. Baba, R. Asano, I. Takigami, T. Takahashi, M. Ohmura, Y. Okada, H. Sugimoto, T. Arika, H. Nishino, T. Okuyama, "*Studies on cancer chemoprevention by traditional folk medicines* XXV. Inhibitory effect of isoliquiritigenin on azoxymethane-induced murine colon aberrant crypt focus formation and carcinogenesis," *Biol. Pharm. Bull.*, Vol. 25, 2002, pp. 247-250.

[7] C.K. Lee, S.H. Son, K.K. Park, J.H. Park, S.S. Lim, W.Y. Chung, "Isoliquiritigenin inhibits tumor growth and protects the kidney and liver against chemotherapy-induced toxicity in a mouse xenograft model of colon carcinoma," *J. Pharmacol. Sci.*, Vol. 106, 2008, pp. 444-451.

[8] Zhan, C., Yang, J., "Protective effects of isoliquiritigenin in transient middle cerebral artery occlusion-induced focal cerebral ischemia in rats," *Pharmacol. Res.*, Vol. 53, No. 3, 2006, pp. 303-309.

[9] Iha Park, Kwang-Kyun Park, Jung Han Yoon Park, Won-Yoon Chung. "Isoliquiritigenin induces G2 and M phase arrest by inducing DNA damage and by inhibiting the metaphase/ anaphase transition," *Cancer Letters*, Vol., 277 No. 2, 2009, pp. 174-181.

[10] Defang Li, Zhenhua Wang, Hongmei Chen, Jingying Wang, Qiusheng Zheng, Jing Shang, Ji Li. "Isoliquiritigenin induces monocytic differentiation of HL-60," *cells Free Radic Biol*, Vol. 46, No. 6, 2009**,** pp. 731-736.

[11] D.C. Carter, J.X. Ho. "Structure of Serum Albumin". *Adv. Protein Chem.*, Vol. 45, 1994, pp.153-203.

[12] R.E. Olson, D.D. Christ. "Plasma protein binding of drugs,"*Ann. Rep. Med. Chem.*, Vol. 31, 1996, pp. 327–337. pp. 57-58.

[13] J.R. Lakowicz, "*Principles of Fluorescence Spectroscopy*," second ed. [M].Plenum Press, New York, 1999.

[14] J.R. Lakowicz, G. Weber, "Quenching of protein fluorescence by oxygen. Detection of structural fluctuations in proteins on the nanosecond time scale" *Biochemistry*, Vol. 21, No, 21, 1973, pp. 4161-4170.

[15] D.P. Ross, S. "Thermodynamics of protein association reactions: forces contributing to stability. Subramanian,"*Biochemistry*, Vol. 81, 2019, pp. 3096-3102.

[16] T. Förster. "Intermolecular Energy Migration and Fluorescence," *Ann. Phys.*, Vol. 2, 1948, pp. 55-75.

[17] L.A. Sklar, B.S. Hudson, R.D. "Conjugated polyene fatty acids as fluorescent probes: synthetic phospholipid membrane Studies. Simoni," *Biochemistry*, Vol. 16, 1977, pp. 819-828.

[18] L. Cyril, J.K. Earl, W.M. Sperry, "*Biochemists' Handbook,*" E. & F. N. Spon, London, 1961, pp. 84.

[19] B. Valeur, J.C. Brochon, "*New Trends in Fluorescence Spectroscopy,"* sixth ed. Springer Press, Berlin, 1999, pp. 25.

978-1-61896-030-6 © 2012 SciRes.

[20] B. Valeur, "Molecular Fluorescence: *Principles and Applications*," Wiley Press, New York, 2001, pp. 250.
[21] G.Z. Chen, X.Z. Huang, Z.Z. Zheng, J.G. Xu, Z.B. Wang, "*Fluorescence Analytical Method,"* second ed. Science Press, Beijing, 1990. pp.78.
[22] J.N. Miller. "Recent advances in molecular luminescence analysis," *Anal. Proc*., Vol. 16, 1979, pp: 203-209.
[23] K.H. Ulrich. "Molecular aspects of ligand binding to serum albumin," *Pharmacol Rev.*, Vol. 33, No.1, pp. 17-53.

Promising Future and Resource of Qinghuajiao-Economic Forest of Sichuan

Meng YE[1], Biao PU[1], Xuan LIU[2], Wensheng LIU[3]
[1]*College of Forestry, Sichuan Agricultural University, Sichuan, China*
[2]*College of Food Science Sichuan Agricultural University, Sichuan, China*
[3]*Bureau of Agriculture Leshan City, Sichuan, China*
Email: yemeng5581@yahoo.com.cn

Abstract: It's revealed the phenomenon of Homonym and synonym in Qinghuajiao, the names of which such as Jinyang Qinghuajiao, Vine pepper and Jiuyeqing are usually used in market and consumption, but all of which are *Z. armatum*. in biology. There are two main production area, Jinyang in southwest of Sichuan (Liangshan) and Hongya, Emei in Sichuan basin. The market and consumption of Qinghuajiao extend in China.

Keywords: Qinghuajiao; promising future; resource; market; economic

1 Introduction

Pepper of Sichuan (Rutaceae, *Zanthoxylum*), the homo-source both in food and drug [1,2], a traditional spices, Chinese herbal medicine, economical forest in China having been utilized for 2000 years[3]. In recent years, Green Prickleyash with green fruits is widely planted in Sichuan and Chongqing province in China which is welcomed by people as their rich aroma and mellow flavor of numb-taste. Why people enjoy them and how about its market? In order to answer these questions and aimed to support the exploiture of Green Prickleyash and learn more about it, investigations and studies had been done in counties of Sichuan where there are pepper of Sichuan being planted widely, including Hongya, Emei, Jinyang, Leshan, Danling, Meishan, Santai Lezhi, Pengxi, Yaan, Hanyuan and Ebian.

2 Characters and Distribution of Green Prickleyash Resource

2.1 Homonym and Synonym Phenomenon of Green Prickleyash

People usually call pepper of *Z. armatum* with green fruits Green Prickleyash which is a popular name[4]. It's shown in the investigations that edible Green Prickleyashes are *Z. armatum* and *Z.schinifolium*, different in morphology but similar in fruits character and the wild resources of both are found in Sichuan. *Z. armatum* is planted as economic tree in Sichuan and Chongqing, while the *Z.schinifolium* planted sporadically and grown mixed with *Z. armatum* isn't large-scale planted because of its peculiar taste. *Z.schinifolium* cited in many papers is actually *Z. armatum*. Thus, the homonym phenomenon of Green Prickleyash leads to the misuse of its name, which shows that the studies on these two kinds of pepper resources are so weak that its taxonomic status is not clear.

Another pepper called vine pepper is existed in regions of plantation, where people regard vine pepper and Green Prickleyash as two kinds. Researches in aspects of tree shape, branches, compound leaves, fruits and its ingredients show that vine pepper is just another name of Green Prickleyash.

2.2 The Breed of Green Prickleyash

There are three breeds of Qinghuajiao registered by the National or Provincial Forest Cultivar Registration Board. They are Jinyang Qinghuajiao[5] from Jinyang county, vine pepper[6] from Hongya county and Jiu Yeqing[7] from Jiangjin City in Chongqing. In fact all of them are *Z. armatum* in academy.

2.3 The Distributions of Qinghuajiao in Sichuan and the Climate Characters of These Regions

The resources of Qinghuajiao are particularly rich in Sichuan. According to the relief and climate, two kinds of region can be generalized that subtropical monsoon climate s in mountains and ubtropical humid climate in basin. In Tab1 characters of the two regions (Jinyang and Hongya) are shown on aspects of physiognomy types, annual average temperature, sunshine, precipitation and altitude. The feature of Jinyang is dry, hot and rich in sunshine contrast with Hongya, which illustrates that the two varieties in the two regions have adapted the local environments.

978-1-61896-030-6

Table 1. Characters of regions producing Qinghuajiao

Breed	Jinyang Qinghuajiao	Vine pepper
Prodition place	Jinyang	Hongya
Relief	Mountains in southwest Sichuan	Sichuan Basin
Climate type	Subtropical monsoon climate	Subtropical humid climate
Annual average temperature（℃）	21～13.3	16.6
Annual sunshine（h）	1600	1006.1
Annual frost-free period（d）	280～300	307
Annual rainfall（mm）	800	1435.5
Altitude（m）	500～1800	410～1300

Figure 1. Distribution of the *Z.armatum* in Sichuan

The Figure1 reveals that Qinghuajiao is mainly distributed in Sichuan Basin (Hongya, Emei, Leshan, Ebian) and Liangshan yi autonomous prefecture in mountains of southwest Sichuan (Jinyang, Leibo). Jinyang County is the biggest production region in Sichuan and also in China. The 70% population of which is Yi peoples. It is a needy county of State-level. As the pillar industry of the county, the Green Prickeyash is along the Jinsha river valley dry and hot and the plantation area of Green Prickeyash is more than 5 acres. The forestation of Jinyang Green Prickeyash in dry and hot river valley is with great dominance both in ecology and economy.

Vine pepper with characters of barren resistance and fertility concentrated in Hongya, Emei, Ebian and Danling adapts the rich rainfall and less sunshine in the Sichuan basin well, While Jiu Yeqing is mainly distributed in Yibin, Zigong, Mianyang and Deyang.

3 The Marketing Demands and Promising Future of Qinghuajiao

3.1 The Marketing Demands of Qinghuajiao

Huajiao is integral to Sichuan cuisine which is famous for numbing and burning sensation, so that its percapita consumption is first in China. Generally, the rational collecting period of huajiao is full ripe but qinghuajiao is not, commonly knowing “wanshuqi”. Because of its immaturity and insufficiently accumulation of numbing matter ,the distinctive numbing sensation is lighter than huajiao,for which it is easier for people to accept and develop qinghuajiao gradually, in addition to rich aroma, special flavor, refreshing taste and obviously enhancing appetite,so that the consumption of Qinghuajiao is rising continuously. Especially, its pure greenness also has a strongly decorative effect.

There are nearly 10 processed products of Qinghuajiao but the main products are fresh and drying preservation which account for 60%-70% on the market, meanwhile, the essential oil is 20% and other products is 10%.

Table 2. The products and market price of Qinghuajiao

The processed products	Price（￥）
Oil of fresh Huajiao	30
Huajiao flavor	500
Seed oil	14
Micropowder of linolenic acid	50
Purify dry Huajiao	75
Essential oil of fresh Huajiao	700
Microcapsule Huajiao powder	80
Linolenic acid capsule	500
Qinghuajiao flavor	700

3.2 Promising Future of Qinghuajiao

3.2.1 Enhance National and International Markets of Qinghuajiao Products

Qinghuajiao has a distinctive taste and a fresh-comfortable aroma. Compared with traditional Pepper of Sichuan, Qinghuajiao is consumed by humans, because the outstanding points of Qinghuajiao involve their rich-fresh aroma and lower numb-taste. A number of edible Qinghuajiao, previously known of as unacquainted ones, began to receive more attentions. Along with exploiting more new edible Qinghuajiao menu and cultivating more consumers, gradually, the domestic markets of Qinghuajiao will be expanded.

Exporting traditional Pepper of Sichuan Time is over. Recent years, the rate of export of Qinghuajiao is growing in Southeast Asia, Japan, Korea, etc. Owing to a wide range of applied fields, traditional Pepper of Sichuan is entering Euro-American market also, as Sichuan is one of exporting Pepper provinces. Besides supply of Qinghuajiao fails to meet the demand in national market, Qinghuajiao products are commanded a

ready market in Korea, Japan, Southeast Asia, America, etc. The price of Qinghuajiao is higher than the 15 to 20 dollars/kg in New Yorkmarket and fresh green pepper and frozen green pepper have been well received in Japan market.

3.2.2 The Ways of Deep Processing and Exploiting Qinghuajiao

The future development of Qinghuajiao mainly depends on the ways of deep process and exploitage. Modern medical research indicates that the extractives of Qinghuajiao have marked antiphlogistic and bacteriostatic action and lots. With the analysis of composition, separating composition and deep exploiting extractive techniques, Qinghuajiao product will has a promising future. The future of condiment products will be located in varieties, complex convenience and nutritive health.

3.2.3 Enhance Its Ecological and Economic Effects

Qinghuajiao is a variety of ecological and economic trees. The resistibility of Qinghuajiao is better than traditional Pepper of Sichuan's, especially Jinyang Green Prickeyash adapts in dry and hot river valley and Vine pepper adapts in the rich rainfall and less sunshine regions. The effects of Qinghuajiao are to improve the income of the farmers in similar ecological region and enhance national unity and harmony.

References

[1] Editorial committee of Flora of China, Flora of China, 1997, 43(2): 43.

[2] The notice of the management of regulating the raw materials of health food ulteriorly of the Ministry of Health, supervision and publication of the law of Ministry of Health[2002]51.

[3] Lin Hongrong. Preliminary inquiry of the History of Pepper, Journal of Sichuan Forestry Sicence and Technology, 1985(1) 35-36.

[4] Zhang Hua, Ye Meng. Research Status on the Taxonomic and Component of Green Zanthoxylumbungeanum Maxim, Northern Horticulture, 2010, (14): 199-203.

[5] Qinghuajiao of Jinyang（ChuanR-SV-ZA-019-2009）,The notice of Forestry Department of Sichuan (2010,1). In.

[6] Tengjiao(ChuanR-SV-ZA-005-2007), The notice of Forestry Department of Sichuan (2008, 1). In.

[7] Qinghuajiao of Jiuye(State S-SV-ZA-020-2005), The introduction of Tree Seeds by the Conference of Forest tree species belong to The States in 2005.

978-1-61896-030-6 © 2012 SciRes.

Purification and Analysis of Chemical Compositions on Glycosaminoglycan from *Bullacta exarata*

Chunying YUAN, Jianglu XU, Qingman CUI, Huifang SUN, Guangjing LI
Key Laboratory for Marine Chemistry and Resource, Tianjin, China
College of Marine Science and Engineering,TianjinUniversity of Science & Technology, Tianjin, China
Email:yuanchunying2000@yahoo.com.cn

Abstract: The purity of crude glycosaminoglycan(GAG) from *Bullacta exarata* was 90.82% through ultrafiltration and CTAB precipitation, its purity was detected by UV scanning and agarose gel electrophoresis, meanwhile the chemical composition of purified glycosaminoglycan were determinated using gelatin $BaCl_2$, carbazole reaction and modified Elson-Morgan methods, the results showed that sulfate content was 3.95%, uronic acid content was 25.83% and amino sugar content was 14.19% in glycosaminoglycan from *Bullacta exarata*.

Keywords: *Bullacta exarata*; glycosaminoglycan; purification; chemical composition analysis

1 Introduction

Glycosaminoglycans are structurally diverse linear polysaccharides which composed of repeating disaccharide units. Glycosaminoglycans are widely located at cell-surface and in the extracellular matrix.As a kind of important biomacromolecule in vivo, glycosaminoglycans participate in a variety of important biological functions, such as cell proliferation, cell differentiation and immunoregulation by combining with kinds of enzyme, growth factor and adhesionmolecules [1]. Scholars have isolated glycosamglycans from some marine animal, chondroitin sulfate, acid mucopolysaccharide and glycoprotein were isolated from cartilage of shark [2], integument of sea star and stichopus japonicas [3,4], mollush(such as scallop, clam, abalone and sea hare) [5] respectively.Cassaro's [6] reaearch showed that mollush were rich in glycosaminoglycans. China is abound in *Bullacta exarata* which is a typical kind of intertidal zoobenthos.

Bullacta exarata has lots of nutritive material as well as some medical functions. According to the "Supplement to the Compendium of Materia Medica", *Bullacta exarata* have functions of tonifying liver, moistening lung,improving eyesight and regenerating fluid [7,8]. Up to date, there is no report about glycosaminoglycan from *Bullacta exarata*. On the basis of optimal extractive condition of glycosaminoglycan from *Bullacta exarata*, this paper did some research about purification and analysis of chemical compositions on glycosaminoglycan from *Bullacta exarata* which will surely lay the foundation for further study on structure and functions analysis of glycosaminoglycan from *Bullacta exarata*.

2 Materials and Methods

Bullacta exarata were gathered from bathing beach of Tianjin.

Hollow fiber membrane was from Tianjin Motimo Membrane Technology Co.,Ltd;TGL-16M high speed freezing centrifuge was from Changsha Xiangyi Centrifuge Instrument Co.,Ltd; TU1810 UV-visible spectrophotometer was from Beijing Purkinje Instrument Co.,Ltd; SAGA-10TJ laboratory ultrapure water instrument was from Nanjing Eped Technology Development Co.,Ltd; Agarose horizontal electrophoresis tank and DC regulated power were from Beijing Liuyi Instrument Factory; Rotary Evaporators was from Shanghai Yarong Instrument Factory.

Extraction process of glycosaminoglycan from *Bullacta exarata*:

Bullactaexarata→shelling→homogenate→enzymolysis→inactivation of enzyme by boiling→decoloration withhydrogenperoide→pHadjustment→deproteinization by centrifugation→ethanolprecipitation→precipitation separation by centrifugation→washing by ethanol and acetone respectively→drying→crude glycosaminoglycan

Purification of glycosaminoglycan:

Deproteiniztion→ultrafiltration→ethanolprecipitation

Dissolved crude glycosaminoglycan in ultrapure water, removed insoluble substance by centrifugation, added trichloroacetic acid to the supernatant until the trichloroacetic acid content was 5%，removed the deposits by centrifugation, ultrafiltrated the supernatant using hollow fiber membrane (interception molecular mass of 10000), ethanol precipitated the filtrate using ethanol-sodium acetate(mixed ethanol with 5% sodium acetate aqueous solution, ethanol content 60%,v/v), stewing 24h at 4℃,removed the supernatant by syphonage,collected precipitate,gained first-step purification of glycosaminoglycan(GAG-1) after drying.

CTAB(cetyl trimethyl ammonium bromide) precipitation

Gained second-step purification of glycosaminoglycan (GAG-2) by CTAB precipitation.

Purity detecting of glycosaminoglycan

Ultraviolet absorption spectrum

In order to compare protein content and nucleic acid content between crude glycosaminoglycan and purified glycosaminoglycan, scaning crude glycosaminoglycan aqueous solution and purified glycosaminoglycan aqueous solution by TU1810 ultraviolet-visible spectrophotometer respectively.

Agarose gel electrophoresis

Used the method recorded in reference [9] .

Analysis of chemical composition on glycosaminoglycan

Sulfate Content

Used the method of gelatin- $BaCl_2$ [10].

Uronic acid conten

Used the method of colorimetry of carbazole [11].

Hexosamine content

Used the method of improved Elson-Morgan [12].

3 Results and Analysis

Purification of Glycosaminoglycan from *Bullacta exarata*

The yield rate, recovery rate and content of GAG were showed in table 1.The GAG content in crude was 21.50%,after first-step purification, the content was 65.20% and the rate of recovery was 47.75%,after second-step purification, the content raised to 90.82% and the rate of recovery was 82.14%.

Table 1. The purification results of Glycosaminoglycan

GAG	Yield rate（%）(relative to fresh meterial)	Recovery rate（%）	Content of GAG（%）
Crude GAG	1.22		21.50
GAG-1	0.096	47.75	65.20
GAG-2	0.0648	82.14	90.82

Purity Detecting of Glycosaminoglycan

Ultraviolet Absorption Spectrum

The spectrograms were showed as follow. Figure1 showed that crude GAG had absorption peaks of 280nm and 260nm which meant that crude GAG contained lots of protein and nucleic acids. Figure2 showed that purificated GAG didn't have absorption peaks of 280nm and 260nm.Both figure1 and figure2 had intense absorption peak at 206nm.The purity of GAG was high after purification.

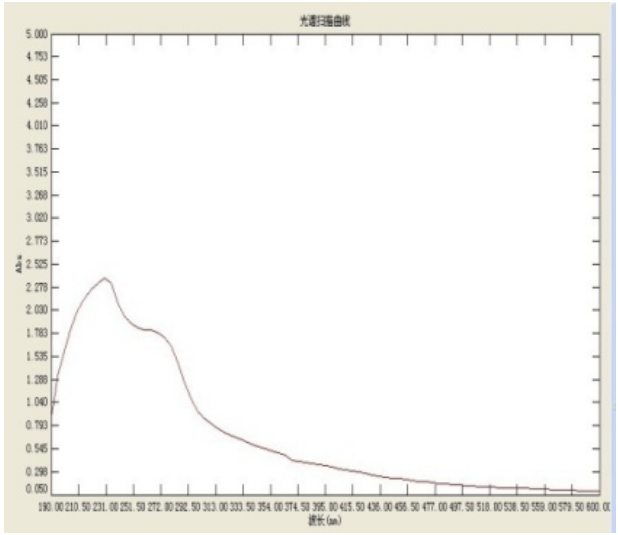

Figure 1. Ultraviolet absorption spectrum of crude GAG

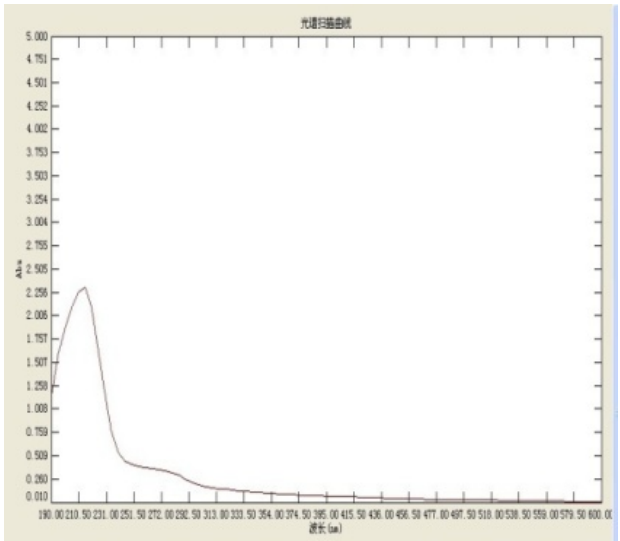

Figure 2. Ultraviolet absorption spectrum of purified GAG

Agarose Gel Electrophoresis

Purified glycosaminoglycan was analysed with agarose gel electrophoresis using heparin sodium and chondroitin sulfate as standard samples, the result was plate1, plate1showed that two standard samples and GAG-2 had positive reaction with toluidine blue and they could migrated to anode under the action of electric field，this meant that GAG-2 had the characteristics of polyanion as standard samples.Both heparin sodium and chondroitin sulfate were of single pure component, of which the electrophoretogram spots were concentrative and clear. The electrophoretogram of GAG-2 had smearing.It might be analyzed that the glycosaminoglycan species were uniform or had large dispersion of molecular mass. plate1 also showed that migrating distance of GAG-2

978-1-61896-030-6 © 2012 SciRes.

was shorter than standard samples which may be concerned with low sulfate content.

Analysis of Chemical Composition on Glycosaminoglycan

The chemical composition of glycosaminoglycan was analysed by chemical methods. The results showed that sulfate content was 3.95%, uronic acid content was 25.83% and amino sugar content was 14.19% in glycosaminoglycan from *Bullacta exarata*(table2). Sheng Wenjing, et al [13] had analysed the chemical composition of the polysaccharides from the sea cucumber, sulfate content was 19.54-29.28%, uronic acid content was 9.85-13.38%, hexosamine content was 4.92-10.18%. Wang Changyun, et al [14] had analysed the chemical composition of glycosaminoglycan from *Argopecten Irradians*, sulfate content was 6.66%, uronic acid content was 23.20%, hexosamine content was 22.60%. It is easy to be known that chemical composition of glycosaminoglycan from different mollusca are of great difference. Study showed that bioactivity of glycosaminoglycans was closely linked with sulfate and acetyl, anticoagulant activity and antiviral activity of heparin sodium and chondroitin sulfate depended on position and connection type of sulfate. Heparin sodium with high degree of sulfation had high lipid-lowering activity and anticoagulant activity while heparin sodium with high degree of acetylation had low anticoagulant activity [15].

Plate 1. Agarose gel electrophoresis spectrum of *Bullacta exarata* GAG

From left to right: 1. *Bullacta exarata* GAG; 2. heparin sodium; 3. chondroitin sulfate

Table 2. The chemical composition of Glycosaminoglycan

Composition	Sulfate	Uronic acid	Hexosamine
GAG	3.95	25.83	14.19

4 Conclusion

The purity of GAG from *Bullacta exarata* could reach 90.82% after two steps of purification;The chemical composition of glycosaminoglycan was analysed by chemical methods, the content of sulfate, uronic acid content and hexosamine was 3.95%, 25.83%and14.19%.

Acknowledgement

This research was financially supported by the Tianjin Program of Revitalization the Sea by Science and Technology (Grant NO. KX2010-0003).

References

[1] HaoWang，Guangli Yu, Xia Zhao, et al. Sorts and disaccharide composition analysis of glycosaminoglycans from rat kidney[J].Spectroscopy and Spectral Analysis, 2010, 30(9): 2484-2487.

[2] Jiahe Li，Yingshi Wang，Weiguo Wang，et al. Extraction of 6-chondroitin sulfate from whaleshark[J]. Journal of Marine Drugs, 1986, 5(2):7-9.

[3] Wenmei Shen，Chuanhuan Luo，Yi Luo，et al., Physicaland chemical properties of acid mucopolysaccharide fromAsteriasAmurensis[J].Journal of Marine Drugs,1986, 5(2):1-6.

[4] Huizeng, Fan，Judi Chen，Kezhong. Lin.An acidic mucopolysaccharide isolated fromStichopus Japonicas Selenka and its physical and chemical properties[J]. Acta Pharmaceutica Sinica, 1980, 5:263-269.

[5] Qianqun Gu，Yuchun Fang，Changyun Wang,et al. The chemical composition of chondrusocellatus and the anti-tumor activities of glycoprotein from Scallop Skirt[J].ChineseJournal of Marine Drugs, 1998,6 (3):23-25.

[6] Cassro C M F,Dietrich C P. Distribution of sulphated Mucopolysaccharides ininvertebrates[J].J.Biol.Chem., 1977, 252: 2254-2261.

[7] Shuguo Li, Biology of Bullacta exarata[J]. Reservoir Fisheries, 2005, 25(4):15-19.

[8] Yuhai Jia.China pharmaceutics of marine lakes and marshes [M]. Beijing:Xueyuan Press, 1996:125.

[9] Chuanying, Yuan，Qingman Cui，Huifang Sun, et al. Study on purification and functional activity of glycosaminoglycan from Mactra Quadrangularis[J]. Journal of Anhui Agricultural Sciences, 2011, 39(10): 5882-5884.

[10] Dodgson K,Price R. A note on the determination of the ester sulfate content of sulfated polysaccharides [J]. Biochem, 1962, 84: 106.

[11] Bitter T,Muir HM. A modified uronic acid carbazole reaction [J].Anal Biochem, 1962, 4:330.

[12] Ressing J L,Strominger LJ,,Leloir FL. A Modified Calorimetric method for the estimation of N-acetylamino sugars[J]. Biol Chem, 1955, 217:959.

[13] Wenjing Sheng，Changhu Xue，Qingxi Zhao,et al. Chemical component analysis of polysaccharides from different seacucumbers[J].Chin J Mar Drugs, 2007, 26(1): 44-49.

[14] Changyun Wang，Huashi Guan. Extraction and purification of glycosaminoglycans from Argopecten Irradiand Larmarck[J]. Journal of Ocean University of Qingdao, 1995, sp.Issue, 209-214.

[15] Shuangli, Xiong, Zhengyu Jin.Analysis and identification method of glycosaminoglycan[J]. Journal of Anhui Agricultural Sciences, 2005, 33(12):2372-2375.

Study on Anti-Oxidative Effect of Polyphenol from *Malus asiatica* Nakai on Mice

Dan ZHU[1], Guangcai NIU[2]
[1]*College of Life Science and Technology, Heilongjiang Bayi Agricultural University, Daqing, China*
[2]*Food college, Heilongjiang Bayi Agricultural University, Daqing, China*
Email: guangcainiu@yahoo.com.cn

Abstract: In order to observe the effect of polyphenol from *Malus asiatica* Nakai (PM) on the changes of SOD activity and MDA content in the liver, brain tissue and serum of mice, totally 50 Kunming mice, which male and female was fifty-fifty, were divided into five groups (n=10) randomly: control group (physiological saline), 100 mg/(Kg·d) group, 200 mg/(Kg·d) group, 400 mg/(Kg·d) group, and 800 mg/(Kg·d) group, mice in different dosage groups were administered for 35 days successively, SOD activities and MDA contents in the liver, brain tissue and serum were detected. The results indicated that PM could increase the SOD activities in the liver, brain tissue and serum significantly, decrease MDA contents in the liver, brain tissue and serum significantly. It showed that PM has better anti-oxidative activities, it is concluded that PM may be exploited as a good natural antioxidant as well as an important base material of functional foods and biomedicinals.

Keywords: Polyphenol from *Malus asiatica* Nakai (PM); mice; anti-oxidation; superoxides dismutase (SOD); malondialdehyde (MDA)

1 Introduction

Polyphenolic substance was a group of compound with remarkable antioxidation activity. Meanwhile, it was an excellent and natural antioxidant. The contents of apple and its pomace were extraordinarily rich source of polyphenolic substance. Plant polyphenols, the general name of polyphenolic substances, including proanthocyanidins, flavonols, phenolic acids, catechins, anthocyanins, dihydrochalcone and so on[1]. At present, finding the natural polyphenolic substance is a new hotspot in borne and abroad[2]. It was concerned about biological activity and health function of polyphenolic substance, especially the biological function of scavenging free radical, anti-lipid peroxidantion, delaying senility, preventing cardiovascular disease, anti-tumor, anti-irradiation, and so on[3,4].

Malus asiatica Nakai is also known as *Malus pumila* var. *rinki* Koidz., *Malus domestica* var. *asiatica* (Nakai) Ponomar, and so on. The plant widely distributed in the northeast of China, the polyphenolic constituents are rich in *Malus asiatica* Nakai[5]. At present, there have been many reports on biological activity evaluation on apple polyphenols[6,7], however, polyphenols from *Mnalus asiatica* Nakai (PM) have been not made a systematical and profound study on biological activity. In order to better develop and utilize *Malus asiatica* Nakai resources, polyphenols from *Malus asiatica* Nakai (PM) and mice were used to study on anti-oxidative effects of PM on mice by determining SOD activity and MDA content in liver, brain, and serum, so as to provide theoretical basis to screen antioxidative drugs.

The project was funded by Daqing science and technology bureau of Heilongjiang province (No. 2008-33).

2 Materials and Methods

2.1 Materials and Instruments

Malus asiatica Nakai pomace, provided by Daqing longhead food Co.,Ltd, dried and crumbled at 50℃, sieved by 40 eyes sifter and reserved; polyphenols from *Malus asiatica* Nakai (PM), prepared by microwave method, the total polyphenol content was 45.73%; The kits of superoxide dismutase (SOD) and maldondialdehyde (MDA) were provided by the Nanjing Jiancheng Bioengineering Institute; alcohol (analytical reagent).

RE-52 rotary evaporation instrument (Shanghai yarong biochemical instrument factory); SHZ-IIIB-circulating water vacuum pump (Shanghai medical apparatus factory); UV-1100 UV-Vis spectrophotometer (Beijing rayleigh analytical instrument Co., Ltd.); HWC-3L Microwave extraction Equipment (Tianshui Huayuan Pharmaceutical Equipment Technological Co.,Ltd); TGL-16G high speed centrifuge, ShangHai Anting Scientific Instrument Factory; Vacuum freezing drier (Beijing sihuan scientific instrument factory).

2.2 Animals

Healthy mice of the species in Kunming, weight 20±2 g, were purchased from Harbin Veterinary Research Institute, Chinese Academy of Agricultural Sciences.

978-1-61896-030-6

2.3 Methods

2.3.1 Preparation of Polyphenols from *Malus asiatica* Nakai (PM)

Malus asiatica Nakai pomace →Crumbled →Sieved →Extracting by Microwave→ Centrifuged →Supernatant →Vacuum concentration →Vacuum freeze-drying →PM

Main points of operation.

2.3.1.1 Extracting

The ratio of *Malus asiatica* Nakai pomace to ethanol solvent (50%) 1:20, extracting 2 min in 540W and 2450MHz microwave conditions, then extracting 20 min at 80℃, the extracts were obtained.

2.3.1.2 Centrifuging

The extracts were centrifuged at 4000r/min for 10 minutes to remove fine particles and powder.

2.3.1.3 Concentrating & Vacuum Freeze-Drying

The extracts were concentrated by rotary evaporation, and polyphenol from *Malus asiatica* Nakai (PM) was obtained by vacuum freeze-drying.

2.3.2 Animal Grouping

After a week normal diet, totally 50 Kunming mice, which male and female was fifty-fifty, were divided into five groups (n=10) randomly: control group (physiological saline), 100 mg/(Kg·d) group, 200 mg/(Kg·d) group, 400 mg/(Kg·d) group, and 800 mg/(Kg·d) group. Mice in different dosage groups were administered with the same volume solution of 100mg/ Kg·d bw, 200mg/ Kg·d bw and 400mg/ Kg·d bw, and 800mg/ Kg·d bw respectively once a day, the same volume physiological saline was administered to the control group. The above actions were to be done for 35 days successively. All mice were stopped eating 1 d before killing, but could drink water freely.

2.3.3 Sample Collecting and Preparation

The eyeball was taken and blood flowed into centrifugal tube, after standing, the serum was obtained by centrifuging at 2200r/min for 10 minutes. The mice were executed by isolating head to take out liver and brain tissue by douching of 4℃ physiological saline. The liver and brain tissue were mixed by 9 times volume 4℃ physiological saline respectively, the 10% homogenates were obtained by grinding, the supernatant was collected by centrifuging at 3000r/min for 10 minutes and preserved at low temperature.

2.3.4 Detection of Indexes

Superoxide dismutase (SOD) and maldondialdehyde (MDA) were detected by the kits of SOD and MDA provided by the Nanjing Jiancheng Bioengineering Institute. SOD activities and MDA contents of mice liver, brain tissue and serum were detected exactly according to the operation instruction.

2.3.5 Data Analysis

The results were measured by $\bar{X}$ ±S. The data obtained were analyzed for ANOVA using SPSS 12.0 software. There was statistical significance ($P < 0.05$).

3 Results and Analysis

3.1 Effects of PM on Activity of SOD and Content of MDA in the Liver Tissue of Mice

SOD activity in the liver tissue of all dosage groups was higher than that in the control group, SOD activity of 100 mg/Kg·d, 200 mg/Kg·d and 400 mg/Kg·d groups reached the remarkable level ($P< 0.05$), 800 mg/Kg·d dosage group reached the extremely remarkable level ($P< 0.01$). MDA content in the liver tissue of all dosage groups mice was lower than that in the control group, 100 mg/Kg·d group reached the remarkable level ($P< 0.05$), 200 mg/Kg·d, 400mg/Kg·d, and 800 mg/Kg·d dosage groups reached the extremely remarkable level ($P< 0.01$). The results showed a dosage effect relationship between increasing SOD activity and decreasing MDA content in the liver tissue of mice.

Table 1. Effect of PM on SOD activity and MDA content in the liver tissue of mice (n=10)

Groups	Dosage (mg/Kg·d)	SOD activity (U/mg pro)	MDA content (nm/mg pro)
Control	0	155.5850±9.71464	3.2550±0.43870
Treatment	100	159.9175±13.15023*	2.6913±0.21755*
	200	164.8063±11.97014*	2.2763±0.29981**
	400	170.1413±11.49618*	1.9950±0.47011**
	800	186.1150±10.90741**	1.6250±0.36622**

Compared with control group, *p<0.05, **p<0.01.

3.2 Effects of PM on Activity of SOD and Content of MDA in the Brain Tissue of Mice

Compared with control group, excluding the 100 mg/Kg·d dosage group ($P> 0.05$), SOD activities in the brain tissue of the rest 3 groups were higher than that in the control group, in which, 200 mg/Kg·d group reached the remarkable level ($P< 0.05$), 400 mg/Kg·d and 800 mg/Kg·d dosage groups reached the extremely remarkable level ($P< 0.01$). MDA content in the brain tissue of all dosage groups mice was lower than that in the control group, 100 mg/Kg·d group reached the remarkable level ($P< 0.05$), 200 mg/Kg·d, 400 mg/Kg·d, and 800 mg/Kg·d dosage groups reached the extremely remarkable level ($P< 0.01$).

Table 2. Effect of PM on SOD activity and MDA content in the brain tissue of mice (n=10)

Groups	Dosage (mg/Kg·d)	SOD activity (U/mg pro)	MDA content (nm/mg pro)
Control	0	165.8688±28.59068	6.6788±0.55256
Treatment	100	172.6775±14.69545	5.1113±0.39621*
	200	194.0125±15.59863*	4.3088±0.52878**
	400	236.6600±14.35399**	4.0175±0.70785**
	800	282.4463±12.05785**	2.3688±0.72383**

Compared with control group, *p<0.05, **p<0.01.

3.3 Effects of PM on Activity of SOD and Content of MDA in the Serum of Mice

SOD activity in the serum of all dosage groups was higher than that in the control group, SOD activity of 100 mg/Kg·d group reached the remarkable level (P<0.05), and SOD activity of 200 mg/Kg·d, 400 mg/Kg·d, 800 mg/Kg·d dosage group reached the extremely remarkable level (P< 0.01). MDA content in the serum of all dosage groups mice was lower than that in the control group, 100 mg/Kg·d group reached the remarkable level (P< 0.05), 200 mg/Kg·d, 400 mg/Kg·d, and 800 mg/Kg·d dosage groups reached the extremely remarkable level (P< 0.01). The results showed that PM could improve the activity of SOD, and decrease the content of MDA in the serum of mice significantly.

Table 3. Effect of PM on SOD activity and MDA content in the serum of mice (n=10)

Groups	Dosage (mg/Kg·d)	SOD activity (U/mL)	MDA content (nm/mL)
Control	0	108.6100±10.54189	6.9963±0.74548
Treatment	100	117.1863±9.17063*	5.6350±0.63209*
	200	127.6375±7.56385**	4.5900±0.69129**
	400	132.2263±8.10067**	3.4650±0.48051**
	800	140.1225±4.69301**	2.0388±0.75106**

Compared with control group, *p<0.05, **p<0.01.

4 Discussion

Metabolism of free radical will lose its balance when it was affected by many factors, such as senescence, environmental pollution, pesticide, radiation, and so on, the imbalance will lead to the accumulation of free radical, activity decreasing of enzyme scavenging free radical, the structure and function of biological macromolecules were attacked and damaged by free radical, the content of malondialdehyde (MDA) produced by lipid peroxidation increased. Exogenous antioxidant was used to adjust and treat imbalance of free radical, it is the new focus of nutrition and health, repairing the body damage and preventing and curing diseases in future[8].

The polyphenol, which is considered as the most antioxidant got from the diet, widely occurs in fruits and vegetables. It has been demonstrated in many studies that polyphenolic substance has biological activity of scavenging free radical, anti-lipid peroxidantion, and so on[9-11]. Mice were administered with apple polyphenol (AP) extract of 100 mg/(Kg·d), 200 mg/(Kg·d), 400 mg/(Kg·d) and 800 mg/(Kg·d), the results showed that AP could increase the activity of SOD, and decrease the contents of MDA in the heart, liver, brain, kidney and serum of mice significantly (Jin ying, 2006) [12].

In our study, mice in different dosage groups were administered with the same volume solution of 100mg/ Kg·d bw, 200mg/ Kg·d bw, 400mg/ Kg·d bw, and 800mg/ Kg·d bw respectively once a day for 35 days successively, the animal physiological status was normal during the study period. Compared with control group, the contents of MDA in the liver, brain tissue and the serum of mice treated decreased significantly, and the activity of SOD increased significantly, it showed a dosage effect relationship, but the polyphenol played the main role.

5 Conclusion

SOD activities of all dosage groups were higher than that in the control group, excluding the 100 mg/Kg·d dosage group of the brain tissue (P> 0.05), SOD activities of the rest groups were higher than that in the control group significantly. MDA contents in the liver, brain tissue and serum of all dosage groups mice were lower than that in the control group, in which, 100 mg/Kg·d group reached the remarkable level (P< 0.05), 200 mg/Kg·d, 400 mg/Kg·d, and 800 mg/Kg·d dosage groups reached the extremely remarkable level (P< 0.01). It showed that PM has better anti-oxidative effect on mice.

References

[1] Giacalone Marilù, Di Sacco Filippo, Traupe Ippolito, et al. "Antioxidant and neuroprotective properties of blueberry polyphenols: a critical review," *Nutritional Neuroscience*, Vol. 14, No. 3, 2011, pp119-125.

[2] Pérez-Jiménez J., Neveu V., Vos F., et al. "Identification of the 100 richest dietary sources of polyphenols: an application of the Phenol-Explorer database," *European Journal of Clinical Nutrition*, Vol. 64, Supplement,2010, ppS112-S120.

[3] Vauzour David, Rodriguez-Mateos Ana, Corona Giulia, et al. "Polyphenols and human Health: prevention of disease and mechanisms of action," *Nutrients*, Vol. 2, No.11, 2010, pp1106-1131.

[4] Visioli, Francesco, Lastra, Catalina Alarcon De La, Andres-Lacueva, Cristina, et al. "Polyphenols and Human Health: A Prospectus," *Critical Reviews in Food Science & Nutrition*, Vol. 51, No. 6, 2011, pp524-546.

978-1-61896-030-6 © 2012 SciRes.

[5] Li Shufen, Zhu Dan, Niu Guangcai,et al. "Optimization of microwave extraction of polyphenols from Malus asiatica pomace by response surface methodology," *China Food Additives*, No. 2, 2011, pp157-161.
[6] Khanizadeh Shahrokh, Tsao Rong, Rekika Djamila, et al. "Polyphenol composition and total antioxidant capacity of selected apple genotypes for processing," *Journal of Food Composition & Analysis*, Vol. 21, No.5, 2008, pp396-401.
[7] Oszmiański, Jan, Wojdyło, Aneta. "Polyphenol content and antioxidative activity in apple purées with rhubarb juice supplement," *International Journal of Food Science & Technology*, Vol. 43, No. 3, 2008, pp501-509.
[8] Wang Hao, Zhang Zesheng, Guo, Ying, et al. "Hawthorn fruit increases the antioxidant capacity and reduces lipid peroxidation in senescence-accelerated mice," *European Food Research & Technology*, Vol. 232, No. 5, 2011, pp743-751.
[9] Bae Song-Hwan, Suh Hyung-Joo. "Antioxidant activities of five different mulberry cultivars in Korea," *LWT - Food Science & Technology*, Vol. 40, No. 6,2007, pp955-962.
[10] Kaviarasan S., Sivakumar A. S.. "Potent radical scavenging ability of sunphenon: a green tea extract," *Journal of Food Biochemistry*, Vol. 35, No. 2, 2011, pp596-612.
[11] Gupta Sheetal, Prakash Jamuna. "Studies on Indian green leafy vegetables for their antioxidant activity," *Plant Foods for Human Nutrition*, Vol. 64, No. 1, 2009, pp39-45.
[12] Jin ying, Sun Aidong. "Study on anti-oxidative effects of polyphenols from apple on mice," *Food and Nutrition in China*, No. 1, 2006, pp 31-33.

Study on the Changes of Active Ingredients of American Ginseng in Preservation

Dejing CHEN
Provincial Key Laboratory of Bio-Resource, Shaanxi University of Technology, Hanzhong, China
Email:cdjlsg@126.com

Abstract: The changes of active ingredients of American ginseng (Panax quinquefolium L.) were analyzed in this paper. Active ingredient in imitation of ecological preservation conditions change, in order to evaluate the quality of fresh ginseng. The results showed that total sugar in American ginseng decreased by 16.14% after preservation for 180 days, polysaccharide decreased by 1.97%, total saponins decreased by 0.08%, the main saponin Rg1 decreased by 0.02%, Re decreased by 0.13%, Rb1 increased by 0.04%, and the content of amino acids increased by 0.66%.

Keywords: American ginseng; preservation; active ingredient; change

1 Introduction

American ginseng (Panax quinquefoiuml L.) is a kind of perennial medicinal plant in Panax of Araliaceae, which is originally produced in USA and Canada and then transferred into China [1]. American ginseng was successfully introduced and cultivated in China in 1975, and it has been cultivated for more than 10 thousands acres. Its annual yield is more than 500 tons, which accounts for 6% of the total yield all over the world and ranks the third in the world [2]. The major active ingredients of American ginseng are American ginseng saponins, polysaccharides, polypeptides, amino acids, volatile oils and others [3,4], therefore, it has certain effects in preventing fatigue, reinforcing immunity, reducing blood sugar, improving memory and inhibiting tumor growth, and it has become one of the frequently used healthcare foods in our daily life [5,6]. American ginseng is mainly sold in the forms of dry ginseng and processed products, and preserved fresh ginseng has not been directly marketed now. People in south China like to cook soups with fresh ginsengs to nourish their bodies, and thus the requirements continuously increase since the smell of fresh American ginseng is strong. During the preservation of American ginseng, the major active ingredients of American ginseng, namely saponins, polysaccharides and amino acids change differently. Shibate S. (1966)[7] reported that the enzymatic activities in dry American ginseng increased at proper temperature due to moistening, and the saponin compounds were hydrolyzed and thus the therapeutic efficacy was reduced. Yang et al. [8] presumed that the contents of Rg1 and Re1 in American ginseng gradually increased with the prolongation in the preservation duration. Yue et al. [9] reported that the accumulation of amino acids in the roots of Panax ginseng and Panax quinquefolium L. showed a typical "V" shape. Panax quinquefolium L. contained 17 kinds of amino acids and 7 kinds of essential amino acids for human body, and the content of amino acids in the germination period was the highest. Wei Yongdi reported that the total content of amino acids in American ginseng was 5.98% [10], and the sequence for total content of individual amino acid was arginine > glutamate > aspartic acid, and amino acids and polypeptides had certain effects in the healthcare functions of American ginseng. Li et al. [11] utilized sand preservation and combination of antistaling agents and refreshing bags to preserve American ginseng for 180 days. The content of panaxsaponin in the American ginseng from sand preservation was maintained at a relatively high level, while the contents of crude polysaccharides and free amino acids changed mildly during the preservation period for 135 days and then showed relatively significant increases after 180 days; however, the content of crude polysaccharides in the American ginseng that was processed with antistaling agents and refreshing bags significantly decreased after it was preserved for 90 days, while the content of free amino acids did not change significantly. Since general investigations on the changes in the active ingredients during the preservation of American ginseng are still deficient, understandings and opinions on the quality of preserved ginseng are different.

2 The Model

2.1 Materials and Instruments

Fresh American ginseng (which was provided by Jiashisen Traditional Chinese Medicine Development Company of Liuba County), refreshing bags (which were produced by Suzhou Deep Breath Refreshing Co., Ltd.).

Sulphuric acid, hydrochloric acid, barium hydroxide, oxalic acid, anthrone, sodium citrate, glucose, perchloric acid, n-butanol, phosphoric acid, triketohydrindene

978-1-61896-030-6

hydrate (they were all analytical pure grade), vanillin (which was produced by Shanghai Chemical Reagent Company of China Pharmaceutical Group), methanol (chromatographic pure), acetonitrile (chromatographic pure), 17 kinds of control preparations for amino acids (SIGMA Company), control preparations for panaxsaponin Rg1, Re and Rb1, and the purity was higher than 97% (National Institute for the Control of Pharmaceutical and Biological Products of China).

Ozone sterilizing machine DHC12 (Shandong Lvbang Photoelectricity Equipment Co., Ltd.), high performance liquid chromatogram (HP1100), UV-2500 ultraviolet spectrophotometer (Shimazu, Japan), L-8900 automatic amino acid analyzer (Hitachi, Japan).

2.2 Experimental Methods

2.2.1 American Ginseng of Imitative Ecological Preservation

American ginseng of four years were collected in the middle of October and the sediments were washed out, then American ginseng was immersed in 5 mg/L ozone water for two hours in order to eliminate the microorganisms on the surface of American ginseng and prevent mould development and corruption. The moisture content on the surface of American ginseng was air-dried and American ginseng was transferred into 0.5 mmm compound refreshing bags, then the mixed gas containing 6% oxygen, 2% carbon dioxide and 92% nitrogen gas was filled in for sealing, and American ginseng was preserved, transported and marketed at 3℃±1℃, and imitative ecological preservation was carried out under the environmental conditions to mimic the dormancy of American ginseng in winter, the preservation duration was 180 days, the sprout of American ginseng was well-stacked and the fibrous roots were intact.

2.2.2 Determination of Respiratory Intensity by Using Titration Technique

A small bottle containing 50 ml barium oxide solution was placed in a brown bottle and a certain amount of fresh American ginseng was weighed and transferred into the brown bottle for every 45 days, subsequently the bottle was sealed with a piece of plastic membrane and kept in a refrigerator of 3℃ for 48 hours, and another bottle was prepared as the blank. Barium hydroxide solution can absorb the carbon dioxide that was released from the respiration of American ginseng, and the remaining barium hydroxide was titrated with oxalic acid, then the oxalic acid consumed in the blank experiment was subtracted and thus the released carbon dioxide from each kilogram of American ginseng per hour can be calculated, and that was the respiratory intensity of American ginseng.

2.2.3 Determination of Total Sugar and Polysaccharide Contents by Using Anthrone-Sulphuric Acid Method

Total sugar extraction: American ginseng was subjected to vacuum drying at 50℃ for every 45 days and grinded into powder, subsequently 1g powder sample was weighed, immersed with 500ml purified water for 12 hours and extracted for 3 hours by heating; the solution was metered to a final volume of 500ml and then filtrated, and 4ml of this filtered solution was metered to a final volume of 50ml for further determination.

Polysaccharide extraction: 1g American ginseng powder was weighed and wrapped in a piece of filter paper and transferred into a round bottomed flask, then it was extracted with 80% ethanol in a water bath of 70℃ for one hour, and the ethanol solution was discarded after centrifugation and the residues were rainsed with hot ethanol for three times, subsequently the filter paper bag was opened and the American ginseng residues were extracted with deionized water in a boiling water bath for three hours, and metered to a final volume of 500ml. 3ml of this solution was metered in a volumetric flask of 10ml for further determination.

0.0926g standard preparation of glucose that had been dried to constant weight was accurately weighted and dissolved in distilled water, then metered to a final volume of 100ml as the stock solution. 1ml, 2 ml, 3 ml, 4ml and 5ml stock solution of glucose was accurately transferred into five clean volumetric flasks of 50ml respectively, then they were metered with distilled water and prepared into standard glucose solutions in different concentration gradient (18.52 μg/ml, 37.04 μg/ml, 55.56 μg/ml, 74.08 μg/ml and 92.60μg/ml).

Six test tubes were prepared, among them 2ml distilled water was added in a test tube as the blank control and 2ml glucose solutions in different concentrations were added in the remaining five test tubes respectively; 8ml freshly prepared anthrone-sulphuric acid solution was added in each test tube respectively, and the six test tubes were heated in a boiling water bath for 10min, and the absorbance was determined at 625nm on a ultraviolet spectrophotometer after cooling, finally the standard curve was plotted. y=0.00971x+0.01226, R=0.99939.

2ml sample solution for total sugar determination was transferred into a test tube, then 8ml anthrone- sulphuric acid solution was added, and the test method was the same to that for standard curve preparation, finally the

absorbance was determined and the total sugar content in the sample was calculated.

Test method for polysaccharide content: the polysaccharide extract was used to determine the polysaccharide content according to the test method for total sugar.

2.2.4 Determination of Total Saponin by Using Vanillin Method, Determination of Rg1, Re and Rb1 by Using High Performance Liquid Chromatography

2.2.4.1 Determination of Total Saponin by Using Vanillin Method

Standard preparation of panaxsaponin Rb1 was precisely weighed and dissolved in 50% methanol to prepare the standard solution in 0.56mg/ml, subsequently 40, 80 and 160μl standard solution was accurately transferred into volumetric flasks of 10ml respectively, then 0.2ml 5% vanillin-acetic acid solution and 0.8ml perchloric acid were accurately added, and the solutions were then fully mixed. The volumetric flasks were kept in a water bath at 60℃ for 15min and then immediately kept on an ice bath for 2 min. 5ml acetic acid was accurately added. Corresponding solvent was used as the blank and the absorbance was determined on the ultraviolet spectrophotometer at 546nm. The concentrations of the standard solutions were used as the X-axis and the absorbance was used as the Y-axis, and the standard curve was thus plotted. The linear equation was as followed: y=0.01046x＋0.004, correlation coefficient: r=0.99983.

2.2.4.2 Determination of Rg1, Re and Rb1 by Using High Performance Liquid Chromatography

Chromatographic column: C18 (4.6×150mm, 5μm), detection wavelength: 203nm, flow rate: 1.0ml/min, column temperature: 25℃, sample size: 20μL. Moving phase: acetonitrile for pump A and 0.1% phosphoric acid for pump B, and gradient elution was carried out.

Table 1. The conditions of the gradient elution

Time (min)	Moving phase A (%)	Moving phase B (%)
0～10	18→20	82→80
10～26	20→22	80→78
26～50	22→40	78→60
50～60	40→18	60→82

One gram dried American ginseng powder was weighed and transferred into conical flasks with lids for every 45 days, then 50ml water saturated n-butanol was accurately added and the total weight was determined. The mixture was subjected to heat reflux extraction in a water bath for one hour, and the weight was measured again after cooling, then water saturated n-butanol was added to make up for the weight loss, and the solution was fully mixed and filtered. 25ml filtrate was accurately measured and transferred into a evaporating dish, and after the filtrate was evaporated to dryness and the residues were dissolved in proper amount of 50% methanol, and the solution was then transferred into a volumetric flask of 10ml and metered with 50% methanol to the scale, subsequently the solution was filtered after fully mixing and the filtrate was used for further determination.

0.0069g standard preparation of panaxsaponin Rg_1 was accurately weighed (the purity was 97.7%), then dissolved and metered to a final volume of 10ml as the stock solution (the concentration was 674.1μg/ml), subsequently 0.5ml, 1ml, 1.5ml and 2ml solutions were transferred and metered in volumetric flasks of 5ml respectively, and thus a concentration gradient was prepared (67.41μg/ml, 134.82μg/ml, 202.2μg/ml and 269.64μg/ml). The equation was as followed: Y=6.71956×X-13.5548, R=0.99964.

0.0064g standard preparation of panaxsaponin Re was accurately weighed, then dissolved and metered to a final volume of 10 ml as the stock solution (the concentration was 640 μg/ml), subsequently 0.5ml, 1 ml, 1.5 ml and 2ml solutions were transferred and metered in volumetric flasks of 5 ml respectively, and thus a concentration gradient was prepared (64 μg/ml, 128μg/ml, 192μg/ml, 256μg/ml). The equation was as followed:
Y=5.51095×X-11.14316, R=0.99988.

0.0061g standard preparation of panaxsaponin Rb_1 was accurately weighed, then dissolved and metered to a final volume of 10ml as the stock solution (the concentration was 610μg/ml), subsequently 1ml solution was metered to a final volume of 10ml, then 1ml and 2ml diluted solution was further metered to a final volume of 5ml respectively, and thus a concentration gradient was prepared (61μg/ml, 122μg/ml and 244μg/ml). The equation was as followed:
Y=4.92638×X-16.49978, R=0.99942.

20μL sample solution was subjected to high performance liquid chromatography according to the chromatographic conditions in ①, and the contents of panaxsaponin Rg_1, Re and Rb_1 were calculated respectively according to the standard curves.

2.2.5 Determination of Amino Acids in American Ginseng by Using Amino Acid Automatic Analysis

American ginseng was dried, grinded and sieved for every 45 days, and certain amount of powder was transferred into hydrolysis tubes, then the powder was frozen with 10ml 6 mol/L hydrochloric acid and three drops of newly distilled hydroxybenzene for 3 minutes, and the sample was subjected to evacuation followed by intro-

978-1-61896-030-6 © 2012 SciRes.

duction of high purity nitrogen gas, then it was subjected to evacuation and introduction of nitrogen gas for another two times, and the hydrolysis tubes were sealed at the presence of nitrogen gas. The tubes were kept in a thermostatic incubator at 110℃ for hydrolysis for 22 hours, then they were taken out and cooled. Subsequently the hydrolysis tubes were opened and the digests were filtered, and the hydrolysis tubes were rinsed with deionized water for several times; the digests were all transferred into and metered in volumetric flasks of 50 ml. 1ml filtrates were transferred into volumetric flasks of 5ml respectively and dried at 50℃ in a vacuum drying oven, then the residues were hydrolyzed with 1ml hydrochloric acid and dried, and this procedure was repeated twice and the solutions were finally evaporated to dryness, and the residues were dissolved in 1ml citrate buffer solution *pH*2.2 for further determination.

0.200ml standard solution of amino acids was accurately measured and diluted to a final volume of 5 ml with the buffer *pH*2.2, and the standard dilution concentration 5.00nmol/50μL was used as the standard for amino acids for the determination, and the content of amino acids in the sample solution was determined on the amino acid automatic analyzer by using the external reference method. The formula for calculating the content of amino acids was shown as below:

$$X = \frac{2S \times N \times V \times W}{M}$$

In this formula:

X-Amino acid percentage content, %

S- Concentration of amino acids in the standard solution, nmol/μL

N-dilution facto

V- metered volume after hydrolysis,mL

W- molecular weight of amino acids

M- Mass of the sample,g

3 Results and Analysis

3.1 The Respiratory Intensity of American Ginseng

The respiratory intensity during the imitative ecological preservation of American ginseng: the respiratory intensity of unpackaged American ginseng at 3℃ was 14.5 mgCO2·kg-1·h-1, and the respiratory intensity slightly increased (14.9 mgCO2·kg-1·h-1) after the sample was filled in the preservation bags for 45 days, the respiratory intensity was the lowest at 90 d (11.8 mgCO2·kg-1·h-1) and gradually increased from 135 d to 180 d, and the changing tendency was shown in Figure 1.

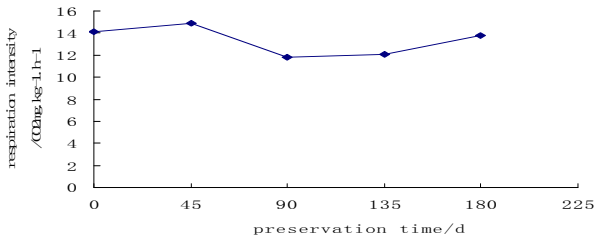

Figure 1. Changes in the respiratory intensity during the preservation of American ginseng

3.2 Total Sugar and Polysaccharide Contents in the Preserved American Ginseng

The total sugar content in the American ginseng during the preservation decreased from 44.83% to 28.69%, and the loss in total sugar was relatively significant, while the content of polysaccharides decreased from 10.71% to 8.74% (which decreased by 1.97%), thus it can be found that the consumptions were mainly monosaccharides and starch other than polysaccharides, which may be attributed to the hydrolysis of starch and monosaccharides and the production of carbon dioxide and water due to the respiration during the preservation of American ginseng, and the changing tendency was shown in Figure 2.

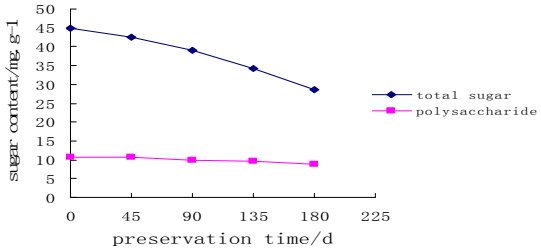

Figure 2. Changes in saccharide content during the preservation of American ginseng

3.3 Saponin Content in Preserved American Ginseng

During the preservation of American ginseng, total saponin content increased from the beginning to 135 d, then it began to decrease from 5.56% to 5.48% (which decreased by 0.08%). The major saponin ingredient Rg decreased from 10.19% to 0.17%, Re content decreased from 1.18% to 1.15%, while Rb1 content increased from 2.89% to 2.95%, which was mainly resulted from the consumption of saccharides and subsequent increase in relative content of saponin during the preservation, but not the increase in total saponin content in American ginseng. The changes in saponins in American ginseng were shown in Figure 3.

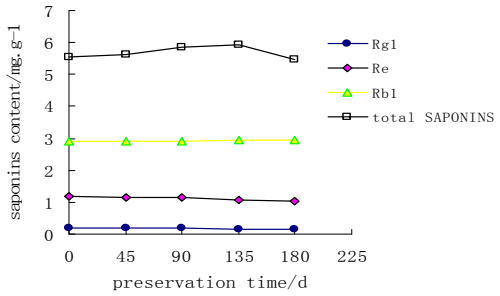

Figure 3. Changes in saponins during the preservation of American ginseng

3.4 Amino Acid Contents in the Preserved American Ginseng

Sixteen kinds of amino acids were detected during the preservation of American ginseng, and the amino acid with the highest concentration was arginine, followed by glutamate and aspartate, and tyrosine was not detected, among them seven kinds of amino acids were essential amino acids for human body, which accounted for 20.12% of the total content. The contents of amino acids increased from 5.89% to 6.64%, and it showed a significant increase at 135 d, which can be attributed to the decrease in saccharides partly, while the metabolic activities were relatively low during the dormancy of American ginseng, and American ginseng stopped to grow and the consumption of amino acids was very low. The changes in amino acid contents were shown in Table 2.

Table 2. Amino acid contents in the preserved American ginseng

Types of amino acids	Preservation time /d				
	0	45	90	135	180
Asp	1.01	0.98	1.01	1.08	1.07
Thr	0.16	0.15	0.15	0.2	0.19
Ser	0.15	0.14	0.14	0.14	0.13
Glu	1.15	1.03	1.08	1.18	1.16
Pro	0.42	0.43	0.44	0.47	0.46
Gly	0.48	0.51	0.51	0.57	0.54
Ala	0.25	0.28	0.28	0.29	0.29
Cys	0.11	0.11	0.11	0.11	0.10
Val	0.22	0.25	0.26	0.26	0.24
Met	0.01	0.02	0.01	0.03	0.02
Iso	0.13	0.14	0.14	0.15	0.15
Leu	0.12	0.25	0.25	0.26	0.26
Tyr	-	-	-	-	-
Phe	0.11	0.12	0.13	0.15	0.14
Lys	0.26	0.31	0.32	0.33	0.34
His	0.2	0.19	0.19	0.22	0.21
Arg	1.2	1.21	1.23	1.33	1.34
Total amino acid	5.98	6.12	6.25	6.77	6.64

4 Conclusion and Discussion

(1) The respiratory intensity of American ginseng from imitative ecological preservation was generally maintained at a relatively low level. The respiratory intensity increased from the beginning to 45 days, which may be attributed to the adaptive physiological changes of American ginseng in the preservation bag, subsequently the respiratory intensity increased after 135 days, which may be attributed to the functions of hormones and enzymes in American ginseng as well as germination and budding of American ginseng in March in the next year, and the change in respiratory intensity also reflected the metabolic changes in endogenous substances.

(2) During the respiration of American ginseng during preservation, saccharide consumption was significant and the consumed substances were mainly starch and monosaccharides, which the decrease in polysaccharides was not significant, thus the effects on the polysaccharides as active ingredients of American ginseng were not significant and their efficacy can not significantly decrease.

(3) During the preservation of American ginseng, total saponin in American ginseng slightly increased in the first 135 days and then began to decrease, but the content was higher than the requirement (2%) in Pharmacopeia of China; the major saponin varieties Rg1 and Re slightly decreased, while Rb1 content increased. In fact, the total mass of American ginseng decreased and the changes in saponins were not significant, saponin contents increased relatively, however, the total content of saponins and the contents of major saponins decreased when they were calculated in comparison to the mass of raw materials.

(4) Amino acid contents continuously increased during the preservation of American ginseng, which may be attributed to the consumption of saccharides during the respiration of American ginseng, and the relative contents increased due to the decrease in dry matter and they showed significant increases after preservation for 135 days, which was related to the metabolism due to endogenous physiological activity during germination and budding of American ginseng in March in the next year.

References

[1] He Yongming. Investigations on the history of ginseng as herbs. [J]. Chinese Traditional Patent Medicine, 2001, 23(5): 384-386.

[2] Cao Lijun, Xu Yonghua, Yu Shulian, et al. Current situation for the development of American ginseng industry in our country. [J]. Ginseng Research.2002, 14(1):36-38.

[3] Chen Lili, Cui Ning. Advancement in the investigations on chemical ingredients in American ginseng. [J]. Lishizhen Medicine and Materia Medica 2002, 13(10): 652-633.

[4] Li Xianggao. Investigations on chemical ingredients in different parts from American ginseng. [J]. Collection for scientific theses

978-1-61896-030-6 © 2012 SciRes.

on ginseng. [A] Changchun: Press of Jilin Agricultural University, 1998.

[5] Huang Taikang, Editor. Manual for ingredients and pharmacology for frequently used traditional Chinese medicines. [M. Beijing: China.Medico-Pharmaceutical Science and Technology Publishing House, 1994.2.

[6] Ma Xiuli, Zhao Dechao, Sun Yunxiu, et al. Investigations on polysaccharides in active American ginseng. [J]. Ginseng Research, 1996, 3: 37-38.

[7] Shibate S.Ando T,Tannka O Chemical studies on the oriental plant drugs .XVII.The prosapogenin of the ginseng saponins (ginsenosides –Rb1,-Rb2,and -Rc)[J] Chem Pharm Bull (tokyo)(Japan),, 1999,14(10):1157-1161.

[8] Yang Ming, Wang Chengfang, Cui Yunzhi, et al. Analysis on saponin contents in American ginseng from soft package and radiation preservation in liquids. [J].Modern Technology, 2006(11): 5-8.

[9] Yue Bing. Investigations on the accumulative rules for amino acids in the root of ginseng and American ginseng. [A]. Thesis for master candidate, Jilin Agricultural University, 2008).

[10] Wei Yongdi, Song Junchun, Wu Guangyi, et al. Determination of amino acids in wild ginseng, garden cultivated ginseng and American ginseng. [J]. Journal of Norman Bethune University of Medical Science, 1987, 13(6):503-505.

[11] Li Yuan, Wang Yun, Zhang Guozhen, et al. Effects of different preservation treatments on the quality and the ingredients in fresh roots of American ginseng. [J]. China Journal of Chinese Materia Medica, 2010, 35(6):145-148.

Author Index

(According to Alphabet)

M

N

P

Q

R

S

T

W

X

Y

Z